NEW INSIGHTS INTO THE TRANSMISSION DYNAMICS AND CONTROL OF ANTIMICROBIAL RESISTANCE TO LAST-RESORT ANTIBIOTICS

EDITED BY: Zhi Ruan, Ye Feng, Yi-Wei Tang, Shaolin Wang and Anne-Catrin Uhlemann

PUBLISHED IN: Frontiers in Microbiology

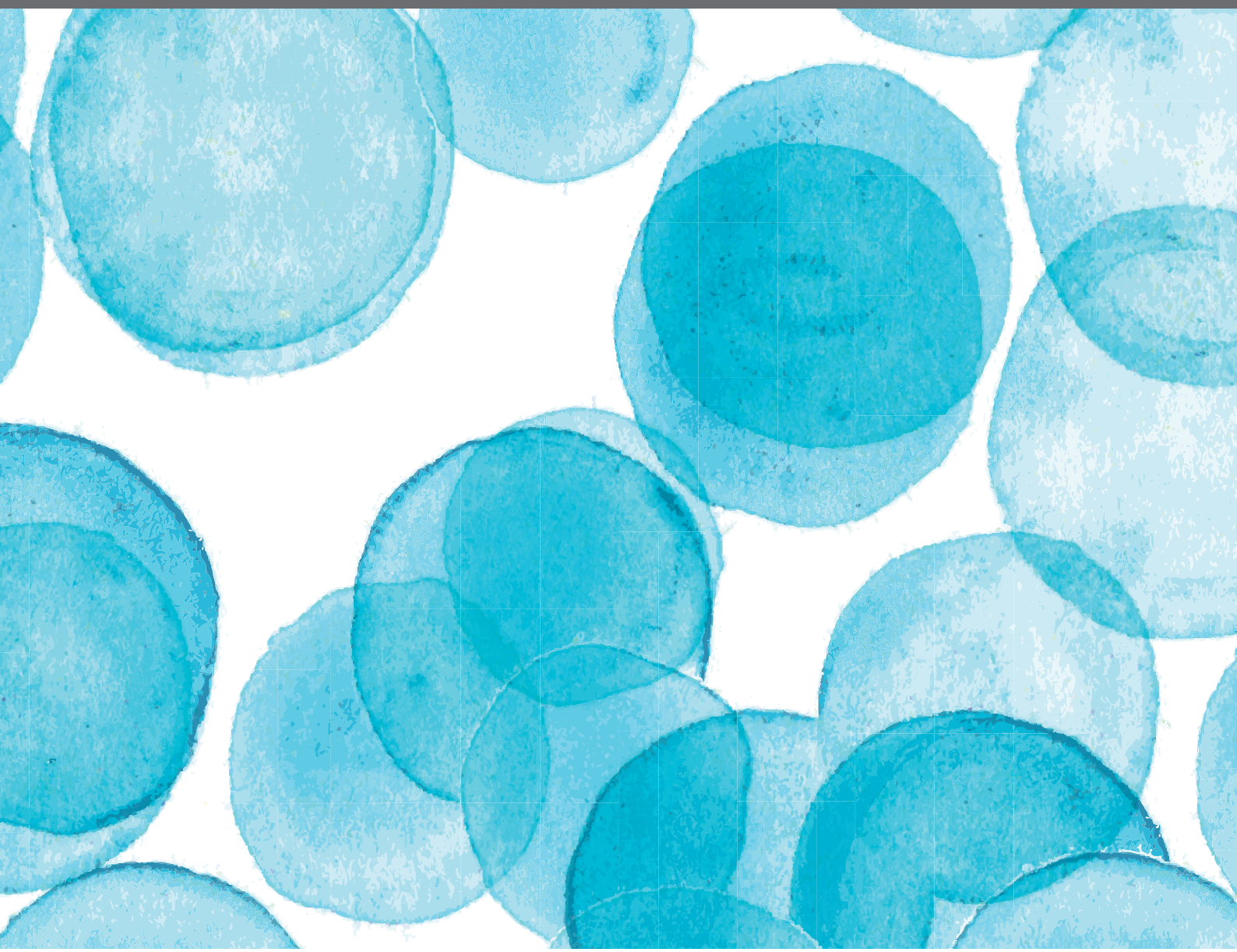

frontiers Research Topics

ISSN 1664-8714
ISBN 978-2-88974-883-9
DOI 10.3389/978-2-88974-883-9

About Frontiers

Frontiers is more than just an open-access publisher of scholarly articles: it is a pioneering approach to the world of academia, radically improving the way scholarly research is managed. The grand vision of Frontiers is a world where all people have an equal opportunity to seek, share and generate knowledge. Frontiers provides immediate and permanent online open access to all its publications, but this alone is not enough to realize our grand goals.

Frontiers Journal Series

The Frontiers Journal Series is a multi-tier and interdisciplinary set of open-access, online journals, promising a paradigm shift from the current review, selection and dissemination processes in academic publishing. All Frontiers journals are driven by researchers for researchers; therefore, they constitute a service to the scholarly community. At the same time, the Frontiers Journal Series operates on a revolutionary invention, the tiered publishing system, initially addressing specific communities of scholars, and gradually climbing up to broader public understanding, thus serving the interests of the lay society, too.

Dedication to Quality

Each Frontiers article is a landmark of the highest quality, thanks to genuinely collaborative interactions between authors and review editors, who include some of the world's best academicians. Research must be certified by peers before entering a stream of knowledge that may eventually reach the public - and shape society; therefore, Frontiers only applies the most rigorous and unbiased reviews.
Frontiers revolutionizes research publishing by freely delivering the most outstanding research, evaluated with no bias from both the academic and social point of view. By applying the most advanced information technologies, Frontiers is catapulting scholarly publishing into a new generation.

What are Frontiers Research Topics?

Frontiers Research Topics are very popular trademarks of the Frontiers Journals Series: they are collections of at least ten articles, all centered on a particular subject. With their unique mix of varied contributions from Original Research to Review Articles, Frontiers Research Topics unify the most influential researchers, the latest key findings and historical advances in a hot research area! Find out more on how to host your own Frontiers Research Topic or contribute to one as an author by contacting the Frontiers Editorial Office: frontiersin.org/about/contact

NEW INSIGHTS INTO THE TRANSMISSION DYNAMICS AND CONTROL OF ANTIMICROBIAL RESISTANCE TO LAST-RESORT ANTIBIOTICS

Topic Editors:
Zhi Ruan, Zhejiang University, China
Ye Feng, Zhejiang University, China
Yi-Wei Tang, Cepheid (United States), United States
Shaolin Wang, China Agricultural University, China
Anne-Catrin Uhlemann, Columbia University Irving Medical Center, United States

Citation: Ruan, Z., Feng, Y., Tang, Y.-W., Wang, S., Uhlemann, A.-C., eds. (2022). New Insights Into the Transmission Dynamics and Control of Antimicrobial Resistance to Last-resort Antibiotics. Lausanne: Frontiers Media SA.
doi: 10.3389/978-2-88974-883-9

Table of Contents

frontiers | Frontiers in Microbiology

EDITORIAL
published: 18 May 2022
doi: 10.3389/fmicb.2022.914978

Editorial: New Insights Into the Transmission Dynamics and Control of Antimicrobial Resistance to Last-Resort Antibiotics

Zhuoren Ling[1,2] *and Shaolin Wang*[1]*

[1] *Beijing Key Laboratory of Detection Technology for Animal-Derived Food Safety, College of Veterinary Medicine, China Agricultural University, Beijing, China,* [2] *Department of Zoology, University of Oxford, Oxford, United Kingdom*

Keywords: antibiotics, antimicrobial resistance, transmission, control, plasmid

Editorial on the Research Topic

New Insights Into the Transmission Dynamics and Control of Antimicrobial Resistance to Last-Resort Antibiotics

OPEN ACCESS

Edited and reviewed by:
Rustam Aminov,
University of Aberdeen,
United Kingdom

***Correspondence:**
Shaolin Wang
shaolinwang@cau.edu.cn

Specialty section:
This article was submitted to Antimicrobials, Resistance and Chemotherapy, a section of the journal Frontiers in Microbiology

Received: *07 April 2022*
Accepted: *08 April 2022*
Published: *18 May 2022*

Citation:
Ling Z and Wang S (2022) Editorial: New Insights Into the Transmission Dynamics and Control of Antimicrobial Resistance to Last-Resort Antibiotics. Front. Microbiol. 13:914978. doi: 10.3389/fmicb.2022.914978

Antimicrobial Resistance (AMR) is one of the most alarming public health issues around the world. Carbapenem, colistin, and tigecycline are currently the last-resort antibiotics for the treatment against multidrug resistant bacteria. This Research Topic integrates recent studies on the transmission dynamics and control strategies of AMR to these important drugs. It is about the mechanism of spread and the mitigation approaches of AMR.

DYNAMIC TRANSMISSION OF AMR

In this Research Topic collection, nearly half of the articles covered the critical role of plasmids in AMR dissemination.

On the one hand, plasmids carrying resistant genes acted as vehicles for horizontal gene transfer. Taking colistin resistance as an example, a well-documented gene, *mcr-1* has been frequently harbored on multiple transferable plasmids and spread worldwide. This gene encoded the MCR-1 enzyme that modified LPS and attenuated bacterial affinity with colistin (Liu et al., 2016). To better understand the interactome profile of MCR-1 with bacterial proteins, Li et al., using co-immunoprecipitation and mass spectrometry, found that MCR-1 affected protein biosynthesis by interacting with ribosomal proteins. Besides, they discovered that multidrug efflux pump AcrA-TolC was also involved in MCR-1-mediated colistin resistance. These data provided valuable information to a deeper understanding of MCR-1 function. Another study by Zhu et al. revealed that under colistin pressure, although *mcr-1* did not facilitate the evolution of high-level colistin resistance in *K. pneumoniae* and *E. coli*, it still improved the survival rates of the above species. Besides, high-level colistin resistance (HLCR) was more likely to emerge in *K. pneumoniae* than *E. coli* when exposed to colistin. This result partly explained why HLCR was more common in *K. pneumoniae* than *E. coli* in clinical sections.

Concerning tigecycline resistance, the plasmid-borne *tet*(X3) and *tet*(X4) were recently reported, alarming the possible horizontal spread of resistance (He et al., 2019; Zhang et al., 2020). This was further demonstrated by the research of Li et al. which identified one conjugative IncX1 plasmid habouring *tet*(X4) in *Escherichia fergusonii*, along with two chromosome-bearing *tet*(X6) in *Proteus cibarius*, from chicken feces. Apart from *tet*(X) and its variants, Xu et al. revealed that *tet*(A) mutation occurred under selective pressure could also lead to tigecycline resistance in *K. pneumoniae*. In their study, induction experiment was performed in which 71.4% (20/28) of *tet*(A)-carrying tigecycline resistance *K. pneumoniae* developed *tet*(A) mutations. And twelve (12/20) of them successfully transferred their *tet*(A)-mutant plasmids to *E. coli* EC600 by conjugation and led to an elevated level of tigecycline MIC in recipients (Xu et al.). These data indicated that mutations of *tet*(A) in conjugative plasmids may contribute to the tigecycline resistance in *K. pneumoniae* and *E. coli*.

To better understand the evolution of plasmids related to carbapenem resistance, one study by Liu et al. analyzed 84 non-duplicate IncX3 plasmids reported across China from 2011 to 2021. And all these plasmids harbored carbapenemase genes, among which 81 were bla_{NDM} carrying and 3 were $bla_{\mathrm{OXA-181}}$-carrying. In those NDM-positive plasmids, the NDM-5-positive ones were dominant and recovered from diverse sources, including clinical specimens, animals, environment and retail food, suggesting the wide spread of NDM-5-producing isolates through the transfer of IncX3 plasmids. However, NDM-1-positive IncX3 plasmids were mainly identified in the hospital section, which was disseminated at a limited level compared with NDM-5. The genetic context of bla_{NDM} on IncX3 plasmid could be classified into five subtypes, two of which have been identified in *Enterobacter cloacae* chromosome and IncF & IncA/C plasmids, respectively. This indicated that the bla_{NDM} gene environment could be transmitted by different plasmids and bacterial species. The other two studies reported KPC-2-carrying plasmids in China from *P. aeruginosa* (pP33-2, non-conjugative) and *E. coli* (pEC2341-KPC conjugative; pEC2547-KPC non-conjugative), respectively (Cai et al.; Wu et al.). In all the three plasmids, KPC-2 was bracketed by Insertion Sequence (IS), suggesting the potential role of IS in promoting the spread of KPC-2 among different plasmids.

On the other hand, plasmid could also act as a "lending library," integrating its sequence into bacterial chromosome and promoting the vertical transmission of AMR. Zhang et al. found that, to cause colistin-resistance in *K. pneumoniae* under drug pressure, IS*Kpn72* on a plasmid could be inserted into *mgrB* gene with a higher efficiency than the IS*Kpn72* from chromosome. More importantly, this plasmid was conjugative, providing a clue about the widespread of *mgrB* inactivation among *K. pneumoniae* in hospitals (Cannatelli et al., 2014). In another research, Wang et al. reported the first detection of clinical *E. coli* (ST131) with a $bla_{\mathrm{KPC-2}}$ in chromosome. Interestingly, sequence analysis showed that the chromosomal $bla_{\mathrm{KPC-2}}$ was carried in a 24 kb IS with high similarity to the $bla_{\mathrm{KPC-2}}$-habouring plasmids in *P. mirabilis* (Hua et al., 2020). This result suggested that the $bla_{\mathrm{KPC-2}}$ was probably transferred from the *P. mirabilis* plasmid to *E. coli* chromosome through IS element. Once incorporated into chromosome, AMR mechanism would largely be maintained in bacterial replication and worth clinical attention.

In recent years, the progress in whole genome sequencing (WGS) made it easier to study the AMR transmission in a deeper level. Using this technique, two studies investigated the evolution of AMR isolates. Gostev et al. uncovered the existence of three international lineage of linezolid-resistant *S. epidermidis*. And Zhao et al. sequenced 99 Carbapenem-Resistant *Klebsiella pneumoniae* (CRKP) from the intensive care unit (ICU) and provided a glimpse of intraspecies replacement in the hospital. According to phylogenetic analysis, both ST4496-KL47 and ST11-KL64 were likely to originated from ST11-KL47. However, ST4496-KL47 was less competitive than ST11-KL64 and disappeared after 6 months. While ST11-KL64 increased virulence by capsule biosynthesis locus recombination and acquired the potential to be the dominant CRKP in hospital. In addition, the serotype was found to be associated with antimicrobial resistance in this Research Topic. The study by Luo et al. indicated that, for clinical Salmonella isolates in China, colistin resistance mainly distributed in *S. Enteritidis* (83.9%, 125/149) and *S. Typhimurium* (15.3%, 9/59), while the resistant rate of the former was significantly higher than that of the latter.

CONTROL OF ANTIMICROBIAL RESISTANCE

To put AMR under control, various strategies need to be executed, including constant surveillance of drug resistance, fast diagnosis of AMR bacteria infections and development of novel therapy.

Firstly, the spread of drug resistance needs to be put under surveillance. The work by Chang et al. revealed the epidemiology and change of antimicrobial resistance rates in children patients with non-typhoidal Salmonella infection from 2012 to 2019. And the report by Paveenkittiporn et al. provided comprehensive information to the prevalence of *mcr*-positive Carbapenem-Resistant Enterobacteriaceae (CRE) among patients in Thailand from 2016 to 2019. Another study by Ma et al. investigated AMR in clinical *Ureaplasma* spp. and addressed the lack of data in this field in China. In their research, the most active antibiotics were azithromycin, josamycin, and clarithromycin. These data provided updates of the prevalence of AMR in hospitals and facilitated clinicians for the rational use of antibiotics.

Secondly, reliable methods for rapid detection of AMR are of great importance in helping clinicians selecting effective antibiotics precisely, optimizing the treatment and preventing the aggravation of infection by Multi-Drug Resistant (MDR) microbes. To compare the currently available methods for fast carbapenemase detection, Han et al. investigated the performance of three lateral flow chromatographic assays (NG-test Carba 5, RESIST-5 O.O.K.N.V., and IMP K-SeT) in determining carbapenemases among CRE. As a result, the NG-test Carba 5 detected all of its targeted carbapenemases (KPC, NDM, VIM, IMP and OXA-48-like) in 15 min with both sensitivity and specificity at 100%. The RESIST-5 O.O.K.N.V.

detected KPC, NDM, VIM and OXA-48-like with the sensitivity and specificity at 99.4 and 100%, respectively. The IMP K-SeT, as a complementary test of RESIST-5 O.O.K.N.V for IMP determination, detected all six IMP producers in the research. This result showed that all the above detection methods could simplify the complex workflow for carbapenemases identification for infection control purposes and epidemiological surveillance. For upgrading detection approaches, Jia et al. developed an AI-Blue-Carba test, an improved version of Blue-Carba, to determine carbapenemase-producing Gram-negative bacteria. In this research, "deep learning" was innovatively combined with traditional Blue-Carba, which allowed elevated efficiency for the detection of carbapenemases (within 15 min) and was user-friendly. Through using AI-Blue-Carba, the author planned to create a co-networking platform with a hospital which would promisingly facilitate the monitoring of carbapenemases and infection treatment in clinical sections. Another study explored a method for fast detection of *Staphylococcus aureus* from patients with diabetic foot infections (Chen et al.). In this method, loop-mediated isothermal amplification (LAMP) and clustered regularly interspaced short palindromic repeats (CRISPR) techniques were coupled. Through targeting *nuc* and *mecA*, the CRISPR-LAMP assay successfully identified *S. aureus* strains and distinguished methicillin-resistant *S. aureus* (MRSA) from methicillin-resistant *S. aureus* (MSSA) in clinical samples. Due to its visualized fluorescent result with easy interpretation criteria, this method could help the point-of-care diagnosis against MRSA. More tools are worth being investigated for fast and precise diagnosis of AMR, like aptamers and CRISPR-Cas suggested in the review by Pereira et al. The former (aptamers) could recognize bacteria through binding to cell surface receptors, antigens or unknown targets, while the latter (CRISPR-Cas) could recognize and cleave the targeted bacterial nucleic acid. Their application for diagnostics has been demonstrated in different studies to offer shorter turnaround time comparing with the conventional AMR phenotypic tests (Pereira et al.), highlighting the potential of these techniques to be refined and used as guidance to clinical antimicrobial prescriptions.

Thirdly, the development of innovative therapies are urgently needed for anti-infective purpose. One straight forward way is selecting new antimicrobial candidates. A novel antibiotic, named lefamulin, has been approved by the U.S. Food and Drug Administration in 2019 against community-acquired bacterial pneumonia (CABP). And Wu et al. evaluated its *in vitro* antibiogram by testing the minimum inhibitory concentrations (MICs) of lefamulin against 634 clinical respiratory pathogens across China. They demonstrated that lefamulin had excellent antimicrobial activity with a broad-spectrum coverage of respiratory pathogens, including MRSA/MSSA, methicillin-resistant/sensitive *S. epidermidis* (MRSE/MSSE), *Streptococcus. pneumoniae*, β-hemolytic *Streptococcus*, *Haemophilus influenzae*, *H. parainfluenzae*, *Morazella catarrhalis,* and *Mycoplasma. pneumoniae*. The *in vitro* activity of lefamulin supported the use of this drug as an alternative treatment option for CABP in China. Apart from new drugs, a reasonable combination of currently available antibiotics is another choice. Chen et al. found that CRKP developed resistance in tigecycline-induced descendants, while in the meantime, also presented stable hypersensitivities to other antibiotics, especially aminoglycosides, showing significantly lower MICs. Further genetic analysis suggested that the loss of AMR plasmids may play a role in this phenomenon. These new findings supported the combination therapy of tigecycline and aminoglycosides against CRKP infections.

To summarize, this Research Topic brought together a number of articles addressing the dynamics of AMR transmission and novel strategies of controlling AMR bacteria infection. Based on these new insights, plasmids were re-emphasized as a critical driving force in the spread and evolution of bacterial drug resistance, not only as mobile gene carriers, but also gene lenders to chromosomes. To overcome the problem of AMR, medical progress is being made in the fields of novel therapies and fast infection diagnosis which promotes the rational use of antimicrobials in the future.

AUTHOR CONTRIBUTIONS

All authors listed have made a substantial, direct, and intellectual contribution to the work and approved it for publication.

FUNDING

This work was supported by the Laboratory of Lingnan Modern Agriculture Project (NT2021006) and China Agriculture Research System (CARS-36).

ACKNOWLEDGMENTS

We would like to acknowledge reviewers for their thoughtful comments and all those involved for their high-quality contributions.

REFERENCES

Cannatelli, A., Giani, T., D'Andrea, M. M., Di Pilato, V., Arena, F., Conte, V., et al. (2014). MgrB inactivation is a common mechanism of colistin resistance in KPC-producing Klebsiella pneumoniae of clinical origin. *Antimicrob. Agents Chemother.* 58, 5696–5703. doi: 10.1128/aac.03110-14

He, T., Wang, R., Liu, D., Walsh, T. R., Zhang, R., Lv, Y., et al. (2019). Emergence of plasmid-mediated high-level tigecycline resistance genes in animals and humans. *Nat. Microbiol.* 4, 1450–1456. doi: 10.1038/s41564-019-0445-2

Hua, X., Zhang, L., Moran, R. A., Xu, Q., Sun, L., van Schaik, W., et al. (2020). Cointegration as a mechanism for the evolution of a KPC-producing multidrug resistance plasmid in Proteus mirabilis. *Emerg. Microbes Infect.* 9, 1206–1218. doi: 10.1080/22221751.2020.1773322

Liu, Y. Y., Wang, Y., Walsh, T. R., Yi, L. X., Zhang, R., Spencer, J., et al. (2016). Emergence of plasmid-mediated colistin resistance mechanism MCR-1 in animals and human beings in China: a microbiological and molecular biological study. *Lancet Infect. Dis.* 16, 161–168. doi: 10.1016/S1473-3099(15)00424-7

Zhang, R., Dong, N., Shen, Z., Zeng, Y., Lu, J., Liu, C., et al. (2020). Epidemiological and phylogenetic analysis reveals Flavobacteriaceae as potential ancestral source of tigecycline resistance gene tet(X). *Nat. Commun.* 11, 4648. doi: 10.1038/s41467-020-18475-9

Conflict of Interest: The authors declare that the research was conducted in the absence of any commercial or financial relationships that could be construed as a potential conflict of interest.

Publisher's Note: All claims expressed in this article are solely those of the authors and do not necessarily represent those of their affiliated organizations, or those of the publisher, the editors and the reviewers. Any product that may be evaluated in this article, or claim that may be made by its manufacturer, is not guaranteed or endorsed by the publisher.

frontiers in Microbiology

ORIGINAL RESEARCH
published: 14 August 2020
doi: 10.3389/fmicb.2020.01940

Emergence of Carbapenem- and Tigecycline-Resistant *Proteus cibarius* of Animal Origin

Yan Li[1], Qian Wang[1], Kai Peng[1], Yuan Liu[1,2,3], Ruichao Li[1,2,3] and Zhiqiang Wang[1,3]**

[1] College of Veterinary Medicine, Yangzhou University, Yangzhou, China, [2] Institute of Comparative Medicine, Yangzhou University, Yangzhou, China, [3] Jiangsu Co-innovation Center for Prevention and Control of Important Animal Infectious Diseases and Zoonoses, Yangzhou University, Yangzhou, China

The emergence of *tet*(X) and carbapenemase genes in Enterobacterales pose significant challenges to the treatment of infectious diseases. Convergence of these two categories of genes in an individual pathogen would deteriorate the antimicrobial resistance (AMR) crisis furthermore. Here, tigecycline-resistant Enterobacterales strains were isolated and detected with carbapenemase genes, characterized by antimicrobial susceptibility testing, PCR, conjugation assay, whole genome sequencing, and bioinformatics analysis. Three tigecycline-resistant isolates consisting of one plasmid-mediated *tet*(X4)-bearing *Escherichia fergusonii* and two chromosomal *tet*(X6)-bearing *Proteus cibarius* were recovered from chicken feces. The *tet*(X4) was located on a conjugative IncX1 plasmid pHNCF11W-tetX4 encoding the identical structure as reported *tet*(X4)-bearing IncX1 plasmids in *Escherichia coli*. Among two *P. cibarius* strains, *tet*(X6) was located on two similar chromosomal MDR regions with genetic contexts IS*26*-*aac(3)-IVa*-*aph(4)-Ia*-IS*Ec59*-*tnpA*-*tet*(X6)-*orf*-*orf*-IS*CR2*-*virD2*-*floR*-IS*CR2*-*glmM*-*sul2* and IS*26*-*aac(3)-IVa*-*aph(4)-Ia*-IS*Ec59*-*tnpA*-*tet*(X6)-*orf*-*orf*-IS*CR2*-*glmM*-*sul2*. Apart from *tet*(X6), *P. cibarius* HNCF44W harbored a novel transposon Tn*6450b* positive for bla_{NDM-1} on a conjugative plasmid. This study probed the genomic basis of three *tet*(X)-bearing, tigecycline-resistant strains, one of which coharbored bla_{NDM-1} and *tet*(X6), and identified *P. cibarius* as the important reservoir of *tet*(X6) variants. Emergence of *P. cibarius* encoding both bla_{NDM-1} and *tet*(X6) reveals a potential public health risk.

Keywords: tigecycline resistance, carbapenem resistance, coexistence, plasmid, chromosome

OPEN ACCESS

Edited by:
Zhi Ruan,
Zhejiang University, China

Reviewed by:
Séamus Fanning,
University College Dublin, Ireland
Fang He,
Zhejiang Provincial People's Hospital, China
Congming Wu,
China Agricultural University, China

****Correspondence:***
Ruichao Li
rchl88@yzu.edu.cn
Zhiqiang Wang
zqwang@yzu.edu.cn

Specialty section:
This article was submitted to Antimicrobials, Resistance and Chemotherapy, a section of the journal Frontiers in Microbiology

Received: *09 June 2020*
Accepted: *23 July 2020*
Published: *14 August 2020*

Citation:
Li Y, Wang Q, Peng K, Liu Y, Li R and Wang Z (2020) Emergence of Carbapenem- and Tigecycline-Resistant Proteus cibarius of Animal Origin. Front. Microbiol. 11:1940. doi: 10.3389/fmicb.2020.01940

INTRODUCTION

Antimicrobial resistance (AMR) is a serious threat to public health globally. Carbapenem and tigecycline are regarded as vital antimicrobials reserved for clinical use due to their broad antibacterial spectrum. However, the increasing spread of carbapenemase-encoding genes has rendered carbapenem-resistant Enterobacteriaceae (CRE) infection a great threat (Du et al., 2018; Tacconelli et al., 2018). Plasmid-mediated resistance genes *tet*(X3) and *tet*(X4) conferring high-level resistance to tigecycline in Enterobacterales and *Acinetobacter* has been found to be ubiquitous in animals and food of animal origin (Bai et al., 2019; He et al., 2019; Sun et al., 2019; Li et al., 2020c). This undermines the efficacy of tigecycline as the last-resort drug in treating MDR bacterial infections, especially those caused by carbapenem-resistant, Gram-negative bacteria, such as CRE.

Initially, *tet*(X) genes were mainly found in *Bacteroides* species and bacteria derived from environmental microbiota (Forsberg et al., 2015; Tian et al., 2019). Alarmingly, novel *tet*(X) variants are being identified from the pathogens of animal, food, and human origins (Li et al., 2019; Wang et al., 2019; He D. et al., 2020; Liu et al., 2020; Peng et al., 2020), which implies that *tet*(X) is expanding from commensals to pathogens (Aminov, 2013). Thus, the convergence of mobile tigecycline-resistant *tet*(X) and carbapenem-resistant genes in Enterobacterales may be inevitable. *Acinetobacter* strains coharboring *tet*(X) and bla_{NDM-1} were identified from samples of waterfowl and dairy cows recently (Cui et al., 2020; He T. et al., 2020), highlighting the potential convergence risk of both critical resistance genes among bacteria. However, Enterobacterales carrying both *tet*(X) and bla_{NDM-1} is unknown, which constitutes a more severe concern. To cover this knowledge gap, we performed a tigecycline-resistant Enterobacterales screening pilot program and identified a *Proteus cibarius* coharboring both *tet*(X6) and bla_{NDM-1}, implying that wide surveillance of Enterobacterales conferring resistance to carbapenems and tigecycline among bacteria should be performed worldwide.

MATERIALS AND METHODS

Bacterial Isolates

A total of 16 chicken fecal samples were collected from four chicken farms in Henan province, China, in 2019. Tigecycline-resistant Enterobacterales were selected on MacConkey agar plates containing tigecycline (4 mg/L). The species of purified tigecycline-resistant isolates was identified by 16S rRNA gene sequencing and further confirmed by analyzing WGS data. The *tet*(X) and carbapenem-resistant genes were determined by PCR with reported primers (Dallenne et al., 2010; He et al., 2019).

Antimicrobial Susceptibility Testing

The antimicrobial susceptibility testing (AST) of *tet*(X)-positive tigecycline-resistant strains against 13 antibiotics was performed based on the broth microdilution method with *Escherichia coli* ATCC 25922 as the quality control and interpreted according to CLSI guidelines (CLSI, 2018). The tigecycline non-susceptibility in Enterobacterales was interpreted with an MIC of $\geq$4 mg/L (Marchaim et al., 2014).

Conjugation Assay and S1-PFGE

A conjugation assay was conducted using rifampicin-resistant *E. coli* C600 (Rif^r) as the recipient to investigate the transferability of *tet*(X) and bla_{NDM-1}. The donor and recipient strains were mixed at a ratio of 1:4 on a filter, followed by culturing on LB agar plates at 30 and 37°C, respectively, overnight and screening on MacConkey plates containing tigecycline (4 mg/L) or meropenem (2 mg/L) with rifampicin (300 mg/L). Transconjugants were confirmed with PCR. S1 nuclease pulsed-field gel electrophoresis (S1-PFGE) was utilized to characterize the plasmid profiles.

Whole Genome Sequencing and Bioinformatics Analysis

Genomid DNA (gDNA) was purified with the TIANamp Genomic DNA Kit and quantified by Qubit 4 Fluorometer. Short-read Illumina sequencing and long-read Nanopore sequencing were combined to generate complete genome sequences (Li et al., 2018). The *de novo* assembled sequences were annotated by RAST[1]. Antibiotic resistance genes (ARGs) and plasmid replicon types were determined using the ResFinder and PlasmidFinder[2]. BRIG and Easyfig were used to compare the plasmid and MDR structures (Alikhan et al., 2011; Sullivan et al., 2011).

Functional Confirmation of *tet*(X6) and Phylogenetic Analysis

To confirm the resistance function of the identified *tet*(X6) variant, TA-cloning and AST were performed. Briefly, the new variant, together with its natural promoter sequence, was amplified by PCR using primers HNCF44W-F/AGCGAACAAGAATATGACTTTACT and HNCF44W-R/CGCCTTTCTGTTTTATAGATTCAT, cloned into a pMD19-T vector and transformed chemically into *E. coli* DH5α. The resistance phenotype of *tet*(X6) was tested by measuring the MICs of different tetracycline antibiotics. Phylogenetic analysis of Tet(X) amino acid sequences were conducted in MEGA X using the neighbor-joining method (Kumar et al., 2018).

Nucleotide Sequence Accession Numbers

The complete sequences obtained in this study have been deposited in the GenBank database under BioProject number PRJNA625637. The novel bla_{NDM-1}-bearing Tn*6450b* was also deposited in the NCBI database (MT701524).

RESULTS AND DISCUSSION

Identification of Tigecycline-Resistant Enterobacterales

Three tigecycline-resistant, *tet*(X)-positive Enterobacterales strains were isolated from 16 samples (18.8%), which consisted of *Escherichia fergusonii* HNCF11W carrying *tet*(X4), *P. cibarius* HNCF43W, and HNCF44W positive for a *tet*(X6) variant. Notably, HNCF44W also carried the bla_{NDM-1} gene. Antimicrobial susceptibility testing revealed that the three tigecycline-resistant strains were resistant to multiple antibiotics, including kanamycin, florfenicol, amoxicillin, and tetracyclines, showing high-level resistance to tigecycline (**Supplementary Table S1**). In addition, the NDM-producing strain HNCF44W was also resistant to meropenem (>16 mg/L). S1-PFGE indicated that two plasmids of ca. 130 and 55 kb were observed in *tet*(X4)-bearing *E. fergusonii* HNCF11W, and one plasmid of ca. 140 kb existed in *tet*(X6)-bearing *P. cibarius* HNCF44W, but no plasmid

[1]https://rast.nmpdr.org/

[2]http://www.genomicepidemiology.org/

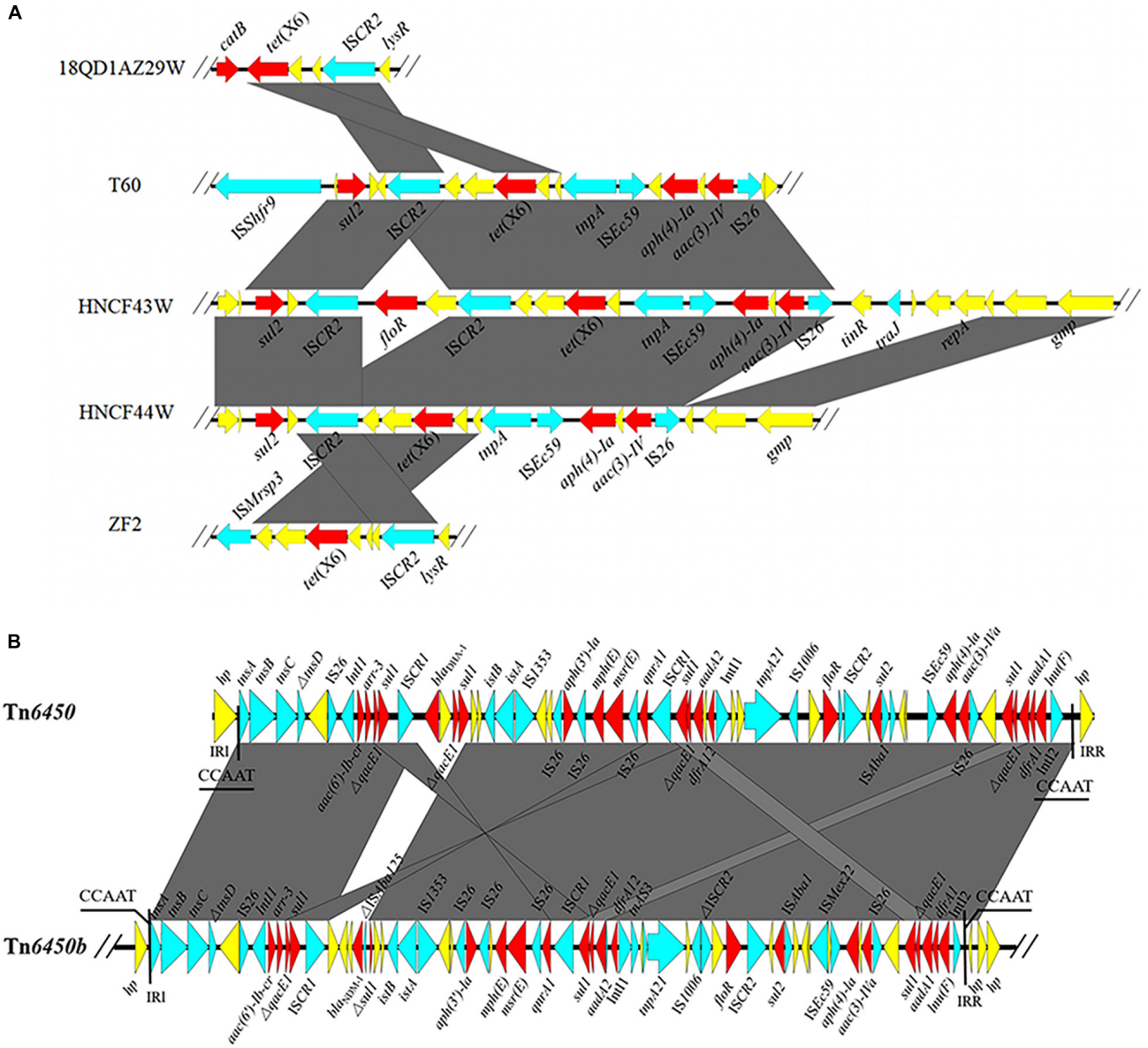

FIGURE 1 | (A) Genetic environments of *tet*(X6) from different strains. **(B)** Linear alignment of bla_{NDM-1}-bearing Tn*6450b* in pHNCF44W_NDM-1 and reported Tn*6450*. The red arrows denote the resistance genes; the blue arrows represent the mobile elements; the yellow arrows signify other CDSs. The shadow parallelograms stand for homologous genetic regions.

existed in *P. cibarius* HNCF43W (**Supplementary Figure S1**). To uncover the genetic locations of *tet*(X) and bla_{NDM-1}, complete genome sequences of the three strains were finished successfully.

Genome Characterization of Tigecycline-Resistant *E. fergusonii*

The *tet*(X4)-bearing *E. fergusonii* harbored one chromosome (4,584,794 bp, ST10543); one p0111-like plasmid pHNCF11W-130 kb (130,643 bp) harboring *aadA1*, *floR*, *tet*(A), *dfrA14*, $bla_{TEM-209}$, bla_{OXA-10}, *cmlA1*, *arr-3*, and *qnrS1*; and one typical IncX1 plasmid pHNCF11W-tetX4 (57,105 bp) encoding *tet*(X4) in the genetic structure of IS*26*-*abh*-*tet*(X4)-IS*CR2*-*virD2*-*floR*-△IS*CR2* coupled with *aadA2*, *lnu(F)*, *tet*(A), and bla_{SHV-12}. A BLASTn search of pHNCF11W-tetX4 against the nr database retrieved other *tet*(X4)-bearing plasmids p1916D18-1 (59,353 bp), p1916D6-2 (59,351 bp), and pYY76-1-2 (57,104 bp) of swine and cattle origins, sharing nearly identical sequences (**Supplementary Figure S2**). Both pHNCF11W-tetX4 and pHNCF11W-130 kb were transferred into the recipient strain, demonstrating that IncX1-type *tet*(X4)-bearing plasmids were mobilizable and spread in Enterobacterales of animal origin (Chen et al., 2019). Although *tet*(X4) was initially found in plasmids of IncFIB and IncQ1 types (He et al., 2019; Sun et al.,

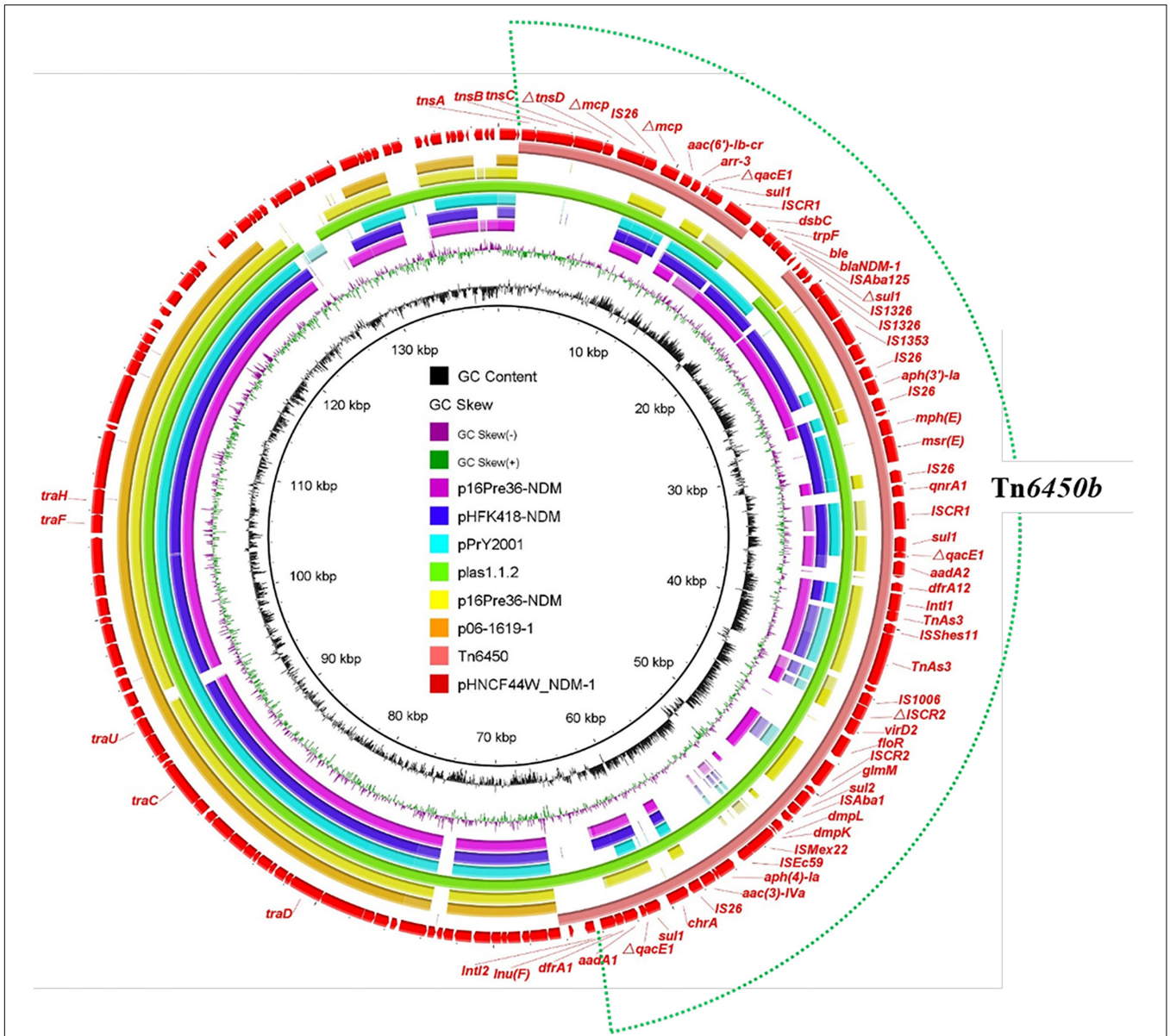

FIGURE 2 | Alignment of the plasmid pHNCF44W_NDM-1 identified in this study with other similar plasmids. The outermost red circle denotes the reference plasmid pHNCF44W_NDM-1. The location of Tn*6450b* is highlighted in the dotted circle.

2019), IncX1 plasmids are common in various Enterobacterales and associated with various resistance genes (Dobiasova and Dolejska, 2016; Li et al., 2020b), which potentially increases the transmission of *tet*(X4) between different Enterobacterales.

Characterization of *Proteus cibarius* Coharboring *tet*(X6) and *bla*$_{NDM-1}$

HNCF43W harbored a 3,965,977 bp chromosome. HNCF44W contained a 3,929,176 bp chromosome and one *bla*$_{NDM-1}$-bearing plasmid pHNCF44W_NDM-1 of 139,490 bp in size. A conjugation assay failed to recover transconjugants positive for *tet*(X6). The *tet*(X6) gene was located on large MDR regions (IS*26*-*aac(3)-IVa*-*aph(4)-Ia*-IS*Ec59*-*tnpA*-*tet*(X6)-*orf*-*orf*-IS*CR2*-*virD2*-*floR*-IS*CR2*-*glmM*-*sul2* and IS*26*-*aac(3)-IVa*-*aph(4)-Ia*-IS*Ec59*-*tnpA*-*tet*(X6)-*orf*-*orf*-IS*CR2*-*glmM*-*sul2,* respectively) embedded in chromosomes of both *P. cibarius* strains (**Figure 1A**), and the MDR regions may derive from recombination of *tet*(X6)-bearing elements and reported plasmids p19110F47-2 (CP046044) and pJXP9 (MK673549) (**Supplementary Figure S3**). The two *tet*(X6)-bearing MDR regions differed by *virD2*-*floR*-IS*CR2*, which was a potential mobile segment (Doublet et al., 2005). IS*CR2* is the major mobile element associated with *tet*(X3), *tet*(X4), and *tet*(X5) (Bai et al., 2019; He et al., 2019; Sun et al., 2019; Li et al., 2020a). Recently, three reports demonstrated *tet*(X6) could be embedded in ICEs

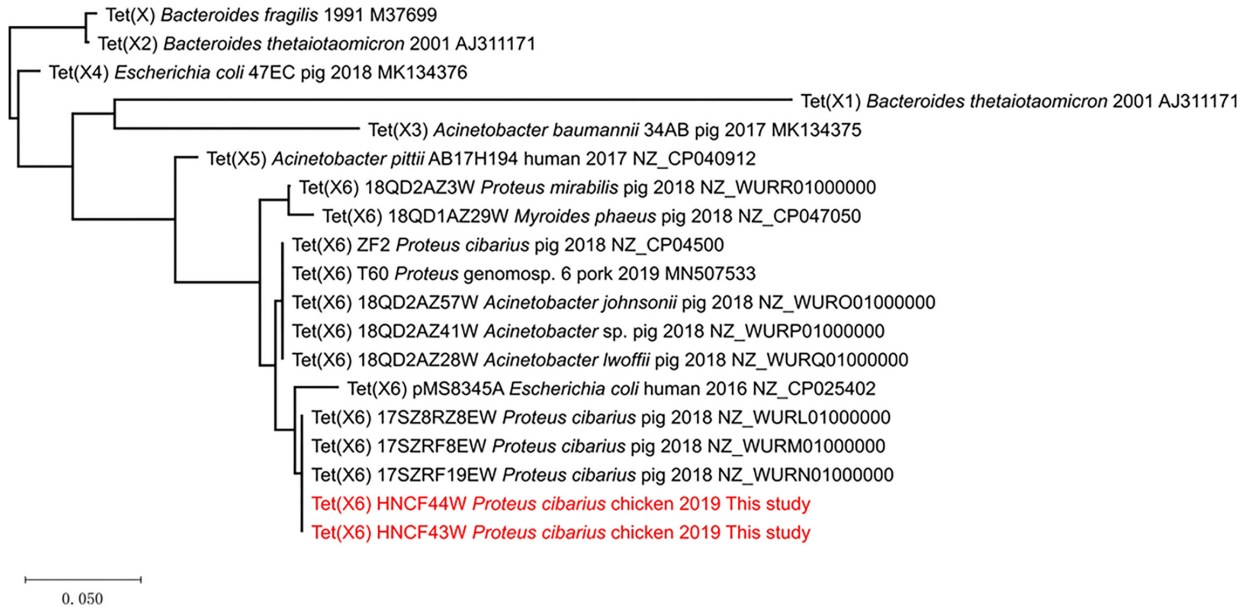

FIGURE 3 | The phylogenetic tree of Tet(X) variants. The tree is drawn to scale with branch lengths in the same units as those of the evolutionary distances used to infer the phylogenetic tree. The evolutionary distances were computed using MEGA X and are in the units of the number of amino acid substitutions per site.

or other MDR regions, all of which harbor IS*CR2* (He D. et al., 2020; Liu et al., 2020; Peng et al., 2020), suggesting it may facilitate the transfer of *tet*(X6) to other plasmids or chromosomes.

The bla_{NDM-1} gene in HNCF44W was located on an MDR plasmid pHNCF44W_NDM-1 carrying resistance genes *aac(6′)-Ib, arr-3, qacE1, sul1, sul2, aph(3′)-la, mph(E), msr(E), qnrA1, aadA1, aadA2, dfrA1, dfrA12, floR, aac(3)-IVa,* and *lnu(F)*. No plasmid replicon was identified, but pHNCF44W_NDM-1 was very similar to plasmid plas1.1.2 (CP047114) from *Proteus mirabilis* of swine origin; it differed mainly in the bla_{NDM-1}-bearing region (**Figure 2**). The bla_{NDM-1} gene and other resistance genes were found in a 65-kb MDR region, showing high similarity to transposon Tn*6450* but with bla_{DHA-1} replaced by bla_{NDM-1} (Chen et al., 2018), designated as Tn*6450b* here (**Figure 1B**). Other similar plasmids or transposons were found in the nr database, including p16Pre36-NDM from *Providencia rettgeri*, pHFK418-NDM from *P. mirabilis*, pPrY2001 from *P. rettgeri*, p16Pre36-NDM from *P. rettgeri*, p06-1619-1 from *P. rettgeri*, and Tn*6450* from *P. mirabilis*. The plasmid pHNCF44W_NDM-1 carrying bla_{NDM-1} was successfully transferred into *E. coli* EC600 at 30°C. Notably, IS*CR2-lysR-floR-virD2-*△IS*CR2* structure in pHNCF44W_NDM-1 was also found in a *tet*(X6)-bearing chromosomal segment, rendering this a Tn*6450b*-bearing plasmid with the potential ability to capture *tet*(X6) under certain circumstances, which warrants further surveillance.

Functional Analysis of *tet*(X6) and Its Evolution

Recently, several reports have characterized different *tet*(X6) variants from diverse bacteria (He D. et al., 2020; Liu et al., 2020; Peng et al., 2020; Xu et al., 2020). The *tet*(X6) variant carried by HNCF44W and HNCF43W is the same as that reported in *P. cibarius* from swine (Liu et al., 2020). The expression of *tet*(X6) in the cloning vector pMD19-T-tet(X6) in *E. coli* DH5α conferred resistance to tetracycline (64 mg/L) and tigecycline (16 mg/L) with 32-fold increments compared to that of DH5α-pMD19-T, indicating that this *tet*(X6) variant can confer tigecycline resistance (**Supplementary Table S2**). The 1137 bp *tet*(X6) variant encoded 378 amino acids and showed 84.7, 66.3, 84.9, 79.9, 87.8, 93.7, and 98.7% amino acid sequence identity to Tet(X), Tet(X1), Tet(X2), Tet(X3), Tet(X4), Tet(X5), and Tet(X6), respectively (**Figure 3**) with 5, 8, and 16 amino acid substitutions to Tet(X6) (MN507533, T60), Tet(X6) (CP025402, pMS8345A), and Tet(X6) (NZ_CP047050, 18QD1AZ29W).

Phylogenetic analysis of Tet(X) indicated that of all reported Tet(X6) variants clustered in a clade, most related to Tet(X5) (**Figure 3**). Although most *tet*(X6) variants were found in *Proteus* and *Acinetobacter* spp., analysis of the NCBI database shows that *E. coli* positive for *tet*(X6) existed as early as 2003 in Denmark (JWJM01000174), indicating the transmission of *tet*(X6) occurred previously. Furthermore, chromosomal *tet*(X6)-bearing ICEs and MDRs are found in *Proteus*, *Acinetobacter*, and *Myroides phaeus* (He D. et al., 2020; Liu et al., 2020; Peng et al., 2020). Plasmid-mediated *tet*(X6) in *Proteus*, *Acinetobacter*, and *E. coli* also emerged according to published reports (Cui et al., 2020; Li et al., 2020c; Xu et al., 2020), implying *tet*(X6) is at the stage of being expanded via different mobile elements. This highlights that *tet*(X6) variants would be the next possible prominent *tet*(X) allele, approaching the widespread situation of *tet*(X4) in *E. coli* (Bai et al., 2019; He et al., 2019; Sun et al., 2019). Nomenclature of *tet*(X) by different allele numbers is not recommended because many of the alleles are 85–100% aa

identical[3], but an identical *tet*(X) naming system may not benefit research communications and AMR surveillance, especially as different *tet*(X) alleles possess different resistance phenotypes, genetic contexts, hosts, and evolutionary routes as more research reveals. For example, *tet*(X4) was found to be more common in *E. coli* than *tet*(X6) owing to the fact that *tet*(X4) has merged into conjugative plasmids adapted in *E. coli*. Also, the plasmids coharboring both bla_{NDM-1} and *tet*(X) in *Acinetobacter* spp. (Cui et al., 2020) could be divided into *tet*(X3)- or *tet*(X6)-bearing plasmids, which could make it difficult to decipher the accurate different genetic contexts if only *tet*(X) represented the two alleles simultaneously. To better investigate the molecular epidemiology, genomic evolution, and functional analysis and avoid confusion in *tet*(X) designations, a clear nomenclature scheme acceptable to researchers worldwide should be proposed as soon as possible. Because *mcr* genes exist in certain bacterial species as housekeeping genes and certain alleles leap over species boundary limits to Enterobacterales via mobile elements like Tn*6330* (Li et al., 2016; Shen et al., 2020), *tet*(X) genes may behave similarly because they exist as core genes in certain bacteria and transfer to Enterobacterales by mobile elements like IS*CR2*. Thus, the *mcr* nomenclature scheme may be a good example when it comes to *tet*(X) designation (Partridge et al., 2018). More research should be performed to put forward a widely accepted *tet*(X) allele numbering system to facilitate research communications.

CONCLUSION

To conclude, we characterized three *tet*(X)-bearing Enterobacterales strains of chicken origin and found that one *P. cibarius* coharbored both bla_{NDM-1} and *tet*(X6). To the best of our knowledge, this is the first report of convergence of *tet*(X6) and bla_{NDM-1} genes in Enterobacterales, highlighting the importance of continuous surveillance of tigecycline- and carbapenem-resistant Enterobacterales of animal origin, which may act as the potential reservoir of clinical Enterobacterales resistant to tigecycline and carbapenems.

[3]http://faculty.washington.edu/marilynr/

DATA AVAILABILITY STATEMENT

The datasets presented in this study can be found in online repositories. The names of the repository/repositories and accession number(s) can be found in the article/ **Supplementary Material**.

AUTHOR CONTRIBUTIONS

RL and ZW: conceptualization, writing – review and editing, and supervision. YaL and RL: methodology. YaL and QW: investigation. QW, KP, and YuL: data curation and visualization. YaL: writing – original draft preparation. All authors have read and agreed to the published version of the manuscript.

FUNDING

This work was supported by grants from the Natural Science Foundation of Jiangsu Province (BK20180900), the National Natural Science Foundation of China (31872523), and the Priority Academic Program Development of Jiangsu Higher Education Institutions (PAPD).

SUPPLEMENTARY MATERIAL

The Supplementary Material for this article can be found online at: https://www.frontiersin.org/articles/10.3389/fmicb.2020.01940/full#supplementary-material

REFERENCES

Alikhan, N. F., Petty, N. K., Ben Zakour, N. L., and Beatson, S. A. (2011). BLAST ring image generator (BRIG): simple prokaryote genome comparisons. *BMC Genomics* 12:402. doi: 10.1186/1471-2164-12-402

Aminov, R. I. (2013). Evolution in action: dissemination of tet(X) into pathogenic microbiota. *Front. Microbiol.* 4:192. doi: 10.3389/fmicb.2013.00192

Bai, L., Du, P., Du, Y., Sun, H., Zhang, P., Wan, Y., et al. (2019). Detection of plasmid-mediated tigecycline-resistant gene tet(X4) in *Escherichia coli* from pork, Sichuan and Shandong Provinces, China, February 2019. *Euro Surveill.* 24:1900340.

Chen, C., Wu, X. T., He, Q., Chen, L., Cui, C. Y., Zhang, Y., et al. (2019). Complete sequence of a tet(X4)-harboring IncX1 plasmid, pYY76-1-2, in *Escherichia coli* from a cattle sample in China. *Antimicrob. Agents Chemother.* 63:e01528-19.

Chen, Y. P., Lei, C. W., Kong, L. H., Zeng, J. X., Zhang, X. Z., Liu, B. H., et al. (2018). Tn6450, a novel multidrug resistance transposon characterized in a *Proteus mirabilis* isolate from chicken in China. *Antimicrob. Agents Chemother.* 62:e02192-17.

CLSI (2018). *Performance Standards for Antimicrobial Susceptibility Testing. 28th ed. CLSI Supplement M100*. Wayne, PA: CLSI.

Cui, C. Y., Chen, C., Liu, B. T., He, Q., Wu, X. T., Sun, R. Y., et al. (2020). Co-occurrence of plasmid-mediated tigecycline and carbapenem resistance in Acinetobacter spp. from waterfowls and their neighboring environment. *Antimicrob. Agents Chemother.* 64:e02502-19.

Dallenne, C., Da Costa, A., Decre, D., Favier, C., and Arlet, G. (2010). Development of a set of multiplex PCR assays for the detection of genes encoding important beta-lactamases in *Enterobacteriaceae*. *J. Antimicrob. Chemother.* 65, 490–495. doi: 10.1093/jac/dkp498

Dobiasova, H., and Dolejska, M. (2016). Prevalence and diversity of IncX plasmids carrying fluoroquinolone and beta-lactam resistance genes in *Escherichia coli* originating from diverse sources and geographical areas. *J. Antimicrob. Chemother.* 71, 2118–2124. doi: 10.1093/jac/dkw144

Doublet, B., Schwarz, S., Kehrenberg, C., and Cloeckaert, A. (2005). Florfenicol resistance gene floR is part of a novel transposon. *Antimicrob. Agents Chemother.* 49, 2106–2108. doi: 10.1128/aac.49.5.2106-2108.2005

Du, X., He, F., Shi, Q., Zhao, F., Xu, J., Fu, Y., et al. (2018). The rapid emergence of tigecycline resistance in blaKPC-2 harboring *Klebsiella pneumoniae*, as mediated in vivo by mutation in tetA during tigecycline treatment. *Front. Microbiol.* 9:648. doi: 10.3389/fmicb.2018.00648

Forsberg, K. J., Patel, S., Wencewicz, T. A., and Dantas, G. (2015). The tetracycline destructases: a novel family of tetracycline-inactivating enzymes. *Chem. Biol.* 22, 888–897. doi: 10.1016/j.chembiol.2015.05.017

He, D., Wang, L., Zhao, S., Liu, L., Liu, J., Hu, G., et al. (2020). A novel tigecycline resistance gene, tet(X6), on an SXT/R391 integrative and conjugative element

in a *Proteus* genomospecies 6 isolate of retail meat origin. *J. Antimicrob. Chemother.* 75, 1159–1164. doi: 10.1093/jac/dkaa012

He, T., Li, R., Wei, R., Liu, D., Bai, L., Zhang, L., et al. (2020). Characterization of *Acinetobacter indicus* co-harbouring tet(X3) and blaNDM-1 of dairy cow origin. *J. Antimicrob. Chemother.* 2020:dkaa182.

He, T., Wang, R., Liu, D., Walsh, T. R., Zhang, R., Lv, Y., et al. (2019). Emergence of plasmid-mediated high-level tigecycline resistance genes in animals and humans. *Nat. Microbiol.* 4, 1450–1456. doi: 10.1038/s41564-019-0445-2

Kumar, S., Stecher, G., Li, M., Knyaz, C., and Tamura, K. (2018). MEGA X: molecular evolutionary genetics analysis across computing platforms. *Mol. Biol. Evol.* 35, 1547–1549. doi: 10.1093/molbev/msy096

Li, R., Liu, Z., Peng, K., Liu, Y., Xiao, X., and Wang, Z. (2019). Cooccurrence of Two tet(X) variants in an empedobacter brevis strain of shrimp origin. *Antimicrob. Agents Chemother.* 63:e01636-19.

Li, R., Lu, X., Liu, Z., Liu, Y., Xiao, X., and Wang, Z. (2020a). Rapid detection and characterization of tet(X4)-positive *Escherichia coli* strains with nanopore sequencing. *J. Antimicrob. Chemother.* 75, 1068–1070. doi: 10.1093/jac/dkz528

Li, R., Lu, X., Peng, K., Liu, Z., Li, Y., Liu, Y., et al. (2020b). Deciphering the structural diversity and classification of the mobile tigecycline resistance gene tet (X)-bearing plasmidome among bacteria. *mSystems* 5:e00134-20.

Li, R., Peng, K., Li, Y., Liu, Y., and Wang, Z. (2020c). Exploring tet(X)-bearing tigecycline-resistant bacteria of swine farming environments. *Sci. Total Environ.* 733:139306. doi: 10.1016/j.scitotenv.2020.139306

Li, R., Xie, M., Dong, N., Lin, D., Yang, X., Wong, M. H. Y., et al. (2018). Efficient generation of complete sequences of MDR-encoding plasmids by rapid assembly of MinION barcoding sequencing data. *Gigascience* 7, 1–9.

Li, R., Xie, M., Lv, J., Wai-Chi Chan, E., and Chen, S. (2016). Complete genetic analysis of plasmids carrying mcr-1 and other resistance genes in an *Escherichia coli* isolate of animal origin. *J. Antimicrob. Chemother.* 72, 696–699.

Liu, D., Zhai, W., Song, H., Fu, Y., Schwarz, S., He, T., et al. (2020). Identification of the novel tigecycline resistance gene tet(X6) and its variants in Myroides, Acinetobacter and *Proteus* of food animal origin. *J. Antimicrob. Chemother.* 75, 1428-1431.

Marchaim, D., Pogue, J. M., Tzuman, O., Hayakawa, K., Lephart, P. R., Salimnia, H., et al. (2014). Major variation in MICs of tigecycline in gram-negative *Bacilli* as a function of testing method. *J. Clin. Microbiol.* 52, 1617–1621. doi: 10.1128/jcm.00001-14

Partridge, S. R., Di Pilato, V., Doi, Y., Feldgarden, M., Haft, D. H., Klimke, W., et al. (2018). Proposal for assignment of allele numbers for mobile colistin resistance (mcr) genes. *J. Antimicrob. Chemother.* 73, 2625–2630. doi: 10.1093/jac/dky262

Peng, K., Li, R., He, T., Liu, Y., and Wang, Z. (2020). Characterization of a porcine *Proteus cibarius* strain co-harbouring tet(X6) and cfr. *J. Antimicrob. Chemother.* 75, 1652–1654. doi: 10.1093/jac/dkaa047

Shen, Y., Zhang, R., Schwarz, S., Wu, C., Shen, J., Walsh, T. R., et al. (2020). Farm animals and aquaculture: significant reservoirs of mobile colistin resistance genes. *Environ. Microbiol.* 22, 2469–2484. doi: 10.1111/1462-2920.14961

Sullivan, M. J., Petty, N. K., and Beatson, S. A. (2011). Easyfig: a genome comparison visualizer. *Bioinformatics* 27, 1009–1010. doi: 10.1093/bioinformatics/btr039

Sun, J., Chen, C., Cui, C. Y., Zhang, Y., Liu, X., Cui, Z. H., et al. (2019). Plasmid-encoded tet(X) genes that confer high-level tigecycline resistance in *Escherichia coli*. *Nat. Microbiol.* 4, 1457–1464. doi: 10.1038/s41564-019-0496-4

Tacconelli, E., Carrara, E., Savoldi, A., Harbarth, S., Mendelson, M., Monnet, D. L., et al. (2018). Discovery, research, and development of new antibiotics: the WHO priority list of antibiotic-resistant bacteria and tuberculosis. *Lancet Infect. Dis.* 18, 318–327.

Tian, Z., Liu, R., Zhang, H., Yang, M., and Zhang, Y. (2019). Developmental dynamics of antibiotic resistome in aerobic biofilm microbiota treating wastewater under stepwise increasing tigecycline concentrations. *Environ. Int.* 131:105008. doi: 10.1016/j.envint.2019.105008

Wang, L., Liu, D., Lv, Y., Cui, L., Li, Y., Li, T., et al. (2019). Novel plasmid-mediated tet(X5) gene conferring resistance to tigecycline, eravacycline, and omadacycline in a clinical *Acinetobacter baumannii* isolate. *Antimicrob. Agents Chemother.* 64:e01326-19.

Xu, Y., Liu, L., and Feng, Y. (2020). A new tet(X6) tigecycline resistance determinant co-carried with mcr-1 by a single plasmid. *bioRxiv* [Preprint]. doi: 10.1101/2020.03.06.981738

Conflict of Interest: The authors declare that the research was conducted in the absence of any commercial or financial relationships that could be construed as a potential conflict of interest.

frontiers in Microbiology

ORIGINAL RESEARCH
published: 16 September 2020
doi: 10.3389/fmicb.2020.578824

In vitro Activity of Lefamulin Against the Common Respiratory Pathogens Isolated From Mainland China During 2017–2019

*Shi Wu[1,2], Yonggui Zheng[1,2], Yan Guo[1,2], Dandan Yin[1,2], Demei Zhu[1,2] and Fupin Hu[1,2]**

[1] *Institute of Antibiotics, Huashan Hospital, Fudan University, Shanghai, China,* [2] *Key Laboratory of Clinical Pharmacology of Antibiotics, Ministry of Health, Shanghai, China*

Purpose: Lefamulin is a novel antibiotic approved by the U.S. Food and Drug Administration in 2019 for the treatment of community-acquired bacterial pneumonia (CABP). In this study we evaluated the *in vitro* antimicrobial activity of lefamulin in order to better understand its antibiogram.

Methods: The test strains were isolated from patients across China during the period from 2017 to 2019, including 634 strains of respiratory pathogens. The minimum inhibitory concentrations (MICs) of lefamulin and comparators were determined by broth microdilution method.

Results: Lefamulin showed potent activity against *Streptococcus pneumoniae* and *Staphylococcus* evidenced by 100% inhibition at 0.25 mg/L, and favorable $MIC_{50/90}$ (0.125/0.125 mg/L) against *S. pneumoniae* (penicillin MIC $\geq$ 2 mg/L), $MIC_{50/90}$ ($\leq$0.015/0.125 mg/L) against methicillin-resistant *S. aureus*, and $MIC_{50/90}$ ($\leq$0.015/0.06 mg/L) against methicillin-resistant *S. epidermidis*. Lefamulin also had good activity against *Streptococcus pyogenes* and *Streptococcus agalactia* ($MIC_{50/90}$: $\leq$0.015/$\leq$0.015 mg/L), β-lactamase-producing *Haemophilus influenzae* ($MIC_{50/90}$: 0.5/1 mg/L), β-lactamase-negative *H. influenzae* ($MIC_{50/90}$: 1/1 mg/L), *Moraxella catarrhalis* ($MIC_{50/90}$: 0.25/0.25 mg/L), and *Mycoplasma pneumoniae* ($MIC_{50/90}$: 0.03/0.03 mg/L) regardless of resistance to azithromycin. Lefamulin was generally more active than the comparators against the test strains.

Conclusion: In summary, lefamulin has good and broad-spectrum coverage of respiratory pathogens (methicillin-sensitive and -resistant *Staphylococcus*, *S. pneumoniae*, β-hemolytic *Streptococcus*, *H. influenzae*, *M. catarrhalis* and *M. pneumoniae*). *In vitro* activity supports the use of lefamulin in the treatment of CABP in China.

Keywords: lefamulin, antimicrobial susceptibility test, minimum inhibitory concentration, community-acquired bacterial pneumonia, *Mycoplasma pneumoniae*

OPEN ACCESS

Edited by:
Shaolin Wang,
China Agricultural University, China

Reviewed by:
Anusak Kerdsin,
Kasetsart University, Thailand
László Majoros,
University of Debrecen, Hungary

***Correspondence:**
Fupin Hu
hufupin@fudan.edu.cn

Specialty section:
This article was submitted to Antimicrobials, Resistance and Chemotherapy, a section of the journal Frontiers in Microbiology

Received: *01 July 2020*
Accepted: *27 August 2020*
Published: *16 September 2020*

Citation:
Wu S, Zheng Y, Guo Y, Yin D, Zhu D and Hu F (2020) In vitro Activity of Lefamulin Against the Common Respiratory Pathogens Isolated From Mainland China During 2017–2019. Front. Microbiol. 11:578824. doi: 10.3389/fmicb.2020.578824

INTRODUCTION

Pleuromutilin is a natural antimicrobial substance first found in 1950s. It can be obtained from *Clitopilus scyphoides*, *Clitopilus passeckerianus*, or other *Clitopilus* species in basidiomycota. Lefamulin is the first-in-class semi-synthetic pleuromutilin antibiotic for systemic use. Its molecular formula is $C_{28}H_{45}NO_5S$ (molecular weight 567.79 g). Lefamulin inhibits bacterial protein synthesis by binding to "A" and "P" sites of the peptidyl transferase center (PTC) of the 23s rRNA of the 50S ribosomal subunit of bacterial cell. The binding is through the mutilin core and C-14 side chain in the forms of hydrogen bonds, hydrophobic interactions, and conformational change to prevent correct orientation of tRNA's 3'-CCA ends for peptide transfer (Veve and Wagner, 2018; Rodvold, 2019). The resistance to lefamulin may be related to the mutations in *rplC* gene and *cfr* gene of *Staphylococcus aureus*, Vga (AV) coded by the transposon Tn5406 and *vga(A)* carried by plasmids (encoding ABC transporter) (Mendes et al., 2019; Rodvold, 2019). So far, it is known that lefamulin has no cross resistance to the antimicrobial agents in clinical use.

Studies have shown that lefamulin has good coverage of the pathogens of community-acquired respiratory tract infections, including antibiotic-resistant strains, such as penicillin-resistant *Streptococcus pneumoniae* (PRSP), macrolide-resistant *Mycoplasma pneumoniae*, and methicillin-resistant *S. aureus* (MRSA) (Veve and Wagner, 2018; Rodvold, 2019). In August 2019, lefamulin was approved by the U.S. Food and Drug Administration (FDA) for the treatment of community-acquired bacterial pneumonia (CABP) patients based on its good pharmacodynamic results, pharmacokinetic, and safety profiles in clinical trials.

The antibacterial spectrum and activity of lefamulin have been studied in the United States and Europe (Paukner et al., 2013, 2019), but it is not clear about its antimicrobial activity against the clinical isolates in China. For better understanding the antimicrobial activity of lefamulin against the common respiratory pathogens recently isolated in China, we studied the *in vitro* activity of lefamulin against a broad range of respiratory pathogens.

MATERIALS AND METHODS

A total of 634 non-duplicate strains of respiratory pathogens were tested, including 580 strains of bacteria and 54 strains of *Mycoplasma pneumoniae*. These strains were isolated from 29 hospitals across China, representing 23 provinces and municipalities, during the period from October 2017 to July 2019. Specifically, the test strains included *S. aureus* (n = 121), *S. epidermidis* (n = 30), β-lactamase-producing *Haemophilus influenzae* (n = 48), β-lactamase-negative *H. influenzae* (n = 48), *Haemophilus parainfluenzae* (n = 10), *Moraxella catarrhalis* (n = 54), *S. pneumoniae* (n = 172), *Streptococcus pyogenes* (n = 30), and *Streptococcus agalactiae* (n = 13). All the strains were re-identified before susceptibility testing. Species identification was confirmed by MALDI-TOF/MS system (bioMérieux, France), and antimicrobial susceptibility testing were controlled with reference strains *S. aureus* ATCC29213, *S. pneumoniae* ATCC49619, *H. influenzae* ATCC49247, and *M. pneumoniae* ATCC 29342.

The minimum inhibitory concentrations (MICs) of lefamulin and the comparators were determined by broth microdilution method according to the Clinical and Laboratory Standards Institute (CLSI) (2018) M07-11th Edition (CLSI, 2018). The MICs against *M. pneumoniae* were measured according to the methods for antimicrobial susceptibility testing for human mycoplasmas described in CLSI document M43-A (2011) (CLSI, 2011). The antimicrobial comparators included tigecycline, moxifloxacin, linezolid, penicillin, ampicillin, oxacillin, ceftriaxone, levofloxacin, vancomycin, trimethoprim-sulfamethoxazole, erythromycin, and azithromycin. The concentrations of the test antimicrobial agents ranged from 32 mg/L to 0.015 mg/L.

WHONET 5.6 software and the breakpoints of CLSI M100-29th Edition (CLSI, 2019) were used to interpret and analyze the results of antimicrobial susceptibility test. Lefamulin and tigecycline were analyzed according to the breakpoints recommended by FDA[1]. The breakpoints of lefamulin was ≤0.25 mg/L active against methicillin-sensitive *S. aureus*, ≤0.5 mg/L against *S. pneumoniae*, and ≤2 mg/L against *H. influenzae*. The breakpoint of tigecycline was ≤0.5 mg/L active against *S. aureus*, and ≤0.25 mg/L against *H. influenzae*.

Ethics Statement

The study protocol was approved by the Ethics Committee of Huashan Hospital, Fudan University (Number: 2019-319).

RESULTS

Lefamulin at 0.25 mg/L inhibited the growth of all *Staphylococcus* strains (**Table 1** and **Figure 1**). The MIC_{90} value of lefamulin was 0.125 mg/L against MRSA, 0.06 mg/L against methicillin-resistant *S. epidermidis* (MRSE), 0.06 mg/L against methicillin-sensitive *S. aureus* (MSSA), and 0.03 mg/L against methicillin-sensitive *S. epidermidis* (MSSE). Lefamulin displayed MIC values ranging from ≤0.015 mg/L to 0.25 mg/L (MIC_{90}: ≤0.25 mg/L) against 172 strains of *S. pneumoniae*, including penicillin-susceptible (PSSP) strains (penicillin MIC ≤0.06 mg/L), penicillin-intermediate (PISP) strains (penicillin MIC: 0.125 mg/L–1 mg/L), and penicillin-resistant (PRSP) strains (penicillin MIC ≥ 2 mg/L). Lefamulin inhibited the growth of all PSSP strains at ≤0.015 mg/L and all PISP and PRSP strains at 0.25 mg/L. The $MIC_{50/90}$ values of lefamulin were ≤0.015/≤0.015 mg/L against *S. pyogenes* and ≤0.015/0.06 mg/L against *S. agalactiae*. Lefamulin inhibited the growth of all the *S. pyogenes* and *S. agalactiae* strains at 0.06 mg/L (**Table 2** and **Figure 1**).

[1] www.fda.gov/drugs/development-resources/antibacterial-susceptibility-test-interpretive-criteria

TABLE 1 | *In vitro* activity of lefamulin and comparators against *Staphylococcus*.

Organism (No. of strains)	Antimicrobial agent	MIC (mg/L)			R%	S%
		MIC Range	MIC_{50}	MIC_{90}		
MRSA (*n* = 60)	Lefamulin	≤0.015–0.25	≤0.015	0.125	–	–
	Oxacillin	32 – >32	>32	>32	100	0
	Levofloxacin	0.125–>32	8	>32	53.3	45
	Moxifloxacin	0.03–16	1	8	48.3	48.3
	Erythromycin	0.25–>32	>32	>32	85.0	11.7
	Azithromycin	0.5–>32	>32	>32	85.0	15.0
	Vancomycin	0.5–2	1	1	0	100
	Linezolid	0.5–4	2	2	0	100
	Tigecycline	0.06–0.5	0.125	0.25	–	100
MSSA (*n* = 61)	Lefamulin	≤0.015–0.125	0.06	0.06	–	100
	Oxacillin	0.25–2	1	2	0	100
	Levofloxacin	0.125–8	0.25	0.5	3.3	96.7
	Moxifloxacin	≤0.015–2	0.06	0.25	3.3	96.7
	Erythromycin	0.25–>32	>32	>32	55.7	44.3
	Azithromycin	0.5–>32	>32	>32	55.7	44.3
	Vancomycin	0.5–1	1	1	0	100
	Linezolid	1–4	2	4	0	100
	Tigecycline	0.06–0.25	0.125	0.25	–	100
MRSE (*n* = 15)	Lefamulin	≤0.015–0.125	≤0.015	0.06	–	–
	Oxacillin	1–>32	4	32	100	0
	Levofloxacin	0.125–>32	8	>32	73.3	20
	Moxifloxacin	0.03–32	2	32	53.3	20
	Erythromycin	0.25–>32	>32	>32	86.7	13.3
	Azithromycin	0.25–>32	>32	>32	80.0	20.0
	Vancomycin	1–2	1	2	0	100
	Linezolid	0.25–1	1	1	0	100
	Tigecycline	0.06–0.25	0.06	0.25	–	–
MSSE (*n* = 15)	Lefamulin	≤0.015–0.06	≤0.015	0.03	–	–
	Oxacillin	0.06–0.125	0.125	0.125	0	100
	Levofloxacin	0.125–4	0.25	4	13.3	80
	Moxifloxacin	0.03–1	0.06	0.5	0	93.3
	Erythromycin	0.125–>32	32	>32	60.0	40.0
	Azithromycin	0.125–>32	32	>32	60.0	40.0
	Vancomycin	1–2	1	2	0	100
	Linezolid	0.5–2	1	1	0	100
	Tigecycline	0.06–0.25	0.125	0.25	–	–

MIC, minimum inhibitory concentration; MIC_{50}, MIC for inhibiting 50% of the isolates; MIC_{90}, MIC for inhibiting 90% of the isolates; R, resistant; S, susceptible; MRSA, methicillin-resistant S. aureus; NA, not available; MSSA, methicillin-susceptible S. aureus; MRSE, methicillin-resistant S. epidermidis; MSSE, methicillin-susceptible S. epidermidis.

The $MIC_{50/90}$ values of lefamulin ≤ 1/ ≤ 1 mg/L against *H. influenzae* and *H. parainfluenzae*, regardless of β-lactamase production. Lefamulin inhibited the growth of all the *Haemophilus* strains at 2 mg/L (**Table 3** and **Figure 1**). Lefamulin showed $MIC_{50/90}$ of 0.25/0.25mg/L against *M. catarrhalis*. Lefamulin inhibited the growth of all *M. catarrhalis* strains at 0.5 mg/L (**Table 3** and **Figure 1**).

Lefamulin inhibited the growth of all *M. pneumoniae* strains at 0.03 mg/L. The MIC ranged from ≤0.015 to 0.03 mg/L ($MIC_{50/90}$: 0.03/0.03 mg/L). Its activity was comparable to moxifloxacin and significantly superior to erythromycin and azithromycin (**Table 4** and **Figure 1**).

DISCUSSION

In the present study, lefamulin displayed excellent antimicrobial activity against all the respiratory pathogens, including MRSA, MSSA, MRSE, MSSE, *S. pneumoniae*, β-hemolytic *Streptococcus*, *Haemophilus*, *M. catarrhalis*, and *M. pneumoniae*. Our results are consistent with the reports of Susanne Paukner et al. on the antimicrobial activity of lefamulin against 1,473 and 2,661 strains of *S. pneumoniae*, 3,923 and 2,919 strains of *S. aureus* in the SENTRY Antimicrobial Surveillance Program 2010 and 2015–2016 (Paukner et al., 2013, 2019). The MIC_{90} of lefamulin was 0.25 mg/L and 0.12 mg/L against *S. pneumoniae*, regardless

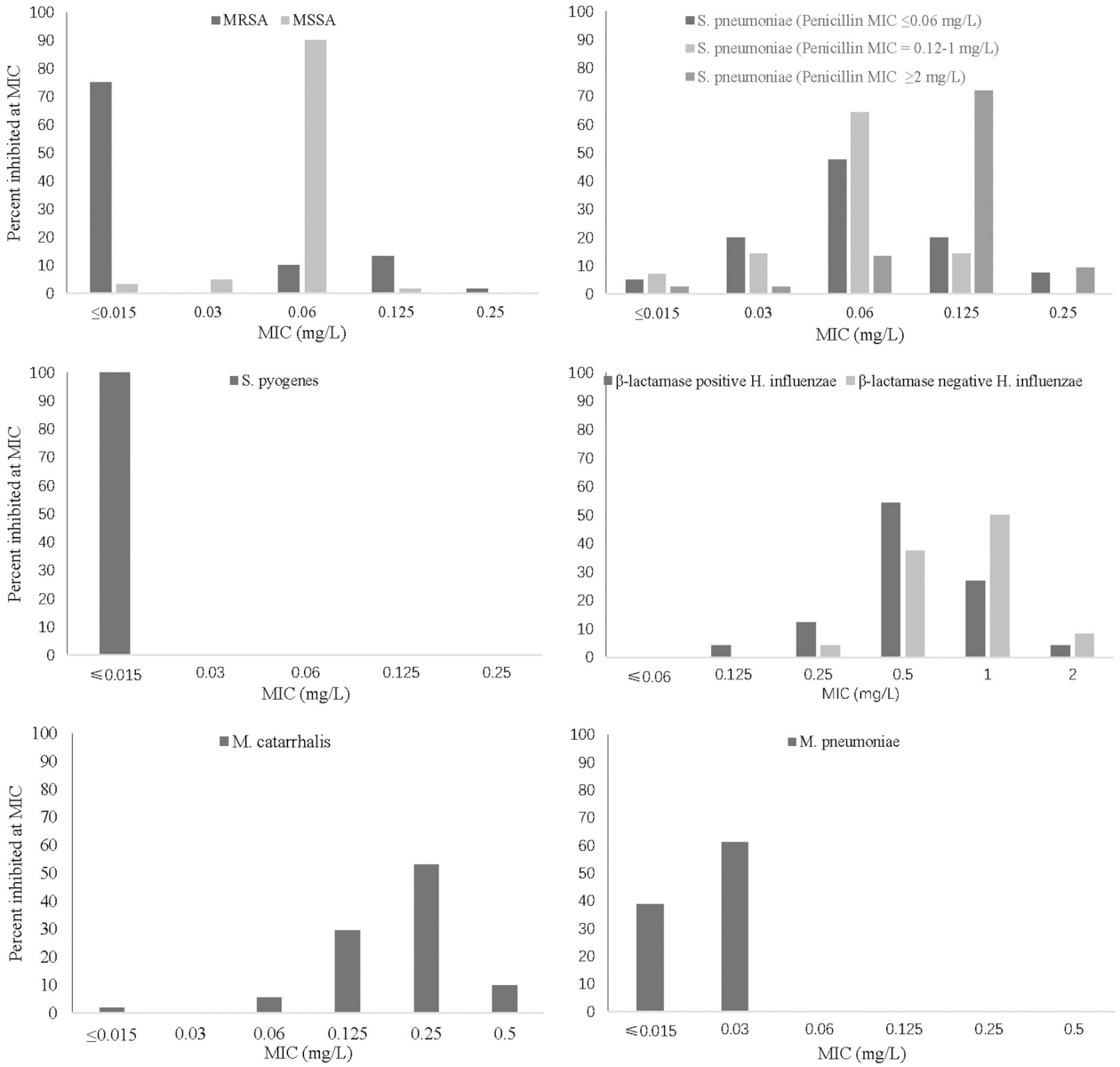

FIGURE 1 | MIC frequency distribution of lefamulin against respiratory pathogens. MRSA (n = 60), MSSA (n = 61), *S. pneumoniae* strains (penicillin MIC ≤ 0.06 mg/L, n = 40; penicillin MIC = 0.12–1 mg/L, n = 40; penicillin MIC ≥ 2 mg/L, n = 118), *S. pyogenes* (n = 30), *H. influenzae* (β-lactamase-positive strains, n = 48; β-lactamase-negative strains, n = 48), *M. catarrhalis* (n = 54), and *M. pneumoniae* (n = 54). MIC, minimum inhibitory concentration; MRSA, methicillin-resistant *S. aureus*; MSSA, methicillin-susceptible *S. aureus*.

of resistance to penicillin, ceftriaxone and/or levofloxacin. The $MIC_{50/90}$ was 0.12/0.12 mg/L against MRSA and MSSA. They also reported that the MIC value of lefamulin was 2–>16 mg/L against two MRSA isolates and 5 MSSA isolates in 2010, whereas the MIC value of lefamulin against 11 *S. aureus* isolates in 2015–2016 was higher than its epidemiological cutoff value. However, all the *Staphylococcus* strains tested in the present study were sensitive to lefamulin. All the *Staphylococcus* strains were also susceptible to tigecycline, vancomycin, and linezolid. However, lefamulin inhibited the growth of all *Staphylococcus* strains at concentration of ≤0.25 mg/L, which is far lower than the concentration of 1–2, 1–4, and 0.25–0.5 mg/L required by the above three comparators for 100% inhibition of bacterial growth. Lefamulin was also superior to quinolones (only inhibited 80–96.7% of the strains) in this respect.

Lefamulin also displayed high antimicrobial activity against *Haemophilus* and *M. catarrhalis*. Lefamulin was comparable to ceftriaxone in activity against *S. pneumoniae* strains (PSSP, PISP) and β-hemolytic *Streptococcus*, but better than ceftriaxone against PRSP, better than penicillin against PISP and PRSP, and similar to penicillin against β-hemolytic *Streptococcus*. Lefamulin had similar activity as moxifloxacin, vancomycin,

TABLE 2 | *In vitro* activity of lefamulin and comparators against *Streptococcus* species.

Organism (No. of strains)	Antimicrobial agent	MIC (mg/L)			R%	S%
		MIC Range	MIC_{50}	MIC_{90}		
Streptococcus pneumoniae (penicillin MIC ≤ 0.06 mg/L) (*n* = 40)	Lefamulin	≤0.015–≤0.015	≤0.015	≤0.015	–	100
	Ceftriaxone	≤0.015–0.03	≤0.015	≤0.015	0	100
	Penicillin	≤0.015–≤0.015	≤0.015	≤0.015	0	100
	Levofloxacin	0.125–0.25	0.25	2	3.3	97.5
	Moxifloxacin	0.03–0.25	0.06	0.125	0	97.5
	Erythromycin	0.03–>32	>32	>32	97.5	2.5
	Azithromycin	0.06–>32	>32	>32	97.5	2.5
	Vancomycin	≤0.015–0.5	0.25	0.5	0	100
	Linezolid	0.125–1	1	1	0	100
Streptococcus pneumoniae (penicillin MIC = 0.12–1 mg/L) (*n* = 40)	Lefamulin	0.03–0.25	0.125	0.25	–	100
	Ceftriaxone	0.03–1	0.125	0.5	0	100
	Penicillin	0.125–1	0.5	1	–	–
	Levofloxacin	0.5–2	1	1	0	100
	Moxifloxacin	0.125–0.25	0.125	0.25	0	100
	Erythromycin	2–>32	>32	>32	100	0
	Azithromycin	2–>32	>32	>32	100	0
	Vancomycin	0.06–0.5	0.25	0.5	–	100
	Linezolid	0.25–1	1	1	–	100
Streptococcus pneumoniae (penicillin MIC ≥ 2 mg/L) (*n* = 118)	Lefamulin	≤0.015–0.25	0.125	0.125	–	100
	Ceftriaxone	0.5–>32	2	4	45.8	47.5
	Penicillin	2–32	8	8	100	0
	Levofloxacin	0.125–32	1	1	1.7	98.3
	Moxifloxacin	0.06–8	0.125	0.25	0.8	98.3
	Erythromycin	2–>32	> 32	>32	100	0
	Azithromycin	2–>32	>32	>32	100	0
	Vancomycin	0.125–1	0.25	0.5	–	100
	Linezolid	0.25–2	1	1	–	100
Streptococcus pyogenes (*n* = 30)	Lefamulin	≤0.015–≤0.015	≤0.015	≤0.015	–	–
	Ceftriaxone	≤0.015–0.03	≤0.015	≤0.015	0	100
	Penicillin	≤0.015–≤0.015	≤0.015	≤0.015	0	100
	Levofloxacin	0.125–0.25	0.25	2	3.3	96.7
	Moxifloxacin	0.03–0.25	0.06	0.125	–	–
	Erythromycin	0.03–>32	>32	>32	93.3	6.7
	Azithromycin	0.06–>32	>32	>32	93.3	6.7
	Vancomycin	0.25–0.5	0.25	0.5	0	100
	Linezolid	0.5–2	1	1	0	100
Streptococcus agalactiae (*n* = 13)	Lefamulin	≤0.015–0.03	≤0.015	0.03	–	–
	Ceftriaxone	≤0.015–0.06	≤0.015	0.06	0	100
	Penicillin	0.06–0.125	0.06	0.06	0	100
	Levofloxacin	0.5–1	1	1	0	100
	Moxifloxacin	0.125–0.25	0.125	0.25	–	–
	Erythromycin	0.06–>32	2	>32	69.2	30.8
	Azithromycin	0.06 –>32	16	>32	69.2	30.8
	Vancomycin	0.5–0.5	0.5	0.5	–	100
	Linezolid	1–2	1	2	–	100

MIC, minimum inhibitory concentration; MIC_{50}, MIC for inhibiting 50% of the isolates; MIC_{90}, MIC for inhibiting 90% of the isolates; R, resistant; S, susceptible.

and linezolid against *Streptococcus*. It inhibited the growth of all *Streptococcus* species at 0.125 mg/L, which was lower than the above mentioned three agents. Lefamulin was significantly better than erythromycin and azithromycin in the activity against *S. pneumoniae* and β-hemolytic *Streptococcus*.

In this study, lefamulin also had good antimicrobial effect on the gram-negative bacilli commonly found in CABP. Lefamulin was similar to ceftriaxone, tigecycline, levofloxacin, and moxifloxacin, and better than ampicillin, azithromycin, and trimethoprim-sulfamethoxazole in the activity against

TABLE 3 | *In vitro* activity of lefamulin and comparators against *Haemophilus influenzae* and *Moraxella catarrhalis.*

Organism (No. of strains)	Antimicrobial agent	MIC (mg/L)			R%	S%
		MIC Range	MIC_{50}	MIC_{90}		
Haemophilus influenzae (β-lactamase positive) (*n* = 48)	Lefamulin	0.125–2	0.5	1	–	100
	Ceftriaxone	≤0.015–1	0.03	0.125	–	100
	Ampicillin	8–>32	>32	>32	100	0
	Levofloxacin	≤0.015–1	≤0.015	0.5	–	100
	Moxifloxacin	≤0.015–1	≤0.015	0.5	–	100
	Erythromycin	4–>32	>32	>32	–	NA
	Azithromycin	1–>32	>32	>32	–	27.1
	Tigecycline	0.06–0.25	0.125	0.25	–	100
	Trimethoprim-sulfamethoxazole	0.06/1.14–32/608	8/152	16/304	77.1	16.7
Haemophilus influenzae (β-lactamase negative) (*n* = 48)	Lefamulin	0.25–2	1	1	–	100
	Ceftriaxone	≤0.015–0.25	≤0.015	0.06	–	100
	Ampicillin	≤0.015–1	0.5	1	0	100
	Levofloxacin	≤0.015–1	≤0.015	0.5	–	100
	Moxifloxacin	≤0.015–1	≤0.015	0.5	–	100
	Erythromycin	2–>32	8	8	–	NA
	Azithromycin	0.5–>32	2	2	–	97.9
	Tigecycline	0.125–0.25	0.25	0.25	–	100
	Trimethoprim-sulfamethoxazole	0.03/0.57–16/304	4/76	16/304	56.2	37.5
Haemophilus parainfluenzae (*n* = 10)	Lefamulin	0.015–2	0.5	1	–	–
	Ceftriaxone	0.015–0.25	0.03	0.125	0	100
	Ampicillin	≤0.015–8	0.125	4	30.0	70.0
	Levofloxacin	0.03–8	0.125	4	0	80.0
	Moxifloxacin	0.125–16	0.25	4	0	60.0
	Erythromycin	2 –>32	2	8	–	–
	Azithromycin	0.25–16	1	2	0	90
	Tigecycline	0.125–1	0.5	0.5	–	–
	Trimethoprim-sulfamethoxazole	0.015/0.285–16/304	0.125/2.375	2/38	10	70
Moraxella catarrhalis (*n* = 54)	Lefamulin	≤0.015–0.5	0.25	0.25	–	–
	Ceftriaxone	≤0.015–2	0.5	1	0	100
	Ampicillin	≤0.015–>32	1	4	–	–
	Levofloxacin	≤0.015–1	0.06	0.06	0	100
	Moxifloxacin	≤0.015–0.5	0.06	0.06	–	–
	Erythromycin	0.125–>32	1	>32	–	–
	Azithromycin	0.03–>32	0.25	>32	0	66.7
	Tigecycline	0.03–2	0.06	0.125	–	–
	Trimethoprim-sulfamethoxazole	0.03/0.57 –>32/608	0.5/9.5	4/76	11.1	64.8

MIC, minimum inhibitory concentration; MIC_{50}, MIC for inhibiting 50% of the isolates; MIC_{90}, MIC for inhibiting 90% of the isolates; R, resistant; S, susceptible; NA, not available.

TABLE 4 | *In vitro* activity of lefamulin and comparators against *M. pneumoniae.*

Organism (no. of strains)	Antimicrobial agent	MIC (mg/L)			R%	S%
		MIC Range	MIC_{50}	MIC_{90}		
Mycoplasma pneumoniae (*n* = 54)	Lefamulin	≤0.015 –0.03	0.03	0.03	–	–
	Erythromycin	≤0.015–>32	32	>32	94.4	5.6
	Azithromycin	≤0.015–32	8	16	94.4	5.6
	Moxifloxacin	0.06–0.125	0.06	0.125	–	100

MIC, minimum inhibitory concentration; MIC_{50}, MIC for inhibiting 50% of the isolates; MIC_{90}, MIC for inhibiting 90% of the isolates; R, resistant; S, susceptible; NA, not available.

β-lactamase-producing *H. influenzae* and *M. catarrhalis*. As for the β-lactamase-negative strains, lefamulin provided significantly better activity than azithromycin. Lefamulin was comparable to tigecycline, ceftriaxone, and levofloxacin, and significantly superior to azithromycin and trimethoprim-sulfamethoxazole in the activity against *M. catarrhalis*. These results are consistent with those reports from other countries (Paukner et al., 2013, 2019).

It has been reported that the *M. pneumonia*e strains isolated from China are highly resistant to macrolides. Our results also confirmed the previous reports. About 94.4% of the 54 *M. pneumoniae* strains were resistant to erythromycin and azithromycin in this study. However, lefamulin still showed MIC range from ≤0.015 to 0.03 mg/L, which was not affected by resistance to macrolides. This MIC range is consistent with that from other countries (MIC_{90}: 0.002 mg/L) (Waites et al., 2017).

Lefamulin is the first semi-synthetic pleuromutilin antimicrobial agent approved for the treatment of CABP patients. Clinical trials have proved the excellent therapeutic effect of lefamulin. The MIC_{90} value of lefamulin was 0.5 μg/mL against the 50 strains of *S. pneumoniae* isolated from the patients in phase III clinical trial LEAP 1 (File et al., 2019) and 0.25 μg/mL against the 123 strains of *S. pneumoniae* isolated from the patients in clinical trial LEAP 2 (Alexander et al., 2019). The MIC_{90} against *S. aureus* isolates (10 and 13 strains) was 0.12–0.25 μg/mL. The post-treatment bacterial clearance rate was up to 100%. Research results at home and abroad have shown that lefamulin had similar antimicrobial activity against *S. epidermidis* and *S. aureus* (Paukner et al., 2013, 2019).

The above results support the excellent antimicrobial activity of lefamulin against CABP pathogens, especially antibiotic-resistant pathogens, such as PRSP, macrolide-resistant *M. pneumoniae* and MRSA. The major parameter driving efficacy for both *S. aureus* and *S. pneumoniae* is the 24h area under the drug concentration–time curve (AUC) over the MIC (24 h AUC/MIC). Lefamulin achieves rapid and predictable penetration into human tissues, with a mean 5.7-fold higher concentration in the pulmonary epithelial lining fluid compared with plasma. Percent probabilities of attaining the median AUCELF/MIC ratio targets associated with a 1-log10 CFU reduction from baseline by MIC were 97.0% at a MIC of 0.5 μg/mL for *S. pneumoniae* and 99.4% at a MIC of 0.25 μg/mL for *S. aureus* (Falcó et al., 2020). The unique mechanism of action, lack of cross resistance, good and broad coverage of respiratory pathogens regardless of resistance to other antimicrobial agent (Abbas et al., 2017; Lee and Jacobs, 2019) will surely make lefamulin a promising alternative treatment option in Chinese patients with CABP, especially those caused by PRSP, MRSA, or macrolide-resistant *M. pneumoniae*.

DATA AVAILABILITY STATEMENT

The raw data supporting the conclusions of this article will be made available by the authors, without undue reservation.

ETHICS STATEMENT

The study protocol was approved by the Ethics Committee of Huashan Hospital, Fudan University (Number: 2019-319).

AUTHOR CONTRIBUTIONS

DZ and FH designed the study. SW, YZ, YG, and DY performed the experimental work. SW and YZ collected the data. FH analyzed the data. All authors read and approved the final manuscript, contributed to the article, and approved the submitted version.

FUNDING

This work was supported by Sinovant Sciences, Major Research and Development Project of Innovative Antibiotics, Ministry of Science and Technology of China (No. 2017ZX09304005), National Mega-project for Innovative Drugs (2019ZX09721001-006-004), and CHINET Antimicrobial Surveillance Network (grant number WI207259).

REFERENCES

Abbas, M., Paul, M., and Huttner, A. (2017). New and improved? a review of novel antibiotics for Gram-positive bacteria. *Clin. Microbiol. Infect* 23, 697–703. doi: 10.1016/j.cmi.2017.06.010

Alexander, E., Goldberg, L., Das, A. F., Moran, G. J., Sandrock, C., Gasink, L. B., et al. (2019). Oral lefamulin vs moxifloxacin for early clinical response among adults with community-acquired bacterial pneumonia: the LEAP 2 randomized clinical trial. *JAMA* 2019 322, 1661–1671. doi: 10.1001/jama.2019.15468

CLSI (2011). *Methods for Antimicrobial Susceptibility Testing for Human Mycoplasmas; Approved Guideline (M43-A)*. Wayne, PA: Clinical and Laboratory Standards Institute.

CLSI (2018). *Methods for Dilution Antimicrobial Susceptibility Tests for Bacteria That Grow Aerobically (M07)*. Wayne, PA: Clinical and Laboratory Standards Institute.

CLSI (2019). *Performance standards for antimicrobial susceptibility testing (M100-S29)*. Wayne, PA: Clinical and Laboratory Standards Institute.

Falcó, V., Burgos, J., and Almirante, B. (2020). An overview of lefamulin for the treatment of community acquired bacterial pneumonia. *Expert Opin. Pharmacother.* 21, 629–636. doi: 10.1080/14656566.2020.1714592

File, T. M., Goldberg, L., Das, A., Sweeney, C., Saviski, J., Gelone, S. P., et al. (2019). Efficacy and safety of intravenous-to-oral lefamulin, a pleuromutilin antibiotic, for the treatment of community-acquired bacterial pneumonia: the phase III Lefamulin Evaluation Against Pneumonia (LEAP 1) trial. *Clin. Infect. Dis.* 69, 1856–1867. doi: 10.1093/cid/ciz090

Lee, Y. R., and Jacobs, K. L. (2019). Leave it to lefamulin: a Pleuromutilin treatment option in community-acquired bacterial pneumonia. *Drugs* 79, 1867–1876. doi: 10.1007/s40265-019-01219-5

Mendes, R. E., Paukner, S., Doyle, T. B., Gelone, S. P., Flamm, R. K., and Sader, H. S. (2019). Low prevalence of gram-positive isolates showing elevated lefamulin MIC results during the SENTRY surveillance program for 2015-2016 and characterization of resistance mechanisms. *Antimicrob. Agents Chemother* 63:e02158-18. doi: 10.1128/AAC.02158-18

Paukner, S., Gelone, S. P., Arends, S. J. R., Flamm, R. K., and Sader, H. S. (2019). Antibacterial activity of lefamulin against pathogens most commonly causing community-acquired bacterial pneumonia: SENTRY antimicrobial surveillance program (2015–2016). *Antimicrob. Agents Chemother* 63:e02161-18. doi: 10.1128/AAC.02161-18

Paukner, S., Sader, H. S., Ivezic-Schoenfeld, Z., and Jones, R. N. (2013). Antimicrobial activity of the pleuromutilin antibiotic BC-3781 against bacterial pathogens isolated in the SENTRY antimicrobial surveillance program in 2010. *Antimicrob. Agents Chemother* 57, 4489–4495. doi: 10.1128/aac.00358-13

Rodvold, K. A. (2019). Introduction: lefamulin and pharmacokinetic/pharmacodynamics rationale to support the dose selection of lefamulin. *J. Antimicrob. Chemother* 74(Suppl. 3), i2–i4.

Veve, M. P., and Wagner, J. L. (2018). Lefamulin: review of a promising novel pleuromutilin antibiotic. *Pharmacotherapy* 38, 935–946. doi: 10.1002/phar.2166

Waites, K. B., Crabb, D. M., Duffy, L. B., Jensen, J. S., Liu, Y., and Paukner, S. (2017). In vitro activities of lefamulin and other antimicrobial agents against macrolide-susceptible and macrolide-resistant mycoplasma pneumoniae from the United States, Europe, and China. *Antimicrob Agents Chemother* 61:e02008-16. doi: 10.1128/AAC.02008-16

Conflict of Interest: The authors declare that the research was conducted in the absence of any commercial or financial relationships that could be construed as a potential conflict of interest.

frontiers in Microbiology

ORIGINAL RESEARCH
published: 13 November 2020
doi: 10.3389/fmicb.2020.586764

Emergence of a Clinical *Escherichia coli* Sequence Type 131 Strain Carrying a Chromosomal bla_{KPC-2} Gene

Dairong Wang[1,2†], Xinli Mu[1,3†], Ying Chen[1,3], Dongdong Zhao[1,3], Ying Fu[3,4], Yan Jiang[1,3], Yiwei Zhu[1,3], Jingjing Quan[1,3], Xiaoting Hua[1,3], Guofeng Mao[5], Xi Li[6] and Yunsong Yu[1,3]**

[1] Department of Infectious Diseases, Sir Run Run Shaw Hospital, College of Medicine, Zhejiang University, Hangzhou, China, [2] Blood Center of Zhejiang Province, Hangzhou, China, [3] Key Laboratory of Microbial Technology and Bioinformatics of Zhejiang Province, Zhejiang Institute of Microbiology, Hangzhou, China, [4] Department of Clinical Laboratory, Sir Run Run Shaw Hospital, College of Medicine, Zhejiang University, Hangzhou, China, [5] Department of Laboratory Medicine, Shaoxing People's Hospital, Shaoxing, China, [6] Centre of Laboratory Medicine, Zhejiang Provincial People's Hospital, People's Hospital of Hangzhou Medical College, Hangzhou, China

Objectives: Bacteria carrying the *Klebsiella pneumoniae* carbapenemase genes have rapidly spread worldwide and have become a great threat to public health. The bla_{KPC-2} gene has been primarily located on plasmids cocirculating in various strains. However, chromosomal integration of the bla_{KPC-2} gene in *Escherichia coli* has not been reported. In the present study, we report the detection of the first clinical strain of *E. coli* ST131 with a bla_{KPC-2} gene, which integrated in the chromosome. *E. coli* strain EC3385 was identified and subjected to susceptibility testing and genotyping. The complete genome sequences of this strain and four *Proteus mirabilis* strains were obtained. Chromosomal integration of the bla_{KPC-2} gene was confirmed using a combination of short- and long-read sequencing. Comparative genetic analyses were performed and the origin of the chromosomal location of the bla_{KPC-2} gene was further analyzed. Whole-genome sequencing revealed that strain EC3385 belonged to the ST131 type and possessed various resistance and virulence genes. Sequence analysis showed that the bla_{KPC-2} gene was carried in a 24-kb insertion sequence on the chromosome. This insertion sequence possessed high sequence similarity to previously reported bla_{KPC-2}-habouring plasmids of *P. mirabilis* in China. To the best of our knowledge, this is the first report of a clinical ST131 *E. coli* strain carrying bla_{KPC-2} on the chromosome. The bla_{KPC-2} gene was probably horizontally transferred from the *P. mirabilis* plasmid to the *E. coli* chromosome by the *IS*26 element, indicating that *P. mirabilis* might be an important reservoir of bla_{KPC-2} gene for *E. coli*. Furthermore, the *E. coli* ST131 strain carrying the chromosomal bla_{KPC-2} gene could be further spread due to its carbapenem resistance and high virulence. It is imperative to perform active surveillance to prevent further dissemination of KPC-2 type carbapenemase-producing isolates.

Keywords: *E. coli*, KPC-2, cre, resistance mechanism, whole genome sequencing

OPEN ACCESS

Edited by:
Yi-Wei Tang,
Cepheid, United States

Reviewed by:
Fupin Hu,
Fudan University, China
Siqiang Niu,
First Affiliated Hospital of Chongqing Medical University, China
Charles William Stratton,
Vanderbilt University Medical Center, United States

****Correspondence:***
Xi Li
lixi_0611@163.com
Yunsong Yu
yvys119@zju.edu.cn

† These authors have contributed equally to this work and share first authorship

Specialty section:
This article was submitted to Antimicrobials, Resistance and Chemotherapy, a section of the journal Frontiers in Microbiology

Received: *24 July 2020*
Accepted: *26 October 2020*
Published: *13 November 2020*

Citation:
Wang D, Mu X, Chen Y, Zhao D, Fu Y, Jiang Y, Zhu Y, Quan J, Hua X, Mao G, Li X and Yu Y (2020) Emergence of a Clinical Escherichia coli Sequence Type 131 Strain Carrying a Chromosomal bla_{KPC-2} Gene. Front. Microbiol. 11:586764. doi: 10.3389/fmicb.2020.586764

INTRODUCTION

Bacteria carrying the *Klebsiella pneumoniae* carbapenemase genes (*bla$_{KPC}$*) have rapidly spread worldwide and have become a great threat to public health because these bacteria are often associated with high morbidity and mortality (Wang et al., 2016; An et al., 2018). KPC-2 is the main type of KPC carbapenemase and is most common in *K. pneumoniae* bacteria. In China, clonal spreading is a main mode of transfer of KPC-2 type carbapenemase-producing *K. pneumonia.* Our previous research demonstrated that multilocus sequence type 11 (ST11) originated from a successful lineage of KPC-2 type carbapenemase-producing *K. pneumonia* in China (Qi et al., 2011).

In contrast to *K. pneumoniae*, *E. coli* strains have rarely been reported to carry the *bla$_{KPC-2}$* gene. However, recent reports found that the number of *E. coli* strains carrying the *bla$_{KPC-2}$* gene has increased. In addition, unlike *K. pneumoniae*, clonal spread has not been found for the *bla$_{KPC-2}$* gene of *E. coli* (Chen et al., 2014). These strains also have different clone types, such as ST131, ST410, ST2281, ST43, ST721, ST4385, and ST8 (Kim et al., 2012; Mavroidi et al., 2012; Tian et al., 2020). Notably, among these clone types, *E. coli* ST131, an international multidrug-resistant high-risk clone, has gained a further selective advantage as a result of acquiring carbapenem resistance (Rogers et al., 2011; Kim et al., 2012) and *E. coli* ST131 may become a successful lineage of KPC-2 type carbapenemase-producing *E. coli*.

In addition, *K. pneumoniae* carbapenemase genes have been primarily located on plasmids cocirculating with various strains (Nordmann et al., 2011). They are considered a major mechanism responsible for the dramatic increase in the prevalence of carbapenem-resistant *Enterobacteriaceae* isolates. Plasmid DNA can act as a temporary "lending library" allowing vital genes to survive various selective pressures (Harrison et al., 2015). Notably, *in vitro* data demonstrated that once a gene is incorporated into a chromosome, it is maintained through replication without being subject to selective pressures, and gene loss from bacterial populations is rare (Bergstrom et al., 2000; Bahl et al., 2009; Carraro et al., 2015). Interestingly, the earliest observed chromosomal *bla$_{KPC}$* gene integration events have been sporadic in gram-negative bacteria, such as *Pseudomonas aeruginosa* in 2006 (Villegas et al., 2007), *Raoultella spp.* in 2008 (Castanheira et al., 2009) and *Acinetobacter baumannii* in 2009 (Martínez et al., 2014). Recently, chromosomal integration has been described in four *K. pneumoniae* ST258 isolates (Conlan et al., 2014; Chen et al., 2015; Mathers et al., 2017). However, *bla$_{KPC-2}$* gene chromosomal integration events in *E. coli* have not been reported.

In the present study, we report the detection of the first clinical strain of *E. coli* ST131 with a chromosomal *bla$_{KPC-2}$* gene integrated in the chromosome. In addition, the genetic origin of this gene was further analyzed using whole-genome sequencing.

MATERIALS AND METHODS

Patient and Strain Data

A patient was admitted to the hospital for a craniocerebral infarction in 2017. A carbapenem-resistant strain of *E. coli* EC3385 was isolated from sputum because the patient developed hospital-acquired pneumonia (HAP) secondary to postoperative intubation during the hospitalization. In addition, four *P. mirabilis* strains isolated at the same period (**Table 1**) as *E. coli* EC3385 in the ICU department were analyzed retrospectively. These strains were preliminary identified by the VITEK 2 system (Sysmex-bioMérieux, Marcy l'Etoile, France) and further confirmed by 16S rRNA sequencing.

Antibiotic Susceptibility Test

Antibiotic susceptibility was determined using the VITEK 2 system and broth microdilution method and the results were interpreted according to the Clinical and Laboratory Standard Institute (CLSI) guidelines (CLSI, 2017) except for tigecycline and colistin, which were interpreted according to the European Committee on Antimicrobial Susceptibility Testing breakpoints for *Enterobacteriaceae*[1].

Whole-Genome Sequencing and Assembly

Total genomic DNA extraction and analysis were performed as previously described (Li et al., 2018). Briefly, *E. coli* strain EC3385 and four *P. mirabilis* strains were cultured to mid-logarithmic phase in 50 ml of MH medium at 37°C. The

[1]http://www.eucast.org/clinical_breakpoints

TABLE 1 | Strains collection date and Vitek-2 antibiotic susceptibility.

Isolates	Collection day	MICs (mg/L)											
		AMK	CZA[a]	CRO	CST[a] CIP	ETP	GEN	IPM[a]	LEV	TGC[a]	SXT	TGC	TZP
E. coli EC3385	10-03-2017	≤2	0.25	≥64	0.25 ≥ 4	≥8	≤1	64	≥8	0.125	≤1/19	≤0.5	≥128
PM380	10-03-2017	≤2	0.125	≥64	- ≥ 4	≥8	≥16	64	≥8	-	≥16/304	-	64
PM906	21-03-2017	≤2	0.125	≥64	- ≥ 4	≥8	≥16	64	≥8	-	≥16/304	-	64
PM431	11-03-2017	≤2	0.125	≥64	- ≥ 4	≥8	≥16	64	≥8	-	≥16/304	-	64
PM187	08-02-2017	≤2	0.125	≥64	- ≥ 4	≥8	≥16	64	≥8	-	≥16/304	-	64
E. coli ATCC 25922	NA	≤2	≤0.125	≤1	0.125 ≤0.25	≤0.5	≤1	≤1	≤0.25	0.125	≤1/19	≤0.5	≤4

[a] *Drug susceptibility was determined with broth microdilution method according to the Clinical Laboratory Standards Institute (CLSI) guidelines. NA, not applicable. AMK, amikacin; CZA, Ceftazidime-avibactam; CRO, ceftriaxone; CST, colistin; CIP, Ciprofloxacin; ETP, ertapenem; GEN, gentamicin; IPM, imipenem; LEV, levofloxacin; SXT, trimethoprim-sulfamethoxazole. TGC, Tigecycline, TZP, piperacillin-tazobactam.*

TABLE 2 | Genome and plasmids of *E. coli* EC3385.

Genomic structure	Size (bp)	GC content(%)	CDS no.	rRNA no.	tRNA no.	Accession no.	Resistance genes	Virulence genes	Incompatibility
EC3385 chromosome	4,910,422	50.9	4749	66	267	CP029420	*bla*$_{KPC-2}$	*iss*, *gad*,*lpfA*,*chuA* *fyuA*,*irp2*,*kpsMII_K5* *ompT*,*sitA*,*terC*,*traT*, *Usp*,*yfcV*	–
EC3385-P1 plasmid	101,340	46.3	121	–	9	CP029421	–	–	incFIB
EC3385-P2 plasmid	89,323	50.5	132	–	–	CP029422	*bla*$_{TEM-1B}$	–	incFIA

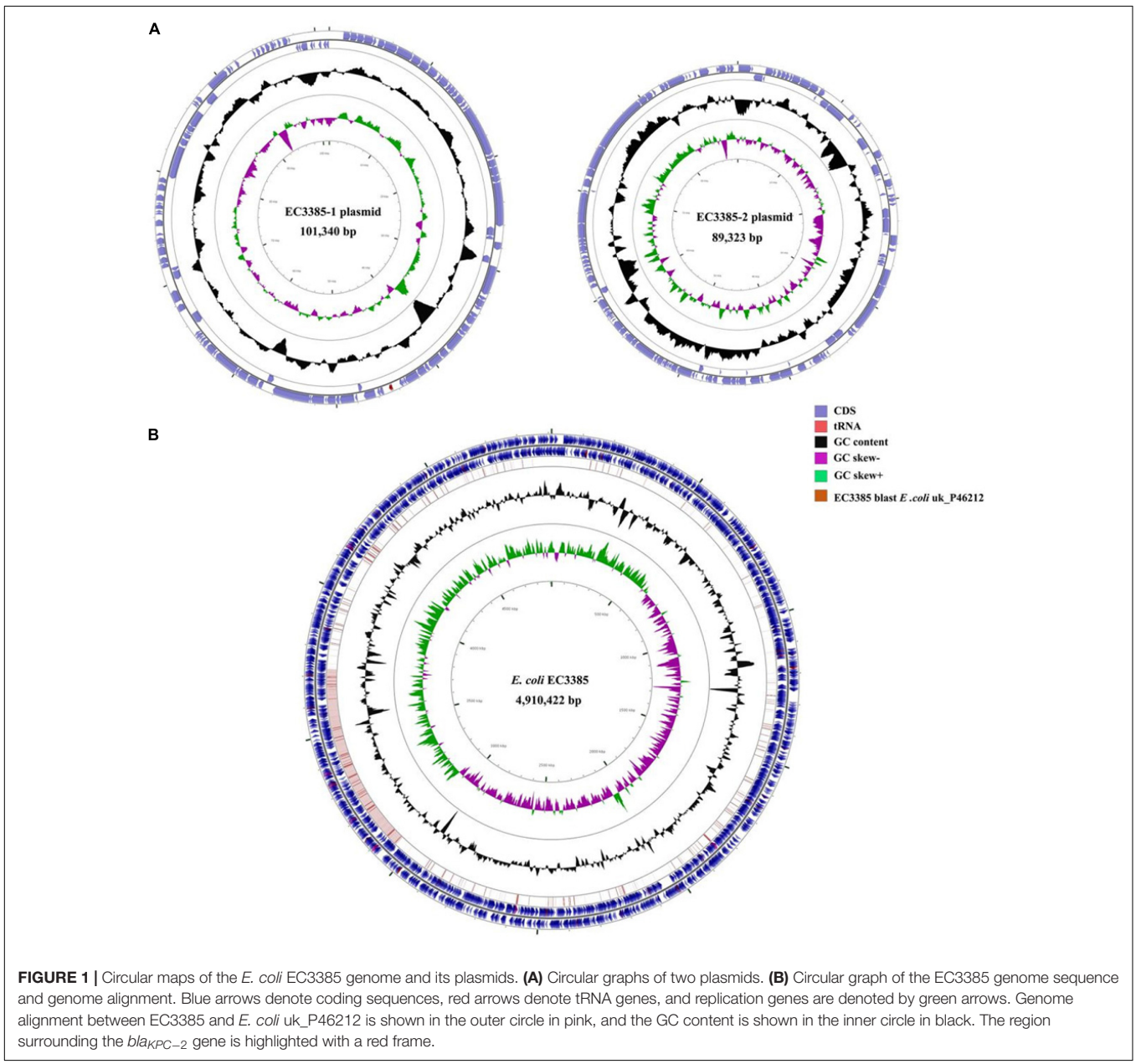

FIGURE 1 | Circular maps of the *E. coli* EC3385 genome and its plasmids. **(A)** Circular graphs of two plasmids. **(B)** Circular graph of the EC3385 genome sequence and genome alignment. Blue arrows denote coding sequences, red arrows denote tRNA genes, and replication genes are denoted by green arrows. Genome alignment between EC3385 and *E. coli* uk_P46212 is shown in the outer circle in pink, and the GC content is shown in the inner circle in black. The region surrounding the *bla*$_{KPC-2}$ gene is highlighted with a red frame.

genomic DNA of these strains was extracted using a QIAamp DNA MiniKit (Qiagen, Valencia, CA, United States) following the manufacturer's recommendations. The DNA library was prepared using a Nextera XT DNA library preparation kit (Illumina, Inc., Cambridge, United Kingdom), and genomic DNA was sequenced on an Illumina HiSeq 4000 instrument with

a 150-bp paired-end approach at a depth of approximately 200 × . The raw reads of the strains were assembled into draft genomes using the CLC Genomics Workbench 10.0.

In addition, *E. coli* EC3385 strain sequencing was further performed via a single molecule real-time (SMRT) technique using a PacBio RS II platform and the resulting sequences were assembled *de novo* using the hierarchical genome assembly process (HGAP) with the default settings of the SMRT Analysis v2.3.0 software package (Shen et al., 2017).

Genome Annotation and *in silico* Analyses

The Rapid Annotation using Subsystems Technology (RAST) annotation website server[2] was used to annotate the genomes. Multi-locus sequence typing (MLST) of resistance genes and the Inc-type plasmid of the strain were performed using the MLST 1.8 server, ResFinder 3.0, Virulence Finder 1.5, and Plasmid Finder 1.3, which are available at the Center for Genomic Epidemiology[3]. Graphical maps were generated by the CGView server[4]. A comparison of the insert sequence of this strain and its related plasmids was performed with EasyFig 2.2.2 (Sullivan et al., 2011).

Phylogenetic Analysis

Phylogenetic analysis of these *P. mirabilis* strains was performed. Genome sequences of other *P. mirabilis* strains were downloaded from the RefSeq database. Our strains were annotated by Prokka (Seemann, 2014) using the *P. mirabilis* proteins from the RefSeq database as a prior reference. The core genome was determined by Roary (Page et al., 2015) using Mafft for multiple sequence alignment. A maximum-likelihood phylogenetic tree was inferred by RAxML (Stamatakis, 2014) using the GTRGAMMA model for nucleotide substitution and running with 100 bootstraps. The phylogenetic tree was visualized by iTOL (Letunic and Bork, 2019).

[2]http://rast.nmpdr.org/rast/cgi

[3]http://www.genomicepidemiology.org/

[4]http://stothard.afns.ualberta.ca/cgview_server/

Nucleotide Sequence Accession Numbers

The complete nucleotide sequences of the chromosome and three plasmids of *E. coli* strain EC3385 reported in the present study were deposited in the GenBank nucleotide database under accession numbers CP029420, CP029421, and CP029422, respectively.

Sequence data from four *P. mirabilis* strains were also deposited in GenBank as follows:

CAV1042, CP018671.1; CAV1392, CP011578.1; CAV1453, CP018356.1.

RESULTS AND DISCUSSION

Clinical Microbiologic Characteristics

The antimicrobial susceptibility test results showed that *E. coli* strain EC3385 was resistant to multiple antimicrobial agents, including cephalosporins, carbapenems and fluoroquinolones, but it was susceptible to aminoglycosides, ceftazidime-avibactam, colistin, and tigecycline (**Table 1**).

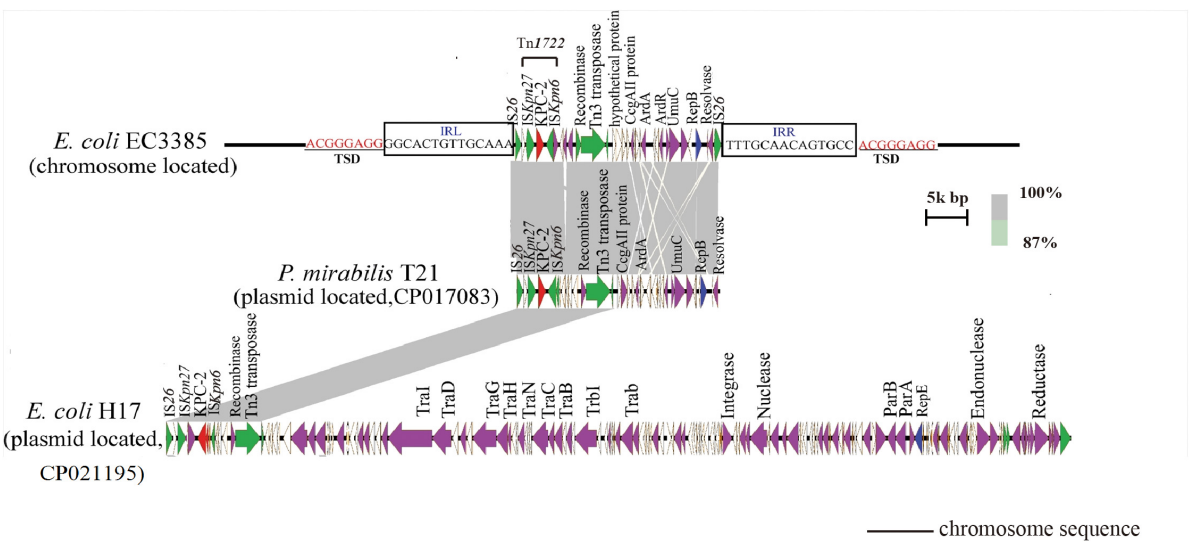

FIGURE 2 | Linear comparison of the 24-kb insertion sequence with closely related plasmids. The gray regions between plasmids indicate nucleotide identity (87–100%) determined by BLASTn. Arrows indicate predicted open reading frames (ORFs). The primary structural characteristics of the 24-kb insertion sequence are compared to plasmids pT21 (CP017083) and pH17 (CP021195). Colored arrows represent ORFs, with red, purple, yellow, green, and white representing antibiotic resistance genes; replication, recombination and repair genes; plasmid stability genes; mobile elements and plasmid transfer related-genes; and genes with unknown function genes, respectively.

Multi-locus sequence typing analysis showed that this strain belonged to the ST131 type. The ST131-type *E. coli* clonal group emerged in the mid-2000s and has since spread extensively throughout the world (Can et al., 2015). Currently, the ST131 type is a very successful pandemic clone associated with community- and hospital-acquired infections. Many studies have demonstrated that this clone has high virulence potential and is associated with treatment failure (Can et al., 2015). In this study, VirulenceFinder analysis showed the presence of multiple potential virulence factors, such as *iss* (increased serum survival), *lpfA* (long polar fimbriae), and *gad* (glutamate decarboxylase) (**Table 2**). In addition, this clone is responsible for the rapid increase in β-lactam resistance among *E. coli*, mainly due to the production of CTX-M type extended spectrum β-lactamase enzymes (ESBLs) (Nicolas-Chanoine et al., 2014).

Interestingly, the isolate in this study did not carry additional genes encoding the CTX-M enzyme. A recent study reported that ESBL-negative ST131 strains have also been isolated worldwide (Ripabelli et al., 2020). In this study, no ESBL-encoding gene was detected in *E. coli* strain EC3385; instead, the *bla*$_{KPC-2}$ gene, which encodes the KPC-2 type β-lactamase was identified by PCR amplification and sequencing.

Chromosomal Integration of the *bla*$_{KPC-2}$ Gene

Escherichia coli strain EC3385 carried the *bla*$_{KPC-2}$ gene, which is primarily located on plasmids. However, further plasmid transfer and location experiments were not successful (data not shown), suggesting that the *bla*$_{KPC-2}$ gene was located on

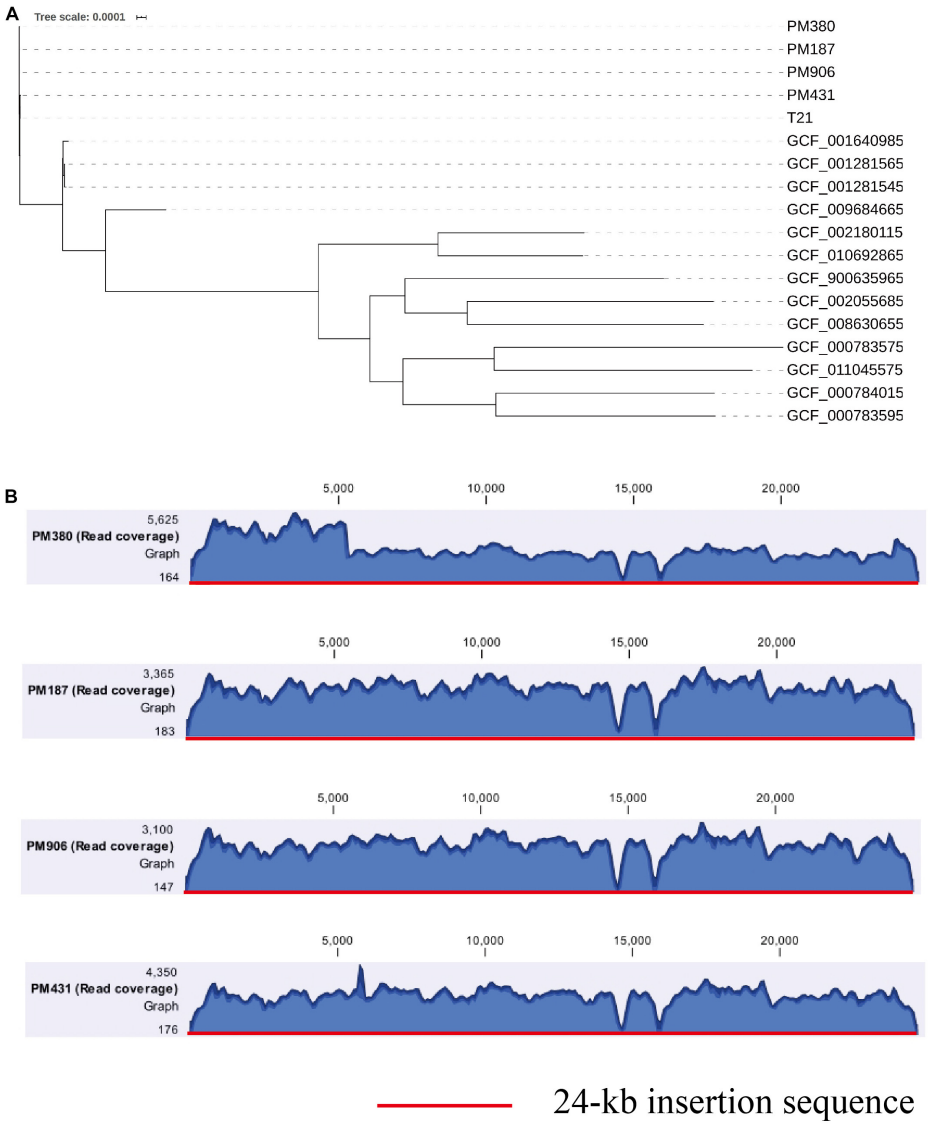

FIGURE 3 | (A) A maximum-likelihood phylogenetic analysis of *P. mirabilis* strains. **(B)** Coverage of Illumina reads for four *P. mirabilis* strains (PM380, PM187, PM906, and PM431) mapped to the 24-kb insertion shown in **Figure 2**. The mean coverage for each strain is denoted by a curve (blue).

the chromosome. Notably, a CTX-M type β-lactamase gene was found to be integrated in the chromosome of a high-risk *E. coli* ST131 clone by vertical transmission (Cerquetti et al., 2010; Stoesser et al., 2016), indicating that the ST131 type *E. coli* strain might have the ability to integrate resistance genes into chromosomes.

To determine the gene location, whole-genome sequencing was performed. The whole-genome sequencing data were assembled, and a circular chromosome and two plasmids were generated (**Table 2**). The size of the genome was 4,910,422 bp, with a GC content of 50.9%, 66 rRNA operons, 267 tRNAs, and 4749 predicted protein-coding sequences (**Table 2**). Two plasmids approximately 89 to 101 kb in size and having a GC content between 50.5 and 46.3% were grouped into identifiable replicon types (**Table 2** and **Figure 1**). Notably, the chromosomal location of the bla_{KPC-2} gene was determined using PacBio sequencing. Furthermore, the resequencing results further confirmed that the bla_{KPC-2} gene was located on the chromosome.

To evaluate the molecular basis of chromosomal integration, the chromosomal region encompassing the bla_{KPC-2} gene in the closed PacBio assembly of the ST131 type EC3385 isolate was aligned to reference the strain *E. coli* uk_P46212 (GenBank accession number CP013658), which belongs to the ST131 clone type. Relative to the reference, the EC3385 strain had a 24-kb insertion sequence in the chromosome, which included Tn1722 and several *IS*s (**Figure 2**).

The bla_{KPC-2} gene in the *E. coli* EC3385 strain was carried on this 24-kb composite transposon-like element flanked by two *IS*26 elements, which undergo replicative transposition with 8-bp target site duplication (TSD) (ACGGGAGG). This finding suggests the mobilization of this bla_{KPC-2} gene by the composite transposon formed by *IS*26 (**Figure 2**). *IS*26 has been demonstrated to undergo frequent intramolecular transposition. The structure of the insert sequence leads to the speculation that the *IS*26 element may facilitate recombination between the plasmid and chromosome (He et al., 2015).

A further BLAST search of the 24-kb insertion sequence against the GenBank database[5] revealed that this sequence is highly similar to plasmid pT21 (GenBank accession no.CP017083), which was described in a KPC-2 type carbapenemase- producing *P. mirabilis* strain isolated in Zhejiang, China (Hua et al., 2020), with 99.9% query coverage and a maximum of 100% identity (**Figure 2**). In contrast, this 24-kb insertion sequence is only partly similar (47% query coverage and a maximum of 100% identity) to plasmid pH17-2 (GenBank accession no. CP021195) of a KPC-2 type carbapenemase-producing *E. coli* strain isolated in China (**Figure 2**; Zhao et al., 2018), indicating that capture of the chromosomal bla_{KPC-2} gene from *P. mirabilis* by plasmids is possible.

Possible Origin of the Chromosomal bla_{KPC-2} Gene

To further clarify the origin of the bla_{KPC-2} gene, four bla_{KPC-2}-producing *P. mirabilis* strains isolated during the same period (approximately 2 months, **Table 1**) as *E. coli* EC3385 in the ICU department were analyzed retrospectively. These four *P. mirabilis* strains were all isolated from the sputum of different patients. Notably, a maximum-likelihood phylogenetic analysis between the four *P. mirabilis* strains and *P. mirabilis* T21 carrying the pT21 plasmid revealed that these strains were clustered together and belonged to the same clone (**Figure 3A**). Moreover, the whole-genome sequence analysis revealed that the four *P. mirabilis* strains all possessed a 24-kb insertion sequence (**Figure 3B**), indicating that this 24-kb insertion sequence that integrated into the chromosome of the *E. coli* EC3385 strain may have been acquired from *P. mirabilis* strains. In addition, two *P. mirabilis* strains were isolated before the *E. coli* EC3385 strain was identified, indicating that KPC-2 type carbapenemase-producing *P. mirabilis* strains may have spread in this ICU department. A limitation of this study is the lack of the direct links regarding the transmission between KPC-2 type carbapenemase- producing *P. mirabilis* and *E. coli* EC3385 strains. However, because the patients had stayed in the same department, it is most likely they were exposed to a common source.

CONCLUSION

In summary, to the best of our knowledge, this is the first report of a clinical ST131 *E. coli* strain carrying the bla_{KPC-2} gene in the chromosome. The bla_{KPC-2} gene was probably horizontally transferred from the *P. mirabilis* plasmid to the *E. coli* chromosome by the *IS*26 mobile element, indicating that *P. mirabilis* might be an important reservoir of the bla_{KPC-2} gene for *E. coli*. Furthermore, the discovery of a chromosomal the bla_{KPC-2} gene in an *E. coli* strain is alarming. This gene will be maintained through replication without being subject to selective pressures, as the loss of chromosomal elements from bacterial populations is rare. Therefore, the *E. coli* ST131 strain carrying the bla_{KPC-2} gene in the chromosome would be further spread due to its own carbapenem resistance and high virulence. It is imperative to perform active surveillance to prevent further dissemination of KPC-2 type carbapenemase-producing isolates.

DATA AVAILABILITY STATEMENT

The datasets presented in this study can be found in online repositories. The names of the repository/repositories and accession number(s) can be found in the article/supplementary material.

AUTHOR CONTRIBUTIONS

YY and XL conceived and designed the experiments. DW, XM, and YC performed the experiments. DZ, YZ, XH, GM, JQ, and YF analyzed the data. DW, XL, and YJ wrote the manuscript. All authors read and approved the final manuscript.

[5]http://blast.ncbi.nlm.nih.gov/Blast.cgi

FUNDING

This study was supported by the National Natural Science Foundation of China (31700125) and The Project Supported by Zhejiang Provincial Natural Science Foundation of China (Grant no. LY20H200007 and LGF20H200004) and the Medical and Health Research Project of Zhejiang Province, China (2018KY229 and 2020KY420). The funders had no role in the study design, data collection and analysis, decision to publish, or preparation of the manuscript.

REFERENCES

An, J., Lai, K., Ma, Y., Guo, L., Ye, L., Luo, Y., et al. (2018). Emergence of multiple carbapenemase-producing organisms in single patients: an increasing threat to treatment of infection. *J. Antimicrob. Chemother.* 73, 544–546. doi: 10.1093/jac/dkx411

Bahl, M. I., Hansen, L. H., and Sørensen, S. J. (2009). Persistence mechanisms of conjugative plasmids. *Methods Mol. Biol.* 532, 73–102. doi: 10.1007/978-1-60327-853-9_5

Bergstrom, C. T., Lipsitch, M., and Levin, B. R. (2000). Natural selection, infectious transfer and the existence conditions for bacterial plasmids. *Genetics* 155, 1505–1519.

Can, F., Azap, O. K., Seref, C., Ispir, P., Arslan, H., and Ergonul, O. (2015). Emerging *Escherichia coli* O25b/ST131 clone predicts treatment failure in urinary tract infections. *Clin. Infect. Dis.* 60, 523–527. doi: 10.1093/cid/ciu864

Carraro, N., Poulin, D., and Burrus, V. (2015). Replication and active partition of integrative and conjugative elements (ICEs) of the SXT/R391 family: the line between ICEs and conjugative plasmids is getting thinner. *PLoS Genet.* 11:e1005298. doi: 10.1371/journal.pgen.1005298

Castanheira, M., Deshpande, L. M., DiPersio, J. R., Kang, J., Weinstein, M. P., and Jones, R. N. (2009). First descriptions of blaKPC in *Raoultella* spp. (*R. planticola* and *R. ornithinolytica*): report from the sentry antimicrobial surveillance program. *J. Clin. Microbiol.* 47, 4129–4130. doi: 10.1128/jcm.01502-09

Cerquetti, M., Giufrè, M., García-Fernández, A., Accogli, M., Fortini, D., Luzzi, I., et al. (2010). Ciprofloxacin-resistant, CTX-M-15-producing *Escherichia coli* ST131 clone in extraintestinal infections in Italy. *Clin. Microbiol. Infect.* 16, 1555–1558. doi: 10.1111/j.1469-0691.2010.03162.x

Chen, L., Chavda, K. D., DeLeo, F. R., Bryant, K. A., Jacobs, M. R., Bonomo, R. A., et al. (2015). Genome sequence of a *Klebsiella pneumoniae* sequence type 258 isolate with prophage-encoded *K. pneumoniae* carbapenemase. *Genome Announc.* 3:e659-15. doi: 10.1128/genomeA.00659-15

Chen, L., Hu, H., Chavda, K. D., Zhao, S., Liu, R., Liang, H., et al. (2014). Complete sequence of a KPC-producing IncN multidrug-resistant plasmid from an epidemic *Escherichia coli* sequence type 131 strain in China. *Antimicrob. Agents Chemother.* 58, 2422–2425. doi: 10.1128/aac.02587-13

CLSI (2017). *Performance Standards for Antimicrobial Susceptibility Testing*, 27th Edn. CLSI Supplement M100. Wayne, PA: Clinical and Laboratory Standards Institute.

Conlan, S., Deming, C., Tsai, Y. C., Lau, A. F., Dekker, J. P., Korlach, J., et al. (2014). Complete genome sequence of a *Klebsiella pneumoniae* isolate with chromosomally encoded carbapenem resistance and colibactin synthesis loci. *Genome Announc.* 2, e1332–e1314. doi: 10.1128/genomeA.01332-14

Harrison, E., Guymer, D., Spiers, A. J., Paterson, S., and Brockhurst, M. A. (2015). Parallel compensatory evolution stabilizes plasmids across the parasitism-mutualism continuum. *Curr. Biol.* 25, 2034–2039. doi: 10.1016/j.cub.2015.06.024

He, S., Hickman, A. B., Varani, A. M., Siguier, P., Chandler, M., Dekker, J. P., et al. (2015). Insertion sequence IS26 reorganizes plasmids in clinically isolated multidrug-resistant bacteria by replicative transposition. *mBio* 6:e00762. doi: 10.1128/mBio.00762-15

Hua, X., Zhang, L., Moran, R. A., Xu, Q., Sun, L., van Schaik, W., et al. (2020). Cointegration as a mechanism for the evolution of a KPC-producing multidrug resistance plasmid in *Proteus mirabilis*. *Emerg. Microbes Infect.* 9, 1206–1218. doi: 10.1080/22221751.2020.1773322

Kim, Y. A., Qureshi, Z. A., Adams-Haduch, J. M., Park, Y. S., Shutt, K. A., and Doi, Y. (2012). Features of infections due to *Klebsiella pneumoniae* carbapenemase-producing *Escherichia coli*: emergence of sequence type 131. *Clin. Infect. Dis.* 55, 224–231. doi: 10.1093/cid/cis387

Letunic, I., and Bork, P. (2019). Interactive tree of life (iTOL) v4: recent updates and new developments. *Nucleic Acids Res.* 47, W256–W259. doi: 10.1093/nar/gkz239

Li, X., Fu, Y., Shen, M., Huang, D., Du, X., Hu, Q., et al. (2018). Dissemination of blaNDM-5 gene via an IncX3-type plasmid among non-clonal *Escherichia coli* in China. *Antimicrob. Resist. Infect. Control* 7:59. doi: 10.1186/s13756-018-0349-6

Martínez, T., Vázquez, G. J., Aquino, E. E., Martínez, I., and Robledo, I. E. (2014). ISEcp1-mediated transposition of blaKPC into the chromosome of a clinical isolate of *Acinetobacter baumannii* from puerto rico. *J. Med. Microbiol.* 63(Pt 12), 1644–1648. doi: 10.1099/jmm.0.080721-0

Mathers, A. J., Stoesser, N., Chai, W., Carroll, J., Barry, K., Cherunvanky, A., et al. (2017). Chromosomal integration of the *Klebsiella pneumoniae* Carbapenemase Gene, bla(KPC), in *Klebsiella* species is elusive but not rare. *Antimicrob. Agents Chemother.* 61, e1823–e1816. doi: 10.1128/aac.01823-16

Mavroidi, A., Miriagou, V., Malli, E., Stefos, A., Dalekos, G. N., Tzouvelekis, L. S., et al. (2012). Emergence of *Escherichia coli* sequence type 410 (ST410) with KPC-2 β-lactamase. *Int. J. Antimicrob. Agents* 39, 247–250. doi: 10.1016/j.ijantimicag.2011.11.003

Nicolas-Chanoine, M. H., Bertrand, X., and Madec, J. Y. (2014). *Escherichia coli* ST131, an intriguing clonal group. *Clin. Microbiol. Rev.* 27, 543–574. doi: 10.1128/cmr.00125-13

Nordmann, P., Naas, T., and Poirel, L. (2011). Global spread of carbapenemase-producing *Enterobacteriaceae*. *Emerg. Infect. Dis.* 17, 1791–1798. doi: 10.3201/eid1710.110655

Page, A. J., Cummins, C. A., Hunt, M., Wong, V. K., Reuter, S., Holden, M. T., et al. (2015). Roary: rapid large-scale prokaryote pan genome analysis. *Bioinformatics* 31, 3691–3693. doi: 10.1093/bioinformatics/btv421

Qi, Y., Wei, Z., Ji, S., Du, X., Shen, P., and Yu, Y. (2011). ST11, the dominant clone of KPC-producing *Klebsiella pneumoniae* in China. *J. Antimicrob. Chemother.* 66, 307–312. doi: 10.1093/jac/dkq431

Ripabelli, G., Sammarco, M. L., Scutellà, M., Felice, V., and Tamburro, M. (2020). Carbapenem-resistant KPC- and TEM-producing *Escherichia coli* ST131 isolated from a hospitalized patient with urinary tract infection: first isolation in molise region, Central Italy, July 2018. *Microb. Drug Resist.* 26, 38–45. doi: 10.1089/mdr.2019.0085

Rogers, B. A., Sidjabat, H. E., and Paterson, D. L. (2011). *Escherichia coli* O25b-ST131: a pandemic, multiresistant, community-associated strain. *J. Antimicrob. Chemother.* 66, 1–14. doi: 10.1093/jac/dkq415

Seemann, T. (2014). Prokka: rapid prokaryotic genome annotation. *Bioinformatics* 30, 2068–2069. doi: 10.1093/bioinformatics/btu153

Shen, P., Yi, M., Fu, Y., Ruan, Z., Du, X., Yu, Y., et al. (2017). Detection of an *Escherichia coli* sequence type 167 strain with two tandem copies of blaNDM-1 in the chromosome. *J. Clin. Microbiol.* 55, 199–205. doi: 10.1128/jcm.01581-16

Stamatakis, A. (2014). RAxML version 8: a tool for phylogenetic analysis and post-analysis of large phylogenies. *Bioinformatics* 30, 1312–1313. doi: 10.1093/bioinformatics/btu033

Stoesser, N., Sheppard, A. E., Pankhurst, L., De Maio, N., Moore, C. E., Sebra, R., et al. (2016). Evolutionary history of the global emergence of the *Escherichia coli* epidemic clone ST131. *mBio* 7:e02162. doi: 10.1128/mBio.02162-15

Sullivan, M. J., Petty, N. K., and Beatson, S. A. (2011). Easyfig: a genome comparison visualizer. *Bioinformatics* 27, 1009–1010. doi: 10.1093/bioinformatics/btr039

Tian, X., Zheng, X., Sun, Y., Fang, R., Zhang, S., Zhang, X., et al. (2020). Molecular mechanisms and epidemiology of carbapenem-resistant *Escherichia coli* isolated from Chinese patients during 2002-2017. *Infect. Drug. Resist.* 13, 501–512. doi: 10.2147/idr.s232010

Villegas, M. V., Lolans, K., Correa, A., Kattan, J. N., Lopez, J. A., and Quinn, J. P. (2007). First identification of *Pseudomonas aeruginosa*

isolates producing a KPC-type carbapenem-hydrolyzing beta-lactamase. *Antimicrob. Agents Chemother.* 51, 1553–1555. doi: 10.1128/aac.01405-06

Wang, Q., Zhang, Y., Yao, X., Xian, H., Liu, Y., Li, H., et al. (2016). Risk factors and clinical outcomes for carbapenem-resistant *Enterobacteriaceae* nosocomial infections. *Eur. J. Clin. Microbiol. Infect. Dis.* 35, 1679–1689. doi: 10.1007/s10096-016-2710-0

Zhao, D., Zhou, Z., Hua, X., Zhang, H., Quan, J., Li, X., et al. (2018). Coexistence of mcr-1, bla(KPC-2) and two copies of fosA3 in a clinical *Escherichia coli* strain isolated from urine. *Infect. Genet. Evol.* 60, 77–79. doi: 10.1016/j.meegid.2018.02.025

Conflict of Interest: The authors declare that the research was conducted in the absence of any commercial or financial relationships that could be construed as a potential conflict of interest.

frontiers in Microbiology

METHODS
published: 20 November 2020
doi: 10.3389/fmicb.2020.585417

AI-Blue-Carba: A Rapid and Improved Carbapenemase Producer Detection Assay Using Blue-Carba With Deep Learning

Ling Jia[1,2], Lu Han[1,2], He-Xin Cai[3], Ze-Hua Cui[1,2], Run-Shi Yang[1,2], Rong-Min Zhang[1,2], Shuan-Cheng Bai[1,2], Xu-Wei Liu[1,2], Ran Wei[1,2], Liang Chen[4], Xiao-Ping Liao[1,2], Ya-Hong Liu[1,2,5], Xi-Ming Li[3] and Jian Sun[1,2]**

[1] National Risk Assessment Laboratory for Antimicrobial Resistance of Animal Original Bacteria, South China Agricultural University, Guangzhou, China, [2] Guangdong Provincial Key Laboratory of Veterinary Pharmaceutics Development and Safety Evaluation, South China Agricultural University, Guangzhou, China, [3] College of Mathematics and Informatics, South China Agricultural University, Guangzhou, China, [4] Public Health Research Institute Tuberculosis Center, New Jersey Medical School, Rutgers University, Newark, NJ, United States, [5] Jiangsu Co-Innovation Center for Prevention and Control of Important Animal Infectious Diseases and Zoonoses, Yangzhou, China

OPEN ACCESS

Edited by:
Shaolin Wang,
China Agricultural University, China

Reviewed by:
Daniel Manoil,
Karolinska Institutet, Sweden
Hua Zhou,
Zhejiang University, China

***Correspondence:**
Xi-Ming Li
liximing@scau.edu.cn
Jian Sun
jiansun@scau.edu.cn

Specialty section:
This article was submitted to Antimicrobials, Resistance and Chemotherapy, a section of the journal Frontiers in Microbiology

Received: 20 July 2020
Accepted: 26 October 2020
Published: 20 November 2020

Citation:
Jia L, Han L, Cai H-X, Cui Z-H, Yang R-S, Zhang R-M, Bai S-C, Liu X-W, Wei R, Chen L, Liao X-P, Liu Y-H, Li X-M and Sun J (2020) AI-Blue-Carba: A Rapid and Improved Carbapenemase Producer Detection Assay Using Blue-Carba With Deep Learning. Front. Microbiol. 11:585417. doi: 10.3389/fmicb.2020.585417

A rapid and accurate detection of carbapenemase-producing Gram-negative bacteria (CPGNB) has an immediate demand in the clinic. Here, we developed and validated a method for rapid detection of CPGNB using Blue-Carba combined with deep learning (designated as AI-Blue-Carba). The optimum bacterial suspension concentration and detection wavelength were determined using a Multimode Plate Reader and integrated with deep learning modeling. We examined 160 carbapenemase-producing and non-carbapenemase-producing bacteria using the Blue-Carba test and a series of time and optical density values were obtained to build and validate the machine models. Subsequently, a simplified model was re-evaluated by descending the dataset from 13 time points to 2 time points. The best suitable bacterial concentration was determined to be 1.5 optical density (OD) and the optimum detection wavelength for AI-Blue-Carba was set as 615 nm. Among the 2 models (LRM and LSTM), the LSTM model generated the higher ROC-AUC value. Moreover, the simplified LSTM model trained by short time points (0–15 min) did not impair the accuracy of LSTM model. Compared with the traditional Blue-Carba, the AI-Blue-Carba method has a sensitivity of 95.3% and a specificity of 95.7% at 15 min, which is a rapid and accurate method to detect CPGNB.

Keywords: carbapenemase-producing gram-negative bacteria, rapid detection, Blue-Carba, deep learning, OD value

INTRODUCTION

Antimicrobial resistance (AMR) poses a serious global threat to human, animal, and environment health, as multidrug resistant bacteria continue to emerge and spread worldwide. Carbapenems are one of the last-resort antibiotics to treat infections caused by multidrug-resistant Gram-negative pathogens. Carbapenem resistance in Gram-negative bacteria is

primarily due to the production of various carbapenemases, which leaves the clinicians with limited therapeutic options. Carbapenemase-producers showed broad spectrum enzyme activity for various β-lactam substrates, and were associated with resistance to other antibiotic classes, and demonstrated rapid transmission in healthcare facilities, animals and the environments (Codjoe and Donkor, 2017). Notably, carbapenemase genes are frequently located on mobile genetic elements and plasmids, therefore facilitating the horizontal of resistance to other bacteria (Dortet et al., 2014; Nordmann and Poirel, 2014). It is of paramount importance to develop reliable methods for rapid detection and characterization of carbapenemase-producers.

Different phenotypic and molecular-based methods have been used to identify these carbapenemase producers. For known mechanisms, molecular methods of gene detection are usually fast and accurate. However, molecular detection of carbapenemase genes can be costly and may require substantial expertise, and more importantly they fail to detect unknown or novel carbapenemase genes (Stuart et al., 2012). A solution to this problem is the detection of carbapenem enzymatic degradation, using Matrix Assisted Laser Desorption Ionization-Time of Flight Mass Spectrometry (MALDI-TOF MS) (Yu et al., 2018); or by chromogenic agar or UV spectrophotometry (e.g., Carba NP and Blue Carba) (Bernabeu et al., 2012); or the rapid Carbapenem Inactivation Method (Muntean et al., 2018).

In 2012, Nordmann et al. developed the Carba NP test which is based on visual monitoring of medium acidification of a mixture containing bacterial cells, a carbapenem and the pH indicator phenol red (Dortet et al., 2012). However, some subtle color variations could be hard to differentiate by visual interpretation. This method was then adapted to microtiter plates and spectrophotometric measurement of optical density and interpreted using a pre-programmed Excel spreadsheet (Surre et al., 2018). However, the assay was not comprehensive enough and the data analysis of this assay is still not straightforward.

In this study, a deep learning approach was used to predict carbapenemase production, taking into consideration the similarity in the OD value distributions at different time points, instead of only the best hit. Deep learning has been proven to be the most powerful machine learning approach to date for many applications, including image processing (LeCun et al., 2015), biomedical signaling (Tabar and Halici, 2017), speech recognition (Hinton et al., 2012), and genomic related analysis, such as the predicting antibiotic resistance genes from metagenomic data (Pan and Shen, 2017; Li et al., 2018). Particularly in the case of predicting new genetic markers, the deep learning model surpasses all known binding site for prediction approaches (Drouin et al., 2016).

To the best our knowledge, this is the first time that contact the carbapenemase detection method with Deep learning. Here we describe the AI-Blue-Carba test, an improved variant of Blue-Carba to determine carbapenemase producers using a uniform standard.

MATERIALS AND METHODS

Sample Collection and Bacterial Strains

In this study, we mainly collected fecal samples from animals (anal swabs and feces). These fecal samples were randomly collected from pigs, chickens, ducks, and goose, if possible, the soil, dust, sewage and vegetable samples were also collected. These samples were screened from 14 animal farms (pig farms, $n = 5$; chicken houses, $n = 5$; duck farms, $n = 3$; goose farms, $n = 1$) in 6 provinces (Guangxi, Guangdong, Heilongjiang, Jiangsu, Jiangxi, and Zhejiang provinces) in China. In total, 498 strains were collected from June 2016 to Nov 2017 and subjected to selection onto MacConkey (MAC) agars containing meropenem (1 mg l-1). In order to enrich the diversity of carbapenem-resistant strains and genes, we also collected some strains from human and flower sources. Sixty clinical isolates were collected from the hospitals of Guangdong and Shandong provinces. In addition, 273 strains were isolated from flowers including carnations, roses and lilies which were collected from Mar 2018 to Apr 2018 in Guangzhou Flower Market and selected on MAC plates without any antibiotics.

We utilized 130 among the 831 collected strains from different sources above, including 49 isolates from animal anal swabs and feces samples which were characterized, 60 clinical isolates collected from two hospitals in Guangdong and Shandong provinces, and then 21 isolates from flowers. Carbapenemase genes were characterized by PCR and Sanger sequencing (Rahman et al., 2013). Strains from different Enterobacteriaceae species (*E. coli, Klebsiella pneumoniae*, *Citrobacter freundii, Enterobacter cloacae*, etc.) as well as *Pseudomonas spp.* were included. We identified 107 carbapenem-resistant strains able to produce at least one carbapenem-hydrolyzing β-lactamase, whereas the remaining 23 carbapenem-susceptible strains were carbapenemase negative (**Table 1**). The MICs for ertapenem, meropenem, and imipenem were determined by agar dilution and interpreted according to the Clinical and Laboratory Standards Institute guidelines (CLSI, 2018).

Blue-Carba Test

The Blue-Carba test was performed and interpreted as previously described (Pires et al., 2013). Briefly, 5 μL loopfuls of bacteria cultured on Mueller-Hinton agar (HuanKai, Guangzhou, China) were suspended in 0.04% bromothymol blue (Macklin, Shanghai, China) solution containing (test) or lacking (control) 3 mg/mL imipenem (MedChemExpress, New Jersey, United States) and 0.1 mM ZnSO4 (Damao, Tianjin, China). Color changes were registered after incubation at 37°C for 2 h. The result was considered positive when the solution containing imipenem became green or yellow and differed from the negative control. The result was negative if the solution lacking antibiotic presented the same or a stronger color change as the solution containing imipenem. A previously characterized NDM-5 producer (CQ02-121) was used as positive control (Sun et al., 2016) and a test tube containing only bacterial inoculum (*E. coli* ATCC 25922) and Blue-Carba solution was used as negative control for each isolate tested.

TABLE 1 | Results of carbapenemase and non-carbapenemase producers' PCR and MIC.

Species	MIC(μg/ml)			No. of isolates with a positive test/no. of isolates tested for 2 h		
	Carbapenemase content	MEM	IPM	ERT	AI-Blue-Carba	Blue-Carba
Carbapenemase producers *E. coli* (47)	NDM-5(43)	1–64	1- >64	>64	41/43	41/43
	NDM-1(4)	4–8	8–16	16–64	4/4	4/4
***Pseudomonas putida*(7)**	VIM-2(6)	≥64	8-≥64	>64	6/6	6/6
	IMP-4(1)	>64	8	>64	1/1	1/1
***Klebsiella pneumoniae* (44)**	NDM-1(15)	2–32	2–32	8- >64	13/15	13/15
	NDM-5(4)	2–64	4- >64	16–64	4/4	4/4
	NDM-1 + IMP-4(2)	32	8- ≥64	>64	1/1	1/1
	KPC-2(23)	32	>64	>64	23/23	23/23
***Citrobacter freundii* (1)**	NDM-1(1)	16	8	64	1/1	1/1
***Enterobacter cloacae* (5)**	IMP-4(1)	8	16	64	1/1	1/1
	NDM-1(3)	16	16–32	32- >64	3/3	3/3
	VIM-1(1)	1	2	2	1/1	1/1
***Providencia rettgeri* (4)**	NDM-1(4)	2- ≥64	4	8	4/4	4/4
***Enterobacter mucus* (2)**	NDM-1(2)	32	32	>64	2/2	2/2
***Pseudomonas aeruginosa* (1)**	NDM-5(1)	64	>64	>64	1/1	1/1
Non-carbapenemase producers						
E. coli (10)	CTX-M	<0.0625	<0.0625–4	<0.0625–2	0/10	0/10
Citrobacter freundii (8)	CTX-M	<0.0625	<0.0625–4	<0.0625–2	0/8	0/8
Enterobacter cloacae (4)	CTX-M	<0.0625	<0.0625–4	<0.0625–2	0/4	0/4
Providencia rettgeri (1)	CTX-M	<0.0625	<0.0625–4	<0.0625–2	0/1	0/1

MEM, meropenem; IPM, imipenem; ERT, ertapenem.

Experiment Condition of AI-Blue-Carba

In order to overcome the limitation of lower the sensitivity with visual interpretation, we used the OD values to indicate the color's change of the Blue-Carba result. To obtain a stable OD value, the optimum wavelength for detection of CPGNB was determined using a wavelength scan of test solutions generated using known carbapenemase producers up to 2 h in a Multimode Plate Reader (PerkinElmer, Hamburg, Germany) to obtain the absorbance maxima corresponding to yellow and blue (negative control).

Bacteria were diluted in 500 μL phosphate buffered saline (PBS, pH 7.4) and distilled water, respectively, the OD600 nm was adjusted to 1.0, 1.5, and 2.0 and the 100 μL of the bacteria suspension was used for testing. The wells were scanned and the OD was recorded every 5 min for 2 h at 37°C in the plate reader.

Deep Learning

The problem of distinguishing carbapenemase and non-carbapenemase producers based on the OD values and the results of the Blue-Carba test can be formalized as a machine learning or supervised learning question. It is assumed that a data sample S that contains m machine learning examples were given at the beginning. These examples are pairs (x, y), where x represents OD values detected over time and y is a label that corresponds to one of the two possible results (positive or negative). In addition, we assume that $x \in \{a_1, a_2 \ldots a_{13}\}$ which corresponds to the set of all 13 OD values and that $\mathrm{y} \in \{0, 1\}$. Label $\mathrm{y} = 1$ is assigned to the carbapenemase producers group and $\mathrm{y} = 0$ is assigned to the non-carbapenemase producers group. We assumed the examples in S are drawn independently from an unknown and fixed data generating distribution D, resulting in the equation of $\mathrm{S} \stackrel{\mathrm{def}}{=} \left\{\left(x_1, y_1\right), \ldots \left(x_m, y_m\right)\right\} \sim D^m$.

Usually, learning algorithms are designed to learn from a vector representation of the data. In order to learn from detected OD values, a function $\emptyset : \{x_1, x_2, \ldots x_m\}^* \rightarrow R^d$ is defined, which takes time as input and maps it to some d dimensional vector space. Then a learning algorithm can be applied to the set $S' \stackrel{\mathrm{def}}{=} \left\{\emptyset\left(x_1\right), y_1, \ldots \emptyset\left(x_m, y_m\right)\right\}$ to obtain a model h : $R^d \rightarrow \{0, 1\}$. The model is a function which maps the feature representation of OD values over time to the associated results of the carbapenemase producers. Our objective is to achieve a model h that has a good generalization performance, i.e., that minimizes the probability, $\mathrm{R}\left(h\right)$, of making a prediction error for any example drawn according to the distribution D, where

$$\mathrm{R}\left(h\right) \stackrel{\mathrm{def}}{=} Pr^R_{(x,y)\sim D}\left[h\left(\emptyset\left(x\right)\right) \neq y\right] \quad (1)$$

Construct Models

The LSTM (Long Short-Time Memory) cells store and access information over long periods of time using multiplicative gates (Hochreiter and Schmidhuber, 1997). It retains useful long-term information through the threshold mechanism and removes useless short-term information to realize the mining of timing information. In this work, the rules were individual units that detect the carbapenemase-producer using OD values over time. These rules are Boolean-valued, i.e., the output is either positive or negative. The models learned by the LSTM are

logical combinations of such rules, which can be conjunctions (logical-AND) or disjunctions (logical-OR). To predict the results of detection of carbapenemase producers using OD values over time, each rule in the model was evaluated and the results were aggregated to obtain the prediction.

Real-time prediction of data traffic requires continuous data input and learning. The dataset was therefore split into a training set (80% of the OD values) to construct the LSTM model that can output a y value randomly (0 or 1 which represent the positive or negative results of carbapenemase producer) if input a group of OD values. In addition, a separate testing set (20% of the data) were used with the results of Blue-Carba to validate and evaluate LSTM's prediction accuracy. In this study, we used a 10-fold cross validation to test the prediction model and select the best hyperparameter (Webb et al., 2019).

In order to display data characteristics to more accurately predict the carbapenemase-producing strains, we compared the LSTM with LRM (Linear Regression model). The LRM is a linear approach to find the relationship between a scalar response and one or more explanatory variables (Kumaresan and Riyazuddin, 2007). In this paper, LRM modeled the relation between OD values and Blue-Carba test.

Evaluation Metrics

We evaluated the performance of the two models using the confusion matrix assessment method. The prediction quality was evaluated by the following evaluation metrics: The ROC curve describes the classifier's True Positive Rate (TPR, the ratio of the number of positive samples correctly classified by the classifier to the total number of positive samples) and False Positive Rate (FPR, the number of negative samples that the classifier misclassified accounts for the total negative samples) Ratio of the number). Recall [Equation 2] shows the number of correct positive results divided by the number of all relevant samples that were identified as positive. Precision [Equation 3] expresses the number of correct positive results divided by the number of positive results predicted by the classifier. F1 Score [Equation 4] indicates the Harmonic Mean between Precision and Recall that tells you how precise your models is. The possible outcomes of a classification model include: true positive, TP; false positive, FP; true negative, TN; false negative, FN.

$$\text{Recall} = \frac{\text{TP}}{\text{TP} + \text{FN}} \tag{2}$$

$$\text{Precision} = \frac{\text{TP}}{\text{TP} + \text{FP}} \tag{3}$$

$$\text{F1} - \text{score} = \frac{2\text{TP}}{2\text{TP} + \text{FP} + \text{FN}} \tag{4}$$

Model Simplification

To achieve the purpose for rapid detection of a carbapenemase producer, we choose the OD values at 12 time points groups: 2 time points,3 time points, and so on 13 time points (**Figure 1B**) to optimize the best model from the above LSTM. We then evaluated the performance of the 12 models on the basis of the 12 sets of time points (OD value data set) using the above evaluation metrics to get the optimal detection time.

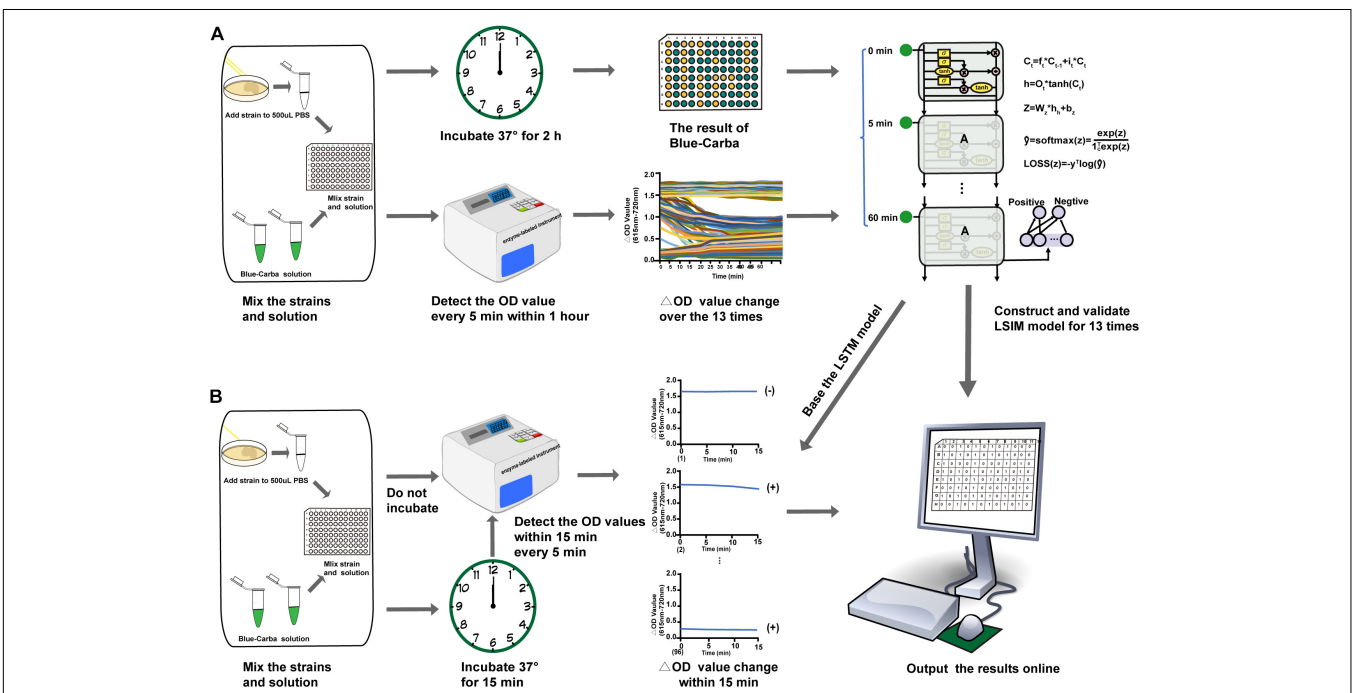

FIGURE 1 | Rapid detection of carbapenemase producers by AI-Blue-Carba. **(A)**. Process to construct and validate the AI model; **(B)** Process to optimize the AI-Blue-Carba.

RESULTS

Optimum Conditions for AI-Blue-Carba Test

The scanning results of positive and negative carbapenemase producers indicated a maximum absorption peak at 615 nm and this was chosen as the detection wavelength in following experiments (**Supplementary Figure S1A**). At the same time, we chose 720 nm as the detection wavelength of negative carbapenemase producers due to its stable absorption after 700 nm (**Supplementary Figure S1B**) to stabilize the OD values. Finally, the experimental data was the difference in OD (ΔOD) values between 615 and 720 nm.

We next examined differing bacterial concentrations and diluents at these wavelengths and found that the ΔOD values varied. The general trend in ΔOD values over time showed a more rapid decrease using the PBS diluent vs. ultrapure water at different bacterial concentrations (**Supplementary Figures S2A–F**). The weak carbapenemase producers showed a more rapid decrease in OD values as the bacterial concentration increased. However, when the bacterial concentration was set at 2.0 OD (at 600 nm), the strong carbapenemase producers generated with an ascending pattern over time (**Supplementary Figures S2C,F**). As such, we choose 1.5 OD (at 600 nm) for the bacterial concentration in PBS as the most appropriate testing condition for the AI-Blue-Carba test, due to more reliable stable OD values were acquired for both strong and weak carbapenemase producers.

We measured the OD values every 5 min up to 1 h (13 time points) using our 160 isolates (**Table 1**) to obtain the data characteristics. In brief, the trend in the ΔOD values of non-carbapenemase producers over time demonstrated a smooth linear pattern and ranged from 1.5 OD to 2.0 OD. The strong carbapenemase-producers generated a trend of ΔOD values over time that were also smooth lines, but the range was 0.2 OD – 0.4 OD while for weak carbapenemase producers, the trend of ΔOD values decreased gradually over time (**Figure 1A**).

TABLE 2 | Prediction results for the majority prediction rule of four models.

Model	ACC	F1	REC	PRE
LRM	0. 93	0.93	0.62	0.94
LSTM	0.98	0.98	0.98	0.98

ACC, Accuracy; PRE, Precision; REC, Recall; F1, F1-score.

Construction and Evaluation of Deep Learning Model

In the following, we discuss the results of a 10-fold cross-validation study on the entire data set of 2 models. Across all cross-validation folds, predictor performance generalizes well to independent data. The degree of certainty of a read prediction can be measured by the prediction probability (see Methods). As **Table 2** shows, the REC of LSTM is bigger (0.98) than LRM (0.62), other parameter values (ACC, REC, F1) of LSTM still higher than LRM. The model receiver operating characteristic (ROC) curves with the performances of LRM and LSTM (**Figure 2A**). The ROC-AUC of LSTM (0.99) was also better than LRM (0.94). Considering these factors, the LSTM model is the optimal model to detect the carbarpenemase producers.

The Simplified Model

In order to determine the earliest time required to accurately detect carbapenemase producers, we used OD values with lesser time points and constructed and evaluated the models in a manner similar to that described above. To find a suitable model for specific application, we get the corresponding ACC, PRE, REC, and F1 values, sensitivity, specificity to adjust the threshold

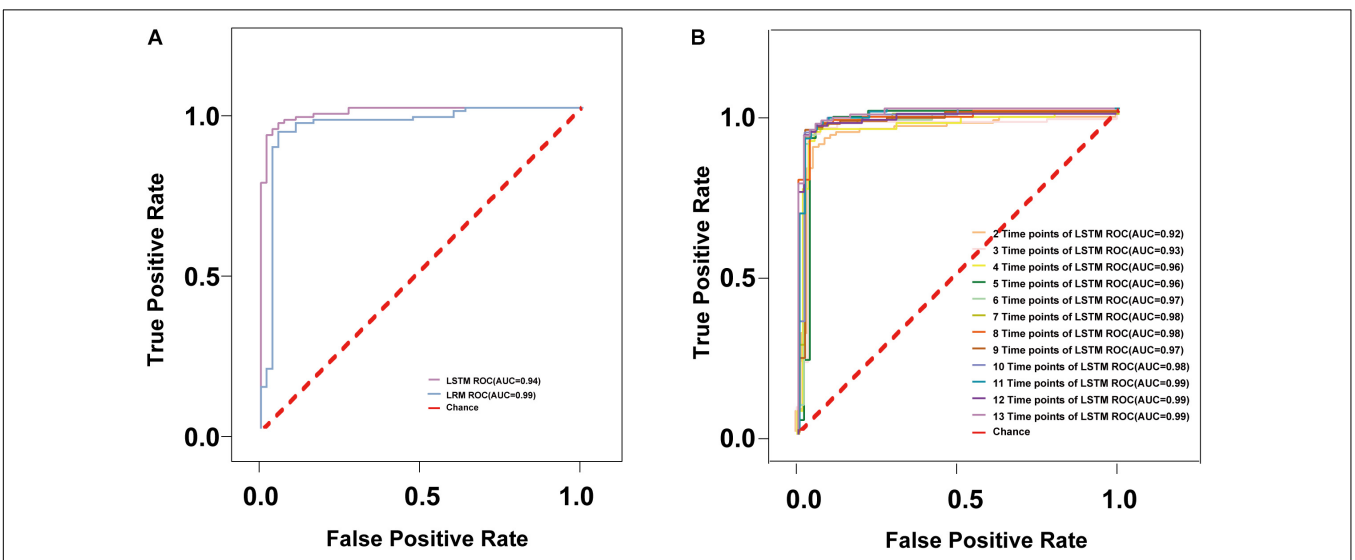

FIGURE 2 | The ROC curves of different models. **(A)** The ROC curves are shown for the models trained with the multispecies data sets of Linear Regression model and LSTM model; **(B)** The ROC curves of different time points of LSTM.

of the model, the ACC, PRE, REC, and F1 values of 12 optimized LSTM models were all >96% after 20 min in **Table 3**. In addition, the ROC-AUC values of the 12 time points group was >96% after 15 min (**Figure 2B**). Additionally, the 95.3% specificity and 95.7% sensitivity of AI-Blue-Carba were higher than Blue-Carba at 0–15 min. Consequently, we used the 0–15 min internal for rapid detecting the carbapenemase producers.

We examined some weak (*Klebsiella pneumonia* E-3F3 and *Citrobacter freundii* 2N3001), strong (*E. coli* FS89) and non-carbapenemase producers (*E. coli* ATCC 25922) using the Blue-Carba test. Isolates FS89 and ATCC 25922 could be detected in 0 min, while E-3F3 and 2N3001 could be accurately judged after 30 min but the confirmation of the final results took 2 h by Blue-Carba. The ΔOD values for FS89 and 25922 from 0–15 min, 0–30 min and 0–60 min were consistent with the trend of the 13-time points taken over 1 h. This indicated that the strong carbapenemase and the non-carbapenemase producers can be rapidly detected within 15 min. For E-3F3 and 2N3001, the ΔOD values for the 13-time points was relatively slow for the 0–15 min, 0–30 min, and 0–60 min intervals (**Figure 3A**). The colors change of Blue-Carba (**Figure 3B**) and the results of AI-Blue-Carba (**Figure 3C**) were consistent with the PCR results.

TABLE 3 | Prediction results for the different time groups by LSTM model.

Time Group	ACC	F1	REC	PRE
0–5 min	0.87	0.87	0.88	0.89
0–10 min	0.90	0.92	0.92	0.92
0–15 min	0.93	0.93	0.94	0.94
0–20 min	0.96	0.96	0.96	0.96
0–25 min	0.97	0.97	0.97	0.97
0–30 min	0.98	0.98	0.98	0.98
0–35 min	0.97	0.97	0.97	0.97
0–40 min	0.97	0.97	0.97	0.97
0–45 min	0.97	0.97	0.97	0.97
0–50 min	0.97	0.97	0.96	0.97
0–55 min	0.97	0.97	0.97	0.97
0–60 min	0.98	0.98	0.98	0.98

DISCUSSION

The rapid increase of carbapenem resistance in Gram-negative bacilli is of great concern worldwide (Zhang et al., 2018). Public health surveillance for a disease is traditionally viewed as the first step in disease prevention and data obtained from surveillance help to enforce public health action. Therefore, rapid and user-friendly assays are crucial.

To rapidly and efficiently detect carbapenemase producers, the Carba NP test was modified according to CLSI guidelines by measuring the *in vitro* hydrolysis of imipenem to produce a color change within 2 h (Dortet et al., 2012). The RAPID ECCARBA NP test could be useful for screening carbapenemase producers from colonized patients (Poirel and Nordmann, 2015). The commercially available β CARBA test is based on the change of color of an undisclosed chromogenic substrate in the presence of carbapenem-hydrolyzing activity. The test is simple to perform and interpret by non-specialized staff members (Mancini et al., 2017). In addition, the CarbAcineto NP test, which is rapid and reproducible, detects all types of carbapenemases including *Acinetobacter spp.* with a sensitivity of 94.7% and a specificity of 100%. Its use will facilitate its recognition and prevent its spread.

All these modified Carba NP tests have an obvious shortcoming that the color intensity is somewhat low, so we choose the LSTM model to correct this deficiency. Carbapenemase detection by spectrophotometric assays is a more accurate approach for the detection of carbapenemases and has

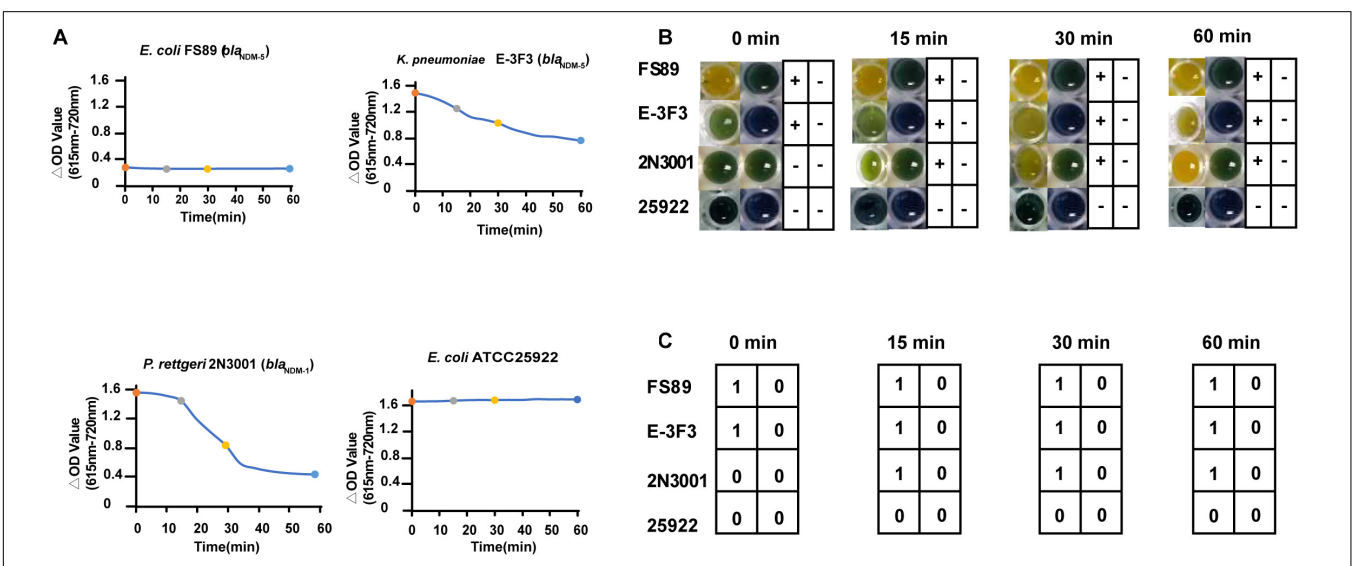

FIGURE 3 | Comparison of the result of AI-Blue-Carba and Blue-Carba. **(A)** shows the ΔOD values' change of different time points (within in 0 min, 0–15 min, 0–30 min, 0–60 min); **(B)** shows the results of carbapenamase producer by Blue-Carba; **(C)** shows the results of carbapenamase producer by AI -Blue-Carba within.

excellent sensitivity and specificity for the Enterobacteriaceae. The results are usually comparable between different labs and were suggested to be implemented in national reference laboratories (Nordmann et al., 2012). Moreover, all the above methods can use these tools (OD values and the LSTM model) to improve their sensitivity and specificity.

A pioneering study illustrated the huge potential of using Big Data for epidemiology in which the epidemics can be detected early by tracking online queries on disease symptoms using social media such as Google Search and Twitter (Deiner et al., 2016). We introduce a "deep learning" approach to improve the objectivity and efficiency of detecting carbapenemase producers. The deep learning model can be applied to new data to make decisions after training, and decision making can involve detection, discrimination, and classification. Therefore, we trained the LRM and LSTM models using OD values generated by the Blue Carba test and compared the evaluation metrics of the four models. The results presented below could not be notably improved by further parameter tuning or feature selection efforts. An auxiliary assessment further shows that our classifiers are very robust. We chose LSTM to construct the website because it was optimized by the evaluation metrics independent of the values of the F1-scores. As we expected, its advantages are most pronounced for problems requiring the use of long-range contextual information. Consequently, LSTM has also been applied to various real-world problems, such as protein secondary structure prediction, music generation, reinforcement learning, speech recognition, and handwriting recognition. Furthermore, similar to any software systems, updating this classification system or model can be conducted at regular intervals whenever new dataset/information/evidence is available.

To achieve the aim of the rapid detection of the carbapenemase producers, we simplified the LSTM model by reducing detection times and chose 15 min as test interval. The deep learning analysis platform illustrates that ΔOD values change over time intuitively and then judges the strength of carbapenemase production by the test strains. In addition, you only need to input the OD values to the model and the result is the number of carbapenemase producers. The data can be output directly to reduce the time for manual entry and analysis of data. Lastly, the model gives a standard procedure for reading experimental results of carbapenemase producers and climates reading errors. In the next step, we will create a website platform that co-networking with hospitals and research laboratories, the results of carbapenemase producers in different areas can be compared to effectively monitor the prevalence of carbapenemases in the region. By providing actionable data directly to governments, a website that could analyze those areas containing CPGNB could forewarn healthcare facilities to take the appropriate infection control measures.

We evaluated a deep learning method (AI-Blue-Carba) which allows detection of CPGNB in less than 15 min. This test can be used as the first step in detecting the carbapenemase activity of candidate isolates. In addition, it is also useful for checking carbapenemase activity as part of the infection control process for outbreaks caused by carbapenemase producers. AI-Blue-Carba is a robust assay which user-friendly (no need for trained staff), high in performance (sensitive and specific), and low in cost.

DATA AVAILABILITY STATEMENT

The original contributions presented in the study are included in the article/**Supplementary Material**, further inquiries can be directed to the corresponding authors.

AUTHOR CONTRIBUTIONS

JS and X-ML conceived of the study. LJ, LH, and S-CB performed the experiments. LJ and H-XC constructed models. LJ, Z-HC, R-SY, and R-MZ analyzed the data. LJ, X-WL, and RW made the figures. LJ wrote the manuscript. JS, LC, X-ML, and X-PL edited and revised the manuscript. Y-HL coordinated the whole project. All authors have read and approved the final manuscript.

FUNDING

This work was jointly supported by the National Key Research and Development Program of China (2016YFD0501300), the National Natural Science Foundation of China (31972735), the Program for Innovative Research Team in the University of Ministry of Education of China (IRT_17R39), and the 111 Project (D20008).

SUPPLEMENTARY MATERIAL

The Supplementary Material for this article can be found online at: https://www.frontiersin.org/articles/10.3389/fmicb.2020.585417/full#supplementary-material

REFERENCES

Bernabeu, S., Poirel, L., and Nordmann, P. (2012). Spectrophotometry-based detection of carbapenemase producers among *Enterobacteriaceae*. *Diagn. Microbiol. Infect. Dis.* 74, 88–90. doi: 10.1016/j.diagmicrobio.2012.05.021

CLSI (2018). *Performance Standards for Antimicrobial Susceptibility Testing*, 28th Edn. ClSI Supplement. M100. Wayne, PA: Clinical and Laboratory Standards Institute. .

Codjoe, F. S., and Donkor, E. S. (2017). Carbapenem resistance: a review. *Med Sci* 6:1. doi: 10.3390/medsci6010001

Deiner, M. S., Lietman, T. M., Mcleod, S. D., Chodosh, J., and Porco, T. C. (2016). Surveillance tools emerging from search engines and social media data for determining eye disease patterns. *JAMA Ophthalmol.* 134, 1024–1030. doi: 10.1001/jamaophthalmol.2016.2267

Dortet, L., Poirel, L., and Nordmann, P. (2012). Rapid identification of carbapenemase types in *Enterobacteriaceae* and *Pseudomonas* spp. by using a biochemical test. *Antimicrob. Agents Chemother.* 56, 6437–6440. doi: 10.1128/aac.01395-12

Dortet, L., Poirel, L., and Nordmann, P. (2014). Worldwide dissemination of the NDM-type carbapenemases in Gram-negative bacteria. *Biomed. Res. Int.* 2014:249856.

Drouin, A., Giguere, S., Deraspe, M., Marchand, M., Tyers, M., Loo, V. G., et al. (2016). Predictive computational phenotyping and biomarker discovery using reference-free genome comparisons. *BMC Genomics* 17:754. doi: 10.1186/s12864-016-2889-6

Hinton, G., Deng, L., Yu, D., Dahl, G. E., Mohamed, A. R., Jaitly, N., et al. (2012). Deep neural networks for acoustic modeling in speech recognition. *IEEE Signal Process. Mag.* 29, 82–97.

Hochreiter, S., and Schmidhuber, J. (1997). Long short-term memory. *Neural Comput.* 9, 1735–1780.

Kumaresan, M., and Riyazuddin, P. (2007). Factor analysis and linear regression model (LRM) of metal speciation and physico-chemical characters of groundwater samples. *Environ. Monit. Assess.* 138, 65–79. doi: 10.1007/s10661-007-9761-8

LeCun, Y., Bengio, Y., and Hinton, G. (2015). Deep learning. *Nature* 521, 436–444.

Li, L. G., Yin, X., and Zhang, T. (2018). Tracking antibiotic resistance gene pollution from different sources using machine-learning classification. *Microbiome* 6:93.

Mancini, S., Kieffer, N., Poirel, L., and Nordmann, P. (2017). Evaluation of the RAPIDEC(R) CARBA NP and beta-CARBA(R) tests for rapid detection of Carbapenemase-producing *Enterobacteriaceae*. *Diagn. Microbiol. Infect. Dis.* 88, 293–297. doi: 10.1016/j.diagmicrobio.2017.05.006

Muntean, M. M., Muntean, A. A., Gauthier, L., Creton, E., Cotellon, G., Popa, M. I., et al. (2018). Evaluation of the rapid carbapenem inactivation method (rCIM): a phenotypic screening test for carbapenemase-producing *Enterobacteriaceae*. *J. Antimicrob. Chemother.* 73, 900–908. doi: 10.1093/jac/dkx519

Nordmann, P., Gniadkowski, M., Giske, C. G., Poirel, L., Woodford, N., Miriagou, V., et al. (2012). Identification and screening of carbapenemase-producing *Enterobacteriaceae*. *Clin. Microbiol. Infect.* 18, 432–438. doi: 10.1111/j.1469-0691.2012.03815.x

Nordmann, P., and Poirel, L. (2014). The difficult-to-control spread of carbapenemase producers among *Enterobacteriaceae* worldwide. *Clin. Microbiol. Infect.* 20, 821–830. doi: 10.1111/1469-0691.12719

Pan, X., and Shen, H. B. (2017). RNA-protein binding motifs mining with a new hybrid deep learning based cross-domain knowledge integration approach. *BMC Bioinformatics* 18:136. doi: 10.1186/s12859-017-1561-8

Pires, J., Novais, A., and Peixe, L. (2013). Blue-carba, an easy biochemical test for detection of diverse carbapenemase producers directly from bacterial cultures. *J. Clin. Microbiol.* 51, 4281–4283. doi: 10.1128/jcm.01634-13

Poirel, L., and Nordmann, P. (2015). RAPIDEC(R) CARBA NP test for rapid detection of carbapenemase producers. *J. Clin. Microbiol.* 53, 3003–3008. doi: 10.1128/jcm.00977-15

Rahman, M., Uddin, M., Sultana, R., Moue, A., and Setu, M. (2013). Polymerase chain reaction (PCR): a short review. *Anwer Khan Mod. Med. Coll. J.* 4, 30–36.

Stuart, J. C., Voets, G., Scharringa, J., Fluit, A. C., and Leverstein-Van Hall, M. A. (2012). Detection of carbapenemase-producing *Enterobacteriaceae* with a commercial DNA microarray. *J. Med. Microbiol.* 61, 809–812. doi: 10.1099/jmm.0.041673-0

Sun, J., Yang, R. S., Zhang, Q., Feng, Y., Fang, L. X., Xia, J., et al. (2016). Co-transfer of blaNDM-5 and mcr-1 by an IncX3-X4 hybrid plasmid in *Escherichia coli*. *Nat. Microbiol.* 1:16176.

Surre, J., Canard, I., Bourne-Branchu, P., Courbiere, E., Franceschi, C., Chatellier, S., et al. (2018). Enhanced detection of carbapenemase-producing *Enterobacteriaceae* by an optimized phenol red assay. *Diagn. Microbiol. Infect. Dis.* 90, 11–17. doi: 10.1016/j.diagmicrobio.2017.09.005

Tabar, Y. R., and Halici, U. (2017). A novel deep learning approach for classification of EEG motor imagery signals. *J. Neural Eng.* 14:016003. doi: 10.1088/1741-2560/14/1/016003

Webb, C. A., Trivedi, M. H., Cohen, Z. D., Dillon, D. G., Fournier, J. C., Goer, F., et al. (2019). Personalized prediction of antidepressant *v*. placebo response: evidence from the EMBARC study. *Psychol. Med.* 49, 1118–1127. doi: 10.1017/S0033291718001708

Yu, J., Liu, J., Li, Y., Yu, J., Zhu, W., Liu, Y., et al. (2018). Rapid detection of carbapenemase activity of *Enterobacteriaceae* isolated from positive blood cultures by MALDI-TOF MS. *Ann. Clin. Microbiol. Antimicrob.* 17:22.

Zhang, H., Ma, G., Zhu, Y., Zeng, L., Ahmad, A., Wang, C., et al. (2018). Active-Site Conformational Fluctuations Promote the Enzymatic Activity of NDM-1. *Antimicrob. Agents Chemother.* 62:e1579-18.

Conflict of Interest: The authors declare that the research was conducted in the absence of any commercial or financial relationships that could be construed as a potential conflict of interest.

frontiers in Microbiology

ORIGINAL RESEARCH
published: 18 December 2020
doi: 10.3389/fmicb.2020.592146

Serotype Is Associated With High Rate of Colistin Resistance Among Clinical Isolates of *Salmonella*

*Qixia Luo[1], Yuan Wang[1], Hao Fu[1], Xiao Yu[1], Beiwen Zheng[1], Yunbo Chen[1], Björn Berglund[1,2] and Yonghong Xiao[1]**

[1] State Key Laboratory for Diagnosis and Treatment of Infectious Diseases, National Clinical Research Center for Infectious Diseases, The First Affiliated Hospital, College of Medicine, Zhejiang University, Hangzhou, China, [2] Department of Clinical and Experimental Medicine, Linköping University, Linköping, Sweden

To investigate the prevalence, probable mechanisms and serotype correlation of colistin resistance in clinical isolates of *Salmonella* from patients in China, *Salmonella* isolates were collected from fecal and blood samples of patients. In this study, 42.8% (136/318) clinical isolated *Salmonella* were resistant to colistin. MIC distribution for colistin at serotype level among the two most prevalent serotypes originating from humans in China indicated that *Salmonella* Enteritidis (83.9% resistance, 125/149) were significantly less susceptible than *Salmonella* Typhimurium (15.3% resistance, 9/59, $P < 0.01$). *mcr* genes and mutations in PmrAB confer little for rate of colistin resistant *Salmonella* isolated from human patients. Phylogenetic tree based on core-genome single nucleotide polymorphisms (SNPs) was separately by the serotypes and implied a diffused distribution of MICs in the same serotype isolates. Relatvie expression levels of colistin resistant related *pmr* genes were significantly higher in non-*mcr* colistin resistant *S.* Typhimurium than in colistin sensitive *S.* Typhimurium, but no discernable differences between colistin resistant and sensitive *S.* Enteritidis, indicating a different mechanism between colistin resistant *S.* Typhimurium and *S.* Enteritidis. In conclusion, colistin susceptibility and colistin resistant mechanism of clinical isolated *Salmonella* were closely associated with specific serotypes, at least in the two most prevalent serotype Enteritidis and Typhimurium. We suggest clinical microbiology laboratory interpreting *Salmonella* colistin MIC results in the serotype level.

Keywords: *Salmonella* enterica, serotype, colistin susceptibility, clinical isolates, phylogenetic analysis, *pmr* genes

OPEN ACCESS

Edited by:
Shaolin Wang,
China Agricultural University, China

Reviewed by:
Xiaodong Xia,
Northwest A&F University, China
Soraya Chaturongakul,
Mahidol University, Thailand

****Correspondence:***
Yonghong Xiao
xiaoyonghong@zju.edu.cn;
xiao-yonghong@163.com

Specialty section:
This article was submitted to Antimicrobials, Resistance and Chemotherapy, a section of the journal Frontiers in Microbiology

Received: *06 August 2020*
Accepted: *16 November 2020*
Published: *18 December 2020*

Citation:
Luo Q, Wang Y, Fu H, Yu X, Zheng B, Chen Y, Berglund B and Xiao Y (2020) Serotype Is Associated With High Rate of Colistin Resistance Among Clinical Isolates of Salmonella. Front. Microbiol. 11:592146. doi: 10.3389/fmicb.2020.592146

INTRODUCTION

Polymyxins, which include polymyxin B and colistin, are cyclic polypeptide antibiotics that are synthesized by members of the *Paenibacillus* genus (Olaitan et al., 2014). As an old class of antimicrobials, polymyxins have been increasingly revitalized as a last resort drug to combat infections caused by multidrug-resistant (MDR) and carbapenem-resistant bacteria (Poirel et al., 2017). The target of polymyxins is the outer membrane lipopolysaccharide (LPS) of Gram-negative bacteria. Binding of polymyxin to the LPS increases the permeability of the bacterial membrane,

leading to leakage of the cytoplasmic content and ultimately cell death (Olaitan et al., 2014). Resistance to polymyxins can be conferred via mutations in chromosomal genes, such as genes involved in the PmrAB/PhoPQ two-component systems, which promote the expression of LPS modification related genes, such as *pmrC*, *pmrE*, and *pmrHFJKLM* operon (Olaitan et al., 2014; Poirel et al., 2017). Plasmid-mediated colistin resistance genes (*mcr*) have since discovery in 2015 been frequently observed, and their continued widespread dissemination has became a challenge to public health worldwide (Liu et al., 2016; Luo et al., 2020).

Salmonella is one of the most important causes of foodborne diarrheal disease, even bloodstream infection (Ashton et al., 2017; Mohan et al., 2019). Although colistin is not a standardized option for treating infections caused by *Salmonella* in humans, the increasing reports of MDR and carbapenem-resistant *Salmonella*, in particular strains harboring *mcr*-genes isolated from patients (Kock et al., 2018; Lu et al., 2019; Sun et al., 2020), indicate that these pathogens constitute a public health concern which calls more attention to the epidemic characteristics of colistin resistance. Colistin resistance in *Salmonella* spp. can be conferred by mutations in *pmrAB*, or more rarely, by the colistin resistance gene *mcr* (Cui et al., 2017). Interestingly, our daily experimental results indicated the rate of colistin resistance among clinical isolates of *Salmonella* spp. are considerably higher compared to other Enterobacteriaceae, such as *Escherichia coli* and *Klebsiella pneumoniae* (Zhang et al., 2017). The objective of this study was to investigate the prevalence and probable mechanisms of colistin resistance in clinical isolates of *Salmonella* in China.

MATERIALS AND METHODS

Collection of *Salmonella* Isolates and Serotyping

A total of 318 isolates of *Salmonella* spp. were collected from clinical samples nationwide in China from 2014 to 2018, including 218 isolates from bloodstream infection and 100 isolates from fecal samples that were derived from diarrhea patients (**Supplementary Table 1**). *Salmonella* serotyping was conducted according to the White–Kauffmann–Le Minor scheme (9th Edition) by performing a slide agglutination test (State Serum Institute (SSI), Copenhagen, Denmark).

Colistin Susceptibility Testing

Cation-adjusted Mueller-Hinton Broth (Oxoid, Basingstoke, United Kingdom) dilutions were used for colistin MIC determination according to the CLSI-EUCAST joint recommendations. *E. coli* ATCC 25922 was used as a control. The experiment was conducted in duplicate on at least two separate occasions. The higher MIC was accepted for analysis in the duplicative test within one double dilution difference, or a third replicate would be measured (Kulengowski et al., 2019). The results were interpreted according to the EUCAST colistin breakpoint for Enterobacteriaceae (MIC > 2 mg/L, resistant).

Anlaysis of Colistin Resistance Mechanisms

The isolates were screened by using primers targeting *mcr-1* to *mcr-9* from previous studies (Luo et al., 2017; Borowiak et al., 2020). For the colistin-resistant isolates, *pmrA* and *pmrB* were amplified by primers *pmrAB*-F and *pmrAB*-R (**Supplementary Table 2**). The positive PCR products were sequenced with Sanger sequencing for verification. The sequences of *pmrA* and *pmrB* were compared to that of *S.* Typhimurium LT2 (GenBank: GCA_000006945.2), a colistin-susceptible *Salmonella* reference strain.

Whole-Genome Sequencing and Bioinformatic Analysis

Genomic DNA of 136 randomly selected *Salmonella* spp. isolates (including 64 colistin resistant and 72 susceptible isolates) were extracted using Gentra Puregene Yeast/Bact. Kit (Qiaqen, Hilden, Germany). Genomes were sequenced using the Illumina HiSeq 2500-PE150 platform (Illumina, San Diego, CA, United States). Quality-trimmed raw sequence data was assembled by using SPAdes 3.13.0. Annotation was performed by uploading the data to the RAST server (rast.nmpdr.org). All the assembled genomes were deposited in NCBI, the genome accession numbers were listed in **Supplementary Table 1**.

A phylogenetic tree based on SNPs in the core-genome was constructed via kSNP version 3.0 (Gardner et al., 2015). iTOL (V4) was used for the display, manipulation and annotation of phylogenetic trees (Letunic and Bork, 2019). Multi-sequence typing (MLST) were identified using BacWGSTdb (Ruan and Feng, 2016). All whole-genome sequenced *Salmonella* genomes were analyzed by using the SeqSero 1.2 software (Zhang et al., 2015)[1] for serotype prediction. The results from SeqSero were compared to the traditional Kauffman-White serotyping. When the serotype of one isolate from SeqSero 1.2 was inconsistent with the serotyping from the slide agglutination test, the serotype

[1]https://cge.cbs.dtu.dk/services/SeqSero/

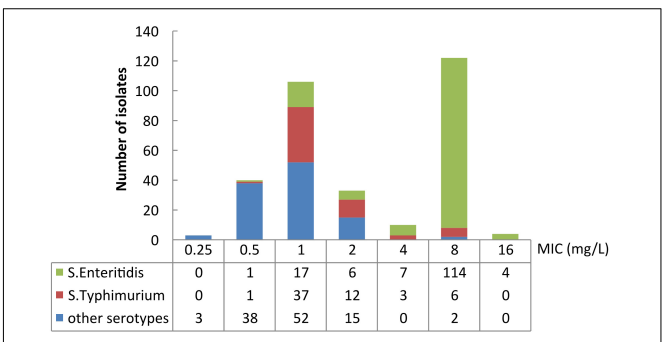

FIGURE 1 | Number of isolates and MIC distribution of different serotypes of *Salmonella*. "Other serotypes" presents serotypes except for Enteritidis and Typhimurium.

was determined according to the phylogenetic clusters using core-genome SNPs.

Reverse Transcription-Quantitative PCR (qRT-PCR)

Overnight cultures of the target *Salmonella* isolates were diluted 1:100 and subcultured in MH medium for ∼4 h at 37°C (OD_{600} ∼0.6). Cells were collected at 4°C by centrifuging at 10,000 rpm for 1 min, and RNA was extracted using TRIzol Reagent (Invitrogen). DNase I-treated RNA was obtained using an RNeasy Mini Kit (QIAGEN, No. 75142), and mRNA expression levels of the target genes were examined using real-time PCR primers listed in **Supplementary Table 2**. qRT-PCR was performed using an ABI 7300 96-well system (Applied Biosystems) with SYBR Premix Ex Taq II (cat. no. RR820A; TaKaRa). Expression levels of target genes were normalized against the 16S rRNA gene of *S. enterica* using the standard curve method.

Statistical Analysis

Hypothesis testing was performed by stratifying the analyses for isolates of *Salmonella* Enteritidis and *Salmonella* Typhimurium. Due to the low prevalence of isolates with other serotypes, these were excluded from the analyses. Fisher's exact tests were used to determine if resistant and susceptible phenotypes were equally distributed in *S.* Enteritidis and *S.* Typhimurium, and among isolates from blood and intestinal samples. A Mann-Whitney test was performed to determine if MICs were equally distributed among isolates of *S.* Enteritidis and *S.* Typhimurium. For the statistical analysis of relative expression levels of *pmr* genes, values are presented as means ± standard deviation (SD). Rank-sum tests were performed for pair-wise

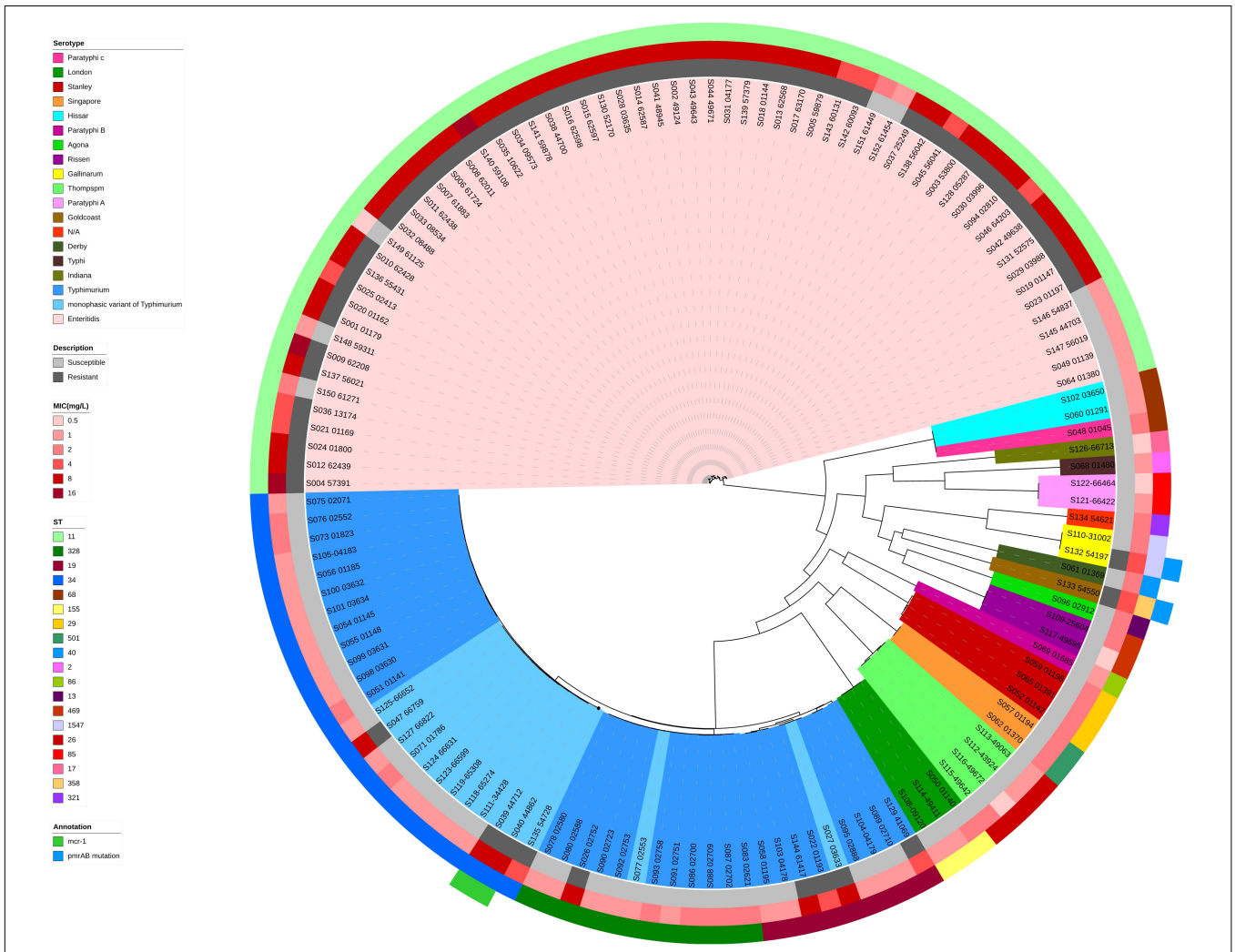

FIGURE 2 | Maximum parsimony tree of the whole-genome sequenced 136 clinical *Salmonella* isolates. MICs (mg/L) and sequence types of colistin among different serotype *Salmonella* isolates were shown. Maximum parsimony tree were generated based on core-genome SNPs by kSNP 3.0. Isolates with different serotypes are indicated in the inner ring with different colors. Colistin MICs in mg/L are shown, along with corresponding *mcr-1* gene and *pmrAB* mutations known to be associated with phenotypic resistance. For the description of colistin susceptibility, resistance corresponds to MIC > 2 mg/L and susceptible corresponds to MIC ≤ 2 mg/L.

comparisons of groups, and $P < 0.05$ (two-tailed) was considered significant.

RESULTS

Colistin MICs and Resistance Mechanisms Among *Salmonella* Isolated From Human Patients

The colistin MICs of the tested *Salmonella* spp. isolates ranged from 0.25 mg/L to 16 mg/L (**Figure 1**). The two most prevalent MICs were 8 mg/L (38.4%, 122/318) and 1 mg/L (33.3%, 106/318). 42.8% (136/318) of colistin MICs of the isolates were measured as > 2 mg/L. MIC_{50} and MIC_{90} of the isolates were 2 and 8 mg/L, respectively. 48.6% (106/218) of the bloodstream infection isolates were identified as colistin-resistant, whereas 30% (30/100) of the isolates from intestinal samples were determined as colistin-resistant.

Resistance mechanisms of all the colistin-resistant isolates were investigated by screening for *mcr* genes and sequencing of *pmrA* and *pmrB*. Out of 136 colistin-resistant isolates, two were as *mcr-1* positive (S039-44712 and S040-44862), none had other *mcr* genes, and two had *pmrAB* mutations which affected the amino acid sequence (S132-54197 and S133-54550). The isolates with *pmrAB* mutations carried a missense point mutation in *pmrA* (T89S), and five missense mutations in *pmrB* (M15T, G73S, V74I, I83V, A111T). However, none of the mutations were predicted to affect the protein function.

Relation Between Serotypes and Colistin Susceptibility

18 serotypes were identified among the 318 isolates. *S.* Enteritidis (n = 149) and *S.* Typhimurium (n = 59) were found to be the overall most prevalent. *S.* Enteritidis (122/218) was the most common among isolates from bloodstream infection samples, followed by *S.* Typhimurium (12/218), whereas the inverse was

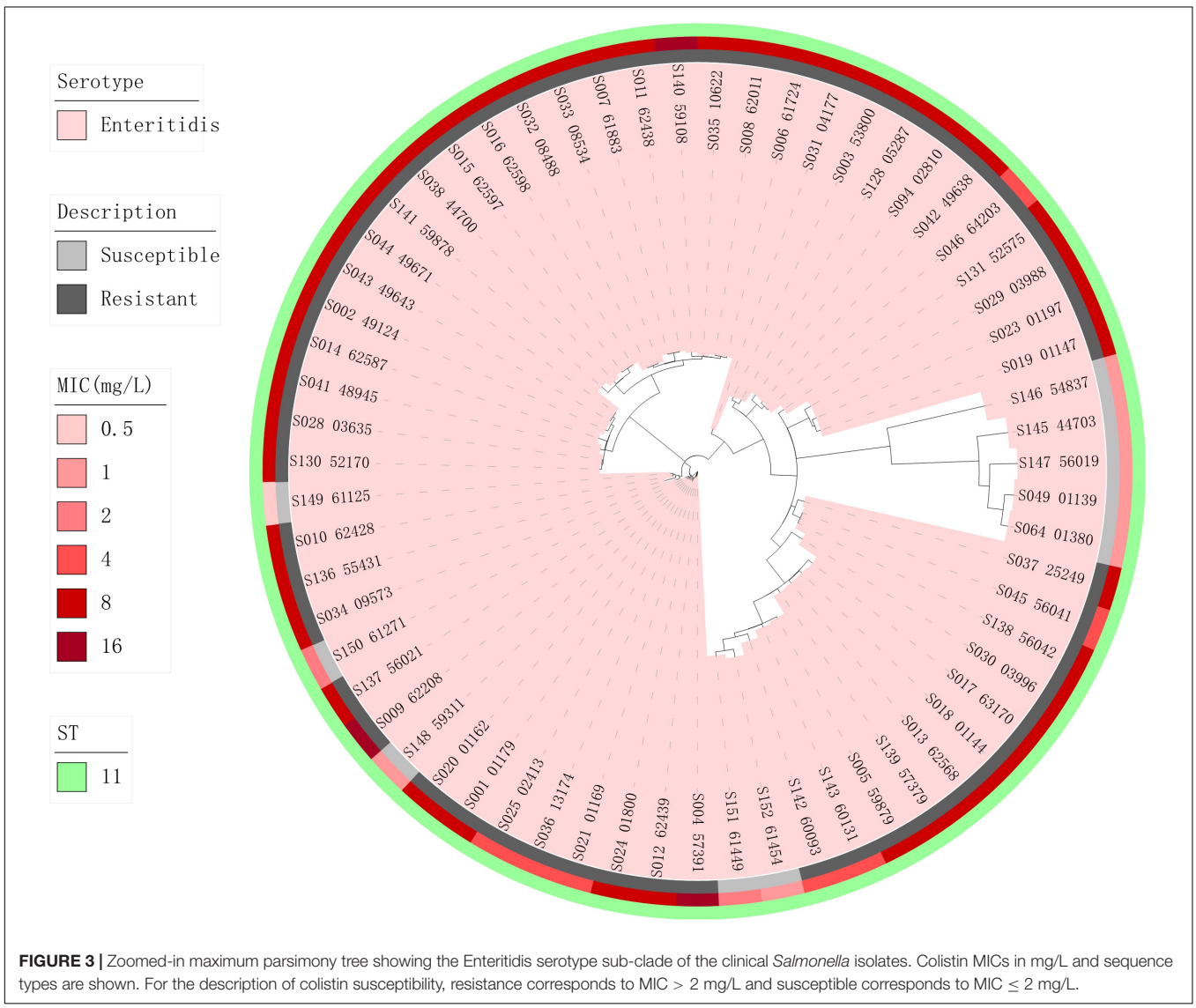

FIGURE 3 | Zoomed-in maximum parsimony tree showing the Enteritidis serotype sub-clade of the clinical *Salmonella* isolates. Colistin MICs in mg/L and sequence types are shown. For the description of colistin susceptibility, resistance corresponds to MIC > 2 mg/L and susceptible corresponds to MIC ≤ 2 mg/L.

true among isolates from patients with intestinal infections, with 27.0% (27/100) *S.* Enteritidis and 47.0% (47/100) *S.* Typhimurium ($P < 0.01$).

The rate of colistin-resistant *S.* Enteritidis and *S.* Typhimurium were 83.9% (125/149) and 15.3% (9/59), respectively. Isolates of *S.* Enteritidis were significantly less susceptible than isolates of *S.* Typhimurium ($P < 0.01$) and had significantly higher MICs ($P < 0.01$). *S.* Enteritidis was most prevalent among the colistin-resistant isolates, representing 91.9% (125/136) of all with the resistance phenotype, followed by *S.* Typhimurium (6.6%, 9/136). All colistin-resistant isolates were *S.* Enteritidis and *S.* Typhimurium, except for the two isolates (S132-54197 and S133-54550) which were identified as *Salmonella* Gallinarum (1/2) and *Salmonella* Goldcoast (1/1), respectively.

Serotype Comparison and Phylogenetic Analysis

In order to discover the relation between *Salmonella* serotypes, phylogenetic evolution and MICs, *Salmonella* serotypes were confirmed and phylogenetic trees based on core-genome SNPs were generated. The whole-genome sequenced isolates were predicted serotypes using SeqSero 1.2 and were compared to the traditional Kauffman-White serotyping. Phylogenetic analysis was employed to confirm the serotyping, by using core-genome SNPs as described above. 63 *S.* Enteritidis, 45 *S.* Typhimurium and 28 isolates of other serotypes were identified from the 136 whole-genome sequenced isolates, and were 98.4% (63/64), 97.8% (45/46), and 92.9% (28/30) identical to the traditional Kauffman-White serotyping, respectively.

Phylogenetic trees based on core-genome SNPs were generated for WGS isolates of all serotypes (**Figure 2**), for all *S.* Enteritidis isolates (**Figure 3**) and for all *S.* Typhimurium isolates (**Figure 4**). The relation between serotypes, sequence types and MICs was inferred in the phylogenetic tree (**Figure 2**). The isolates clustered by serotypes and sequence types in the phylogenetic tree but not by MICs. The *S.* Enteritidis isolates showed little variation in their core genomes. The numbers of SNPs of serotype Enteritidis isolates ranged

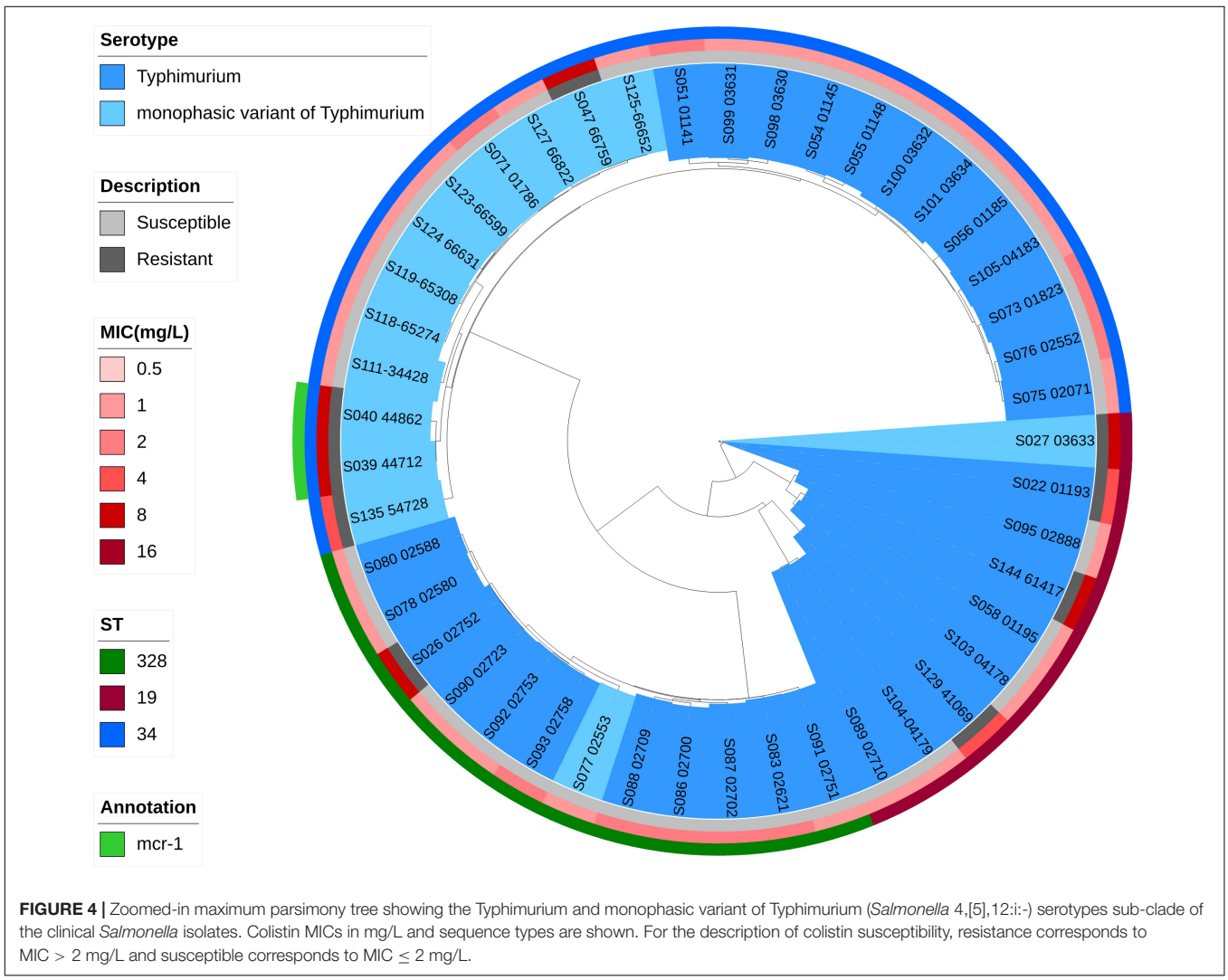

FIGURE 4 | Zoomed-in maximum parsimony tree showing the Typhimurium and monophasic variant of Typhimurium (*Salmonella* 4,[5],12:i:-) serotypes sub-clade of the clinical *Salmonella* isolates. Colistin MICs in mg/L and sequence types are shown. For the description of colistin susceptibility, resistance corresponds to MIC > 2 mg/L and susceptible corresponds to MIC ≤ 2 mg/L.

from 1 to 236, which was very closely in evolution, but did not constitute a single clone. Sequence type of all serotype Enteritidis were ST11 (**Figure 3**). Five colistin-susceptible isolates (S049, S064, S145, S146, S147) clustered together while the remaining five colistin-susceptible isolates (S148, S149, S150, S151, S152) were more diffusely distributed (**Figure 3**). In contrast, isolates of *S.* Typhimurium showed a considerable diversity in their core genomes (**Figure 4**). The two *mcr-1* positive *S.* Typhimurium isolates were both monophasic variant of Typhimurium and clustered together, while the other colistin-resistant *S.* Typhimurium isolates were more dispersed.

Comparision of Expression Levels of *pmr* genes in Colistin Resistant and Sensitive *S.* Typhimurium or *S.* Enteritidis

In order to discover if there are different mechanisms between colistin resistant *S.* Typhimurium and *S.* Enteritidis, expression levels of LPS modification related *pmr* genes (*pmrC*, *pmrD*, *pmrE*, and *pmrHFJKLM* operon) in colistin sensitive *S.* Typhimurium or *S.* Enteritidis were compared with non-*mcr* colistin resistant *S.* Typhimurium or *S.* Enteritidis, respectively. Seven isolates of each serotype were colistin resistance (**Supplementary Table 1**) and seven were colistin sensitive (**Supplementary Table 1**). Relatvie expression levels of all *pmr* genes were enhanced in colistin resistant *S.* Typhimurium than in colistin sensitive *S.* Typhimurium ($P < 0.05$), but no discernable differences between colistin resistant and sensitive *S.* Enteritidis (**Figure 5**), indicating a different mechanism between colistin resistant *S.* Typhimurium and *S.* Enteritidis.

DISCUSSION

Previous studies on colistin susceptibility of *Salmonella* spp. utilizing surveillance data from poultry, food and human clinical sources in European countries and the United States, have indicated a correlation between *Salmonella* serotype and colistin MICs (Tyson et al., 2018; Alvarez et al., 2019). Though the occurrence of *Salmonella* serotypes vary from different countries and sources, the inhomogeneity was confirmed in the current study in which the high rate of colistin resistance of *Salmonella* spp. isolated from human patients from China was clearly linked to specific serotypes.

S. Enteritidis and *S.* Typhimurium were the predominant serotypes overall (with *S.* Enteritidis being the most prevalent), however, there was a sizeable and significant difference in colistin susceptibility and MICs between isolates of the two serotypes. Interestingly, the colistin resistance rate of bloodstream infection isolates was significantly higher compared to that of isolates from intestinal samples ($P < 0.01$). This difference was attributable to that *S.* Enteritidis were significantly more common among bloodstream isolates compared to the *S.* Typhimurium ($P < 0.01$). This indicates that not only is *S.* Enteritidis more likely to be colistin-resistant compared to *S.* Typhimurium, but also more frequently cause severe infections in China.

Carriage of *mcr* genes and missense mutations causing amino acid substitutions in PmrAB are the most commonly reported colistin resistance mechanisms in *Salmonella* spp. Surprisingly, in this study, only four isolates were observed with either of these resistance mechanisms, including two *S.* Typhimurium isolates carried *mcr-1* and two isolates had missense mutations in *pmrAB*. According to previous studies in China, *S.* Typhimurium appear to more easily acquire *mcr* genes compared to *S.* Enteritidis (Li et al., 2016; Cui et al., 2017; Luo et al., 2020). This may be because *S.* Typhimurium in general is more susceptible to colistin than *S.* Enteritidis, and so tend to acquire *mcr* genes in order to adapt to colistin selection pressure. No *pmrAB* mutations were found in colistin resistant *S.* Enteritidis, though the high rate of colistin resistance were observed in this serotype. Relatvie expression levels of *pmr* genes were enhanced in colistin resistant *S.* Typhimurium than in colistin sensitive *S.* Typhimurium, but no discernable differences between colistin

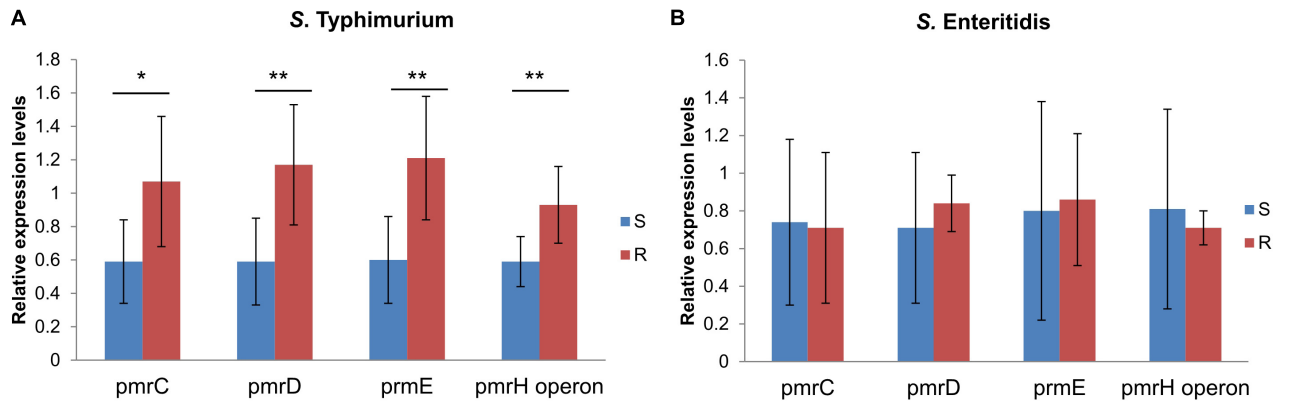

FIGURE 5 | Relative expression levels of *pmrC*, *pmrD*, *pmrE* and *pmrHFJKLM* operon in colistin resistant and sensitive isolates of serotype Typhimurium **(A)** and Enteritidis **(B)**. Gene expression levels of each target gene were identified and compared with 16s rRNA expression levels of each isolates. Relative gene expression levels of colistin sensitive (S) group and colistin resistant (R) group in serotype Typhimurium and Enteritidis were compared using *p*-values calculated by Statistical Package for the Social Sciences (SPSS) using rank-sum tests, respectively (*$P < 0.05$, **$P < 0.01$).

resistant and sensitive *S.* Enteritidis, which indicating a *pmr* related mechanism that confers to colistin resistance to non-*mcr S.* Typhimurium, but a *pmr* unrelated mechanism in colistin resistant *S.* Enteritidis. The large proportion of isolates with unknown resistance mechanisms in the current study indicate that other, as of yet uncharacterized, resistance mechanisms may be more important for *Salmonella* spp.

Aside from that unknown colistin resistance mechanisms could account for the difference in colistin resistance rates of *S.* Enteritidis and *S.* Typhimurium in this study, there could also be intrinsic differences between the serotypes which play an important role. The target of polymyxins is the outer membrane LPS of Gram-negative bacteria. These suggests that the O-antigen (surface LPS of the cell) might play a role in colistin susceptibility. Whether and how different O-antigen confer a different colistin susceptibility phenotype of *Salmonella* needs to be further investigation.

An epidemiological cut-off value for colistin regarding *Salmonella* spp. is lacking in the data presented by EUCAST; currently, only the MIC distribution of *S.* Dublin is presented. The results in this study indicate a very high rate of colistin resistance among *S.* Enteritidis in clinical isolates in China, and this could be associated to elevated wild type MICs compared to other serotypes. Further studies including isolates of *S.* Enteritidis from other countries and other sources are warranted to explore this possibility.

DATA AVAILABILITY STATEMENT

The original contributions presented in the study are publicly available. This data can be found in NCBI under accession Nos. WPIS00000000-WPNX00000000.

ETHICS STATEMENT

The studies involving human participants were reviewed and approved by the Ethics Committee of the First Affilated Hospital of Zhejiang University. The patients/participants provided their written informed consent to participate in this study.

AUTHOR CONTRIBUTIONS

QL and YX conceived and designed the experiments. YW, HF, XY, and YC performed the experiments. QL, BB, and BZ analyzed the data. QL wrote the manuscript. All authors contributed to the article and approved the submitted version.

FUNDING

This work was supported by the National Key R&D Program of China (2017YFC1600100), the National Natural Science Foundation of China (81702040), the National Science Foundation of Zhejiang province, China (LY20H190002), the Swedish Research Council for Environment, Agricultural Sciences and Spatial Planning (Formas) (2016-00640), and the Swedish Foundation for International Cooperate in Research and Higher Education (STINT) (CH2016-6707).

ACKNOWLEDGMENTS

We thank Jinru Ji, Chaoqun Ying, and Yunhui Fang, for the support of technical support and quality control.

SUPPLEMENTARY MATERIAL

The Supplementary Material for this article can be found online at: https://www.frontiersin.org/articles/10.3389/fmicb.2020.592146/full#supplementary-material

REFERENCES

Alvarez, J., Lopez, G., Muellner, P., de Frutos, C., Ahlstrom, C., Serrano, T., et al. (2019*). Identifying emerging trends in antimicrobial resistance using *Salmonella* surveillance data in poultry in Spain. *Transbound. Emerg. Dis.* 67, doi: 10.1111/tbed.13346

Ashton, P. M., Owen, S. V., Kaindama, L., Rowe, W. P. M., Lane, C. R., Larkin, L., et al. (2017). Public health surveillance in the UK revolutionises our understanding of the invasive *Salmonella* typhimurium epidemic in Africa. *Genome Med.* 9:92. doi: 10.1186/s13073-017-0480-487

Borowiak, M., Baumann, B., Fischer, J., Thomas, K., Deneke, C., Hammerl, J. A., et al. (2020). Development of a novel mcr-6 to mcr-9 multiplex PCR and assessment of mcr-1 to mcr-9 occurrence in colistin-resistant *Salmonella enterica* isolates from environment, feed, animals and food (2011-2018) in Germany. *Front. Microbiol.* 11:80. doi: 10.3389/fmicb.2020.00080

Cui, M., Zhang, J., Gu, Z., Li, R., Chan, E. W., Yan, M., et al. (2017). Prevalence and molecular characterization of mcr-1-positive *Salmonella* strains recovered from clinical specimens in China. *Antimicrob Agents Chemother* 61:e02471-16. doi: 10.1128/AAC.02471-2416

Gardner, S. N., Slezak, T., and Hall, B. G. (2015). kSNP3.0: SNP detection and phylogenetic analysis of genomes without genome alignment or reference genome. *Bioinformatics* 31, 2877–2878. doi: 10.1093/bioinformatics/btv271

Kock, R., Daniels-Haardt, I., Becker, K., Mellmann, A., Friedrich, A. W., Mevius, D., et al. (2018). Carbapenem-resistant *enterobacteriaceae* in wildlife, food-producing, and companion animals: a systematic review. *Clin. Microbiol. Infect.* 24, 1241–1250. doi: 10.1016/j.cmi.2018.04.004

Kulengowski, B., Ribes, J. A., and Burgess, D. S. (2019). Polymyxin B EtestR compared with gold-standard broth microdilution in carbapenem-resistant *Enterobacteriaceae* exhibiting a wide range of polymyxin B MICs. *Clin. Microbiol. Infect.* 25, 92–95. doi: 10.1016/j.cmi.2018.04.008

Letunic, I., and Bork, P. (2019). Interactive Tree Of Life (iTOL) v4: recent updates and new developments. *Nucleic Acids Res.* 47, 256–259. doi: 10.1093/nar/gkz239

Li, X. P., Fang, L. X., Song, J. Q., Xia, J., Huo, W., Fang, J. T., et al. (2016). Clonal spread of mcr-1 in PMQR-carrying ST34 *Salmonella* isolates from animals in China. *Sci. Rep.* 6:38511. doi: 10.1038/srep38511

Liu, Y. Y., Wang, Y., Walsh, T. R., Yi, L. X., Zhang, R., Spencer, J., et al. (2016). Emergence of plasmid-mediated colistin resistance mechanism MCR-1 in

animals and human beings in China: a microbiological and molecular biological study. *Lancet Infect Dis.* 16, 161–168. doi: 10.1016/s1473-3099(15)00424-427

Lu, X., Zeng, M., Xu, J., Zhou, H., Gu, B., Li, Z., et al. (2019). Epidemiologic and genomic insights on mcr-1-harbouring *Salmonella* from diarrhoeal outpatients in Shanghai. China, 2006–2016. *EBioMedicine* 42, 133–144. doi: 10.1016/j.ebiom.2019.03.006

Luo, Q., Wan, F., Yu, X., Zheng, B., Chen, Y., Gong, C., et al. (2020). MDR *Salmonella enterica* serovar Typhimurium ST34 carrying mcr-1 isolated from cases of bloodstream and intestinal infection in children in China. *J. Antimicrob. Chemotherapy* 75, 92–95. doi: 10.1093/jac/dkz415

Luo, Q., Yu, W., Zhou, K., Guo, L., Shen, P., Lu, H., et al. (2017). Molecular epidemiology and colistin resistant mechanism of mcr-positive and mcr-negative clinical isolated *Escherichia coli*. *Front. Microbiol.* 8:2262. doi: 10.3389/fmicb.2017.02262

Mohan, A., Munusamy, C., Tan, Y. C., Muthuvelu, S., Hashim, R., Chien, S. L., et al. (2019). Invasive *Salmonella* infections among children in Bintulu, Sarawak, Malaysian Borneo: a 6-year retrospective review. *BMC Infect Dis.* 19:330. doi: 10.1186/s12879-019-3963-x

Olaitan, A. O., Morand, S., and Rolain, J. M. (2014). Mechanisms of polymyxin resistance: acquired and intrinsic resistance in bacteria. *Front. Microbiol.* 5:643. doi: 10.3389/fmicb.2014.00643

Poirel, L., Jayol, A., and Nordmann, P. (2017). Polymyxins: antibacterial activity, susceptibility testing, and resistance mechanisms encoded by plasmids or chromosomes. *Clin. Microbiol. Rev.* 30, 557–596. doi: 10.1128/CMR.00064-16

Ruan, Z., and Feng, Y. (2016). BacWGSTdb, a database for genotyping and source tracking bacterial pathogens. *Nucleic Acids Res.* 44, 682–687. doi: 10.1093/nar/gkv1004

Sun, R. Y., Ke, B. X., Fang, L. X., Guo, W. Y., Li, X. P., Yu, Y., et al. (2020). Global clonal spread of mcr-3-carrying MDR ST34 *Salmonella enterica* serotype Typhimurium and monophasic 1,4,[5],12:i:- variants from clinical isolates. *J. Antimicrob Chemother* 75, 1756–1765. doi: 10.1093/jac/dkaa115

Tyson, G. H., Bodeis-Jones, S., Caidi, H., Cook, K., Dessai, U., Haro, J., et al. (2018). Proposed epidemiological cutoff values for ceftriaxone, cefepime, and colistin in *Salmonella*. *Foodborne Pathog Dis.* 15, 701–704. doi: 10.1089/fpd.2018.2490

Zhang, R., Liu, L., Zhou, H., Chan, E. W., Li, J., Fang, Y., et al. (2017). Nationwide surveillance of clinical carbapenem-resistant *Enterobacteriaceae* (CRE) strains in China. *EBioMedicine* 19, 98–106. doi: 10.1016/j.ebiom.2017.04.032

Zhang, S., Yin, Y., Jones, M. B., Zhang, Z., Deatherage Kaiser, B. L., Dinsmore, B. A., et al. (2015). *Salmonella* serotype determination utilizing high-throughput genome sequencing data. *J. Clin. Microbiol.* 53, 1685–1692. doi: 10.1128/JCM.00323-315

Conflict of Interest: The authors declare that the research was conducted in the absence of any commercial or financial relationships that could be construed as a potential conflict of interest.

frontiers in Microbiology

ORIGINAL RESEARCH
published: 11 January 2021
doi: 10.3389/fmicb.2020.586368

Whole-Genome Sequencing of Clinically Isolated Carbapenem-Resistant Enterobacterales Harboring *mcr* Genes in Thailand, 2016–2019

*Wantana Paveenkittiporn[1], Watcharaporn Kamjumphol[1], Ratchadaporn Ungcharoen[2] and Anusak Kerdsin[2]**

[1] National Institute of Health, Department of Medical Sciences, Ministry of Public Health, Nonthaburi, Thailand, [2] Faculty of Public Health, Kasetsart University, Nakhon, Thailand

OPEN ACCESS

Edited by:
Shaolin Wang,
China Agricultural University, China

Reviewed by:
Mehmet Demirci,
Beykent University, Turkey
Ye Feng,
Zhejiang University, China
Lu-chao Lv,
South China Agricultural University, China

***Correspondence:**
Anusak Kerdsin
Anusak.ke@ku.th

Specialty section:
This article was submitted to Antimicrobials, Resistance and Chemotherapy, a section of the journal Frontiers in Microbiology

Received: 23 July 2020
Accepted: 16 November 2020
Published: 11 January 2021

Citation:
Paveenkittiporn W, Kamjumphol W, Ungcharoen R and Kerdsin A (2021) Whole-Genome Sequencing of Clinically Isolated Carbapenem-Resistant Enterobacterales Harboring mcr Genes in Thailand, 2016–2019. Front. Microbiol. 11:586368. doi: 10.3389/fmicb.2020.586368

Mobile colistin-resistant genes (*mcr*) have become an increasing public health concern. Since the first report of *mcr-1* in Thailand in 2016, perspective surveillance was conducted to explore the genomic characteristics of clinical carbapenem-resistant Enterobacterales (CRE) isolates harboring *mcr* in 2016–2019. Thirteen (0.28%) out of 4,516 CRE isolates were found to carry *mcr* genes, including 69.2% (9/13) of *E. coli* and 30.8% (4/13) of *K. pneumoniae* isolates. Individual *mcr-1.1* was detected in eight *E. coli* (61.5%) isolates, whereas the co-occurrence of *mcr-1.1* and *mcr-3.5* was seen in only one *E. coli* isolate (7.7%). No CRE were detected carrying *mcr-2, mcr-4,* or *mcr-5* through to *mcr-9*. Analysis of plasmid replicon types carrying *mcr* revealed that IncX4 was the most common (61.5%; 8/13), followed by IncI2 (15.4%; 2/13). The minimum inhibitory concentration values for colistin were in the range of 4–16 μg/ml for all CRE isolates harboring *mcr*, suggesting they have 100% colistin resistance. Clermont phylotyping of nine *mcr*-harboring carbapenem-resistant *E. coli* isolates demonstrated phylogroup C was predominant in ST410. In contrast, ST336 belonged to CC17, and the KL type 25 was predominant in carbapenem-resistant *K. pneumoniae* isolates. This report provides a comprehensive insight into the prevalence of *mcr*-carrying CRE from patients in Thailand. The information highlights the importance of strengthening official active surveillance efforts to detect, control, and prevent *mcr*-harboring CRE and the need for rational drug use in all sectors.

Keywords: *mcr*, carbapenem-resistant Enterobacterales, Thailand, colistin, genome

INTRODUCTION

The global spread of carbapenem-resistant Enterobacterales (CRE) has become a leading public health concern. The lack of accessible treatment has resulted in the use of colistin, an outmoded antibiotic, as a last-resort therapeutic drug for human infections by gram-negative bacteria. The widespread use of colistin in humans and animals has led to the emergence of colistin resistance in gram-negative bacteria, and the rates of resistance are continuously increasing

(Kempf et al., 2016; Elbediwi et al., 2019). In 2017, the World Health Organization acknowledged that CRE are a serious priority in a published list of globally important of 12 antimicrobial-resistant pathogens (World Health Organization, 2017). Of particular concern is the spread of *mcr* genes into CRE, which would create strains that are potentially pan-drug resistant (PDR).

A common mechanism of colistin resistance is thought to be associated with chromosomal mediation (Meletis and Skoura, 2018). The discovery of the first plasmid-mediated colistin resistance gene *mcr-1* in an *Escherichia coli* strain isolated from a pig in China led to an increasing number of reports on the identification of *mcr* in many bacterial species worldwide (Liu et al., 2016; Elbediwi et al., 2019). Thus far, 10 variants of *mcr* (*mcr-1* through to *mcr-10*) have been reported (Gharaibeh and Shatnawi, 2019; Wang et al., 2020). The *mcr* gene has been shown to encode a phosphoethanolamine transferase that alters lipid A in the lipopolysaccharide of the bacterial outer membrane by adding a phosphoethanolamine (Gharaibeh and Shatnawi, 2019). This reduces the attachment of colistin to the bacterial outer membrane and, therefore, prevents cell lysis.

The presence of *mcr* has been reported in different gram-negative bacteria isolated worldwide from animal and human sources (Elbediwi et al., 2019; Gharaibeh and Shatnawi, 2019). In Thailand, the first reported *mcr-1*-harboring *E. coli* were isolated from the stool of an asymptomatic person in 2012 (Olaitan et al., 2016). There has since been documentation of *mcr- 1-*, *mcr- 2-*, and *mcr-3*-carrying *E. coli* and *Klebsiella pneumoniae* strains isolated from patients (Paveenkittiporn et al., 2017; Srijan et al., 2018; Kamjumphol et al., 2019; Malchione et al., 2019). The current study investigated the genomic characterization of antimicrobial resistance genes and antimicrobial susceptibility of CRE isolated from patients in Thailand during a laboratory-based surveillance program in 2016–2019.

MATERIALS AND METHODS

Identification of CRE and Detection of Antimicrobial Resistance Genes

In total, 6,996 multidrug-resistant (MDR) bacterial isolates were collected from individuals during 2016–2019 from a hospital network in 24 provinces throughout Thailand (**Figure 1**). There were 666, 2,763, 2,618, and 949 MDR isolates surveyed in 2016–2019, respectively. Conventional biochemical tests described elsewhere were used for the species identification of Enterobacterales (Abbott, 2011). The presence of carbapenemase (bla_{IMP}, bla_{KPC}, bla_{NDM}, and $bla_{\text{OXA-48-like}}$) and *mcr-1* genes was determined using multiplex PCR (Hatrongjit et al., 2018). The *mcr* genes (*mcr-1* to *mcr-9*) were detected using PCR, as described elsewhere (Rebelo et al., 2018; Wang et al., 2018; Yang et al., 2018; Yuan et al., 2019). All *mcr*-positive isolates were subjected to whole-genome sequencing.

Antimicrobial Susceptibility Testing

Analysis of the minimal inhibitory concentration (MIC) of antimicrobials for *mcr*-harboring CRE isolates was performed using the Epsilometer test (*E* test) and interpreted according to the 2020 Clinical and Laboratory Standards Institute guidelines (Clinical and Laboratory Standards Institute, 2020), and *E. coli* ATCC 25922 was used as the control. The *E* test was based on ampicillin, amoxicillin-clavulanate, ampicillin-sulbactam, piperacillin-tazobactam, cefazolin, cefepime, cefotaxime, cefoxitin, ertapenem, meropenem, imipenem, gentamicin, amikacin, ciprofloxacin, levofloxacin, trimethoprim, fosfomycin, nitrofurantoin, chloramphenicol, tetracycline, aztreonam, and azithromycin. Additionally, a modified carbapenem inactivation method (mCIM) was applied to all CRE isolates according to 2020 CLSI M100-S30.

Broth microdilution was used to determine the MIC of colistin using colistin sulfate (Merck, Germany) at 1, 2, 4, 8, 16, and 32 μg/ml, respectively. According to 2020 CLSI M100-S30, an MIC of $\leq$2 μg/ml was interpreted as intermediate susceptibility, whereas an MIC of $\geq$4 μg/ml was considered to indicate resistance.

Whole-Genome Sequencing and Analysis

DNA from 13 *mcr*-carrying CRE isolates was extracted from nutrient agar plate cultures using a DNeasy blood & tissue kit (Qiagen, Hilden, Germany) following the manufacturer's recommendations, and the concentration was determined using the Qubit dsDNA BR assay kit (Invitrogen, Oregon, United States). Sequence libraries were prepared using a Qiagen QIAseq FX DNA library kit (Qiagen, Hilden, Germany) according to the manufacturer's protocol. The prepared libraries were sequenced on the Illumina Miseq platform with Illumina MiSeq 2X 250 base paired-end chemistry (Illumina, CA, United States) according to the manufacturer's instructions. The genomes for each strain were *de novo* assembled using CLC Genomics Workbench v12.0.2 (Qiagen, Aarhus, Denmark) with mostly default settings, except that the minimum contig size threshold was set to 500 bp.

Analysis of the whole-genome sequence data was performed as described elsewhere (Kerdsin et al., 2019). Briefly, the isolates were identified to species level using KmerFinder 3.1 (Larsen et al., 2014)[1]. Antimicrobial resistance genes were identified using ResFinder 4.1 (Zankari et al., 2012)[2] and the Comprehensive Antibiotic Resistance Database (CARD) (Alcock et al., 2020)[3]. We investigated chromosome-mediated colistin resistance by analyzing the *mgrB*, *phoPQ*, *pmrAB, crrB,* and *rpoN* genes. The gene sequences were analyzed using local BLAST + and Clustal W, including *K. pneumoniae* MGH78578 (GenBank accession number NC_009648.1) and *E. coli* K12 sub-strain MG1655 (GenBank accession number U00096) genomes as colistin-susceptible references.

Plasmid replicons were analyzed using PlasmidFinder (Carattoli et al., 2014)[4]. Phylogrouping for *E. coli* and

[1]https://cge.cbs.dtu.dk/services/KmerFinder/

[2]https://cge.cbs.dtu.dk/services/ResFinder/

[3]https://card.mcmaster.ca/

[4]https://cge.cbs.dtu.dk/services/PlasmidFinder/

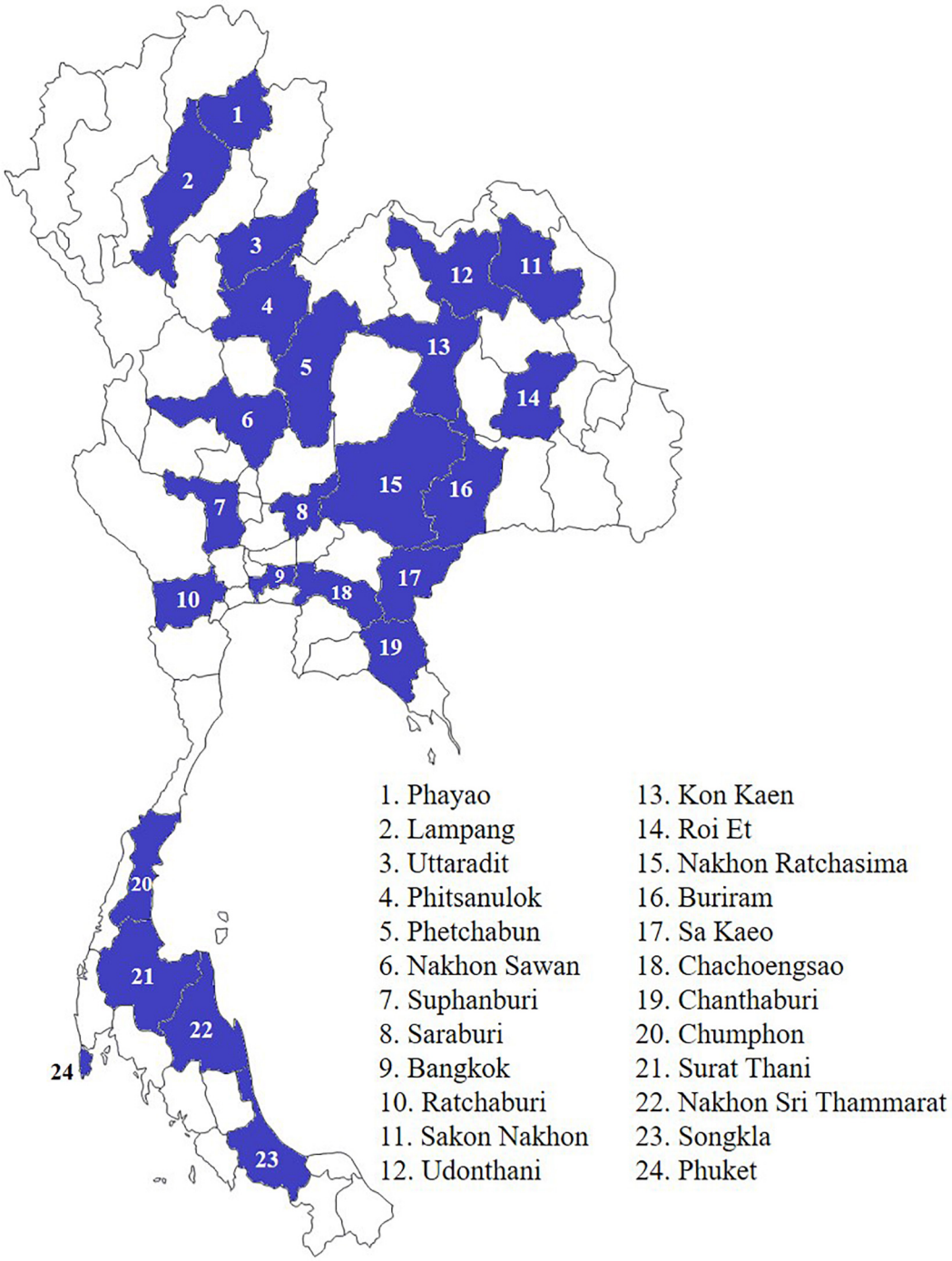

FIGURE 1 | Location of hospital network in 24 provinces throughout Thailand.

the KL type of *K. pneumoniae* were based on analysis using ClermonTyping (Beghain et al., 2018)[5] and Kaptive (Wick et al., 2018)[6]. The virulence genes of *E. coli* and *K. pneumoniae* were analyzed using VirulenceFinder 2.0 (Joensen et al., 2014)[7] and Institut Pasteur[8], respectively.

For multilocus sequence typing (MLST) analysis of the sequence types (STs) of *E. coli* and *K. pneumoniae*, we used MLST

[5]http://clermontyping.iame-research.center/
[6]http://kaptive.holtlab.net
[7]https://cge.cbs.dtu.dk/services/VirulenceFinder/
[8]https://bigsdb.pasteur.fr/klebsiella/klebsiella.html

2.0 (Larsen et al., 2012)[9]. The genomic comparison of 13 *mcr*-harboring CRE isolates was conducted using a modular Single Genome Analysis to search for the genetically closest relatives in the database following the single nucleotide polymorphism (SNP) approach with BacWGSTdb (Feng et al., 2020)[10]. A phylogenetic tree was constructed using REALPHY and MEGA X via the neighbor-joining method with 500 bootstrap replicates by applying the Tamura three-parameter model (Bertels et al., 2014; Kumar et al., 2018). The tree was visualized and annotated using Interactive Tree of Life (iTOL) v4 (Letunic and Bork, 2016). *E. coli* K12 substrain MG1655 (accession no. U00096) and *K. pneumoniae* HS11286 (accession no. CP003200) were used as the reference sequences for SNP analysis. Details of the other genomes used for comparison with our isolates are shown in the **Supplementary Materials**.

Statistical Analysis

The associations between *mcr* genes, *mcr*-harboring *E. coli* isolates, and non-*E. coli* isolates were analyzed by calculating the odds ratios (OR) and *p*-values using the STATA version 14 software package, with $p < 0.05$ considered to be statistically significant.

Accession Number

The assembled genomic sequences were deposited under the BioProject accession number PRJNA525849 with BioSample accessions: SAMN15497997-SAMN15498009. The accession numbers for each *mcr-1*-harboring CRE isolate are provided in **Table 2**.

RESULTS

Genomic Analysis of CRE Isolates Harboring *mcr* Genes

Of the 6,996 MDR isolates, 4,516 were identified as CRE (64.5%). Of these, 4,235 (93.7%) isolates were classified as carbapenemase-producing Enterobacterales (CPE) and carried carbapenemase genes (bla_{NDM}, $bla_{\text{OXA-48-like}}$, bla_{IMP}, or coexisting carbapenemase genes) according to the mCIM and PCR results. Of all the CPE isolates, 13 (0.3%) carried *mcr* genes (**Table 1**). The *mcr*-carrying rates among carbapenemase-producing *E. coli* and *K. pneumoniae* were 1.03 and 0.12%, respectively. Statistical analysis revealed a strong association between *mcr* and carbapenemase-producing *E. coli*, with the OR being 11.06 (95% CI, 3.07–49.23) and statistically significant ($p < 0.0001$) (**Table 1**).

The proportions of *E. coli* and *K. pneumoniae* isolates showing *mcr* genes were 69.2% (9/13) and 30.8% (4/13), respectively. Individual *mcr-1.1* genes were detected in eight *E. coli* (61.5%) from 13 *mcr*-carrying CRE isolates, whereas the co-occurrence of *mcr-1.1* and *mcr-3.5* was found in only one *E. coli* isolate (7.7%) (**Table 2**). However, *mcr-2*, *mcr-4*, and *mcr-5* through to

TABLE 1 | Distribution of *mcr* and carbapenemase genes in carbapenemase-producing Enterobacterales (CPE) during 2016–2019.

Species	Total	bla_{NDM}	$bla_{\text{OXA-48-like}}$	bla_{IMP}	bla_{NDM} + $bla_{\text{OXA-48-like}}$	bla_{IMP} + bla_{NDM}	bla_{IMP} + $bla_{\text{OXA-48-like}}$	bla_{NDM} + *mcr*	$bla_{\text{OXA-48-like}}$ + *mcr*	*mcr*-carrying rate	*p-value*	Odd ratio (95% CI)
Escherichia coli	868	695	54	1	108	1		8	1	1.03%	<0.0001	11.06 (3.07–49.23)
Escherichia sp.	2	1	1									
Klebsiella pneumoniae	3129	1206	1341	46	529	1	2	3	1	0.12%		
Klebsiella aerogenes	11	5	6									
Klebsiella oxytoca	3	3										
Enterobacter cloacae	189	108	24	37	12	3	5					
Enterobacter sp.	1	1										
Citrobacter freundii	10	9			1							
Citrobacter sp.	1	1										
Morganella morganii	1	1										
Pantoea agglomerans	4	3			1							
Proteus mirabilis	7	5		1	1							
Proteus vulgaris	2	2										
Providencia sp.	3	1	1		1							
Salmonella enterica	4	2		2								
	4235	2043	1427	87	653	5	7	11	2	0.31%		

[9]https://cge.cbs.dtu.dk/services/MLST/

[10]http://bacdb.org/BacWGSTdb/

TABLE 2 | Distribution of sequence types and antimicrobial resistant genes in carbapenem-resistant *E. coli* and *K. pneumoniae* carrying *mcr* genes.

Strain no.	Genome accession	Species	Isolation year	Sex	Age	Isolation source	Province/Region in Thailand	CC	ST	Clermont phylogroup	KL type	Virulence genes	Plasmid replicon types	Plasmid carrying-*mcr*	*mcr*	*mgrB* mutation	*pmrA* mutation	*pmrB* mutation	*phoP* mutation	*phoQ* mutation	*crrB* mutation	*rpoN* mutation	bla_{NDM}	$bla_{OXA-48-like}$	bla_{CTX-M}	bla_{CMY}	bla_{TEM}	bla_{OXA-1}	bla_{SHV}	*aac(6')-Ib-cr*	*aac(3)-IId*	*aadA*	*aac(3)-VIa*	*aph(3')-Ia*	*aph(3')-Ib*	*aph(3')-VI*	*aph(6)-Id*	*ndf(A)*	*mph(A)*	*mef(B)*	*erm(42)*	*inu(F)*	*catB3*	*floR*	*cmlA1*	*oqxA,B*	*qnrB6*	*qnrS1*	*ARR-3*	*sul*	*tet*	*dfrA*	*fosA*
53037	JACGZL000000000	*E. coli*	2016	F	74	Urine	Bangkok/ Central	23	410	C		*fyuA, gad, hlyF, iroN, irp2, iss, iucC, iutA, lpfA, neuC, ompT, sitA, terC, traT*	IncFIB, IncFII, IncN2, IncX1, IncX4, IncY	IncX4	1.1		S29G, G144S	D283G, Y358N				E150D, I165M	1		55		1B																				2	A		
53360	JACGZM000000000	*E. coli*	2016	M	63	Urine	Phetchabul/ North	23	410	C		*hra, lpfA, papA, terC, traT*	Col, IncC, IncFIA, IncFIB, IncFII, IncQ1, IncX1, IncX4	IncX4	1.1		S29G, G144S	D283G, Y358N				E150D, I165M	1		15	2	1B								5														1,2	B	17	
56511	JACGZN000000000	*E. coli*	2017	M	68	Urine	Saraburi/ Central	23	410	C		*gad, lpfA, terC*	Col, Col440I, IncFIA, IncFIB, IncFII, IncX4, IncY	IncX4	1.1		S29G, G144S	D283G, Y358N				E150D, I165M	5		15	2	1B					2,5																1	B	12,17	
58967	JACGZO000000000	*E. coli*	2018	M	67	Sputum	Phitsanulok/ North	23	410	C		*fyuA, irp2, lpfA, terC*	Col, IncC, IncFIA, IncFIB, IncFII, IncQ1, IncX4	IncX4	1.1		S29G, G144S	D283G, Y358N				E150D, I165M	5		15	2	1B					2,5																1,2	B	12,17	
62122	JACGZP000000000	*E. coli*	2018	M	41	Urine	Buriram/ Northeast	23	410	C		*fyuA, hra, irp2, lpfA, terC*	Col, IncC, IncFIA, IncFIB, IncFII, IncQ1, IncX4, IncY	IncX4	1.1		S29G, G144S	D283G, Y358N				E150D, I165M	5		15	2	1B					2,5																1,2	B,X4	12,17	
54881	JACGZQ000000000	*E. coli*	2017	F	55	Rectal swab	Nan/ North	38	3052	D		*air, chuA, eilA, iss, kpsE, ompT, papA, terC, traT*	Col, IncFII, IncI2, IncN2	IncI2	1.1		S29G	H2R, D283G	I44L			E150D, I165M	1		15		1C					16																1,2	A,B	27	
54882	JACGZR000000000	*E. coli*	2017	F	50	Rectal swab	Nan/ North	38	3052	D		*air, chuA, eilA, iss, kpsE, ompT, papA, terC, traT*	Col, IncFII, IncI2, IncN2	IncI2	1.1		S29G	H2R, D283G	I44L			E150D, I165M	1		15		1C					16																1,2	A,B	27	
60000	JACGZS000000000	*E. coli*	2018	F	66	Rectal swab	Nan/ North	10	10	A		*gad, mcbA, terC, traT*	IncFIB, IncL, IncX1, IncX4, p0111, IncB/O/K/Z	IncX4	1.1		S29G					R217G	1		3		1B		12			2,5																1,2	A,X4	17	
54715	JACGZT000000000	*E. coli*	2017	M	54	Sputum	Bangkok/ Central	10	1287	A		*cia, fyuA, gad, irp2, iss, iucC, iutA, sitA, terC, traT*	IncFIA, IncFIB, IncFII, IncI1-I, IncI2	Unknown	1.1+3.5		S29G			L343V					48							1,2b																3	A	12	
59990	JACXSU000000000	*K. pneumoniae*	2018	F	69	Sputum	Phuket/ South	17	336		K25	*fyuA, irp1, irp2, mrk locus, ybt locus*	ColRNAI, IncFIB, IncFII, IncN2, IncR, IncX4	IncX4	1.1		E57G	T246A			L296Q	F304Y	1						12																					D		
61843	JACGZU000000000	*K. pneumoniae*	2018	F	76	Urine	Phuket/ South	17	336		K25	*fyuA, irp1, irp2, mrk locus, ybt locus*	ColRNAI, IncFIB, IncFII, IncI2, IncN2	Unknown	1.1		E57G	T246A			L296Q	F304Y	1						11																					A,D	12	
2514-18	JADCQU000000000	*K. pneumoniae*	2018	F	61	Urine	Phuket/ South	17	336		K25	*fyuA, irp1, irp2, mrk locus, ybt locus*	ColRNAI, IncFIB, IncFII, IncI2, IncN2	Unknown	1.1		E57G	T246A			L296Q	F304Y	1						11																					A,D	12	
60220	JACGZV000000000	*K. pneumoniae*	2018	M	71	Ascitic fluid	Khon Kaen/ Northeast	258	340		K15	*fyuA, irp1, irp2, mrk locus, ybt locus*	Col440I, ColKP3, IncFIB, IncFII, IncR, IncX3, IncX4	IncX4	1.1			T246A, R256G			L296Q			181	15		1B		182			2																	1	D	12,14	

mcr-9 were not detected. Analysis of the plasmid replicon types carrying *mcr* revealed that IncX4 was the most common (61.5%; 8/13), followed by IncI2 (15.4%; 2/13), as shown in **Table 2**. However, three isolates were unidentified. Six carbapenem-resistant *E. coli* isolates harboring *mcr* carried IncX4, whereas two isolates contained IncI2. Of the four carbapenem-resistant *K. pneumoniae* isolates harboring *mcr*, two carried IncX4 and the other two had unknown plasmid replicon types. The genetic organization of the *mcr* genes in these 13 isolates is outlined in **Figure 2**. A common gene found downstream of *mcr-1.1* in all isolates encoded the PAP2 family protein, whereas the upstream genes varied. However, a DUF2726-domain-containing protein-encoding gene was commonly found in 8 of the 13 isolates (seven *E. coli* and one *K. pneumoniae*). Furthermore, the upstream and downstream genetic organization of *mcr-3.5* was quite different from that of *mcr-1.1*.

As shown in **Table 2**, chromosomal-mediated colistin resistance gene mutations, including those in *mgrB*, *pmrAB*, *phoPQ, crrB,* and *rpoN*, were analyzed. We detected substitutions in *pmrAB* and *rpoN* in almost *mcr*-harboring CRE isolates, whereas *phoPQ* substitutions were found in three isolates, and no mutations were detected in *mgrB.* Substitutions were commonly found in the *pmrA* genes of 12 out of 13 *mcr*-harboring isolates, while *pmrB* and *rpoN* substitutions were detected in 11 isolates. The isolates 54881 and 54882 contained more mutations in the chromosomal-mediated colistin resistance genes than other isolates. Substitution at S29G and E57G in *pmrA* was predominant in *E. coli* and *K. pneumoniae,* respectively. The *pmrB* substitution at D283G was commonly found in *E. coli,* whilst all four *mcr-1*-harboring *K. pneumoniae* contained a T246A substitution. Only one substitution in *phoP* (I44L) and one in *phoQ* (L343V) were detected in *mcr-1*-carrying *E. coli*. Substitution at E150D and I165M in *rpoN* was predominant in *E. coli* isolates, in contrast to those at F304Y which was commonly found in *K. pneumoniae* isolates. In addition, one *crrB* substitution (L296Q) was found in all *K. pneumoniae* isolates. Insertion or deletion in those described genes was not detected in all *mcr-1*-harboring CRE isolates.

As shown in **Table 2**, of the 13 isolates, five and three *mcr*-harboring *E. coli* isolates carried $bla_{\mathrm{NDM-1}}$ and $bla_{\mathrm{NDM-5}}$, respectively. Only one *E. coli* isolate contained $bla_{\mathrm{OXA-48}}$. Three and one *mcr-1.1*-harboring *K. pneumoniae* isolates carried $bla_{\mathrm{NDM-1}}$ and $bla_{\mathrm{OXA-181}}$, respectively. Among the β-lactamase genes, $bla_{\mathrm{CTX-M}}$, bla_{SHV}, or bla_{TEM} were detected in almost all isolates (92.3%, 12/13), and only one *E. coli* isolate had no β-lactamase genes. The predominant $bla_{\mathrm{CTX-M}}$ was $bla_{\mathrm{CTX-M-15}}$, which was detected in 53.8% (7/13) of all isolates. The gene bla_{SHV} was found in all *K. pneumoniae* and one isolate of *E. coli* (**Table 2**). Among the ampC β-lactamase genes, $bla_{\mathrm{CMY-2}}$ only was detected in four *E. coli* isolates (28.6%). The other antimicrobial resistance genes in the *mcr*-carrying CRE isolates, including those for fluoroquinolones, aminoglycosides, rifampicin, macrolides, chloramphenicol, sulfonamide, tetracycline, fosfomycin, and trimethoprim, are shown in **Table 2**.

Antimicrobial Susceptibility of CRE Isolates Harboring *mcr* Genes

As shown in **Table 3**, the colistin MIC values for the *mcr*-harboring isolates were in the range of 4–16 μg/ml. According to the 2020 CLSI M100-S30 guidelines, a microbe with a colistin MIC value of ≥4 μg/ml is resistant, whereas MIC ≤ 2 μg/ml indicates intermediate resistance. Thus, the results indicate that 100% of the *mcr*-carrying CRE isolated from patients were resistant to colistin. The highest MIC value for colistin (16 μg/ml) was found in two carbapenem-resistant *K. pneumoniae* isolates. Most of the *mcr*-harboring *E. coli* had colistin MIC values of 4 μg/ml (8/9; 88.8%).

More than 50% of the *mcr*-harboring CRE isolates were susceptible to amikacin (11/13), fosfomycin (12/13), and nitrofurantoin (7/13). Of the 13 CRE-harboring *mcr* isolates, four *E. coli* isolates and one *K. pneumoniae* isolate were extensively drug-resistant (XDR; 38.5%). Details of the antimicrobial resistance profiles of the 13 isolates are provided in **Table 3**. Moreover, 12 of the 13 *mcr*-harboring CRE isolates were resistant to ciprofloxacin. As shown in **Table 2**, ciprofloxacin resistance may result from the presence of quinolone resistance genes: *oqxA, oqxB, qnrS1, qnrB6,* and *aac(6′)-Ib-cr*.

Molecular Typing of *mcr*-Harboring CRE Isolates

As summarized in **Table 2**, Clermont phylotyping of nine *mcr*-harboring carbapenem-resistant *E. coli* isolates demonstrated that phylogroup C (5/9; 55.6%) was predominant, followed by phylogroups A (2/9; 22.2%) and D (2/9; 22.2%). The Clermont phylogroup was concordant with clonal complexes (CC). Phylogroup C was concordant with CC23, which contained only ST410. Phylogroup D was concordant with CC38, which consisted of ST3052, whereas phylogroup A was concordant with CC10, which contained either ST10 or ST1287. Four carbapenem-resistant *K. pneumoniae* isolates harboring *mcr* were predominantly ST336 (3/4; 75%) and one was ST340 (1/4; 25%). ST336 belonged to CC17 and KL type 25, whereas ST340 belonged to CC258 and KL type 15.

The genetic relationships based on the SNPs of these *mcr*-harboring isolates are demonstrated in **Figures 3**, **4**. Five *E. coli* ST410 isolates were widely distributed in several sub-clusters of the ST410 cluster. Strain no. 53360 was closely related to the strain AMA1167 from Denmark, whereas strain no. 56511 clustered with strains from Norway, India, Lebanon, China, and Denmark (**Figure 3**). Strains no. 58967 and no. 62122 were related to strain KBN10P04869 from South Korea. Strain no. 53037 clustered with strains from Norway, the United States, Brazil, and Germany. Two ST3052 isolates (nos. 54881 and 54882) were closely related to the strain WCHEC020028 from China; they had similar characteristics and were from different individuals in the same hospital ward, indicating that they were likely to have originated from the same source. Strain no. 54715 (ST1287) was related to a strain from the United States (ST617), and these were clustered together with strain no. 6000 (ST10) (**Figure 3**).

TABLE 3 | Antimicrobial susceptibility of *mcr*-harboring carbapenem-resistant *E. coli* and *K. pneumoniae*.

No.		1	2	3	4	5	6	7	8	9	10	11	12	13
Isolate No.		53360	54881	54882	56511	58967	62122	60000	54715	53037	59990	60220	61843	2514-18
Organism		*E. coli*	*E. coli*	*E. coli*	*E. coli*	*E. coli*	*E. coli*	*E. coli*	*E. coli*	*E. coli*	*K. pneumoniae*	*K. pneumoniae*	*K. pneumoniae*	*K. pneumoniae*
Classification		XDR	XDR	MDR	MDR	MDR	XDR	XDR	MDR	MDR	MDR	XDR	MDR	MDR
Penicillin	AMP (μg/ml)	>256 (R)	>256 (R)	>256 (R)	>256 (R)	>256 (R)	>256 (R)	>256 (R)	>256 (R)	>256 (R)	>256 (R)	>256 (R)	>256 (R)	>256 (R)
β-lactam combination	AMC (μg/ml)	>256 (R)	>256 (R)	>256 (R)	>256 (R)	>256 (R)	>256 (R)	>256 (R)	>256 (R)	>256 (R)	>256 (R)	>256 (R)	>256 (R)	>256 (R)
	SAM (μg/ml)	>256 (R)	>256 (R)	>256 (R)	>256 (R)	>256 (R)	>256 (R)	> 256 (R)	> 256 (R)	> 256 (R)	> 256 (R)	> 256 (R)	> 256 (R)	> 256 (R)
	TZP (μg/ml)	> 256 (R)	>256 (R)	> 256 (R)	>256 (R)	> 256 (R)	>256 (R)	> 256 (R)	64 (I)	> 256 (R)	>256 (R)	> 256 (R)	>256 (R)	> 256 (R)
13rd generation Cephalosporins	KZ (μg/ml)	>256 (R)	>256 (R)	>256 (R)	>256 (R)	>256 (R)	>256 (R)	>256 (R)	32 (R)	>256 (R)	>256 (R)	>256 (R)	>256 (R)	>256 (R)
	FEP (μg/ml)	>256 (R)	>256 (R)	>256 (R)	>256 (R)	>256 (R)	>256 (R)	>256 (R)	0125 (S)	>256 (R)	>256 (R)	>256 (R)	96 (R)	96 (R)
	CTX (μg/ml)	>32 (R)	>32 (R)	>32 (R)	>32 (R)	>32 (R)	>32 (R)	>32 (R)	0.25 (S)	>32 (R)	>32 (R)	>32 (R)	>32 (R)	>32 (R)
	FOX (μg/ml)	>256 (R)	>256 (R)	>256 (R)	>256 (R)	>256 (R)	>256 (R)	>256 (R)	8 (S)	>256 (R)	>256 (R)	>256 (R)	>256 (R)	>256 (R)
Carbapenems	ERT (μg/ml)	>32 (R)	>32 (R)	>32 (R)	>32 (R)	>32 (R)	>32 (R)	>32 (R)	0.75 (I)	32 (R)	>32 (R)	>4(R)	>32 (R)	>32 (R)
	MER (μg/ml)	>32 (R)	>32 (R)	>32 (R)	12(R)	12 (R)	8 (R)	>32 (R)	0.5 (S)	8 (R)	>32 (R)	>8(R)	>32 (R)	>32 (R)
	IMP (μg/ml)	>32 (R)	>32 (R)	>32 (R)	1.5 (I)	8 (R)	8 (R)	>32 (R)	0.25 (S)	4 (R)	32 (R)	>8 (R)	>32 (R)	>32 (R)
Aminoglycoside	CN (μg/ml)	64 (R)	32 (R)	0.38 (S)	0.75 (S)	32 (R)	16 (R)	>256 (R)	24 (R)	0.75 (S)	0.5 (S)	0.75 (S)	0.75 (S)	0.75 (S)
	AK (μg/ml)	32 (I)	4 (S)	4 (S)	8 (S)	6 (S)	3 (S)	3 (S)	2 (S)	3 (S)	2 (S)	32 (I)	4 (S)	6 (S)
Quinolone	CIP (μg/ml)	>32 (R)	>32 (R)	3 (R)	>32 (R)	>32 (R)	>32 (R)	>32 (R)	>32 (R)	>32 (R)	0.094 (S)	>32 (R)	1.5 (R)	1 (R)
	LEV (μg/ml)	>32 (R)	>32 (R)	0.75 (S)	>32 (R)	>32 (R)	>32 (R)	>32 (R)	>32 (R)	>32 (R)	0.125 (S)	>32 (R)	0.5 (S)	0.25 (S)
Folate	SXT (μg/ml)	>32 (R)	>32 (R)	>32 (R)	>32 (R)	>32 (R)	>32 (R)	>32 (R)	>32 (R)	0.38 (S)	0.38 (S)	>32 (R)	4 (R)	>32 (R)
Fosfomycin	FOT (μg/ml)	0.75 (S)	6 (S)	0.75 (S)	0.75 (S)	1 (S)	1.5 (S)	0.75 (S)	0.5 (S)	0.38 (S)	24 (S)	64 (S)	96 (S)	>256 (R)
Nitrofuran	N (μg/ml)	32 (S)	16 (S)	16 (S)	24 (S)	48 (S)	64 (I)	64 (I)	32 (S)	16 (S)	128 (R)	>512 (R)	96 (R)	>256 (R)
Phenicol	C (μg/ml)	24 (I)	>256 (R)	16 (I)	12 (S)	24 (I)	64 (R)	>256 (R)	128 (R)	6 (S)	32 (R)	96 (R)	8 (S)	3 (S)
Tetracycline	TE (μg/ml)	>256 (R)	>256 (R)	>256 (R)	>256 (R)	>256 (R)	>256 (R)	96 (R)	48 (R)	64 (R)	>256 (R)	>256 (R)	>256 (R)	>256 (R)
Monobactam	ATM (μg/ml)	>256 (R)	>256 (R)	>256 (R)	>256 (R)	>256 (R)	>256 (R)	>256 (R)	0.047 (S)	48 (R)	96 (R)	>256 (R)	0.064 (S)	0.125 (S)
Macrolide	AZM (μg/ml)	32 (R)	>256 (R)	>256 (R)	32 (R)	>256 (R)	>256 (R)	>256 (R)	32 (R)	>256 (R)	>256 (R)	>256 (R)	>256 (R)	32 (R)
Colistin	COL (μg/ml)	4 (R)	4 (R)	4 (R)	4 (R)	4 (R)	4 (R)	8 (R)	4 (R)	8 (R)	8 (R)	8 (R)	16 (R)	16 (R)

AMP, ampicillin; AMC, amoxicillin/clavulanic acid; SAM, ampicillin-sulbactam; TZP, piperacillin-tazobactam; KZ, Cefazolin; FEP, cefepime; CTX, cefotaxime; FOX, Cefoxitin; ERT, ertapenem; MER, meropenem; IMP, imipenem; CN, gentamicin; AK, amikacin; CIP, ciprofloxacin; LEV, levofloxacin; SXT, trimethoprim; FOT, Fosfomycin; N, nitrofurantoin; C, chloramphenicol; TE, tetracycline; ATM, aztreonam; AZM, azithromycin; COL colistin.

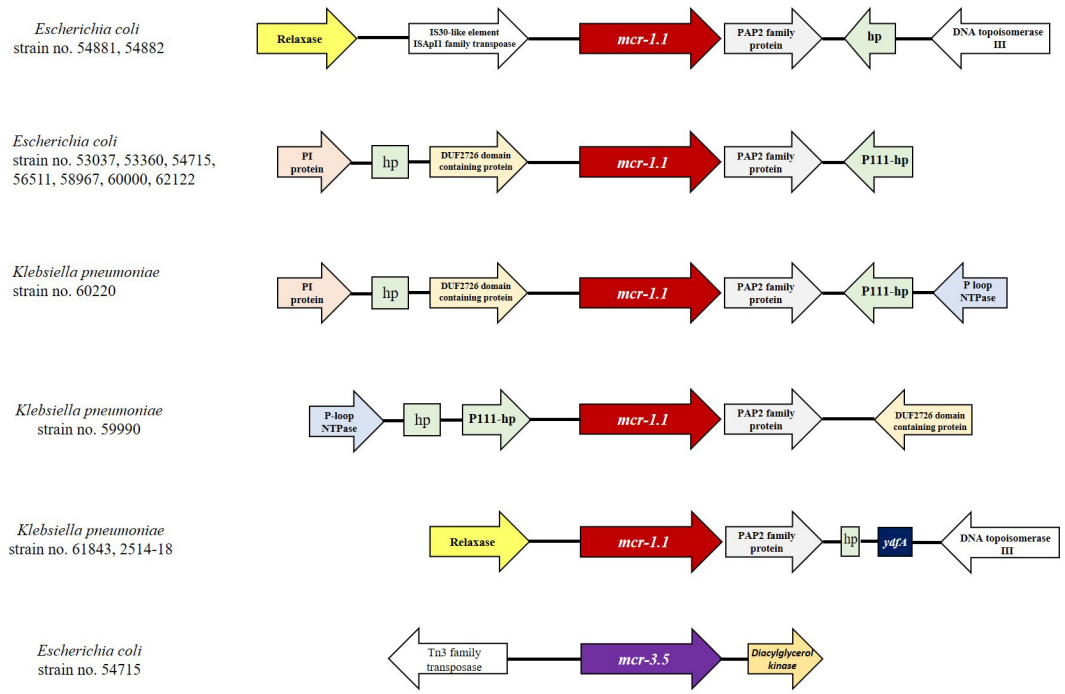

FIGURE 2 | Comparison of the genetic organization of the *mcr* genes in 13 CRE isolates. The schematic shows the genes flanking the *mcr* genes in the isolates.

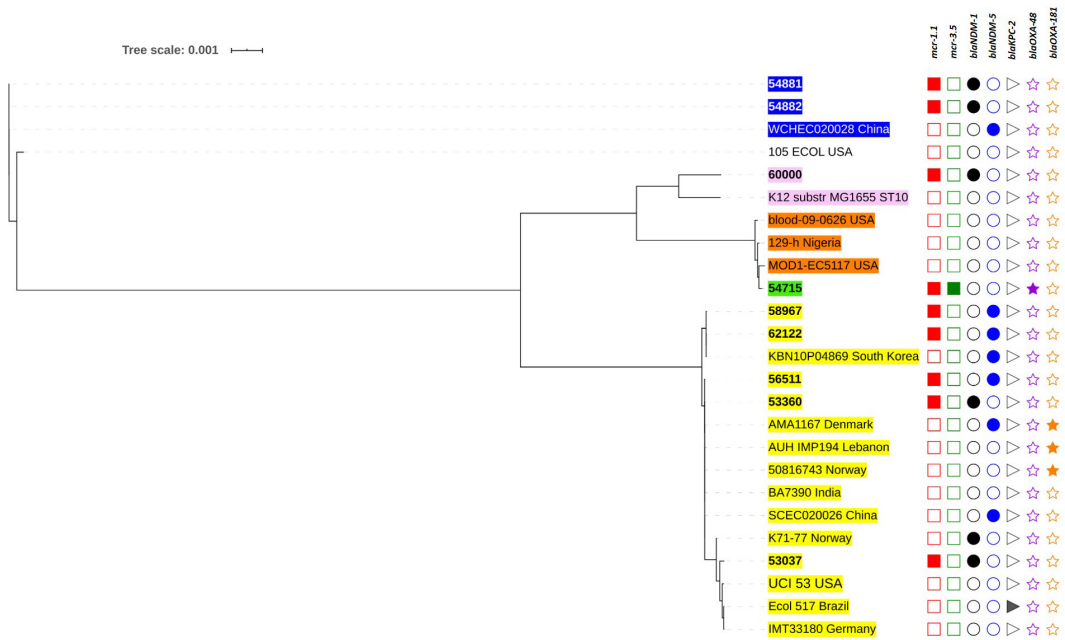

FIGURE 3 | Phylogenetic tree based on single nucleotide polymorphisms (SNP) in *E. coli* using the neighbor-joining method. The tree was visualized and annotated using Interactive Tree of Life (iToL). The tree is annotated based on sequence types (STs; color highlight), *mcr* (square), bla_{NDM} (circle), bla_{KPC} (right triangle), and $bla_{OXA-48-like}$ (star). Presentation of the genes is shown by filled symbols. STs 410, 1287, 617, 10, and 3052 are highlighted in yellow, green, brown, pink, and blue, respectively. The isolates used in this study are shown in bold.

Among the *K. pneumoniae* isolates, the ST336 isolates were closely related and clustered with other ST336 strains isolated in Thailand (**Figure 4**). Interestingly, the Thai-ST336 isolates were in a different cluster from that containing the ST336 isolates from other countries. Similarly, isolate no. 60220 (ST340) in this study was

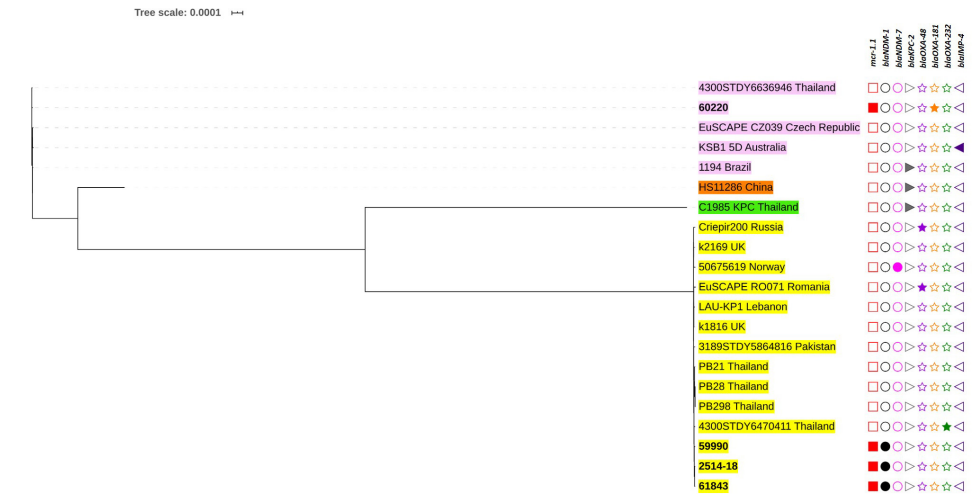

FIGURE 4 | Phylogenetic tree based on single nucleotide polymorphisms (SNP) in *K. pneumoniae* using the neighbor-joining method. The tree was visualized and annotated using Interactive Tree of Life (iToL). The tree is annotated based on sequence types (STs; color highlight), *mcr* (square), bla_{NDM} (circle), bla_{KPC} (right triangle), $bla_{OXA-48-like}$ (star), and bla_{IMP} (left triangle). Presentation of the genes is revealed by filled symbols. STs 336, 340, 11, and 4008 are highlighted in yellow, pink, and brown, and green, respectively. The isolates used in this study are shown in bold.

closely related to strain 4300STDY6636946 circulating in Thailand (**Figure 4**).

DISCUSSION

The discovery that plasmid-mediated colistin resistance is encoded by *mcr* genes and the high prevalence of human isolates harboring these genes are of global concern. A recent report revealed the overall average prevalence of *mcr* genes to be 4.7% (0.1–9.3%) in 47 countries across six continents (Elbediwi et al., 2019), and as many as 10 *mcr* genes (*mcr-1* through to *mcr-10)* have been reported (Gharaibeh and Shatnawi, 2019; Wang et al., 2020). A study of the global prevalence of *mcr* genes revealed that *mcr-1* (4917/5191; 94.7%) is a common gene and has a wider distribution compared with *mcr*-2 through to *mcr-8* (Elbediwi et al., 2019). Human infections with both CRE and non-CRE isolates carrying *mcr-1* have been widely reported (Liu et al., 2016; Mediavilla et al., 2016; Paveenkittiporn et al., 2017; Quan et al., 2017; Mendes et al., 2018; Srijan et al., 2018; Zhong et al., 2018; Elbediwi et al., 2019).

The coexistence of *mcr* and carbapenemase genes, such as bla_{NDM}, $bla_{OXA-48-like}$, and bla_{IMP}, in CRE isolates has been described in countries worldwide (Mediavilla et al., 2016; Arabaci et al., 2019; Huang et al., 2020; Kananizadeh et al., 2020). The current study found the predominant *mcr* gene to be *mcr-1*, which more frequently coexists with bla_{NDM} than $bla_{OXA48-like}$, highlighting the potential dissemination of *mcr-1* and bla_{NDM} among CRE isolates in Thailand. This concurs with a study in China (Huang et al., 2020), where *mcr-1* and bla_{NDM-5} were predominant (78.6%, 11/14). In this study, *mcr-1* and bla_{NDM-1} were the most prevalent resistance genes (61.5%, 8/13). A previous study showed that *mcr-3* had a wide distribution in water, animals, food, and human isolates (Elbediwi et al., 2019). We found a 7.7% (1/13) prevalence for *mcr-3.5*, which co-occurred with *mcr-1* and bla_{OXA-48} in *E. coli.* The phenomenon of double *mcr* genes has been reported in isolates from humans, with *K. pneumoniae* harboring *mcr-3* and *mcr-8* being isolated from the stool of a healthy individual in Laos (Hadjadj et al., 2019).

Our study revealed that the most common type of plasmid replicon carrying *mcr* was IncX4. Previous reports have shown IncX4, IncI2, and IncHI2 to be the major plasmid types driving the global dissemination of *mcr-1* (Wu et al., 2018). A study in Thailand revealed two predominant plasmid types (IncX4 and IncI2) carrying *mcr-1* in CRE (Shanmugakani et al., 2019). This suggests that IncX4 bearing *mcr-1* mediates the transmission of CRE and may promote its circulation throughout Thailand. IncX4 and IncI2 acting as vehicles for *mcr-1* propagation enhance host fitness and provide a competitive advantage over strains with other plasmid replicon types, resulting in greater plasmid stability (Wu et al., 2018).

On the basis of the Clermont phylotyping scheme, *E. coli* species can be divided into eight main phylogroups, termed A, B1, B2, C, D, E, F, and G (Clermont et al., 2019). The nine carbapenem-resistant *E. coli* isolates carrying *mcr* (55.6%) in this study belonged to phylogroup C, whereas the rest belonged to phylogroups A and D (22.2% each). The *E. coli* strains responsible for extra-intestinal infection were more likely to be members of phylogroups B2 or D, which show greater pathogenesis than A, B1, or C (Clermont et al., 2013). Strains belonging to phylogroups A, B1, and C are commonly commensal, suggesting that more than half of the *E. coli* harboring *mcr* isolated from patients in this study were commensal strains.

Our study revealed seven carbapenem-resistant STs that carry *mcr*, of which *E. coli* ST410 (35.7%) and *K. pneumoniae* ST336 (21.4%) isolates were predominant. Elbediwi et al. (2019) reported that *E. coli* ST101 carrying *mcr-1* have been found in

environmental samples, animals, and humans. However, ST10 was the most globally common ST of *E. coli* carrying *mcr-1* (Elbediwi et al., 2019). In Asia, ST116 was found to be the predominant ST that carries *mcr*-1 isolated from humans, followed by ST117, ST10, ST38, ST101, and ST156 (Elbediwi et al., 2019). *E. coli* ST410 is internationally considered a new high-risk clone that can cause several types of infection; it is highly resistant and has a global distribution (Roer et al., 2018). This ST has been described in Southeast Asia following multiple introductions through several independent events and differs from clones detected in Europe and North America (Nadimpalli et al., 2019). SNP phylogenetic analysis in this study revealed that the ST410 isolates were diverse or not closely related to other strains. Instead, they were shown to be related to strains from countries other than Thailand. This adds support to the assumption that there have been multiple dissemination events into this area.

Klebsiella pneumoniae ST336 (CC17) is considered an international clone (Rodrigues et al., 2014; Novović et al., 2017; Palmieri et al., 2020) and has been frequently associated with the worldwide spread of $bla_{\text{CTX-M-15}}$ and $bla_{\text{OXA-48-like}}$ (Rodrigues et al., 2014; Novović et al., 2017; Palmieri et al., 2020). Interestingly, all ST336 isolates in the current study carried $bla_{\text{NDM-1}}$, but not any $bla_{\text{CTX-M}}$ genes, suggesting that they may be from different lineages. To the best of our knowledge, the carbapenem-resistant ST336 isolates in this study are the first to be described as having *mcr-1*. Previous studies revealed that colistin-resistant ST336 resulted from an *mgrB* mutation, and no *mcr* genes have been detected in this ST (Novović et al., 2017; Palmieri et al., 2020). SNP phylogenetic analysis allocated the ST336 isolates to the same cluster as other Thai-ST336 isolates, and this cluster was independent from another ST336 cluster consisting of isolates from other countries. This suggests that Thai-ST336 isolates circulate throughout our country by clonal expansion.

The colistin MIC values (4–16 μg/ml) for our isolates indicated they have 100% resistance. Combinations of *mcr* and chromosome-mediated colistin resistant genes (*pmrAB*, *phoPQ, crrB,* or *recN*) contributed to the colistin resistance of our isolates. It is interesting that substitutions in *pmrAB* and *crrB* in *mcr-1*-carrying *K. pneumoniae* are quite different from previous reports (Olaitan et al., 2014a,b; Wright et al., 2015; Cheng et al., 2016). In addition, substitution of *phoPQ* was not found in our *K. pneumoniae* isolates comparing to those studies (Olaitan et al., 2014a,b; Wright et al., 2015; Cheng et al., 2016). On the other hand, substitutions of *pmrA* (G144S), *pmrB* (H2R, D283G, Y358N), and *phoP* (I44L) in our *mcr-1*-harboring *E. coli* are similar to a study previously described (Choi et al., 2020). In case of *rpoN*, inactivation of this gene resulting in polymyxin resistance has been observed in *Salmonella enterica* (Barchiesi et al., 2009). However, polymyxin resistance via *rpoN* inactivation or substitution is not yet reported in either *E. coli* or *K. pneumoniae*. Although our study detected substitution of *rpoN*, but its role on polymyxin resistance remain to be investigated.

Several studies have shown *mcr-1*-carrying CRE isolated from humans to have high frequencies of colistin resistance, such as 71.4% in China (Huang et al., 2020), 100% in the United States (Mediavilla et al., 2016), and 100% in Turkey (Arabaci et al., 2019). A previous study in Thailand reported colistin resistance rates of 75.0 and 79.1% in carbapenem-resistant *E. coli* and *K. pneumoniae* isolates, respectively (Eiamphungporn et al., 2018). The 13 carbapenem-resistant *mcr-1*-harboring CRE isolates described here showed a high susceptibility (>50%) to the antibiotics amikacin, fosfomycin, and nitrofurantoin. In contrast, the human *mcr-1*-harboring CRE isolate from China was reported to be highly susceptible only to tigecycline, amikacin, and aztreonam (Huang et al., 2020), whereas the isolate from the United States was susceptible to more antibiotics, including amikacin, aztreonam, gentamicin, nitrofurantoin, tigecycline, and trimethoprim-sulfamethoxazole (Mediavilla et al., 2016).

Polymyxins, including colistin, were reintroduced into human medical practice by the WHO in 2012 (World Health Organization, 2012). In China, this antibiotic was approved for clinical use in the treatment of bacterial infections in 2017. Since then, the relative prevalence of CRE carrying *mcr* genes increased from 0.41 to 1.38% (Huang et al., 2020). A study in Singapore revealed that prior exposure to polymyxin (adjusted OR, 21.31; 95% CI, 3.04–150.96) and carbapenem (OR 3.74; CI 1.13–12.44) were independent risk factors for polymyxin-resistant CRE among hospitalized patients (Teo et al., 2019). A study in Thailand demonstrated that chronic kidney diseases (OR 3.95; CI 1.26–12.32) and exposure to antimicrobials for less than 3 months (OR 2.29; CI 0.29–18.21) were risk factors associated with infections by *mcr-1*-carrying Enterobacteriaceae (Shanmugakani et al., 2019). In patients infected with polymyxin-resistant CRE, the 30-day all-cause in-hospital mortality was 50.0% compared with a 38.1% mortality in patients with polymyxin-susceptible CRE (Teo et al., 2019). Therefore, minimizing the use of polymyxin and carbapenem is strongly recommended.

The findings of the current study provide comprehensive insights into the prevalence of *mcr*-carrying CRE in patients in Thailand. In general, *mcr-1* was present in *E. coli* and *K. pneumoniae* isolates. The co-occurrence of two *mcr* genes was also demonstrated in CRE isolated from patients. To slow the emergence of XDR or PDR strains, priority should be given to strengthening official surveillance, active control, and prevention efforts as well as minimizing the dissemination of *mcr* genes among CRE isolates in humans.

DATA AVAILABILITY STATEMENT

The datasets generated for this study can be found in the Raw sequencing data were deposited in the Sequence Read Archive (SRA) of NCBI under the BioProject ID PRJNA380676.

ETHICS STATEMENT

The Human Research Ethics Committee of Department of Medical Sciences, Ministry of Public Health, reviewed this study and judged that the protocol constituted routine public health

activities and therefore did not involve human subject research. Written informed consent for participation was not required for this study in accordance with the national legislation and the institutional requirements.

AUTHOR CONTRIBUTIONS

WP and AK conceived and designed the study, performed the data analysis, drafted the manuscript, and performed critical revisions of the manuscript for intellectual content. WK performed the laboratory experiments and analyzed the data. RU performed the statistical analysis and critical revision of the manuscript for intellectual content. All the authors read, edited, and approved the final manuscript.

FUNDING

This work was supported by the National Institute of Health, Department of Medical Sciences, Ministry of Public Health, Thailand, and the Division of Global Health Protection, Thailand MoPH–U.S. CDC Collaboration.

ACKNOWLEDGMENTS

We would like to thank Dr. Charatdao Bunthi, Division of Global Health Protection, Thailand MoPH–U.S. CDC Collaboration for critical review of the manuscript and the Kasetsart University Research and Development Institute (KURDI), Bangkok, Thailand for English-editing assistance. We also thank Suzanne Leech, Ph.D., from Edanz Group (https://en-author-services.edanzgroup.com/ac) for editing the draft of this manuscript.

SUPPLEMENTARY MATERIAL

The Supplementary Material for this article can be found online at: https://www.frontiersin.org/articles/10.3389/fmicb.2020.586368/full#supplementary-material

REFERENCES

Abbott, S. (2011). "*Klebsiella*, *Enterobacter*, *Citrobacter*, *Serratia*, *Plesiomonas*, and other Enterobacteriaceae," in Manual of Clinical Microbiology, 10th Edn, Vol. 2, eds J. Versalovic, K. C. Carroll, G. Funke, J. H. Jorgensen, M. L. Landry, and D. W. Warnock, (Washington, DC: ASM Press), 639–657.

Alcock, B. P., Raphenya, A. R., Lau, T., Tsang, K. K., Bouchard, M., Edalatmand, A., et al. (2020). CARD 2020: antibiotic resistome surveillance with the comprehensive antibiotic resistance database. *Nucleic Acids Res.* 48, D517–D525. doi: 10.1093/nar/gkz935

Arabaci, Ç, Dal, T., Başyiğit, T., Genişel, N., and Durmaz, R. (2019). Investigation of carbapenemase and *mcr-1* genes in carbapenem-resistant *Klebsiella pneumoniae* isolates. *J. Infect. Dev. Ctries* 13, 504–509. doi: 10.3855/jidc.11048

Barchiesi, J., Espariz, M., Checa, S. K., and Soncini, F. C. (2009). Downregulation of RpoN-controlled genes protects *Salmonella* cells from killing by the cationic antimicrobial peptide polymyxin B. *FEMS Microbiol. Lett.* 291, 73–79. doi: 10.1111/j.1574-6968.2008.01437.x

Beghain, J., Bridier-Nahmias, A., Le Nagard, H., Denamur, E., and Clermont, O. (2018). ClermonTyping: an easy-to-use and accurate in silico method for *Escherichia* genus strain phylotyping. *Microb. Genom.* 4:e000192. doi: 10.1099/mgen.0.000192

Bertels, F., Silander, O. K., Pachkov, M., Rainey, P. B., and van Nimwegen, E. (2014). Automated reconstruction of whole-genome phylogenies from short-sequence reads. *Mol. Biol. Evol.* 31, 1077–1088. doi: 10.1093/molbev/msu088

Carattoli, A., Zankari, E., García-Fernández, A., Voldby Larsen, M., Lund, O., Villa, L., et al. (2014). In silico detection and typing of plasmids using PlasmidFinder and plasmid multilocus sequence typing. *Antimicrob. Agents Chemother.* 58, 3895–3903. doi: 10.1128/AAC.02412-14

Cheng, Y. H., Lin, T. L., Lin, Y. T., and Wang, J. T. (2016). Amino acid substitutions of CrrB responsible for resistance to colistin through CrrC in *Klebsiella pneumoniae*. *Antimicrob. Agents Chemother.* 60, 3709–3716. doi: 10.1128/AAC.00009-16

Choi, Y., Lee, J. Y., Lee, H., Park, M., Kang, K., Lim, S. K., et al. (2020). Comparison of fitness cost and virulence in chromosome- and plasmid-mediated colistin-resistant *Escherichia coli*. *Front. Microbiol.* 11:798. doi: 10.3389/fmicb.2020.00798

Clermont, O., Christenson, J. K., Denamur, E., and Gordon, D. M. (2013). The clermont *Escherichia coli* phylo-typing method revisited: improvement of specificity and detection of new phylo-groups. *Environ. Microbiol. Rep.* 5, 58–65. doi: 10.1111/1758-2229.12019

Clermont, O., Dixit, O. V. A., Vangchhia, B., Condamine, B., Dion, S., Bridier-Nahmias, A., et al. (2019). Characterization and rapid identification of phylogroup G in *Escherichia coli*, a lineage with high virulence and antibiotic resistance potential. *Environ. Microbiol.* 21, 3107–3117. doi: 10.1111/1462-2920.14713

Clinical and Laboratory Standards Institute, (2020). *Performance Standards for Antimicrobial Susceptibility Testing:* CLSI Document M100-S30, 30th Edn. Wayne, PA: Clinical and Laboratory Standards Institute.

Eiamphungporn, W., Yainoy, S., Jumderm, C., Tan-Arsuwongkul, R., Tiengrim, S., and Thamlikitkul, V. (2018). Prevalence of the colistin resistance gene *mcr-1* in colistin-resistant *Escherichia coli* and *Klebsiella pneumoniae* isolated from humans in Thailand. *J. Glob. Antimicrob. Resist.* 15, 32–35. doi: 10.1016/j.jgar.2018.06.007

Elbediwi, M., Li, Y., Paudyal, N., Pan, H., Li, X., Xie, S., et al. (2019). Global burden of colistin-resistant bacteria: mobilized colistin resistance genes study (1980-2018). *Microorganisms.* 7:E461. doi: 10.3390/microorganisms7100461

Feng, Y., Zou, S., Chen, H., Yu, Y., and Ruan, Z. (2020). BacWGSTdb 2.0: a one-stop repository for bacterial whole-genome sequence typing and source tracking. *Nucleic Acids Res.* 3:gkaa821. doi: 10.1093/nar/gkaa821

Gharaibeh, M. H., and Shatnawi, S. Q. (2019). An overview of colistin resistance, mobilized colistin resistance genes dissemination, global responses, and the alternatives to colistin: a review. *Vet. World* 12, 1735–1746. doi: 10.14202/vetworld.2019

Hadjadj, L., Baron, S. A., Olaitan, A. O., Morand, S., and Rolain, J. M. (2019). Co-occurrence of variants of *mcr-3* and *mcr-8* Genes in a *Klebsiella pneumoniae* isolate from Laos. *Front. Microbiol.* 10:2720. doi: 10.3389/fmicb.2019.02720

Hatrongjit, R., Kerdsin, A., Akeda, Y., and Hamada, S. (2018). Detection of plasmid-mediated colistin-resistant and carbapenem-resistant genes by multiplex PCR. *MethodsX* 5, 532–536. doi: 10.1016/j.mex.2018.05.016

Huang, H., Dong, N., Shu, L., Lu, J., Sun, Q., Chan, E. W., et al. (2020). Colistin-resistance gene *mcr* in clinical carbapenem-resistant *Enterobacteriaceae* strains in China, 2014-2019. *Emerg. Microbes Infect.* 9, 237–245. doi: 10.1080/22221751.2020.1717380

Joensen, K. G., Scheutz, F., Lund, O., Hasman, H., Kaas, R. S., Nielsen, E. M., et al. (2014). Real-time whole-genome sequencing for routine typing, surveillance, and outbreak detection of verotoxigenic *Escherichia coli*. *J. Clin. Microbiol.* 52, 1501–1510. doi: 10.1128/JCM.03617-13

Kamjumphol, W., Wongboot, W., Suebwongsa, N., Kluabwang, P., Chantaroj, S., and Okada, K. (2019). Draft genome sequence of a colistin-resistant *Escherichia coli* ST226: a clinical strain harbouring an *mcr-1* variant. *J. Glob. Antimicrob. Resist.* 16, 168–169. doi: 10.1016/j.jgar.2019.01.009

Kananizadeh, P., Oshiro, S., Watanabe, S., Iwata, S., Kuwahara-Arai, K., Shimojima, M., et al. (2020). Emergence of carbapenem-resistant and colistin-susceptible *Enterobacter cloacae* complex co-harboring bla_{IMP-1} and *mcr-9* in Japan. *BMC Infect. Dis.* 20:282. doi: 10.1186/s12879-020-05021-7

Kempf, I., Jouy, E., and Chauvin, C. (2016). Colistin use and colistin resistance in bacteria from animals. *Int. J. Antimicrob. Agents* 48, 598–606. doi: 10.1016/j.ijantimicag.2016.09.016

Kerdsin, A., Deekae, S., Chayangsu, S., Hatrongjit, R., Chopjitt, P., Takeuchi, D., et al. (2019). Genomic characterization of an emerging bla_{KPC-2} carrying *Enterobacteriaceae* clinical isolates in Thailand. *Sci. Rep.* 9:18521. doi: 10.1038/s41598-019-55008-x

Kumar, S., Stecher, G., Li, M., Knyaz, C., and Tamura, K. (2018). Mega X: molecular evolutionary genetics analysis across computing platforms. *Mol. Biol. Evol.* 35, 1547–1549. doi: 10.1093/molbev/msy096

Larsen, M. V., Cosentino, S., Lukjancenko, O., Saputra, D., Rasmussen, S., Hasman, H., et al. (2014). Benchmarking of methods for genomic taxonomy. *J. Clin. Microbiol.* 52, 1529–1539. doi: 10.1128/JCM.02981-13

Larsen, M. V., Cosentino, S., Rasmussen, S., Friis, C., Hasman, H., Marvig, R. L., et al. (2012). Multilocus sequence typing of total-genome-sequenced bacteria. *J. Clin. Microbiol.* 50, 1355–1361. doi: 10.1128/JCM.06094-11

Letunic, I., and Bork, P. (2016). Interactive tree of life (iTOL) v3: an online tool for the display and annotation of phylogenetic and other trees. *Nucleic Acids Res.* 44, W242–W245. doi: 10.1093/nar/gkw290

Liu, Y. Y., Wang, Y., Walsh, T. R., Yi, L. X., Zhang, R., Spencer, J., et al. (2016). Emergence of plasmid-mediated colistin resistance mechanism MCR-1 in animals and human beings in China: a microbiological and molecular biological study. *Lancet Infect. Dis.* 16, 161–168. doi: 10.1016/S1473-3099(15)00424-7

Malchione, M. D., Torres, L. M., Hartley, D. M., Koch, M., and Goodman, J. L. (2019). Carbapenem and colistin resistance in *Enterobacteriaceae* in Southeast Asia: review and mapping of emerging and overlapping challenges. *Int. J. Antimicrob. Agents* 54, 381–399. doi: 10.1016/j.ijantimicag.2019.07.019

Mediavilla, J. R., Patrawalla, A., Chen, L., Chavda, K. D., Mathema, B., Vinnard, C., et al. (2016). Colistin- and carbapenem-resistant *Escherichia coli* harboring *mcr-1* and bla_{NDM-5}, causing a complicated urinary tract infection in a patient from the United States. *mBio* 7:e01191-16. doi: 10.1128/mBio.01191-16

Meletis, G., and Skoura, L. (2018). Polymyxin resistance mechanisms: from intrinsic resistance to *mcr* genes. *Recent Pat. Antiinfect. Drug Discov.* 13, 198–206. doi: 10.2174/1574891X14666181126142704

Mendes, A. C., Novais, Â, Campos, J., Rodrigues, C., Santos, C., Antunes, P., et al. (2018). *mcr-1* in carbapenemase-producing *Klebsiella pneumoniae* with hospitalized patients, Portugal, 2016-2017. *Emerg. Infect. Dis.* 24, 762–766. doi: 10.3201/eid2404.171787

Nadimpalli, M. L., de Lauzanne, A., Phe, T., Borand, L., Jacobs, J., Fabre, L., et al. (2019). *Escherichia coli* ST410 among humans and the environment in Southeast Asia. *Int. J. Antimicrob. Agents* 54, 228–232. doi: 10.1016/j.ijantimicag.2019.05.024

Novović, K., Trudić, A., Brkić, S., Vasiljević, Z., Kojić, M., Medić, D., et al. (2017). Molecular epidemiology of colistin-resistant, carbapenemase-producing *Klebsiella pneumoniae* in Serbia from 2013 to 2016. *Antimicrob. Agents Chemother.* 61:e02550-16. doi: 10.1128/AAC.02550-16

Olaitan, A. O., Chabou, S., Okdah, L., Morand, S., and Rolain, J. M. (2016). Dissemination of the *mcr-1* colistin resistance gene. *Lancet Infect. Dis.* 16:147. doi: 10.1016/S1473-3099(15)00540-X

Olaitan, A. O., Diene, S. M., Kempf, M., Berrazeg, M., Bakour, S., Gupta, S. K., et al. (2014a). Worldwide emergence of colistin resistance in *Klebsiella pneumoniae* from healthy humans and patients in Lao PDR, Thailand, Israel, Nigeria and France owing to inactivation of the PhoP/PhoQ regulator mgrB: an epidemiological and molecular study. *Int. J. Antimicrob. Agents* 44, 500–507. doi: 10.1016/j.ijantimicag.2014.07.020

Olaitan, A. O., Morand, S., and Rolain, J. M. (2014b). Mechanisms of polymyxin resistance: acquired and intrinsic resistance in bacteria. *Front. Microbiol.* 5:643. doi: 10.3389/fmicb.2014.00643

Palmieri, M., D'Andrea, M. M., Pelegrin, A. C., Mirande, C., Brkic, S., Cirkovic, I., et al. (2020). Genomic epidemiology of carbapenem- and colistin-resistant *Klebsiella pneumoniae* isolates from Serbia: predominance of ST101 strains carrying a novel OXA-48 plasmid. *Front. Microbiol.* 11:294. doi: 10.3389/fmicb.2020.00294

Paveenkittiporn, W., Kerdsin, A., Chokngam, S., Bunthi, C., Sangkitporn, S., and Gregory, C. J. (2017). Emergence of plasmid-mediated colistin resistance and New Delhi metallo-β-lactamase genes in extensively drug-resistant *Escherichia coli* isolated from a patient in Thailand. *Diagn. Microbiol. Infect. Dis.* 87, 157–159. doi: 10.1016/j.diagmicrobio.2016.11.005

Quan, J., Li, X., Chen, Y., Jiang, Y., Zhou, Z., Zhang, H., et al. (2017). Prevalence of *mcr-1* in *Escherichia coli* and *Klebsiella pneumoniae* recovered from bloodstream infections in China: a multicentre longitudinal study. *Lancet Infect. Dis.* 17, 400–410. doi: 10.1016/S1473-3099(16)30528-X

Rebelo, A. R., Bortolaia, V., Kjeldgaard, J. S., Pedersen, S. K., Leekitcharoenphon, P., Hansen, I. M., et al. (2018). Multiplex PCR for detection of plasmid-mediated colistin resistance determinants, *mcr-1, mcr-2, mcr-3, mcr-4* and *mcr-5* for surveillance purposes. *Euro. Surveill.* 23:17-00672. doi: 10.2807/1560-7917.ES.2018.23.6.17-00672

Rodrigues, C., Machado, E., Ramos, H., Peixe, L., and Novais, Â (2014). Expansion of ESBL-producing *Klebsiella pneumoniae* in hospitalized patients: a successful story of international clones (ST15, ST147, ST336) and epidemic plasmids (IncR, IncFIIK). *Int. J. Med. Microbiol.* 304, 1100–1108. doi: 10.1016/j.ijmm.2014.08.003

Roer, L., Overballe-Petersen, S., Hansen, F., Schønning, K., Wang, M., Røder, B. L., et al. (2018). *Escherichia coli* sequence type 410 is causing new international high-risk clones. *mSphere* 3:e00337-18. doi: 10.1128/mSphere.00337-18

Shanmugakani, R. K., Akeda, Y., Sugawara, Y., Laolerd, W., Chaihongsa, N., Sirichot, S., et al. (2019). PCR-dipstick-oriented surveillance and characterization of *mcr-1*- and carbapenemase-carrying *Enterobacteriaceae* in a Thai hospital. *Front. Microbiol.* 10:149. doi: 10.3389/fmicb.2019.00149

Srijan, A., Margulieux, K. R., Ruekit, S., Snesrud, E., Maybank, R., Serichantalergs, O., et al. (2018). Genomic characterization of nonclonal *mcr-1*-positive multidrug-resistant *Klebsiella pneumoniae* from clinical samples in Thailand. *Microb. Drug Resist.* 24, 403–410. doi: 10.1089/mdr.2017.0400

Teo, J. Q., Chang, C. W., Leck, H., Tang, C. Y., Lee, S. J., Cai, Y., et al. (2019). Risk factors and outcomes associated with the isolation of polymyxin B and carbapenem-resistant *Enterobacteriaceae* spp.: a case-control study. *Int. J. Antimicrob. Agents* 53, 657–662. doi: 10.1016/j.ijantimicag.2019.03.011

Wang, C., Feng, Y., Liu, L., Wei, L., Kang, M., and Zong, Z. (2020). Identification of novel mobile colistin resistance gene *mcr-10*. *Emerg. Microbes Infect.* 9, 508–516. doi: 10.1080/22221751.2020.1732231

Wang, X., Wang, Y., Zhou, Y., Li, J., Yin, W., Wang, S., et al. (2018). Emergence of a novel mobile colistin resistance gene, *mcr-8*, in NDM-producing *Klebsiella pneumoniae*. *Emerg. Microbes Infect.* 7:122. doi: 10.1038/s41426-018-0124-z

Wick, R. R., Heinz, E., Holt, K. E., and Wyres, K. L. (2018). Kaptive Web: user-friendly capsule and lipopolysaccharide serotype prediction for *Klebsiella* genomes. *J. Clin. Microbiol.* 56:e00197-18. doi: 10.1128/JCM.00197-18

World Health Organization, (2012). *Critically Important Antimicrobials for Human Medicine, 3rd Revision*. Geneva: WHO.

World Health Organization, (2017). *Global Priority List of Antibiotic-Resistant Bacteria to Guide Research, Discovery, and deveLopment of New Antibiotics*. Geneva: WHO.

Wright, M. S., Suzuki, Y., Jones, M. B., Marshall, S. H., Rudin, S. D., van Duin, D., et al. (2015). Genomic and transcriptomic analyses of colistin-resistant clinical isolates of *Klebsiella pneumoniae* reveal multiple pathways of resistance. *Antimicrob. Agents Chemother.* 59, 536–543. doi: 10.1128/AAC.04037-14

Wu, R., Yi, L. X., Yu, L. F., Wang, J., Liu, Y., Chen, X., et al. (2018). Fitness advantage of *mcr-1*-bearing IncI2 and IncX4 plasmids *in vitro*. *Front. Microbiol.* 9:331. doi: 10.3389/fmicb.2018.00331

Yang, Y. Q., Li, Y. X., Lei, C. W., Zhang, A. Y., and Wang, H. N. (2018). Novel plasmid-mediated colistin resistance gene *mcr-7.1* in *Klebsiella pneumoniae*. *J. Antimicrob. Chemother.* 73, 1791–1795. doi: 10.1093/jac/dky111

Yuan, Y., Li, Y., Wang, G., Li, C., Xiang, L., She, J., et al. (2019). Coproduction of *mcr-9* and NDM-1 by colistin-resistant *Enterobacter hormaechei* isolated from bloodstream infection. *Infect. Drug Resist.* 12, 2979–2985. doi: 10.2147/IDR.S217168

Zankari, E., Hasman, H., Cosentino, S., Vestergaard, M., Rasmussen, S., Lund, O., et al. (2012). Identification of acquired antimicrobial resistance genes. *J. Antimicrob. Chemother.* 67, 2640–2644. doi: 10.1093/jac/dks261

Zhong, L. L., Phan, H. T. T., Shen, C., Vihta, K. D., Sheppard, A. E., Huang, X., et al. (2018). High rates of human fecal carriage of mcr-1-positive multidrug-resistant *Enterobacteriaceae* emerge in China in association with successful plasmid families. *Clin. Infect. Dis.* 66, 676–685. doi: 10.1093/cid/cix885

Conflict of Interest: The authors declare that the research was conducted in the absence of any commercial or financial relationships that could be construed as a potential conflict of interest.

frontiers in Microbiology

METHODS
published: 15 January 2021
doi: 10.3389/fmicb.2020.609856

Evaluation of the Immunochromatographic NG-Test Carba 5, RESIST-5 O.O.K.N.V., and IMP *K*-SeT for Rapid Detection of KPC-, NDM-, IMP-, VIM-type, and OXA-48-like Carbapenemase Among *Enterobacterales*

*Renru Han[1,2], Yan Guo[1,2], Mingjia Peng[1,2], Qingyu Shi[1,2], Shi Wu[1,2], Yang Yang[1,2], Yonggui Zheng[1,2], Dandan Yin[1,2] and Fupin Hu[1,2]**

[1] Institute of Antibiotics, Huashan Hospital, Fudan University, Shanghai, China, [2] Key Laboratory of Clinical Pharmacology of Antibiotics, Ministry of Health, Shanghai, China

OPEN ACCESS

Edited by:
Anne-Catrin Uhlemann, Columbia University Irving Medical Center, United States

Reviewed by:
Miriam Cordovana, Bruker Daltonik GmbH, Germany
Wonkeun Song, Hallym University, South Korea

***Correspondence:**
Fupin Hu
hufupin@fudan.edu.cn

Specialty section:
This article was submitted to Antimicrobials, Resistance and Chemotherapy, a section of the journal Frontiers in Microbiology

Received: 24 September 2020
Accepted: 30 November 2020
Published: 15 January 2021

Citation:
Han R, Guo Y, Peng M, Shi Q, Wu S, Yang Y, Zheng Y, Yin D and Hu F (2021) Evaluation of the Immunochromatographic NG-Test Carba 5, RESIST-5 O.O.K.N.V., and IMP K-SeT for Rapid Detection of KPC-, NDM-, IMP-, VIM-type, and OXA-48-like Carbapenemase Among Enterobacterales. Front. Microbiol. 11:609856. doi: 10.3389/fmicb.2020.609856

Background: *Enterobacterales* are the most common pathogens for nosocomial infections. The emergence and spread of KPC, NDM, and OXA-48-like carbapenemase-producing *Enterobacterales* with their extensively drug-resistant characteristics have posed great threats to public health. This study aimed to evaluate the performance of NG-test Carba 5, RESIST-5 O.O.K.N.V., and IMP *K*-SeT for rapid detection of five carbapenemases (KPC, NDM, VIM, IMP, and OXA-48-like) among *Enterobacterales*.

Methods: A total of 186 carbapenem-resistant *Enterobacterales* clinical isolates and 29 reference strains were used in this study. Carbapenemase genes were confirmed by PCR and DNA sequencing. The sensitivities and specificities of these assays were calculated utilizing the VassarStats software.

Results: For clinical isolates, the NG-test Carba 5 detected KPC, NDM, OXA-48-like, IMP, and VIM in less than 15 min with the sensitivity and specificity of 100% and 100%, respectively. The RESIST-5 O.O.K.N.V. detected KPC, NDM, OXA-48-like, and VIM with the sensitivity and specificity of 99.4 and 100%. The IMP *K*-SeT detected all of the IMP producers (6/6). For reference strains, the sensitivity and specificity of NG-test Carba 5, RESIST-5 O.O.K.N.V., and IMP *K*-SeT were all 100 and 100%, respectively.

Conclusion: As efficient, rapid, and convenient diagnostic methods, NG-test Carba 5, RESIST-5 O.O.K.N.V., and IMP *K*-SeT could help to simplify the complex routine workflow for detecting carbapenemases. Rapid and accurate identification of carbapenemase is of significance for both epidemiological and infection control purposes.

Keywords: immunochromatographic assay, carbapenem-resistant *Enterobacterales*, carbapenemase, NG-test Carba 5, RESIST-5 O.O.K.N.V, IMP K-SeT

INTRODUCTION

The emergence and dissemination of carbapenemase-producing *Enterobacterales* (CPE) pose a global health threat (Nordmann et al., 2012a). As the ability of carbapenemases to hydrolyze all β-lactam antibiotics leads to few antibiotics retaining activity against CPE, infections caused by CPE are usually burdened by high mortality and poor prognoses (Falagas et al., 2014; Feil, 2016). Tigecycline, colistin, and ceftazidime-avibactam are the only available antimicrobial agents for the treatment of infections caused by CPE in China. However, unlike tigecycline and colistin, the activity of ceftazidime-avibactam is varied to different CPE. The *in vitro* studies show that ceftazidime-avibactam has excellent *in vitro* activity against ESBL-, AmpC-, KPC-, and OXA-48-producing *Enterobacterales*, but has no activity against metallo-beta-lactamases *Enterobacterales* (Shirley, 2018; Yin et al., 2019). As reported, for the treatment of carbapenem-resistant *Klebsiella pneumoniae* bloodstream infections, initial adequate antibiotic therapy resulted in the only independent factor able to protect against death (Micozzi et al., 2017). Therefore, rapid and accurate identification of carbapenemases is critical for both epidemiological and infection control purposes.

Recently, rapid diagnostic tests, NG-test Carba 5 immunochromatographic assay (NG Biotech, Guipry, France), and RESIST-5 O.O.K.N.V. (CORIS, BioConcept, Gembloux, Belgium) have been developed to detect the five main carbapenemases, namely, KPC, NDM, OXA-48-like, IMP, and VIM. To date, several studies have evaluated the performance of NG-test Carba 5 and demonstrated that it performed well on bacterial colonies and positive blood cultures with overall sensitivity and specificity that ranged from 97.3 to 100% and 95.3 to 100%, respectively (Boutal et al., 2018; Hopkins et al., 2018; Bodendoerfer et al., 2019; Giordano et al., 2019). The RESIST-5 O.O.K.N.V. detected KPC-type and OXA-48-like carbapenemases from blood cultures with a sensitivity of 100% for both, but 50.0 and 52.2% for NDM- and VIM-type carbapenemases, respectively (Bianco et al., 2020). Comparative studies evaluating the performance of different lateral flow chromatographic assays to detect carbapenemase from bacterial colonies are lacking in China. In this study, we investigated the performance of NG-test Carba 5, RESIST-5 O.O.K.N.V., and IMP *K*-SeT assay to detect carbapenemases among CPE.

MATERIALS AND METHODS

Strains

From January 2016 to December 2018, 186 non-duplicate clinical isolates were collected from 32 hospitals of 22 provinces or cities across China, and 29 reference strains were purchased from the American Type Culture Collection[1]. These clinical isolates were resistant to at least one of the carbapenem antibiotics (ertapenem, meropenem, or imipenem), including 124 *K. pneumoniae,* 26 *Escherichia coli,* 23 *Enterobacter cloacae,* 5 *Klebsiella oxytoca*, 2 *Citrobacter freundi*, 2 *Enterobacter aerogenes*, 2 *Serratia marcescens*, 1 *Morganella morganii*, and 1 *Providencia rettgeri*. Twenty-nine reference strains (including 17 *K. pneumoniae*, 8 *E. coli*, 1 *E. cloacae*, 1 *K. oxytoca*, 1 *P. rettgeri*, and 1 *Enterobacter hormaechei*) with or without carbapenemase were involved in this study (**Table 1**). All tested isolates were identified to the species level using matrix-assisted laser desorption/ionization-time of flight mass spectrometry (bioMérieux, France).

Detection of Carbapenemase genes

For 186 carbapenem-resistant *Enterobacterales* (CRE) clinical strains, carbapenemase genes (bla_{KPC}, bla_{NDM}, $bla_{OXA-48-like}$, bla_{IMP}, and bla_{VIM}) were detected by polymerase chain reaction (PCR) with specific primers and conditions as described previously (Poirel et al., 2011). The positive PCR amplicons were sequenced and compared with the reported sequences from GenBank by Blast[2]. As a result, 172 were positive for carbapenemase genes, including bla_{KPC-2} (n = 70), bla_{NDM-1} (n = 35), bla_{NDM-5} (n = 23), bla_{NDM-7} (n = 1), bla_{NDM-9} (n = 1), $bla_{OXA-232}$ (n = 20), $bla_{OXA-181}$ (n = 2), bla_{OXA-48} (n = 2), bla_{IMP-4} (n = 5), bla_{IMP-6} (n = 1), bla_{VIM} (n = 1), bla_{KPC-2} plus bla_{NDM-1} (7/7), bla_{KPC-2} plus bla_{NDM-5} (1/1), bla_{NDM-5} plus bla_{OXA-48} (1/1), bla_{NDM-1} plus bla_{IMP-4} (1/1), and bla_{NDM-1} plus bla_{IMP-6} (1/1). Fourteen CRE clinical strains were carbapenemase-negative.

Immunochromatographic Assays

The NG-Test Carba 5 assay consists of an independent cassette (targets KPC-, NDM-, VIM-, and IMP-type and OXA-48-like five main carbapenemases). RESIST-5 O.O.K.N.V. consists of two independent K-SeTs (one for the detection of OXA-163, OXA-48-like, and KPC; another for the detection of VIM and NDM). Both cassettes are provided in a single package and are to be used in parallel on the same bacterial lysis preparation. IMP K-SeT consists of a K-SeT for the detection of IMP metallo-β-lactamase, which was performed as a complementary test of RESIST-5 O.O.K.N.V.

These tests were performed according to the manufacturer's instructions in parallel. Firstly, one single isolated colony of overnight growth was harvested from the plate to an Eppendorf tube or tube with extraction buffer and suspended thoroughly to perform the lysis step. Subsequently, approximately 100 μl of the mixture was loaded on the sample region of the cassette and allowed to migrate for 15 min. Finally, the results were read until the control line turned red in the control region and then recorded whether the lines turned red in the test region of the cassette 15 min later.

Statistical Analysis

The sensitivity and specificity of the assay and upper and lower limits of the 95% confidence intervals (CIs) were calculated utilizing the VassarStats software[3].

[1]https://www.atcc.org

[2]www.ncbi.nlm.nih.gov/blast/

[3]http://www.vassarstats.net/

TABLE 1 | Reference strains used in this study.

Reference Strains	Species	β-lactamase genes	NG-test Carba 5	RESIST-5O.O.K.N.V. /IMP *K*-SeT
ATCC BAA 2146	*K. pneumoniae*	NDM-1	NDM	NDM
ATCC BAA 2452	*E. coli*	NDM-1	NDM	NDM
ATCC BAA 2469	*E. coli*	NDM-1	NDM	NDM
ATCC BAA 2470	*K. pneumoniae*	NDM-1	NDM	NDM
ATCC BAA 2471	*E. coli*	NDM-1	NDM	NDM
ATCC BAA 2473	*K. pneumoniae*	NDM-1	NDM	NDM
ATCC BAA 1705	*K. pneumoniae*	KPC-2	KPC	KPC
ATCC BAA 1899	*K. pneumoniae*	KPC-2	KPC	KPC
ATCC BAA 1900	*K. pneumoniae*	KPC-2	KPC	KPC
ATCC BAA 1902	*K. pneumoniae*	KPC-2	KPC	KPC
ATCC BAA 1903	*K. pneumoniae*	KPC-2	KPC	KPC
ATCC BAA 1904	*K. pneumoniae*	KPC-2	KPC	KPC
ATCC BAA 1905	*K. pneumoniae*	KPC-2	KPC	KPC
ATCC BAA 2341	*E. cloacae*	KPC-2	KPC	KPC
ATCC BAA 2342	*K. pneumoniae*	KPC-2	KPC	KPC
ATCC BAA 2343	*K. pneumoniae*	KPC-2	KPC	KPC
ATCC BAA 2344	*K. pneumoniae*	KPC-2	KPC	KPC
ATCC BAA 2082	*E. hormaechei*	KPC-2	KPC	KPC
ATCC BAA 2340	*E. coli*	KPC-2	KPC	KPC
ATCC BAA 2078	*K. pneumoniae*	KPC-2	KPC	KPC
ATCC BAA 2523	*E. coli*	OXA-48	OXA	OXA
ATCC BAA 2524	*K. pneumoniae*	OXA-48	OXA	OXA
ATCC BAA 2525	*P. rettgeri*	OXA-181	OXA	OXA
ATCC 51983	*K. oxytoca*	ESBL	NEG	NEG
ATCC BAA 204	*E. coli*	ESBL	NEG	NEG
ATCC BAA 198	*E. coli*	ESBL	NEG	NEG
NCTC 13440	*K. pneumoniae*	VIM-1	VIM	VIM
NCTC 13476	*E. coli*	IMP-1/70	IMP	IMP
NCTC 13439	*K. pneumoniae*	VIM-1	VIM	VIM

RESULTS

The NG-test Carba 5 and RESIST-5 O.O.K.N.V. showed the detection of 100% of KPC-2 (70/70), NDM-5 (23/23), NDM-7 (1/1), VIM (1/1), OXA-232 (20/20), OXA-181 (2/2), and OXA-48 (2/2) with no false positive. This study also demonstrated that 100% of IMP-4 (5/5) and IMP-6 (1/1) were correctly detected by NG-test Carba 5 and IMP *K*-SeT. NG-test Carba 5 showed the detection of 100% of NDM-1 (35/35), whereas RESIST-5 O.O.K.N.V. showed the detection of 97.1% of NDM-1 (34/35) except one *P. rettgeri*. Moreover, NG-test Carba 5 and RESIST-5 O.O.K.N.V. were able to detect double carbapenemases-producers simultaneously, and the results showed 100% of KPC-2 plus NDM-1 (7/7)-, KPC-2 plus NDM-5 (1/1)-, and NDM-5 plus OXA-48 (1/1)-producing isolates with two red positive lines in the test region. All of the non-carbapenemase (0/14) producers were negative in the tests (**Table 2**). Overall, the sensitivity and specificity of NG-test Carba 5 to detect five main carbapenemases were both 100%. The sensitivity and specificity of RESIST-5 O.O.K.N.V. were 99.4 and 100%, respectively (**Table 2**).

For the 29 reference strains, NG-test Carba 5, RESIST-5 O.O.K.N.V., and IMP *K*-SeT detected all KPC-2 (14/14), NDM-1 (6/6), OXA-48 (2/2), OXA-181 (1/1), VIM-1 (2/2), and IMP-1 producers (1/1) (**Table 1**). Three ESBL producers were negative without cross-reaction. The overall sensitivity and specificity of NG-test Carba 5, RESIST-5 O.O.K.N.V., and IMP *K*-SeT detecting carbapenemases were all 100 and 100%, respectively (**Table 2**).

DISCUSSION

Of note, the rapid detection and identification of carbapenemase can help to prevent the spread and infection control of carbapenemase-producing isolates in health facilities (Boutal et al., 2018; Takissian et al., 2019). A nationwide survey indicated that $bla_{\text{KPC-2}}$ (57% and 627/1,105) and bla_{NDM} (31% and 343/1,105) were the most common carbapenemase genes among carbapenem-resistant *Enterobacterales* clinical isolates in China (Zhang et al., 2017; Han et al., 2020). Rapid identification of the carbapenemase type can help to guide therapy for the treatment of infection caused by carbapenemase-producing isolates. As reported, most KPC-2 or OXA-48-like carbapenemase-producing isolates are susceptible to ceftazidime-avibactam (Falcone and Paterson, 2016; Bassetti et al., 2018; Stewart et al., 2018; Zou et al., 2019). On the contrary, ceftazidime-avibactam has no activities against metallo-β-lactamase (NDM-, VIM-, or IMP-type) producers; thus other therapeutic options have to be considered, such as tigecycline, colistin, or other available antimicrobial agents (Davido et al., 2017; Zusman et al., 2017;

TABLE 2 | Rapid identification of carbapenemases by NG-test Carba 5, RESIST-5 O.O.K.N.V., and IMP *K*-SeT.

Strains	β -lactamase	No. of positive tests/total no. of strains			Sensitivity [% (95% CI)]	Specificity [% (95% CI)]
		NG-test Carba 5	RESIST-5 O.O.K.N.V.	IMP *K*-SeT		
Clinical strains						
	KPC-2	70/70	70/70	0/70	100 (93.5–100)	100 (96.0–100)
	NDM	60/60			100 (92.5–100)	100 (96.3–100)
			59/60	0/60	98.3 (89.7–100)	100 (96.3–100)
	NDM-1	35/35	34/35			
	NDM-5	23/23	23/23			
	NDM-7	1/1	1/1			
	NDM-9	1/1	1/1			
	IMP	6/6	0/6	6/6	100 (51.7–100)	100 (97.4–100)
	IMP-4	5/5	0/5	5/5		
	IMP-6	1/1	0/1	1/1		
	OXA-48-like	24/24	24/24	0/24	100 (82.8–100)	100 (97.1–100)
	OXA-232	20/20	20/20			
	OXA-48	2/2	2/2			
	OXA-181	2/2	2/2			
	VIM-1	1/1	1/1	0/1	100 (5.5–100)	100 (97.5–100)
	Multiple carbapenemases	11/11	11/11	2/11	100 (67.9–100)	100 (97.3–100)
	KPC-2 + NDM-1	7/7	7/7			
	KPC-2 NDM-5	1/1	1/1			
	NDM-5 OXA-48	1/1	1/1			
	NDM-1 IMP-4	1/1	1/1			
	NDM-1 IMP-6	1/1	1/1			
	Carbapenemase-negative	0/14	0/14	0/14		
	Total	172/186			100 (97.3–100)	100 (73.2–100)
			165/186	6/186	99.4 (96.2–100)	100 (80.0–100)
Reference strains						
	KPC-2	14/14	14/14	0/14		
	NDM-1	6/6	6/6	0/6		
	IMP-1/70	1/1	0/1	1/1		
	VIM-1	2/2	2/2	0/2		
	OXA-48-like	3/3	3/3	0/3		
	OXA-48	2/2	2/2			
	OXA-181	1/1	1/1			
	ESBL	0/3	0/3	0/3		
	Total	26/29			100 (84.0–100)	100 (31.0–100)
			25/29	1/1	100 (83.4–100)	100 (39.6–100)

Jayol et al., 2018; Emeraud et al., 2019; Yin et al., 2019; Zou et al., 2019).

Currently, several phenotypic methods have been developed for the detection and identification of carbapenemases. Modified carbapenem inactivation methods (mCIMs) had sensitivities ranging from 93 to 100% and specificities from 97 to 100% for the detection of CPE, and excellent reproducibility was shown across laboratories (Pierce et al., 2017; Tsai et al., 2020). The mCIM and EDTA-CIM detected metallo-carbapenemases with a sensitivity of 89.3% and a specificity of 98.7% (Tsai et al., 2020). The mCIM was easy to perform and interpret for *Enterobacterales*, but time-consuming (overnight incubation). Besides, invalid or uncertain results may occur with some isolates, and certain carbapenemase types are not detected consistently.

Carba NP test detected most carbapenemases with high sensitivities from 73 to 100% among *Enterobacterales*, but with low sensitivity in detecting OXA-48-like carbapenemase producers (Nordmann et al., 2012b; Tijet et al., 2013; Vasoo et al., 2013; Yusuf et al., 2014; Papagiannitsis et al., 2015; Tamma et al., 2017). The modified Carba NP test had a sensitivity of 99% (Tamma et al., 2017). One limitation of the manual versions of the Carba NP test and its variants was frequent reagent preparation due to the short shelf life of the imipenem-containing solution. Other commercially available assays, including the Rapidec Carba NP test, the Neo-Rapid Carb screen, and the Rapid Carb Blue screen have sensitivities ranging from 89 to 98% and specificities approaching 100% (Tamma et al., 2017). Similar to the Carba NP test, the limitations of these commercial

assays are as follows: false-negative results occurred with OXA-48-like carbapenemase and the interpretation of results can be subjective due to slight color changes (Tamma and Simner, 2018). The sensitivites of the modified Hodge test (MHT) have been reported to be between 93 and 98% in KPC producers, but low sensitivites for metallo-beta-lactamases (Girlich et al., 2012; Mathers et al., 2013; Vasoo et al., 2013; Tsai et al., 2020). Reported sensitivities and specificities of MALDI-TOF MS ranged from 77 to 100% and 94 to 100%, respectively, with a turnaround time of within 4 h (Knox et al., 2014; Papagiannitsis et al., 2015; Oho et al., 2020). Carbapenemase inhibition tests with boronic acid derivatives (BA) and dipicolinic acid (DPA)/EDTA were tested in *Enterobacterales*. The sensitivity for identification of class A, B, and OXA-48 carbapenemases was 95, 90, and 100%, with 96 to 100% specificity (van Dijk et al., 2014).

Compared with the phenotypic method, the multiplex immunochromatographic assay for the detection of KPC-, NDM-, VIM-, IMP-, and OXA-48-like carbapenemases was easy to perform and only relatively little hands-on time (no more than 5 min) was required. Several studies assessing the immunochromatographic for the detection of common carbapenemases showed high sensitivity and specificity results in bacteria (Boutal et al., 2018; Hopkins et al., 2018; Bodendoerfer et al., 2019). The NG-test Carba 5 has evaluated the detection of CPE from spiked blood cultures with a sensitivity and specificity of 97.7 to 98.3% and 96.1 to 100%, respectively (Giordano et al., 2019; Takissian et al., 2019). The RESIST-5 O.O.K.N.V. detected KPC-type and OXA-48-like carbapenemases from blood cultures with a high sensitivity of 100%, but with low sensitivities of 50.0 and 52.2% in detecting NDM- and VIM-type carbapenemases, respectively, and the results were quite different from our research of NDM metallo-beta-lactamases (97.1% sensitivity) (Bianco et al., 2020).

The results of our study indicated that the NG-test Carba 5 showed the detection of 100% of KPC-2, NDM, VIM, and OXA-48-like with no false positive. The RESIST-5 O.O.K.N.V. showed 100% detection of KPC-2, OXA-48-like, IMP, and VIM, whereas it showed 97.1% detection of NDM-1 (34/35) with one false-negative result. We speculated that this might be associated with the mean intensity of NDM bands; NG-Test Carba 5 was 2.2 times higher than RESIST-4 O.K.N.V. (Bogaerts et al., 2020). Additionally, NG-test Carba 5, RESIST-5 O.O.K.N.V., and IMP *K-SeT* were also able to detect two carbapenemases simultaneously with a sensitivity of 100%. Of concern, NG-test Carba 5 was not able to distinguish OXA-48-like variants (OXA-48-, OXA- 181-, OXA- 163-, OXA- 232-, and OXA-405-type carbapenemase), and the OXA-163- and the OXA-405-producing strains might be considered as false-negative results for OXA-48-like carbapenemase producers (Boutal et al., 2018; Takissian et al., 2019). In this case, the RESIST-5 O.O.K.N.V. assay could fill this gap by specifically detecting OXA-163 (OXA-48-like variants) with a sensitivity of 100%, which was an updated version of the RESIST-3 O.O.K. *K*-SeT (Coris BioConcept) and the OXA-163/48 *K*-SeT (Coris BioConcept) (Meunier et al., 2016; Pasteran et al., 2016). Due to a lack of OXA-163 producers, we could not evaluate the ability of RESIST-5 O.O.K.N.V. in detecting OXA-163. The limited detection ranges of these assays cover only common carbapenemases, which lead to the neglect of rare carbapenemases like GES, IMI, and GIM.

Our study had three limitations. The first limitation is including only six bla_{IMP}-positive strains and one bla_{VIM}-positive strain. Second, there is a lack of other KPC- and OXA-48-like variant carbapenemases such KPC-3 and OXA-163 in this study; these variants are rare in China. Third, limited non-CPE isolates were used to assess the specificity of the assays, and we need to sufficiently investigate this isolates to evaluate the performance of these assays in this study. Recently, we collected one *K. pneumoniae* harboring a new variant, rare carbapenemase $bla_{\text{KPC-33}}$ (Shi et al., 2020), and we found that immunochromatographic assays cannot detect this new variant. Although other bla_{KPC}-positive strains including $bla_{\text{KPC-3}}$-, $bla_{\text{KPC-33}}$-, or bla_{VIM}-type metallo-β-lactamase positive strains are rare in China, we still need to collect these strains to make a more comprehensive assessment on the performance of immunochromatographic testing for detection of carbapenemases.

CONCLUSION

In conclusion, NG-test Carba 5, RESIST-5 O.O.K.N.V., and IMP *K*-SeT assays could be efficient, rapid, and convenient diagnostic tools for detecting the most common carbapenemases in China. These might help to control the spread of carbapenemase-producing isolates in health facilities.

DATA AVAILABILITY STATEMENT

The original contributions presented in the study are included in the article/supplementary material, further inquiries can be directed to the corresponding author/s.

ETHICS STATEMENT

The study protocol was approved by the Institutional Review Board of Huashan Hospital, Fudan University (Number: 2018-408).

AUTHOR CONTRIBUTIONS

FH designed the study. RH, YG, MP, QS, and SW performed the experimental work. RH, YG, YY, and DY collected the data. FH and RH analyzed the data. All authors read and approved the final manuscript.

FUNDING

This work was supported by the National Natural Science Foundation of China (grant no. 81871690), the China Antimicrobial Surveillance Network (nos. 2018QD099 and 2018QD100), and the National Mega-project for Innovative Drugs (2019ZX09721001-006-004).

REFERENCES

Bassetti, M., Giacobbe, D. R., Giamarellou, H., Viscoli, C., Daikos, G. L., Dimopoulos, G., et al. (2018). Management of KPC-producing *Klebsiella pneumoniae* infections. *Clin. Microbiol. Infect.* 24, 133–144. doi: 10.1016/j.cmi.2017.08.030

Bianco, G., Boattini, M., van Asten, S., Iannaccone, M., Zanotto, E., Zaccaria, T., et al. (2020). RESIST-5 O.O.K.N.V. and NG-Test Carba 5 assays for the rapid detection of carbapenemase-producing Enterobacterales from positive blood cultures: a comparative study. *J. Hosp. Infect.* 105, 162–166. doi: 10.1016/j.jhin.2020.03.022

Bodendoerfer, E., Keller, P. M., and Mancini, S. (2019). Rapid identification of NDM-, KPC-, IMP-, VIM- and OXA-48-like carbapenemase-producing *Enterobacteriales* from blood cultures by a multiplex lateral flow immunoassay. *J Antimicrob Chemother.* 74, 1749–1751. doi: 10.1093/jac/dkz056

Bogaerts, P., Berger, A. S., Evrard, S., and Huang, T. D. (2020). Comparison of two multiplex immunochromatographic assays for the rapid detection of major carbapenemases in Enterobacterales. *J. Antimicrob. Chemother.* 75, 1491–1494. doi: 10.1093/jac/dkaa043

Boutal, H., Vogel, A., Bernabeu, S., Devilliers, K., Creton, E., Cotellon, G., et al. (2018). A multiplex lateral flow immunoassay for the rapid identification of NDM-, KPC-, IMP- and VIM-type and OXA-48-like carbapenemase-producing *Enterobacteriaceae*. *J. Antimicrob. Chemother.* 73, 909–915. doi: 10.1093/jac/dkx521

Davido, B., Fellous, L., Lawrence, C., Maxime, V., Rottman, M., and Dinh, A. (2017). Ceftazidime-Avibactam and Aztreonam, an Interesting Strategy To Overcome beta-Lactam Resistance Conferred by Metallo-beta-Lactamases in *Enterobacteriaceae* and *Pseudomonas aeruginosa*. *Antimicrob. Agents Chemother.* 61:e01008-17. doi: 10.1128/AAC.01008-17

Emeraud, C., Escaut, L., Boucly, A., Fortineau, N., Bonnin, R. A., Naas, T., et al. (2019). Aztreonam plus clavulanate, tazobactam, or avibactam for treatment of infections caused by metallo-beta-lactamase-producing gram-negative bacteria. *Antimicrob. Agents Chemother.* 63:e00010-19. doi: 10.1128/AAC.00010-19

Falagas, M. E., Tansarli, G. S., Karageorgopoulos, D. E., and Vardakas, K. Z. (2014). Deaths attributable to carbapenem-resistant *Enterobacteriaceae* infections. *Emerg. Infect. Dis.* 20, 1170–1175. doi: 10.3201/eid2007.121004

Falcone, M., and Paterson, D. (2016). Spotlight on ceftazidime/avibactam: a new option for MDR Gram-negative infections. *J. Antimicrob. Chemother.* 71, 2713–2722. doi: 10.1093/jac/dkw239

Feil, E. J. (2016). *Enterobacteriaceae*: joining the dots with pan-European epidemiology. *Lancet Infect. Dis.* 17, 118–119. doi: 10.1016/S1473-3099(16)30333-4

Giordano, L., Fiori, B., D'Inzeo, T., Parisi, G., Liotti, F. M., Menchinelli, G., et al. (2019). Simplified testing method for direct detection of carbapenemase-producing organisms from positive blood cultures using the NG-test Carba 5 assay. *Antimicrob. Agents Chemother.* 63:e00550-19. doi: 10.1128/AAC.00550-19

Girlich, D., Poirel, L., and Nordmann, P. (2012). Value of the modified Hodge test for detection of emerging carbapenemases in *Enterobacteriaceae*. *J. Clin. Microbiol.* 50, 477–479. doi: 10.1128/JCM.05247-11

Han, R., Shi, Q., Wu, S., Yin, D., Peng, M., Dong, D., et al. (2020). Dissemination of carbapenemases (KPC, NDM, OXA-48, IMP, and VIM) among carbapenem-resistant *Enterobacteriaceae* isolated from adult and children patients in China. *Front. Cell Infect. Microbiol.* 10:314. doi: 10.3389/fcimb.2020.00314

Hopkins, K. L., Meunier, D., Naas, T., Volland, H., and Woodford, N. (2018). Evaluation of the NG-Test CARBA 5 multiplex immunochromatographic assay for the detection of KPC, OXA-48-like, NDM, VIM and IMP carbapenemases. *J. Antimicrob. Chemoth.* 73, 3523–3526. doi: 10.1093/jac/dky342

Jayol, A., Nordmann, P., Poirel, L., and Dubois, V. (2018). Ceftazidime/avibactam alone or in combination with aztreonam against colistin-resistant and carbapenemase-producing *Klebsiella pneumoniae*. *J. Antimicrob. Chemother.* 73, 542–544. doi: 10.1093/jac/dkx393

Knox, J., Jadhav, S., Sevior, D., Agyekum, A., Whipp, M., Waring, L., et al. (2014). Phenotypic detection of carbapenemase-producing *Enterobacteriaceae* by use of matrix-assisted laser desorption ionization-time of flight mass spectrometry and the Carba NP test. *J. Clin. Microbiol.* 52, 4075–4077. doi: 10.1128/JCM.02121-14

Mathers, A. J., Carroll, J., Sifri, C. D., and Hazen, K. C. (2013). Modified Hodge test versus indirect carbapenemase test: prospective evaluation of a phenotypic assay for detection of *Klebsiella pneumoniae* carbapenemase (KPC) in *Enterobacteriaceae*. *J. Clin. Microbiol.* 51, 1291–1293. doi: 10.1128/JCM.03240-12

Meunier, D., Vickers, A., Pike, R., Hill, R. L., Woodford, N., and Hopkins, K. L. (2016). Evaluation of the K-SeT R.E.S.I.S.T. immunochromatographic assay for the rapid detection of KPC and OXA-48-like carbapenemases: table 1. *J. Antimicrob. Chemother.* 71, 2357–2359. doi: 10.1093/jac/dkw113

Micozzi, A., Gentile, G., Minotti, C., Cartoni, C., Capria, S., Ballar 貌, D., et al. (2017). Carbapenem-resistant *Klebsiella pneumoniae* in high-risk haematological patients: factors favouring spread, risk factors and outcome of carbapenem-resistant *Klebsiella pneumoniae* bacteremias. *BMC Infect. Dis.* 17:203. doi: 10.1186/s12879-017-2297-9

Nordmann, P., Dortet, L., and Poirel, L. (2012a). Carbapenem resistance in *Enterobacteriaceae*: here is the storm! *Trends Mol. Med.* 18, 263–272. doi: 10.1016/j.molmed.2012.03.003

Nordmann, P., Poirel, L., and Dortet, L. (2012b). Rapid detection of carbapenemase-producing *Enterobacteriaceae*. *Emerg. Infect. Dis.* 18, 1503–1507. doi: 10.3201/eid1809.120355

Oho, M., Funashima, Y., Nagasawa, Z., Miyamoto, H., and Sueoka, E. (2020). Rapid detection method of carbapenemase-producing *Enterobacteriaceae* by MALDI-TOF MS with imipenem/cilastatin (KB) disc and zinc sulfate solution. *J. Infect. Chemother.* [Epub ahead of print]. doi: 10.1016/j.jiac.2020.09.013

Papagiannitsis, C. C., Študentová, V., Izdebski, R., Oikonomou, O., Pfeifer, Y., Petinaki, E., et al. (2015). Matrix-assisted laser desorption ionization-time of flight mass spectrometry meropenem hydrolysis assay with NH4HCO3, a reliable tool for direct detection of carbapenemase activity. *J. Clin. Microbiol.* 53, 1731–1735. doi: 10.1128/JCM.03094-14

Pasteran, F., Denorme, L., Ote, I., Gomez, S., De Belder, D., Glupczynski, Y., et al. (2016). Rapid identification of OXA-48 and OXA-163 subfamilies in carbapenem-resistant gram-negative bacilli with a novel immunochromatographic lateral flow assay. *J. Clin. Microbiol.* 54, 2832–2836. doi: 10.1128/JCM.01175-16

Pierce, V. M., Simner, P. J., Lonsway, D. R., Roe-Carpenter, D. E., Johnson, J. K., Brasso, W. B., et al. (2017). Modified carbapenem inactivation method for phenotypic detection of carbapenemase production among *Enterobacteriaceae*. *J. Clin. Microbiol.* 55, 2321–2333. doi: 10.1128/JCM.00193-17

Poirel, L., Walsh, T. R., Cuvillier, V., and Nordmann, P. (2011). Multiplex PCR for detection of acquired carbapenemase genes. *Diagn. Micr. Infect. Dis.* 70, 119–123. doi: 10.1016/j.diagmicrobio.2010.12.002

Shi, Q., Yin, D., Han, R., Guo, Y., Zheng, Y., Wu, S., et al. (2020). Emergence and recovery of ceftazidime-avibactam resistance in bla_{KPC-33}-harboring *Klebsiella pneumoniae* sequence type 11 isolates in China. *Clin. Infect. Dis.* 71, S436–S439. doi: 10.1093/cid/ciaa1521

Shirley, M. (2018). Ceftazidime-avibactam: a review in the treatment of serious gram-negative bacterial infections. *Drugs* 78, 675–692. doi: 10.1007/s40265-018-0902-x

Stewart, A., Harris, P., Henderson, A., and Paterson, D. (2018). Treatment of infections by OXA-48-producing *Enterobacteriaceae*. *Antimicrob. Agents Chemother.* 62:e01195-18. doi: 10.1128/AAC.01195-18

Takissian, J., Bonnin, R. A., Naas, T., and Dortet, L. (2019). NG-test carba 5 for rapid detection of carbapenemase-producing enterobacterales from positive blood cultures. *Antimicrob. Agents Chemother.* 63:e00011-19. doi: 10.1128/AAC.00011-19

Tamma, P. D., Opene, B. N., Gluck, A., Chambers, K. K., Carroll, K. C., and Simner, P. J. (2017). Comparison of 11 phenotypic assays for accurate detection of carbapenemase-producing *Enterobacteriaceae*. *J. Clin. Microbiol.* 55, 1046–1055. doi: 10.1128/JCM.02338-16

Tamma, P. D., and Simner, P. J. (2018). Phenotypic detection of carbapenemase-producing organisms from clinical isolates. *J. Clin. Microbiol.* 56:e01140-18. doi: 10.1128/JCM.01140-18

Tijet, N., Boyd, D., Patel, S. N., Mulvey, M. R., and Melano, R. G. (2013). Evaluation of the Carba NP test for rapid detection of carbapenemase-producing *Enterobacteriaceae* and *Pseudomonas aeruginosa*. *Antimicrob. Agents Chemother.* 57, 4578–4580. doi: 10.1128/AAC.00878-13

Tsai, Y. M., Wang, S., Chiu, H. C., Kao, C. Y., and Wen, L. L. (2020). Combination of modified carbapenem inactivation method (mCIM) and EDTA-CIM (eCIM) for phenotypic detection of carbapenemase-producing *Enterobacteriaceae*. *BMC Microbiol.* 20:315. doi: 10.1186/s12866-020-02010-3

van Dijk, K., Voets, G. M., Scharringa, J., Voskuil, S., Fluit, A. C., Rottier, W. C., et al. (2014). A disc diffusion assay for detection of class A, B and OXA-48 carbapenemases in *Enterobacteriaceae* using phenyl boronic acid, dipicolinic acid and temocillin. *Clin. Microbiol. Infect.* 20, 345–349. doi: 10.1111/1469-0691.12322

Vasoo, S., Cunningham, S. A., Kohner, P. C., Simner, P. J., Mandrekar, J. N., Lolans, K., et al. (2013). Comparison of a novel, rapid chromogenic biochemical assay, the Carba NP test, with the modified Hodge test for detection of carbapenemase-producing Gram-negative bacilli. *J. Clin. Microbiol.* 51, 3097–3101. doi: 10.1128/JCM.00965-13

Yin, D., Wu, S., Yang, Y., Shi, Q., Dong, D., Zhu, D., et al. (2019). Results from the china antimicrobial surveillance network (CHINET) in 2017 of the in vitro activities of ceftazidime-avibactam and ceftolozane-tazobactam against clinical isolates of *Enterobacteriaceae* and *Pseudomonas aeruginosa*. *Antimicrob. Agents Chemother.* 63:e02431-18. doi: 10.1128/AAC.02431-18

Yusuf, E., Van Der Meeren, S., Schallier, A., and Piérard, D. (2014). Comparison of the Carba NP test with the Rapid CARB Screen Kit for the detection of carbapenemase-producing *Enterobacteriaceae* and *Pseudomonas aeruginosa*. *Eur. J. Clin. Microbiol. Infect. Dis.* 33, 2237–2240. doi: 10.1007/s10096-014-2199-3

Zhang, R., Liu, L., Zhou, H., Chan, E. W., Li, J., Fang, Y., et al. (2017). Nationwide surveillance of clinical carbapenem-resistant *Enterobacteriaceae* (CRE) strains in China. *EBioMedicine* 19, 98–106. doi: 10.1016/j.ebiom.2017.04.032

Zou, H., Xiong, S. J., Lin, Q. X., Wu, M. L., Niu, S. Q., and Huang, S. F. (2019). CP-CRE/non-CP-CRE stratification and CRE resistance mechanism determination help in better managing CRE bacteremia using ceftazidime-avibactam and aztreonam-avibactam. *Infect. Drug Resist.* 12, 3017–3027. doi: 10.2147/IDR.S219635

Zusman, O., Altunin, S., Koppel, F., Dishon, B. Y., Gedik, H., and Paul, M. (2017). Polymyxin monotherapy or in combination against carbapenem-resistant bacteria: systematic review and meta-analysis. *J. Antimicrob. Chemother.* 72, 29–39. doi: 10.1093/jac/dkw377

Conflict of Interest: The authors declare that the research was conducted in the absence of any commercial or financial relationships that could be construed as a potential conflict of interest.

frontiers in Microbiology

ORIGINAL RESEARCH
published: 25 January 2021
doi: 10.3389/fmicb.2020.583185

Identification of Functional Interactome of Colistin Resistance Protein MCR-1 in *Escherichia coli*

*Hui Li[1], Yingyu Wang[2], Qiyan Chen[2], Xi Xia[2], Jianzhong Shen[2], Yang Wang[2] and Bing Shao[1,2]**

[1] Beijing Key Laboratory of Diagnostic and Traceability Technologies for Food Poisoning, Beijing Center for Disease Prevention and Control, Beijing, China, [2] Beijing Advanced Innovation Center for Food Nutrition and Human Health, College of Veterinary Medicine, China Agricultural University, Beijing, China

The emergence and worldwide dissemination of plasmid-mediated colistin resistance gene *mcr-1* has attracted global attention. The MCR-1 enzyme mediated colistin resistance by catalyzing phosphoethanolamine (PEA) transfer onto bacterial lipid A. However, the interaction partners of MCR-1 located in membrane protein in *E. coli* are unknown. Co-immunoprecipitation (Co-IP) and Mass Spectrometry were performed to define the interacting proteins of MCR-1. A total of three different anti-MCR-1 monoclonal antibody (mAbs) were prepared and 3G4 mAb was selected as the bait protein by compared their suitability for Co-IP. We identified 53, 13, and 14 interacting proteins in *E. coli* BL21 (DE3) (pET28a-*mcr-1*), *E. coli* BL21 (DE3) (pET28a-*mcr-1-200*), and *E. coli* DH5α (pUC19-*mcr-1*), respectively. Six proteins, including the stress response proteins DnaK (chaperone protein) and SspB (stringent starvation protein B), the transcriptional regulation protein H-NS, and ribosomal proteins (RpsE, RpsJ, and RpsP) were identified in all these three strains. These MCR-1-interacting proteins were mainly involved in ribosome and RNA degradation, suggesting that MCR-1 influences the protein biosynthesis through the interaction with ribosomal protein. Multidrug efflux pump AcrA and TolC were important interacting membrane proteins of MCR-1 referred to drug efflux during the PEA modification of the bacterial cell membrane. Overall, we firstly identified the functional interactome profile of MCR-1 in *E. coli* and discovered that two-component AcrA-TolC multidrug efflux pump was involved in *mcr-1*-mediated colistin resistance.

Keywords: MCR-1, colistin resistance, interactome, co-immunoprecipitation, *E. coli*

OPEN ACCESS

Edited by:
Yi-Wei Tang,
Cepheid (United States), United States

Reviewed by:
Jianfeng Wang,
Jilin University, China
Hong Du,
Soochow University, China

***Correspondence:**
Bing Shao
shaobingch@sina.com

Specialty section:
This article was submitted to Antimicrobials, Resistance and Chemotherapy, a section of the journal Frontiers in Microbiology

Received: *14 July 2020*
Accepted: *30 December 2020*
Published: *25 January 2021*

Citation:
Li H, Wang Y, Chen Q, Xia X, Shen J, Wang Y and Shao B (2021) Identification of Functional Interactome of Colistin Resistance Protein MCR-1 in Escherichia coli. Front. Microbiol. 11:583185. doi: 10.3389/fmicb.2020.583185

INTRODUCTION

mcr-1, as an important plasmid-borne colistin resistant gene, has attracted much attention in recent years for its threat in the clinical efficacy of the last-resort antibiotic when treating multidrug–resistant (MDR) Gram-negative bacterial infections (Liu et al., 2016; Shen et al., 2016; Poirel et al., 2017). *mcr-1* encodes a member of the family of phosphoethanolamine (PEA) transferases that decorates the lipid A headgroups of lipopolysaccharide of the outer membrane of Gram-negative bacteria through the addition of PEA (Anandan et al., 2017; Li et al., 2018). MCR-1 belongs to the alkaline phosphatase superfamily/sulphatase with five transmembrane segments. Many MDR

gram-negative bacteria possess multiple members of this family of enzymes that are engaged in the decoration of lipid A or the conserved inner core of the lipopolysaccharide (Needham and Trent, 2013). The proper function of an organism is orchestrated by highly complex protein networks and the interactome is crucial for understanding structural and functional organization in time and space (Sanchez et al., 1999). Deciphering the interactome profile of MCR-1 may help us in decoding its exact physiological function and various related biological process.

At present, the dissemination and prevalence of *mcr-1* has been widely reported in human, foods, animals, and environment (Gao et al., 2016; Ye et al., 2016; Wang et al., 2017). As an important resistant protein, the functional interactome of membrane protein MCR-1 was poorly understood. Affinity purification based on co-immunoprecipitation (Co-IP) coupled to mass spectrometry has become an important method of identifying protein interactome (Pankow et al., 2016; Maccarrone et al., 2017). Discovering interaction protein is still challenging, however, because a comprehensive interactome analysis requires high yields of the bait protein for robust co-purification of its interactors. In this study, we express and purify the catalytic domain and full-length protein of MCR-1, and prepare three different anti-MCR-1 monoclonal antibody (mAbs). We define the interacting proteins of MCR-1 using Co-IP and mass spectrometry in *E. coli* and characterize the protein-protein interaction (PPI) network of MCR-1.

MATERIALS AND METHODS

Expression and Purification of MCR-1

The gene encoding *mcr-1*, was amplified by polymerase chain reaction (PCR) from *E. coli* strain SHP45 genomic DNA using primers pET28a-mcr-1-F and pET28a-mcr-1-R and cloned into the plasmid pET28a to create a high copy expression vector with a N terminal hexa-histidine tag (pET28a-*mcr-1*) (**Supplementary Table 1**). Then the constructed plasmid pET28a-*mcr-1* was chemically transferred into *E. coli* BL21 (DE3) strains to express the full length MCR-1. For the expression of the catalytic domain of MCR-1, the constructed plasmid pET28a-*mcr-1-200* using primers pET28a-mcr-1-200-F and pET28a-mcr-1-200-R was transformed into *E. coli* BL21 (DE3) strains (**Supplementary Table 1**). Transformants were selected by the inclusion of kanamycin (50 μg/ml) on Luria Broth (LB) agar plates. The construction of *E. coli* cloning strains [*E. coli* DH5α (pUC19) and DH5α (pUC19-*mcr-1*)] was referred to our previous article (Li et al., 2019). The bacterial strains and plasmids used in this study were listed in **Table 1**. A starter culture was prepared by inoculating a single colony into 2 ml LB medium and grown at 37°C overnight. A sufficient volume of the starter culture was used to inoculate 200 ml LB medium and grown at 37°C in a shaking incubator set at 200 rpm until the OD_{600} reached 0.5–0.6. Protein expression was induced by the addition of isopropyl β-D-1-thiogalactopyranoside (IPTG) to a final concentration of 0.5 mM and the culture was continued at 18°C, 160 rpm for a further 14 h. The cells were harvested by centrifuging at 9,000 × *g* for 20 min at 4°C.

The harvested cells were re-suspended in 50 mM sodium phosphate buffer pH8.0 containing 300 mM NaCl, 10 mM imidazole at 4°C. Between 5 and 10 ml was used for each gram of cell pellet and cell lysis was performed using VCX105 ultrasonic instrument (Sonics & Materials, Inc., Newtown, CT, United States). The lysate was centrifuged at 12,000 × *g* for 30 min at 4°C to remove the non-lysed cells. The protein was purified from the supernatant using Ni-NTA agarose beads (Qiagen, Hilden, Germany). Briefly, the supernatant was incubated with pre-equilibrated Ni-NTA agarose beads (1 ml per pellet from a 200 ml culture) for 1 h. The beads were then loaded on a column and washed with 50 mM NaH_2PO_4, 300 mM NaCl, and 20 mM imidazole (pH 8.0). Protein was eluted with four column volumes of 50 mM NaH_2PO_4, 300 mM NaCl, and 150 mM imidazole (pH8.0). Imidazole was removed from the eluted protein by exchanging buffer to 50 mM NaH_2PO_4, 300 mM NaCl, and 1 mM tris (2-carboxyethyl) phosphine (TCEP) (pH8.0) using a PD-10 desalting column (GE Healthcare).

Preparation of MCR-1 mAb

The purified MCR-1 catalytic protein was used for immunization and custom production of the affinity-purified mouse mAb was used for subsequent experiments. All animal treatments were in accordance with Chinese laws and guidelines that were approved by the Animal Ethics Committee of China Agricultural University. Six eight-week old female BALB/c mice were immunized with the immunogen. The mice were immunized three times with an interval of 3 weeks between immunizations. The collected ascites were further purified to obtain the anti-MCR-1 mAb using AKTA Pure 150 system (GE Healthcare, Buckinghamshire, United Kingdom). Specificity of the antibody was determined by SDS-PAGE and Western blot.

Co-immunoprecipitation Assay

To identify the interactome profile associated with MCR-1, three *E. coli* clone strains carrying *mcr-1 gene* [DH5α (pUC19-*mcr-1*), BL21 (DE3) (pET28a-*mcr-1*), and BL21 (DE3) (pET28a-*mcr-1-200*)] and two empty vector strains [DH5α (pUC19) and BL21 (DE3) (pET28a)] were included to pull down MCR-1 and associated proteins using Co-IP assays with anti-MCR-1 mAb 3G4 as the bait. Anti-IgG and empty vector pull-downs were set as negative controls. The Co-IP assays of membrane protein MCR-1 was performed as previously described (Pankow et al., 2016). Briefly, the cells of two cloning strains [(DH5α (pUC19), DH5α (pUC19-*mcr-1*)] and three expressing strains [BL21 (DE3) (pET28a), BL21(DE3) (pET28a-*mcr-1*), and BL21(DE3) (pET28a-*mcr-1-200*)] were lysed by 50 mM Tris–HCl (pH7.5), 300 mM NaCl, 1 mM phenylmethylsulfonyl fluoride (PMSF), and 1% *n*-dodecyl β-D-maltoside (DDM). 1 mg of solubilized proteins were incubated overnight with 250 μg of anti-MCR-1 mAb in a reaction volume of 100 μl at 4°C with gentle mixing. 50 μl of pre-equilibrated *G*-Sepharose (GE Healthcare, Uppsala, Sweden) was added and incubated for 4 h at 4°C with gentle agitation. After centrifugation, samples were washed 5 times with solubilization buffer and co-precipitates were eluted by incubation with 0.2 M glycine (pH2.3) and 0.5% Igepal CA-630

TABLE 1 | Bacterial strains and plasmids used in this study.

Plasmids or strains	Description	Source
General plasmids		
pET28a	T7 *lac* promotor-operator, N-terminal His tag, kan^r	Novagen
pUC19	M13 *lac* promoter-operator, amp^r	Takara
pET28a:His-*mcr-1*	pET28a derivative carrying *mcr-1*	This study
pET28a:His-*mcr-1-200*	pET28a derivative carrying *mcr-1-200* (201–541 bp)	This study
pUC19:*mcr-1*	pUC19 derivative carrying *mcr-1*	Liu et al., 2016
Strains		This study
E.coli		
DH5α	*endA hsdR17 supE44 thi-1 recA1 gyrA relA1*Δ *(lacZYA-argF)U169 deoR* [Φ*80dlac*Δ *(lacZ)M15*]	Takara
BL21 (DE3)	F$^-$ *ompT hsdS$_B$ (r_B^- m_B^-) gal dcm met* (DE3)	Transgen Biotech
DH5α (pUC19)	*E. coli* DH5α strain carrying plasmid pUC19	Liu et al., 2016
DH5α (pUC19-*mcr-1*)	*E. coli* DH5α strain carrying plasmid pUC19:*mcr-1*	Liu et al., 2016
BL21 (DE3) (pET28a-*mcr-1*)	*E. coli* BL21 (DE3) strain carrying pET28a:*mcr-1*	This study
BL21 (DE3) (pET28a-*mcr-1-200*)	*E. coli* BL21 (DE3) strain carrying pET28a:*mcr-1-200* (201–541 bp)	This study

^{r}*Indicates resistance.*

(Sigma-Aldrich, St. Louis, MO, United States). Co-precipitates were separated by SDS-PAGE, and visualized with silver staining. The MCR-1 binding proteins were identified using nano LC-MS/MS analysis. Three biological repeats were conducted in the Co-IP assay.

Nano LC-MS/MS and Data Analysis

The co-precipitates were analyzed on a Q-exactive mass spectrometer equipped with a Dionex Ultimate 3000 Nano (Thermo Fisher Scientific). Peptides were trapped on a Acclaim PePmap 100 (75 μm × 2 cm, nanoviper, C_{18}, 3 μm, Thermo Fisher Scientific) and separated on a Venusil XBP C_{18} (2.1 × 150 mm, 5 μm, Agela Technologies) using a gradient formed between solvent A (0.1% formic acid in water) and solvent B (0.1% formic acid in acetonitrile). The gradient started at 5% solvent B and the concentration of solvent B was increased to 80% within 60 min. Database search was performed using the MASCOT software against the *E. coli* K12 database.

Surface Plasmon Resonance Interaction Analysis of MCR-1 and SspB Protein

The surface plasmon resonance (SPR) interaction analysis was performed using the Reichert 4SPR instrument (Reichert Life Sciences). The MCR-1 and MCR-1-200 protein in PBS buffer were directly immobilized on a Planar Mixed SAM biosensor chip (Reichert Life Sciences), respectively. SspB was sequentially diluted in running buffer PBST (pH7.4, containing 0.05% Tween-20) and injected to be trapped on the chip through the immobilized MCR-1. Evaluation and calculation of the binding parameters were carried out according to the formula: $K_D = K_a/K_d$ (K_a = association rate constant and K_d = dissociation rate constant).

Bioinformatics Analysis

A protein-protein interaction (PPI) network was constructed from the STRING database v11.0 (Szklarczyk et al., 2017) using the set of MCR-1 interacting proteins identified here. The interaction score was set as medium confidence (more than 0.400), and gene ontology (GO) enrichment was calculated by Blast2GO software. Metabolic pathway of MCR-1 interacting proteins was analyzed using KEGG software[1] to facilitate the related biological interpretation.

RESULTS

Protein Expression and mAb Preparation of MCR-1

Recombinant plasmid pET28a-mcr-1 was induced by IPTG to express a 6 × His-tagged recombinant protein at the N-terminus, consisting of 541 amino acids. The molecular weight of MCR-1 full-length protein after fusion expression was about 66 KDa. The catalytic domain of MCR-1 was induced and expressed by recombinant plasmid pET28a-mcr-1-200. The catalytic domain of MCR-1 consisted of 341 amino acids and its molecular weight was about 46 KDa. IgG positive hybridoma cells belonging to three isotypes-IgG1 (3G4, 6G4, and 8H11) were obtained. The anti-MCR-1 mAbs were purified from ascites fluid by protein G resin affinity chromatography. The cell lysate of the constructed *E. coli* DH5α (pUC19-*mcr-1*) strains was used for anti-MCR-1 mAb validation through regular Western blot method. His6-MCR-1 bands were detected by anti-His6 mAb (**Figure 1A**) and MCR-1 were successfully recognized by newly prepared anti-MCR-1 mAbs (**Figure 1B**). Then we compared the suitability of an antibody for Co-IP in a small-scale experiment followed by western blotting. We found that the anti-MCR-1 mAb 3G4 had no cross-linking efficiency and optimal performance in pulling down the target protein (**Figure 1C**).

Interactome Profile of MCR-1

In an effort to better understand the mechanistic role of MCR-1, Co-IP, and mass spectrometry were used to identify the interacting proteins of MCR-1 in *E. coli*. Corresponding strong band at the expected size of MCR-1 and MCR-1-200 and a large

[1]http://www.genome.jp/kegg/

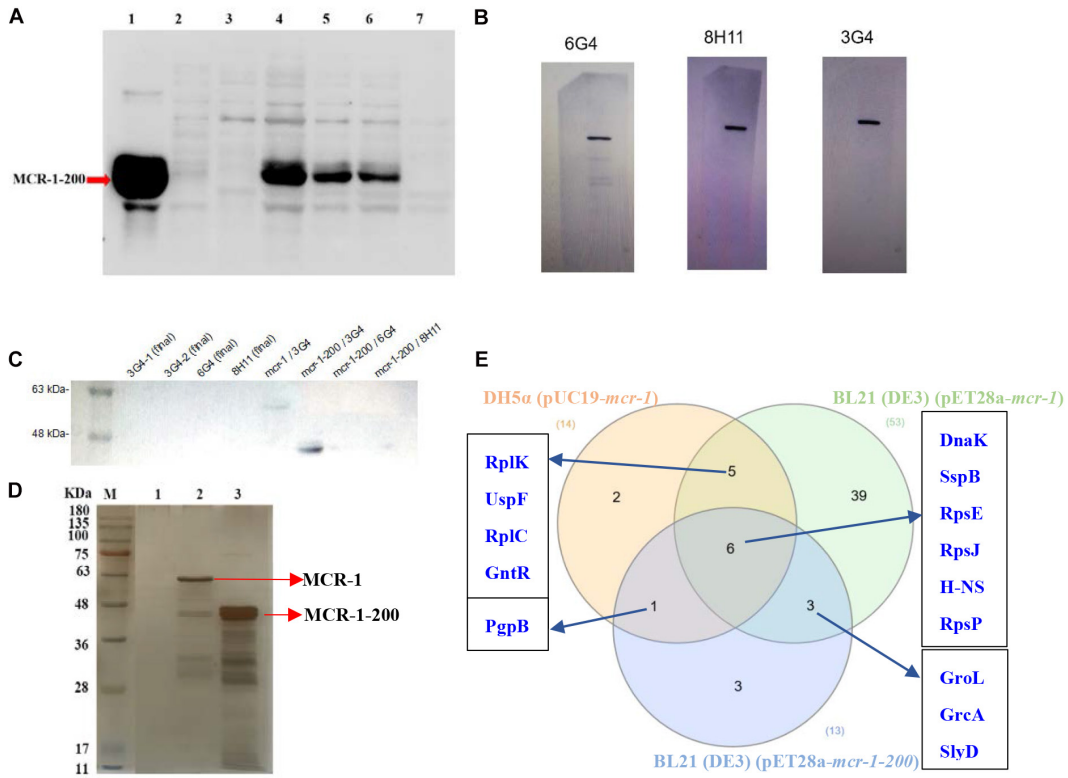

FIGURE 1 | Characterization of the developed Co-IP assays. **(A)** MCR-1 catalytic domain expression in cell lysate. Lane 1–3: purified protein eluted from Ni-NTA column by the elution buffer, wash buffer, and binding buffer, respectively; Lane 4–5: total cellular protein in supernatant and pellets of the sonicated cell lysates, respectively; Lane 6–7: total cellular protein induced expression with IPTG and total cellular protein without induction, respectively. **(B)** Anti-MCR-1 mAbs validation using the cell lysate through regular Western blot method. **(C)** Comparison of the prepared anti-MCR-1 mAbs in Co-IP. **(D)** Representative silver-stained SDS-gel of the eluted binding proteins mixtures using 3G4 mAb bait. M: prestained protein ladder 11–180 KDa; Lanes 1–3: *E. coli* BL21 (DE3) (pET28a), BL21 (DE3) (pET28a-*mcr-1*), and BL21 (DE3) (pET28a-*mcr-1-200*), respectively. **(E)** The Venn diagrams of the identified MCR-1 interacting proteins in three different *E. coli* strains.

number of other immunoprecipitated protein bands were shown using SDS-PAGE and silver stained (**Figure 1D**). We identified a total of 53 interacting proteins linked with ribosomal proteins (RplJ, RplK, RplO, RplL, RplC, RpmC, RplF, RplD, RplI, RpsU, RpsE, RpsJ, RpsP, and RpsN), stress response proteins (DnaK and SspB), metabolism (IDH1, SdhB, AcnB, ATPF0B, and GatB) and drug efflux system (AcrA, Lpp, OmpA, Pal, and TolC) in *E. coli* BL21 (DE3) (pET28a-*mcr-1*) (**Table 2**). In addition, we identified a total of 14 interacting proteins in *E. coli* DH5α (pUC19-*mcr-1*) and these interacting proteins mainly included ribosomal proteins (RpsE, RplK, RpsJ, RpsP, and RplK), DNA-binding proteins (H-NS, GntR, and EF-Tu) and stress response proteins (DnaK, GroL, and SspB) (**Supplementary Table 2**). A total of 13 interacting proteins including ribosomal proteins (RpsJ, RpsE, and RpsP), DNA-binding proteins (H-NS, HupA, HupB, and HofN) and stress response proteins (DnaK and SspB) were identified in the soluble domain expression vector *E. coli* BL21 (DE3) (pET28a-*mcr-1-200*) (**Supplementary Table 3**). The number of MCR-1-interacting proteins identified in full-length protein-expressing strains BL21 (DE3) (pET28a-*mcr-1*) was significantly higher than that in catalytic domain-expressing strains BL21 (DE3) (pET28a-*mcr-1-200*). Next, we analyzed all of the MCR-1-interacting proteins using InteractiVenn software. Of these proteins, six proteins (DnaK, SspB, H-NS, RpsE, RpsJ, and RpsP) were identified in all the three strains (**Figure 1E**).

To elucidate the functional relationships between the MCR-1 interacting proteins, we extracted a PPI network over these proteins from the STRING interaction database. We identified several functional proteins associated with ribosome, DNA replication, and hyperosmotic shock in *E. coli* DH5α (pUC19-*mcr-1*) (**Figure 2A**). The interacting proteins of MCR-1 in *E. coli* BL21 (DE3) (pET28a-*mcr-1*) were mainly involved in ribosome, drug efflux system, DNA binding, and DNA replication (**Figure 2B**). And the MCR-1-interacting proteins in *E. coli* BL21 (DE3) (pET28a-*mcr-1-200*) were mainly related with ribosome and DNA binding (**Figure 2C**). KEGG pathway enrichment analysis of the MCR-1-interacting proteins in *E. coli* DH5α (pUC19-*mcr-1*) found that these proteins were mainly involved in ribosome and RNA degradation (**Figure 2D**). And the KEGG pathway of the MCR-1-interacting proteins identified in *E. coli* BL21 (DE3) (pET28a-*mcr-1*) were referred to ribosome, RNA degradation, and cationic antimicrobial peptide (CAMP) resistance (**Supplementary Figure 1A**). Interestingly, multidrug efflux pump AcrA and TolC was identified important

TABLE 2 | MCR-1 protein interactors identified in *E. coli* BL21 (DE3) (pET28a-mcr-1).

No.	Uniprot ID	Protein	Mass (Da)	Gene
1	P0ACF0	DNA-binding protein HU-alpha	9,529	*hupA*
2	P0ACF8	DNA-binding protein H-NS	15,587	*hns*
3	P0A6Y8	Chaperone protein DnaK	69,130	*dnaK*
4	P0A910	Outer membrane protein A	37,292	*ompA*
5	P0A7W1	30S ribosomal protein S5	17,592	*rpsE*
6	P0AFZ3	Stringent starvation protein B	18,251	*sspB*
7	P0A6N2	Elongation factor Tu	43,457	*tufA*
8	P0ACF4	DNA-binding protein HU-beta	9,220	*hunB*
9	P69776	Major outer membrane lipoprotein Lpp	8,375	*lpp*
10	P02930	Outer membrane protein TolC	53,708	*tolC*
11	P0A7R5	30S ribosomal protein S10	11,728	*rpsJ*
12	P0A9K9	FKBP-type peptidyl-prolyl *cis-trans* isomerase SlyD	21,182	*slyD*
13	P0A7K2	50S ribosomal protein L7/L12	12,288	*rplL*
14	P0ADT8	Uncharacterized protein YgiM	23,062	*ygiM*
15	P0C054	Small heat shock protein IbpA	15,764	*ibpA*
16	P0AEH5	Protein ElaB	11,299	*elaB*
17	P0ADP9	Protein YihD	10,323	*yihD*
18	P0AG55	50S ribosomal protein L6	18,949	*rplF*
19	P0AF36	Cell division protein ZapB	9,629	*zapB*
20	P37903	Universal stress protein F	16,064	*uspF*
21	P0A6Y1	Integration host factor subunit beta	10,645	*ihfB*
22	P45523	FKBP-type peptidyl-prolyl *cis-trans* isomerase FkpA	28,864	*fkpA*
23	P0ADS2	Cell division protein ZapA	12,643	*zapA*
24	Q0TLG8	UPF0325 protein YaeH	15,144	*yaeH*
25	P0A7T3	30S ribosomal protein S16	9,185	*rpsP*
26	P69428	Sec-independent protein translocase protein TatA	9,658	*tatA*
27	P0AG30	Transcription termination factor Rho	47,032	*rho*
28	P0AGE0	Single-stranded DNA-binding protein	18,963	*ssb*
29	P02925	Ribose import binding protein RbsB	30,931	*rbsB*
30	P0A7J7	50S ribosomal protein L11	14,923	*rplK*
31	P64596	Uncharacterized protein YraP	20,073	*yraP*
32	Q0TCG0	50S ribosomal protein L15	14,957	*rplO*
33	Q0TCE1	50S ribosomal protein L3	22,230	*rplC*
34	P0A7M6	50S ribosomal protein L29	7,269	*rpmC*
35	P0A7J3	50S ribosomal protein L10	17,757	*rplJ*
36	P0AG59	30S ribosomal protein S14	11,630	*rpsN*
37	P0ABA0	ATP synthase subunit b	17,310	*atpF*
38	Q0TCE2	50S ribosomal protein L4	22,073	*rplD*
39	P0A6 × 7	Integration host factor subunit alpha	11,347	*ihfA*
40	P0AGJ9	Tyrosine–tRNA ligase	47,896	*tyrS*
41	P0A7R1	50S ribosomal protein L9	15,759	*rplI*
42	P0AEZ3	Septum site-determining protein MinD	29,710	*minD*
43	Q0TD41	30S ribosomal protein S21	8,552	*rpsU*
44	P36683	Aconitate hydratase B	94,009	*acnB*
45	P0AEU7	Chaperone protein Skp	17,677	*skp*
46	P0AE06	Multidrug efflux pump subunit AcrA	42,228	*acrA*
47	P0ACP5	HTH-type transcriptional regulator GntR	36,570	*gntR*
48	Q0TB02	Membrane protein insertase YidC	61,557	*yidC*
49	P07014	Succinate dehydrogenase iron-sulfur subunit	27,379	*sdhB*
50	P37188	Galactitol-specific phosphotransferase enzyme IIB component	10,443	*gatB*
51	P0A912	Peptidoglycan-associated lipoprotein	18,869	*pa1*
52	P0A905	Outer membrane lipoprotein SlyB	15,649	*slyB*
53	P08200	Isocitrate dehydrogenase (NADP)	46,070	*icd*
54	A0A0R6L508	MCR-1	60,428	*mcr-1*

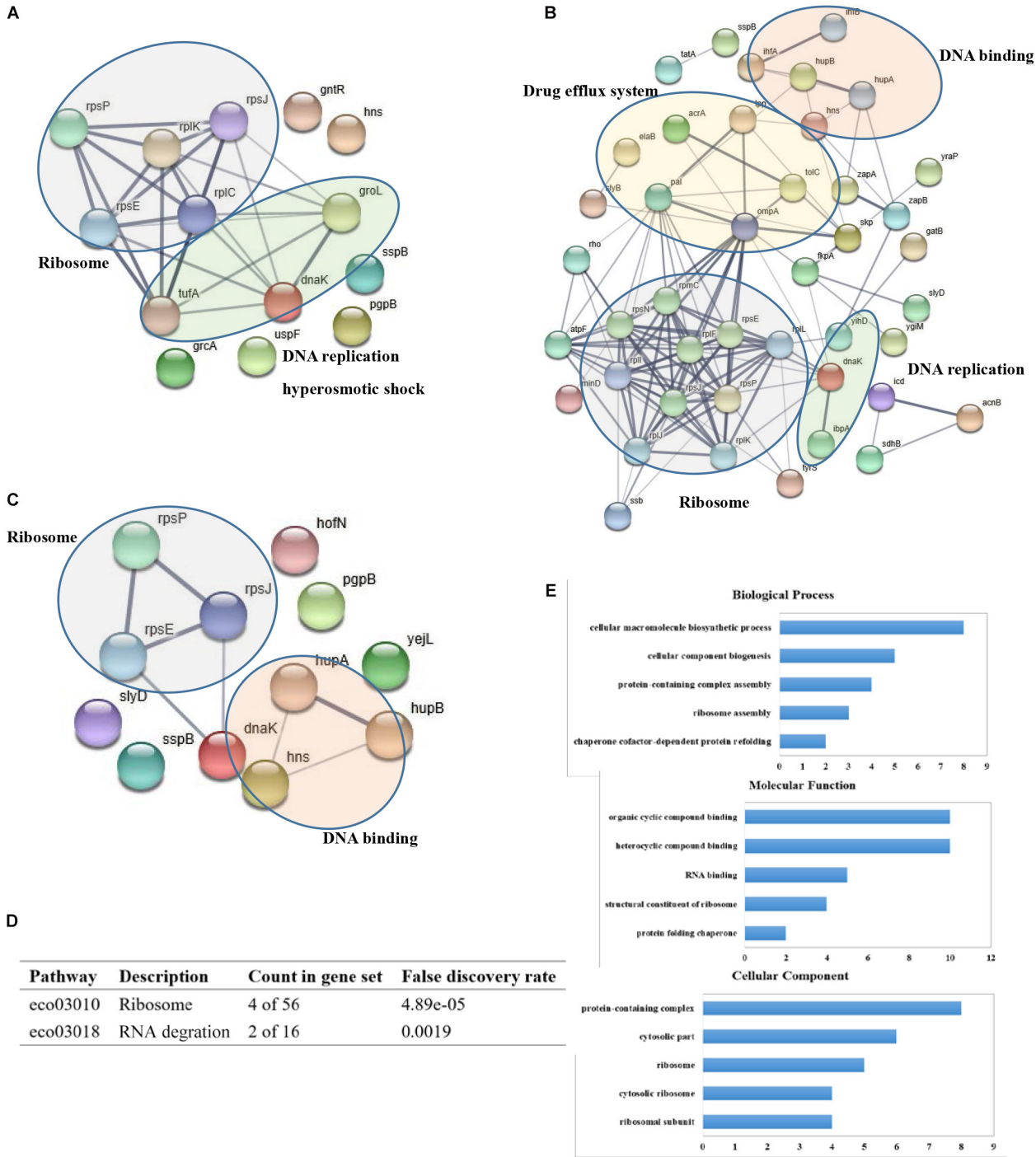

Pathway	Description	Count in gene set	False discovery rate
eco03010	Ribosome	4 of 56	4.89e-05
eco03018	RNA degration	2 of 16	0.0019

FIGURE 2 | Defining the MCR-1 functional interactome. **(A)** PPI network generated for 14 MCR-1 interactors using experimental evidence in STRING database and medium confidence links (>0.400) in *E. coli* DH5α (pUC19-*mcr-1*). Thickness of edges represent strength of evidence supporting interaction; **(B)** PPI network generated for 53 MCR-1 interactors in *E. coli* BL21 (DE3) (pET28a-*mcr-1*); **(C)** PPI network of the 13 MCR-1 interactors in *E. coli* BL21 (DE3) (pET28a-*mcr-1-200*); **(D)** KEGG pathway analysis of the interacting proteins of MCR-1 in *E. coli* DH5α (pUC19-*mcr-1*); **(E)** GO enrichment analysis of the interacting proteins of MCR-1 in *E. coli* DH5α (pUC19-*mcr-1*).

interacting partners of MCR-1 (**Table 2**). Outer membrane lipoprotein SlyB contributes to membrane integrity. YidC is required for the insertion and/or proper folding of integral membrane proteins into the membrane. The discovery of these interacting proteins demonstrated that MCR-1 might affect the expression and regulation of membrane proteins to cause

drug efflux during the PEA modification of bacterial cell membrane lipid A.

To identify putative functional processes associated with MCR-1-interacting proteins, we performed GO analysis. In *E. coli* DH5α (pUC19-*mcr-1*), the top-ranked categories of Biological Process analysis were cellular macromolecule biosynthetic process, cellular component biogenesis, protein-containing complex assembly (**Figure 2E**), suggesting that MCR-1 is related to protein biosynthetic process. In addition, Molecular Function of the MCR-1 interacting partners referred to organic cyclic compound binding, heterocyclic compound binding and RNA binding (**Figure 2E**). It indicates that MCR-1 may be involved in nucleic acid binding. Cellular Component analysis showed that these proteins were related to protein-containing complex, cytosolic part, and ribosome (**Figure 2E**), which implies that MCR-1 is likely to participate in protein biosynthesis. GO analysis of MCR-1-interactiong proteins in *E. coli* BL21 (DE3) (pET28a-*mcr-1*) were shown in **Supplementary Figures 1B–D**.

Interaction Analysis of SspB With MCR-1

To confirm the reliability of the developed Co-IP method and the effects of the identified MCR-1-interacting proteins, we investigated the binding ability of the target protein MCR-1, MCR-1-200, and SspB on the sensor chip. The SPR responses were obtained when the protein solution (0.156–5 μM, twofold dilution) was injected onto the sensor chip. The K_D values for the association between the MCR-1 full length protein and the SspB were 1.40×10^{-4} and 5.13×10^{-6} M for catalytic domain protein MCR-1-200, respectively (**Figures 3A,B**). These results demonstrated that MCR-1 was directly interacted with SspB in colistin-resistant *E. coli* strains.

DISCUSSION

With the rapid spread of the *mcr-1*, its public health problems and human health threats need to be solved urgently. The identification of functional interaction partners is fundamental to understanding the role of proteins and the mechanism of action *in vivo*. This is particularly challenging because bacteria will continue to produce adaptive changes under the pressure of antibiotics. Using a reliable Co-IP assay couple with mass spectrometry, we reported here the first functional interactome of MCR-1 and identified the key interacting proteins in colistin-resistant *E. coli* strains.

Our data indicate that MCR-1 interacts with multiple types of proteins. Among the interacting proteins identified by mass spectrometry, the most enriched groups of proteins associated with MCR-1 were the components of the ribosome and cellular stress response (**Figure 2D**). We speculate that MCR-1 interact with ribosome-associated proteins to affect protein biosynthesis in conferring resistance by modifying the colistin target, catalyzing transfer of phosphoethanolamine (PEA) onto the glucosamine saccharide of lipid A in the bacterial outer membrane. Our previous research indicated that the expression of some ribosomal proteins was disturbed in the construct *E. coli* strains carrying *mcr-1* and the bacteria could enhance protein synthesis in order to adapt to drug selection pressure (Li et al., 2019). Evaluating the likelihood and functional impact of the ribosome-associated interacting partners of MCR-1 will be an interesting follow up of this study.

As known, AcrAB-TolC multidrug resistance pump provides the Gram-negative bacteria with the necessary means to adapt drug pressure (Nikaido and Takatsuka, 2009). AcrA is the adapter component that associates the inner membrane pump with the TolC outer membrane channel (Fralick, 1996; Symmons et al., 2009). Our previous research found that MCR-1 not only caused the PEA modification of bacterial cell membrane lipid A, but also affected the efflux of polymyxin through disturbing the expression of efflux pump proteins involved in CAMP resistance pathway (Li et al., 2019). This study further confirmed that AcrA and TolC were important interacting membrane proteins of MCR-1 referred to drug efflux process. This finding indicated that MCR-1 might cause bacterial cell membrane to undergo the PEA molecule modification, which might also cause efflux pumps to participate in this biological process. The identification of the interacting partners SlyB and YidC showed that the importance of membrane protein integrity in *mcr-1*-mediated colistin resistance

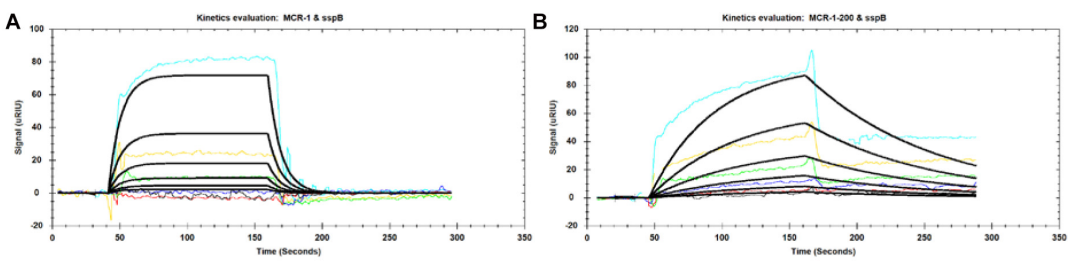

Ka (1/(m*s))	Kd(1/s)	K_D(M)
2.32E+03	3.25E-01	1.40E-04

Ka (1/(m*s))	Kd(1/s)	K_D(M)
2.06E+03	1.06E-02	5.13E-06

FIGURE 3 | SPR interaction analysis of MCR-1 and SspB protein. **(A)** Kinetic evaluation of MCR-1 full length protein and SspB; **(B)** Kinetic evaluation of MCR-1-200 catalytic domain protein and SspB. The SspB was diluted with PBST running buffer in the concentration range of 0.156–5 μM with twofold dilution series.

in *E. coli*. Lpp was a protein required for maintaining structural and functional integrity of bacterial cell envelope (Stenberg et al., 2005). Lpp was an integral component of cell outer membrane and seemed to interact with TolB, Pal, and TonB. We also found that H-NS interacted with DnaK, Lpp, HupA, and HupB in our study (**Figure 2B**). The regulatory protein H-NS controlled the lipid A palmitoylation mediated by the PagP enzyme (Chalabaev et al., 2014). Future work is needed to uncover the role of the promiscuous interaction of MCR-1 with two-component efflux pump AcrA-TolC and the contribution of other membrane proteins of the MCR-1 interactome during colistin resistance.

The stringent response is a general bacterial stress response that allows bacteria to adapt and survive adverse conditions. The cellular response to stress is orchestrated by the expression of a family of proteins termed heat shock proteins (e.g., DnaK) that are involved in the stabilization of basic cellular processes to preserve cell viability and homeostasis. Here, we found DnaK was a chaperone protein that interacted with MCR-1 (**Figure 1E** and **Table 2**). Chaperone protein DnaK was a multifunctional chaperone of highly conserved HSP70 family which assisted in protein folding, disaggregation, and remodeling of protein complexes (Calloni et al., 2012; Zahn et al., 2013). DnaK functions as a central hub to interact with a large number of proteins to regulate ribosomal biogenesis in *E. coli* (Zhang et al., 2016). DnaK has been proven to play an important role in the stress resistance of microorganism and may associate with the fitness cost reduction for *mcr-1*-carrying plasmids (Genevaux et al., 2007; Ma et al., 2018). We elucidate that DnaK might assist in the regulation of ribosomal biogenesis and affect the lipopolysaccharide modification. SspB, another protein that has been shown to interact with MCR-1 using Co-IP and SPR (**Figure 3**). Stringent starvation protein B (SspB) enhanced recognition of SsrA-tagged proteins by the ClpX-ClpP protease and regulated the protein expression during exponential and stationary-phase growth (Levchenko et al., 2000). H-NS was a global DNA-binding transcriptional dual regulator and implicated in transcriptional repression. RpsE, RpsJ, and RpsP are components of 30S ribosomal subunit and play an important role in ribosome biosynthesis. RpsE linked to the functional center of the 30S ribosomal subunit and was implicated in translational accuracy (Wimberly et al., 2000; Kirthi et al., 2006). RpsJ is involved in the regulation of ribosomal RNA biosynthesis by transcriptional antitermination (Luo et al., 2008; Weisberg, 2008). RpsP is essential for the viability of *E. coli* and plays an important role in the assembly of the 30S ribosomal subunits (Persson et al., 1995). So we predicted that MCR-1 interacted with H-NS to inhibit the DNA transcription and linked with ribosome proteins (RpsE, RpsJ, RpsP, etc.). Importantly, the identification and validation of MCR-1 interaction partner SspB with proven relevance demonstrate the power of our new Co-IP assay and provide reliable protein targets to advance our understanding of the *mcr-1*-mediated colistin resistance.

In conclusion, we define the functional interactome profile of colistin resistant protein MCR-1 in *E. coli* strains using Co-IP and mass spectrometry. Our study has uncovered a conceivable mechanism that MCR-1 influences the protein biosynthesis through the interaction with ribosomal protein. Multidrug efflux pump AcrA and TolC involved in the cationic antimicrobial peptide (CAMP) resistance pathway were identified as important interacting partners of MCR-1. Our data illustrates the interacting network of MCR-1 in colistin resistance and can provide valuable information to accurately understand its function and the mechanism of action at a deeper level.

DATA AVAILABILITY STATEMENT

The datasets presented in this study can be found in online repositories. The names of the repository/repositories and accession number(s) can be found in the article/ **Supplementary Material**.

ETHICS STATEMENT

The animal study was reviewed and approved by Chinese laws and guidelines that were approved by the Animal Ethics Committee of China Agricultural University.

AUTHOR CONTRIBUTIONS

BS, JS, YW, and XX conceived and designed the experiments. HL, YW, and QC performed the experiments. HL, YW, QC, and XX analyzed the data. HL, YW, and BS wrote the manuscript. All authors contributed to the article and approved the submitted version.

FUNDING

This work was supported by National Natural Science Foundation of China (Grant Nos. 31602107 and 81861138051), Capital's Funds for Health Improvement and Research (Grant No. 2018-4-3017), and National Key Research and Development Program of China (2017YFC1600305).

ACKNOWLEDGMENTS

We thank Xiya Zhang for the help in the preparation of monoclonal antibody of anti-MCR-1.

SUPPLEMENTARY MATERIAL

The Supplementary Material for this article can be found online at: https://www.frontiersin.org/articles/10.3389/fmicb.2020.583185/full#supplementary-material

REFERENCES

Anandan, A., Evans, G. L., Condic-Jurkic, K., O'mara, M. L., John, C. M., Phillips, N. J., et al. (2017). Structure of a lipid A phosphoethanolamine transferase suggests how conformational changes govern substrate binding. *Proc. Natl. Acad. Sci. U.S.A.* 114, 2218–2223. doi: 10.1073/pnas.1612927114

Calloni, G., Chen, T., Schermann, S. M., Chang, H. C., Genevaux, P., Agostini, F., et al. (2012). DnaK functions as a central hub in the *E. coli* chaperone network. *Cell Rep.* 1, 251–264. doi: 10.1016/j.celrep.2011.12.007

Chalabaev, S., Chauhan, A., Novikov, A., Iyer, P., Szczesny, M., Beloin, C., et al. (2014). Biofilms formed by gram-negative bacteria undergo increased lipid a palmitoylation, enhancing *in vivo* survival. *mBio* 5:e01116-14.

Fralick, J. A. (1996). Evidence that TolC is required for functioning of the Mar/AcrAB efflux pump of *Escherichia coli*. *J. Bacteriol.* 178, 5803–5805. doi: 10.1128/jb.178.19.5803-5805.1996

Gao, R., Hu, Y., Li, Z., Sun, J., Wang, Q., Lin, J., et al. (2016). Dissemination and mechanism for the *MCR-1* colistin resistance. *PLoS Pathog.* 12:e1005957. doi: 10.1371/journal.ppat.1005957

Genevaux, P., Georgopoulos, C., and Kelley, W. L. (2007). The Hsp70 chaperone machines of *Escherichia coli*: a paradigm for the repartition of chaperone functions. *Mol. Microbiol.* 66, 840–857. doi: 10.1111/j.1365-2958.2007.05961.x

Kirthi, N., Roy-Chaudhuri, B., Kelley, T., and Culver, G. M. (2006). A novel single amino acid change in small subunit ribosomal protein S5 has profound effects on translational fidelity. *RNA* 12, 2080–2091. doi: 10.1261/rna.302006

Levchenko, I., Seidel, M., Sauer, R. T., and Baker, T. A. (2000). A specificity-enhancing factor for the ClpXP degradation machine. *Science* 289, 2354–2356. doi: 10.1126/science.289.5488.2354

Li, H., Wang, Y., Meng, Q., Wang, Y., Xia, G., Xia, X., et al. (2019). Comprehensive proteomic and metabolomic profiling of *mcr-1*-mediated colistin resistance in *Escherichia coli*. *Int. J. Antimicrob. Agents* 53, 795–804. doi: 10.1016/j.ijantimicag.2019.02.014

Li, H., Yang, L., Liu, Z., Yin, W., Liu, D., Shen, Y., et al. (2018). Molecular insights into functional differences between *mcr-3*- and *mcr-1*-mediated colistin resistance. *Antimicrob. Agents Chemother.* 62:e0366-18.

Liu, Y.-Y., Wang, Y., Walsh, T. R., Yi, L.-X., Zhang, R., Spencer, J., et al. (2016). Emergence of plasmid-mediated colistin resistance mechanism *MCR-1* in animals and human beings in China: a microbiological and molecular biological study. *Lancet Infect. Dis.* 16, 161–168. doi: 10.1016/s1473-3099(15)00424-7

Luo, X., Hsiao, H. H., Bubunenko, M., Weber, G., Court, D. L., Gottesman, M. E., et al. (2008). Structural and functional analysis of the *E. coli NusB-S10* transcription antitermination complex. *Mol. Cell* 32, 791–802. doi: 10.1016/j.molcel.2008.10.028

Ma, K., Feng, Y., and Zong, Z. (2018). Fitness cost of a *mcr-1*-carrying IncHI2 plasmid. *PLoS One* 13:e0209706. doi: 10.1371/journal.ppat.0209706

Maccarrone, G., Bonfiglio, J. J., Silberstein, S., Turck, C. W., and Martins-De-Souza, D. (2017). Characterization of a protein interactome by Co-immunoprecipitation and shotgun mass spectrometry. *Methods Mol. Biol.* 1546, 223–234. doi: 10.1007/978-1-4939-6730-8_19

Needham, B. D., and Trent, M. S. (2013). Fortifying the barrier: the impact of lipid A remodelling on bacterial pathogenesis. *Nat. Rev. Microbiol.* 11, 467–481. doi: 10.1038/nrmicro3047

Nikaido, H., and Takatsuka, Y. (2009). Mechanisms of RND multidrug efflux pumps. *Biochim. Biophys. Acta* 1794, 769–781. doi: 10.1016/j.bbapap.2008.10.004

Pankow, S., Bamberger, C., Calzolari, D., Bamberger, A., and Yates, J. R. III (2016). Deep interactome profiling of membrane proteins by co-interacting protein identification technology. *Nat. Protoc.* 11, 2515–2528. doi: 10.1038/nprot.2016.140

Persson, B. C., Bylund, G. O., Berg, D. E., and Wikström, P. M. (1995). Functional analysis of the ffh-trmD region of the *Escherichia coli* chromosome by using reverse genetics. *J. Bacteriol.* 177, 5554–5560. doi: 10.1128/jb.177.19.5554-5560.1995

Poirel, L., Jayol, A., and Nordmann, P. (2017). Polymyxins: antibacterial activity, susceptibility testing, and resistance mechanisms encoded by plasmids or chromosomes. *Clin. Microbiol. Rev.* 30, 557–596. doi: 10.1128/cmr.00064-16

Sanchez, C., Lachaize, C., Janody, F., Bellon, B., Röder, L., Euzenat, J., et al. (1999). Grasping at molecular interactions and genetic networks in Drosophila melanogaster using FlyNets, an Internet database. *Nucleic Acids Res.* 27, 89–94. doi: 10.1093/nar/27.1.89

Shen, Z., Wang, Y., Shen, Y., Shen, J., and Wu, C. (2016). Early emergence of *mcr-1* in *Escherichia coli* from food-producing animals. *Lancet Infect. Dis.* 16:293. doi: 10.1016/s1473-3099(16)00061-x

Stenberg, F., Chovanec, P., Maslen, S. L., Robinson, C. V., Ilag, L. L., Von Heijne, G., et al. (2005). Protein complexes of the *Escherichia coli* cell envelope. *J. Biol. Chem.* 280, 34409–34419.

Symmons, M. F., Bokma, E., Koronakis, E., Hughes, C., and Koronakis, V. (2009). The assembled structure of a complete tripartite bacterial multidrug efflux pump. *Proc. Natl. Acad. Sci. U.S.A.* 106, 7173–7178. doi: 10.1073/pnas.0900693106

Szklarczyk, D., Morris, J. H., Cook, H., Kuhn, M., Wyder, S., Simonovic, M., et al. (2017). The STRING database in 2017: quality-controlled protein-protein association networks, made broadly accessible. *Nucleic Acids Res.* 45, D362–D368.

Wang, Y., Zhang, R., Li, J., Wu, Z., Yin, W., Schwarz, S., et al. (2017). Comprehensive resistome analysis reveals the prevalence of NDM and MCR-1 in Chinese poultry production. *Nat. Microbiol.* 2: 16260.

Weisberg, R. A. (2008). Transcription by moonlight: structural basis of an extraribosomal activity of ribosomal protein S10. *Mol. Cell* 32, 747–748. doi: 10.1016/j.molcel.2008.12.010

Wimberly, B. T., Brodersen, D. E., Clemons, W. M. Jr., Morgan-Warren, R. J., and Carter, A. P. (2000). Structure of the 30S ribosomal subunit. *Nature* 407, 327–339.

Ye, H., Li, Y., Li, Z., Gao, R., Zhang, H., Wen, R., et al. (2016). Diversified *mcr-1*-harbouring plasmid reservoirs confer resistance to colistin in human gut microbiota. *mBio* 7:e00177.

Zahn, M., Berthold, N., Kieslich, B., Knappe, D., Hoffmann, R., and Strater, N. (2013). Structural studies on the forward and reverse binding modes of peptides to the chaperone DnaK. *J. Mol. Biol.* 425, 2463–2479. doi: 10.1016/j.jmb.2013.03.041

Zhang, H., Yang, J., Wu, S., Gong, W., Chen, C., and Perrett, S. (2016). Glutathionylation of the bacterial Hsp70 chaperone DnaK provides a link between oxidative stress and the heat shock response. *J. Biol. Chem.* 291, 6967–6981. doi: 10.1074/jbc.m115.673608

Conflict of Interest: The authors declare that the research was conducted in the absence of any commercial or financial relationships that could be construed as a potential conflict of interest.

frontiers in Microbiology

ORIGINAL RESEARCH
published: 15 February 2021
doi: 10.3389/fmicb.2021.619369

Mobile Plasmid Mediated Transition From Colistin-Sensitive to Resistant Phenotype in *Klebsiella pneumoniae*

Baoyue Zhang[1,2], Bing Yu[3], Wei Zhou[1,2], Yue Wang[4], Ziyong Sun[4], Xiaojun Wu[5], Shiyun Chen[1], Ming Ni[6] and Yangbo Hu[1]**

[1] CAS Key Laboratory of Special Pathogens and Biosafety, Center for Biosafety Mega-Science, Wuhan Institute of Virology, Chinese Academy of Sciences, Wuhan, China, [2] University of Chinese Academy of Sciences, Beijing, China, [3] Department of Pathogen Biology, School of Basic Medicine, Tongji Medical College, Huazhong University of Science and Technology, Wuhan, China, [4] Department of Laboratory Medicine, Tongji Hospital, Tongji Medical College, Huazhong University of Science and Technology, Wuhan, China, [5] Department of Respiratory and Critical Medicine, Renmin Hospital of Wuhan University, Wuhan, China, [6] Department of Infectious Diseases, Tongji Hospital, Tongji Medical College, Huazhong University of Science and Technology, Wuhan, China*

OPEN ACCESS

Edited by:
Christophe Merlin, Université de Lorraine, France

Reviewed by:
Ning Dong, City University of Hong Kong, Hong Kong
Hua Zhou, Zhejiang University, China

***Correspondence:**
Ming Ni
niming@tjh.tjmu.edu.cn
Yangbo Hu
ybhu@wh.iov.cn

Specialty section:
This article was submitted to Antimicrobials, Resistance and Chemotherapy, a section of the journal Frontiers in Microbiology

Received: *20 October 2020*
Accepted: *27 January 2021*
Published: *15 February 2021*

Citation:
Zhang B, Yu B, Zhou W, Wang Y, Sun Z, Wu X, Chen S, Ni M and Hu Y (2021) Mobile Plasmid Mediated Transition From Colistin-Sensitive to Resistant Phenotype in Klebsiella pneumoniae. Front. Microbiol. 12:619369. doi: 10.3389/fmicb.2021.619369

Multidrug-resistant bacteria, including carbapenem-resistant *Klebsiella pneumoniae* (CRKP), are becoming an increasing health crisis worldwide. For CRKP, colistin is regarded as "the last treatment option." In this study, we isolated a clinical CRKP strain named as *K. pneumoniae* R10-341. Phenotyping analysis showed that this strain could transit from a colistin-sensitive to a resistant phenotype by inserting an IS*4* family IS*Kpn72* element into the colistin-resistance associated *mgrB* gene. To investigate the mechanism of this transition, we performed genome sequencing analysis of the colistin-sensitive parental strain and found that 12 copies of IS*Kpn72* containing direct repeats (DR) are located on the chromosome and 1 copy without DR is located on a multidrug-resistant plasmid pR10-341_2. Both types of IS*Kpn72* could be inserted into the *mgrB* gene to cause colistin-resistance, though the plasmid-derived IS*Kpn72* without DR was in higher efficiency. Importantly, we demonstrated that colistin-sensitive *K. pneumoniae* strain transferred with the IS*Kpn72* element also obtained the ability to switch from colistin-sensitive to colistin-resistant phenotype. Furthermore, we confirmed that the IS*Kpn72*-containing pR10-341_2 plasmid was able to conjugate, suggesting that the ability of causing colistin-resistant transition is transferable through common conjugation. Our results point to new challenges for both colistin-resistance detection and CRKP treatment.

Keywords: multidrug resistance, CRKP, mgrB, colistin, phenotype transition

INTRODUCTION

Multidrug-resistant pathogenic bacteria, such as carbapenem-resistant *Klebsiella pneumoniae* (CRKP), are increasingly becoming a health crisis worldwide (Nordmann et al., 2011; Pitout et al., 2015). Polymyxins, including polymyxin B and polymyxin E (colistin), have been regarded as "the last treatment option" for CRKP (Biswas et al., 2012). Polymyxins are lipopeptide antibiotics targeting the lipopolysaccharide (LPS) of the bacterial outer membrane, the main component of the Gram-negative bacterial cell wall (Hancock, 1997; Li et al., 2006).

The increase in infections by polymyxin-resistant bacteria has become a great challenge to clinical treatment (Antoniadou et al., 2007; Bogdanovich et al., 2011; Macesic et al., 2020). In *K. pneumoniae*, the most common polymyxin-resistance mechanism is achieved by LPS modification, which decreases the negative charge of LPS and reduces its affinity to polymyxins (Velkov et al., 2014; Liu et al., 2017). The mobile colistin resistance gene (*mcr-1*) is the first reported plasmid-mediated colistin resistance gene (Liu et al., 2016), which encodes a phosphoethanolamine-lipid A transferase catalyzing the addition of phosphoethanolamine (PEtN) to lipid A (Liu et al., 2016, 2017). To date, 10 variants (*mcr*1-10) have been identified on a wide variety of transferable plasmids (Wang et al., 2018, 2020; Yang et al., 2018; Zhong et al., 2018; Lei et al., 2020), leading to the widespread diffusion of *mcr*-mediated colistin-resistance (Zhong et al., 2018; Nang et al., 2019). Chromosome-mediated colistin-resistance has also been characterized by the involvement of a small transmembrane protein MgrB and the two-component systems (TCSs) PhoPQ, PmrAB, and CrrAB (Gunn and Miller, 1996; Olaitan et al., 2014). To the best of our knowledge, in contrast to *mcr* genes, chromosome-mediated colistin-resistance mechanisms are considered to be stable and have not been reported to be transferred or mobile to other bacteria. However, inactivation of the *mgrB* gene has been widely identified from clinical colistin-resistant clinical *K. pneumoniae* strains (Cannatelli et al., 2013; Gaibani et al., 2014; Olaitan et al., 2014).

In this study, we isolated a multidrug resistant *K. pneumoniae* strain named R10-341 with high frequency ($\sim 10^{-6}$) of colistin heteroresistance (El-Halfawy and Valvano, 2015; Halaby et al., 2016). Genetic and molecular analyses identified that insertion of an IS*Kpn72* element into the *mgrB* gene was responsible for the acquisition of colistin resistance. We further analyzed IS*Kpn72* copies in this strain and demonstrated that the IS*Kpn72* element is derived from a mobile plasmid and suggested that this mobile plasmid has the ability to render transition from colistin-sensitive to resistant phenotype in *K. pneumoniae*.

MATERIALS AND METHODS

Bacterial Strains, Plasmids, and Primers

The *K. pneumoniae* strains named R10-341 and 7097 used in this study were isolated from the sputum samples collected from the Tongji Hospital, Hubei Province, China. The *K. pneumoniae* strains were grown in LB medium with 100 μg/mL ampicillin at 37°C.

For plasmid constructions, the p15A *ori* from plasmid pACYC184 (Rose, 1988) and the streptomycin-resistance gene from pTargetF (Jiang et al., 2015) were PCR amplified, respectively. These two fragments were assembled as the linearized vector p15A-Sm by overlap PCR, which was then cloned with IS*pla* (IS fragment from pR10-341_2) or IS*chr* (IS fragment from chromosome) fragment using the ClonExpress II One Step Cloning Kit (Vazyme) to generate two plasmids named p15A-Sm-IS*pla* and p15A-Sm-IS*chr* respectively. All primers used in this study are listed in **Supplementary Table 1**.

Sequence Typing and Colistin Resistant Gene Detection

Multilocus sequence typing (MLST) for the *K. pneumoniae* R10-341 strain was performed as described (Diancourt et al., 2005).[1] Colistin resistance associated genes were detected by PCR. Each of the *mcr* genes was amplified using two pairs of primers. Genes encoding the two-component systems were amplified by PCR and confirmed by DNA sequencing in comparison with the *K. pneumoniae* HS11286 strain (Accession: NC_016845). All primers are listed in **Supplementary Table 1**.

Drug Susceptibility Test

MICs of antibiotics (except colistin) for *K. pneumoniae* R10-341 were determined using the broth microdilution method according to the Clinical and Laboratory Standards Institute (CLSI) guidelines (CLSI document M100-S28)[2]. The susceptibility to colistin was tested according to the guidelines of European Committee on Antimicrobial Susceptibility Testing (EUCAST)[3]. Briefly, 100 μL Cation-adjusted Mueller-Hinton Broth containing 2-fold diluted antibiotics was added to a 96-well plate, followed by the addition of 100 μL bacterial cells ($10^5 \sim 10^6$ CFU/mL) to each well. The 96-well plate was incubated at 37°C for 16–24 h. The lowest concentration of antibiotic with complete inhibition (clear broth) was regarded as the MIC.

Genome DNA Extraction, Whole Genome Sequencing, and Bioinformatics Analysis

The *K. pneumoniae* R10-341 strain was first spread onto a LB plate. A single colony was selected and cultured in LB medium at 37°C. Genomic DNA was extracted using a bacterial genomic DNA extraction Kit (Tiangen). Genome DNA sequencing was performed by both Hiseq X Ten (Illumina) and MinION (Oxford Nanopore Technologies) platforms according to a standard protocol provided by Illumina and Oxford Nanopore Technologies. The off-machine data of Nanopore sequencing is converted to fastq format through the Albacore software in the MinKNOW software package[4] (Payne et al., 2019). After filtering to obtain clean reads, these reads are randomly selected and aligned with the Nucleotide Sequence Database. *De novo* genome assembly was performed with Unicycler v0.4.7 (Wick et al., 2017). NCBI Prokaryotic Genomes Annotation Pipeline (PGAP) was used to annotate assembled genome sequence and to identify genes related to conjugation (Tatusova et al., 2016). Antibiotic resistance genes and plasmid replicons were respectively identified by ResFinder v3.0 (Zankari et al., 2012) and PlasmidFinder v2.0 (Carattoli et al., 2014) from the Center for Genomic Epidemiology website[5]. Sequence reads for the whole-genome sequencing are available from the NCBI Sequence Read Archive (PRJNA655367).

[1] https://bigsdb.pasteur.fr/klebsiella/

[2] https://clsi.org/standards/products/microbiology/documents/m100-preorder/

[3] https://www.eucast.org/fileadmin/src/media/PDFs/EUCAST_files/General_documents/Recommendations_for_MIC_determination_of_colistin_March_2016.pdf

[4] https://github.com/Albacore/albacore

[5] http://www.genomicepidemiology.org/

IS Element Analysis

For analyzing the IS elements in *K. pneumoniae* R10-341, the IS element inserted into the *mgrB* gene in colistin resistant colonies was first identified by PCR and DNA sequencing. This IS element sequence was analyzed in ISfinder database[6] and was named as IS*Kpn72* based on suggestion from ISfinder. The sequence of the ISKpn72 element was then aligned with the *K. pneumoniae* R10-341 genome sequence using BLASTn.

Amino acid sequences of transposases used in the phylogenetic tree analyses of the IS elements were downloaded from ISfinder database. Phylogenetic tree was constructed based on average distance using Jalview 2.11 (Waterhouse et al., 2009).

Conjugation Analysis

Since *K. pneumoniae* R10-341 is resistant to several antibiotics but is relatively sensitive to tetracycline, we constructed a tetracycline-resistant (TcR) *E. coli* K-12 strain as the recipient in conjugation experiment using a CRISPR/Cas9 system (Jiang et al., 2015). Briefly, the *E. coli* K-12 strain was first transformed with a Cas9 expressing plasmid pCas, and the sgRNA expressing plasmid pTargetF-EclacZ (targeting the *lacZ* gene) was then co-transformed with a DNA repairing fragment containing tetracycline-resistance gene from pACYC184 plasmid (Rose, 1988). The colonies resistant to tetracycline were screened. A single colony from 50 μg/ml tetracycline-containing LB agar plate was confirmed by DNA sequencing and was named as K12-TcR for subsequent conjugation tests.

Conjugation was performed by mixing an overnight donor (*K. pneumoniae* R10-341) and logarithmic phase recipient (K12-TcR) at a ratio of 4:1 in a total volume of 1 mL as described (Wu et al., 2019). The mixture was then concentrated and spotted onto LB agar without antibiotics at 37°C for 2–4 h to allow conjugation to occur. Since the pR10-341_2 plasmid contains streptomycin resistance gene (**Table 1**), the conjugated bacterial mixture was plated on LB agar containing 50 μg/ml tetracycline and 50 μg/ml streptomycin to screen for transconjugants carrying plasmid pR10-341_2. Transconjugants were confirmed by PCR using primers paired to *K. pneumoniae* R10-341 (Kpn-F-FR), K12-TcR (Ec-F-FR), and pR10-341_2 plasmid (P-F-FR), respectively.

[6]http://www-is.biotoul.fr

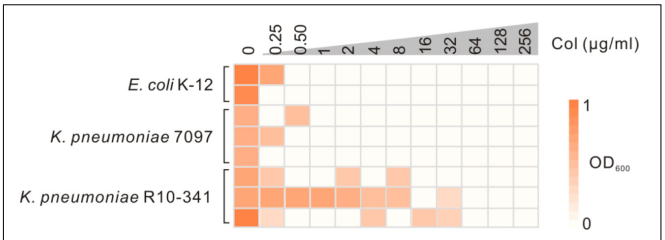

FIGURE 1 | Sensitivity test of the *K. pneumoniae* R10-341 strain to colistin. *E. coli* K-12 and *K. pneumoniae* 7097 were used as control strains. The depth of the color increases with the OD_{600} values.

RESULTS

Characterization of a Multi-Drug Resistant *Klebsiella pneumoniae* R10-341 Strain

The *K. pneumoniae* R10-341 strain was a clinical isolate from a sputum sample collected before antibiotic treatment from Tongji Hospital in Wuhan, China. This *K. pneumoniae* R10-341 strain was classified as ST11 and was resistant to different classes of antibiotics, including beta lactams, aminoglycosides, chloramphenicol, rifamycin, quinolones, sulfonamides and macrolides (summarized in **Table 1**). When testing the minimal inhibitory concentration (MIC) of colistin for this strain, we observed that some of the wells in the 96-well plate tested were resistant, while other wells showed colistin-sensitive phenotype (**Figure 1**). To exclude the possibility that the tested strain was a mixture of colistin sensitive and resistant, DNA sequences of known colistin resistance associated genes were tested in *K. pneumoniae* R10-341 parental strain. As summarized in **Table 2**, *phoPQ*, *pmrAB*, *crrAB,* and *mgrB* genes were the same as those in drug-sensitive strain, and the *mcr1-8* genes could not be successfully amplified in *K. pneumoniae* R10-341 strain. To further exclude the possibility of bacterial contamination, we streaked the R10-341 strain onto LB plate and selected different single colonies. Similar results were obtained for all these single colonies (data not shown), which suggested that the appearance of colistin resistant colonies for *K. pneumoniae* R10-341 strain was due to a colistin heteroresistance (CHR).

TABLE 1 | MIC values of different antibiotics to *K. pneumoniae* R10-341.

Antibiotic name	Antibiotic class	MIC (μg/ml)	Resistance gene	Gene location
Ampicillin	Beta lactams	>256	*bla*SHV-11 *bla*KPC-2 *bla*CTX-M-27	Chromosome pR10-341_2
Kanamycin	Aminoglycoside	128	–	–
Streptomycin	Aminoglycoside	256	*aadA*	pR10-341_2
Gentamicin	Aminoglycoside	>128	–	–
Rifampin	Rifamycin	>256	*arr-2*	pR10-341_2
Chloramphenicol	Chloramphenicol	128	*cat3*	Chromosome
Ciprofloxacin	Quinolones	>256	*qnrB*	pR10-341_2
Trimethoprim	Sulfonamides	>256	*dfrA12*	pR10-341_2
Tetracycline	Tetracyclines	16	–	–
Erythromycin	Macrolides	>256	–	–

TABLE 2 | Genes related to colistin resistance in *K. pneumoniae* R10-341.

Resistance mechanism	Gene	Gene functions	Detection results
Lipid A assembly PEtN	*mcr-1*	Phosphatidylethanolamine-lipid A transferase	No product
	mcr-2		No product
	mcr-3		No product
	mcr-4		No product
	mcr-5		No product
	mcr-6		No product
	mcr-7		No product
	mcr-8		No product
L-Ara4N and PEtN synthesis and modified LPS pathway	*mgrB*	PhoPQ negative-regulate protein	WT*
	phoPQ	TCS (Two-Component System)	WT*
	pmrAB	TCS	WT*
	crrAB	TCS	WT*

**WT indicates gene had the 100% DNA sequence identity in coding region and a ∼150 bp promoter region as these in the reference strain K. pneumoniae HS11286.*

Insertion of an IS*4* Family Transposon Element Into *mgrB* Gene Generated Colistin-Resistant Colonies

To further characterize the *K. pneumoniae* R10-341 strain, we tested the growth of this strain on LB plates containing 100 μg/mL colistin. Consistent with MIC testing, some colonies ($\sim 10^{-6}$) grew on the plate containing colistin, but no colonies were obtained from *E. coli* K-12 nor from another clinical isolate named *K. pneumoniae* 7097 on the colistin-containing plate (**Figure 2A**). To test the mechanism of this colistin resistance, we selected two colonies of the *K. pneumoniae* R10-341 strain from LB plate without colistin and then streaked onto LB plates containing 100 μg/mL colistin. Again, some colonies from both strains can grow on LB plates containing colistin. We then isolated four colonies from each of these two colistin-containing plates and sequenced the *phoPQ*, *pmrAB,* and *mgrB* genes (**Figure 2B**). Surprisingly, the amplified *mgrB* fragments from colistin-resistant colonies were all ∼1.4 kb longer than that from parental colistin-sensitive strains (**Figures 2B,C**).

Next, we sequenced this ∼1.4 kb inserted fragment. Sequence alignment in the NCBI database showed this fragment encodes an IS*4* family transposase. Further analysis of this ∼1.4 kb inserted fragment in ISfinder suggested that this insertion sequence could be named as IS*Kpn72* and classified into the IS*10* group in the IS*4* family, as its sequence is >95% identical to IS*10R* (**Figure 2D**). In accordance with this analysis, we identified 22 bp inverted repeats (IR) at both the left and right ends of this insertion fragment and 9 bp direct repeats (DR) around the insertion site (**Figure 2C**).

K. pneumoniae R10-341 Carries the IS*Kpn72* Element Both in the Chromosome and Plasmid DNA

The R10-341 strain can become colistin-resistant by inserting the IS*Kpn72* element into the *mgrB* gene, but we do not know the source of the IS*Kpn72* element. We therefore sequenced the genome of the original colistin-sensitive *K. pneumoniae* R10-341 strain. We obtained a 5.3 Mb chromosome DNA and two plasmid sequences (named pR10-341_1 and pR10-341_2, respectively), which are 5.3Mb, 10.06 kb, and 236.3 kb with G + C contents of 57.46, 55.07, and 52.72%, respectively. According to the PlasmidFinder database, pR10-341_1 and pR10-341_2 harbored ColRNAI and IncR replicon sequence, respectively. Several antibiotic resistance genes were identified both on the chromosome and plasmids, which were in consistent with our drug resistance tests (**Table 1**). Genome sequencing analysis confirmed that colistin-resistance related genes, including *mgrB*, *phoPQ,* and *pmrAB*, were all the same as the *K. pneumoniae* reference strain HS11286 (Genome accession: NC_016845), which further supports our hypothesis that the colistin-sensitive strain acquired resistance in the presence of colistin.

In searching for the IS*Kpn72* element sequence in the whole genome we obtained, we found 12 copies of this IS*Kpn72* element on the chromosome, and 1 copy on the plasmid pR10-341_2. Similar to that observed in the colistin-resistant R10-341 strain, all copies of the IS*Kpn72* element contain a pair of 22 bp-length imperfect terminal inverted repeats (IR) (**Figure 3A**). Surrounding the 12 copies of the IS*Kpn72* element located on the chromosome are 9-bp direct repeated (DR) sequences. In contrast, the plasmid encoding the IS*Kpn72* element only contains IR sequences but not the 9 bp-DR sequences (**Figure 3A**). Therefore, we assumed that the copy without DR on pR10-341_2 might be the root of all the IS*Kpn72* copies on the chromosome. These analyses suggested that the IS*Kpn72* element had already been inserted into the chromosome in the parental colistin-sensitive strain.

Both the DR-Containing and DR-Missing IS*Kpn72* Elements Can Be Inserted Into the *mgrB* Gene

Whether these existing IS*Kpn72* elements could be inserted into the *mgrB* gene to cause colistin-resistance is the next question. We transformed plasmids cloned with either the IS*Kpn72* element from pR10-341_2 or an IS*Kpn72* element from the *K. pneumoniae* R10-341 chromosome (named as IS*pla* and IS*chr*, respectively) into the colistin-sensitive strain *K. pneumoniae* 7097 (**Figure 3B**). In contrast to the parental *K. pneumoniae* 7097 strain, the transformation of the plasmid containing either

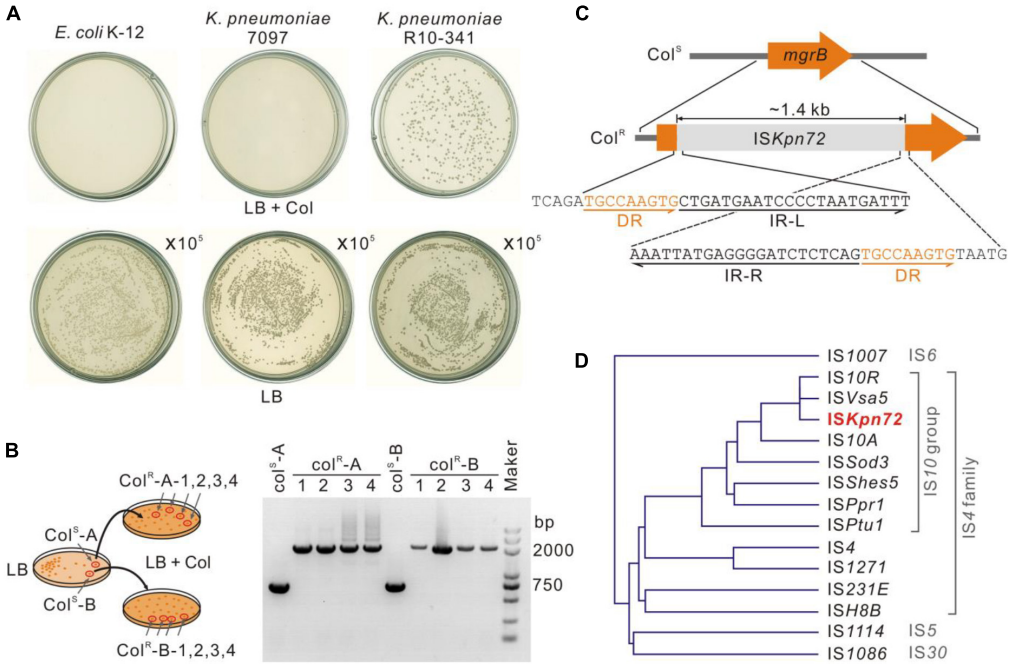

FIGURE 2 | Insertion of an IS*Kpn72* transposon element into the *mgrB* gene in colistin-resistant strain**. (A)** Colonies of *E. coli* K-12, *K. pneumoniae* 7097 and *K. pneumoniae* R10-341 streaked on LB plates containing 100 μg/mL colistin. Each plate was streaked with 100 μL of logarithmic phase bacteria. As a control, 100 μL of 10^5 diluted bacteria was also spread onto LB plates without colistin. **(B)** Confirmation of acquisition of colistin resistance for the *K. pneumoniae* R10-341 strain. Two separated colistin-sensitive colonies were spread onto two LB plates containing 100 μg/mL colistin. Fragment insertions of the *mgrB* gene in four colonies from each plate were tested by PCR. **(C)** Insertion of the IS*Kpn72* element into the *mgrB* gene in *K. pneumoniae* R10-341 colistin-resistant colonies. **(D)** Phylogenetic tree of the IS elements based on amino acid sequences of transposases.

IS*pla* or IS*chr* into this colistin-sensitive strain resulted in the growth of some colistin-resistant colonies. Colony forming units (CFU) on LB agar containing 100 μg/mL colistin revealed that the plasmid-derived IS*Kpn72* was more efficient than the chromosome-derived one in inserting into the *mgrB* gene to acquire colistin-resistance (**Figure 3C**). These data suggest that both IS*pla* and IS*chr* can be inserted into *mgrB* gene to acquire the colistin-resistance phenotype and IS*pla* without DRs had a higher efficiency.

The Resistance-Acquiring Mechanism May Be Potently Disseminated Among Bacteria

The next question is whether the IS*Kpn72* element on the pR10-341_2 plasmid could be horizontally transferred to acquire the colistin-resistant phenotype. Sequence alignment of the pR10-341_2 plasmid from the NCBI database showed high similarity to the conjugative multidrug resistant plasmid pR46-270 in a *K. pneumoniae* R46 isolate (GenBank: CP035776.1). Accordingly, a conjugative system consisting of *tra*, *trb,* and *finO* genes were encoded by the plasmid (**Figure 4A**). To confirm the transferability of the pR10-341_2, we used *K. pneumoniae* R10-341 as the donor and a tetracycline-resistant *E. coli* K12-TcR strain as the recipient to verify plasmid conjugation (**Figure 4B**). As expected, the *E. coli* K12-TcR strain containing the pR10-341_2 plasmid was successfully obtained (**Figure 4C**), suggesting the pR10-341_2 plasmid was transferable. Together, these results demonstrated that the *K. pneumoniae* R10-341 was able to disseminate the ability to switch from colistin-sensitive to resistant phenotype by transferring an IS containing plasmid.

DISCUSSION

Colistin-resistant bacteria are becoming an increasing threat to healthcare especially in hospitals (Antoniadou et al., 2007; Bogdanovich et al., 2011; Zhong et al., 2018; Nang et al., 2019). Previous studies have focused on mechanisms of drug-resistance and how to detect these resistant strains (Olaitan et al., 2014; Poirel et al., 2017). In this study, we identified a colistin-sensitive *K. pneumoniae* R10-341 strain with high frequency ($\sim 10^{-6}$) of colistin heteroresistance. The *K. pneumoniae* R10-341 strain was classified as ST11, which is the most widely prevalent CRKP genotype in China and contains the *bla*KPC-2 gene, which encodes the KPC family carbapenem-hydrolyzing class A beta-lactamase (Qi et al., 2011; Liu et al., 2018). We showed that this *K. pneumoniae* R10-341 strain could transit from a colistin-sensitive to a resistant phenotype by the insertion of an IS*Kpn72* element into the *mgrB* gene. Importantly, we characterized this IS*Kpn72* element in a mobile plasmid, which showed high similarity to the conjugative plasmid pR46-270 (Wu et al., 2019).

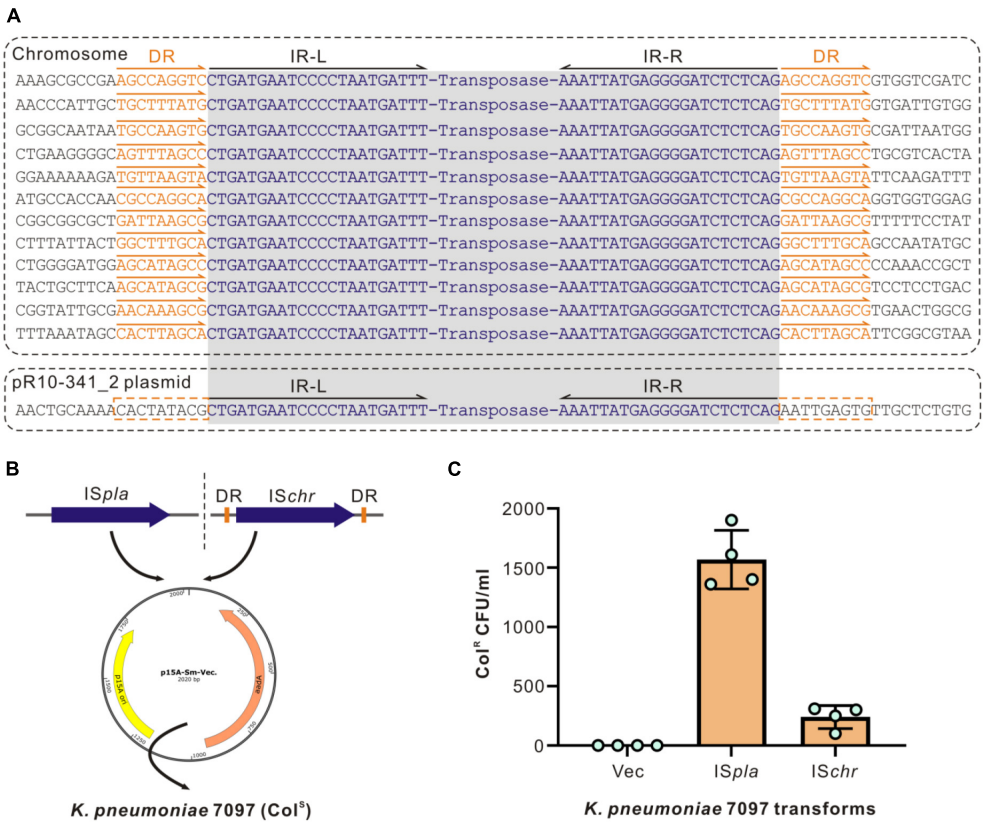

FIGURE 3 | Different types of ISs have different insertion efficiencies. **(A)** Schematic diagram of IS*Kpn72* elements located on chromosome and P2 plasmid. IR sequences are shown in blue and the DR sequences are indicated in orange. **(B)** Schematic diagram for cloning two forms of the IS*Kpn72* element into colistin-sensitive *K. pneumoniae* 7097 strain. **(C)** Acquired colistin-resistance for *K. pneumoniae* 7097 strain transformed with different IS*Kpn72* elements. Overnight grown bacteria were spread onto plates containing 100 μg/mL colistin, and bacterial colony forming unit (CFU) numbers were calculated. Representative data from two-independent experiments with four technique replicates are shown.

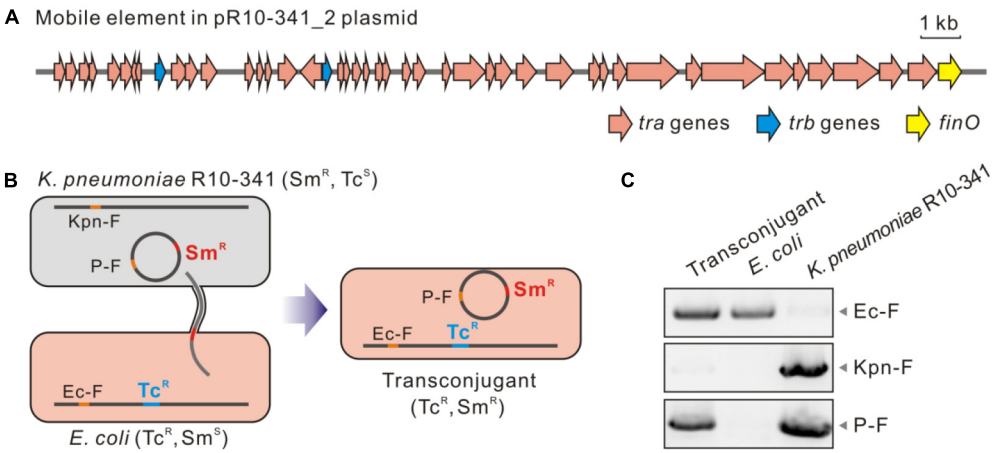

FIGURE 4 | Transconjugation of the pR10-341_2 plasmid from *K. pneumoniae* R10-341. **(A)** Genes involved in mobility of the pR10-341_2 plasmid. **(B)** Strategy used in conjugation transfer analysis. **(C)** PCR confirmation of transconjugant. Data of amplified products for Ec-F, Kpn-F, and P2-F are shown.

These analyses suggest that the ability of transiting from colistin-sensitive to resistant may be disseminated through plasmid transfer.

Heteroresistance has been reported to lead to failures in antibiotic treatment (Band et al., 2016; Band et al., 2019). In CRKP, colistin heteroresistance could be achieved by inserted

inactivation and deletion or point mutations in *mgrB*, *phoP*, *phoQ*, *lpxM,* and *yciM* genes (Jayol et al., 2015; Halaby et al., 2016). Similar as previous studies, we found that the colistin heteroresistance in *K. pneumoniae* R10-341 was also caused by inactivation of chromosomal encoded *mgrB* gene, but we characterized that this inactivation was mediated by a mobile plasmid derived IS element. Therefore, our result is the first to report that the colistin heteroresistance is able to be transferred or spread via plasmid mobilization.

Colistin-resistance in *K. pneumoniae* can be achieved by chromosome- or plasmid-encoded genes (Ah et al., 2014; Olaitan et al., 2014; Rebelo et al., 2018). Chromosome-encoded mutations are considered to be stable (Gunn et al., 1998), while plasmid encoded *mcr* genes can be potentially transferred across bacterial species to cause direct colistin-resistance (Liu et al., 2016; Zhong et al., 2018). Being different from spreading of drug-resistance genes, we characterized the spread of the ability to become colistin-resistance via mobile plasmid. The IS*Kpn72*-containing mobile plasmid enables the strain to transit from colistin-sensitive to resistant phenotype by inactivating the *mgrB* gene, which may also explain the widespread of *mgrB* gene inactivation in clinical samples (Cannatelli et al., 2014; Gaibani et al., 2014). Interestingly, all copies of the IS*Kpn72* element contain a pair of 22 bp-length imperfect terminal inverted repeats (IR), which is a characteristic feature of the IS element in bacteria (Rezsöhazy et al., 1993; Mahillon and Chandler, 1998); but only the 12 copies of the IS*Kpn72* element located on the chromosome contain 9-bp direct repeated (DR) sequences, which are considered as a marker of IS insertion (Mahillon and Chandler, 1998). These observations indicate that the copies of IS*Kpn72* on the chromosome are probably inserted from the DR-missing IS*Kpn72* element on the pR10-341_2 plasmid. In addition, we observed a colistin-resistance acquirement of IS*chr* transformers (**Figure 3C**), which indicated that the bacteria also can store the ability to become colistin-resistance by inserting IS in chromosome. The ability to transit to colistin-resistant can be both stored at chromosome and disseminated through mobile plasmids.

The mechanism of a mobile plasmid-mediated transfer of the ability to transit from a colistin-sensitive to resistant phenotype brings not only challenges to colistin-resistance detection, but also raises concerns to the use of colistin in clinical treatment. Firstly, this type of colistin-resistant phenotype was generated by the insertion of an IS*Kpn72* element into the *mgrB* gene, which means the parental strain may be mis-classified as colistin-sensitive in drug-resistant genotyping or phenotyping assays. Secondly, the IS*Kpn72* and other IS elements widely exist in prokaryotes (Mahillon and Chandler, 1998; Frost et al., 2005), suggesting transition to colistin-resistance may be widely occurred (Cannatelli et al., 2013, 2014). Different methods have been deployed for antibiotic resistance analysis and prediction, including traditional antimicrobial susceptibility testing (AST) (Jorgensen and Ferraro, 1998) and bioinformatics tools (Zankari et al., 2012; Boolchandani et al., 2019). It is still a challenge to identify whether a strain is able to acquiring inheritable or transmissible antibiotic-resistance, or under specific conditions due to the wide existence of IS elements. Additionally, the frequency of the IS*Kpn72* insertion into the *mgrB* gene characterized in our study can reach $\sim 10^{-6}$, indicating that the IS insertion, especially the IS*4* family, should receive more attention in the clinical use of colistin.

DATA AVAILABILITY STATEMENT

The datasets presented in this study can be found in online repositories. The names of the repository/repositories and accession number(s) can be found in the article/**Supplementary Material**.

AUTHOR CONTRIBUTIONS

MN and YH conceptualized and designed the study. BZ and BY performed the experiments. BZ, WZ, XW, and SC analyzed the data. YW and ZS provided the materials. BZ, MN, and YH drafted the manuscript. BY and SC critically revised the manuscript. All authors read and approved the final manuscript.

FUNDING

This work was supported by the Open Research Fund Program of National Biosafety Laboratory, Wuhan (2018SPCAS001 to MN and YH) and the Youth Innovation Promotion Association CAS (Y201750 to YH).

ACKNOWLEDGMENTS

We thank the Core Facility and Technical Support of Wuhan Institute of Virology for help in this study.

SUPPLEMENTARY MATERIAL

The Supplementary Material for this article can be found online at: https://www.frontiersin.org/articles/10.3389/fmicb.2021.619369/full#supplementary-material

REFERENCES

Ah, Y. M., Kim, A. J., and Lee, J. Y. (2014). Colistin resistance in *Klebsiella pneumoniae*. *Int. J. Antimicrob. Agent.* 44, 8–15.

Antoniadou, A., Kontopidou, F., Poulakou, G., Koratzanis, E., Galani, I., Papadomichelakis, E., et al. (2007). Colistin-resistant isolates of *Klebsiella pneumoniae* emerging in intensive care unit patients: first report of a multiclonal cluster. *J. Antimicrob. Chemother.* 59, 786–790. doi: 10.1093/jac/dkl562

Band, V. I., Crispell, E. K., Napier, B. A., Herrera, C. M., Tharp, G. K., Vavikolanu, K., et al. (2016). Antibiotic failure mediated by a resistant subpopulation in *Enterobacter cloacae*. *Nat. Microbiol.* 1:16053.

Band, V. I., Hufnagel, D. A., Jaggavarapu, S., Sherman, E. X., Wozniak, J. E., Satola, S. W., et al. (2019). Antibiotic combinations that exploit heteroresistance

to multiple drugs effectively control infection. *Nat. Microbiol.* 4, 1627–1635. doi: 10.1038/s41564-019-0480-z

Biswas, S., Brunel, J.-M., Dubus, J.-C., Reynaud-Gaubert, M., and Rolain, J.-M. (2012). Colistin: an update on the antibiotic of the 21st century. *Expert. Rev. Anti.Infect. Ther.* 10, 917–934. doi: 10.1586/eri.12.78

Bogdanovich, T., Adams-Haduch, J. M., Tian, G. B., Nguyen, M. H., Kwak, E. J., Muto, C. A., et al. (2011). Colistin-resistant, *Klebsiella pneumoniae* carbapenemase (KPC)-producing *Klebsiella pneumoniae* belonging to the international epidemic clone ST258. *Clin. Infec. Dis.* 53, 373–376. doi: 10.1093/cid/cir401

Boolchandani, M., D'souza, A. W., and Dantas, G. (2019). Sequencing-based methods and resources to study antimicrobial resistance. *Nat. Rev. Genet.* 20, 356–370.

Cannatelli, A., D'andrea, M. M., Giani, T., Di Pilato, V., Arena, F., Ambretti, S., et al. (2013). *In vivo* emergence of colistin resistance in *Klebsiella pneumoniae* producing KPC-type carbapenemases mediated by insertional inactivation of the PhoQ/PhoP mgrB regulator. *Antimicrob. Agent. Chemother.* 57, 5521–5526. doi: 10.1128/aac.01480-13

Cannatelli, A., Giani, T., D'andrea, M. M., Di Pilato, V., Arena, F., Conte, V., et al. (2014). MgrB inactivation is a common mechanism of colistin resistance in KPC-producing *Klebsiella pneumoniae* of clinical origin. *Antimicrob. Agent. Chemother.* 58, 5696–5703. doi: 10.1128/aac.03110-14

Carattoli, A., Zankari, E., García-Fernández, A., Voldby Larsen, M., Lund, O., Villa, L., et al. (2014). *In silico* detection and typing of plasmids using plasmidfinder and plasmid multilocus sequence typing. *Antimicrobial. Agent. Chemother.* 58, 3895–3903. doi: 10.1128/aac.02412-14

Diancourt, L., Passet, V., Verhoef, J., Grimont, P. A., and Brisse, S. (2005). Multilocus sequence typing of *Klebsiella pneumoniae* nosocomial isolates. *J. Clin. Microbiol.* 43, 4178–4182. doi: 10.1128/jcm.43.8.4178-4182.2005

El-Halfawy, O. M., and Valvano, M. A. (2015). Antimicrobial heteroresistance: an emerging field in need of clarity. *Clin. Microbiol. Rev.* 28, 191–207. doi: 10.1128/cmr.00058-14

Frost, L. S., Leplae, R., Summers, A. O., and Toussaint, A. (2005). Mobile genetic elements: the agents of open source evolution. *Nat. Rev. Microbiol.* 3, 722–732. doi: 10.1038/nrmicro1235

Gaibani, P., Lombardo, D., Lewis, R. E., Mercuri, M., Bonora, S., Landini, M. P., et al. (2014). *In vitro* activity and post-antibiotic effects of colistin in combination with other antimicrobials against colistin-resistant KPC-producing *Klebsiella pneumoniae* bloodstream isolates. *J. Antimicrobial. Chemother.* 69, 1856–1865. doi: 10.1093/jac/dku065

Gunn, J. S., Lim, K. B., Krueger, J., Kim, K., Guo, L., Hackett, M., et al. (1998). PmrA-PmrB-regulated genes necessary for 4-aminoarabinose lipid a modification and polymyxin resistance. *Mol. Microbiol.* 27, 1171–1182. doi: 10.1046/j.1365-2958.1998.00757.x

Gunn, J. S., and Miller, S. I. (1996). PhoP-PhoQ activates transcription of *pmrAB*, encoding a two-component regulatory system involved in *Salmonella typhimurium* antimicrobial peptide resistance. *J. Bacteriol.* 178, 6857–6864. doi: 10.1128/jb.178.23.6857-6864.1996

Halaby, T., Kucukkose, E., Janssen, A. B., Rogers, M. R. C., Doorduijn, D. J., Van Der Zanden, A. G. M., et al. (2016). Genomic characterization of colistin heteroresistance in *Klebsiella pneumoniae* during a nosocomial outbreak. *Antimicrobial. Agent. Chemother.* 60, 6837–6843. doi: 10.1128/aac.01344-16

Hancock, R. E. (1997). Peptide antibiotics. *Lancet* 349, 418–422.

Jayol, A., Nordmann, P., Brink, A., and Poirel, L. (2015). Heteroresistance to colistin in *Klebsiella pneumoniae* associated with alterations in the PhoPQ regulatory system. *Antimicrobial. Agent. Chemother.* 59, 2780–2784. doi: 10.1128/aac.05055-14

Jiang, Y., Chen, B., Duan, C., Sun, B., Yang, J., Yang, S. et al. (2015). Multigene editing in the *Escherichia coli* genome via the CRISPR-Cas9 system. *Appl. Environ. Microbiol.* 81, 2506–2514. doi: 10.1128/aem.04023-14

Jorgensen, J. H., and Ferraro, M. J. (1998). Antimicrobial susceptibility testing: general principles and contemporary practices. *Clin. Infect. Dis.* 26, 973–980. doi: 10.1086/513938

Lei, C. W., Zhang, Y., Wang, Y. T., and Wang, H. N. (2020). Detection of mobile colistin resistance gene mcr-10.1 in a conjugative plasmid from *Enterobacter* roggenkampii of chicken origin in china. *Antimicrob. Agent. Chemother.* 64, e1120–e1191.

Li, J., Nation, R. L., Turnidge, J. D., Milne, R. W., Coulthard, K., Rayner, C. R., et al. (2006). Colistin: the re-emerging antibiotic for multidrug-resistant Gram-negative bacterial infections. *Lancet Infect. Dis.* 6, 589–601. doi: 10.1016/s1473-3099(06)70580-1

Liu, L., Feng, Y., Tang, G., Lin, J., Huang, W., Qiao, F., et al. (2018). Carbapenem-resistant isolates of the *Klebsiella pneumoniae* complex in western china: the common ST11 and the surprising hospital-specific types. *Clin. Infect. Dis.* 67, S263–S265.

Liu, Y. Y., Chandler, C. E., Leung, L. M., Mcelheny, C. L., Mettus, R. T., Shanks, R. M. Q., et al. (2017). Structural modification of lipopolysaccharide conferred by in gram-negative ESKAPE pathogens. *Antimicrob. Agent. Chemother.* 61, e517–e580.

Liu, Y. Y., Wang, Y., Walsh, T. R., Yi, L. X., Zhang, R., Spencer, J., et al. (2016). Emergence of plasmid-mediated colistin resistance mechanism MCR-1 in animals and human beings in china: a microbiological and molecular biological study. *Lancet Infect. Dis.* 16, 161–168. doi: 10.1016/s1473-3099(15)00424-7

Macesic, N., Nelson, B., Mcconville, T. H., Giddins, M. J., Green, D. A., Stump, S., et al. (2020). Emergence of polymyxin resistance in clinical *Klebsiella pneumoniae* through diverse genetic adaptations: a genomic, retrospective cohort study. *Clin. Infect. Dis.* 70, 2084–2091. doi: 10.1093/cid/ciz623

Mahillon, J., and Chandler, M. (1998). Insertion sequences. *Microbiol. Mol. Biol. Rev.* 62, 725–774.

Nang, S. C., Li, J., and Velkov, T. (2019). The rise and spread of plasmid-mediated polymyxin resistance. *Crit. Rev. Microbiol.* 45, 131–161. doi: 10.1080/1040841x.2018.1492902

Nordmann, P., Naas, T., and Poirel, L. (2011). Global spread of carbapenemase-producing *enterobacteriaceae*. *Emerg. Infec. Dis.* 17, 1791–1798.

Olaitan, A. O., Morand, S., and Rolain, J. M. (2014). Mechanisms of polymyxin resistance: acquired and intrinsic resistance in bacteria. *Front. Microbiol.* 5:643. doi: 10.3389/fmicb.2014.00643

Payne, A., Holmes, N., Rakyan, V., and Loose, M. (2019). BulkVis: a graphical viewer for Oxford nanopore bulk FAST5 files. *Bioinformatics* 35, 2193–2198. doi: 10.1093/bioinformatics/bty841

Pitout, J. D. D., Nordmann, P., and Poirel, L. (2015). Carbapenemase-producing *Klebsiella pneumoniae*, a key pathogen set for global nosocomial dominance. *Antimicrob. Agent. Chemother.* 59, 5873–5884. doi: 10.1128/aac.01019-15

Poirel, L., Jayol, A., and Nordmann, P. (2017). Polymyxins: antibacterial activity, susceptibility testing, and resistance mechanisms encoded by plasmids or chromosomes. *Clin. Microbiol. Rev.* 30, 557–596. doi: 10.1128/cmr.00064-16

Qi, Y., Wei, Z., Ji, S., Du, X., Shen, P., Yu, Y. et al. (2011). ST11, the dominant clone of KPC-producing *Klebsiella pneumoniae* in China. *J. Antimicrob. Chemother.* 66, 307–312. doi: 10.1093/jac/dkq431

Rebelo, A. R., Bortolaia, V., Kjeldgaard, J. S., Pedersen, S. K., Leekitcharoenphon, P., Hansen, I. M., et al. (2018). Multiplex PCR for detection of plasmid-mediated colistin resistance determinants, *mcr*-1, *mcr*-2, *mcr*-3, *mcr*-4 and *mcr*-5 for surveillance purposes. *Euro. Surveill.* 23, 17–00672.

Rezsöhazy, R., Hallet, B., Delcour, J., and Mahillon, J. (1993). The IS4 family of insertion sequences: evidence for a conserved transposase motif. *Mol. Microbiol.* 9, 1283–1295. doi: 10.1111/j.1365-2958.1993.tb01258.x

Rose, R. E. (1988). The nucleotide sequence of pACYC184. *Nucleic Acids Res.* 16:355. doi: 10.1093/nar/16.1.355

Tatusova, T., Dicuccio, M., Badretdin, A., Chetvernin, V., Nawrocki, E. P., Zaslavsky, L., et al. (2016). NCBI prokaryotic genome annotation pipeline. *Nucleic Acids Res.* 44, 6614–6624. doi: 10.1093/nar/gkw569

Velkov, T., Deris, Z. Z., Huang, J. X., Azad, M. A., Butler, M., Sivanesan, S., et al. (2014). Surface changes and polymyxin interactions with a resistant strain of *Klebsiella pneumoniae*. *Innate. Immun.* 20, 350–363. doi: 10.1177/1753425913493337

Wang, C., Feng, Y., Liu, L., Wei, L., Kang, M., and Zong, Z. (2020). Identification of novel mobile colistin resistance gene. *Emerg. Microb. Infec.* 9, 508–516. doi: 10.1080/22221751.2020.1732231

Wang, X., Wang, Y., Zhou, Y., Li, J., Yin, W., Wang, S., et al. (2018). Emergence of a novel mobile colistin resistance gene, mcr-8, in NDM-producing *Klebsiella pneumoniae*. *Emerg. Microb. Infec.* 7:122.

Waterhouse, A. M., Procter, J. B., Martin, D. M. A., Clamp, M., and Barton, G. J. (2009). Jalview Version 2–a multiple sequence alignment editor and analysis workbench. *Bioinformatics* 25, 1189–1191. doi: 10.1093/bioinformatics/btp033

Wick, R. R., Judd, L. M., Gorrie, C. L., and Holt, K. E. (2017). Unicycler: Resolving bacterial genome assemblies from short and long sequencing reads. *PLoS comput. Biol.* 13:e1005595. doi: 10.1371/journal.pcbi.1005595

Wu, F., Ying, Y., Yin, M., Jiang, Y., Wu, C., Qian, C., et al. (2019). Molecular characterization of a multidrug-resistant strain R46 isolated from a rabbit. *Int. J. Genom.* 2019:5459190.

Yang, Y.-Q., Li, Y.-X., Lei, C.-W., Zhang, A.-Y., and Wang, H.-N. (2018). Novel plasmid-mediated colistin resistance gene mcr-7.1 in *Klebsiella pneumoniae*. *J. Antimicrob. Chemother.* 73, 1791–1795. doi: 10.1093/jac/dky111

Zankari, E., Hasman, H., Cosentino, S., Vestergaard, M., Rasmussen, S., Lund, O., et al. (2012). Identification of acquired antimicrobial resistance genes. *J. Antimicrob. Chemother.* 67, 2640–2644. doi: 10.1093/jac/dks261

Zhong, L. L., Phan, H. T. T., Shen, C., Vihta, K. D., Sheppard, A. E., Huang, X., et al. (2018). High rates of human fecal carriage of *mcr*-1-positive multidrug-resistant *Enterobacteriaceae* emerge in china in association with successful plasmid families. *Clin. Infect. Dis.* 66, 676–685. doi: 10.1093/cid/cix885

Conflict of Interest: The authors declare that the research was conducted in the absence of any commercial or financial relationships that could be construed as a potential conflict of interest.

frontiers in Microbiology

REVIEW
published: 19 February 2021
doi: 10.3389/fmicb.2021.606360

Enlarging the Toolbox Against Antimicrobial Resistance: Aptamers and CRISPR-Cas

*Higor Sette Pereira†, Thaysa Leite Tagliaferri† and Tiago Antônio de Oliveira Mendes**

Laboratory of Synthetic Biology and Modelling of Biological Systems, Department of Biochemistry and Molecular Biology, Universidade Federal de Viçosa, Viçosa, Brazil

In the post-genomic era, molecular treatments and diagnostics have been envisioned as powerful techniques to tackle the antimicrobial resistance (AMR) crisis. Among the molecular approaches, aptamers and CRISPR-Cas have gained support due to their practicality, sensibility, and flexibility to interact with a variety of extra- and intracellular targets. Those characteristics enabled the development of quick and onsite diagnostic tools as well as alternative treatments for pan-resistant bacterial infections. Even with such potential, more studies are necessary to pave the way for their successful use against AMR. In this review, we highlight those two robust techniques and encourage researchers to refine them toward AMR. Also, we describe how aptamers and CRISPR-Cas can work together with the current diagnostic and treatment toolbox.

Keywords: antimicrobial resistance, molecular diagnostic, alternative treatments, aptamer, CRISPR-Cas

OPEN ACCESS

Edited by:
Yi-Wei Tang,
Cepheid, United States

Reviewed by:
Wenyuan Han,
Huazhong Agricultural University, China
Yi Wang,
Auburn University, United States

***Correspondence:**
Tiago Antônio de Oliveira Mendes
tiagoaomendes@ufv.br

†These authors share first authorship

Specialty section:
This article was submitted to Antimicrobials, Resistance and Chemotherapy, a section of the journal Frontiers in Microbiology

Received: *14 September 2020*
Accepted: *05 January 2021*
Published: *19 February 2021*

Citation:
Pereira HS, Tagliaferri TL and Mendes TAdO (2021) Enlarging the Toolbox Against Antimicrobial Resistance: Aptamers and CRISPR-Cas. Front. Microbiol. 12:606360. doi: 10.3389/fmicb.2021.606360

ANTIBIOTIC RESISTANCE CRISIS

Despite antimicrobials' impact on modern medicine since their introduction in the first part of the 19th century (Powers, 2004; CDC, 2019), resistant bacteria quickly emerged throughout the decades. Drug resistance to all available antibiotics has been detected in clinical bacteria, threatening all advances achieved within the antibiotic era and urging for alternative treatments (CDC, 2019).

Abbreviations: ALISA, Aptamer-linked immobilized sorbent assay; AMR, Antimicrobial resistance; ARG, Antimicrobial resistance genes; CRISPR-Cas, Clustered regularly interspaced short palindromic repeats, CRISPR-associated enzymes; crRNA, CRISPR RNA; COVID-19, Coronavirus disease 2019; DNA, Deoxyribonucleic acid; FDA, Food and Drug Administration; HIV, Human immunodeficiency virus; KPC, *Klebsiella pneumoniae* carbapenemase; LAMP, Loop-mediated isothermal amplification; MALDI-TOF MS, Matrix-assisted laser desorption/ionization time-of-flight mass spectrometry; MRSA, Methicillin-resistant *Staphylococcus aureus*; NDM, New Delhi metallo-β-lactamase; NGS, Next-generation sequencing; PAM, Protospacer adjacent motif; PBP, Penicillin-binding protein; RNA, Ribonucleic acid; RNP, Ribonucleoprotein; RT-qPCR, quantitative reverse transcription PCR; SARS, Severe acute respiratory syndrome; SARS-CoV-2, Severe acute respiratory syndrome coronavirus 2; SELEX, Systematic evolution of ligands by exponential enrichment; sgRNA, single-guide RNA; siRNA, Small interfering RNA; SNP, Single-nucleotide polymorphism; TALEN, Transcription activator-like effector nucleases; tracrRNA, trans-activating CRISPR RNA.

Bacteria have developed resistance mechanisms to avoid, disrupt, eject, or resist the currently used antimicrobials (**Box 1**). They can be intrinsically resistant to antibiotics by using structural or functional inherent bacterial features or acquire resistance via genetic mutations or by horizontal transference of genetic elements (Blair et al., 2015; Munita and Arias, 2016).

The spread of bacterial resistance mechanisms has been much faster than the development of new treatments. New investments on antimicrobial research have been discouraged due to their elevated production costs and long-term development process (Adams and Brantner, 2010). On top of that, the misuse and over-prescription of antibiotics, which stem from uncertainties in diagnosis, contribute to the antimicrobial resistance (AMR) crisis escalation (Llor and Bjerrum, 2014; Malik and Bhattacharyya, 2019). The lack of rapid diagnostic tools directly affects initial treatment decisions, which might lead to empirical treatment guided only by clinical presentation (Fischer et al., 2004; Leekha et al., 2011).

Phenotypic-based diagnostics are currently considered as gold standards in AMR assessment. The "catch-all" resistance characteristic of phenotypic tests enables the evaluation of microbial susceptibility in a relatively unbiased way (Mitsakakis et al., 2018). Although efforts have been made to provide quick phenotypic tests (∼7 h) (Pancholi et al., 2018) to better guide antibiotic treatment, the most used techniques still require microorganism culture, with a turnaround time of around 18 h. This delays the availability of the AMR profiles, which might be accessible up to 72 h after sample collection (Leekha et al., 2011). Besides time-to-result limitation, phenotypic tests generally require laboratory structure (Mitsakakis et al., 2018). Therefore, quicker and accessible diagnostic tools are imperative to guide the first medical decisions regarding antimicrobial therapy prescription worldwide.

MOLECULAR APPROACHES

The search for more precise molecular diagnostic tools with quicker turnaround times has been encouraged to better guide clinical practice and public health policies. The recent global SARS-CoV-2 (severe acute respiratory syndrome coronavirus 2) outbreak has shown that in a matter of weeks, diagnostic centers have been overloaded with patients' samples and quick result release is required for viral spread control. So far, until 21 December 2020, SARS-CoV-2 virus infected 75,704,857 individuals, with 1,690,061 deaths worldwide[1]. We dare to draw here a parallel between SARS-CoV-2 and the AMR crisis. Currently, AMR infections cause around 700,000 deaths per year (O'Neil, 2016). In both cases, an early diagnosis would give trustworthy information for discrimination and contention of the causative agent. With alarming death numbers, the exploration of alternative treatments and diagnostics comes into the spotlight as an attempt to revert the current scenario caused by AMR.

Different molecular tools have been employed as a diagnostic to identify infectious disease agents and their resistance profile. RT-qPCR (quantitative reverse transcription PCR) and NGS (Next-Generation Sequencing) have been currently playing a key role in the diagnostics of the SARS-CoV-2, different from what happened in the 2002 SARS outbreak (Sheridan, 2020). qPCR is also an outstanding tool for the molecular detection of antimicrobial resistance genes (ARGs) (Waseem et al., 2019) directly from patient samples such as urine, blood, and cerebrospinal fluid (Singh et al., 2017). In addition to qPCR, metagenomic, LAMP (Loop-mediated isothermal amplification), and whole genome sequencing approaches not only characterize pathogens at the species level but also detect ARGs (Zankari et al., 2012; Dekker, 2018; Ota et al., 2019).

The molecular diagnostic tools described above offer an abundant panel to recognize DNA and RNA of infectious microorganisms. Complementarily, proteomics- and metabolomics-based techniques have been gaining momentum into the clinical molecular diagnostic field, for instance, MALDI-TOF MS (Matrix-Assisted Laser Desorption/Ionization Time-of-Flight Mass Spectrometry) (Patrinos et al., 2017). However, these tools require expensive equipment and laboratory structure, hampering their wide implementation as *in loco* diagnostic tools.

Aptamers and CRISPR-Cas (clustered repetitive interspaced short palindromic repeats, CRISPR-associated enzymes) systems have been slowly gaining support in clinical diagnosis and treatment of infectious diseases. Both can be employed as an onsite diagnostic tool with a quick turnaround time, which makes them more interesting than other methods targeting proteins or nucleic acids. Therefore, reviewing these two robust techniques attempts to encourage molecular biologist researchers to develop and refine clinical molecular tools against ARGs. Those methods do not necessarily intend to substitute the already implemented diagnostic approaches, but to stimulate their combination to circumvent antibiotic misuse. Also, their application in therapy will be reviewed to help paving the way for their use as treatments against multidrug-resistant agents.

APPLICATION OF APTAMERS INTO DETECTION AND NEUTRALIZATION OF AMR FACTORS

A substantial boost in aptamer application in research and clinical institutes has been noted worldwide (McKeague et al., 2015). Also called chemical antibodies (Toh et al., 2015), most aptamers interact with their targets in a constant equilibrium with binding affinities up to 1 pM (Ha et al., 2017). They offer a cheap large-scale production with chemical modifications, low or no immunogenicity, small size (close to 3 nm), flexibility in tridimensional structure, and great stability in different conditions of pH, temperature, and organic solvents (Yoon and Rossi, 2018). Also, aptamers interact with high sensitivity toward their targets, being able to discriminate a single amino acid mutation (Chen et al., 2015). Due to their small size, aptamers reach cavities that are often not accessible to monoclonal antibodies and, therefore, penetrate cell tissues more easily (Xiang et al., 2015). In this process, intracellular

[1]https://covid19.who.int/

BOX 1 | Antimicrobial resistance mechanism.

Resistance mechanisms date back to thousands of years and have been probably used to endure the presence of toxic compounds present in nature—including antimicrobials derived from different microorganisms, while they also provide alternative cellular functions (Allen et al., 2010; D'costa et al., 2011). Bacteria can evade antimicrobials via reduction of drug intracellular concentration either by low membrane permeability or through antibiotic efflux; target modification by genetic mutation or post-translational modification; and inactivation of the antibiotic by hydrolysis or its modification (Blair et al., 2015). With the introduction and constant presence of antimicrobials in medical care, agriculture and animal health, the spread of resistant microorganisms and the evolution of their defense strategies have been accelerated (**Figure 1**; CDC, 2019). From all resistance mechanisms, genes responsible for antibiotic inactivation and target alteration (**Figure 1** I and III, respectively) are commonly spread by plasmids and phage transduction (Munita and Arias, 2016; Calero-Caceres et al., 2019). Antibiotic inactivation is a usual strategy adopted for instance against beta-lactams and aminoglycosides. Beta-lactams can be hydrolyzed by enzymes encoded by the *bla* genes (beta-lactamase genes), such as bla_{TEM}, bla_{KPC}, and bla_{OXA}. Aminoglycosides, by its turn, are chemically inactivated by mainly three biochemical reaction, named adenylation, acetylation, and phosphorylation catalyzed by the enzymes nucleotidyltransferases (ANT), acetyltransferases (AAC), and phosphotransferases (APH), respectively (Doi et al., 2016; Munita and Arias, 2016; Bush and Bradford, 2019). An advantage of the hydrolysis over the chemical alteration strategy is the requirement of water instead of chemical compounds as a co-substrate, which ease enzyme activity outside the cell. Target alteration can be achieved by four main strategies, affecting several antimicrobials (not limited to the examples), as follows: (i) Target protection. One of the best-studied examples involves the determinants Tet(M) and Tet(O), which confers resistance to tetracycline. They interact with the ribosome and dislodge the drug from its binding site. (ii) Mutation of the antimicrobial target site. The development of mutations in the chromosomal genes *gyrA-gyrB* and *parC-parE* codifying for DNA gyrase and topoisomerase IV, respectively, promotes resistance against fluoroquinolones. (iii) Enzymatic alteration. Macrolide resistance is acquired by *erm* genes (erythromycin ribosomal methylation), which codify enzymes responsible for 50S ribosomal subunit methylation. This alteration weakens the binding of the erythromycin to the ribosome. (iv) Replacement/bypass of the target. Beta-lactam resistance is frequently acquired by Gram-positive microorganisms via *mec*A gene. The gene encodes an exogen penicillin-binding protein (PBP2a) that has low affinity for the beta-lactams, opposite to what happens to endogen PBPs (Munita and Arias, 2016).

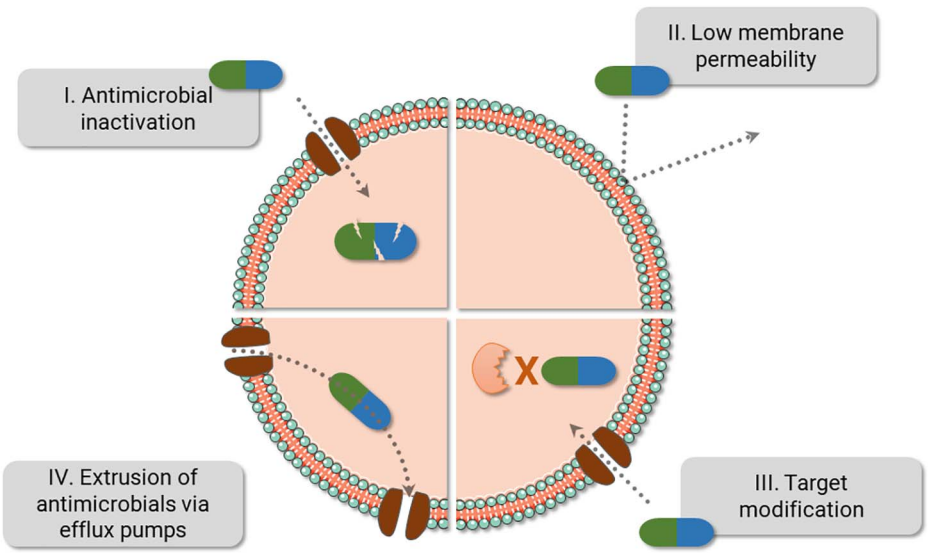

FIGURE 1 | Bacteria fight back antimicrobials. The main bacterial resistance mechanisms are displayed above. Of note, resistance against one class of antibiotics can be achieved using different strategies. For instance, resistance against beta-lactams can be caused by PBP2a (III), beta-lactamase (I), or by a combination of different mechanisms, i.e., reduction of porins (II) and the use of beta-lactamase (I). Also, efflux pumps can expel several antibiotic classes (IV) and are frequently present in multidrug resistance bacteria.

aptamers could be internalized by either a clathrin-dependent or -independent mechanism and co-localized in subcellular compartments, directly associated to its target, as reviewed in Yoon and Rossi (2018; **Figure 2**).

Single-stranded oligonucleotides can assume several secondary conformations such as hairpin, loop, pseudoknot, and G-quadruplex, which assure a unique folding for each sequence and allow interaction with specific sites (Yunn et al., 2015). DNA and RNA aptamers have similar binding characteristics, although DNA nucleotides have lower operating cost and offer greater stability than RNA, which in turn have greater versatility in their three-dimensional structures that directly affect target affinity.

Aptamer selection commonly occurs via a randomized process of systematic evolution of ligands by exponential enrichment (SELEX), firstly reported in 1990 (Ellington and Szostak, 1990; Tuerk and Gold, 1990). SELEX is based on iterative rounds of incubation of the oligonucleotide pool with the target, frequently divided into four stages: incubation, partition, recovery, and amplification. Also, aptamer–target affinity slowly increases alongside the rounds until the most specific aptamer is selected. SELEX allows greater versatility of binding conditions, which favors the adaptation of selected oligonucleotides to different cellular and non-cellular environments (McKeague et al., 2015).

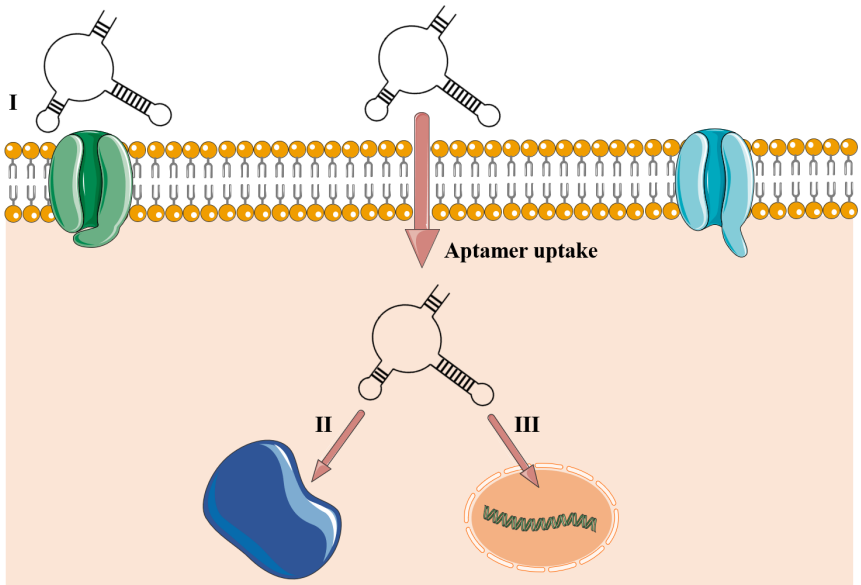

FIGURE 2 | Aptamer–target interactions in extra- and intracellular environments. (I) Aptamer recognizing cell membrane receptor or surface protein. The aptamer is uptaken into the cellular environment and can be located in some subcellular compartments such as lysosome, mitochondria, Golgi, and endoplasmic reticulum or guided to the nucleus in eukaryotic cells (Yoon and Rossi, 2018) or be stored into the cytoplasm of prokaryotic cells. (II) Cytosolic intracellular aptamers recognizing circulating proteins. (III) Nuclear intramers interacting directly with genetic elements. Aptamers' uptake is mediated to the intracellular environment by a clathrin-dependent mechanism. Clathrin is a group of proteins present in membrane cavities that assist in membrane vesicle formation during the molecule internalization by endocytosis.

Aptamer selection against many biological and chemical targets has been described (Qiao et al., 2018; Dalirirad and Steckl, 2020), along with its use in drug development (Esposito et al., 2018), bioimaging (Kim et al., 2019), food inspection (Duan et al., 2016), genetic modulation (Mol et al., 2019), and as a delivery vehicle (Zhuang et al., 2020). In antiviral therapy, G-3 aptamer dually inhibits HIV-1 cell replication both by blocking virus entrance via CCR5 receptor and by delivering a siRNA that decreases HIV-1 cytoplasmatic traffic (Zhou et al., 2015). Also, aptamers blocked quorum sensing and inhibited biofilm formation in *Pseudomonas aeruginosa* infections (Zhao et al., 2019). Even with many progresses, there is currently only one aptamer approved for clinical use, named pegaptanib. It is the main component of Macugen®, released by the FDA in 2004 to treat age-related macular degeneration (Gragoudas et al., 2004). Recently, there have been 10 therapeutic aptamers at different stages of clinical trials (Kaur et al., 2018), most of them employed to inhibit protein–protein interaction or act as antagonist (Yunn et al., 2015). To date, there is no aptamer currently approved by FDA for diagnostic purposes, even though they fit the quality standards of the diagnostic industry: affordable, sensitive, specific, user-friendly, and robust.

Different diagnostic devices based on aptamers have been proposed, including Aptamer-Linked Immobilized Sorbent Assay (ALISA), dot-blot, lateral-flow strips conjugated to nanomaterials, and the promising aptamer-based sensors (Stoltenburg et al., 2016; Shin et al., 2018; Su et al., 2018; Xiong et al., 2020). Aptasensors can be conjugated to a wide diversity of reporter molecules without modification of their activity (McKeague et al., 2015). Signal transducers commonly conjugated to aptasensors include but are not limited to colorimetric, electrochemical, and fluorescent approaches (Bai et al., 2017; Bayrac et al., 2017; Cai et al., 2019). Linking aptamer-based biosensors with nanomaterials can increase specificity and sensitivity of target binding up to 10-fold and offers a platform for rapid point-of-care diagnostic (<1 h) (Dalirirad and Steckl, 2020). Aptasensors have well-established protocols of chemical conjugation of aptamers with color or signal-transductor molecules, such as gold, silver, platinum, iron oxide nanoparticles, or carbon nanotubes and graphene oxide (Duan et al., 2016; Dehghani et al., 2018; Gao et al., 2018; Hua et al., 2018; Das et al., 2019a; Fan et al., 2020). The application of aptasensors for disease diagnosis has been tested in different samples, e.g., plasma and spiked nasal swab (Qiao et al., 2018), cultured bacteria (Maldonado et al., 2020), and urine and serum samples (Su et al., 2018). A lateral-flow paper strip conjugated with a gold nanoparticle aptamer-based sensor was developed to onsite detection of dopamine in urine samples (Dalirirad and Steckl, 2020).

When repurposed to bacteria, aptamers could recognize them by binding to antigens or cell surface receptors, or interacting with the whole cell through unknown targets (Tang et al., 2016; Song M. Y. et al., 2017; Shin et al., 2019). Although there are uncertainties concerning the mechanisms of aptamer uptake in bacteria, a report indicates that aptamers could traffic inside bacterial cells (Afrasiabi et al., 2020), similarly to what is shown in **Figure 2**. From 2016 to 2020, several papers have reported the use of aptamers applied to diagnostics of bacterial infections

(**Table 1**). Nearly all studies employed biosensors based on DNA aptamers, which indicates that for diagnostic purposes, the DNA stability overcomes the advantage of tridimensional possibilities of RNA. It is worth mentioning that only three of these studies targeted resistant bacteria or products of ARGs. First, Fan et al. (2020) made a graphene-oxide aptasensor based on peroxidase-like activity for the detection of purified PBP2a protein, encoded by the *mec*A gene. Also, Maldonado et al. (2020) employed a fast and label-free photonic pegylated aptasensor that recognizes both pure PBP2a protein and methicillin-resistant *Staphylococcus aureus* (MRSA)-infected cells in culture. Finally, Qiao et al. (2018) detected PBP2a in *S. aureus* cells collected in clinical plasma and spiked nasal swab samples infected with MRSA strains using a single bacterial lysis step. Predominantly, the diagnostic approach using aptamer has been focusing on the detection of the whole cell instead of its biological specific components, such as proteins or toxins. Therefore, due to the well-established protein-SELEX approach, there is still room for finding highly specific aptamers that bind to proteins associated with ARGs and enrich the diagnostic toolbox.

CRISPR-CAS AS A TOOL AGAINST ANTIMICROBIAL-RESISTANT PATHOGENS

CRISPR-Cas is a ribonucleoprotein (RNP) prokaryotic complex present in 50% of the bacteria and in most archaea that behaves as a prokaryotic adaptive immune system (Makarova et al., 2015). The system confers protection against mobile genetic elements, i.e., bacteriophages, plasmids, and transposons in three coordinated phases: adaptation, CRISPR RNA (crRNA) biogenesis, and interference (Hille et al., 2018). Nearly all CRISPR-Cas system counts on an ingenious mechanism to prevent self-targeting. This includes the recognition of a short sequence called protospacer adjacent motif (PAM) during adaptation and interference stages, present only in foreign nucleic acids (Mojica et al., 2009; Marraffini and Sontheimer, 2010).

Based mainly on the signature *Cas* genes, the new classification of CRISPR-Cas systems includes two different classes, six types, and 33 subtypes (Makarova et al., 2020). The most widespread class 1 CRISPR-Cas comprises types I, III, and IV. It is characterized by effector complexes with multiple Cas proteins responsible for a coordinated action from pre-crRNA processing to target cleavage. By its turn, class 2 consists of types II, V, and VI, which contains a single-protein effector module able to recognize and cleave the targeting nucleic acid (**Table 2**; Makarova et al., 2020).

Upon unraveling the CRISPR-Cas potential of gene editing in an easier, cheaper, and flexible way compared to previously established tools [for instance, TALENs (transcription activator-like effector nucleases) and Zinc-finger nucleases], the systems have been quickly repurposed to the biomedical and biotechnology fields (Chen and Gao, 2014; Liu et al., 2018; Zhang et al., 2019; Li et al., 2020). Class 2 CRISPR-Cas has been an attractive option for gene editing as a result of the effector module's simpler architecture when compared to class 1 (Makarova et al., 2020). Target specificity and cutting activity of the nucleases can be virtually programmed to any gene of interest by means of the short-length crRNA sequence. The engineering of a single-guide RNA (sgRNA) by fusing Cas9 crRNA and tracrRNA was a benchmark for gene editing (Jinek et al., 2012), but off-target effects still hold back CRISPR-Cas full potential. Several studies have tried to overcome this drawback by employing a plethora of modifications to increase the system specificity for gene editing (Kleinstiver et al., 2016; Slaymaker et al., 2016; Chen et al., 2017; Casini et al., 2018; Lee et al., 2018). Similarly, collateral effects of some Cas enzymes, i.e., the ability to indiscriminately (*trans*-) cleave ssDNA/ssRNA unleashed by site-specific DNA/RNA (*cis*-) bound by the crRNA, may also be a limitation for gene editing. However, here, this feature has been exploited for diagnostic purposes.

The collateral effect of Cas12 and Cas13 has been used as a key step to create several diagnostic platforms, such as DETECTR, HOLMES (both using Cas12), SHERLOCK, and CARMEN-Cas13 (the last two using Cas13) (Gootenberg et al., 2017; Chen et al., 2018; Li S. Y. et al., 2018; Ackerman et al., 2020). All platforms have similar diagnostic strategies, which involve the incubation of Cas enzymes (Cas12/Cas13) along with the target nucleic acid and fluorescent ssDNA/ssRNA reporters. By detecting the target nucleic acid, the Cas enzymes *trans*-cleave the quenched-fluorescent ssDNA/ssRNA reporters inserted into the platform, generating a robust fluorescent signal from around 1-h incubation (**Figure 3**) with a good correlation with PCR-based methods (Gootenberg et al., 2017; Chen et al., 2018; Gootenberg et al., 2018). In order to achieve attomolar sensitivity, the nucleic acid detection platforms were coupled to DNA amplification steps (i.e., PCR, recombinase polymerase amplification, and loop-mediated amplification) or reverse transcriptase combined with a DNA amplification step and T7 transcription for RNA targets (Gootenberg et al., 2017; Chen et al., 2018; Gootenberg et al., 2018; Li S. Y. et al., 2018; Ackerman et al., 2020; Broughton et al., 2020). To further enhance signal sensitivity, CRISPR type III effector nuclease Csm6, responsible for non-specific RNA degradation, can be combined with Cas13 activity (Gootenberg et al., 2018).

CARMEN-Cas13 and SHERLOCK have also been explored for multiplexing assays. The first one was specifically developed for this purpose and uses droplets containing either sample or detection solution, arranged pairwise. CARMEN can test more than 4500 crRNA–target pairs on a single microfluidic chip, which represents a simultaneous detection of around 170 agents (Ackerman et al., 2020). SHERLOCK, however, explored different *trans*-cleavage ssRNA preferences of Cas13 orthologs to develop a four-channel single-reaction multiplexing (Gootenberg et al., 2018). A different multiplexing strategy is employed by FLASH, a platform that uses Cas9 to enrich low-abundance targets from complex backgrounds (including clinical specimens) before NGS (**Figure 3**; Quan et al., 2019). Both CARMEN-Cas13 and FLASH offered an important multiplexing capacity but rely on robust laboratory structure, which may impar its implementation in less developed regions. SHERLOCK, however, has demonstrated its feasibility also as a paper-based test, which

TABLE 1 | Report of literature aptamers applied in the diagnostic of bacterial infections from 2016 to 2020.

Target	Oligo	Binding affinity or LOD	References
Acinetobacter baumannii isolates	DNA	7.547 ± 1.353 pM	Rasoulinejad and Gargari, 2016
Bacillus subtilis, Citrobacter freundii, Escherichia coli, Enterobacter aerogenes, Klebsiella pneumoniae, and Staphylococcus epidermidis cells	DNA	9.22–38.5 nM	Song M. Y. et al., 2017
Campylobacter jejuni cells	DNA	100 CFU ml−1	Dehghani et al., 2018
Escherichia coli and *Staphylococcus aureus* pathogenic cells	DNA	100 CFU ml−1	Xu et al., 2018
Escherichia coli ATCC cells	DNA	11.97 ± 2.94 nM	Marton et al., 2016
Escherichia coli cells	DNA	3 CFU ml−1	Jin et al., 2017
Escherichia coli cells	DNA	0.66 CFU ml−1	Hua et al., 2018
Escherichia coli O157 cells	DNA	107.6 ± 67.8 pM	Amraee et al., 2017
Escherichia coli O157:H7 cells	DNA	1.46 × 103 CFU ml−1	Yu et al., 2018
Escherichia coli whole cells	RNA	2 × 104 CFU ml−1	Dua et al., 2016
Escherichia coli whole-cells	DNA	102 CFU ml−1	Wu et al., 2017
Glycolipid antigen of *Mycobacterium tuberculosis*	DNA	668 ± 159 nM	Tang et al., 2016
Gram-negative outer membrane vesicles	DNA	25 ng/ml	Shin et al., 2019
HspX protein in tuberculous meningitis	DNA	10 pg	Das et al., 2019b
Listeria monocytogenes cells	DNA	2.5 CFU ml−1	Suh et al., 2018
Methicillin-resistant *Staphylococcus aureus* strains	DNA	1.38 × 103 CFU ml−1	Qiao et al., 2018
MPT64 antigen of *Mycobacterium tuberculosis*	DNA	0.2 fg ml−1	Bai et al., 2017
MPT64 antigen of *Mycobacterium tuberculosis*	DNA	100 CFU ml−1	Li N. et al., 2018
Mycobacterium tuberculosis cells	DNA	100 CFU ml−1	Zhang et al., 2017
Mycobacterium tuberculosis H37Ra cells	DNA	5.09 ± 1.43 nM	Mozioglu et al., 2016
Mycolactone in Buruli ulcer	RNA	1.59–73.0 μM	Sakyi et al., 2016
Mycoplasma-infected cells	DNA	Not informed	Liu et al., 2019
Neisseria meningitidis serogroup B	DNA	28.3–39.1 pM	Mirzakhani et al., 2017
PBP2a detection	DNA	20 nM	Fan et al., 2020
PBP2a in nosocomial infections	DNA	29 CFU ml^{-1}	Maldonado et al., 2020
Protein A of *Staphylococcus aureus*	DNA	11.3 nM	Stoltenburg et al., 2016
Protein A of *Staphylococcus aureus*	DNA	10 CFU ml^{-1}	Reich et al., 2017
Pseudomonas aeruginosa cells	DNA	100 CFU ml^{-1}	Gao et al., 2018
Pseudomonas aeruginosa cells	DNA	60 CFU ml^{-1}	Das et al., 2019a
Salmonella enterica serovar *typhimurium* in milk samples	DNA	3.37 × 10^2 CFU ml^{-1}	Zhang et al., 2018
Salmonella enteritidis cells	DNA	0.309 μM	Bayrac and Oktem, 2017
Salmonella enteritis cells	DNA	25 CFU ml^{-1}	Chinnappan et al., 2017
Salmonella typhimurium cells	DNA	10 CFU ml^{-1}	Duan et al., 2016
Salmonella typhimurium cells	DNA	123 ± 23 nM	Lavu et al., 2016
Salmonella Typhimurium cells	DNA	1 CFU ml^{-1}	Ren et al., 2019
Salmonella Typhimurium cells	DNA	80 CFU ml^{-1}	Wang et al., 2020
Salmonella Typhimurium cells	DNA	10 CFU ml^{-1}	Appaturi et al., 2020
Shigella sonnei cells	DNA	15.89 ± 1.77 nM	Song M. S. et al., 2017
Staphylococcus aureus and *Escherichia coli* cells	DNA	10–2,000 CFU ml^{-1}	Shen et al., 2016
Staphylococcus aureus cells	DNA	16 CFU ml^{-1}	Kurt et al., 2016
Staphylococcus aureus cells	DNA	10^3 CFU ml^{-1}	Bayrac et al., 2017
Staphylococcus aureus cells	DNA	39 CFU ml^{-1}	Cai et al., 2019
Streptococcus pyogenes cells	DNA	7 nM	Hamula et al., 2016
Streptococcus pyogenes serotype M3 cell	DNA	7.47 ± 1.72 pM	Alfavian et al., 2017
Vibrio parahaemolyticus cells	DNA	2.04e^{-9} ± 0.12 M	Ahn et al., 2018
Vibrio parahaemolyticus cells	DNA	10 CFU ml^{-1}	Sun et al., 2019

Papers recovered on the PUBMED NCBI website. Binding affinity and Limit of Detection (LOD) were represented by K_d and CFU counting, respectively.

amplifies its potential to become a widely spread quick-and-cheap ($0.61 per test) diagnostic method (Gootenberg et al., 2017). The addition of an extra step called HUDSON before SHERLOCK protocol enabled the viral detection directly from bodily fluids, contributing to the creation of a field-deployable diagnostic platform (Myhrvold et al., 2018). Its efficiency to detect bacteria directly from patient samples, however, is yet to be defined. Also, SHERLOCK might benefit from Cas13 engineering

TABLE 2 | General features of CRISPR-Cas systems based on the most well-characterized subtypes.

Type	Multisubunity RNP complex	Single protein	Signature enzyme	Seed sequence	Most common substrates		Cleavage
					RNA	DNA	
I	X		Cas3	1–5 nt and 7–8 nt		X	Single-stranded DNA cleavage
II		X	Cas9	10–12 nt		X	Blunt double-stranded DNA break
III	X		Cas10	Not defined*	X	X	Specific and non-specific ssRNA cleavage. Double-stranded DNA break
IV	Defective CRISPR-Cas loci typically lacking the effector nuclease and the adaptation module						
V		X	Cas12	~18 nt		X	Double-stranded DNA break with staggered overhangs, non-specific ssDNA break
VI		X	Cas13	Not defined#	X		Specific and non-specific ssRNA cleavage

*Seed sequence: PAM-proximal sequence in which full complementarity is required for CRISPR-Cas interference. As (i) some CRISPR-Cas subtypes have promiscuous PAM sequences, (ii) the site sequence varies among the subtypes; the PAM sequences have not been displayed in this table. Gleditzsch et al. (2019) review the PAM recognition strategies for all CRISPR-Cas types and engineering approaches to change the PAM recognition sequence. *Inconsistent conclusions regarding the seed region of CRISPR type III: absence of seed or its presence in the 5′ end (Cao et al., 2016) or 3′ end (Peng et al., 2015). #Central seed region proposed for Cas13a (Abudayyeh et al., 2016; Liu et al., 2017). Table based on Semenova et al. (2011); Chen et al. (2018), Hille et al. (2018), and Makarova et al. (2020).*

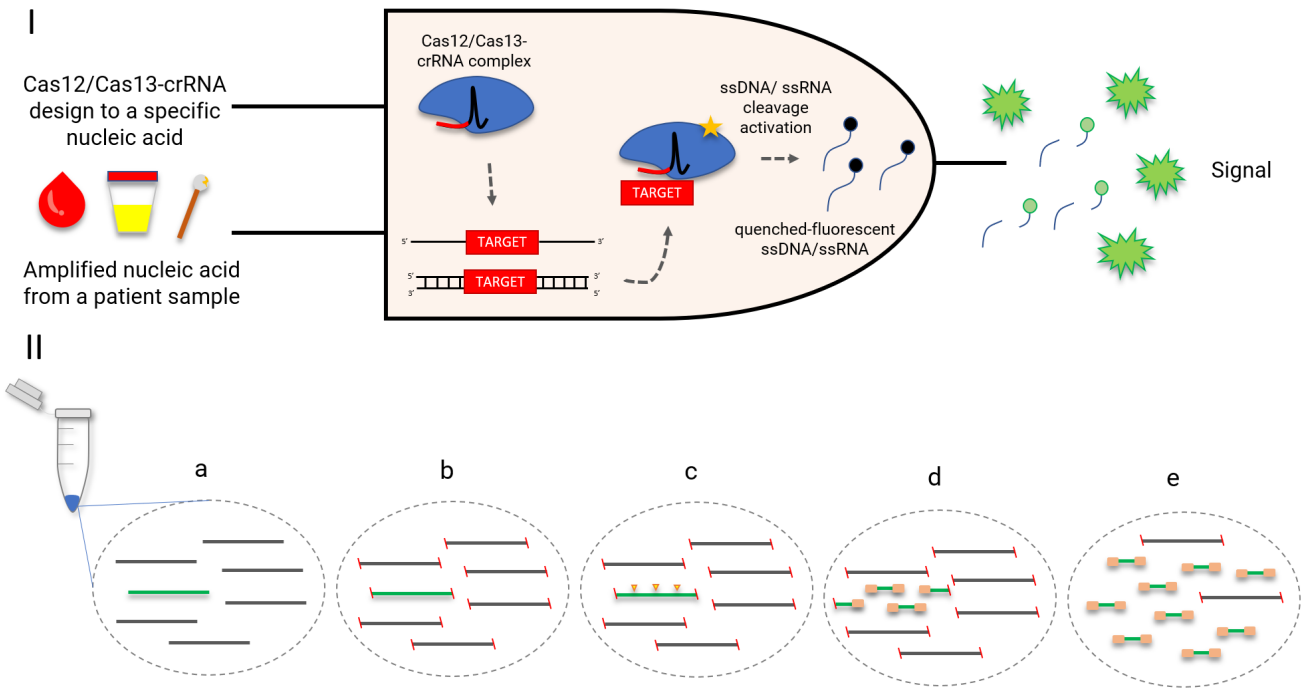

FIGURE 3 | CRISPR-Cas-based diagnostics. (I) A logic gate type "AND" of CRISPR-Cas12/13-based diagnostics. Amplified nucleic acid from patient samples can be used as input. Attomolar concentrations of RNA extracted from serum or urine samples could be detected. Without purification, Cas13 could detect RNA in samples containing up to 2% serum. The diagnostic could be performed also in cfDNA liquid biopsy samples and DNA extracted from anal swabs (Gootenberg et al., 2017; Chen et al., 2018; Gootenberg et al., 2018). A specific crRNA design to match a desired target, for instance, an antimicrobial resistance gene, is coupled with the Cas12/Cas13 as a second necessary input for the diagnostic. Once the target-positive sample is identified by the Cas12/Cas13-crRNA complex, the fluorescent output is generated. The fluorescent signal is a result of a collateral *trans*-cleavage of the quenched-fluorescent ssDNA/ssRNA by Cas12/Cas13, respectively. (II) CRISPR-Cas9 enrichment for NGS detection (Quan et al., 2019). (a) DNA or cDNA sequences containing the gene of interest (green); (b) blockage of DNA extremities; (c) CRISPR-Cas9 cleaves the target gene into fragments appropriately sized for NGS (yellow arrows); (d) ligation of universal sequencing adapters; (e) enrichment of the target sequence, which is now ready for NGS.

in order to increase target preference options and therefore the multiplexing panel.

When focusing on ARGs, *Klebsiella pneumoniae* carbapenemase (KPC) and New Delhi metallo-β-lactamase (NDM) were precisely detected and distinguished from five clinical isolates of *K. pneumoniae* (Gootenberg et al., 2017). Also, HIV drug resistance mutations from 22 patient samples could be identified (Ackerman et al., 2020). As an advantage, these platforms offer a highly specific detection of single-nucleotide polymorphisms (SNPs), which can be valuable to precisely

distinguish any desired resistance gene variant (Li S. Y. et al., 2018; Myhrvold et al., 2018).

Of note, the power of the platforms to face real-world challenges has been demonstrated with the detection of SARS-CoV-2 during the COVID-19 pandemic (Ackerman et al., 2020; Broughton et al., 2020) and with the FDA emergency authorization for CRISPR SARS-CoV-2 Rapid Diagnostic using SHERLOCK platform (Guglielmi, 2020).

When employed against AMR, CRISPR-Cas9, Cas3, and Cas13 have been explored as a powerful sequence-specific antimicrobial. Cell death is an expected outcome when sgRNA is directed to genes on the chromosome or plasmids containing a toxin–antitoxin system. For vectors without toxin–antitoxin, plasmid clearance or drastic copy number reduction can be achieved when targeting plasmids up to 300 copies/cell (Bikard et al., 2014; Citorik et al., 2014; Yosef et al., 2015; Kiga et al., 2020; Tagliaferri et al., 2020). Consequently to plasmid clearance in clinical isolates, other non-targeting ARGs harbored on the target vector were also eliminated, and antibiotic reusability could be confirmed in a *Galleria mellonella* infection model (Tagliaferri et al., 2020). Several variants or sub-variants of the resistance gene can be covered with one sgRNA/crRNA directed to a conserved genetic region (Kim et al., 2016; Tagliaferri et al., 2020), while selecting a sequence from a variable region may be a strategy to achieve a narrow-spectrum effect. CRISPR-Cas-mediated interference can also be fine-tuned according to the delivery approach. CRISPR-Cas delivery can be mediated by bacteriophages, and the specificity of phage–host interactions is an advantage when the target is placed in complex environments, such as microbiota (Bikard et al., 2014; Citorik et al., 2014; Yosef et al., 2015). Alternatively, the CRISPR-Cas system can be delivered via conjugative plasmid (Citorik et al., 2014; Rodrigues et al., 2019; Ruotsalainen et al., 2019). Opposite to the phage-mediated approach, lack of specific receptors for plasmid uptake during conjugation is considered as an advantage over phage delivery, as mutations in the receptors may lead to phage resistance. On the other hand, the conjugation rate is slower when compared to transduction (Ruotsalainen et al., 2019).

DISCUSSION AND FUTURE DIRECTIONS

Even with eminent demand, little has been explored of CRISPR-Cas and aptamer potential toward treatment of bacterial infection. As for CRISPR-Cas approach, Cas9 immunogenicity must be considered (Crudele and Chamberlain, 2018), as well as the definition of the most appropriate delivery method to optimize CRISPR-Cas effect in targeting bacteria within complex microbial communities. Environmental assessments may be required to evaluate risks involved on plasmid clearance and bacterial death, which can affect the frequency of non-targeting bacterial species and non-targeting plasmids. Also, with the ordinary or induced death of the targeting bacteria, CRISPR-Cas nucleic acid will naturally be released into the environment and strategies to prevent spread and horizontal transference of CRISPR-Cas system still need to be developed.

Important limitations of *in vivo* use of aptamers stem from their susceptibility to nuclease degradation and rapid elimination due to renal filtration, but chemical adjustments to the oligonucleotide structure have contributed to decrease those shortcomings (Rohloff et al., 2014). As an FDA-approved aptamer-based therapy is already a reality, we believe that the extension of this technology to other fields, including AMR, is a matter of time.

In contrast to treatment application, CRISPR-Cas-mediated diagnostic has been recently FDA-approved for detecting SARS-CoV-2, paving the way for further applications. Its high scalability and multiplexing properties are of great value for the detection and surveillance of the wide varieties of ARGs. A limitation of this approach is the target of either DNA or RNA, which confirms the presence but not the functionality of the ARGs. Aptamers by their turn target ARG products, but in order to be used as an independent diagnostic tool, increased sensitivity to attomolar levels may be required to bacterial detection in bloodstream (Kelley, 2017). As a counterpoint, the target flexibility of CRISPR-Cas, its simplicity, and the rational design of sgRNA/crRNA can be an advantage over the more complex and randomized process of aptamer selection.

We envisioned that, in the near future, CRISPR-Cas and aptamers can be combined to treat and/or diagnose resistant bacterial infections due to their aforementioned complementary characteristics. Together, those strategies have already shown to reduce CRISPR-Cas-related off-target effects in the HEK293 cell line (Zhao et al., 2020) and to increase the delivery selectivity in liver cells (Zhuang et al., 2020), and the combination was a powerful and reliable molecular sensor able to detect nasopharyngeal carcinoma biomarkers (Li et al., 2021). Whether their combined characteristics will also be beneficial for AMR diagnostics and for treating infections caused by resistant bacteria is yet to be determined. A recent study developed a strategy to recognize surface proteins on MRSA strains by aptamer and CRISPR-Cas12a-assisted rolling circle amplification (Xu et al., 2020). Still, there is a gallery of CRISPR-Cas/aptamer combinations and target bacteria to be tested, as well as further optimizations to achieve attomolar sensitivity.

Studies employing aptamer and CRISPR-Cas for diagnostics have demonstrated their ability to provide shorter turnaround time results than the gold standard AMR phenotypic tests, which can take up to 72 h to be released. This, along with the possibility of developing paper-based diagnostics, highlights the techniques' potential to be employed as a first guidance to clinical decisions related to antimicrobial use. Altogether, the molecular approaches may offer a suitable solution to circumvent antibiotic misuse in the first antibiotic prescription, currently guided only by empirical decisions.

AUTHOR CONTRIBUTIONS

HP, TT, and TM designed and wrote the manuscript. HP and TT analyzed the data. All authors contributed to the article and approved the submitted version.

FUNDING

The group received funding from Conselho Nacional de Desenvolvimento Científico e Tecnológico (CNPq), Coordenação de Aperfeiçoamento de Pessoal de Nível Superior (CAPES), Fundação de Amparo à Pesquisa do Estado de Minas Gerais (FAPEMIG), Fundação Arthur Bernardes, and the Bill and Melinda Gates Foundation (Grant No. OPP1193112). HP was supported by CNPq Ph.D. Fellowship. TT was supported by CNPq Postdoc Fellowship—Brazil (160598/2019-2).

REFERENCES

Abudayyeh, O. O., Gootenberg, J. S., Konermann, S., Joung, J., Slaymaker, I. M., Cox, D. B., et al. (2016). C2c2 is a single-component programmable RNA-guided RNA-targeting CRISPR effector. *Science* 353:aaf5573. doi: 10.1126/science.aaf5573

Ackerman, C. M., Myhrvold, C., Thakku, S. G., Freije, C. A., Metsky, H. C., Yang, D. K., et al. (2020). Massively multiplexed nucleic acid detection using Cas13. *Nature* 582, 277–282. doi: 10.1038/s41586-020-2279-8

Adams, C. P., and Brantner, V. V. (2010). Spending on new drug development1. *Health Econ.* 19, 130–141. doi: 10.1002/hec.1454

Afrasiabi, S., Pourhajibagher, M., Raoofian, R., Tabarzad, M., and Bahador, A. (2020). Therapeutic applications of nucleic acid aptamers in microbial infections. *J. Biomed. Sci.* 27:6.

Ahn, J. Y., Lee, K. A., Lee, M. J., Sekhon, S. S., Rhee, S. K., Cho, S. J., et al. (2018). Surface plasmon resonance aptamer biosensor for discriminating pathogenic bacteria vibrio parahaemolyticus. *J. Nanosci. Nanotechnol.* 18, 1599–1605. doi: 10.1166/jnn.2018.14212

Alfavian, H., Mousavi Gargari, S. L., Rasoulinejad, S., and Medhat, A. (2017). Development of a DNA aptamer that binds specifically to group a streptococcus serotype M3. *Can. J. Microbiol.* 63, 160–168. doi: 10.1139/cjm-2016-0495

Allen, H. K., Donato, J., Wang, H. H., Cloud-Hansen, K. A., Davies, J., and Handelsman, J. (2010). Call of the wild: antibiotic resistance genes in natural environments. *Nat. Rev. Microbiol.* 8, 251–259. doi: 10.1038/nrmicro2312

Amraee, M., Oloomi, M., Yavari, A., and Bouzari, S. (2017). DNA aptamer identification and characterization for *E. coli* O157 detection using cell based SELEX method. *Anal. Biochem.* 536, 36–44. doi: 10.1016/j.ab.2017.08.005

Appaturi, J. N., Pulingam, T., Thong, K. L., Muniandy, S., Ahmad, N., and Leo, B. F. (2020). Rapid and sensitive detection of Salmonella with reduced graphene oxide-carbon nanotube based electrochemical aptasensor. *Anal. Biochem.* 589:113489. doi: 10.1016/j.ab.2019.113489

Bai, L., Chen, Y., Bai, Y., Chen, Y., Zhou, J., and Huang, A. (2017). Fullerene-doped polyaniline as new redox nanoprobe and catalyst in electrochemical aptasensor for ultrasensitive detection of *Mycobacterium tuberculosis* MPT64 antigen in human serum. *Biomaterials* 133, 11–19. doi: 10.1016/j.biomaterials.2017.04.010

Bayrac, C., and Oktem, H. A. (2017). Evaluation of *Staphylococcus aureus* DNA aptamer by enzyme-linked aptamer assay and isothermal titration calorimetry. *J. Mol. Recognit.* 30, 1–9.

Bayrac, C., Eyidogan, F., and Avni Oktem, H. (2017). DNA aptamer-based colorimetric detection platform for *Salmonella Enteritidis*. *Biosens. Bioelectron.* 98, 22–28. doi: 10.1016/j.bios.2017.06.029

Bikard, D., Euler, C. W., Jiang, W., Nussenzweig, P. M., Goldberg, G. W., Duportet, X., et al. (2014). Exploiting CRISPR-Cas nucleases to produce sequence-specific antimicrobials. *Nat. Biotechnol.* 32, 1146–1150. doi: 10.1038/nbt.3043

Blair, J. M., Webber, M. A., Baylay, A. J., Ogbolu, D. O., and Piddock, L. J. (2015). Molecular mechanisms of antibiotic resistance. *Nat. Rev. Microbiol.* 13, 42–51.

Broughton, J. P., Deng, X., Yu, G., Fasching, C. L., Servellita, V., Singh, J., et al. (2020). CRISPR-Cas12-based detection of SARS-CoV-2. *Nat Biotechnol.* 38, 870–874.

Bush, K., and Bradford, P. A. (2019). Interplay between beta-lactamases and new beta-lactamase inhibitors. *Nat. Rev. Microbiol.* 17, 295–306. doi: 10.1038/s41579-019-0159-8

Cai, R., Yin, F., Zhang, Z., Tian, Y., and Zhou, N. (2019). Functional chimera aptamer and molecular beacon based fluorescent detection of *Staphylococcus aureus* with strand displacement-target recycling amplification. *Anal. Chim. Acta* 1075, 128–136. doi: 10.1016/j.aca.2019.05.014

Calero-Caceres, W., Ye, M., and Balcazar, J. L. (2019). Bacteriophages as environmental reservoirs of antibiotic resistance. *Trends Microbiol.* 27, 570–577. doi: 10.1016/j.tim.2019.02.008

Cao, L., Gao, C. H., Zhu, J., Zhao, L., Wu, Q., Li, M., et al. (2016). Identification and functional study of type III-A CRISPR-Cas systems in clinical isolates of *Staphylococcus aureus*. *Int. J. Med. Microbiol.* 306, 686–696. doi: 10.1016/j.ijmm.2016.08.005

Casini, A., Olivieri, M., Petris, G., Montagna, C., Reginato, G., Maule, G., et al. (2018). A highly specific SpCas9 variant is identified by in vivo screening in yeast. *Nat. Biotechnol.* 36, 265–271. doi: 10.1038/nbt.4066

CDC, (2019). *Antibiotic Resistance Threats in the United States*. Atlanta: CDC.

Chen, J. S., Dagdas, Y. S., Kleinstiver, B. P., Welch, M. M., Sousa, A. A., Harrington, L. B., et al. (2017). Enhanced proofreading governs CRISPR-Cas9 targeting accuracy. *Nature* 550, 407–410. doi: 10.1038/nature24268

Chen, J. S., Ma, E., Harrington, L. B., Da Costa, M., Tian, X., Palefsky, J. M., et al. (2018). CRISPR-Cas12a target binding unleashes indiscriminate single-stranded DNase activity. *Science* 360, 436–439. doi: 10.1126/science.aar6245

Chen, K., and Gao, C. (2014). Targeted genome modification technologies and their applications in crop improvements. *Plant Cell Rep.* 33, 575–583. doi: 10.1007/s00299-013-1539-6

Chen, L., Rashid, F., Shah, A., Awan, H. M., Wu, M., Liu, A., et al. (2015). The isolation of an RNA aptamer targeting to p53 protein with single amino acid mutation. *Proc. Natl. Acad. Sci. U.S.A.* 112, 10002–10007. doi: 10.1073/pnas.1502159112

Chinnappan, R., Alamer, S., Eissa, S., Rahamn, A. A., Abu Salah, K. M., and Zourob, M. (2017). Fluorometric graphene oxide-based detection of *Salmonella enteritis* using a truncated DNA aptamer. *Mikrochim. Acta* 185:61.

Citorik, R. J., Mimee, M., and Lu, T. K. (2014). Sequence-specific antimicrobials using efficiently delivered RNA-guided nucleases. *Nat. Biotechnol.* 32, 1141–1145. doi: 10.1038/nbt.3011

Crudele, J. M., and Chamberlain, J. S. (2018). Cas9 immunity creates challenges for CRISPR gene editing therapies. *Nat. Commun.* 9:3497.

Dalirirad, S., and Steckl, A. J. (2020). Lateral flow assay using aptamer-based sensing for on-site detection of dopamine in urine. *Anal. Biochem.* 596:113637. doi: 10.1016/j.ab.2020.113637

Das, R., Dhiman, A., Kapil, A., Bansal, V., and Sharma, T. K. (2019a). Aptamer-mediated colorimetric and electrochemical detection of *Pseudomonas aeruginosa* utilizing peroxidase-mimic activity of gold NanoZyme. *Anal. Bioanal. Chem.* 411, 1229–1238. doi: 10.1007/s00216-018-1555-z

Das, R., Dhiman, A., Mishra, S. K., Haldar, S., Sharma, N., Bansal, A., et al. (2019b). Structural switching electrochemical DNA aptasensor for the rapid diagnosis of tuberculous meningitis. *Int. J. Nanomed.* 14, 2103–2113. doi: 10.2147/ijn.s189127

D'costa, V. M., King, C. E., Kalan, L., Morar, M., Sung, W. W., Schwarz, C., et al. (2011). Antibiotic resistance is ancient. *Nature* 477, 457–461.

Dehghani, Z., Hosseini, M., Mohammadnejad, J., Bakhshi, B., and Rezayan, A. H. (2018). Colorimetric aptasensor for *Campylobacter jejuni* cells by exploiting the peroxidase like activity of Au@Pd nanoparticles. *Mikrochim. Acta* 185:448.

Dekker, J. P. (2018). Metagenomics for clinical infectious disease diagnostics steps closer to reality. *J. Clin. Microbiol.* 56:e00850-18.

Doi, Y., Wachino, J. I., and Arakawa, Y. (2016). Aminoglycoside resistance: the emergence of acquired 16S ribosomal RNA methyltransferases. *Infect. Dis. Clin. North Am.* 30, 523–537.

Dua, P., Ren, S., Lee, S. W., Kim, J. K., Shin, H. S., Jeong, O. C., et al. (2016). Cell-SELEX based identification of an RNA aptamer for *Escherichia coli* and its use in various detection formats. *Mol. Cells* 39, 807–813. doi: 10.14348/molcells.2016.0167

Duan, N., Xu, B., Wu, S., and Wang, Z. (2016). Magnetic nanoparticles-based aptasensor using gold nanoparticles as colorimetric probes for the detection of *Salmonella typhimurium*. *Anal. Sci.* 32, 431–436. doi: 10.2116/analsci.32.431

Ellington, A. D., and Szostak, J. W. (1990). In vitro selection of RNA molecules that bind specific ligands. *Nature* 346, 818–822. doi: 10.1038/346818a0

Esposito, C. L., Nuzzo, S., Catuogno, S., Romano, S., De Nigris, F., and De Franciscis, V. (2018). STAT3 gene silencing by aptamer-siRNA chimera as selective therapeutic for glioblastoma. *Mol. Ther. Nucleic Acids* 10, 398–411. doi: 10.1016/j.omtn.2017.12.021

Fan, Y., Cui, M., Liu, Y., Jin, M., and Zhao, H. (2020). Selection and characterization of DNA aptamers for constructing colorimetric biosensor for detection of PBP2a. *Spectrochim. Acta A Mol. Biomol. Spectrosc.* 228:117735. doi: 10.1016/j.saa.2019.117735

Fischer, J. E., Harbarth, S., Agthe, A. G., Benn, A., Ringer, S. A., Goldmann, D. A., et al. (2004). Quantifying uncertainty: physicians' estimates of infection in critically ill neonates and children. *Clin. Infect. Dis.* 38, 1383–1390. doi: 10.1086/420741

Gao, R., Zhong, Z., Gao, X., and Jia, L. (2018). Graphene oxide quantum dots assisted construction of fluorescent aptasensor for rapid detection of *Pseudomonas aeruginosa* in food samples. *J. Agric. Food Chem.* 66, 10898–10905. doi: 10.1021/acs.jafc.8b02164

Gleditzsch, D., Pausch, P., Muller-Esparza, H., Ozcan, A., Guo, X., Bange, G., et al. (2019). PAM identification by CRISPR-Cas effector complexes: diversified mechanisms and structures. *RNA Biol.* 16, 504–517. doi: 10.1080/15476286.2018.1504546

Gootenberg, J. S., Abudayyeh, O. O., Kellner, M. J., Joung, J., Collins, J. J., and Zhang, F. (2018). Multiplexed and portable nucleic acid detection platform with Cas13. Cas12a, and Csm6. *Science* 360, 439–444. doi: 10.1126/science.aaq0179

Gootenberg, J. S., Abudayyeh, O. O., Lee, J. W., Essletzbichler, P., Dy, A. J., Joung, J., et al. (2017). Nucleic acid detection with CRISPR-Cas13a/C2c2. *Science* 356, 438–442. doi: 10.1126/science.aam9321

Gragoudas, E. S., Adamis, A. P., Cunningham, E. T. Jr., Feinsod, M., and Guyer, D. R. (2004). Pegaptanib for neovascular age-related macular degeneration. *N. Engl. J. Med.* 351, 2805–2816.

Guglielmi, G. (2020). First CRISPR test for the coronavirus approved in the United States. *Nature* doi: 10.1038/d41586-020-01402-9 Online ahead of print.

Ha, N. R., Jung, I. P., La, I. J., Jung, H. S., and Yoon, M. Y. (2017). Ultra-sensitive detection of kanamycin for food safety using a reduced graphene oxide-based fluorescent aptasensor. *Sci. Rep.* 7:40305.

Hamula, C. L., Peng, H., Wang, Z., Tyrrell, G. J., Li, X. F., and Le, X. C. (2016). An improved SELEX technique for selection of DNA aptamers binding to M-type 11 of *Streptococcus pyogenes*. *Methods* 97, 51–57. doi: 10.1016/j.ymeth.2015.12.005

Hille, F., Richter, H., Wong, S. P., Bratovic, M., Ressel, S., and Charpentier, E. (2018). The biology of CRISPR-Cas: backward and forward. *Cell* 172, 1239–1259. doi: 10.1016/j.cell.2017.11.032

Hua, R., Hao, N., Lu, J., Qian, J., Liu, Q., Li, H., et al. (2018). A sensitive Potentiometric resolved ratiometric Photoelectrochemical aptasensor for *Escherichia coli* detection fabricated with non-metallic nanomaterials. *Biosens. Bioelectron.* 106, 57–63. doi: 10.1016/j.bios.2018.01.053

Jin, B., Wang, S., Lin, M., Jin, Y., Zhang, S., Cui, X., et al. (2017). Upconversion nanoparticles based FRET aptasensor for rapid and ultrasenstive bacteria detection. *Biosens. Bioelectron.* 90, 525–533. doi: 10.1016/j.bios.2016.10.029

Jinek, M., Chylinski, K., Fonfara, I., Hauer, M., Doudna, J. A., and Charpentier, E. (2012). A programmable dual-RNA-guided DNA endonuclease in adaptive bacterial immunity. *Science* 337, 816–821. doi: 10.1126/science.1225829

Kaur, H., Bruno, J. G., Kumar, A., and Sharma, T. K. (2018). Aptamers in the therapeutics and diagnostics pipelines. *Theranostics* 8, 4016–4032. doi: 10.7150/thno.25958

Kelley, S. O. (2017). What are clinically relevant levels of cellular and biomolecular analytes? *ACS Sens.* 2, 193–197. doi: 10.1021/acssensors.6b00691

Kiga, K., Tan, X. E., Ibarra-Chavez, R., Watanabe, S., Aiba, Y., Sato'o, Y., et al. (2020). Development of CRISPR-Cas13a-based antimicrobials capable of sequence-specific killing of target bacteria. *Nat. Commun.* 11:2934.

Kim, H. J., Park, J. Y., Lee, T. S., Song, I. H., Cho, Y. L., Chae, J. R., et al. (2019). PET imaging of HER2 expression with an 18F-fluoride labeled aptamer. *PLoS One* 14:e0211047. doi: 10.1371/journal.pone.0211047

Kim, J. S., Cho, D. H., Park, M., Chung, W. J., Shin, D., Ko, K. S., et al. (2016). CRISPR/Cas9-mediated re-sensitization of antibiotic-resistant *Escherichia coli* harboring extended-spectrum beta-lactamases. *J. Microbiol. Biotechnol.* 26, 394–401. doi: 10.4014/jmb.1508.08080

Kleinstiver, B. P., Pattanayak, V., Prew, M. S., Tsai, S. Q., Nguyen, N. T., Zheng, Z., et al. (2016). High-fidelity CRISPR-Cas9 nucleases with no detectable genome-wide off-target effects. *Nature* 529, 490–495. doi: 10.1038/nature16526

Kurt, H., Yuce, M., Hussain, B., and Budak, H. (2016). Dual-excitation upconverting nanoparticle and quantum dot aptasensor for multiplexed food pathogen detection. *Biosens. Bioelectron.* 81, 280–286. doi: 10.1016/j.bios.2016.03.005

Lavu, P. S., Mondal, B., Ramlal, S., Murali, H. S., and Batra, H. V. (2016). Selection and characterization of aptamers using a modified whole cell bacterium SELEX for the detection of *Salmonella enterica* serovar Typhimurium. *ACS Comb. Sci.* 18, 292–301. doi: 10.1021/acscombsci.5b00123

Lee, J. K., Jeong, E., Lee, J., Jung, M., Shin, E., Kim, Y. H., et al. (2018). Directed evolution of CRISPR-Cas9 to increase its specificity. *Nat. Commun.* 9:3048.

Leekha, S., Terrell, C. L., and Edson, R. S. (2011). General principles of antimicrobial therapy. *Mayo Clin. Proc.* 86, 156–167. doi: 10.4065/mcp.2010.0639

Li, H., Xing, S., Xu, J., He, Y., Lai, Y., Wang, Y., et al. (2021). Aptamer-based CRISPR/Cas12a assay for the ultrasensitive detection of extracellular vesicle proteins. *Talanta* 221:121670. doi: 10.1016/j.talanta.2020.121670

Li, H., Yang, Y., Hong, W., Huang, M., Wu, M., and Zhao, X. (2020). Applications of genome editing technology in the targeted therapy of human diseases: mechanisms, advances and prospects. *Signal Transduct. Target. Ther.* 5:1.

Li, N., Huang, X., Sun, D., Yu, W., Tan, W., Luo, Z., et al. (2018). Dual-aptamer-based voltammetric biosensor for the *Mycobacterium tuberculosis* antigen MPT64 by using a gold electrode modified with a peroxidase loaded composite consisting of gold nanoparticles and a Zr(IV)/terephthalate metal-organic framework. *Mikrochim. Acta* 185:543.

Li, S. Y., Cheng, Q. X., Wang, J. M., Li, X. Y., Zhang, Z. L., Gao, S., et al. (2018). CRISPR-Cas12a-assisted nucleic acid detection. *Cell Discov.* 4:20.

Liu, H. L. C., Zhao, Y., Han, X., Zhou, Z., Wang, C., Li, R., et al. (2018). Comparing successful gene knock-in efficiencies of CRISPR/Cas9 with ZFNs and TALENs gene editing systems in bovine and dairy goat fetal fibroblasts. *J. Integr. Agric.* 17, 406–414. doi: 10.1016/s2095-3119(17)61748-9

Liu, L., Li, X., Ma, J., Li, Z., You, L., Wang, J., et al. (2017). The molecular architecture for RNA-guided RNA cleavage by cas13a. *Cell* 170:e710.

Liu, Y., Jiang, W., Yang, S., Hu, J., Lu, H., Han, W., et al. (2019). Rapid detection of mycoplasma-infected cells by an ssDNA aptamer probe. *ACS Sens.* 4, 2028–2038. doi: 10.1021/acssensors.9b00582

Llor, C., and Bjerrum, L. (2014). Antimicrobial resistance: risk associated with antibiotic overuse and initiatives to reduce the problem. *Ther. Adv. Drug Saf.* 5, 229–241. doi: 10.1177/2042098614554919

Makarova, K. S., Wolf, Y. I., Alkhnbashi, O. S., Costa, F., Shah, S. A., Saunders, S. J., et al. (2015). An updated evolutionary classification of CRISPR-Cas systems. *Nat. Rev. Microbiol.* 13, 722–736.

Makarova, K. S., Wolf, Y. I., Iranzo, J., Shmakov, S. A., Alkhnbashi, O. S., Brouns, S. J. J., et al. (2020). Evolutionary classification of CRISPR-Cas systems: a burst of class 2 and derived variants. *Nat. Rev. Microbiol.* 18, 67–83. doi: 10.1038/s41579-019-0299-x

Maldonado, J., Estevez, M. C., Fernandez-Gavela, A., Gonzalez-Lopez, J. J., Gonzalez-Guerrero, A. B., and Lechuga, L. M. (2020). Label-free detection of nosocomial bacteria using a nanophotonic interferometric biosensor. *Analyst* 145, 497–506. doi: 10.1039/c9an01485c

Malik, B., and Bhattacharyya, S. (2019). Antibiotic drug-resistance as a complex system driven by socio-economic growth and antibiotic misuse. *Sci. Rep.* 9:9788.

Marraffini, L. A., and Sontheimer, E. J. (2010). Self versus non-self discrimination during CRISPR RNA-directed immunity. *Nature* 463, 568–571. doi: 10.1038/nature08703

Marton, S., Cleto, F., Krieger, M. A., and Cardoso, J. (2016). Isolation of an Aptamer that Binds Specifically to *E. coli*. *PLoS One* 11:e0153637. doi: 10.1371/journal.pone.0153637

McKeague, M., De Girolamo, A., Valenzano, S., Pascale, M., Ruscito, A., Velu, R., et al. (2015). Comprehensive analytical comparison of strategies used for small molecule aptamer evaluation. *Anal. Chem.* 87, 8608–8612. doi: 10.1021/acs.analchem.5b02102

Mirzakhani, K., Mousavi Gargari, S. L., Rasooli, I., and Rasoulinejad, S. (2017). Development of a DNA Aptamer for screening *Neisseria meningitidis* serogroup B by cell selex. *Iran Biomed. J.* 22, 193–201.

Mitsakakis, K., Kaman, W. E., Elshout, G., Specht, M., and Hays, J. P. (2018). Challenges in identifying antibiotic resistance targets for point-of-care diagnostics in general practice. *Future Microbiol.* 13, 1157–1164. doi: 10.2217/fmb-2018-0084

Mojica, F. J. M., Diez-Villasenor, C., Garcia-Martinez, J., and Almendros, C. (2009). Short motif sequences determine the targets of the prokaryotic CRISPR defence system. *Microbiology* 155, 733–740. doi: 10.1099/mic.0.023960-0

Mol, A. A., Groher, F., Schreiber, B., Ruhmkorff, C., and Suess, B. (2019). Robust gene expression control in human cells with a novel universal TetR aptamer splicing module. *Nucleic Acids Res.* 47:e132. doi: 10.1093/nar/gkz753

Mozioglu, E., Gokmen, O., Tamerler, C., Kocagoz, Z. T., and Akgoz, M. (2016). Selection of Nucleic acid aptamers specific for *Mycobacterium tuberculosis*. *Appl. Biochem. Biotechnol.* 178, 849–864. doi: 10.1007/s12010-015-1913-7

Munita, J. M., and Arias, C. A. (2016). Mechanisms of antibiotic resistance. *Microbiol. Spectr.* 4, 1–24.

Myhrvold, C., Freije, C. A., Gootenberg, J. S., Abudayyeh, O. O., Metsky, H. C., Durbin, A. F., et al. (2018). Field-deployable viral diagnostics using CRISPR-Cas13. *Science* 360, 444–448. doi: 10.1126/science.aas8836

O'Neil, J. (2016). *Tackling Drug-Resistant Infections Globally: Final Report and Recommendations [Online]*. Available online at: http://amr-review.org (accessed July 19, 2020).

Ota, Y., Furuhashi, K., Nanba, T., Yamanaka, K., Ishikawa, J., Nagura, O., et al. (2019). A rapid and simple detection method for phenotypic antimicrobial resistance in *Escherichia coli* by loop-mediated isothermal amplification. *J. Med. Microbiol.* 68, 169–177. doi: 10.1099/jmm.0.000903

Pancholi, P., Carroll, K. C., Buchan, B. W., Chan, R. C., Dhiman, N., Ford, B., et al. (2018). Multicenter evaluation of the accelerate phenotest BC kit for rapid identification and phenotypic antimicrobial susceptibility testing using morphokinetic cellular analysis. *J. Clin. Microbiol.* 56:e01329-17.

Patrinos, G. P., Danielson, P. B., and Ansorge, W. J. (2017). "Molecular diagnostics: past, present, and future," in *Molecular Diagnostic* ed. G.P. Patrinos, (Amsterdam: Elsevier), 520.

Peng, W., Feng, M., Feng, X., Liang, Y. X., and She, Q. (2015). An archaeal CRISPR type III-B system exhibiting distinctive RNA targeting features and mediating dual RNA and DNA interference. *Nucleic Acids Res.* 43, 406–417. doi: 10.1093/nar/gku1302

Powers, J. H. (2004). Antimicrobial drug development–the past, the present, and the future. *Clin. Microbiol. Infect* 10(Suppl. 4), 23–31. doi: 10.1111/j.1465-0691.2004.1007.x

Qiao, J., Meng, X., Sun, Y., Li, Q., Zhao, R., Zhang, Y., et al. (2018). Aptamer-based fluorometric assay for direct identification of methicillin-resistant *Staphylococcus aureus* from clinical samples. *J. Microbiol. Methods* 153, 92–98. doi: 10.1016/j.mimet.2018.09.011

Quan, J., Langelier, C., Kuchta, A., Batson, J., Teyssier, N., Lyden, A., et al. (2019). FLASH: a next-generation CRISPR diagnostic for multiplexed detection of antimicrobial resistance sequences. *Nucleic Acids Res.* 47:e83. doi: 10.1093/nar/gkz418

Rasoulinejad, S., and Gargari, S. L. M. (2016). Aptamer-nanobody based ELASA for specific detection of *Acinetobacter baumannii* isolates. *J. Biotechnol.* 231, 46–54. doi: 10.1016/j.jbiotec.2016.05.024

Reich, P., Stoltenburg, R., Strehlitz, B., Frense, D., and Beckmann, D. (2017). Development of an impedimetric aptasensor for the detection of *Staphylococcus aureus*. *Int. J. Mol. Sci.* 18:2484. doi: 10.3390/ijms18112484

Ren, J., Liang, G., Man, Y., Li, A., Jin, X., Liu, Q., et al. (2019). Aptamer-based fluorometric determination of *Salmonella Typhimurium* using Fe3O4 magnetic separation and CdTe quantum dots. *PLoS One* 14:e0218325. doi: 10.1371/journal.pone.0218325

Rodrigues, M., Mcbride, S. W., Hullahalli, K., Palmer, K. L., and Duerkop, B. A. (2019). Conjugative delivery of CRISPR-Cas9 for the selective depletion of antibiotic-resistant enterococci. *Antimicrob. Agents Chemother.* 63:e01454-9.

Rohloff, J. C., Gelinas, A. D., Jarvis, T. C., Ochsner, U. A., Schneider, D. J., Gold, L., et al. (2014). Nucleic acid ligands with protein-like side chains: modified aptamers and their use as diagnostic and therapeutic agents. *Mol. Ther. Nucleic Acids* 3:e201. doi: 10.1038/mtna.2014.49

Ruotsalainen, P., Penttinen, R., Mattila, S., and Jalasvuori, M. (2019). Midbiotics: conjugative plasmids for genetic engineering of natural gut flora. *Gut Microbes* 10, 643–653. doi: 10.1080/19490976.2019.1591136

Sakyi, S. A., Aboagye, S. Y., Otchere, I. D., Liao, A. M., Caltagirone, T. G., and Yeboah-Manu, D. (2016). RNA aptamer that specifically binds to mycolactone and serves as a diagnostic tool for diagnosis of buruli ulcer. *PLoS Negl. Trop Dis.* 10:e0004950. doi: 10.1371/journal.pntd.0004950

Semenova, E., Jore, M. M., Datsenko, K. A., Semenova, A., Westra, E. R., Wanner, B., et al. (2011). Interference by clustered regularly interspaced short palindromic repeat (CRISPR) RNA is governed by a seed sequence. *Proc. Natl. Acad. Sci. U.S.A.* 108, 10098–10103.

Shen, H., Wang, J., Liu, H., Li, Z., Jiang, F., Wang, F. B., et al. (2016). Rapid and selective detection of pathogenic bacteria in bloodstream infections with aptamer-based recognition. *ACS Appl. Mater Interfaces* 8, 19371–19378. doi: 10.1021/acsami.6b06671

Sheridan, C. (2020). Coronavirus and the race to distribute reliable diagnostics. *Nat. Biotechnol.* 38, 382–384. doi: 10.1038/d41587-020-00002-2

Shin, H. S., Gedi, V., Kim, J. K., and Lee, D. K. (2019). Detection of gram-negative bacterial outer membrane vesicles using DNA aptamers. *Sci. Rep.* 9:13167.

Shin, W. R., Sekhon, S. S., Rhee, S. K., Ko, J. H., Ahn, J. Y., Min, J., et al. (2018). Aptamer-based paper strip sensor for detecting vibrio fischeri. *ACS Comb Sci.* 20, 261–268. doi: 10.1021/acscombsci.7b00190

Singh, R. K., Dhama, K., Karthik, K., Tiwari, R., Khandia, R., Munjal, A., et al. (2017). Advances in diagnosis, surveillance, and monitoring of Zika virus: an update. *Front. Microbiol.* 8:2677.

Slaymaker, I. M., Gao, L., Zetsche, B., Scott, D. A., Yan, W. X., and Zhang, F. (2016). Rationally engineered Cas9 nucleases with improved specificity. *Science* 351, 84–88. doi: 10.1126/science.aad5227

Song, M. S., Sekhon, S. S., Shin, W. R., Kim, H. C., Min, J., Ahn, J. Y., et al. (2017). Detecting and discriminating Shigella sonnei using an aptamer-based fluorescent biosensor platform. *Molecules* 22:825. doi: 10.3390/molecules22050825

Song, M. Y., Nguyen, D., Hong, S. W., and Kim, B. C. (2017). Broadly reactive aptamers targeting bacteria belonging to different genera using a sequential toggle cell-SELEX. *Sci. Rep.* 7:43641.

Stoltenburg, R., Krafcikova, P., Viglasky, V., and Strehlitz, B. (2016). G-quadruplex aptamer targeting protein a and its capability to detect *Staphylococcus aureus* demonstrated by Elona. *Sci. Rep.* 6:33812.

Su, Y., Shao, C., Huang, X., Qi, J., Ge, R., Guan, H., et al. (2018). Extraction and detection of bisphenol a in human serum and urine by aptamer-functionalized magnetic nanoparticles. *Anal. Bioanal. Chem.* 410, 1885–1891. doi: 10.1007/s00216-017-0801-0

Suh, S. H., Choi, S. J., Dwivedi, H. P., Moore, M. D., Escudero-Abarca, B. I., and Jaykus, L. A. (2018). Use of DNA aptamer for sandwich type detection of *Listeria monocytogenes*. *Anal. Biochem.* 557, 27–33. doi: 10.1016/j.ab.2018.04.009

Sun, Y., Duan, N., Ma, P., Liang, Y., Zhu, X., and Wang, Z. (2019). Colorimetric aptasensor based on truncated aptamer and trivalent DNAzyme for *Vibrio parahemolyticus* determination. *J. Agric. Food Chem.* 67, 2313–2320. doi: 10.1021/acs.jafc.8b06893

Tagliaferri, T. L., Guimaraes, N. R., Pereira, M. P. M., Vilela, L. F. F., Horz, H. P., Dos Santos, S. G., et al. (2020). Exploring the potential of CRISPR-Cas9 under challenging conditions: facing high-copy plasmids and counteracting beta-lactam resistance in clinical strains of *Enterobacteriaceae*. *Front. Microbiol.* 11:578.

Tang, X. L., Wu, S. M., Xie, Y., Song, N., Guan, Q., Yuan, C., et al. (2016). Generation and application of ssDNA aptamers against glycolipid antigen ManLAM of *Mycobacterium tuberculosis* for TB diagnosis. *J. Infect.* 72, 573–586. doi: 10.1016/j.jinf.2016.01.014

Toh, S. Y., Citartan, M., Gopinath, S. C., and Tang, T. H. (2015). Aptamers as a replacement for antibodies in enzyme-linked immunosorbent assay. *Biosens. Bioelectron.* 64, 392–403. doi: 10.1016/j.bios.2014.09.026

Tuerk, C., and Gold, L. (1990). Systematic evolution of ligands by exponential enrichment: RNA ligands to bacteriophage T4 DNA polymerase. *Science* 249, 505–510. doi: 10.1126/science.2200121

Wang, L., Huo, X., Qi, W., Xia, Z., Li, Y., and Lin, J. (2020). Rapid and sensitive detection of *Salmonella Typhimurium* using nickel nanowire bridge for electrochemical impedance amplification. *Talanta* 211:120715. doi: 10.1016/j.talanta.2020.120715

Waseem, H., Jameel, S., Ali, J., Saleem, Ur Rehman, H., Tauseef, I., et al. (2019). Contributions and challenges of high throughput qPCR for determining antimicrobial resistance in the environment: a critical review. *Molecules* 24:163. doi: 10.3390/molecules24010163

Wu, G., Dai, Z., Tang, X., Lin, Z., Lo, P. K., Meyyappan, M., et al. (2017). Graphene field-effect transistors for the sensitive and selective detection of *Escherichia coli* Using Pyrene-tagged DNA aptamer. *Adv. Healthc Mater* 6:1700736.

Xiang, D., Zheng, C., Zhou, S. F., Qiao, S., Tran, P. H., Pu, C., et al. (2015). Superior Performance of aptamer in tumor penetration over antibody: implication of aptamer-based theranostics in solid tumors. *Theranostics* 5, 1083–1097. doi: 10.7150/thno.11711

Xiong, Y., Zhang, J., Yang, Z., Mou, Q., Ma, Y., Xiong, Y., et al. (2020). Functional DNA regulated CRISPR-Cas12a sensors for point-of-care diagnostics of non-nucleic-acid targets. *J. Am. Chem. Soc.* 142, 207–213. doi: 10.1021/jacs.9b09211

Xu, L., Dai, Q., Shi, Z., Liu, X., Gao, L., Wang, Z., et al. (2020). Accurate MRSA identification through dual-functional aptamer and CRISPR-Cas12a assisted rolling circle amplification. *J. Microbiol. Methods* 173:105917. doi: 10.1016/j.mimet.2020.105917

Xu, Y., Wang, H., Luan, C., Liu, Y., Chen, B., and Zhao, Y. (2018). Aptamer-based hydrogel barcodes for the capture and detection of multiple types of pathogenic bacteria. *Biosens. Bioelectron.* 100, 404–410. doi: 10.1016/j.bios.2017.09.032

Yoon, S., and Rossi, J. J. (2018). Aptamers: uptake mechanisms and intracellular applications. *Adv. Drug Deliv. Rev.* 134, 22–35. doi: 10.1016/j.addr.2018.07.003

Yosef, I., Manor, M., Kiro, R., and Qimron, U. (2015). Temperate and lytic bacteriophages programmed to sensitize and kill antibiotic-resistant bacteria. *Proc. Natl. Acad. Sci. U.S.A.* 112, 7267–7272. doi: 10.1073/pnas.1500107112

Yu, X., Chen, F., Wang, R., and Li, Y. (2018). Whole-bacterium SELEX of DNA aptamers for rapid detection of *E.coli O*157:H7 using a QCM sensor. *J. Biotechnol.* 266, 39–49. doi: 10.1016/j.jbiotec.2017.12.011

Yunn, N. O., Koh, A., Han, S., Lim, J. H., Park, S., Lee, J., et al. (2015). Agonistic aptamer to the insulin receptor leads to biased signaling and functional selectivity through allosteric modulation. *Nucleic Acids Res.* 43, 7688–7701. doi: 10.1093/nar/gkv767

Zankari, E., Hasman, H., Cosentino, S., Vestergaard, M., Rasmussen, S., Lund, O., et al. (2012). Identification of acquired antimicrobial resistance genes. *J. Antimicrob. Chemother.* 67, 2640–2644. doi: 10.1093/jac/dks261

Zhang, J., Liu, J., Yang, W., Cui, M., Dai, B., Dong, Y., et al. (2019). Comparison of gene editing efficiencies of CRISPR/Cas9 and TALEN for generation of MSTN knock-out cashmere goats. *Theriogenology* 132, 1–11. doi: 10.1016/j.theriogenology.2019.03.029

Zhang, X., Feng, Y., Yao, Q., and He, F. (2017). Selection of a new *Mycobacterium tuberculosis* H37Rv aptamer and its application in the construction of a SWCNT/aptamer/Au-IDE MSPQC H37Rv sensor. *Biosens. Bioelectron.* 98, 261–266. doi: 10.1016/j.bios.2017.05.043

Zhang, Y., Luo, F., Zhang, Y., Zhu, L., Li, Y., Zhao, S., et al. (2018). A sensitive assay based on specific aptamer binding for the detection of *Salmonella enterica* serovar Typhimurium in milk samples by microchip capillary electrophoresis. *J. Chromatogr. A* 1534, 188–194. doi: 10.1016/j.chroma.2017.12.054

Zhao, J., Inomata, R., Kato, Y., and Miyagishi, M. (2020). Development of aptamer-based inhibitors for CRISPR/Cas system. *Nucleic Acids Res.* doi: 10.1093/nar/gkaa865 Online ahead of print.

Zhao, M., Li, W., Liu, K., Li, H., and Lan, X. (2019). C4-HSL aptamers for blocking qurom sensing and inhibiting biofilm formation in *Pseudomonas aeruginosa* and its structure prediction and analysis. *PLoS One* 14:e0212041. doi: 10.1371/journal.pone.0212041

Zhou, J., Satheesan, S., Li, H., Weinberg, M. S., Morris, K. V., Burnett, J. C., et al. (2015). Cell-specific RNA aptamer against human CCR5 specifically targets HIV-1 susceptible cells and inhibits HIV-1 infectivity. *Chem. Biol.* 22, 379–390. doi: 10.1016/j.chembiol.2015.01.005

Zhuang, J., Tan, J., Wu, C., Zhang, J., Liu, T., Fan, C., et al. (2020). Extracellular vesicles engineered with valency-controlled DNA nanostructures deliver CRISPR/Cas9 system for gene therapy. *Nucleic Acids Res.* 48, 8870–8882. doi: 10.1093/nar/gkaa683

Conflict of Interest: The authors declare that the research was conducted in the absence of any commercial or financial relationships that could be construed as a potential conflict of interest.

frontiers in Microbiology

ORIGINAL RESEARCH
published: 24 February 2021
doi: 10.3389/fmicb.2021.644949

The Plasmid-Borne *tet*(A) Gene Is an Important Factor Causing Tigecycline Resistance in ST11 Carbapenem-Resistant *Klebsiella pneumoniae* Under Selective Pressure

*Juan Xu[1], Zhongliang Zhu[2], Yanmin Chen[2], Weizhong Wang[2] and Fang He[2]**

[1] School of Public Health, Hangzhou Medical College, Hangzhou, China, [2] Department of Clinical Laboratory, Zhejiang Provincial People's Hospital, People's Hospital of Hangzhou Medical College, Hangzhou, China

The emergence and prevalence of tigecycline-resistant *Klebsiella pneumoniae* have seriously compromised the effectiveness of antimicrobial agents in the treatment of infections. To explore the role of the plasmid-borne *tet*(A) gene in tigecycline resistance in carbapenem-resistant *K. pneumoniae* (CRKP), a total of 63 CRKP isolates were collected from a tertiary hospital in Hangzhou, China. The minimum inhibitory concentration (MIC) of tigecycline, mutation rate of *tet*(A) gene, genetic surroundings of *tet*(A)-carrying transmissible plasmid and the contribution of *tet*(A) mutation to tigecycline resistance were analyzed using antimicrobial susceptibility test, whole-genome sequencing, tigecycline resistance evolution experiment, and plasmid conjugation experiment. Our results showed that 52.4% (33 isolates) of the test isolates carried the *tet*(A) gene; among them, 75.8% (25 isolates) exhibited a tigecycline non-susceptible phenotype (MIC = 4 mg/L). Three clonal groups (cluster I, cluster II, and cluster III) were identified in these *tet*(A)-bearing isolates. All 17 isolates belonged to serotype KL21 (cluster I), which differed by only 13 SNPs, suggesting a clonal spread of *tet*(A)-positive ST11 *K. pneumoniae* with serotype KL21 occurred in the sampling hospital. The induction of tigecycline resistance experiments showed that 71.4% of strains evolved *tet*(A) mutations and developed a high-level tigecycline resistance. Eight amino acid substitutions were identified in these mutants. The most common amino acid substitution was A370V, followed by S251A and G300E. Twelve isolates carrying *tet*(A) mutants succeeded in the filter mating experiment with a conjugation efficiency of 10^{-3}–10^{-8}. Tigecycline MICs in *E. coli* EC600 transconjugants with a mutated *tet*(A) were 2 to 8-fold higher than those in *E. coli* EC600 transconjugants with a wild-type *tet*(A). One ColRNAI/IncFII type and two IncFII type *tet*(A)-bearing conjugative plasmids were identified in this study, including a class 1 integron containing multiple antibiotic resistance genes, i.e., *tet*(A), *qnrS1*, bla_{LAP-2}, *catA2*, *sul2*, and *dfrA14*. Our study revealed the wide-spread situation of plasmid-borne *tet*(A) gene in clinical CRKP, and mutation of *tet*(A) is a potential driven force that lead to tigecycline resistance.

Keywords: mutation, plasmid-bearing, tigecycline, *tet*(A), *Klebsiella pneumoniae*

OPEN ACCESS

Edited by:
Zhi Ruan,
Zhejiang University, China

Reviewed by:
Ning Dong,
City University of Hong Kong, Hong Kong
Shangshang Qin,
Zhengzhou University, China

****Correspondence:***
Fang He
hetrue@163.com

Specialty section:
This article was submitted to Antimicrobials, Resistance and Chemotherapy, a section of the journal Frontiers in Microbiology

Received: *22 December 2020*
Accepted: *02 February 2021*
Published: *24 February 2021*

Citation:
Xu J, Zhu Z, Chen Y, Wang W and He F (2021) The Plasmid-Borne tet(A) Gene Is an Important Factor Causing Tigecycline Resistance in ST11 Carbapenem-Resistant Klebsiella pneumoniae Under Selective Pressure. Front. Microbiol. 12:644949. doi: 10.3389/fmicb.2021.644949

INTRODUCTION

Carbapenem-resistant *Klebsiella pneumoniae* (CRKP) is currently a substantial threat to public health worldwide. CRKP can cause a variety of infections, such as pneumonia, liver abscess, urinary tract infection, and bloodstream infection. CRKP often carry multiple antimicrobial resistance genes in the chromosome and plasmids, enabling the strain to be resistant to almost all antibiotics, except colistin and tigecycline. Tigecycline, the first glycylcycline drug, is an extended-spectrum antibiotic that inhibits protein synthesis by binding to the 30S ribosome and can overcome the mechanisms of tetracycline resistance (Pankey, 2005).

Antibiotics that can treat CRKP infections are limited. Tigecycline remains an important treatment method for CRKP. However, tigecycline resistance has emerged since the approval of this antibiotic and has been reported frequently in Enterobacteriaceae (Hoban et al., 2005). Previous reports have shown that overexpression of resistance-nodulation-cell division (RND)-type efflux pumps is associated with tigecycline resistance in Enterobacteriaceae, such as AcrAB (Ruzin et al., 2005; Keeney et al., 2007; Bratu et al., 2009; He et al., 2015). Ribosomal protein mutation (via the *rpsJ* gene) has also been reported to cause tigecycline resistance in Enterobacteriaceae (Beabout et al., 2015; He et al., 2018; Xu et al., 2020). Recently, the plasmid-mediated mobile tigecycline resistance gene *tet*(X4) and its variants has been reported in Enterobacteriaceae (He et al., 2019; Sun et al., 2019). However, this gene has most often been reported in *Escherichia coli* strains (Zhang et al., 2020), and its role in *K. pneumoniae* is limited.

In 2018, we reported the first case of tigecycline resistance in CRKP mediated by *tet*(A) evolution *in vivo* during tigecycline treatment (Du et al., 2018). Previously, Linkevicius et al. (2016) observed that evolutionary changes in *tet*(A) can cause tigecycline resistance in *E. coli in vitro*. Chiu et al. (2017) considered widespread mutated *tet*(A) gene to be concerning for the possible dissemination of tigecycline resistance in *K. pneumoniae*. To explore the role of *tet*(A) in tigecycline resistance in clinical CRKP isolates, tigecycline minimum inhibitory concentration (MIC) distribution, *tet*(A)-bearing rate, *tet*(A) mutation rate and transmission ability of clinical CRKP isolates were analyzed through antimicrobial susceptibility tests, whole genome sequencing, bioinformatics analysis, and plasmid conjugation experiments.

MATERIALS AND METHODS

CRKP Clinical Isolates

A total of 63 non-repetitive CRKP clinical strains were continuously collected from April 1st to May 30th in 2018 at a tertiary hospital in Hangzhou, China. Strains from different specimens of the same patient or specimens collected from the same patient at different times were considered to be duplicate strains, and only the first strain was selected for subsequent research. **Supplementary Figure 1** outlined the detailed specimen collection information. All of the isolates were identified using the VITEK MS system (bioMérieux, Marcy-l'Étoile, France). The carbapenem resistance genes, bla_{KPC} and bla_{NDM}, as well as the tetracycline resistance gene, *tet*(A), were amplified by PCR and further sent for Sanger sequencing.

Antimicrobial Susceptibility Test

Antimicrobial susceptibility testing was conducted using standard broth microdilution tests and the VITEK 2 system (bioMérieux) with Gram-negative antimicrobial susceptibility testing cards (AST-GN13) following the guidelines of the Clinical and Laboratory Standards Institute (CLSI). Antimicrobial agents: amoxicillin/clavulanate, ceftriaxone, cefepime, cefoxitin, aztreonam, piperacillin/tazobactam, imipenem, meropenem, amikacin, levofloxacin, sulfamethoxazole/trimethoprim, colistin, and tigecycline were used in the test. Antimicrobial susceptibility was determined using breakpoints approved by the CLSI (2019). For tigecycline MIC detection, standard broth microdilution tests were adopted with fresh (<12 h) Mueller-Hinton broth (Cation-adjusted, Oxoid Ltd., Basingstoke, Hampshire, United Kingdom). *E. coli* ATCC 25922 was used for quality control. As there are no CLSI breakpoints for tigecycline, the FDA standard was adopted[1]. The interpretation of colistin MIC was follow by the EUCAST guideline (Breakpoints for 2021)[2].

Quantitative Real-Time PCR

mRNA expression levels of the efflux pump genes, *acrA* and *acrB*, in tigecycline-resistant isolates were examined by quantitative real-time PCR according to our previously published paper (He et al., 2015). The relative expression of each target gene was calibrated against the corresponding expression of *K. pneumoniae* type strain ATCC 13883 (expression = 1), which served as a control with a tigecycline MIC of 0.125 mg/L. Relative expression levels of the two genes were analyzed by the $2^{-\Delta\Delta CT}$ analytical method.

Whole-Genome Sequencing

Isolates confirmed to possess the *tet*(A) gene or resistance to tigecycline were sent for whole-genome sequencing using the Illumina NovaSeq 6000 platform (Illumina Inc., San Diego, CA, United States). In brief, genomic DNA was extracted using a QIAamp DNA Mini Kit (Qiagen, Valencia, CA, United States) and sent for sequencing using the paired-end 2 × 150-bp protocol. The draft genome sequences were assembled using SPAdes 3.13.0. Three strains with *tet*(A) mutants (CRKP52R, CRKP66R, and CRKP78R) were further sent for Nanopore sequencing with a long-read MinION sequencer (Nanopore, Oxford, United Kingdom). Both short Illumina reads and long MinION reads were hybrid assembled using Unicycler (v0.4.7). Complete genome sequences were generated and automatically annotated by the NCBI Prokaryotic Genome Annotation Pipeline (PGAP) server.

[1]https://www.fda.gov/drugs/development-resources/tigecycline-injection-products

[2]https://eucast.org/

Genomic and Phylogenetic Relationship Analysis of *tet*(A)-Positive Isolates

MLST, acquired antibiotic resistance genes (ARGs) and plasmid replicons were analyzed using the BacWGSTdb 2.0 server (Ruan and Feng, 2016; Feng et al., 2020; Ruan et al., 2020). The phylogenetic relationship between *tet*(A)-carrying isolates was analyzed using the (neighbor joining (NJ))/unweighted pair group method with arithmetic mean (UPGMA) phylogeny method (MAFFT version 7) based on a core genome single nucleotide polymorphism strategy (Katoh et al., 2019). A phylogenetic tree was constructed using the resulting SNPs with recombination regions removed using the maximum parsimony algorithm (Jia et al., 2019). The KL type of *K. pneumoniae* was predicted by Kaptive Web (Wick et al., 2018).

Tigecycline Resistance Evolution Experiment *in vitro*

Wild-type *tet*(A)-carrying CRKP clinical isolates were used as parental strains in tigecycline resistance evolution experiments *in vitro*. Tigecycline-resistant mutants were selected by successive passages in MH broth containing increasing concentrations of tigecycline. In brief, one single clone of the parental strain was inoculated in MH broth overnight, and 200 μL of overnight cultures was added to 2 mL of fresh MH broth containing serial concentrations of tigecycline. The selective concentration began at 0.5 mg/L and doubled every 24 h. The protocol was repeated until the mutants grew at a tigecycline concentration of 32 mg/L.

Conjugation Experiment and VITEK MS Identification

Tigecycline-resistant *tet*(A) mutants obtained from tigecycline resistance evolution experiments and their parental strains with wild-type *tet*(A) were used as donors, and rifampicin-resistant *E. coli* EC600 was used as the recipient. Transconjugants were selected on MH agar plates supplemented with tetracycline (16 mg/L) and rifampicin (600 mg/L). *E. coli* EC600 transconjugants were identified using the VITEK MS system, and *tet*(A) gene mutations were further confirmed by PCR and Sanger sequencing. The conjugation efficiency was measured and calculated following the protocol in https://openwetware.org/wiki/conjugation.

Characterization of the *tet*(A)-Bearing Plasmid and Genetic Background of *tet*(A)

Circular comparisons of the *tet*(A)-carrying plasmid were conducted with BLAST Ring Image Generator (BRIG) based on concentric rings (Alikhan et al., 2011). Insertion elements (ISs) located on the plasmids were predicted by application of ISfinder (Siguier et al., 2006). Integrative and conjugative elements (ICEs) were predicted using ICEberg (Liu et al., 2019). The genetic location and background of *tet*(A) were determined by aligning the contigs carrying *tet*(A) with complete genome sequences generated in this study using CLC Genomics Workbench 10.0.1.

Nucleotide Sequence Accession Numbers

We deposited the complete sequences of the CRKP52R, CRKP66R, and CRKP78R *K. pneumoniae* strains and plasmids in GenBank under accession numbers CP066249-CP066253, CP063833-CP063838, and CP066254-CP066259. The draft genome sequences of 33 *tet*(A)-positive strains were deposited in GenBank under accession numbers JAEQKY000000000-JAEQME000000000. The sequence with GenBank accession number AJ517790 was used as the reference for the wild-type *tet*(A) gene with the primary start codon of GTG.

RESULTS

Tigecycline MIC Distribution and Mutations in *rpsJ*, *ramR*, and *tet*(A)

The antimicrobial susceptibility testing results are presented in **Supplementary Table 1**. All isolates were multidrug resistant bacteria with a resistance rate greater than 85% compared to β-lactams, quinolones and aminoglycosides but were still highly sensitive to colistin. The tigecycline MIC distribution of the 63 isolates is presented in **Figure 1A**. All 63 isolates carried bla_{KPC-2} gene, and the *in silico* MLST analysis showed that all strains, except three ST437 strains, one ST751 strain, and one ST15 strain, belonged to ST11. The highest MIC was 16 mg/L for isolate CRKP65, and further WGS results showed that this isolate did not harbor the *tet*(A) gene but had a *rpsJ* mutation (V57L). One isolate, namely, CRKP26, had a tigecycline MIC of 8 mg/L. Further WGS results showed that this strain had a *ramR* mutation (GATCCTG insertion at 222–223 resulted in frameshift mutation) and high expression of the RND efflux pump, AcrAB (**Table 1**), but did not harbor the *tet*(A) gene. Twenty-six isolates had a MIC of 4 mg/L, and among these, 25 isolates harbored wild-type *tet*(A). According to the FDA standard (MIC >2 mg/L for tigecycline non-susceptible), there were 28 tigecycline non-susceptible isolates, and the non-susceptible rate was 44.4%. The expression levels of the RND efflux pump genes, *acrA* and *acrB*, as well as the mutations in *rpsJ*, *ramR*, and *tet*(A) in tigecycline non-susceptible isolates are presented in **Table 1**. Four isolates (CRKP5, CRKP15, CRKP21, and CRKP26) had a high expression (two-fold increase compare to reference strain) of the AcrAB efflux pump.

Characterizations of *tet*(A)-Positive Isolates and Phylogenetic Analysis

The PCR and Sanger sequencing results showed that 33 of the 63 isolates (52.4%) carried the *tet*(A) gene, all of which were wild-type. The tigecycline MIC distribution of the 33 *tet*(A)-positive isolates is presented in **Figure 1B**, and there were 25 isolates with MIC 4 mg/L (75.8%) and eight isolates (24.2%) with MIC 2 mg/L. Compared with *tet*(A)-negative isolates, the tigecycline MIC is generally increased by two-fold. All 33 isolates belonged to ST11. The antimicrobial resistance genes and serotype based on WGS data of these 33 *tet*(A)-bearing isolates are presented in **Figure 2**. In total, 16 antimicrobial resistance genes were found in these

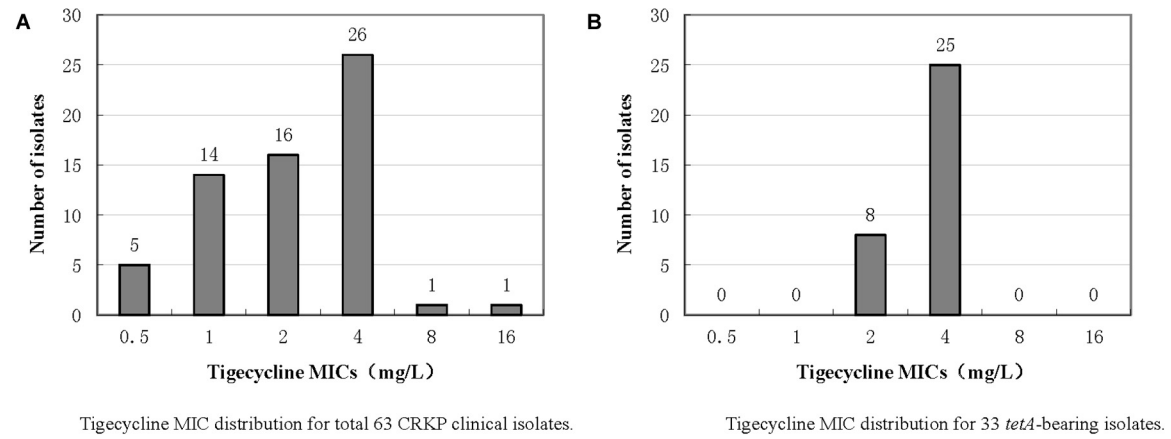

FIGURE 1 | Tigecycline MIC distributions of 63 CRKP clinical isolates and 33 *tet*(A)-bearing isolates.

TABLE 1 | Expression levels of the *acrA* and *acrB* efflux pump genes and mutation of *rpsJ*, *ramR*, and *tet*(A) in tigecycline non-susceptible isolates.

Isolate	MIC (mg/L)[b]	Relative expression[a]		*Tet*(A)[c]	Mutation	
		acrA	*acrB*		*rpsJ*	*ramR*
ATCC 13883	0.125	1	1	ND	–	–
CRKP5	4	2.16 ± 0.10	1.66 ± 0.31	WT	–	–
CRKP8	4	1.18 ± 0.15	1.27 ± 0.03	WT	–	–
CRKP10	4	1.28 ± 0.11	1.08 ± 0.23	WT	–	–
CRKP15	4	2.38 ± 0.39	2.46 ± 0.40	WT	–	–
CRKP17	4	1.44 ± 0.28	0.99 ± 0.12	WT	–	–
CRKP21	4	2.18 ± 0.15	2.07 ± 0.45	WT	–	–
CRKP22	4	1.03 ± 0.05	0.81 ± 0.17	WT	–	–
CRKP24	4	0.89 ± 0.15	0.75 ± 0.05	WT	–	–
CRKP26	8	3.78 ± 0.29	3.56 ± 0.24	ND	–	GATCCTG insertion at 222–223
CRKP29	4	1.99 ± 0.27	1.83 ± 0.12	WT	–	–
CRKP31	4	0.89 ± 0.20	0.80 ± 0.16	ND		–
CRKP34	4	1.94 ± 0.06	1.81 ± 0.24	WT	–	–
CRKP38	4	1.67 ± 0.30	1.00 ± 0.22	WT	–	–
CRKP39	4	1.42 ± 0.23	0.71 ± 0.06	WT	–	–
CRKP41	4	1.31 ± 0.34	0.78 ± 0.06	WT	–	–
CRKP42	4	0.87 ± 0.12	0.89 ± 0.12	WT	–	–
CRKP43	4	0.78 ± 0.06	0.67 ± 0.02	WT	–	–
CRKP45	4	1.20 ± 0.09	0.98 ± 0.12	WT	–	–
CRKP51	4	1.41 ± 0.28	1.14 ± 0.10	WT	–	–
CRKP52	4	1.35 ± 0.15	1.13 ± 0.14	WT	–	–
CRKP55	4	1.79 ± 0.28	1.25 ± 0.15	WT	–	–
CRKP59	4	1.59 ± 0.60	1.17 ± 0.19	WT	–	–
CRKP61	4	0.81 ± 0.14	0.77 ± 0.15	WT	–	–
CRKP62	4	1.02 ± 0.13	0.73 ± 0.06	WT	–	–
CRKP65	16	1.30 ± 0.25	1.14 ± 0.03	ND	G169C (V57L)	–
CRKP72	4	1.03 ± 0.15	1.28 ± 0.28	WT	–	–
CRKP77	4	1.91 ± 0.54	1.32 ± 0.33	WT	–	–
CRKP80	4	1.17 ± 0.34	0.92 ± 0.12	WT	–	–

[a] *Relative expression compared with K. pneumoniae type strain ATCC 13883 (expression = 1). Results represent the means of three runs ± standard deviation.*
[b] *Tigecycline MIC.*
[c] *ND, tet(A) not detected. WT, wild-type tet(A).*

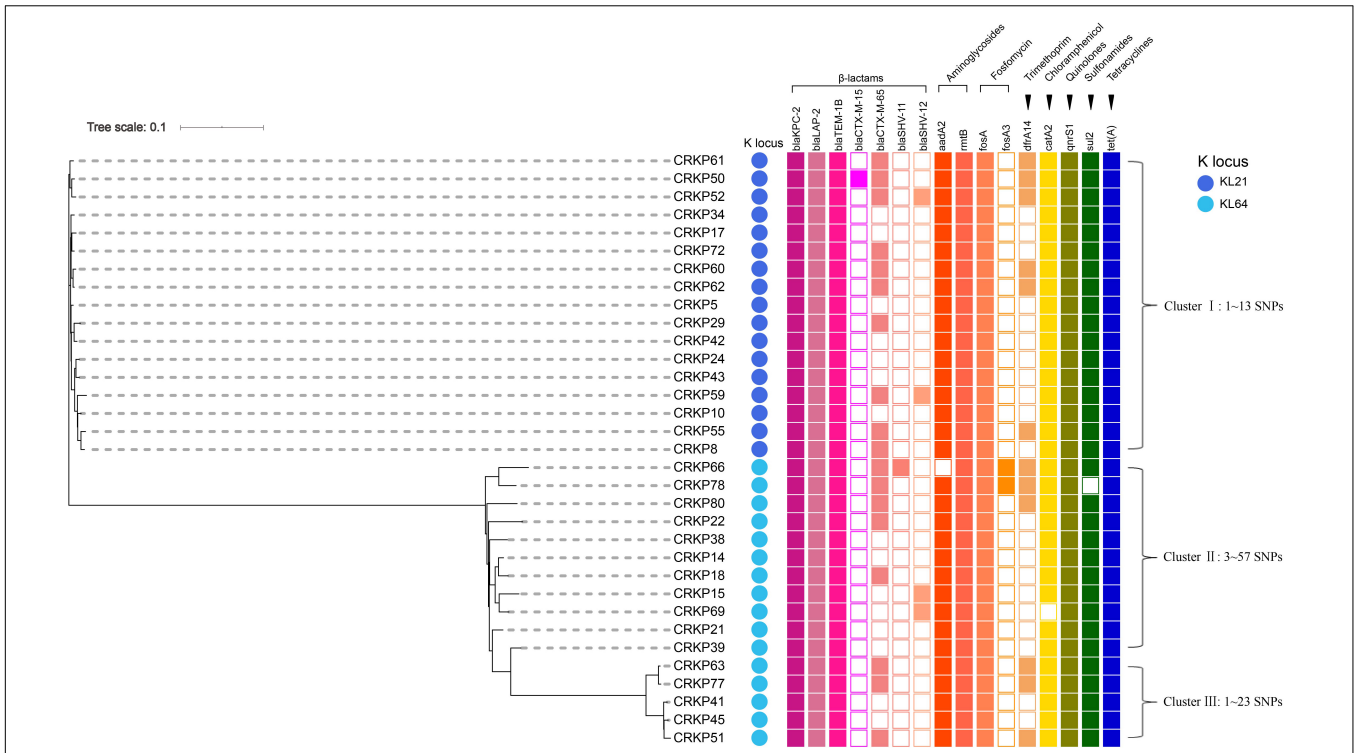

FIGURE 2 | Phylogenetic relationship, antimicrobial resistance genes and serotype analysis based on WGS data of 33 *tet*(A)-bearing CRKP isolates. The cells in different colors indicate the presence of the antimicrobial resistance gene, while the blank cells indicate the absence of the gene. The color of each circle indicates a distinct capsular serotype.

isolates, including bla_{KPC-2}, bla_{LAP-2}, bla_{TEM-1B}, *fosA*, *qnrS1*, *rmtB*, *tet*(A), $bla_{CTX-M-15}$, $bla_{CTX-M-65}$, bla_{SHV-11}, bla_{SHV-12}, *aadA2*, *dfrA14*, *catA2*, *fosA3*, and *sul2*. These isolates were divided into two serotypes (KL21 and KL64). The phylogenetic tree is presented in **Figure 2**, and SNP differences are presented in **Supplementary Figure 2**. Three clonal clusters (cluster I, cluster II, and cluster III) were identified. All 17 isolates belonged to serotype KL21 (cluster I), which differed with 13 SNPs. According to the relatedness criteria recommended for SNP typing schemes of *K. pneumoniae* reported by Schürch et al. (2018), a difference of SNPs $\leq$18 represents epidemiologically related. Therefore, a clonal spread of *tet*(A)-positive ST11 *K. pneumoniae* with serotype KL21 occurred in the sampling hospital.

Mutations of *tet*(A) in the Tigecycline Resistance Evolution Experiment

All 33 wild-type *tet*(A)-carrying CRKP isolates were subjected to tigecycline resistance evolution experiments *in vitro*. Under successive passages of tigecycline induction in MH broth for approximately 2 weeks, 28 isolates were induced to develop resistance with a tigecycline MIC $\geq$32 mg/L. PCR and Sanger sequencing detected 20 of the 28 isolates that evolved *tet*(A) mutations (**Table 2**), and the mutation rate was 71.4%. The following eight amino acid substitutions were identified in these mutants: A264V, I248L, A370V, S251A, G300E, G300V, A53G, and G237V. The most common amino acid substitution was A370V, which appeared six times, followed by S251A and G300E (appeared four times each). All 20 *tet*(A) mutants were subjected to conjugation experiments in which they were used as donors, and *E. coli* EC600 was the recipient. Twelve mutants succeeded in the conjugation experiment, and the conjugation efficiency was at a frequency of 10^{-3}–10^{-8} (**Table 2**). The MICs of tigecycline and tetracycline of *E. coli* EC600 transconjugants of *tet*(A) mutants and wild-type *tet*(A) are presented in **Table 2**. In general, tigecycline MICs in *E. coli* EC600 transconjugants of mutated *tet*(A) were 2- to 8-fold higher than *E. coli* EC600 transconjugants of wild-type *tet*(A), and the MICs of tetracycline also increased in eight strains.

Characterization of the *tet*(A)-Bearing Plasmid and Genetic Background of *tet*(A)

The complete genome sequences of three *tet*(A) mutants (CRKP52R, CRKP66R, and CRKP78R) were obtained using Nanopore sequencing. CRKP52R, CRKP66R, and CRKP78R were tigecycline-resistant *tet*(A) mutants collected in the tigecycline resistance evolution experiment. The parental strains of CRKP52R, CRKP66R, and CRKP78R were *K. pneumoniae* strains CRKP52, CRKP66, and CRKP78, respectively. *tet*(A) was located on plasmids in these strains, and three *tet*(A)-bearing plasmids were identified in CRKP52R, CRKP66R, and CRKP78R. The plasmid from CRKP52R was a ColRNAI/IncFII plasmid

TABLE 2 | Tigecycline and tetracycline MICs of *E. coli* EC600 transconjugants of *tet*(A) mutants or wild-type *tet*(A).

Isolates	TGC[c] MICs (mg/L)	*tet*(A)[a]	TGC MICs after tigecycline induction (mg/L)	*tet*(A) mutation after tigecycline induction[b]		Conjugation efficiency	*E. coli* EC600 transconjugant of *tet*(A) mutant[c]		*E. coli* EC600 transconjugant of wild-type *tet*(A)[c]	
				Nucleotide change	Amino acid change		TGC (mg/L)	TC (mg/L)	TGC (mg/L)	TC (mg/L)
CRKP5	4	WT	64	–	–	–	–	–	–	–
CRKP8	4	WT	64	C791T	A264V	$(1.4 \pm 0.6) \times 10^{-4}$	1	64	0.25	64
CRKP10	4	WT	64	–	–	–	–	–	–	–
CRKP14	2	WT	64	A742C	I248L	$(4.8 \pm 1.9) \times 10^{-6}$	2	>256	0.5	128
CRKP15	4	WT	64	–	–	–	–	–	–	–
CRKP17	4	WT	64	–	–	–	–	–	–	–
CRKP18	2	WT	64	–	–	–	–	–	–	–
CRKP21	4	WT	64	–	–	–	–	–	–	–
CRKP22	4	WT	4	–	–	–	–	–	–	–
CRKP24	4	WT	64	C1109T	A370V	Failed	NA	NA	NA	NA
CRKP29	4	WT	64	T751G	S251A	$(6.0 \pm 3.4) \times 10^{-6}$	1	256	0.25	128
CRKP34	4	WT	4	–	–	–	–	–	–	–
CRKP38	4	WT	64	T751G	S251A	$(1.8 \pm 0.9) \times 10^{-3}$	1	64	0.25	64
CRKP39	4	WT	64	G899T	G300V	Failed	NA	NA	NA	NA
CRKP41	4	WT	4	–	–	–	–	–	–	–
CRKP42	4	WT	64	C1109T	A370V	Failed	NA	NA	NA	NA
CRKP43	4	WT	64	G710T T751G	G237V S251A	Failed	NA	NA	NA	NA
CRKP45	4	WT	4	–	–	–	–	–	–	–
CRKP50	2	WT	64	C791T	A264V	$(7.7 \pm 3.3) \times 10^{-7}$	1	128	0.5	64
CRKP51	4	WT	64	G899A	G300E	$(3.7 \pm 1.9) \times 10^{-6}$	2	>256	0.25	128
CRKP52	4	WT	64	G899A	G300E	$(5.2 \pm 2.5) \times 10^{-8}$	1	256	0.25	128
CRKP55	4	WT	64	C1109T	A370V	$(3.2 \pm 1.4) \times 10^{-5}$	1	128	0.5	128
CRKP59	4	WT	64	C1109T	A370V	$(1.1 \pm 0.7) \times 10^{-5}$	1	>256	0.25	128
CRKP60	2	WT	64	G899A	G300E	Failed	NA	NA	NA	NA
CRKP61	4	WT	64	–	–	–	–	–	–	–
CRKP62	4	WT	4	–	–	–	–	–	–	–
CRKP63	2	WT	32	–	–	–	–	–	–	–
CRKP66	2	WT	64	C1109T	A370V	$(1.4 \pm 1.2) \times 10^{-6}$	1	64	0.25	64
CRKP69	2	WT	64	G899A	G300E	$(1.1 \pm 0.5) \times 10^{-4}$	4	>256	0.5	128
CRKP72	4	WT	64	C158G	A53G	Failed	NA	NA	NA	NA
CRKP77	4	WT	64	C1109T	A370V	Failed	NA	NA	NA	NA
CRKP78	2	WT	64	T751G	S251A	$(4.7 \pm 2.8) \times 10^{-6}$	4	>256	0.5	128
CRKP80	4	WT	64	C791T	A264V	Failed	NA	NA	NA	NA

[a] *WT, wild-type tet(A).*

[b] *–, no mutation detected in tet(A).*

[c] *TGC, Tigecycline; TC, Tetracycline. NA, Data not available.*

that was 99,066 bp in size and was designated pCRKP52R-4-tetA. Plasmids from CRKP66R and CRKP78R belonged to the IncFII type with sizes of 87,095 and 86,962 bp, and they were designated pCRKP66R-4-tetA and pCRKP78R-4-tetA, respectively (**Table 3**). Similar *tet*(A)-bearing plasmids in the NCBI GenBank database were searched with the Basic Local Alignment Search Tool (BLAST). We found that IncFII-type and IncFIB-type plasmids with sizes of approximately 90 and 120 kb were common plasmids carrying *tet*(A) in *K. pneumoniae* (**Table 3**). The similarity of the plasmid backbone of these plasmids is presented in **Figure 3**. These IncFII-type plasmids have a plasmid backbone similar to that of ARGs, including *qnrS1*, bla_{LAP-2}, *tet*(A), *catA2*, *sul2*, and *dfrA14*. The *tet*(A) genes in the pCRKP52R-4-tetA plasmid were flanked by the *qnrS1* and bla_{LAP-2} resistance genes on the left and the *catA2*, *sul2*, and *dfrA14* resistance genes on the right, and

TABLE 3 | Detailed information of *tet*(A)-bearing plasmids obtained in this study and the NCBI database.

Plasmid name	Plasmid replicon	Plasmid size	Host bacteria	Antimicrobial resistance genes	Accession number
pCRKP52R-4-tetA	ColRNAI/IncFII	99066bp	*K. pneumoniae*	*qnrS1*, bla_{LAP-2}, *tet*(A), *catA2*, *sul2*, *dfrA14*	CP066252 (this study)
pCRKP66R-4-tetA	IncFII	87095bp	*K. pneumoniae*	*qnrS1*, bla_{LAP-2}, *tet*(A), *catA2*, *sul2*, *dfrA14*	CP063836 (this study)
pCRKP78R-4-tetA	IncFII	86962bp	*K. pneumoniae*	*qnrS1*, bla_{LAP-2}, *tet*(A), *catA2*, *sul2*, *dfrA14*	CP066257 (this study)
pKP18-3-8-IncFII	IncFII	87095bp	*K. pneumoniae*	*qnrS1*, bla_{LAP-2}, *tet*(A), *catA2*, *sul2*, *dfrA14*	MT035876 (NCBI)
pKP18-2079_tetA	IncFII	84699bp	*K. pneumoniae*	*qnrS1*, bla_{LAP-2}, *tet*(A), *sul2*, *dfrA14*	MT090960 (NCBI)
pKP13-53-tet(A)	Col/IncFIB	181383bp	*K. pneumoniae*	*qnrS1*, bla_{LAP-2}, *tet*(A), *sul1*, *dfrA1*, *aac(3)-IId*	MN268580 (NCBI)
p71221-tetA	IncFIB	128170bp	*K. pneumoniae*	*tet*(A), *sul1*, *dfrA1*, *mph(A)*, bla_{SHV-12}, *aph(3′)-Ia*	MN310374 (NCBI)
pW08291-tetA	IncFIB	130483bp	*K. pneumoniae*	*tet*(A), *sul1*, *dfrA1*, *mph(A)*, bla_{SHV-12}	MN310376 (NCBI)

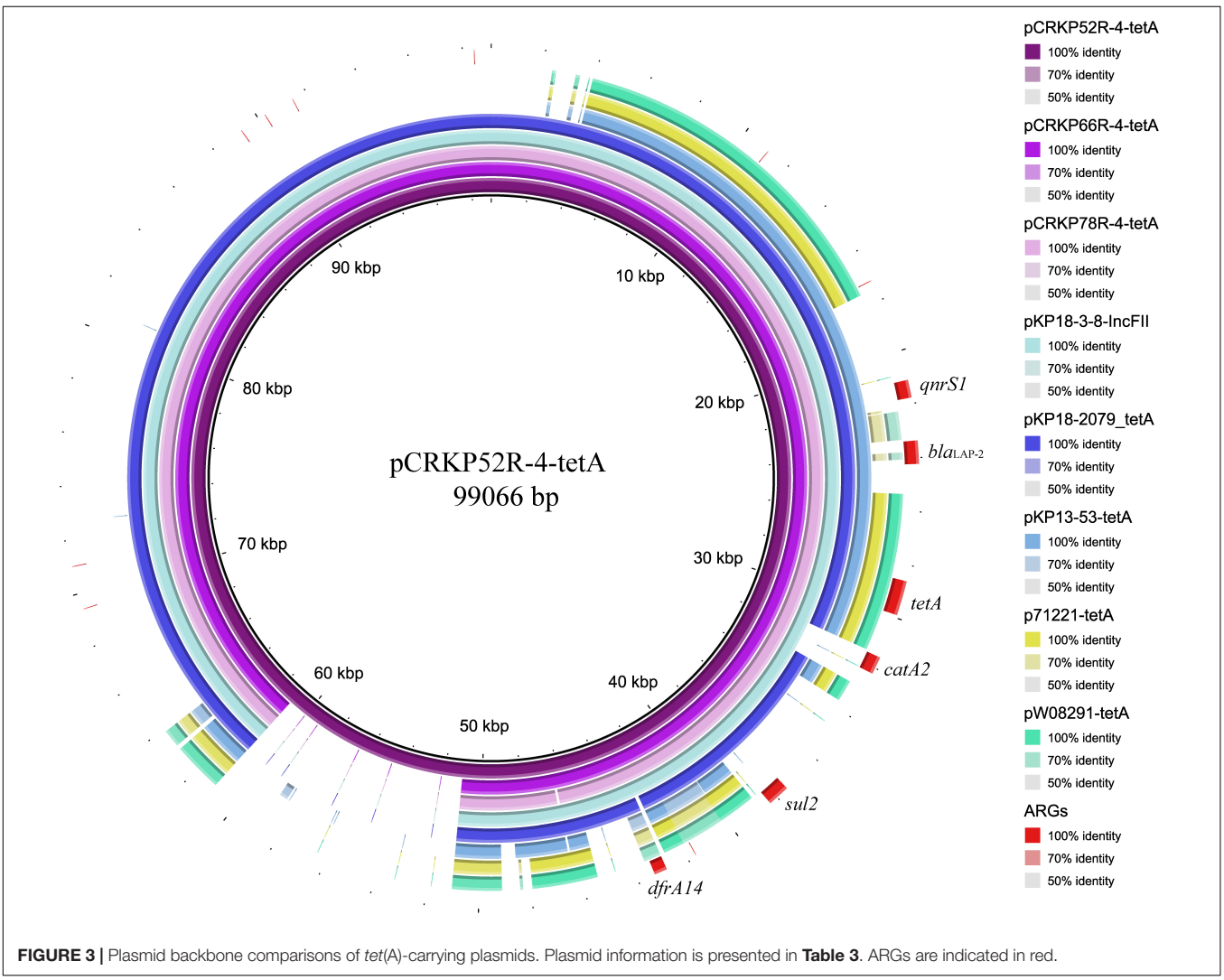

FIGURE 3 | Plasmid backbone comparisons of *tet*(A)-carrying plasmids. Plasmid information is presented in **Table 3**. ARGs are indicated in red.

they were all located in ICEs ranging from 11 to 99 kb in size (**Figure 3**). One class 1 integron (IntI1) was identified in pCRKP52R-4-tetA (from 18944 to 46168 bp), pCRKP66R-4-tetA, and pCRKP78R-4-tetA (**Figure 4**). This integron contains multiple ARGs, including *tet*(A). The *tet*(A) gene was located in the genetic environment, IS*26*-*tetR*-*tet*(A)-*eamA*-*orf*-TnAs1, suggesting that it was acquired by horizontal gene transfer with mobilizable transposons.

DISCUSSION

Carbapenem-resistant *K. pneumoniae* has emerged as an important pathogen worldwide, and the emergence of tigecycline and colistin resistance makes clinical treatment difficult. According to the data obtained in this study, 52.4% of the tested isolates carried the wild-type *tet*(A) gene. Among these isolates, 75.8% of these *tet*(A)-bearing isolates exhibited a tigecycline non-susceptible phenotype. No mutations of *rpsJ* and *ramR* genes were identified in these isolates. We also searched the plasmid-encoded RND efflux pump genes *tmexCD1-toprJ1* in the genome of these strains, but no related genes were found. Compared with *tet*(A)-negative isolates, the tigecycline MIC was generally increased by approximately two-fold in these wild-type *tet*(A)-bearing isolates. Except for three isolates (CRKP5, CRKP15, and CRKP21) had a high expression of the AcrAB efflux pump (**Table 1**), we considered that other undiscovered mechanisms may be utilized in these isolates that work together with wild-type *tet*(A) to mediate tigecycline non-susceptibility. A recent study reported that TetA in synergy with RND-type efflux transporters contribute to tigecycline resistance in *Acinetobacter baumannii* (Foong et al., 2020). This synergy may also exist in *K. pneumoniae*, which warrant further investigation.

tet(A) is a MFS family efflux pump, and mutation in *tet*(A) might result in increased accumulation of tigecycline as a substrate, thus contributing to tigecycline resistance (Linkevicius et al., 2016; Chiu et al., 2017). *tet*(A)-bearing *K. pneumoniae* tended to more easily evolve tigecycline resistance under selective pressure as 71.4% of the strains evolved *tet*(A) mutations and developed high-level tigecycline resistance in our tigecycline resistance evolution experiment *in vitro*. We have previously confirmed the contribution of the S251A Tet(A) variant to tigecycline resistance by transformation experiments (Du et al., 2018). Linkevicius et al. (2016) also confirmed that *tet*(A) mutants of I235F, I248L, S251A, and G300E show increased tigecycline MICs compared to the unmutagenized control. We further conducted transformation experiments on several other mutants (A264V, A370V, G300V, and A53G) identified in this study, and we found these mutants increased the tigecycline MIC in *E. coli* DH5α by 2 to 4-fold compared to the wild-type *tet*(A) control. The degree of tigecycline MIC increase in *E. coli* EC600 transconjugants of *tet*(A) mutants was diverse (**Table 2**), especially for a few transconjugants harboring the same mutation site (e.g., CRKP29, CRKP38, and CRKP78). Linkevicius et al. (2016) confirmed that the magnitude increase of tigecycline MIC depends on the expression level of the *tet*(A) mutant. Thus, we speculated that the difference of the *tet*(A) mutant expression level may be due to the diverse tigecycline MICs in these *E. coli* EC600 transconjugants. *tet*(A) mutants are often located in different types of plasmids, and these plasmids have different promoter and regulatory sequences that may result in different expression levels of *tet*(A).

Multiple types of *tet*(A)-bearing plasmids were retrieved from the NCBI GenBank database, and circular comparison analysis revealed that they have some similar structures, suggesting

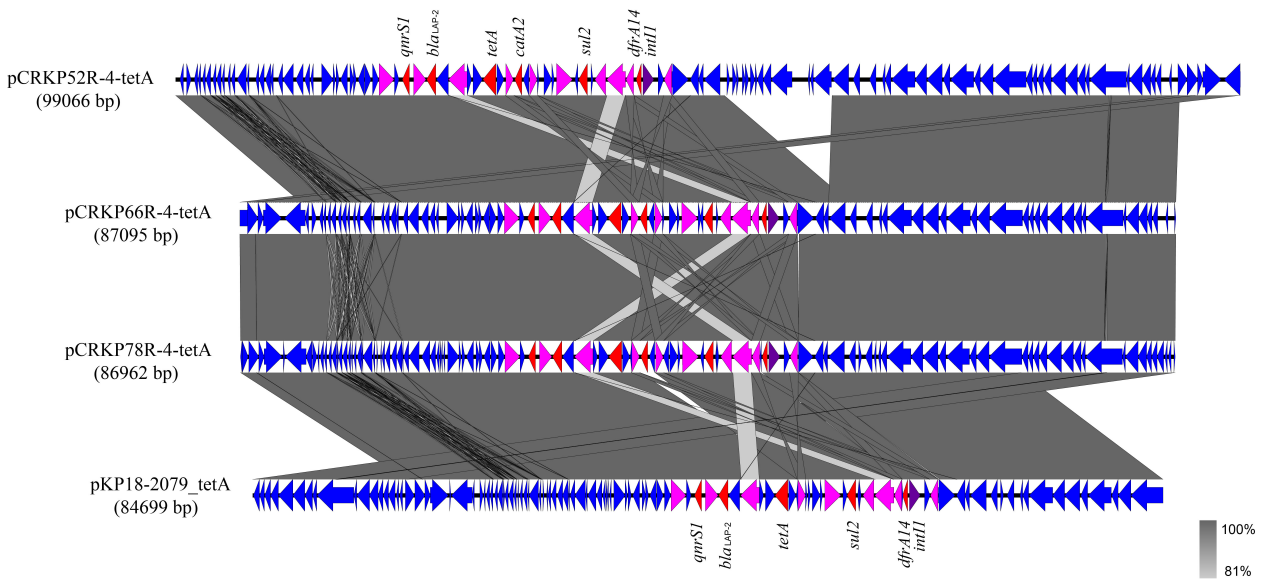

FIGURE 4 | Alignment of integrative elements with *tet*(A) in the pCRKP52R-4-tetA, pCRKP66R-4-tetA, pCRKP78R-4-tetA, and pKP18-2079_tetA plasmids. Resistance genes are indicated in red, and *int1* is indicated in purple. IS elements are indicated in pink, and all other ORFs are indicated in blue.

that genetic exchange and recombination among different types of *tet*(A)-bearing plasmids have occurred (Ribera et al., 2003; Szmolka et al., 2015; Yao et al., 2020). In the three *tet*(A)-bearing plasmids obtained in this study, one class 1 integron containing multiple ARGs, including *tet*(A), was detected. In addition, *tet*(A) mutation occurring under selective pressure may lead to tigecycline treatment failure. Zhang et al. (2019) reported the coexistence of *mcr-1* and the *tet*(A) variant on the same plasmid from a *K. pneumoniae* isolate in human gut, and Yao et al. (2020) also reported an IncFII plasmid co-harboring bla_{IMP-26} and *tet*(A) variant in a clinical *K. pneumoniae* isolate. It seems that *tet*(A) mutants can not only occur in bla_{KPC-2}-carrying plasmids, but also form fusion plasmids with other carbapenem resistance genes and *mcr* gene, which will cause a higher transmission risk of simultaneous resistance to carbapenem, colistin and tigecycline. The emergence and spread of such fusion plasmid needs our attention.

CONCLUSION

In conclusion, our study revealed the wide-spread of plasmid-borne *tet*(A) gene in clinical CRKP, and mutation of *tet*(A) is a potential threat that lead to tigecycline resistance. More attention should be devoted to monitoring the spread of plasmid-borne *tet*(A) in *K. pneumoniae* clinical isolates, especially the emergence of *tet*(A) mutants. Strict administration of tigecycline and classification management of antibiotics must be carried out with precautions.

DATA AVAILABILITY STATEMENT

The data presented in the study are deposited in the GenBank repository, accession numbers CP066249-CP066253, CP063833-CP063838, CP066254-CP066259, and JAEQKY000000000-JAEQME000000000.

ETHICS STATEMENT

This study was conducted in accordance with the Declaration of Helsinki and approved by the Ethics Committee of Zhejiang Provincial People's Hospital. Written informed consent from the patients was exempted by the Ethics Committee of Zhejiang Provincial People's Hospital because the present study only focused on bacteria.

AUTHOR CONTRIBUTIONS

FH designed the experiments. JX and ZZ performed the experiments and were the major contributors in writing the manuscript. YC and WW analyzed the data. All authors read and approved the final manuscript.

FUNDING

This study was supported by grants from the National Natural Science Foundation of China (81702042), Natural Science Foundation of Zhejiang Province (LQ19H200003), Natural Science Foundation of Zhejiang Provincial Department of Education (Y202044471), and Zhejiang Provincial Medical and Health Science and Technology Plan (2019KY311).

SUPPLEMENTARY MATERIAL

The Supplementary Material for this article can be found online at: https://www.frontiersin.org/articles/10.3389/fmicb.2021.644949/full#supplementary-material

Supplementary Figure 1 | Specimen type and department distribution of 63 non-repetitive CRKP clinical isolates.

Supplementary Figure 2 | Phylogenetic analysis of 33 *tet*(A)-bearing isolates based on the core genome SNP strategy.

REFERENCES

Alikhan, N. F., Petty, N. K., Ben Zakour, N. L., and Beatson, S. A. (2011). BLAST Ring Image Generator (BRIG): simple prokaryote genome comparisons. *BMC Genomics* 12:402. doi: 10.1186/1471-2164-12-402

Beabout, K., Hammerstrom, T. G., Perez, A. M., Magalhaes, B. F., Prater, A. G., Clements, T. P., et al. (2015). The ribosomal S10 protein is a general target for decreased tigecycline susceptibility. *Antimicrob. Agents Chemother.* 59, 5561–5566. doi: 10.1128/aac.00547-15

Bratu, S., Landman, D., George, A., Salvani, J., and Quale, J. (2009). Correlation of the expression of acrB and the regulatory genes marA, soxS and ramA with antimicrobial resistance in clinical isolates of *Klebsiella pneumoniae* endemic to New York City. *J. Antimicrob. Chemother.* 64, 278–283. doi: 10.1093/jac/dkp186

Chiu, S. K., Huang, L. Y., Chen, H., Tsai, Y. K., Liou, C. H., Lin, J. C., et al. (2017). Roles of ramR and tet(A) mutations in conferring tigecycline resistance in carbapenem-resistant *Klebsiella pneumoniae* clinical isolates. *Antimicrob. Agents Chemother.* 61:e00391-17.

CLSI (2019). *Performance Standards for Antimicrobial Susceptibility Testing:* Clinical and Laboratory Standards Institute (CLSI) supplement M100, 29th Edn. Wayne, PA: Clinical and Laboratory Standards Institute.

Du, X., He, F., Shi, Q., Zhao, F., Xu, J., Fu, Y., et al. (2018). The rapid emergence of tigecycline resistance in blaKPC-2 harboring *Klebsiella pneumoniae*, as mediated in vivo by mutation in tetA during tigecycline treatment. *Front. Microbiol.* 9:648. doi: 10.3389/fmicb.2018.00648

Feng, Y., Zou, S., Chen, H., Yu, Y., and Ruan, Z. (2020). BacWGSTdb 2.0: a one-stop repository for bacterial whole-genome sequence typing and source tracking. *Nucleic Acids Res.* 49, D644–D650.

Foong, W. E., Wilhelm, J., Tam, H. K., and Pos, K. M. (2020). Tigecycline efflux in *Acinetobacter baumannii* is mediated by TetA in synergy with RND-type efflux transporters. *J. Antimicrob. Chemother.* 75, 1135–1139. doi: 10.1093/jac/dkaa015

He, F., Fu, Y., Chen, Q., Ruan, Z., Hua, X., Zhou, H., et al. (2015). Tigecycline susceptibility and the role of efflux pumps in tigecycline resistance in KPC-producing *Klebsiella pneumoniae*. *PLoS One* 10:e0119064. doi: 10.1371/journal.pone.0119064

He, F., Shi, Q., Fu, Y., Xu, J., Yu, Y., and Du, X. (2018). Tigecycline resistance caused by rpsJ evolution in a 59-year-old male patient infected with KPC-producing *Klebsiella pneumoniae* during tigecycline treatment. *Infect. Genet. Evol.* 66, 188–191. doi: 10.1016/j.meegid.2018.09.025

He, T., Wang, R., Liu, D., Walsh, T. r., Zhang, R., Lv, Y., et al. (2019). Emergence of plasmid-mediated high-level tigecycline resistance genes in animals and humans. *Nat. Microbiol.* 4, 1450–1456. doi: 10.1038/s41564-019-0445-2

Hoban, D. J., Bouchillon, S. K., Johnson, B. M., Johnson, J. L., and Dowzicky, M. J. (2005). In vitro activity of tigecycline against 6792 gram-negative and gram-positive clinical isolates from the global tigecycline evaluation and surveillance trial (TEST Program, 2004). *Diagn. Microbiol. Infect. Dis.* 52, 215–227. doi: 10.1016/j.diagmicrobio.2005.06.001

Jia, H., Chen, Y., Wang, J., Xie, X., and Ruan, Z. (2019). Emerging challenges of whole-genome-sequencing-powered epidemiological surveillance of globally distributed clonal groups of bacterial infections, giving *Acinetobacter baumannii* ST195 as an example. *Int. J. Med. Microbiol.* 309:151339. doi: 10.1016/j.ijmm.2019.151339

Katoh, K., Rozewicki, J., and Yamada, K. D. (2019). MAFFT online service: multiple sequence alignment, interactive sequence choice and visualization. *Brief. Bioinform.* 20, 1160–1166. doi: 10.1093/bib/bbx108

Keeney, D., Ruzin, A., and Bradford, P. A. (2007). RamA, a transcriptional regulator, and AcrAB, an RND-type efflux pump, are associated with decreased susceptibility to tigecycline in *Enterobacter cloacae*. *Microb. Drug Resist.* 13, 1–6. doi: 10.1089/mdr.2006.9990

Linkevicius, M., Sandegren, L., and Andersson, D. I. (2016). Potential of tetracycline resistance proteins to evolve tigecycline resistance. *Antimicrob. Agents Chemother.* 60, 789–796. doi: 10.1128/aac.02465-15

Liu, M., Li, X., Xie, Y., Bi, D., Sun, J., Li, J., et al. (2019). ICEberg 2.0: an updated database of bacterial integrative and conjugative elements. *Nucleic Acids Res.* 47, D660–D665.

Pankey, G. A. (2005). Tigecycline. *J. Antimicrob. Chemother.* 56, 470–480.

Ribera, A., Roca, I., Ruiz, J., Gibert, I., and Vila, J. (2003). Partial characterization of a transposon containing the tet(A) determinant in a clinical isolate of *Acinetobacter baumannii*. *J. Antimicrob. Chemother.* 52, 477–480. doi: 10.1093/jac/dkg344

Ruan, Z., and Feng, Y. (2016). BacWGSTdb, a database for genotyping and source tracking bacterial pathogens. *Nucleic Acids Res.* 44, D682–D687.

Ruan, Z., Yu, Y., and Feng, Y. (2020). The global dissemination of bacterial infections necessitates the study of reverse genomic epidemiology. *Brief. Bioinform.* 21, 741–750. doi: 10.1093/bib/bbz010

Ruzin, A., Visalli, M. A., Keeney, D., and Bradford, P. A. (2005). Influence of transcriptional activator RamA on expression of multidrug efflux pump AcrAB and tigecycline susceptibility in *Klebsiella pneumoniae*. *Antimicrob. Agents Chemother.* 49, 1017–1022. doi: 10.1128/aac.49.3.1017-1022.2005

Schürch, A., Arredondo-Alonso, S., Willems, R., and Goering, R. (2018). Whole genome sequencing options for bacterial strain typing and epidemiologic analysis based on single nucleotide polymorphism versus gene-by-gene-based approaches. *Clin. Microbiol. Infect.* 24, 350–354. doi: 10.1016/j.cmi.2017.12.016

Siguier, P., Perochon, J., Lestrade, L., Mahillon, J., and Chandler, M. (2006). ISfinder: the reference centre for bacterial insertion sequences. *Nucleic Acids Res.* 34, D32–D36.

Sun, J., Chen, C., Cui, C. y, Zhang, Y., Liu, X., Cui, Z. h, et al. (2019). Plasmid-encoded tet(X) genes that confer high-level tigecycline resistance in *Escherichia coli*. *Nat. Microbiol.* 4, 1457–1464. doi: 10.1038/s41564-019-0496-4

Szmolka, A., Lestár, B., Pászti, J., Fekete, P., and Nagy, B. (2015). Conjugative IncF and IncI1 plasmids with tet(A) and class 1 integron conferring multidrug resistance in F18(+) porcine enterotoxigenic *E. coli*. *Acta Vet. Hung.* 63, 425–443. doi: 10.1556/004.2015.040

Wick, R. R., Heinz, E., Holt, K. E., and Wyres, K. L. (2018). Kaptive web: user-friendly capsule and lipopolysaccharide serotype prediction for *Klebsiella* genomes. *J. Clin. Microbiol.* 56:e00197-18.

Xu, J., Zhao, Z., Ge, Y., and He, F. (2020). Rapid emergence of a pandrug-resistant *Klebsiella pneumoniae* ST11 isolate in an inpatient in a teaching hospital in China after treatment with multiple broad-spectrum antibiotics. *Infect Drug Resist.* 13, 799–804. doi: 10.2147/idr.s243334

Yao, H., Cheng, J., Li, A., Yu, R., Zhao, W., Qin, S., et al. (2020). Molecular characterization of an IncFII(k) plasmid co-harboring bla (IMP-26) and tet(A) variant in a clinical *Klebsiella pneumoniae* isolate. *Front. Microbiol.* 11:1610. doi: 10.3389/fmicb.2020.01610

Zhang, R., Dong, N., Shen, Z., Zeng, Y., Lu, J., Liu, C., et al. (2020). Epidemiological and phylogenetic analysis reveals Flavobacteriaceae as potential ancestral source of tigecycline resistance gene tet(X). *Nat. Commun.* 11:4648.

Zhang, R., Hu, Y. Y., Zhou, H. W., Wang, S. L., Shu, L. B., and Chen, G. X. (2019). Emergence of mcr-1 and the tet(A) variant in a *Klebsiella pneumoniae* isolate from the faeces of a healthy person. *J. Med. Microbiol.* 68, 1267–1268. doi: 10.1099/jmm.0.000932

Conflict of Interest: The authors declare that the research was conducted in the absence of any commercial or financial relationships that could be construed as a potential conflict of interest.

frontiers in Microbiology

ORIGINAL RESEARCH
published: 29 March 2021
doi: 10.3389/fmicb.2021.648008

Changing Antimicrobial Resistance and Epidemiology of Non-Typhoidal *Salmonella* Infection in Taiwanese Children

*Yi-Jung Chang[1,2], Yi-Ching Chen[1,2], Nai-Wen Chen[1], Ying-Jie Hsu[1], Hsiao-Han Chu[1], Chyi-Liang Chen[2] and Cheng-Hsun Chiu[1,2,3]**

[1] Department of Pediatrics, Chang Gung Memorial Hospital, College of Medicine, Chang Gung University, Taoyuan, Taiwan, [2] Molecular Infectious Disease Research Center, Chang Gung Memorial Hospital, Taoyuan, Taiwan, [3] Graduate Institute of Clinical Medical Sciences, College of Medicine, Chang Gung University, Taoyuan, Taiwan

OPEN ACCESS

Edited by:
Zhi Ruan,
Zhejiang University, China

Reviewed by:
Christopher Parry,
University of Oxford, United Kingdom
Ursula Panzner,
International Vaccine Institute, South Korea
Samuel Kariuki,
Kenya Medical Research Institute (KEMRI), Kenya

***Correspondence:**
Cheng-Hsun Chiu
chchiu@adm.cgmh.org.tw

Specialty section:
This article was submitted to Antimicrobials, Resistance and Chemotherapy, a section of the journal Frontiers in Microbiology

Received: 31 December 2020
Accepted: 02 March 2021
Published: 29 March 2021

Citation:
Chang Y-J, Chen Y-C, Chen N-W, Hsu Y-J, Chu H-H, Chen C-L and Chiu C-H (2021) Changing Antimicrobial Resistance and Epidemiology of Non-Typhoidal Salmonella Infection in Taiwanese Children. Front. Microbiol. 12:648008. doi: 10.3389/fmicb.2021.648008

Non-typhoidal *Salmonella* (NTS) typically causes self-limiting diarrheal disease but may occasionally lead to invasive infection. This study investigated the epidemiology and antimicrobial resistance of children with NTS infection between 2012 and 2019. We retrospectively analyzed pediatric patients with NTS infections, confirmed by positive cultures, in a tertiary medical center in Taiwan in 2012 and 2019. Clinical features and laboratory data of the patients were collected. Changes in the serogroup category and antimicrobial resistance were also analyzed. Of the total 797 isolates collected, 55 had NTS bacteremia. Compared with the resistance rates in 2012, the rates of resistances to third-generation cephalosporin and ciprofloxacin were significantly higher in 2019 (4.1% vs 14.3%, $P < 0.001$; 1.9% vs 28.6%, $P < 0.001$), especially in groups B, D, and E. Moreover, we observed significantly higher antimicrobial resistance (25.3%) to third-generation cephalosporin, and approximately half the NTS isolates in the infant group were multidrug resistant – a higher rate than those of other age groups in 2019. Invasive NTS often presented with a longer fever duration, lower hemoglobin level and with no elevated C-reactive protein ($P < 0.05$). Non-invasive NTS isolates in 2019 were significantly more resistant to ceftriaxone ($P < 0.001$) and ciprofloxacin ($P < 0.001$) than those in 2012. The antimicrobial resistance of NTS in children has increased progressively in the past decade, and different serogroups exhibited different resistance patterns. During this period, infants showed the highest risk to get a third-generation cephalosporin-resistant NTS infection. The high rates of antimicrobial resistance among children with NTS in Taiwan merit continual surveillance.

Keywords: antimicrobial resistance, bacteremia, *Salmonella*, antibiotics, children

INTRODUCTION

Non-typhoidal *Salmonella* (NTS) infection is a global public health concern; it results in a considerable disease burden in both industrialized and developing countries (Majowicz et al., 2010; Kyu et al., 2018; Roth et al., 2018; Stanaway et al., 2019). NTS typically causes self-limiting diarrheal disease and may also result in invasive NTS (iNTS) infection (Katiyo et al., 2019).

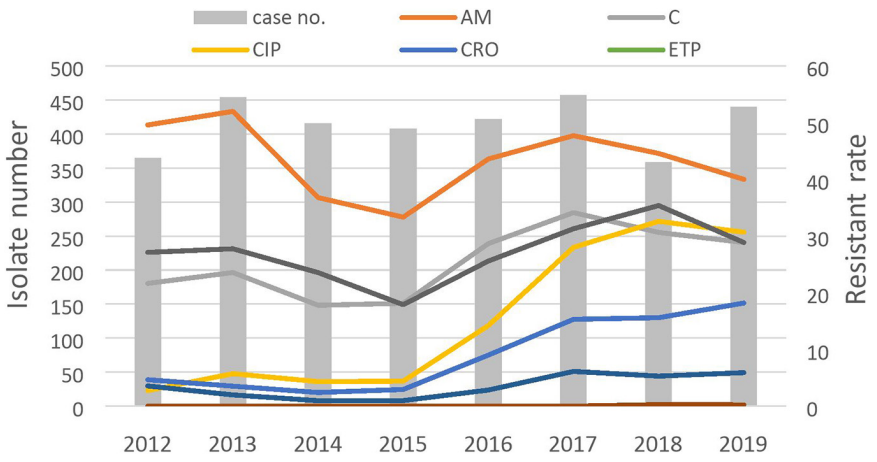

FIGURE 1 | Antibiotic resistant rates of non-typhoidal salmonella from 2012 to 2019.

Approximately 5% of individuals with NTS infection develop invasive diseases, such as bacteremia, meningitis, or septic arthritis, which are especially common in young infants or patients with compromised immune systems (Hohmann, 2001; Feasey et al., 2012). Antimicrobial agents are not recommended for non-severe NTS diarrhea, but they are recommended for people at risk of severe or invasive infection (Ke et al., 2020).

Antimicrobial therapy is the first-line therapy for treating patients with NTS with invasive diseases (Tsai et al., 2011). However, the recognition of NTS bacteremia in children before culture is challenging and rarely reported. Furthermore, resistance to antimicrobial agents has increased worldwide, including in Taiwan (Su et al., 2011; James et al., 2018; Chang et al., 2020). Resistant NTS infection has been reported to be correlated with higher morbidity and mortality (Angelo et al., 2016). Therefore, awareness of changes in antimicrobial resistance and the clinical characteristics of NTS is essential for physicians to arrange effective therapeutic plans to prevent complications.

This study investigated the changing trend of antimicrobial resistance and serogroup distribution in children in northern Taiwan between 2012 and 2019 and the risk factors associated with invasive NTS infection.

MATERIALS AND METHODS

Study Population and Data Collection

The secular trend of antimicrobial resistance of NTS in Chang Gung Memorial Hospital is shown in **Figure 1**. The study enrolled patients aged < 18 years with NTS infection, confirmed by a positive culture, in Chang Gung Memorial Hospital, Linkou, Taiwan, in 2012 and 2019. We retrospectively collected demographic data and clinical characteristics, including patient age, sex, treatment, outcome, serogroup category, and antimicrobial susceptibility from the medical records. In Taiwan, the pediatrician cares patients under 18 of age. In addition, diarrhea is the main cause of morbidity of children under 5 years of age. We stratified participants at different age group, which has been widely validated in many studies. The study was approved by the Research Ethics Committee of Chang Gung Memorial Hospital. (Institutional Review Board Approval No: 201702155B0). All data analyzed were anonymized.

TABLE 1 | Baseline characteristics and clinical features of 797 patients with non-typhoid *Salmonella* infection in 2012 and 2019.

***N* (%)**	**2012 (*N* = 363)**	**2019 (*N* = 434)**	***P* value**
Males (n, %)	200 (55.1%)	239 (55.1%)	0.994
Age(mean) (y/o)	2.1 (SD = 3.8)	2.4 (SD = 3.8)	0.56
Admission proportion	74.2%	62.7%	<0.001
Admission duration (days)	6.9 ± 16.2	5.4 ± 5.9	0.139
Ampicillin use	27/144(18.8%)	8/195 (4.1%)	<0.001
Ceftriaxone use	82/144(56.9%)	155/195(79.5%)	<0.001
iNTS	23/364 (6.3%)	39/434 (7.9%)	0.123
***Salmonella* serogroups**			
Group B	98/364 (26.9%)	100/434 (23%)	0.206
Group C1	20/364 (5.5%)	29/434 (6.7%)	0.486
Group C2	45/364 (12.4%)	56/434 (12.9%)	0.819
Group D	155/364 (42.6%)	185/434 (42.6%)	0.990
Group E	40/364 (11%)	57/434 (13.1%)	0.356
Antimicrobial resistance			
MDR	44/364 (12.2%)	130/434 (30%)	<0.001
Ampicillin	179/364 (49.3%)	174/434 (40.1%)	0.009
Ceftriaxone	15/364 (4.1%)	62/434 (14.3%)	<0.001
Ciprofloxacin	7/364 (1.9%)	124/433 (28.6%)	<0001
TMP-SMX	99/364 (27.3%)	127/432 (29.4%)	0.508
Ertapenem	0/364 (0%)	3/434 (0.7%)	0.255
Imipenem	0/364 (0%)	5/434 (1.2%)	0.067
Chloramphenicol	79/364 (21.8%)	126/403 (31.3%)	0.003
Flomoxef	12/364 (3.3%)	24/403 (6%)	0.084

iNTS, invasive non-typhoidal Salmonella;
MDR, multi-drug resistance, resistant to ≥3 drug classes;
TMP-SMX: trimethoprim-sulphamethoxazole.

Salmonella Strains and Antimicrobial Susceptibility Testing

We collected stool when the patient had gastrointestinal symptoms. The cerebrospinal fluid was sampled when meningitis is suspected. When a person has symptoms such as urinary irritation or needs to rule out a urinary tract infection, a urine culture would be ordered. At the time of admission in our hospital, each child would have a blood sample taken as usual. The blood samples were sent to microbiology laboratory and incubated in the BACTEC FX automatic blood culture system (Becton Dickinson Diagnostic Instrument Systems, Sparks, MD, United States). The BACTEC FX system monitors the production of carbon dioxide every 10 min and uses a fluorescent signal to indicate positive. The stool samples were planted on HE (Hektoen enteric) and EMB (Eosin Methylene Blue) agar medium, and then incubated at 35°C for 20–24 h. If the same participant had several samples, only 1 sample per patient was collected for downstream analyses. If both blood and stool isolates were available from the same patient, only the blood isolate was analyzed. Our hospital identified each *Salmonella* isolate by using a matrix-assisted laser desorption ionization time-of-flight mass spectrometry automated microbiology system. Serogroups of *Salmonella* isolates were examined with O-antigen antisera (Difco Laboratories, Detroit, MI, United States) by employing the slide agglutination method. We then classified *Salmonella* isolates into five serogroups (group B, C1, C2, D, and E) and other serogroups. The antimicrobial susceptibility of NTS isolates was determined using the Kirby–Bauer disk diffusion method and interpreted according to the Standards for Antimicrobial Susceptibility of the Clinical Laboratory Standards Institute. The CLSI versions M100-S29 in 2019 and M100-S22 in 2012 were used in this study (Clinical and Laboratory Standards Institute [CLSI], 2012, 2019). The following antimicrobial agents were examined: ciprofloxacin, ceftriaxone, ampicillin, chloramphenicol, ertapenem, imipenem, flomoxef, and trimethoprim-sulfamethoxazole (TMP-SMX). In MIC determination, the concentration of ceftriaxone resistant was with MIC 4 μg/mL and intermediate was with MIC 1–4 μg/mL. Meanwhile, the concentration of ciprofloxacin resistant was with MIC 1 μg/ml and intermediate was with MIC 0.5 μg/ml. The MIC range of chloramphenicol was 2.0–8.0 μg/mL. For further statistical analysis, intermediate resistance was regarded as the threshold for resistance. Multi-drug resistance (MDR) was defined as concomitant resistance to ≥three antimicrobial drug classes with the same selection, including ampicillin, ceftriaxone, chloramphenicol, ciprofloxacin, imipenem, TMP-SMX, ertapenem, and flomoxef. To analyze factors associated with invasive NTS in children, patients with *Salmonella* bacteremia, meningitis, or septic arthritis and without invasive salmonellosis were analyzed. For clinical features, only children who had both blood and stool culture performed were analyzed. We further divided the study patients into two groups. Those with diarrhea and negative blood culture were categorized as the non-invasive group. Those had positive results either in blood, CSF, or pus culture would be categorized into the invasive group. Patient eligibility was determined according to factors such as clinical manifestations and laboratory data obtained upon admission.

Statistical Analysis

We completed statistical analysis using SPSS for Windows version 22.0 (SPSS Inc., Chicago, IL, United States). Categorical variables including multiple categories were analyzed using the chi-square test, and continuous variables were examined using

TABLE 2 | Changing antimicrobial resistance in different serogroup between 2012 and 2019.

Antimicrobials	2012	2019	*P* value	OR	95% CI
Serogroup B					
MDR	11.2% (11/98)	32% (32/100)	<0.001	3.72	1.74–7.91
Ceftriaxone	5.1% (5/98)	15% (15/100)	0.021	3.28	1.14–9.41
Ciprofloxacin	1% (1/98)	27.3% (27/99)	<0.001	36.3	4.83–273.95
Ampicillin	53.1% (52/98)	43% (43/100)	0.157	1.49	0.85–2.62
TMP-SMX	26.5% (26/98)	35% (35/100)	0.197	0.671	0.365–1.232
Ertapenem	0% (0/98)	1% (1/100)	1.000	NA	NA
Imipenem	0% (0/98)	2% (2/100)	0.498	NA	NA
Serogroup C1					
MDR	10% (2/20)	34.5% (10/29)	0.089	4.73	0.91–24.64
Ceftriaxone	0% (0/20)	20.7% (6/29)	0.069	NA	NA
Ciprofloxacin	0% (0/20)	44.8% (13/29)	<0.001	NA	NA
TMP-SMX	26.3% (5/19)	32.1% (9/28)	0.668	0.754	0.20–2.74
Ampicillin	47.4% (9/19)	44.8% (13/29)	0.863	1.10	0.34–3.53
Ertapenem	0% (0/19)	3.4% (1/29)	1.000	NA	NA
Imipenem	0% (0/19)	3.4% (1/29)	1.000	NA	NA
Serogroup C2					
MDR	8.9% (4/45)	16.1% (9/56)	0.284	1.96	0.56–6.85
Ceftriaxone	4.4% (2/45)	5.4% (3/56)	1.000	1.21	0.19–7.61
Ciprofloxacin	2.2% (1/45)	19.6% (11/56)	0.007	10.75	1.33–86.85
TMP-SMX	31.1% (14/45)	14.3% (8/56)	0.042	2.70	1.01–7.21
Ampicillin	62.6% (28/45)	23.2% (13/56)	<0.001	5.44	2.29–12.93
Ertapenem	0% (0/45)	0% (0/56)	NA	NA	NA
Imipenem	0% (0/45)	0% (0/56)	NA	NA	NA
Serogroup D					
MDR	14.2% (22/155)	31.4% (58/185)	<0.001	2.76	1.59–4.77
Ceftriaxone	5.2% (8/155)	15.1% (28/185)	0.003	3.27	1.44–7.42
Ciprofloxacin	2.6% (4/155)	27.6% (51/185)	<0.001	14.36	5–40.8
TMP-SMX	27.7% (43/155)	30.4% (56/184)	0.587	0.878	0.548–1.406
Ampicillin	45.8% (71/155)	43.2% (80/185)	0.636	1.10	0.72–1.70
Ertapenem	0% (0/155)	0% (0/185)	NA	NA	NA
Imipenem	0% (0/155)	0.5% (1/185)	1.000	NA	NA
Serogroup E					
MDR	12.5% (5/40)	31.6% (18/57)	0.030	3.23	1.08–9.61
Ceftriaxone	0% (0/40)	14% (8/57)	0.019	NA	NA
Ciprofloxacin	2.5% (1/40)	19.6% (19/57)	<0.001	19.5	2.48–152.98
TMP-SMX	27.5% (11/40)	28.1% (16/57)	0951	0.972	0.394–2.398
Ampicillin	42.5% (17/40)	38.6% (22/57)	0.700	1.17	0.51–2.67
Ertapenem	0% (0/40)	0% (0/57)	NA	NA	NA
Imipenem	0% (0/40)	0% (0/57)	NA	NA	NA

MDR, multi-drug resistance, resistant to ≥3 drug classes; TMP-SMX, trimethoprim/sulfamethoxazole; OR, odds ratio; CI, confidence interval; NA, not applicable.

independent *t* tests. A *p* value <0.05 was considered to be statistically significant.

RESULTS

A total of 797 NTS isolates were collected from 781 patients in 2012 and 2019 (363 from 2012 and 434 from 2019), of which 90.7% were isolated from the stool, 6.8% from blood, and 2.5% from other extraintestinal samples (12 isolates from urine, 3 from cerebrospinal fluid, and 2 from pus). The isolates collected from blood and extraintestinal samples were classified as iNTS. The majority (81.5%) of the NTS isolates were obtained from children aged ≤ 3 years, and 36.0% of the isolates were from children aged 1–2 years. The most common serogroup was group D (42.6%), followed by group B (24.8%), serogroup C2 (12.6%), and serogroup E (12.1%). The overall resistance rates were 15.1% to ciprofloxacin, 8% to ceftriaxone, 41.4% to ampicillin, 27.8% to chloramphenicol, 2.3% to ertapenem, 3.9% to flomoxef, 0.6% to imipenem, and 28.2% to sulfamethoxazole. **Table 1** presents a comparison of the baseline characteristics of the patients and antimicrobial resistance rates of NTS between 2012 and 2019. The mean age of the two groups was similar (2.1 years vs 2.4 years, $P = 0.56$). Compared with the resistance rates in 2012, the resistance rates in 2019 to ciprofloxacin (28.6% vs 1.9%, $P < 0.001$), ceftriaxone (14.3% vs 4.1%, $P < 0.001$), chloramphenicol (31.3% vs 21.7%, $P = 0.003$), and sulfamethoxazole (29.4% vs 27.2%, $P < 0.001$) were significantly higher. Moreover, the ampicillin resistance rate was significantly lower in 2019 than in 2012 (49.2% vs 40.1%, $P = 0.01$). No significant difference in resistance rate was observed for ertapenem, imipenem, and flomoxef between those 2 years. The incidence of ampicillin as an empirical antibiotic in 2012 was higher than in 2019 (18.8% vs 4.1%, $P < 0.001$). On the contrary, if directed, most doctors choose ceftriaxone as an empirical antibiotic in 2019 than in 2012 (79.5% vs 56.9%, $P < 0.001$). The evolution of antimicrobial resistance in different serogroups is presented in **Table 2**. The highest resistance rate to ampicillin was noted in group B (48%), and the highest resistance rate to ciprofloxacin was observed in group C1 (27.1%). We noted significantly increased ciprofloxacin, ceftriaxone, and MDR resistance between 2012 and 2019 in the isolates from group B, group D, and group E. In groups C1 and C2, we also noted an increase in ciprofloxacin resistance in 2019 compared with 2012. **Table 3** presents the differences in antimicrobial resistance by age for 2012 and 2019. In 2019, the patients aged < 1 year had a higher resistance rate to ampicillin (50.6%, $P = 0.005$), ceftriaxone (25.3%, $P = 0.002$), TMP-SMX (44.2%, $P = 0.001$), and chloramphenicol (46.3%, $P = 0.003$) than did that other age group. The differences in clinical manifestations and laboratory examination results upon admission between the NTS bacteremia group and the non-iNTS group are listed in **Table 4**. Longer fever duration (3.8 ± 2.7, $P < 0.001$), lower C-reactive protein (CRP) level (39.1 ± 41.8 vs 58.6 ± 55.7, $P < 0.001$), and lower hemoglobin level (11.6 ± 1.4 vs 12.1 ± 1.2, $P = 0.027$) were significant factors associated with the NTS bacteremia group. The main outcomes between children with iNTS and those with diarrhea and a negative blood culture was the prolonged hospital stay in iNTS (9.8 ± 9.5 vs 5.8 ± 12.1 $p = 0.016$). **Table 5** presents the antimicrobial resistance in NTS bacteremia and non-iNTS infections in 2012 and 2019. Non-iNTS isolates in 2019 were significantly more resistant to

TABLE 3 | Changing antimicrobial resistance by different age groups between 2012 and 2019.

AGE	<1 Y	1–2 Y	2–5 Y	>5 Y	*P* value
2012					
MDR	12.1% (12/99)	11.6% (18/155)	14.9% (14/94)	0% (0/15)	0.426
Ampicillin	48.5% (48/99)	54.2% (84/155)	42.3% (22/52)	43.1% (25/58)	0.279
Ceftriaxone	3% (3/99)	5.2% (8/155)	4.3% (4/94)	0% (0/15)	0.575
Ciprofloxacin	2% (2/99)	1.9% (3/155)	2.1% (2/94)	0% (0/15)	0.895
TMP-SMX	25.3% (25/99)	25.8% (40/155)	34% (32/94)	13.3% (2/15)	0.260
Ertapenem	0% (0/99)	0% (0/155)	0% (0/94)	0% (0/15)	
Imipenem	0% (0/99)	0% (0/155)	0% (0/94)	0% (0/15)	
Chloramphenicol	28.3% (28/99)	22.6% (35/155)	16% (15/94)	6.7% (1/15)	0.094
Flomoxef	4% (4/99)	2.6% (4/155)	4.3% (4/94)	0% (0/15)	0.641
2019					
MDR	42.5% (37/87)	22.2% (40/180)	29.6% (37/125)	38.1% (16/42)	0.005
Ampicillin	50.6% (44/87)	32.8% (59/180)	41.6% (52/125)	19.0% (8/42)	0.036
Ceftriaxone	25.3% (22/87)	8.3% (15/180)	13.6% (17/125)	19.0% (8/42)	0.002
Ciprofloxacin	34.9% (30/86)	23.9% (43/180)	28.8% (36/125)	35.7% (15/42)	0.199
TMP-SMX	44.2% (38/86)	22.3% (40/179)	26.4% (33/125)	38.1% (16/42)	0.001
Ertapenem	2.3% (2/87)	0.6% (1/180)	0% (0/125)	0% (0/42)	0.221
Imipenem	3.4% (3/87)	0.6% (1/180)	0% (0/125)	2.4% (1/42)	0.084
Chloramphenicol	46.3% (37/80)	24.4% (39/160)	27.9 (34/122)	39% (16/41)	0.003
Flomoxef	3.8% (3/80)	4.4% (7/160)	8.2% (10/122)	49.8% (4/41)	0.326

MDR, multi-drug resistance, resistant to ≥3 drug classes.

TABLE 4 | Demographic, clinical manifestations and antimicrobial resistance among iNTS and non-iNTS infections in 2012 and 2019.

	iNTS infections (*n* = 62)	Non-iNTS infections (*n* = 555)	*P* value
Male, *n* (%)	53.2% (33)	56.5% (314)	0.582
Age, y/o, mean ± SD	1.7 ± 2.8	2.3 ± 2.3	0.099
Symptoms at admission			
Fever, *n* (%)	58(93.5%)	512(92.8%)	0.930
Diarrhea, *n* (%)	45(72.6%)	376(68.1%)	0.444
Bloody stools, *n* (%)	19(43.2%)	242(58%)	0.059
Abdominal pain, *n* (%)	9(14.5%)	186(33.7%)	0.001
Vomiting, *n* (%)	18(29%)	208(37.3%)	0.087
Fever duration, days, mean ± SD	3.8 ± 2.4	2.7 ± 2.1	< 0.001
Hospital stay, days, mean ± SD	9.8 ± 9.5	5.8 ± 12.1	0.016
Hb, g/dL, mean ± SD	11.6 ± 1.4	12.1 ± 1.2	0.027
CRP, mg/L, mean ± SD	39.1 ± 58.3	58.6 ± 54.8	0.009
Band form, %, mean ± SD	4.7 ± 6.9	6.9 ± 6.9	0.112
WBC, /μl, mean ± SD	10,803 ± 4,420	10,051 ± 4,168	0.192
Antimicrobial resistance			
2019			
Ampicillin	29.7%	41.6%	0.165
Ceftriaxone	5.4%	14.8%	0.119
Ertapenem	2.7%	0.3%	0.209
Imipenem	2.8%	1.0%	0.353
Ciprofloxacin	30.6%	28.5%	0.790
TMP-SMX	20.6%	30.2%	0.240
Chloramphenicol	66.7%	29.9%	0.073
Flomoxef	40%	5.5%	0.030
2012			
Ampicillin	42.1%	49.7%	0.519
Ceftriaxone	10.5%	3.8%	0.182
Ertapenem	0%	0%	NA
Imipenem	0%	0%	NA
Ciprofloxacin	5.3%	1.7%	0.316
TMP-SMX	15.8%	27.9%	0.248
Chloramphenicol	21.1%	21.8%	1.000
Flomoxef	5.3%	3.2%	0.624

iNTS, invasive non-typhoidal Salmonella;
SD, standard deviation;
TMP-SMX, trimethoprim-sulfamethoxazole.

TABLE 5 | Antimicrobial resistance and serogroups between iNTS and non-iNTS infections in 2012 and 2019.

	iNTS			non-iNTS		
	2012	2019	*P* value	2012	2109	*P* value
Antimicrobial resistance						
Ampicillin	42.1%	27.8%	0.282	49.7%	41.2%	0.020
Ceftriaxone	10.5%	5.6%	0.602	3.8%	15.1%	<0.001
Ertapenem	0%	2.8%	1.000	0%	0.5%	0.502
Imipenem	0%	2.8%	1.000	0%	1.0%	0.128
Ciprofloxacin	5.3%	30.6%	0.041	1.7%	28.5%	<0.001
TMP-SMX	15.8%	20.6%	1.000	27.9%	30.2%	0.518
Chloramphenicol	21.2%	60%	0.126	21.8%	30.9%	0.005
Flomoxef	5.3%	40%	0.099	3.2%	5.5%	0.125
MDR	10.5%	13.9%	1.000	12.2%	31.4%	<0.001
Serogroups						
B	15.8%	22.2%	0.730	27.6%	23.1%	0.159
C1	15.8%	2.8%	0.114	4.7%	7%	0.170
C2	5.3%	16.7%	0.401	12.8%	12.6%	0.926
D	52.6%	41.7%	0.437	42.2%	42.7%	0.891
E	10.5%	13.9%	1.000	11%	13.1%	0.401

iNTS, invasive non-typhoidal Salmonella;
MDR, multi-drug resistance, resistant to ≥3 drug classes;
TMP-SMX, trimethoprim-sulfamethoxazole.

ceftriaxone (15.1% vs 3.8%, $P < 0.001$) and ciprofloxacin (28.5% vs 1.7%, $P < 0.001$) than those in 2012.

DISCUSSION

Our results indicated that the antimicrobial susceptibility of NTS has changed during the past decade, with several clinically relevant findings. A particularly crucial finding is the significantly higher prevalence of antimicrobial resistance to third-generation cephalosporin in infants. Additionally, the resistance rate to ciprofloxacin and third-generation cephalosporin increased significantly from 2012 to 2019, especially in groups B, D, and E. Furthermore, we observed that most patients with NTS bacteremia presented with fever lasting more than 4 days at admission with a lower systemic inflammatory reaction. This is the first analysis to reveal that *Salmonella* bacteremia is closely associated with longer fever duration and inconsistent lower systemic inflammatory reaction. By contrast, non-blood isolates (mostly local) were generally more resistant than NTS bacteremia isolates.

Concern has been growing over the past decades regarding antimicrobial resistance in NTS. Our data demonstrated an increase in overall antimicrobial resistance in *Salmonella* from 20 to 30% in 2012 to as high as 70% in 2019. Previous studies have reported high resistance rates to ampicillin in Taiwan. The increasing rates of resistance have resulted in changes to clinical practice guidelines for treating the disease. Therefore, expensive third-generation cephalosporins are currently the first-choice antibiotics for iNTS infection in children. Our data revealed a significant elevation in ceftriaxone resistance from 2012 to 2019, whereas the resistance rate to ampicillin decreased. These results are in accordance with recent studies indicating the emergence and spread of resistance to third-generation cephalosporin in Taiwan and other Asian countries (Lee et al., 2021). Ampicillin resistance significantly decreased in our study period, possibly because of antibiotic choice.

This study explored various NTS serogroups that are closely associated with antimicrobial resistance. More than half the NTS isolates were classified as MDR, with particularly high resistance in groups B, D, and E. These three groups also had the highest resistance rate to third-generation cephalosporin. In Taiwan, self-transferable bla_{CMY-2}-harboring IncI1 plasmids have been identified in several *Salmonella* serotypes belonging to *Salmonella* groups B and D (Lo et al., 2020). Since 2015, northern Taiwan has experienced an increase in *Salmonella* infections caused by

previously rare *Salmonella* Anatum, a serogroup E serotype. Such infections have also been reported in central Taiwan, indicating that this outbreak has already spread throughout the island (Chiou et al., 2019). Coresistance to ceftriaxone and ciprofloxacin is the main feature of the outbreak clone (Feng et al., 2020).

This study highlighted that isolates from infants had significantly higher MDR to ampicillin and third-generation cephalosporin than did isolates from other age groups. This is partly explained by the increase in isolates in infants with serotypes since the early 1990s, which have been associated with MDR (Katiyo et al., 2019). This rather unexpected result may be attributed to human-to-human transmissions. Parents may have more often touched, rinsed, and cooked contaminated meat before feeding other foods to their infants. Moreover, these parents were more willing to purchase meat from traditional markets rather than supermarkets (Feng et al., 2020). One possibility is that parents bought meat from traditional markets, and then, their frequent rinsing spread the *Salmonella* from the surface of the meats to cutting boards, knives, sinks, and finally onto fresh vegetables, fruit, and other ready-to-eat foods that were cross-contaminated and reached the infants through parents or other caregivers. This transmission mode is particularly critical in infants. On the basis of these findings, we recommend that clinicians in Taiwan use third-generation cephalosporins for empirical treatment of NTS bacteremia and determine the exact treatment according to antimicrobial susceptibility results.

Our analyses indicated that ceftriaxone resistance in Taiwan was low in 2012, and our results revealed that the overall resistance rates in the non-iNTS isolates were generally higher than those in the iNTS isolates. We noted significantly lower serum CRP level in patients with NTS bacteremia than in patients without NTS bacteremia. In previous studies, a severity score with CRP served as a guide for prescribing antibiotics for severe NTS infection in children. On the basis of the current findings, we recommend against routinely using antimicrobials to treat uncomplicated NTS gastroenteritis in cases of high CRP level. This finding is consistent with that of Mughini-Gras et al. (2020) who reported that iNTS isolates were generally less resistant than non-iNTS isolates (Mughini-Gras et al., 2020; Ke et al., 2020). NTS bacteremia in this study tended to develop in young children with prolonged fever. The hemoglobin level was also found significantly lower in the invasive group (P = 0.027) in our study. Christenson (2013) had reported that patients with hemolytic anemia, malaria, sickle cell anemia, and thalassemia major were more susceptible to invasive *Salmonella* infection (Christenson, 2013). This finding is consistent with previous reports that revealed a longer duration of symptoms, such as fever and diarrhea, before admission in children with bacteremia (Lee et al., 2021). Thus, fever duration can be a suitable rationale for treatment before receiving antimicrobial susceptibility results.

Adopting an 8-year detailed hospitalization dataset from the largest pediatric hospital in Taiwan enabled us to representatively evaluate the trends and characteristics of antimicrobial resistance in pediatric NTS infections. However, this study has some limitations. First, only serogroup data were available in our research, and serotype data were limited. Disease severity and antimicrobial resistance may be associated with different serotypes; therefore, further analysis of serotypes with clinical manifestations or resistance patterns are required to clarify virulence and impact among different serotypes. Second, this was a single-center study; thus, we could not adequately account for the considerable geographic variability in antimicrobial resistance patterns in NTS. Although the data is from a single hospital, Chang Gung Memorial Hospital is the largest in Taiwan. So, the data can reflect the true epidemiology in Taiwan.

This study revealed that the resistance of NTS to fluoroquinolones and third-generation cephalosporins has been increasing in Taiwan. MDR in serogroups B, D, and E remained high. More importantly, cephalosporin resistance was more common in isolates from infants. Prolonged fever was a single factor associated with bacteremia in children with NTS infection.

DATA AVAILABILITY STATEMENT

The original contributions presented in the study are included in the article/supplementary material, further inquiries can be directed to the corresponding author/s.

AUTHOR CONTRIBUTIONS

C-HC and Y-JC: conception and design of the study. N-WC and Y-JH: implementation and data collection. H-HC and Y-CC: analysis and interpretation of the data. Y-JC, C-LC, and C-HC: writing and critical review of the manuscript. All authors contributed to the article and approved the submitted version.

FUNDING

The funders had no role in study design, data collection and analysis, decision to publish, or preparation of the manuscript.

REFERENCES

Angelo, K., Reynolds, J., Karp, B., Hoekstra, R., Scheel, C. M., and Friedman, C. (2016). Antimicrobial resistance among nontyphoidal *Salmonella* Isolated from blood in the United States, 2003–2013. *J. Infect. Dis.* 214, 1565–1570. doi: 10.1093/infdis/jiw415

Chang, Y. J., Chen, M. C., Feng, Y., Su, L. H., Li, H. C., Yang, H. P., et al. (2020). Highly antimicrobial-resistant nontyphoidal *Salmonella* from retail meats and clinical impact in children, Taiwan. *Pediatr. Neonatol.* 61, 432-438. doi: 10.1016/j.pedneo.2020.03.017

Chiou, C. S., Hong, Y. P., Liao, Y. S., Wang, Y. W., Tu, Y. H., Chen, B. H., et al. (2019). New Multidrug-resistant *Salmonella enterica* serovar Anatum clone, Taiwan, 2015-2017. *Emerg Infect Dis.* 25, 144–147. doi: 10.3201/eid2501.181103

Christenson, J. C. (2013). *Salmonella* infections. *Pediatr Rev.* 34, 375–383. doi: 10.1542/pir.34-9-375

Clinical and Laboratory Standards Institute [CLSI] (2012). *Performance Standards for Antimicrobial Susceptibility Testing; Twenty-Two Informational Supplement. CLSI Document M100-22*. Wayne, PA: Clinical and Laboratory Standards Institute.

Clinical and Laboratory Standards Institute [CLSI] (2019). *Performance Standards for Antimicrobial Susceptibility Testing; Twenty-Ninth Informational Supplement. CLSI Document M100-29*. Wayne, PA: Clinical and Laboratory Standards Institute.

Feasey, N. A., Dougan, G., Kingsley, R. A., Heyderman, R. S., and Gordon, M. A. (2012). Invasive non-typhoidal *Salmonella* disease: an emerging and neglected tropical disease in Africa. *Lancet* 379, 2489-2499. doi: 10.1016/S0140-6736(11)61752-2

Feng, Y., Chang, Y. J., Pan, S. C., Su, L. H., Li, H. C., Yang, H. P., et al. (2020). Characterization and source investigation of multidrug-resistant *Salmonella* Anatum from a sustained outbreak, Taiwan. *Emerg. Infect. Dis.* 26, 2951–2955. doi: 10.3201/eid2612.200147

Hohmann, E. L. (2001). Nontyphoidal salmonellosis. *Clin. Infect. Dis.* 32, 263-9. doi: 10.1086/318457

James, S. L., Abate, D., Abate, K. H., Abay, S. M., Abbafati, C., Abbasi, N., et al. (2018). Global, regional, and national incidence, prevalence, and years lived with disability for 354 diseases and injuries for 195 countries and territories, 1990–2017: a systematic analysis for the Global Burden of Disease Study 2017. *Lancet* 392, 1789–1858. doi: 10.1016/S0140-6736(18)32279-7

Katiyo, S., Muller-Pebody, B., Minaji, M., Powell, D., Johnson, A. P., De Pinna, E., et al. (2019). Epidemiology and outcomes of nontyphoidal *Salmonella* Bacteremias from England, 2004 to 2015. *J. Clin. Microbiol.* 57:e01189-18. doi: 10.1128/JCM.01189-18

Ke, Y., Lu, W., Liu, W., Zhu, P., Chen, Q., and Zhu, Z. (2020). Non-typhoidal *Salmonella* infections among children in a tertiary hospital in Ningbo, Zhejiang, China, 2012-2019. *PLoS Negl. Trop. Dis.* 14:e0008732. doi: 10.1371/journal.pntd.0008732

Kyu, H. H., Abate, D., Abate, K. H., Abay, S. M., Abbafati, C., Abbasi, N., et al. (2018). Global, regional, and national disability-adjusted life-years (DALYs) for 359 diseases and injuries and healthy life expectancy (HALE) for 195 countries and territories, 1990–2017: a systematic analysis for the Global Burden of Disease Study 2017. *Lancet* 392, 1859–1922. doi: 10.1016/S0140-6736(18)32335-3

Lee, C. M., Lee, M. S., Yang, T. L., Lee, K. L., Yen, T. Y., Lu, C. Y., et al. (2021). Clinical features and risk factors associated with bacteremia of nontyphoidal salmonellosis in pediatric patients, 2010-2018. *J. Formos. Med. Assoc.* 120, 196–203. doi: 10.1016/j.jfma.2020.04.022

Lo, H. Y., Lai, F. P., and Yang, Y. J. (2020). Changes in epidemiology and antimicrobial susceptibility of nontyphoid *Salmonella* in children in southern Taiwan, 1997-2016. *J. Microbiol. Immunol. Infect.* 53, 585-591. doi: 10.1016/j.jmii.2018.06.004

Majowicz, S. E., Musto, J., Scallan, E., Angulo, F. J., Kirk, M., O'Brien, S. J., et al. (2010). International collaboration on enteric disease 'Burden of Illness' studies. the global burden of nontyphoidal *Salmonella* gastroenteritis. *Clin. Infect. Dis.* 50, 882-889. doi: 10.1086/650733

Mughini-Gras, L., Pijnacker, R., Duijster, J., Heck, M., Wit, B., Veldman, K., et al. (2020). Changing epidemiology of invasive non-typhoid *Salmonella* infection: a nationwide population-based registry study. *Clin. Microbiol. Infect.* 26, 941.e9-941.e14. doi: 10.1016/j.cmi.2019.11.015

Roth, G. A., Abate, D., Abate, K. H., Abay, S. M., Abbafati, C., Abbasi, N., et al. (2018). Global, regional, and national age-sex-specific mortality for 282 causes of death in 195 countries and territories, 1980–2017: a systematic analysis for the Global Burden of Disease Study 2017. *Lancet* 392, 1736–1788. doi: 10.1016/S0140-6736(18)32203-7

Stanaway, J. D., Parisi, A., Sarkar, K., Blacker, B. F., Reiner, R. C., Hay, S. I., et al. (2019). The global burden of non-typhoidal *Salmonella* invasive disease: a systematic analysis for the Global Burden of Disease Study 2017. *Lancet Infect. Dis.* 19, 1312–1324. doi: 10.1016/S1473-3099(19)30418-9

Su, L. H., Teng, W. S., Chen, C. L., Lee, H. Y., Li, H. C., Wu, T. L., et al. (2011). Increasing ceftriaxone resistance in *Salmonellae*, Taiwan. *Emerg. Infect. Dis.* 17, 1086-1890. doi: 10.3201/eid/1706.101949

Tsai, M. H., Huang, Y. C., Lin, T. Y., Huang, Y. L., Kuo, C. C., and Chiu, C. H. (2011). Reappraisal of parenteral antimicrobial therapy for nontyphoidal *Salmonella enteric* infection in children. *Clin. Microbiol. Infect.* 17, 300–305. doi: 10.1111/j.1469-0691.2010.03230.x

Conflict of Interest: The authors declare that the research was conducted in the absence of any commercial or financial relationships that could be construed as a potential conflict of interest.

frontiers in Microbiology

ORIGINAL RESEARCH
published: 26 April 2021
doi: 10.3389/fmicb.2021.666782

Impact of *mcr-1* on the Development of High Level Colistin Resistance in *Klebsiella pneumoniae* and *Escherichia coli*

Xiao-Qing Zhu[1,2†], Yi-Yun Liu[1,2†], Renjie Wu[1,2], Haoliang Xun[1,2], Jian Sun[1,2], Jian Li[3], Yaoyu Feng[2,4] and Jian-Hua Liu[1,2]*

[1] College of Veterinary Medicine, Guangdong Provincial Key Laboratory of Veterinary Pharmaceutics Development and Safety Evaluation, Key Laboratory of Zoonosis of Ministry of Agricultural and Rural Affairs, National Risk Assessment Laboratory for Antimicrobial Resistance of Microorganisms in Animals, South China Agricultural University, Guangzhou, China, [2] Guangdong Laboratory for Lingnan Modern Agriculture, Guangzhou, China, [3] Biomedicine Discovery Institute and Department of Microbiology, School of Biomedical Sciences, Monash University, Clayton, VIC, Australia, [4] College of Veterinary Medicine, Center for Emerging and Zoonotic Diseases, South China Agricultural University, Guangzhou, China

OPEN ACCESS

Edited by:
Shaolin Wang,
China Agricultural University, China

Reviewed by:
Ruichao Li,
Yangzhou University, China
Mehmet Demirci,
Kırklareli University, Turkey

***Correspondence:**
Jian-Hua Liu
jhliu@scau.edu.cn

[†] These authors have contributed equally to this work

Specialty section:
This article was submitted to Antimicrobials, Resistance and Chemotherapy, a section of the journal Frontiers in Microbiology

Received: 11 February 2021
Accepted: 26 March 2021
Published: 26 April 2021

Citation:
Zhu X-Q, Liu Y-Y, Wu R, Xun H, Sun J, Li J, Feng Y and Liu J-H (2021) Impact of mcr-1 on the Development of High Level Colistin Resistance in Klebsiella pneumoniae and Escherichia coli. Front. Microbiol. 12:666782. doi: 10.3389/fmicb.2021.666782

Plasmid-mediated colistin resistance gene *mcr-1* generally confers low-level resistance. The purpose of this study was to investigate the impact of *mcr-1* on the development of high-level colistin resistance (HLCR) in *Klebsiella pneumoniae* and *Escherichia coli*. In this study, *mcr-1*-negative *K. pneumoniae* and *E. coli* strains and their corresponding *mcr-1*-positive transformants were used to generate HLCR mutants *via* multiple passages in the presence of increasing concentrations of colistin. We found that for *K. pneumoniae,* HLCR mutants with minimum inhibitory concentrations (MICs) of colistin from 64 to 1,024 mg/L were generated. Colistin MICs increased 256- to 4,096-fold for *mcr-1*-negative *K. pneumoniae* strains but only 16- to 256-fold for the *mcr-1*-harboring transformants. For *E. coli*, colistin MICs increased 4- to 64-folds, but only 2- to 16-fold for their *mcr-1*-harboring transformants. Notably, *mcr-1* improved the survival rates of both *E. coli* and *K. pneumoniae* strains when challenged with relatively high concentrations of colistin. In HLCR *K. pneumoniae* mutants, amino acid alterations predominately occurred in *crrB*, followed by *phoQ*, *crrA*, *pmrB*, *mgrB*, and *phoP*, while in *E. coli* mutants, genetic alterations were mostly occurred in *pmrB* and *phoQ*. Additionally, growth rate analyses showed that the coexistence of *mcr-1* and chromosomal mutations imposed a fitness burden on HLCR mutants of *K. pneumoniae*. In conclusion, HLCR was more likely to occur in *K. pneumoniae* strains than *E. coli* strains when exposed to colistin. The *mcr-1* gene could improve the survival rates of strains of both bacterial species but could not facilitate the evolution of high-level colistin resistance.

Keywords: *mcr-1*, *Enterobacterales*, colistin, resistance, fitness cost

INTRODUCTION

Infections caused by multidrug-resistant pathogens pose significant risks to public health worldwide (Ruhnke et al., 2014; Huang et al., 2018). Owing to a limited number of effective antimicrobial agents, colistin has been reused and is considered to be the last therapeutic agent; however, resistance to colistin has been increasingly reported (Liu et al., 2016; Srinivas and Rivard, 2017). Previously, colistin resistance was mainly caused by mutations in chromosomal genes, including *pmrAB*, *phoPQ*, *crrAB*, and the negative regulator *mgrB* (Wright et al., 2015; Poirel et al., 2017; Srinivas and Rivard, 2017), which resulted in the modification of lipid A with positively charged residues, such as phosphoethanolamine and/or 4-amino-4-deoxy-L-arabinose. However, plasmid-mediated colistin resistance genes have also emerged recently. Since, we reported the first case of plasmid-mediated colistin resistance gene (*mcr-1*) in 2015 (Liu et al., 2016), several variants of *mcr* genes (*mcr-2* to *mcr-10*) have been reported worldwide (Shi et al., 2020; Wang et al., 2020).

Similar to plasmid-mediated quinolone resistance genes, *mcr-1* generally confers low-level colistin resistance (2–8 mg/L) (Jeong et al., 2008; Jacoby et al., 2014; Liu et al., 2016). However, it is unknown whether the presence of *mcr-1* can facilitate the selection of a higher level of colistin resistance, as reported for *qnr* family genes (Jeong et al., 2008; Jacoby et al., 2014). Furthermore, the available data show that the prevalence of *mcr-1* is significantly higher in *Escherichia coli* than that in *Klebsiella pneumoniae* (Quan et al., 2017; Eiamphungporn et al., 2018). Additionally, in clinical *K. pneumoniae* isolates, colistin resistance is mostly mediated by chromosomal mutations, which usually confer higher levels of resistance (16–1,024 mg/L) than that conferred by *mcr* (Cannatelli et al., 2014; Liu et al., 2016; Jayol et al., 2017). It seems that *K. pneumoniae* is more likely to generate chromosomal mutations but is less likely to harbor *mcr-1* compared to the phenomenon observed in *E. coli*. Nevertheless, a previous study showed that after a single overnight exposure to twofold minimum inhibitory concentrations (MICs) of colistin, *mcr-1* facilitated the development of high-level colistin resistance (HLCR; MIC $\geq$ 32 mg/L) mutants in *E. coli* but did not affect the HLCR mutation rates in *K. pneumoniae* (Zhang et al., 2019). However, another study reported that MCR-negative strains could be induced to higher level of colistin resistance than MCR-positive strains after step-wise induction (Luo et al., 2019). Thus, the impact of *mcr-1* on the development of high level colistin resistance in *K. pneumoniae* and *E. coli*, and whether similar probability and frequency of mutations will be observed in *E. coli* and *K. pneumoniae* under selection with increasing concentrations of colistin remain unclear.

In this study, we investigated and compared the development of HLCR and chromosomal mutations among strains of *E. coli* and *K. pneumoniae*, with or without *mcr-1*, *via* multiple passages in the presence of increasing colistin concentrations.

MATERIALS AND METHODS

Bacterial Strains and Plasmids

Klebsiella pneumoniae P11, HZ7H152, and YX6P94K and *E. coli* ATCC 25922, C600, and ZYTF186 were used as *mcr-1*-negative parental strains for this study. The sources and resistance phenotypes of these strains are listed in **Supplementary Table 1**. To construct an *mcr-1*-harboring plasmid, *mcr-1* was cloned from pHNSHP45 (GenBank accession number KP347127.1) to pHSG575 using the primer pair listed in **Supplementary Table 2**, which yielded pHSG575-*mcr-1* (Takeshita et al., 1987). The recombinant plasmid was transformed into *E. coli* ATCC 25922 by electroporation, whereas the original plasmid pHNSHP45 was transformed into *K. pneumoniae* P11, HZ7H152, and YX6P94K and *E. coli* C600 and ZYTF186. Transformants were selected on Luria–Bertani (LB) medium containing 2 mg/L colistin. The presence of *mcr-1* in the transformants was confirmed as per previously described methods (Liu et al., 2016).

Whole-Genome Sequencing and Analysis

The whole genomic DNA of four strains, *K. pneumoniae* P11, HZ7H152, and YX6P94K and *E. coli* ZYTF186, was sequenced using Illumina HiSeq 2000 (Illumina, San Diego, CA, United States). Sequence reads were assembled into contigs using SOAPdenovo version 2.04. Resistance genes were explored using ResFinder[1]. The whole-genome sequences of two laboratory strains, *E. coli* C600 and ATCC 25922 (GenBank accession numbers NZ_CP031214.1 and NZ_CP009072.1, respectively), were obtained from NCBI and used as reference genomes.

Antimicrobial Susceptibility Testing

Minimum inhibitory concentrations of colistin were determined using Mueller–Hinton (MH) broth microdilution following the recommendations of the Clinical and Laboratory Standards Institute (Matuschek et al., 2018). *E. coli* ATCC 25922 was used as a reference strain.

Induction of Colistin Resistance by Conducting Serial Passages

Serial passaging was performed as per previously described methods (San Millan et al., 2016), with minor modifications. As shown in **Supplementary Figure 1**, strains were incubated on MH agar plates at 37°C to obtain single colonies. For each strain, 48 colonies were randomly selected and inoculated in separate wells of 96-well plates containing colistin-free LB broth to obtain overnight cultures. The overnight cultures were inoculated in 0.2 mL of LB broth with colistin (0.5 × MIC) in a new 96-well plate. Following a 24-h incubation at 37°C, the cultures were diluted 1:100 and transferred to a new plate containing a double concentration of colistin relative to that used on the previous day. The serial passages were performed until no surviving populations were observed.

[1]https://cge.cbs.dtu.dk//services/ResFinder/

Surviving populations were defined considering growth indicated by OD_{600} (optical density at 600 nm) > 0.10 ± 0.02. The number of surviving populations was recorded for all treatments over time. For each strain, 5–10 surviving populations were selected along the concentration gradient of colistin from low to high, with priority selection of populations that survived at the highest concentration. Subsequently, the populations were separately plated on fresh LB agar to obtain single colonies, and three colonies were randomly selected from each population to determine their susceptibility to colistin and resistance mechanisms.

Genetic Alterations in Colistin-Resistant Mutants

Chromosomal genes (*mgrB*, *pmrAB*, *phoPQ*, and *crrAB*) associated with colistin resistance were amplified by PCR and sequenced using the primers listed in **Supplementary Table 2**. Genetic alterations that occurred in colistin-resistant mutants were determined by comparing the resulting sequences to their corresponding parental reference genomes.

In vitro Growth Rate Assay

Forty-four HLCR K. pneumoniae mutants with different mutations, including equal numbers of *mcr-1*-negative and *mcr-1*-positive derivatives, were selected incubated in fresh MH broth under shaking (180 rpm) conditions at 37°C. The overnight cultures were inoculated in fresh MH broth, and OD_{600} was measured using the Multiskan Spectrum microplate spectrophotometer (Thermo Labsystems, Franklin, MA, United States). The growth rates were determined by plotting the logarithm of OD_{600} versus time. Data analysis was performed using a non-parametric Mann–Whitney *U*-test, followed by Dunn's multiple comparison test (Zwietering et al., 1990).

Accession Numbers

The whole genome sequencing data of *K. pneumoniae* P11, HZ7H152, *K. variicola* YX6P94K (subtype of *K. pneumoniae*) and *E. coli* ZYTF186 have been deposited in GenBank with accession numbers JAFKAD010000000, JAFKAE010000000, JAFKAG010000000, and JAFKAF010000000, respectively.

RESULTS

Development of Resistance to Colistin via Serial Passages of *Escherichia coli*

Colistin-resistant *E. coli* mutants were obtained under increasing colistin pressure. The final induction concentrations of colistin, which inhibited the growth of all *E. coli* strains, ranged from 32 to 64 mg/L. As shown in **Figures 1A–C**, initially, the surviving populations of the *mcr-1*-negative parental strains (ATCC 25922, C600, and ZYTF186) plummeted in response to a challenge with 2 mg/L colistin, while those of their corresponding *mcr-1*-positive derivatives did not show a marked decline until the colistin concentration reached 16 mg/L. Furthermore, when exposed to relatively high concentrations of colistin (16 and 32 mg/L), *mcr-1*-positive derivatives showed higher survival rates than those of their corresponding *mcr-1*-negative strains, demonstrating that *mcr-1* could enhance the survival rate of *E. coli* at higher colistin concentrations.

After the serial colistin challenge, the highest MICs of colistin for *mcr-1*-positive *E. coli* derivatives reached 32 mg/L, while those for *mcr-1*-negative derivatives only reached 16 mg/L (**Figure 2A**). Colistin MIC values for all mutants ranged from 2 to 32 mg/L (n = 9), suggesting that it was difficult for *E. coli* to generate HLCR mutants. Compared with their basal MICs, those for the *mcr-1*-negative strains (ATCC 25922/pHSG575, C600, and ZYTF186) increased 4- to 64-fold, while the MIC values for their corresponding *mcr-1*-positive derivatives merely showed 2- to 16-fold increases, suggesting that the presence of *mcr-1* did not facilitate the generation of higher colistin resistance in *E. coli*.

Development of Resistance to Colistin via Serial Passages of *Klebsiella pneumoniae*

Compared with *E. coli*, *K. pneumoniae* strains, with or without *mcr-1*, were more likely to generate HLCR mutations. *K. pneumoniae* strains could survive up to extremely high concentrations of colistin (256–1,024 mg/L) (**Figures 1D–F**). Notably, the contribution of *mcr-1* in improving the survival odds of *K. pneumoniae* was initially remarkable, however, it was weakened at higher concentrations of colistin. For example, compared with those of the parent strains of *K. pneumoniae* (YX6P94K and HZ7H152), more populations of their *mcr-1*-harboringtransformants survived when the concentrations of colistin were lower than 32 mg/L (**Figures 1E,F**). However, the contribution of *mcr-1* gradually diminished in the presence of >64 mg/L colistin. Furthermore, the number of P11/pHNSHP45 subsets was initially higher but decreased to fewer than that of the parent strain P11 upon exposure to more than 4 mg/L colistin (**Figure 1D**).

After serial passages, the colistin MIC values for *K. pneumoniae* mutants ranged from 64 to >1,024 mg/L (**Figure 2B**). Particularly, the colistin MICs increased 256- to 4,096-fold for *mcr-1*-negative mutants but only 16- to 256-fold for their respective *mcr-1*-harboring transformants.

Genetic Alterations in *pmrAB* and *phoPQ* in *Escherichia coli*

Although most *E. coli* strains failed to generate HLCR, 36 derivatives that survived at relatively high concentrations of colistin (16–32 mg/L), including 18 *mcr-1*-negative and 18 *mcr-1*-positive derivatives, were selected to determine the presence of mutations in key genes related to colistin resistance (*mgrB*, *pmrAB*, and *phoPQ*). As shown in **Supplementary Table 3**, alterations mainly occurred in *pmrB* (21/36, 58.3%), followed by *phoQ* (15/36, 41.7%), and *pmrA* (9/36, 25.0%), most of which were associated with different amino acid substitutions, except frameshift mutations found in the *pmrB* gene (n = 6). No mutations were observed in *phoP* or *mgrB*.

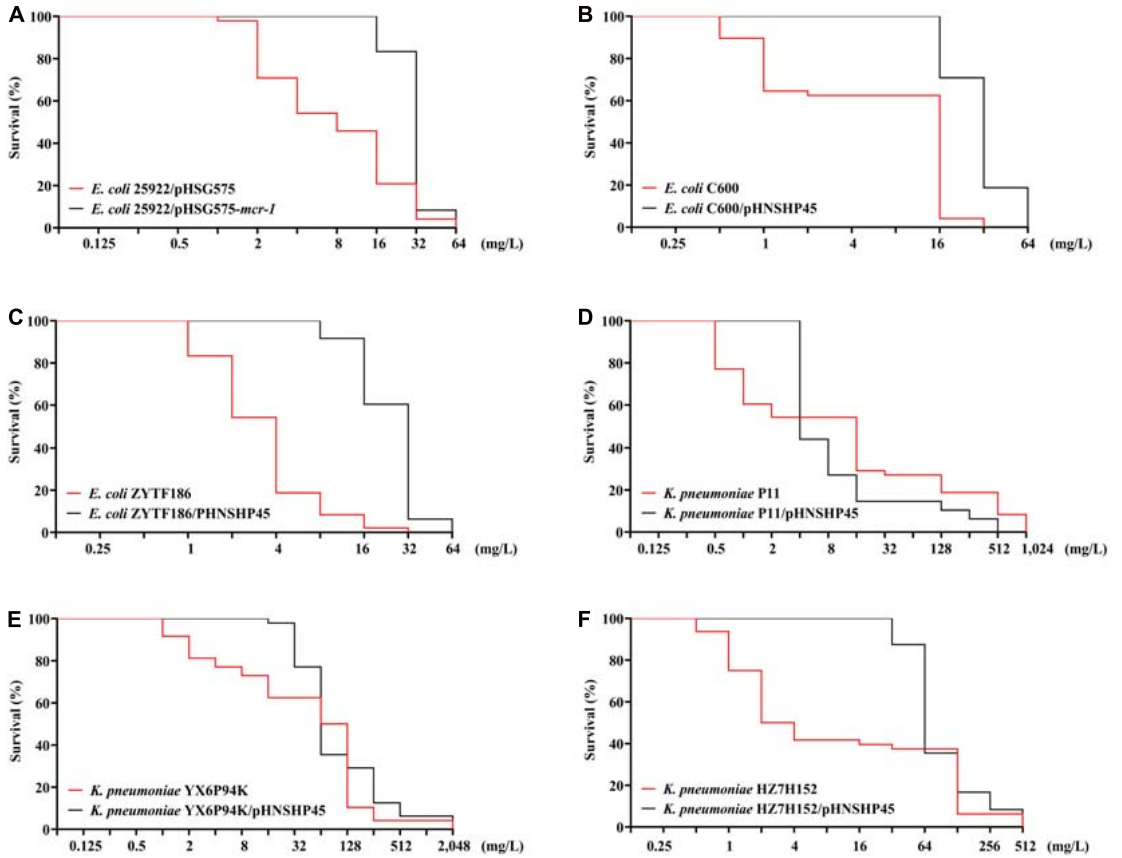

FIGURE 1 | Survival curves of *E. coli* **(A–C)** and *K. pneumoniae* strains **(D–F)** and their *mcr-1*-positive transformants in the presence of increasing concentrations of colistin.

Genetic Alterations in *mgrB*, *pmrAB*, *phoPQ*, and *crrAB* in *Klebsiella pneumoniae*

A total of 156 HLCR *K. pneumoniae* mutants, including 75 *mcr-1*-negative and 81 *mcr-1*-positive derivatives, were examined for the presence of mutations in the *mgrB*, *pmrAB*, *phoPQ*, and *crrAB* genes. The HLCR mutants showed a remarkable multiplicity of mutations in these genes (**Figure 3**, **Table 1**, and **Supplementary Table 4**). Among these mutants, genetic changes predominately occurred in *crrB* (62/156, 39.7%), followed by *phoQ* (41/156, 26.3%), *crrA* (35/156, 22.4%), *pmrB* (28/156, 17.9%), *mgrB* (27/156, 17.3%), and *phoP* (23/156, 14.7%). In 55 mutants, mutations were occurred in two or three genes (**Table 1**). No mutations were observed in *pmrA*.

There were evident differences in mutations between the *mcr-1*-negative and *mcr-1*-positive isolates (**Figure 3A**, **Table 1**, and **Supplementary Table 4**). *phoQ* and *mgrB* alterations were more frequent in the *mcr-1*-negative derivatives (41.3 and 32.0%, respectively) than in the *mcr-1*-positive derivatives (12.3 and 3.7%, respectively). By contrast, the *mcr-1*-positive derivatives predominantly harbored mutations in *crrA* (26/81, 32.1%) and *pmrB* (19/81, 23.5%), both of which only occurred in 12.0% (9/75) of the *mcr-1*-negative derivatives. Moreover, of the 55 mutants with genetic change(s) in two or three genes, 34 (34/75, 45.3%) were *mcr-1*-negative derivatives and 21 (21/81, 25.9%) were *mcr-1*-positive derivatives (**Table 1**).

Regarding mutational patterns, alterations were mainly associated with amino acid substitutions or frameshift mutations (**Table 1** and **Supplementary Table 4**), except for insertion sequences (ISs), which were almost exclusively associated with *mgrB* (**Table 1** and **Supplementary Table 4**). Among 27 derivatives with alterations in *mgrB*, 18 (66.7%) were characterized by insertional inactivation of *mgrB*, which was truncated by one of the ISs, namely IS*Kpn26* (n = 3), IS*903B* (n = 6), IS*Kpn14* (n = 3), IS*Ecp1* (n = 3), or IS*1R* (n = 3) (**Supplementary Figure 2**). Additionally, *crrB* was first observed to be truncated by IS*1R* in three derivatives (**Supplementary Figure 2**).

Impacts of Mutations on the Growth of HLCR *Klebsiella pneumoniae* Strains

To determine whether the genetic changes in *mgrB*, *pmrAB*, *phoPQ*, and *crrAB* could impose a fitness cost on *K. pneumoniae* strains, we determined the growth rates of HLCR mutants harboring different mutations. In the *mcr-1*-negative groups, most of the HLCR mutants showed subtle advantages in the

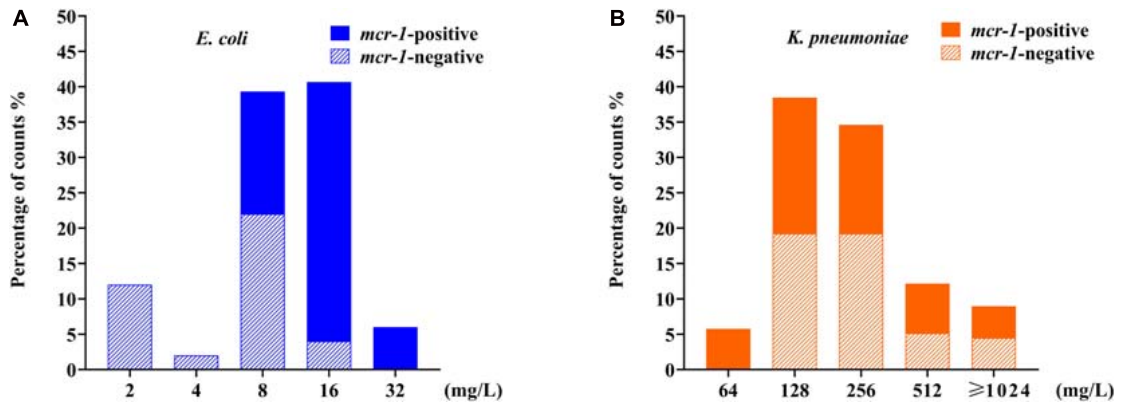

FIGURE 2 | Distributions of colistin minimum inhibitory concentration (MIC) values among *E. coli* and *K. pneumoniae* mutants after induction of colistin resistance *in vitro*. **(A)** Data for 90 *mcr-1*-positive and 60 *mcr-1*-negative *E. coli* derivatives. **(B)** Data for 81 *mcr-1*-positive and 75 *mcr-1*-negative *K. pneumoniae* derivatives. *E. coli* data are indicated in blue, and *K. pneumoniae* data are indicated in orange.

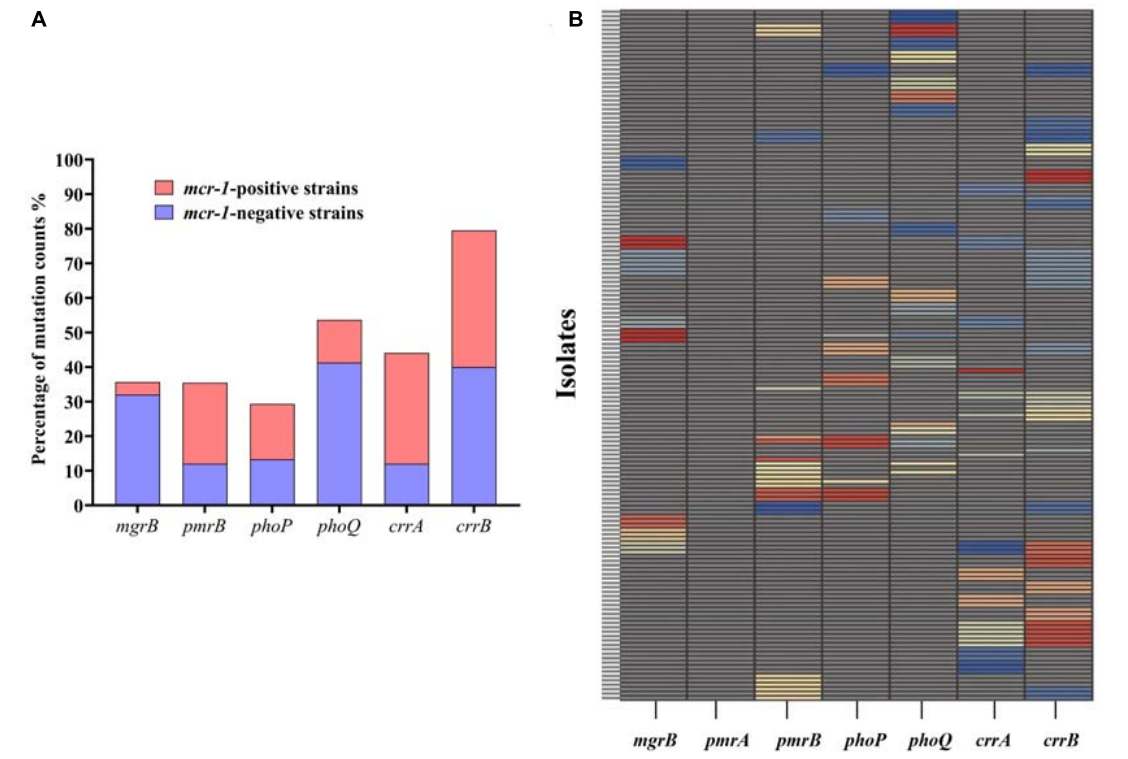

FIGURE 3 | Occurrence of genetic alterations in *mgrB*, *pmrAB*, *phoPQ*, and *crrAB* in *K. pneumoniae*. **(A)** Distribution of mutations in different genes in 81 *mcr-1*-positive and 75 *mcr-1*-negative *K. pneumoniae* derivatives. **(B)** Profiles of genetic alterations in key genes related to colistin resistance, with 53 unique combinations in the 156 colistin-resistant *K. pneumoniae* derivatives. Each unique mutation in each colistin resistance gene is represented by a different color. Specific information on the mutations can be found in **Supplementary Table 4**.

growth rates compared with those of their wild-type parent strains (**Figure 4A**), except for one mutant (*phoQ* V38G), which exhibited a substantial reduction in the growth rate ($p < 0.01$), and three isolates (13.6%) with different mutations, which showed significant advantages in the growth rates ($p < 0.05$). Conversely, among the *mcr-1*-positive HLCR mutants, none exhibited remarkable growth advantages, and most mutants showed slow growth rates compared to their corresponding parent strains (**Figure 4B**). Additionally, 13 individual mutants (59.1%) exhibited significant biological costs for growth ($n = 1$, $p < 0.05$; $n = 9$, $p < 0.01$; $n = 3$, $p < 0.001$). Overall, most chromosomal mutations alone resulted in no burden on growth of HLCR mutants; however, the fitness cost was observed in most *mcr-1*-harboring HLCR mutants.

TABLE 1 | Number of *K. pneumoniae* derivatives with genomic mutation(s) in colistin resistance genes after stepwise induction.

Genome alterations on single gene	Genetic alterations	No. of strains	No. of *mcr-1*-negative strains	No. of *mcr-1*-positive strains
mgrB	Insertional inactivation by ISs	9	6	3
	FMs	2	2	0
pmrB	FMs	5	0	5
	Amino acid substitutions	3	0	3
phoP	Amino acid substitutions	3	0	3
	FMs	3	0	3
phoQ	Amino acid substitutions	33	27	6
crrA	Amino acid substitutions	9	0	9
	FMs	8	0	8
crrB	Amino acid substitutions	21	6	15
	Amino acid substitution, FM	1	0	1
	FM	1	0	1
	Insertional inactivation by ISs, amino acid substitutions	3	0	3
Total strains with mutations in single gene		64.7% (101)	54.7% (41/75)	74.1% (60/81)
Genome alterations on two or three genes	*pmrB* and *phoQ* amino acid substitutions	5	3	2
	phoP and *crrB* amino acid substitutions	9	9	0
	pmrB and *crrB* amino acid substitutions	3	3	0
	mgrB FMs, *crrA* amino acid substitutions	6	6	0
	mgrB FMs, *crrB* amino acid substitutions	6	6	0
	mgrB FM, *phoPQ* amino acid substitution	1	1	0
	crrA FMs, *crrB* amino acid substitutions	3	0	3
	pmrB amino acid substitution and FM, *phoP* amino acid substitution	1	0	1
	pmrB and *phoPQ* amino acid substitution	1	0	1
	phoPQ amino acid substitution	1	0	1
	pmrB amino acid substitution, *phoP* FM	1	0	1
	pmrB and *phoP* amino acid substitutions	3	0	3
	pmrB FMs, *crrB* amino acid substitutions	6	3	3
	mgrB insertional inactivation by ISs, *crrAB* amino acid substitutions	3	3	0
	crrA amino acid substitutions, *crrB* FMs	6	0	6
Total strains associate with mutations in two or more genes		35.3% (55/156)	45.3% (34/75)	25.9% (21/81)

IS, insertion sequence; FM, frameshift mutation.

DISCUSSION

Although the presence of *mcr-1* confers low-level resistance to colistin, there is a concern regarding whether the presence of *mcr-1* can accelerate the development of HLCR. In this study, we found that *mcr-1* did not potentiate the development of HLCR in *E. coli* and *K. pneumoniae,* as the colistin MICs for *mcr-1*-negative derivatives obtained *via* serial colistin challenges were similar to those of their corresponding *mcr-1*-harboring transformants. Moreover, the fold increases in the colistin MICs were higher for *mcr-1*-negative strains than those for their *mcr-1*-harboring transformants. Although the presence of *mcr-1* could not facilitate the evolution of colistin resistance in these two species of bacteria, *mcr-1* could improve their survival rates upon exposure to relatively high concentrations of colistin (16–32 mg/L), which indicated that the presence of *mcr-1* might enhance the survival ability of bacteria under clinical colistin pressure, thereby potentially leading to treatment failure.

Previous reports have shown that the mechanisms of resistance to colistin significantly vary between clinical *K. pneumoniae* and *E. coli* isolates. In *K. pneumoniae*, colistin resistance, including HLCR, is usually caused by chromosomal mutations (Cannatelli et al., 2014; Jayol et al., 2017), whereas in *E. coli*, colistin resistance is mainly associated with the presence of *mcr-1* (Huang et al., 2017). Herein, we demonstrated that compared with *E. coli*, *K. pneumoniae* strains were more likely to develop HLCR by genetic alterations of the two-component systems (TCSs, e.g., PmrAB and PhoPQ) and their regulators (MgrB and CrrAB) when exposed to increasing concentrations of colistin *in vitro*. Previous studies have demonstrated that the TCSs play crucial roles in regulating the expression of genes for lipid A modifications in both *K. pneumoniae* and *E. coli* strains (Poirel et al., 2017; Srinivas and Rivard, 2017). This result partly explains the clinical phenomenon of HLCR being more common in *K. pneumoniae* compared to *E. coli* isolates. However, the mechanism underlying why TCSs and their regulators in

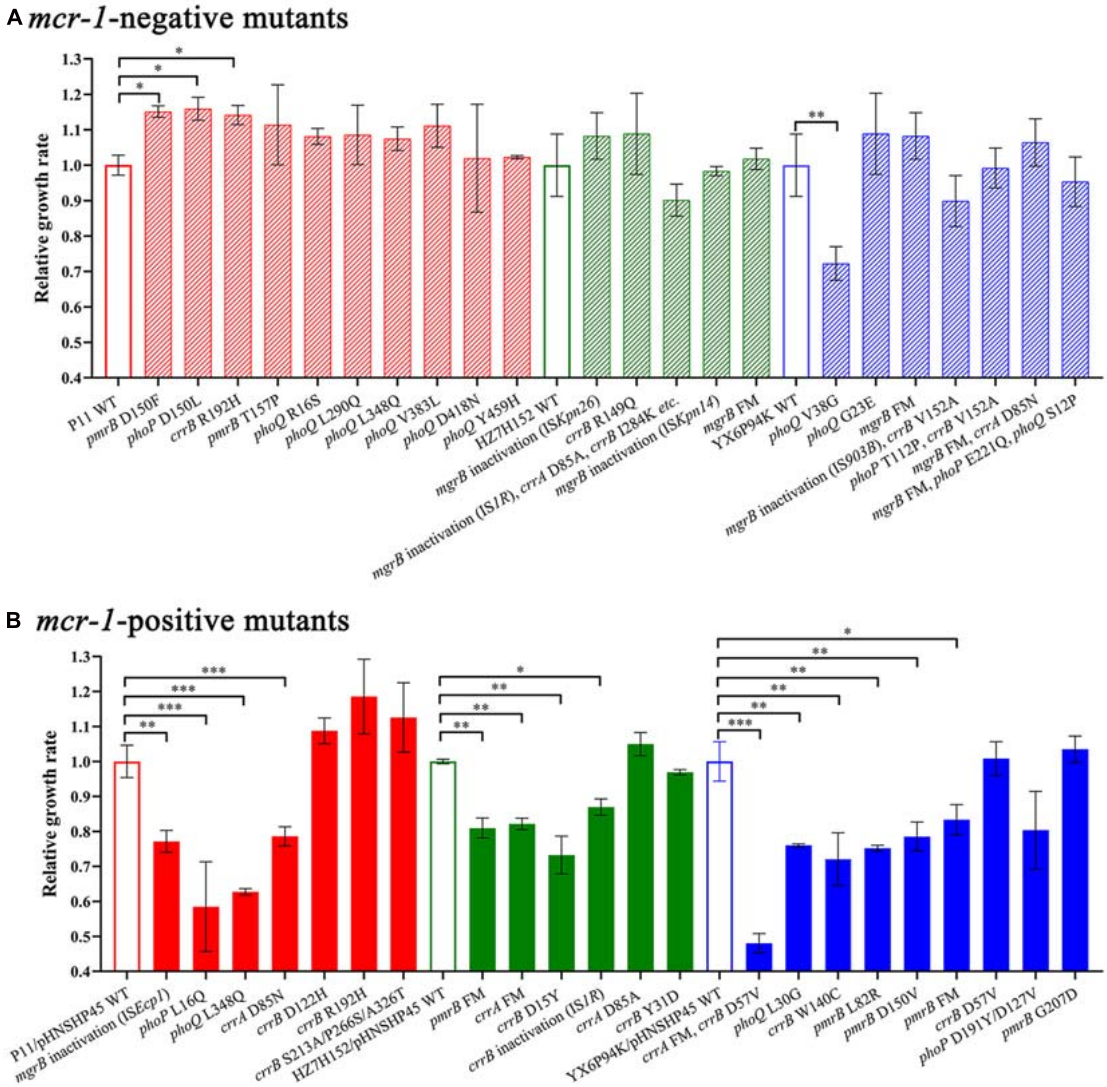

FIGURE 4 | Relative growth rates of *mcr-1*-negative **(A)** and *mcr-1*-positive **(B)** *K. pneumoniae* mutants and their parental strains. The maximal growth rates are presented as relative values compared with the wild-type growth rate (set to 1.0). The relevant mutated genes of each strain are indicated below the chart. $^{*}p < 0.05$; $^{**}p < 0.01$; $^{***}p < 0.001$. Error bars represent standard deviation values. WT, wild-type; FM, frameshift mutation.

K. pneumoniae are more likely to occur genetic alteration under the selective pressure of colistin than those in *E. coli* is unclear and needs further study.

After colistin exposure, alterations were detected in genes (*mgrB*, *pmrAB*, *phoPQ*, and *crrAB*) associated with colistin resistance. In *E. coli*, alterations mainly occurred in *pmrB*, followed by *phoQ*, and no mutations were observed in the *mgrB* or *phoP* gene. However, in HLCR *K. pneumoniae* variants, mutations were more complex and diverse and occurred in all the indicated genes, except *pmrA*. Genetic changes mainly occurred in *crrB* and *phoQ* (**Figure 3A**), in contrast to a previous report which stated that alterations in *mgrB* played a primary role in colistin resistance in *K. pneumoniae* (Cannatelli et al., 2014). However, consistent with previous reports (Kim et al., 2019; Yang et al., 2020), in both *E. coli* and *K. pneumoniae,* the histidine kinase genes *crrB*, *pmrB*, and *phoQ* seemed to be more common sites for mutations compared to the response regulatory genes *crrA*, *pmrA*, and *phoP*. It is possible that the sensor kinases can directly sense environmental stimuli and are therefore more likely to undergo mutations to confer protection against adverse stimuli, such as colistin pressure (Huang et al., 2020). The detected *mgrB*-disrupting ISs, IS*Kpn26*, IS*903B*, IS*Kpn14*, IS*Ecp1*, and IS*1R*, were similar to those found in other studies (Shamina et al., 2020; Yang et al., 2020). Although recent studies have shown that amino acid substitution mutations in *crrB* or IS disruptions are responsible for HLCR (Wright et al., 2015; Jayol et al., 2017; McConville et al., 2020), mutations in *crrAB* in clinical isolates have rarely been reported, possibly due to few tests performed for this newly identified two-component system and the deletion of *crrAB* in some *K. pneumoniae* strains (Wright et al., 2015).

Moreover, most of the mutations observed in this study have not been previously reported; thus, further studies are warranted to elucidate the potential contributions of these novel mutations to colistin resistance.

Remarkably, there were differences in the occurrence of chromosomal mutations in *mcr-1*-positive and *mcr-1*-negative *K. pneumoniae* isolates. In most (74.1%) *mcr-1*-positive derivatives, genetic alteration(s) only occurred in single gene involved in colistin resistance, while half of the *mcr-1*-negative derivatives harbored multiple mutations, thereby implying that the coexistence of chromosomal mutations and *mcr-1* might impose a severe fitness burden on *K. pneumoniae*. To test this hypothesis, we compared the growth rates of *mcr-1*-positive and *mcr-1*-negative strains with those of their relevant HLCR mutants and found that HLCR mutants derived from *mcr-1*-negative strains exhibited almost no fitness cost, while HLCR mutants of *mcr-1*-positive strains showed an evident fitness cost. Previous studies have shown that the fitness cost attributed to chromosomal mutations or the acquisition of wild-type *mcr-1*-harboring plasmids seemed to be insignificant (Cannatelli et al., 2015; Wu et al., 2018); however, increased expression of *mcr-1* could impose a significant fitness burden on host bacteria (Yang et al., 2017; Liu et al., 2020). Our results demonstrated that the coexistence of chromosomal mutations and *mcr-1* was disadvantageous for *K. pneumoniae*, which might partly explain the lack of clinical strains with both chromosomal mutations and *mcr-1* (Nang et al., 2018).

In conclusion, we demonstrated that compared with *E. coli*, *K. pneumoniae* was more likely to develop HLCR by acquiring chromosomal mutations. Although *mcr-1* could not facilitate the selection of HLCR mutants, it could improve the survival rates of bacteria at relatively high concentrations of colistin, which might result in treatment failure.

DATA AVAILABILITY STATEMENT

The whole genome sequencing data of *K. pneumoniae* P11, HZ7H152, *Klebsiella variicola* YX6P94K (subtype of *K. pneumoniae*) and *E. coli* ZYTF186 have been deposited at GenBank with accession numbers JAFKAD000000000, JAFKAE000000000, JAFKAG000000000, and JAFKAF000000000, respectively.

AUTHOR CONTRIBUTIONS

J-HL designed the study. X-QZ, RW, and HX performed the experiments and collected the data. X-QZ, Y-YL, RW, and HX analyzed and interpreted the data. X-QZ and Y-YL wrote the draft of the manuscript. J-HL, Y-YL, X-QZ, JS, JL, and YF edited and revised the manuscript. All authors have read and approved the manuscript. J-HL coordinated the whole project.

FUNDING

This work was supported in part by the National Natural Science Foundation of China (No. 31830099 and 31625026), the Guangdong Local Innovation Team Program (No. 2019BT02N054), the 111 Project (No. D20008), and the Innovation Team Project of Guangdong University (No. 2019KCXTD001).

SUPPLEMENTARY MATERIAL

The Supplementary Material for this article can be found online at: https://www.frontiersin.org/articles/10.3389/fmicb.2021.666782/full#supplementary-material

REFERENCES

Cannatelli, A., Giani, T., D'Andrea, M. M., Di Pilato, V., Arena, F., Conte, V., et al. (2014). MgrB inactivation is a common mechanism of colistin resistance in *KPC*-producing *Klebsiella pneumoniae* of clinical origin. *Antimicrob. Agents Chemother.* 58, 5696–5703. doi: 10.1128/aac.03110-14

Cannatelli, A., Santos-Lopez, A., Giani, T., Gonzalez-Zorn, B., and Rossolini, G. M. (2015). Polymyxin resistance caused by *mgrB* inactivation is not associated with significant biological cost in *Klebsiella pneumoniae*. *Antimicrob. Agents Chemother.* 59, 2898–2900. doi: 10.1128/aac.04998-14

Eiamphungporn, W., Yainoy, S., Jumderm, C., Tan-Arsuwongkul, R., Tiengrim, S., and Thamlikitkul, V. (2018). Prevalence of the colistin resistance gene *mcr-1* in colistin-resistant *Escherichia coli* and *Klebsiella pneumoniae* isolated from humans in Thailand. *J. Glob. Antimicrob. Resist.* 15, 32–35. doi: 10.1016/j.jgar.2018.06.007

Huang, J., Li, C., Song, J., Velkov, T., Wang, L., Zhu, Y., et al. (2020). Regulating polymyxin resistance in Gram-negative bacteria: roles of two-component systems PhoPQ and PmrAB. *Future Microbiol.* 15, 445–459. doi: 10.2217/fmb-2019-0322

Huang, X., Yu, L., Chen, X., Zhi, C., Yao, X., Liu, Y., et al. (2017). High prevalence of colistin resistance and *mcr-1*gene in *Escherichia coli* isolated from food animals in China. *Front. Microbiol.* 8:562. doi: 10.3389/fmicb.2017.00562

Huang, Y. H., Chou, S.-H., Liang, S.-W., Ni, C.-E., Lin, Y.-T., Huang, Y. W., et al. (2018). Emergence of an XDR and carbapenemase-producing hypervirulent *Klebsiella pneumoniae* strain in Taiwan. *J. Antimicrob. Chemother.* 73, 2039–2046. doi: 10.1093/jac/dky164

Jacoby, G. A., Strahilevitz, J., and Hooper, D. C. (2014). Plasmid-mediated quinolone resistance. *Microbiol. Spectr.* 2:10.

Jayol, A., Nordmann, P., Brink, A., Villegas, M. V., Dubois, V., and Poirel, L. (2017). High-level resistance to colistin mediated by various mutations in the *crrB* gene among carbapenemase-producing *Klebsiella pneumoniae*. *Antimicrob. Agents Chemother.* 61:e01423-17.

Jeong, J. Y., Kim, E. S., Choi, S. H., Kwon, H. H., Lee, S. R., Lee, S. O., et al. (2008). Effects of a plasmid-encoded *qnr*A1 determinant in *Escherichia coli* strains carrying chromosomal mutations in the *acrAB* efflux pump genes. *Diagn. Microbiol. Infect. Dis.* 60, 105–107. doi: 10.1016/j.diagmicrobio.2007.07.015

Kim, S., Woo, J. H., Kim, N., Kim, M. H., Kim, S. Y., Son, J. H., et al. (2019). Characterization of chromosome-mediated colistin resistance in *Escherichia coli* isolates from livestock in Korea. *Infect. Drug Resist.* 12, 3291–3299. doi: 10.2147/idr.s225383

Liu, Y. Y., Wang, Y., Walsh, T. R., Yi, L. X., Zhang, R., Spencer, J., et al. (2016). Emergence of plasmid-mediated colistin resistance mechanism MCR-1 in animals and human beings in China: a microbiological and molecular biological study. *Lancet Infect. Dis.* 16, 161–168. doi: 10.1016/s1473-3099(15)00424-7

Liu, Y. Y., Zhu, Y., Wickremasinghe, H., Bergen, P. J., Lu, J., Zhu, X. Q., et al. (2020). Metabolic perturbations caused by the over-expression of *mcr-1* in *Escherichia coli*. *Front. Microbiol.* 11:588658. doi: 10.3389/fmicb.2020.588658

Luo, Q., Niu, T., Wang, Y., Yin, J., Wan, F., Yao, M., et al. (2019). In vitro reduction of colistin susceptibility and comparative genomics reveals multiple differences between MCR-positive and MCR-negative colistin-resistant *Escherichia coli*. *Infect. Drug Resist.* 12, 1665–1674. doi: 10.2147/idr.s210245

Matuschek, E., Åhman, J., Webster, C., and Kahlmeter, G. (2018). Antimicrobial susceptibility testing of colistin - evaluation of seven commercial MIC products against standard broth microdilution for *Escherichia coli*, *Klebsiella pneumoniae*, *Pseudomonas aeruginosa*, and *Acinetobacter spp*. *Clin. Microbiol. Infect.* 24, 865–870. doi: 10.1016/j.cmi.2017.11.020

McConville, T. H., Annavajhala, M. K., Giddins, M. J., Macesic, N., Herrera, C. M., Rozenberg, F. D., et al. (2020). CrrB positively regulates high-level polymyxin resistance and virulence in *Klebsiella pneumoniae*. *Cell Rep.* 33:108313. doi: 10.1016/j.celrep.2020.108313

Nang, S. C., Morris, F. C., Mcdonald, M. J., Han, M. L., Wang, J., Strugnell, R. A., et al. (2018). Fitness cost of *mcr-1*-mediated polymyxin resistance in *Klebsiella pneumoniae*. *J. Antimicrob. Chemother.* 73, 1604–1610. doi: 10.1093/jac/dky061

Poirel, L., Jayol, A., and Nordmann, P. (2017). Polymyxins: antibacterial activity, susceptibility testing, and resistance mechanisms encoded by plasmids or chromosomes. *Clin. Microbiol. Rev.* 30, 557–596. doi: 10.1128/cmr.00064-16

Quan, J., Li, X., Chen, Y., Jiang, Y., Zhou, Z., Zhang, H., et al. (2017). Prevalence of *mcr-1* in *Escherichia coli* and *Klebsiella pneumoniae* recovered from bloodstream infections in China: a multicentre longitudinal study. *Lancet Infect. Dis.* 17, 400–410. doi: 10.1016/s1473-3099(16)30528-x

Ruhnke, M., Arnold, R., and Gastmeier, P. (2014). Infection control issues in patients with haematological malignancies in the era of multidrug-resistant bacteria. *Lancet Oncol.* 15:e0606-19.

San Millan, A., Escudero, J. A., Gifford, D. R., Mazel, D., and Maclean, R. A. (2016). Multicopy plasmids potentiate the evolution of antibiotic resistance in bacteria. *Nat. Ecol. Evol.* 1:10.

Shamina, O. V., Kryzhanovskaya, O. A., Lazareva, A. V., Alyabieva, N. M., Polikarpova, S. V., Karaseva, O. V., et al. (2020). Emergence of a ST307 clone carrying a novel insertion element MITE *Kpn1* in the *mgrB* gene among carbapenem-resistant *Klebsiella pneumoniae* from Moscow, Russia. *Int. J. Antimicrob. Agents* 55:105850. doi: 10.1016/j.ijantimicag.2019.11.007

Shi, X., Li, Y., Yang, Y., Shen, Z., Wu, Y., and Wang, S. (2020). Global impact of mcr-1-positive *Enterobacteriaceae* bacteria on "one health". *Crit. Rev. Microbiol.* 46, 565–577. doi: 10.1080/1040841x.2020.1812510

Srinivas, P., and Rivard, K. (2017). Polymyxin resistance in gram-negative pathogens. *Curr. Infect. Dis. Rep.* 19:38.

Takeshita, S., Sato, M., Toba, M., Masahashi, W., and Hashimoto-Gotoh, T. (1987). High-copy-number and low-copy-number plasmid vectors for *lacZ* alpha-complementation and chloramphenicol- or kanamycin-resistance selection. *Gene* 61, 63–74. doi: 10.1016/0378-1119(87)90365-9

Wang, C., Feng, Y. A.-O., Liu, L., Wei, L., Kang, M., and Zong, Z. A.-O. X. (2020). Identification of novel mobile colistin resistance gene *mcr-10*. *Emerg. Microb. Infect.* 9, 508–516. doi: 10.1080/22221751.2020.1732231

Wright, M. S., Suzuki, Y., Jones, M. B., Marshall, S. H., Rudin, S. D., Van Duin, D., et al. (2015). Genomic and transcriptomic analyses of colistin-resistant clinical isolates of *Klebsiella pneumoniae* reveal multiple pathways of resistance. *Antimicrob. Agents Chemother.* 59, 536–543. doi: 10.1128/aac.04037-14

Wu, R., Yi, L. X., Yu, L. F., Wang, J., Liu, Y., Chen, X., et al. (2018). Fitness Advantage of *mcr-1*-bearing IncI2 and IncX4 plasmids in vitro. *Front. Microbiol.* 9:331. doi: 10.3389/fmicb.2018.00331

Yang, Q., Li, M., Spiller, O. B., Andrey, D. A.-O., Hinchliffe, P., Li, H., et al. (2017). Balancing *mcr-1* expression and bacterial survival is a delicate equilibrium between essential cellular defence mechanisms. *Nat. Commun.* 8:2054.

Yang, T. Y., Wang, S. F., Lin, J. E., Griffith, B. T. S., Lian, S. H., Hong, Z. D., et al. (2020). Contributions of insertion sequences conferring colistin resistance in *Klebsiella pneumoniae*. *Int. J. Antimicrob. Agents* 55:105894. doi: 10.1016/j.ijantimicag.2020.105894

Zhang, H., Zhao, D., Quan, J., Hua, X., and Yu, Y. (2019). *mcr-1* facilitated selection of high-level colistin-resistant mutants in *Escherichia coli*. *Clin. Microbiol. Infect.* 25:517.e1-e4.

Zwietering, M. H., Jongenburger, I., Rombouts, F. M., and Van 'T Riet, K. (1990). Modeling of the bacterial growth curve. *Appl. Environ. Microbiol.* 56, 1875–1881.

Conflict of Interest: The authors declare that the research was conducted in the absence of any commercial or financial relationships that could be construed as a potential conflict of interest.

frontiers in Microbiology

ORIGINAL RESEARCH
published: 02 July 2021
doi: 10.3389/fmicb.2021.674502

Acquisition of Tigecycline Resistance by Carbapenem-Resistant *Klebsiella pneumoniae* Confers Collateral Hypersensitivity to Aminoglycosides

Hua-le Chen[1,2†], Yan Jiang[3†], Mei-mei Li[3], Yao Sun[1], Jian-ming Cao[4], Cui Zhou[1], Xiao-xiao Zhang[1], Yue Qu[5] and Tie-li Zhou[1]**

[1] Department of Clinical Laboratory, The First Affiliated Hospital of Wenzhou Medical University, Wenzhou, China, [2] Department of Laboratory Medicine, The Second Affiliated Hospital of Wenzhou Medical University, Wenzhou, China, [3] Department of Infectious Diseases, Sir Run Run Shaw Hospital, Zhejiang University School of Medicine, Hangzhou, China, [4] School of Laboratory Medicine and Life Science, Wenzhou Medical University, Wenzhou, China, [5] Biomedicine Discovery Institute, Department of Microbiology, Faculty of Medicine, Nursing and Health Sciences, Monash University, Clayton, VIC, Australia

OPEN ACCESS

Edited by:
Shaolin Wang,
China Agricultural University, China

Reviewed by:
Hua Zhou,
Zhejiang University, China
Mehmet Demirci,
Kırklareli University, Turkey

***Correspondence:**
Tie-li Zhou
wyztli@163.com
Yue Qu
yue.qu@monash.edu

[†] These authors have contributed equally to this work

Specialty section:
This article was submitted to Antimicrobials, Resistance and Chemotherapy, a section of the journal Frontiers in Microbiology

Received: 01 March 2021
Accepted: 10 June 2021
Published: 02 July 2021

Citation:
Chen H-l, Jiang Y, Li M-m, Sun Y, Cao J-m, Zhou C, Zhang X-x, Qu Y and Zhou T-l (2021) Acquisition of Tigecycline Resistance by Carbapenem-Resistant Klebsiella pneumoniae Confers Collateral Hypersensitivity to Aminoglycosides. Front. Microbiol. 12:674502. doi: 10.3389/fmicb.2021.674502

Tigecycline is a last-resort antibiotic for infections caused by carbapenem-resistant *Klebsiella pneumoniae* (CRKP). This study aimed to broaden our understanding of the acquisition of collateral hypersensitivity by CRKP, as an evolutionary trade-off of developing resistance to tigecycline. Experimental induction of tigecycline resistance was conducted with tigecycline-sensitive CRKP clinical isolates. Antimicrobial susceptibility testing, microbial fitness assessment, genotypic analysis and full-genome sequencing were carried out for these clinical isolates and their resistance-induced descendants. We found that tigecycline resistance was successfully induced after exposing CRKP clinical isolates to tigecycline at gradually increased concentrations, at a minor fitness cost of bacterial cells. Quantitative reverse transcription-polymerase chain reaction (RT-PCR) found higher expression of the efflux pump gene *acrB* (5.3–64.5-fold) and its regulatory gene *ramA* (7.4–65.8-fold) in resistance-induced strains compared to that in the tigecycline-sensitive clinical isolates. Stable hypersensitivities to aminoglycosides and other antibiotics were noticed in resistance-induced strains, showing significantly lowered MICs (X 4 – >500 times). Full genome sequencing and plasmid analysis suggested the induced collateral hypersensitivity might be multifaceted, with the loss of an antimicrobial resistance (AMR) plasmid being a possible major player. This study rationalized the sequential combination of tigecycline with aminoglycosides for the treatment of CRKP infections.

Keywords: collateral sensitivity, CRKP, aminoglycosides, tigecycline, antimicrobial resistance

INTRODUCTION

Carbapenem-resistant *Klebsiella pneumoniae* (CRKP) has emerged as one of the deadliest causes of hospital-acquired infections and poses a serious therapeutic concern (Petrosillo et al., 2013). Overproduction of various carbapenemases in CRKP, such as *Klebsiella pneumoniae* carbapenemase (KPC) and metallo-β-lactamases (MBLs), renders the bacteria resistant to nearly

all β-lactam antibiotics including carbapenems (Petrosillo et al., 2013).

Tigecycline and colistin are the very few options in the antibiotic arsenal for infections caused by carbapenem-resistant Enterobacteriaceae (Stein and Babinchak, 2013; Sun et al., 2013). Resistance to tigecycline of *Klebsiella* or other Enterobacteriaceae has emerged after its wide use in clinical settings, either as a monotherapy or in combination with other antibiotics (Woodford et al., 2007; Poulakou et al., 2009; Hirsch and Tam, 2010; Sekowska and Gospodarek, 2010; Stein and Babinchak, 2013; Sun et al., 2013; Gonzalez-Padilla et al., 2015). Underlying molecular mechanisms of tigecycline resistance are complex, with the upregulation of resistance-nodulation-division (RND) efflux pumps being a major contributor. Efflux pump systems related to tigecycline resistance include AcrAB-TolC and its positive regulators, *ramA*, SoxS, MarA or its negative regulator r*amR* (Hentschke et al., 2010; Roy et al., 2013; Villa et al., 2014; He et al., 2015; Juan et al., 2016; Xu et al., 2016), OqxAB and its positive regulator *rarA* and negative regulator *oqxR* (Zhong et al., 2014; Juan et al., 2016), and KpgABC (Nielsen et al., 2014; Juan et al., 2016). Structural alteration of the 30S ribosomal subunit protein S10 is another important resistance mechanism, mediated by mutations in the *rpsJ* gene and consequential target site modifications (Villa et al., 2014). A unique enzymatic inactivation mechanism mediated by Tet(X3) and Tet(X4), has also been associated with tigecycline resistance of numerous carbapenems-resistant Enterobacteriaceae (He et al., 2019; Sun et al., 2019).

Development of collateral sensitivity is a widespread evolutionary trade-off that occurs in many Gram-negative and Gram-positive bacteria (Barbosa et al., 2017; Lozano-Huntelman et al., 2020). Only a limited number of studies have examined collateral sensitivity in *Klebsiella pneumoniae*. Du et al. (2018) found that *K. pneumoniae* synchronously regained susceptibility to imipenem and meropenem when the patient developed resistance to tigecycline after long-term antibiotic treatment (Du et al., 2018). Villa et al. (2013) reported a reversion to susceptibility to carbapenems of a CRKP clinical isolate under the pressure of tigecycline (Villa et al., 2013). Proposed mechanisms mediating collateral sensitivity include plasticity of mobile elements in the host bacterium (Stohr et al., 2020), change of global gene expression associated with mutations in resistance genes (Maltas and Wood, 2019), amino acid deletions/substitutions that might result in reduced antibiotic hydrolase activity (Frohlich et al., 2019), and resistance mutations in regulatory genes for efflux pumps (Villa et al., 2013; Barbosa et al., 2017). Membrane-potential-altering mutations may also contribute to reversion of bacterial susceptibility to several unrelated classes of antibiotics, by changing the proton-motive force (PMF) and diminishing the activity of PMF-dependent major efflux pumps (Pal et al., 2015; Furusawa et al., 2018).

Recent emergence of CRKP clinical isolates that are resistant to both tigecycline and colistin, and discovery of a plasmid-mediated colistin resistance gene *mcr-1* highlight the pressing need of developing more effective antimicrobial strategies for CRKP infections (Zhang et al., 2018). This study aimed to establish a comprehensive understanding of collateral sensitivity that accompany the development of tigecycline resistance in CRKP, and to rationalize the combination antibiotic therapy using tigecycline and aminoglycosides for CRKP infections.

MATERIALS AND METHODS

Bacterial Isolates

Fifty CRKP isolates were from patients visiting the First Affiliated Hospital of Wenzhou Medical University and clinically diagnosed with CRKP infections between December 2013 and 2014. These clinical isolates were identified to a species level using the following tests: the Vitek II Identification System (bioMérieux Vitec Inc., Hazelwood, MO, United States) and MALDI Biotyper Identification System (MALDI-TOF MS, BioMérieux, Craponne, France).

Pulsed-Field Gel Electrophoresis Analysis

Genomic DNA of *K. pneumoniae* clinical isolates was digested with restriction endonuclease *Xba*I (Takara Bio, Dalian, China). DNA fragments were separated in a Pulsed-field gel electrophoresis (PFGE) CHEF-Mapper XA system (Bio-Rad, Hercules, CA, United States) in 0.5 × Tris-borate-EDTA buffer at 14°C and 120 V for 19 h, with pulse times ranging from 5 s to 35 s. PFGE results were analyzed using Quantity One 1-D Analysis 4.6.9 (Bio-Rad, Hercules, CA, United States) Software.

Antimicrobial Susceptibility Test

Antimicrobial susceptibility of 50 CRKP isolates to 15 first-line antibiotics were initially tested with the Vitek II Identification System (bioMérieux Vitec Inc., Hazelwood, MO, United States) and then confirmed by the CLSI recommended broth microdilution or agar dilution methods. The MICs of tigecycline for *K. pneumoniae* clinical isolates and resistance-induced strains were interpreted using breakpoints recommended by the European Committee on Antimicrobial Susceptibility Testing (EUCAST) criteria (susceptible, $\leq$1.0 μg/ml; medium, 1.0–2.0 μg/ml; resistant, $>$2.0 μg/ml) (European Committee on Antimicrobial Susceptibility Testing Steering, 2006). Susceptibility of other antimicrobial agents for *K. pneumoniae* was determined by the agar dilution method according to the Clinical and Laboratory Standards Institute (M100-S24, 2014). *Escherichia coli* ATCC 25922 was used as a quality control.

In vitro Induction of Tigecycline Resistance

Four clinical isolates susceptible to tigecycline (K467, K43, K521, and K428) and one tigecycline-resistant clinical isolate (K537) were used to study tigecycline resistance induction and collateral sensitivity of CRKP. These five clinical isolates were assigned to sequence types by Multilocus sequence typing (MLST), according to the *K. pneumoniae* MLST website.[1] Tigecycline resistance was induced for the tigecycline-susceptible clinical

[1]https://bigsdb.pasteur.fr/klebsiella/klebsiella.html

isolates, by gradually exposing them to tigecycline at serially increasing concentrations at a 24 h interval (1/4 MIC to a higher concentration at which there was no bacterial growth) (Liu et al., 2011).

Examining General Antimicrobial-Resistance Determinants for Tigecycline Resistance

Polymerase chain reaction (PCR) and sequencing were carried out to examine the presence of common antimicrobial-resistant genes in these 5 CRKP clinical isolates and four resistance-induced strains, including ESBLs genes ($bla_{CTX-M-1}$, $bla_{CTX-M-9}$, bla_{TEM}, bla_{SHV}, bla_{VEB} and bla_{PER}), AmpC genes (bla_{CMY}, bla_{FOX}, bla_{MOX}, bla_{DHA}), carbapenemase genes (bla_{KPC}, bla_{SPM}, bla_{IMP}, bla_{VIM}, bla_{GES}, bla_{NDM}, bla_{OXA-23}, bla_{OXA-48}), PMQR genes (*qnrA, qnrB, qnrC, qnrD, qnrS, qepA, aac(6′)-Ib-cr, oqxA, oqxB*), and 16S-RMTase genes (*armA, rmtA, rmtB, rmtC, rmtD, rmtE*). The mutation of chromosomal genes *gyrA* and *parC* was also examined. Primer sequences for PCR assays were adapted from other published studies (Doi and Arakawa, 2007; Dallenne et al., 2010; Park et al., 2012) and are available on request. Nucleotide sequences were compared by BLAST to align drug-resistance gene nucleotide sequences[2].

Outer Membrane Proteins Analysis

A crude outer membrane fraction of CRKP clinical isolates and resistance-induced strains was obtained by growing the bacteria to a mid-log phase, followed by sonication. Outer membrane proteins (OMPs) were separated by sodium dodecyl sulfate polyacrylamide gel electrophoresis (SDS-PAGE). *K. pneumoniae* ATCC 13883 was used as a control for OMP profiling (Shi et al., 2013). The outer membrane protein encoding genes were further amplified using multiple primer pairs among the 4 paired strains (Zhang et al., 2014).

Inhibition of Efflux Pumps With CCCP

Efflux pump inhibitor carbonyl cyanide m-chlorophenylhydrazone (CCCP, 10 mg/l) was used to examine the impact of efflux pumps on tigecycline resistance (Zhong et al., 2014). Minimum inhibitory concentrations of tigecycline for CRKP clinical isolates and resistance-induced strains were determined by the broth microdilution method in the presence or absence of CCCP. Four times or greater reduction of tigecycline MICs in the presence of CCCP was adopted as a significant inhibition effect for efflux pumps (He et al., 2015).

Analysis of *acrR*, *ramR* and *oqxR* Mutations

Efflux pump regulator encoding genes including *acrR*, *ramR* and *oqxR* were amplified by PCR with specific primers (Bialek-Davenet et al., 2011; Lin et al., 2016). The nucleotide sequences of *acrR*, *ramR* and *oqxR* were analyzed using a basic local alignment search tool (BLAST)[3] with *K. pneumoniae* subsp. pneumoniae MGH 78578 as the reference strain (GenBank accession no. CP000647) (Hentschke et al., 2010).

Quantitative Real-Time PCR

The relative expression levels of genes encoding efflux pumps AcrB and OqxB and their regulators *ramA* and *rarA* were evaluated using a 7500 Real-Time PCR (RT-PCR) system and *rpoB* as the housekeeping gene (Stein and Babinchak, 2013; He et al., 2015). All experiments were performed in triplicate. The relative expression of the target genes was analyzed using the comparative Ct method ($2^{-\Delta\Delta Ct}$) with the Agilent MxPro software.

Genome Sequencing and Annotation

Whole-genome shotgun sequencing was carried out for 5 CRKP clinical isolates and 4 resistance-induced strains, using a standard run of Illumina HiSeq2000 sequencing using a generating 2×100 paired-end libraries (500-bp insert size) sequencing strategy according to the manufacturer's instructions. Clean reads were assembled into scaffolds using Velvet version 1.2.07. Post-Assembly Genome Improvement Toolkit (PAGIT) was then used to extend the initial contiguous sequences (contigs) and correct sequencing errors. Open reading frames (ORFs) were identified using Glimmer version 3.0. Protein-coding sequences were further BLAST-searched against the Antimicrobial Resistance Database (ARDB).

Plasmid Analysis

Plasmids of 5 CRKP clinical isolates and 4 resistance-induced strains were analyzed by S1-nuclease pulsed-field gel electrophoresis (S1-PFGE). Plasmid DNA was extracted using a QIAGEN Plasmid Midi Kit (Qiagen, shanghai, China) according to the manufacturer's instructions, and was separated by electrophoresis in 0.8% agarose at 120 V for 1 h. The plasmids of *E. coli* V517 served as a size marker.

Data Analysis and Statistical Methods

One-way ANOVA or a non-parametric test (Mann-Whitney *U* test) was carried out to compare two means, depending on the data distribution. Statistical significance was assumed at p value of less than 0.05. Data analysis was performed using Minitab 16 software (Minitab, State College, PA, United States).

RESULTS

Microbiological Characteristics of CRKP Clinical Isolates

Pulsed-field gel electrophoresis analysis of 50 CRKP clinical isolates showed five clusters, suggesting clonally distinct nature of these isolates (**Figure 1A**). Antimicrobial susceptibility tests showed that all CRKP isolates were resistant to first-line antibiotics except tigecycline and colistin; one isolate was found to be resistant to tigecycline (K537, MIC 8 mg/L, see **Table 1**). One representative strain from each cluster (designated as K537, K521, K467, K428, and K43) was chosen for further

[2]http://blast.ncbi.nlm.nih.gov/Blast.cgi

[3]http://www.ncbi.nlm.nih.gov/BLAST

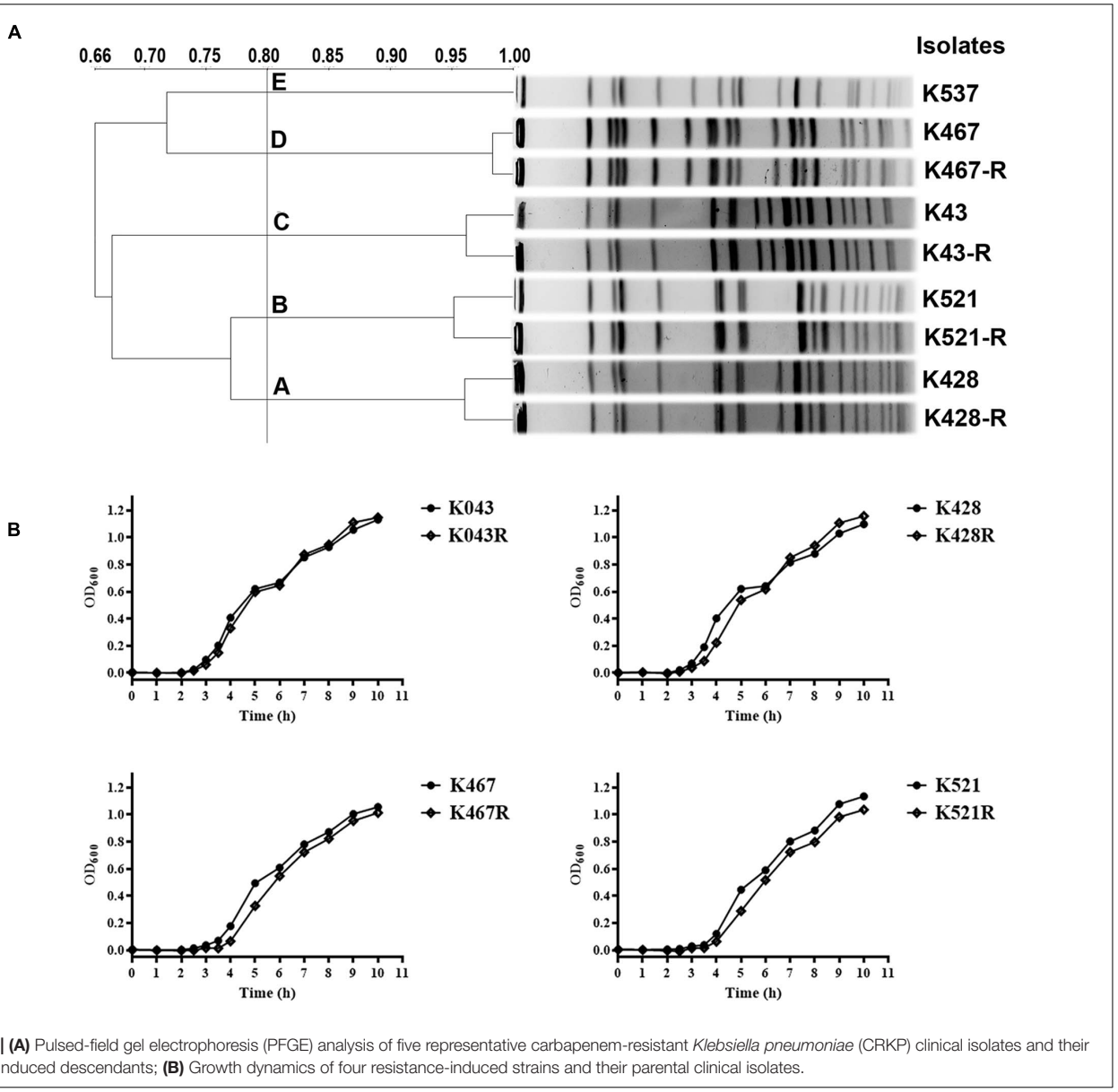

FIGURE 1 | (A) Pulsed-field gel electrophoresis (PFGE) analysis of five representative carbapenem-resistant *Klebsiella pneumoniae* (CRKP) clinical isolates and their resistance-induced descendants; **(B)** Growth dynamics of four resistance-induced strains and their parental clinical isolates.

TABLE 1 | Antimicrobial susceptibility of five CRKP clinical isolates and four resistance-induced descendant strains.

Isolates	Minimum inhibitory concentrations (μg/ml)															
	AMK	CRO	CTX	CAZ	IPM	MEM	ETP	LEV	CIP	TOB	GEN	C	FOS	PB	TGC	TGC + CCCP
K537	>256	>256	>256	>256	64	128	256	16	64	256	>128	>256	>1024	1	8	4
K467	>256	>256	>256	256	128	256	>256	16	64	256	>128	>256	>1024	0.5	0.5	0.5
K467-R	<0.25	128	>256	128	64	128	128	32	64	<0.25	0.5	>256	128	0.5	16	4
K521	>256	>256	>256	>256	128	256	>256	16	64	256	>128	>256	>1024	1	0.5	0.25
K521-R	<0.25	128	256	32	128	128	>256	32	64	<0.25	<0.25	>256	256	1	16	4
K428	>256	>256	>256	>256	32	128	>256	16	64	256	>128	>256	>1024	1	0.5	0.5
K428-R	0.5	32	8	256	0.25	0.25	0.25	16	64	128	8	>256	4	0.5	16	4
K43	>256	>256	>256	64	32	256	256	16	64	128	>128	>256	>1024	1	0.5	0.5
K43-R	<0.25	0.25	2	1	0.25	1	8	0.25	1	0.5	1	>256	16	1	32	8

AMK, amikacin; CRO, ceftriaxone; CTX, cefotaxime; CAZ, ceftazidime; IPM, imipenem; MEM, meropenem; ETP, ertapenem; LEV, levofloxacin; CIP, ciprofloxacin; TOB, tobramycinl; GEN, gentamicin; C, chloramphenicol; FOS, fosfomycin; PB, polymyxin B; TGC + CCCP, tigecycline with CCCP.

studies. MLST found that the tigecycline-resistant clinical isolate K537 and tigecycline-sensitive isolates K521, K467, K428, and K43 belonged to sequence types ST39, ST11, ST11, ST37, and ST3623, respectively.

Experimental Induction of Tigecycline Resistance in CRKP

Four tigecycline-sensitive clinical isolates (K467, K521, K428, and K43) were treated with tigecycline at gradually increased concentrations to induce tigecycline resistance. Significant increases in the MICs of tigecycline (32- – 64- fold) were achieved for the descendant strains in comparison with their parental clinical isolates (**Table 1**). PFGE analysis further confirmed the origin of the resistance-induced CRKP strains (**Figure 1A**). The induced tigecycline-resistance remained stable after sixteen passages of CRKP in an antibiotic-free growth medium. Comparing the growth dynamics of tigecycline-sensitive clinical isolates and their resistance-induced descendant strains showed a minor but universal fitness loss (**Figure 1B**).

Molecular Mechanisms Underpinning Experimental Induction of Tigecycline Resistance

We examined the role of adenosine triphosphate (ATP)-driven efflux pumps in the resistance of CRKP to many antibiotics including tigecycline. Using the efflux pump inhibitor CCCP partially restored the susceptibility of all five tigecycline-resistant strains (**Table 1**). Gene expression of pump- and regulator-encoding genes including *acrB*, *ramA*, *oqxB*, and *rarA* was evaluated (**Figure 2**). All tigecycline-resistant strains showed higher expression of *acrB* (6. 9-, 19. 3-, 15. 6-, 5. 3-, 64.5-fold for K537, K467-R, K521-R, K428-R, and K43-R, respectively) and its regulator gene *ramA* (7. 4-, 12. 2-, 13. 5-, 34. 5-, 65.8-fold, respectively). Over-expression of *oqxB* and *rarA* was seen in K43-R (12.5-fold and 2.5-fold) and K521-R (2.7-fold and 5.9-fold).

We also sequenced genes encoding other important regulators of efflux pumps, including *acrR*, *ramR*, and *oqxR*. No mutation was identified in *acrR* and *ramR*. Mutations in *oqxR* were found; no difference between tigecycline-sensitive clinical isolates and their resistance-induced counterparts indicated no direct link between *oqxR* mutation and experimentally induced tigecycline resistance (**Table 2**). SDS-PAGE was carried out to study the role of three major OMPs (ompK34, ompK35, and ompK36) on tigecycline resistance, that may affect the diffusion of tigecycline to its target sites. Using the porin profile of *K. pneumoniae* ATCC 13883 as a control, OmpK36 was missing on SDS-PAGE and amplification of its encoding gene with PCR was unsuccessful (**Figure 3**), suggesting that a deletion and/or rearrangement of its encoding gene might have occurred in strains with clinical background. Same SDS-PAGE results for tigecycline-sensitive clinical isolates and resistance-induced descendant strains, again suggested no direct association between these OMPs and induced tigecycline resistance.

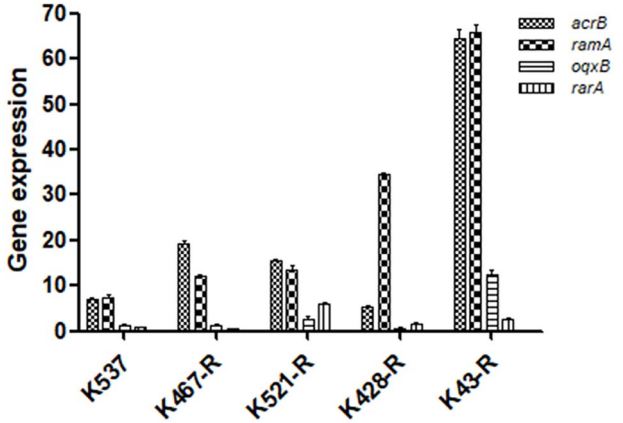

FIGURE 2 | Expression of pump and regulator encoding genes including *acrB*, *ramA*, *oqxB*, and *rarA* in five tigecycline-resistant CRKP strains. The values were expressed as mean ± standard deviation (SD).

Emergence of Collateral Sensitivity in Tigecycline-Resistant CRPK

Interestingly, prolonged exposure of CRKP to tigecycline reversed their resistance to all tested antibiotics except chloramphenicol and tigecycline; significantly lowered MICs of different antibiotics were found for all resistance-induced descendant strains (**Table 1**). The level of acquired hypersensitivity seemed to be antibiotic and strain dependent. Up to 2048-fold decreases in the MIC of cephalosporins and carbapenems were observed when tigecycline-sensitive clinical isolates were converted into tigecycline-resistant descendant strains; up to 64-fold and 512-fold decreases in the MIC were found when fluoroquinolones and fosfomycin were tested, respectively. At least 2 out of 4 tigecycline-sensitive and tigecycline-resistant pairs showed relatively small changes in the MIC of these non-aminoglycoside antibiotics ($\leq$4-fold for cephalosporins and carbapenems, $\leq$2-fold for fluoroquinolones, and $\leq$16-fold for fosfomycin). More significant decreases in the MIC were noticed for aminoglycosides when compared with other antibiotics (**Table 1**). Most resistance-induced strains had MICs of amikacin, tobramycin and gentamicin 250-fold lower than that of their parental clinical isolates. The induced hypersensitivity of CRKP to aminoglycosides and other antibiotics remained stable after regrowth in an antibiotic-free medium for 16 passages.

Evaluating Common Antibiotic Resistance Determinants for Collateral Hypersensitivity of CRKP

Some common antibiotic resistance determinants were examined for 5 CRKP clinical isolates and 4 resistance-induced descendent strains. All isolates harbored the KPC-2 carbapenemase-encoding gene (bla_{KPC-2}) and genes encoding other β-lactamases including SHV (sulf-hydryl variable) and TEM (Temoniera in). Genes encoding CTX-M-type ESBLs were only found in the K467 pairs and K521 pairs. Some other

TABLE 2 | Mutations of *acrR*, *ramR* and *oqxR* in five clinical isolates and four resistance-induced descendant strains.

Strain no.	*acrR* mutation	*ramR* mutation	*oqxR* mutation
K537	No mutation	No mutation	Missense mutation: R152H, M224T
K43	No mutation	No mutation	Missense mutation: R152H, M224T
K43-R	No mutation	No mutation	Missense mutation: R152H, M224T
K428	No mutation	No mutation	Silent mutation: P108P; Missense mutation: R152H, M224T, G317D
K428-R	No mutation	No mutation	Silent mutation: P108P; Missense mutation: R152H, M224T, G317D
K467	No mutation	No mutation	Silent mutation: P108P; Missense mutation: R152H, M224T, G317D
K467-R	No mutation	No mutation	Silent mutation: P108P; Missense mutation: R152H, M224T, G317D
K521	No mutation	No mutation	Silent mutation: P108P; Missense mutation: R152H, M224T, G317D
K521-R	No mutation	No mutation	Silent mutation: P108P; Missense mutation: R152H, M224T, G317D

common AMR genes conferring antibiotic resistance in CRKP were sequenced, including *gyrA* encoding the DNA gyrase and *parC* encoding DNA topoisomerase that are responsible for fluoroquinolone resistance. An amino acid substitution of S83I was detected in *gyrA* in all 9 strains and S80I was detected in *parC* in the K428, K467, and K521 pairs. *gyrA* mutation D87G was found in the K467 and K521 pairs. The plasmid-carrying quinolone resistance gene *qnrS* was also detected in K537 and K467 pairs. Interestingly, the 16S-rRNA methylase encoding gene *rmtB*, a gene that confers resistance to most clinically relevant aminoglycosides, was found in K467 and K521 but missing in their resistance-induced counterparts.

Whole Genome Sequencing Broadened Our Understanding of Collateral Sensitivity in CRKP

Common genetic determinants seemed to be inadequate to explain the induced hypersensitivity to aminoglycosides of CRKP. We thus performed a next-generation full genome sequencing for all nine strains selected for this study, intending to identify molecular determinants that differ between the tigecycline-sensitive and tigecycline-resistant groups. Despite the significant difference in the bacterial resistance to multiple antibiotics including aminoglycosides, no obvious chromosome-related genetic difference was found (**Supplementary Figure 1** and **Supplementary Table 1**, for reviewers' information only). Full genome sequencing of CRKP revealed several antibiotic-resistance related mutations that were not unique to the tigecycline-sensitive parental strains or their tigecycline-resistant descendants, including: 1) a 4bp mutation in non-coding region between *ybhN* and *ybhL* in the K428 pairs, 2) a 11bp insertion in the non-coding region between *garK-1* and *tRNA_anti-like,* a 10bp insertion in the non-coding region between *kp467_02292* and *kp467_02293* and a 4bp mutation in the gene encoding DNA polymerase IV (*dinB_4)* in the K467 pairs, 3) and a 12bp insertion in the non-coding region between *kp521_05022* and *kp521_05023* in the K521 pairs (**Table 3**). Several key AMR mobile elements were found in the parental clinical isolates but not the descendants, including *rmtB* (K467 and K521 pairs), bla_{TEM-1E} (K521 pair), *fosA3* (K467 and K521 pairs) (**Supplementary Figure 1**). As *rmtB* and *fosA3* are often co-carried on a large AMR plasmid, we hypothesized that loss of an AMR plasmid might have occurred to compensate the fitness cost. S1-PFGE revealed that all clinical isolates contained multiple plasmids ranging from 2.1 kb to 54.2 kb in size (**Figure 4**). One plasmid of 54.2–5.6 kb was absent in K43-R but present in K43, and one plasmid of approximately 2.1 kb was missing in K467-R but not the parental clinical isolate.

DISCUSSION

Extended spectrum beta lactamase-producing CRKP are now among the most critical pathogens advised by the recent WHO global priority list of antibiotic-resistant bacteria (WHO, 2020). The overuse of tigecycline and colistin in clinical settings has promoted CRKP to develop resistance to both last-resort antibiotics (Zhang et al., 2018), highlighting a pressing clinical need for alternative strategies such as antibiotic combination therapy. This study intended to increase our understanding of collateral sensitivity in CRKP that tolerates tigecycline treatment, and such knowledge might serve as the foundation of a promising combination therapy for otherwise "untreatable" CRKP infections.

Carbapenem-resistant *Klebsiella pneumoniae* isolates used in this study have distinct PFGE patterns and belong to different sequence types, supporting the non-dominant clonal nature of CRKP encountered in a hospital environment (Chiu et al., 2017). Development of resistance or non-susceptibility to tigecycline has been linked to prolonged use of tigecycline or other antibiotics (Lin et al., 2016). Our mechanistic study of tigecycline resistance only found an association between the reduced tigecycline susceptibility and the overexpression of *acrB*/*ramA* in CRKP. No significant difference in the expression of *oqxB* and *rarA*, or missense/silent mutations in *oqxR*, *acrR* or *ramR* was found when comparing tigecycline-sensitive clinical isolates and their resistance-induced descendants.

Enterobacteriaceae is known to be able to regain collateral sensitivity to many first-line antibiotics when developing resistance to tigecycline, in particular aminoglycosides (Fang et al., 2016; Barbosa et al., 2017). The underlying mechanisms of collateral sensitivity have been proposed but not been fully disclosed (Barbosa et al., 2017). Barbosa et al. (2017) reported that resistance mutation in the regulatory genes of efflux pumps such as *nalC* or *mexZ* might resensitize β-lactam-adapted bacterial

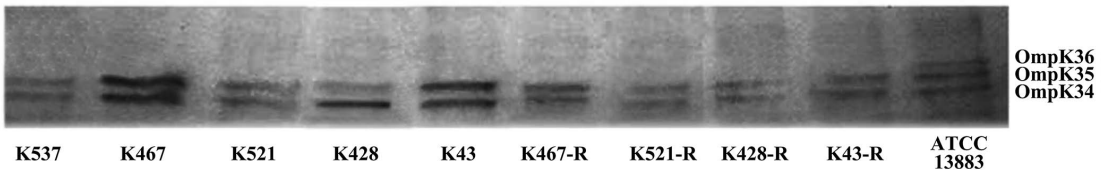

FIGURE 3 | Sodium dodecyl sulfate polyacrylamide gel electrophoresis (SDS-PAGE) of outer membrane proteins (OMPs) in five CRKP clinical isolates and four resistance-induced descendants.

TABLE 3 | Mutations observed in the four clinical isolates and their resistance-induced descendant strains.

Strain	Nearest gene(s)	Reference position (nt)	Reference sequence	Mutant sequence	Mutation type	Predicted effect
K428/ K428-R	ybhN and ybhL	171782	GGGC	AAAT	MNV	Non-coding region
K467/ K467-R	*garK-1* and *tRNA_anti-like*	149888	–	GCTATACCAAA	Insertion	Non-coding region
	kp467_02292 and *kp467_02293*	1318	–	CGAAAAATTT	Insertion	Non-coding region
	dinB_4	1703	GGAA	ATCC	MNV	DNA polymerase IV
K521/ K521-R	*kp521_05022* and *kp521_05023*	1318	–	CGAAAAATTTTT	Insertion	Non-coding region

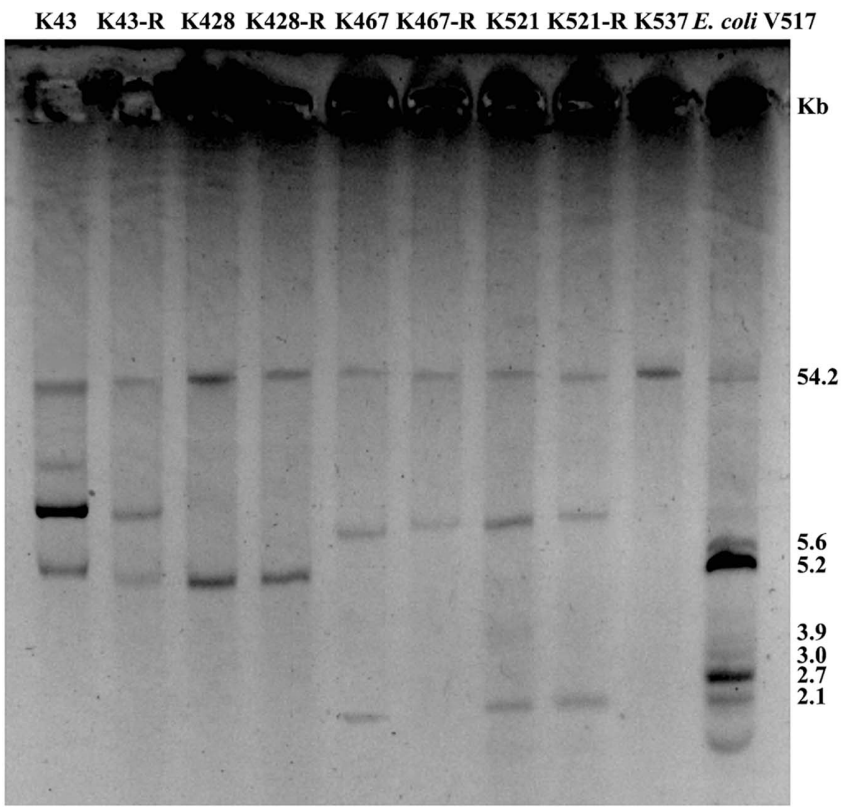

FIGURE 4 | Plasmid analysis of five CRKP clinical isolates and four resistance-induced strains. *Escherichia coli* V517 was used as a control.

populations to aminoglycosides (Barbosa et al., 2017). Previously reported collateral sensitivity in *K. pneumoniae* was supported by mild decreases in MICs of several first-line antibiotics, by 2–10 times (Fang et al., 2016). We, however, found dramatic changes in MICs of aminoglycosides (>100 times) for all 4 experimentally induced tigecycline-resistant strains. Current mechanisms of aminoglycoside resistance do not seem to sufficiently explain the much greater level of collateral sensitivity of CRKP found in this study (Wachino et al., 2020). We hypothesized that accumulative mechanisms drove the development of collateral hypersensitivity of tigecycline-resistant CRKP. We assessed such trade-offs through whole-genome sequencing of clinical isolates

and experimentally induced resistant strains. Genomes of our clinical isolates and resistance-induced descendent strains have high similarity to CRKP clinical isolates of different ST (ST15, ST512, ST11 and ST17) sequenced by others (Hua et al., 2014; Villa et al., 2014; Xu et al., 2017; Du et al., 2018); no major chromosome-related genetic difference were found (Fang et al., 2016). We did find loss of a major AMR plasmid in at least two laboratory evolved strains (K43-R and K467-R). It has been proposed that the co-carriage of various important AMR determinants such as bla_{KPC-2}, bla_{TEM-1}, $bla_{CTX-M-14}$, and *rmtB* on one plasmid could provide evolutionary benefits to bacteria in an antibiotic-rich environment (Sheng et al., 2012). *K. pneumoniae* is an opportunistic pathogen that is well-known for its diversity of antibiotic resistance genes, with significantly more varied DNA composition, and higher plasmid burden than other Gram-negative pathogens (Wyres and Holt, 2018). The high burden of plasmid carriage in *K. pneumoniae*, however, may result in a comparatively lower fitness of the bacterium (Wyres and Holt, 2018). The complex bacterium-plasmid interaction results in not only the adaption of the host to plasmid, but also specific adaption of plasmid to the host. We thus reasoned the voluntary loss of an AMR plasmid under the long-term pressure of tigecycline might also offer survival advantages to the bacterium (Sheng et al., 2012).

Limitations of this study include that only a small number of isolates were used and the structure of the AMR plasmids involved in collateral sensitivity was not further investigated, due to the limited time frame of this study. Another evident limitation is that tigecycline-resistant clinical isolate failed to show any sensitivity to aminoglycoside or other antibiotics and did not provide direct support to the proposed theory. However, theory raised from this experimental study was supported by findings of several recent clinical studies. Stohr et al. (2020) reported loss of the KPC-gene carrying plasmid and plasmid recombination in KPC-producing *K. pneumoniae* clinical isolates from two patients in a hospital outbreak (Stohr et al., 2020). Fang et al. (2016) also isolated tigecycline non-susceptible clinical isolates that had a 2–4-fold decreases in the MICs to aminoglycosides relative to its tigecycline-sensitive ancestral isolates (Fang et al., 2016).

CONCLUSION

Carbapenem-resistant *Klebsiella pneumoniae* may develop collateral hypersensitivity to aminoglycosides and other antibiotics, accompanying the development of bacterial resistance to tigecycline. This experimental study provides a proof of concept to support the sequentially combinational use of tigecycline and aminoglycosides for the treatment of CRKP infections. Antimicrobial susceptibility tests of CRKP should be frequently repeated to provide more specific and accurate guidance for its treatment (Stohr et al., 2020).

DATA AVAILABILITY STATEMENT

The datasets presented in this study can be found in online repositories. The names of the repository/repositories and accession number(s) can be found below: https://www.ncbi.nlm.nih.gov/, PRJNA706839.

AUTHOR CONTRIBUTIONS

YQ and T-LZ: conceptualization and supervision. H-LC, YJ, and M-ML: methodology and validation. H-LC, YJ, and YQ: software. H-LC and M-ML: formal analysis, investigation, and writing—original draft preparation. H-LC, J-MC, and CZ: resources. H-LC and YJ: data curation. CZ, X-XZ, and YQ: writing—review and editing. YS, T-LZ, and YQ: funding acquisition. All authors have read and agreed to the published version of the manuscript.

FUNDING

This work was supported by the National Natural Science Foundation of China (grant number 81802069), the Zhejiang Provincial Natural Science Foundation of China (grant number LY14H190005), the Planned Science and Technology Project of Wenzhou (grant number Y20150312), and Zhejiang Province Program for the Cultivation of High-level Innovative Health Talents.

ACKNOWLEDGMENTS

We are grateful to the reviewers who helped to improve this paper.

SUPPLEMENTARY MATERIALS

The Supplementary Material for this article can be found online at: https://www.frontiersin.org/articles/10.3389/fmicb.2021.674502/full#supplementary-material

Supplementary Figure 1 | Schematic diagram of comparison of chromosome-harboring or plasmid- harboring resistance genes between tigecycline-sensitive and -resistant pairs (K467 and K521 only). The white arrows illustrate the resistance genes among which the red framed arrows indicate the loss of genes in tigecycline-resistant strains.

REFERENCES

Barbosa, C., Trebosc, V., Kemmer, C., Rosenstiel, P., Beardmore, R., Schulenburg, H., et al. (2017). Alternative evolutionary paths to bacterial antibiotic resistance cause distinct collateral effects. *Mol. Biol. Evol.* 34, 2229–2244. doi: 10.1093/molbev/msx158

Bialek-Davenet, S., Marcon, E., Leflon-Guibout, V., Lavigne, J. P., Bert, F., Moreau, R., et al. (2011). In vitro selection of ramR and soxR mutants overexpressing efflux systems by fluoroquinolones as well as cefoxitin in *Klebsiella pneumoniae*. *Antimicrob. Agents Chemother.* 55, 2795–2802. doi: 10.1128/AAC.00156-11

Chiu, S. K., Chan, M. C., Huang, L. Y., Lin, Y. T., Lin, J. C., Lu, P. L., et al. (2017). Tigecycline resistance among carbapenem-resistant *Klebsiella Pneumoniae*:

clinical characteristics and expression levels of efflux pump genes. *PLoS One* 12:e0175140. doi: 10.1371/journal.pone.0175140

Dallenne, C., Da Costa, A., Decre, D., Favier, C., and Arlet, G. (2010). Development of a set of multiplex PCR assays for the detection of genes encoding important beta-lactamases in *Enterobacteriaceae*. *J. Antimicrob. Chemother.* 65, 490–495. doi: 10.1093/jac/dkp498

Doi, Y., and Arakawa, Y. (2007). 16S ribosomal RNA methylation: emerging resistance mechanism against aminoglycosides. *Clin. Infect. Dis.* 45, 88–94. doi: 10.1086/518605

Du, X., He, F., Shi, Q., Zhao, F., Xu, J., Fu, Y., et al. (2018). The rapid emergence of tigecycline resistance in blaKPC-2 harboring *Klebsiella pneumoniae*, as mediated in vivo by mutation in tetA during tigecycline treatment. *Front. Microbiol.* 9:648. doi: 10.3389/fmicb.2018.00648

European Committee on Antimicrobial Susceptibility Testing Steering (2006). EUCAST technical note on tigecycline. *Clin. Microbiol. Infect.* 12, 1147–1149. doi: 10.1111/j.1469-0691.2006.01578.x

Fang, L., Chen, Q., Shi, K., Li, X., Shi, Q., He, F., et al. (2016). Step-wise increase in tigecycline resistance in *Klebsiella pneumoniae* associated with mutations in ramR, lon and rpsJ. *PLoS One* 11:e0165019. doi: 10.1371/journal.pone.0165019

Frohlich, C., Sorum, V., Thomassen, A. M., Johnsen, P. J., Leiros, H. S., and Samuelsen, O. (2019). OXA-48-mediated ceftazidime-avibactam resistance is associated with evolutionary trade-offs. *mSphere* 4:e00024-19. doi: 10.1128/mSphere.00024-19

Furusawa, C., Horinouchi, T., and Maeda, T. (2018). Toward prediction and control of antibiotic-resistance evolution. *Curr. Opin. Biotechnol.* 54, 45–49. doi: 10.1016/j.copbio.2018.01.026

Gonzalez-Padilla, M., Torre-Cisneros, J., Rivera-Espinar, F., Pontes-Moreno, A., Lopez-Cerero, L., Pascual, A., et al. (2015). Gentamicin therapy for sepsis due to carbapenem-resistant and colistin-resistant *Klebsiella pneumoniae*. *J. Antimicrob. Chemother.* 70, 905–913. doi: 10.1093/jac/dku432

He, F., Fu, Y., Chen, Q., Ruan, Z., Hua, X., Zhou, H., et al. (2015). Tigecycline susceptibility and the role of efflux pumps in tigecycline resistance in KPC-producing *Klebsiella pneumoniae*. *PLoS One* 10:e0119064. doi: 10.1371/journal.pone.0119064

He, T., Wang, R., Liu, D., Walsh, T. R., Zhang, R., Lv, Y., et al. (2019). Emergence of plasmid-mediated high-level tigecycline resistance genes in animals and humans. *Nat. Microbiol.* 4, 1450–1456. doi: 10.1038/s41564-019-0445-2

Hentschke, M., Wolters, M., Sobottka, I., Rohde, H., and Aepfelbacher, M. (2010). ramR mutations in clinical isolates of *Klebsiella pneumoniae* with reduced susceptibility to tigecycline. *Antimicrob. Agents Chemother.* 54, 2720–2723. doi: 10.1128/AAC.00085-10

Hirsch, E. B., and Tam, V. H. (2010). Detection and treatment options for *Klebsiella pneumoniae* carbapenemases (KPCs): an emerging cause of multidrug-resistant infection. *J. Antimicrob. Chemother.* 65, 1119–1125. doi: 10.1093/jac/dkq108

Hua, X., Chen, Q., Li, X., Feng, Y., Ruan, Z., and Yu, Y. (2014). Complete genome sequence of *Klebsiella pneumoniae* sequence type 17, a multidrug-resistant strain isolated during tigecycline treatment. *Genome Announc.* 2:e01337-14. doi: 10.1128/genomeA.01337-14

Juan, C. H., Huang, Y. W., Lin, Y. T., Yang, T. C., and Wang, F. D. (2016). Risk factors, outcomes, and mechanisms of tigecycline-nonsusceptible *Klebsiella pneumoniae* bacteremia. *Antimicrob. Agents Chemother.* 60, 7357–7363. doi: 10.1128/AAC.01503-16

Lin, Y. T., Huang, Y. W., Huang, H. H., Yang, T. C., Wang, F. D., and Fung, C. P. (2016). In vivo evolution of tigecycline-non-susceptible *Klebsiella pneumoniae* strains in patients: relationship between virulence and resistance. *Int. J. Antimicrob. Agents* 48, 485–491. doi: 10.1016/j.ijantimicag.2016.07.008

Liu, Y., Li, J., Du, J., Hu, M., Bai, H., Qi, J., et al. (2011). Accurate assessment of antibiotic susceptibility and screening resistant strains of a bacterial population by linear gradient plate. *Sci. China Life Sci.* 54, 953–960. doi: 10.1007/s11427-011-4230-6

Lozano-Huntelman, N. A., Singh, N., Valencia, A., Mira, P., Sakayan, M., Boucher, I., et al. (2020). Evolution of antibiotic cross-resistance and collateral sensitivity in *Staphylococcus epidermidis* using the mutant prevention concentration and the mutant selection window. *Evol. Appl.* 13, 808–823. doi: 10.1111/eva.12903

Maltas, J., and Wood, K. B. (2019). Pervasive and diverse collateral sensitivity profiles inform optimal strategies to limit antibiotic resistance. *PLoS Biol.* 17:e3000515. doi: 10.1371/journal.pbio.3000515

Nielsen, L. E., Snesrud, E. C., Onmus-Leone, F., Kwak, Y. I., Aviles, R., Steele, E. D., et al. (2014). IS5 element integration, a novel mechanism for rapid in vivo emergence of tigecycline nonsusceptibility in *Klebsiella pneumoniae*. *Antimicrob. Agents Chemother.* 58, 6151–6156. doi: 10.1128/AAC.03053-14

Pal, C., Papp, B., and Lazar, V. (2015). Collateral sensitivity of antibiotic-resistant microbes. *Trends Microbiol.* 23, 401–407. doi: 10.1016/j.tim.2015.02.009

Park, K. S., Kim, M. H., Park, T. S., Nam, Y. S., Lee, H. J., and Suh, J. T. (2012). Prevalence of the plasmid-mediated quinolone resistance genes, aac(6')-Ib-cr, qepA, and oqxAB in clinical isolates of extended-spectrum beta-lactamase (ESBL)-producing *Escherichia coli* and *Klebsiella pneumoniae* in Korea. *Ann. Clin. Lab. Sci.* 42, 191–197.

Petrosillo, N., Giannella, M., Lewis, R., and Viale, P. (2013). Treatment of carbapenem-resistant *Klebsiella pneumoniae*: the state of the art. *Expert Rev. Anti Infect. Ther.* 11, 159–177. doi: 10.1586/eri.12.162

Poulakou, G., Kontopidou, F. V., Paramythiotou, E., Kompoti, M., Katsiari, M., Mainas, E., et al. (2009). Tigecycline in the treatment of infections from multi-drug resistant gram-negative pathogens. *J. Infect.* 58, 273–284. doi: 10.1016/j.jinf.2009.02.009

Roy, S., Datta, S., Viswanathan, R., Singh, A. K., and Basu, S. (2013). Tigecycline susceptibility in *Klebsiella pneumoniae* and *Escherichia coli* causing neonatal septicaemia (2007-10) and role of an efflux pump in tigecycline non-susceptibility. *J. Antimicrob. Chemother.* 68, 1036–1042. doi: 10.1093/jac/dks535

Sekowska, A., and Gospodarek, E. (2010). Susceptibility of *Klebsiella* spp. to tigecycline and other selected antibiotics. *Med. Sci. Monit.* 16, BR193–BR196.

Sheng, J. F., Li, J. J., Tu, S., Sheng, Z. K., Bi, S., Zhu, M. H., et al. (2012). blaKPC and rmtB on a single plasmid in *Enterobacter* amnigenus and *Klebsiella pneumoniae* isolates from the same patient. *Eur. J. Clin. Microbiol. Infect. Dis.* 31, 1585–1591. doi: 10.1007/s10096-011-1481-x

Shi, W., Li, K., Ji, Y., Jiang, Q., Wang, Y., Shi, M., et al. (2013). Carbapenem and cefoxitin resistance of *Klebsiella pneumoniae* strains associated with porin OmpK36 loss and DHA-1 beta-lactamase production. *Braz. J. Microbiol.* 44, 435–442. doi: 10.1590/S1517-83822013000200015

Stein, G. E., and Babinchak, T. (2013). Tigecycline: an update. *Diagn. Microbiol. Infect. Dis.* 75, 331–336. doi: 10.1016/j.diagmicrobio.2012.12.004

Stohr, J., Verweij, J. J., Buiting, A. G. M., Rossen, J. W. A., and Kluytmans, J. (2020). Within-patient plasmid dynamics in *Klebsiella pneumoniae* during an outbreak of a carbapenemase-producing *Klebsiella pneumoniae*. *PLoS One* 15:e0233313. doi: 10.1371/journal.pone.0233313

Sun, J., Chen, C., Cui, C. Y., Zhang, Y., Liu, X., Cui, Z. H., et al. (2019). Plasmid-encoded tet(X) genes that confer high-level tigecycline resistance in *Escherichia coli*. *Nat. Microbiol.* 4, 1457–1464. doi: 10.1038/s41564-019-0496-4

Sun, Y., Cai, Y., Liu, X., Bai, N., Liang, B., and Wang, R. (2013). The emergence of clinical resistance to tigecycline. *Int. J. Antimicrob. Agents* 41, 110–116. doi: 10.1016/j.ijantimicag.2012.09.005

Villa, L., Capone, A., Fortini, D., Dolejska, M., Rodriguez, I., Taglietti, F., et al. (2013). Reversion to susceptibility of a carbapenem-resistant clinical isolate of *Klebsiella pneumoniae* producing KPC-3. *J. Antimicrob. Chemother.* 68, 2482–2486. doi: 10.1093/jac/dkt235

Villa, L., Feudi, C., Fortini, D., Garcia-Fernandez, A., and Carattoli, A. (2014). Genomics of KPC-producing *Klebsiella pneumoniae* sequence type 512 clone highlights the role of RamR and ribosomal S10 protein mutations in conferring tigecycline resistance. *Antimicrob. Agents Chemother.* 58, 1707–1712. doi: 10.1128/AAC.01803-13

Wachino, J. I., Doi, Y., and Arakawa, Y. (2020). Aminoglycoside resistance: updates with a focus on acquired 16S Ribosomal RNA methyltransferases. *Infect. Dis. Clin. North Am.* 34, 887–902. doi: 10.1016/j.idc.2020.06.002

WHO (2020). *Essential Medicines and Health Products*. Available online at: http://www.who.int/medicines/publications/global-priority-list-antibiotic-resistant-bacteria (accessed February 15, 2021).

Woodford, N., Hill, R. L., and Livermore, D. M. (2007). In vitro activity of tigecycline against carbapenem-susceptible and -resistant isolates of *Klebsiella* spp. and *Enterobacter* spp. *J. Antimicrob. Chemother.* 59, 582–583. doi: 10.1093/jac/dkl514

Wyres, K. L., and Holt, K. E. (2018). *Klebsiella pneumoniae* as a key trafficker of drug resistance genes from environmental to clinically important bacteria. *Curr. Opin. Microbiol.* 45, 131–139. doi: 10.1016/j.mib.2018.04.004

Xu, H., Zhou, Y., Zhai, X., Du, Z., Wu, H., Han, Y., et al. (2016). Emergence and characterization of tigecycline resistance in multidrug-resistant *Klebsiella pneumoniae* isolates from blood samples of patients in intensive care units in northern China. *J. Med. Microbiol.* 65, 751–759. doi: 10.1099/jmm.0.000299

Xu, J., Gao, M., Hong, Y., and He, F. (2017). Draft genome sequence of a tigecycline-resistant KPC-2-producing *Klebsiella pneumoniae* ST15 clinical isolate from China. *J. Glob. Antimicrob. Resist.* 11, 156–158. doi: 10.1016/j.jgar.2017.10.017

Zhang, R., Dong, N., Huang, Y., Zhou, H., Xie, M., Chan, E. W., et al. (2018). Evolution of tigecycline- and colistin-resistant CRKP (carbapenem-resistant *Klebsiella pneumoniae*) in vivo and its persistence in the GI tract. *Emerg. Microbes Infect.* 7:127. doi: 10.1038/s41426-018-0129-7

Zhang, Y., Jiang, X., Wang, Y., Li, G., Tian, Y., Liu, H., et al. (2014). Contribution of beta-lactamases and porin proteins OmpK35 and OmpK36 to carbapenem resistance in clinical isolates of KPC-2-producing *Klebsiella pneumoniae*. *Antimicrob. Agents Chemother.* 58, 1214–1217. doi: 10.1128/AAC.02045-12

Zhong, X., Xu, H., Chen, D., Zhou, H., Hu, X., and Cheng, G. (2014). First emergence of acrAB and oqxAB mediated tigecycline resistance in clinical isolates of *Klebsiella pneumoniae* pre-dating the use of tigecycline in a Chinese hospital. *PLoS One* 9:e115185. doi: 10.1371/journal.pone.0115185

Conflict of Interest: The authors declare that the research was conducted in the absence of any commercial or financial relationships that could be construed as a potential conflict of interest.

frontiers in Microbiology

ORIGINAL RESEARCH
published: 05 July 2021
doi: 10.3389/fmicb.2021.674974

Co-harboring of Novel *bla*$_{KPC-2}$ Plasmid and Integrative and Conjugative Element Carrying Tn*6203* in Multidrug-Resistant *Pseudomonas aeruginosa*

Heng Cai[1,2,3], *Yiwei Zhu*[1,2,3], *Dandan Hu*[1,2,3], *Yue Li*[1,2,3], *Sebastian Leptihn*[1,4], *Belinda Loh*[4], *Xiaoting Hua*[1,2,3]* and *Yunsong Yu*[1,2,3]*

[1]Department of Infectious Diseases, Sir Run Run Shaw Hospital, Zhejiang University School of Medicine, Hangzhou, China, [2]Key Laboratory of Microbial Technology and Bioinformatics of Zhejiang Province, Hangzhou, China, [3]Regional Medical Center for National Institute of Respiratory Diseases, Sir Run Run Shaw Hospital, Zhejiang University School of Medicine, Hangzhou, China, [4]Zhejiang University-University of Edinburgh Institute, Zhejiang University, Haining, China

OPEN ACCESS

Edited by:
Miklos Fuzi, Semmelweis University, Hungary

Reviewed by:
Huiluo Cao, The University of Hong Kong, China
Rodolpho M. Albano, Rio de Janeiro State University, Brazil

***Correspondence:**
Yunsong Yu
yvys119@zju.edu.cn
Xiaoting Hua
xiaotinghua@zju.edu.cn

Specialty section:
This article was submitted to Antimicrobials, Resistance and Chemotherapy, a section of the journal Frontiers in Microbiology

Received: *02 March 2021*
Accepted: *31 May 2021*
Published: *05 July 2021*

Citation:
Cai H, Zhu Y, Hu D, Li Y, Leptihn S, Loh B, Hua X and Yu Y (2021) Co-harboring of Novel bla$_{KPC-2}$ Plasmid and Integrative and Conjugative Element Carrying Tn6203 in Multidrug-Resistant Pseudomonas aeruginosa. Front. Microbiol. 12:674974. doi: 10.3389/fmicb.2021.674974

Many strains of the opportunistic pathogen *Pseudomonas aeruginosa* have acquired resistance to multiple antibiotics. Carbapenem-resistant *P. aeruginosa* poses a global healthcare problem due to limited therapeutic options for the treatment of infections. Plasmids and integrative and conjugative elements (ICEs) are the major vectors of antibiotic-resistance gene transfer. In our study, four carbapenem-resistant strains of *P. aeruginosa* were isolated from the same patient in a tertiary referral hospital in China, one of these was resistant to gentamicin and tobramycin. In this strain P33, we observed a non-transferable plasmid, pP33-2, carrying a novel *bla*$_{KPC-2}$ gene segment (IS*Kpn27*-*bla*$_{KPC-2}$-IS*Kpn6*-*korC*-ORF-*klcA*-IS*26*), which we concluded to have been formed by IS*26*-mediated gene cluster translocation. In addition, by comparing the chromosomes of the *P. aeruginosa* strains that belong to the same sequence type, we identified an ICE, ICEP33, adjacent to a prophage. The *att*L site of ICEP33 is identical to the terminal part of the *att*R site of the prophage. The ICEP33 element contains the transposon Tn*6203*, which encodes antibiotic and metal resistance genes. The insertion of ICEP33 in the chromosome mediates resistance to multiple antibiotics. Our study contributes to the understanding of the acquisition of antibiotic resistance in *P. aeruginosa* facilitated by mobile genetic elements.

Keywords: plasmid, KPC-2, integrative and conjugative element, prophage, *Pseudomonas aeruginosa*

INTRODUCTION

Multidrug-resistant (MDR) *Pseudomonas aeruginosa* poses a threat to human health, causing severe acute and chronic infections in hospitalized and immunocompromised patients (Horcajada et al., 2019). Due to the increasing resistance levels globally, the World Health Organization has listed this bacteria as a "critical" pathogen of which research and development for new

antibiotics are urgently required (Tacconelli et al., 2018). While carbapenems are currently one of the most important classes of antibiotics for the treatment of MDR *P. aeruginosa* strains, they are ineffective in nearly 30% of clinical cases in China (Hu et al., 2019a).

The acquisition of carbapenemase genes is one of the main mechanisms of resistance to carbapenems (van Duin and Doi, 2017). *Klebsiella pneumoniae* carbapenemases (KPCs), belonging to Ambler's class A beta-lactamases, have spread extensively and are often horizontally transferred *via* plasmids (Munoz-Price et al., 2013; Chen et al., 2014b). The previous reports have documented KPC-2-producing *P. aeruginosa* ST463 in Hangzhou, China, and typically, the bla_{KPC-2} genes were plasmid located (Hu et al., 2015b, 2019b). In addition to intrinsic resistances and chromosomal mutations, mobile genetic elements, such as plasmids and integrative and conjugative elements (ICEs), are responsible for spreading resistance genes to *P. aeruginosa* strains (Botelho et al., 2019).

Integrative and conjugative elements are key players in transmitting antibiotic resistance by conjugation like plasmids and then integrating into the chromosome and being replicated as part of the host genome like bacteriophage (Carraro and Burrus, 2015). They carry certain genes that are required for excision, maintenance, conjugative transfer, and integration into the host genome. ICEs may also carry cargo genes that confer diverse phenotypes on the organisms including pathogenicity islands containing virulence-associated genes (Wurdemann and Tummler, 2007; Kung et al., 2010; Roy Chowdhury et al., 2017).

In this study, we found a clinical *P. aeruginosa* isolate carrying a novel bla_{KPC-2} plasmid, pP33-2, markedly different from the bla_{KPC-2} carrying plasmids reported previously. This strain also harbored an ICE, ICEP33 containing a Tn*6203* transposon with several resistance genes.

MATERIALS AND METHODS

Clinical Isolates and Identification

Four isolates, P20, P22, P23, and P33, were cultured from a patient's rectal and throat swabs and tracheotomy tube using Pseudomonas Isolation Agar (Peptone 20 g/l, $MgCl_2$ 1.4 g/l, K_2SO_4 10 g/l, Triclosan 25 mg/l, Agar 13.6 g/l, and Glycerol 20 ml/l.). Bacterial species were identified by the matrix-assisted laser desorption ionization-time of flight mass spectrometry (MALDI-TOF MS; Bruker Daltonik GmbH, Bremen, Germany) and 16S rRNA gene sequencing.

Antimicrobial Susceptibility Testing

Antimicrobial susceptibility testing was performed by broth microdilution. Antibiotics included: piperacillin; piperacillin-tazobactam; ceftazidime; ceftazidime-avibactam; cefepime; aztreonam; imipenem; meropenem; gentamicin; tobramycin; amikacin; ciprofloxacin; levofloxacin; and colistin. The results were interpreted according to Clinical and Laboratory Standards Institute guidelines (CLSI; M100, 30th Edn.; CLSI, 2020). *P. aeruginosa* strain ATCC 27853 was used as the quality control.

Genome Sequencing and Analysis

Genomic DNA was extracted by the QIAamp DNA Mini Kit (Qiagen, Germany) and sequenced by HiSeq (Illumina, San Diego, CA, United States). The paired-end reads were assembled by CLC genomics workbench (version 12). Multilocus sequence typing was identified by the PubMLST[1] (Jolley et al., 2018). Antibiotic resistance genes were identified by the ResFinder 4.1[2] (Zankari et al., 2012) and were further confirmed by PCR. The genomic DNA of P23 and P33 was additionally prepared by the Gentra Puregene Yeast/Bact. Kit (Qiagen) and Nanopore sequencing was performed by a MinION sequencer (Oxford Nanopore Technologies, Oxford, United Kingdom). *De novo* assembly of the Illumina and Nanopore reads was performed using the Unicycler v0.4.8 (Wick et al., 2017). The genome sequence was annotated by Prokka[3] (Seemann, 2014) and manually refined by NCBI Blast (Camacho et al., 2009). The nucleotide polymorphism (SNP) tree was built by snippy-multi and FastTree,[4] visualized by ggtree v2.0.4 (Yu, 2020). Conjugative apparatus was predicted by oriTfinder[5] and MOBscan (Li et al., 2018; Garcillan-Barcia et al., 2020). ICEs were predicted by ICEfinder[6] (Liu et al., 2019).

Conjugation

Conjugation assays were conducted using rifampicin-resistant *Escherichia coli* EC600 and a spontaneous rifampicin-resistant mutant of *P. aeruginosa* PAO1 as the recipient strain. Strain P33 was used as the donor. The selective Mueller-Hinton agar plates contained rifampicin (300 μg/ml) combined with meropenem (0.5 μg/ml) or meropenem (4 μg/ml). Each conjugation experiment was repeated at least three times.

Accession Numbers

The complete sequences of the chromosomes and plasmids from *P. aeruginosa* strain P23 and P33 have been deposited in the GenBank nucleotide database under accession numbers CP065417-CP065418 and CP065412-CP065416, respectively. The genome sequences of *P. aeruginosa* strains P20 and P22 have been deposited in the GenBank database under accession numbers JAEMVM000000000 and JAEMVL000000000, respectively.

RESULTS AND DISCUSSION

Case Report

In August 2019, a 69-year-old man was hospitalized in Sir Run Run Shaw Hospital (Mayo Clinic Care Network) in Hangzhou, China. The patient had been suffering from a severe cough with expectoration for 5 months, in addition to fever and hypotension that began approximately 1 month

[1]https://pubmlst.org/organisms/pseudomonas-aeruginosa
[2]https://cge.cbs.dtu.dk/services/ResFinder/
[3]https://github.com/tseemann/prokka
[4]https://github.com/tseemann/snippy
[5]https://tool-mml.sjtu.edu.cn/oriTfinder
[6]https://db-mml.sjtu.edu.cn/ICEfinder

before hospitalization. The patient's medical history included hypertension, cerebral infarction, and multiple pulmonary infections. Several months before hospitalization, the patient suffered from a bloodstream infection by *P. aeruginosa*. After this renewed hospitalization, the patient's symptoms were controlled by antibiotics and other supportive treatment, such as mechanical ventilation and fluid therapy. The course of antibiotics used is listed in chronological order as follows: cefoperazone-sulbactam, cefuroxime, piperacillin-tazobactam, and cefuroxime. After 1 month, his condition improved and he was discharged. Four *P. aeruginosa* strains P20, P22, P23, and P33 were isolated from different anatomical locations or at different time points during hospitalization (**Table 1**). Specifically, P20 was isolated from the rectal swab on the day of admission; P22 and P23 were isolated from the rectal swab and throat swab on the fifth day after admission, respectively; and P33 was isolated from the tracheotomy tube on the twelfth day.

Results of Antimicrobial Susceptibility Testing

The four *P. aeruginosa* isolates were all resistant to penicillins, β-lactam/β-lactamase inhibitor combination agents, cephems, monobactams, carbapenems, and fluoroquinolones and intermediate to colistin. P20, P22, and P23 were susceptible to aminoglycosides while P33 was susceptible to amikacin but resistant to gentamicin and tobramycin (**Table 1**).

Genetic Relationship and Antibiotic Resistance Genes of the Strains

P20, P22, P23, and P33 were all identified as ST463. An analysis based on SNP showed that P33 was more genetically distant from the other three strains (**Figure 1**). P33 differed from P20 in 315 SNPs, from P22 in 314 SNPs, and from P23 in 306 SNPs. Taking the large number of varied SNPs into consideration, it seems that P33 unlikely evolved from the other three strains recently, i.e., during the hospitalization.

The antimicrobial resistance genes of P33 were different from the other isolates. The genome of P33 contained genes that conferred resistance to β-lactams (bla_{CARB-2}), aminoglycosides (*aac(6')−IIa*, *ant(2")−Ia*), and sulfonamide (*sul1*), which were absent in P20, P22, and P23. While P33 lacked $bla_{OXA-468}$, the other three strains contained the gene. All of four strains had *aph(3')−IIb*, bla_{KPC-2}, $bla_{PDC-374}$, *catB7*, *crpP*, and *fosA* (**Figure 1**). The genes *aac(6')−IIa* and *ant(2")−Ia* are likely to confer the resistance in P33 to gentamicin and tobramycin. Nanopore sequencing and subsequent analysis showed that the carbapenem-resistant gene bla_{KPC-2} is located in a plasmid found in P23 and P33, respectively. Sequence analysis indicated that P20, P22, and P23 carry a closely related bla_{KPC-2} plasmid, while the one in the P33 is different. The nucleotide sequence of the bla_{KPC-2} plasmid in P33 is about in 30% identical to those in others.

The observations of our study reveal differences in SNP and antimicrobial susceptibility among the strains of the same sequence type (ST463). We speculate that the P33 strain could have acquired the mobile elements carrying the relevant antibiotic resistance genes by exchanging genes with other bacteria in the host microbiome during the long-term repeated infection.

Characterization of Plasmids in P33

Employing Nanopore sequencing, we were able to identify four plasmids in P33, named pP33-1, pP33-2, pP33-3, and pP33-4. Plasmid pP33-1 is 49,654 bp long with an average GC content of 59% and 58 predicted open reading frames (ORFs). Plasmid pP33-2 has a length of 48,306 bp, with an average GC content of 59%. Sequence annotation predicted 64 ORFs. Plasmid pP33-3 is smaller with 3,014 bp, an average GC content of 61% and only three predicted ORFs. Finally, pP33-4 was predicted to contain three ORFs on a similarly sized plasmid (2,953 bp) with an average GC content of 65%.

The genetic structure of pP33-2 can be divided into the general maintenance and the bla_{KPC-2} segment. The general maintenance includes the replication initiation (*repA*), partitioning

TABLE 1 | Summary of antimicrobial susceptibility testing for four strains.

	Antibiotics	P20 (rectal swab, day 0)	P22 (rectal swab, day 5)	P23 (throat swab, day 5)	P33 (tracheotomy tube, day 12)
MIC (μg/ml)	Piperacillin	>256 (R)	>256 (R)	>256 (R)	>256 (R)
	Piperacillin-tazobactam	>256/4 (R)	>256/4 (R)	>256/4 (R)	>256/4 (R)
	Ceftazidime-avibactam	32/4 (R)	16/4 (R)	16/4 (R)	16/4 (R)
	Ceftazidime	256 (R)	256 (R)	256 (R)	128 (R)
	Cefepime	>256 (R)	>256 (R)	>256 (R)	>256 (R)
	Aztreonam	>128 (R)	>128 (R)	>128 (R)	>128 (R)
	Imipenem	>128 (R)	>128 (R)	>128 (R)	>128 (R)
	Meropenem	>128 (R)	>128 (R)	>128 (R)	>128 (R)
	Colistin	0.5 (I)	0.5 (I)	0.5 (I)	0.5 (I)
	Gentamicin	1 (S)	1 (S)	1 (S)	>64 (R)
	Tobramycin	0.5 (S)	0.5 (S)	0.5 (S)	>64 (R)
	Amikacin	4 (S)	4 (S)	4 (S)	8 (S)
	Ciprofloxacin	16 (R)	16 (R)	16 (R)	16 (R)
	Levofloxacin	>64 (R)	>64 (R)	>64 (R)	>64 (R)

S, sensitive; I, intermediate; and R, resistant.

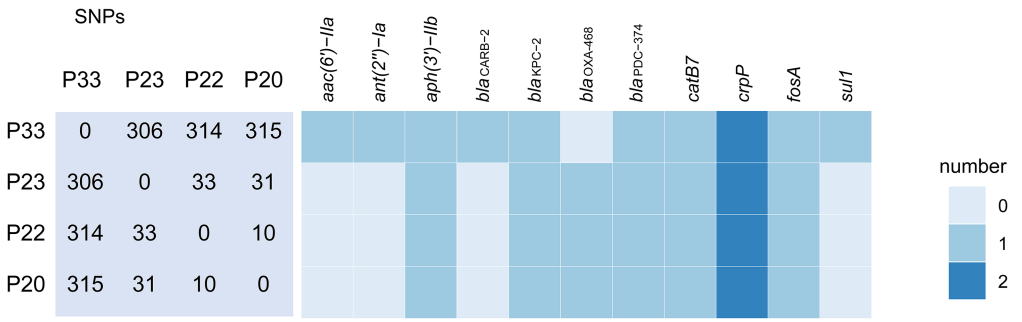

FIGURE 1 | SNP difference matrix and heat map of predicted antibiotic resistance genes of four *Pseudomonas aeruginosa* strains. The numbers in the matrix are the number of variant SNPs between the strains. The indicator denotes the cope number of genes by different color.

(*parAB*), and genes for plasmid maintenance. The plasmid pP33-2 is classified as an unidentified incompatibility (Inc.) type. BLAST analysis showed that pP33-2 is similar to plasmid ID40_1 (LR700249.1), pPA7790 (CP015000.1), pPB353_1 (CP025052.1), pPB354_1 (CP025054.1), pMS14403A (CP049162.1), pJUPA4295 (LC586269.1), and an unnamed plasmid in strain AR_0230 (CP027175.1), with query coverage ranging from 59 to 78% and an identity of 95.24–98.51%. After removing the bla_{KPC-2} cluster, pP33-2 shares 97–100% coverage with the plasmid sequences mentioned above. Thus, while these plasmids share similar backbones, only pP33-2 carries the bla_{KPC-2} gene, indicating that pP33-2 is a novel bla_{KPC-2} plasmid in *P. aeruginosa*.

Plasmid pP33-1 encodes four components of a conjugative apparatus: an origin of transfer (oriT), a relaxase (R), a type IV coupling protein (T4CP), and a type IV secretion system (T4SS; Smillie et al., 2010), while pP33-2 was predicted to harbor only a MOB_C family relaxase and part of T4SS. Although pP33-1 was included as a conjugative helper, conjugation experiments with pP33-2 failed several times, suggesting that pP33-2 might be not transferable.

Evolution of the bla_{KPC-2} Gene Cluster Within the Strains

Strain P23 harbors the bla_{KPC-2} gene-containing plasmid pP23, which is very similar to plasmid YLH6_p3 (MK882885.1) and pPA1101 (MH734334.1; Hu et al., 2019b). The accessory modules of bla_{KPC-2} were different in pPA1101, pP23, and pP33-2 (**Figure 2**). In pPA1101, there was a core module Tn3-IS*Kpn27*-bla_{KPC-2}-IS*Kpn6*-*korC*-ORF-*klcA*-ORF-ORF with two inverted IS*26* elements at both ends. The core module Tn3-IS*Kpn27*-bla_{KPC-2}-IS*Kpn6* was frequently identified as the bla_{KPC-2} gene cluster in China (Shen et al., 2009; Cai et al., 2014; Chen et al., 2014a; Li et al., 2015). Occasionally, the core module was observed to be interrupted by the IS*26*-based composite transposons (Chen et al., 2014c). When comparing pP23 to pPA1101, a part of the core module appeared to be reversed (**Figure 2**). Due to the intramolecular replicative transposition in inverse orientation, the segment between the original IS*26* and the targeted site on *tnp*A was reversed. An indication that supports our interpretation is that we observed 8-bp sequences (5'-CGATATTT-3') reverse complements of each other that flank the two IS*26* copies (Harmer et al., 2014; He et al., 2015; Partridge et al., 2018).

Unlike sequences reported previously, IS*Kpn27*-bla_{KPC-2}-IS*Kpn6*-*korC*-ORF-*klcA*-IS*26* was found in the KPC module of pP33-2. The gene cluster *korC*-ORF-*klcA* is commonly connected with the core module IS*Kpn27*-bla_{KPC-2}-IS*Kpn6* as mentioned above (Shen et al., 2009; Dai et al., 2016; Shi et al., 2018). However, unilateral IS*26* element insertion is rarely observed. A possible explanation for this is if IS*26* and the adjacent region that included IS*Kpn27*-bla_{KPC-2}-IS*Kpn6*-*korC*-ORF-*klcA*, formed a transferable unit (TU). This TU might then have inserted into another plasmid. Normally, the integration results in two copies IS*26* in direct orientation, one at each boundary between the two participating molecules (Harmer et al., 2014; Harmer and Hall, 2015; Varani et al., 2021). However, we observe only one IS*26* in pP33-2; the other might possibly have been lost through a deletion event.

Blast search results identified plasmid pPA7790 (Nascimento et al., 2016), which was isolated from a patient in Brazil, as being most similar to pP33-2 with 78% query coverage and 98.51% identity. Comparing pP33-2 to pPA7790, the backbone is similar, yet the bla_{KPC-2} segment in pP33-2 substituted a part of T4SS module in pPA7790 (**Figure 2**).

The mechanism of how the bla_{KPC-2}-carrying plasmid originated has not been completely established. However, it is very plausible that the IS*26* facilitated the spread of KPC among different plasmids in *P. aeruginosa*. The *P. aeruginosa* strain with novel bla_{KPC-2} plasmid described here might become an important regional epidemic clone.

Integration of ICEP33 Brings Resistance Genes

Among the four clinical isolates, P23 and P33 have the closest genetic relationship (**Figure 1**). A comparison of the chromosomes of P23 and P33 showed there is an 110,131-bp-long insertion downstream of the gene encoding the integrase family protein on the P33 chromosome (**Figure 3**). ICEfinder predicted it to be a putative ICE, hereafter named ICEP33. Within this element, we found the aminoglycosides-resistant genes *aac(6')-IIa* and *ant(2")-Ia* together with bla_{CARB-2} and *sul1*, which were only found in P33.

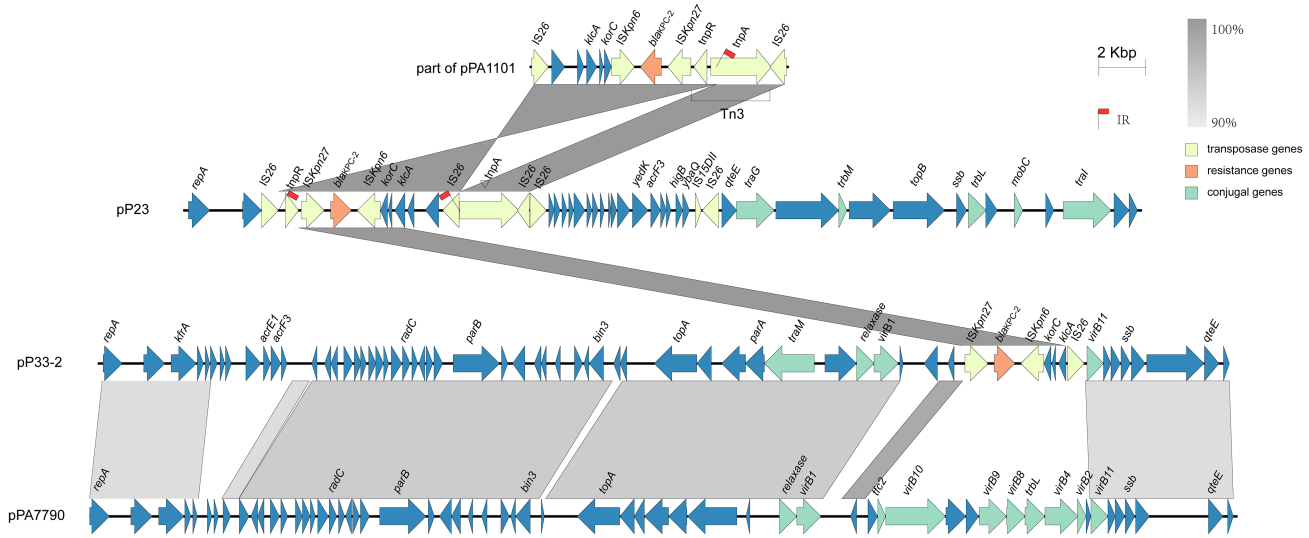

FIGURE 2 | Detailed structure and comparison of the bla_{KPC-2} gene cluster within the strains. Yellow, orange, and green arrows represent transposase, resistance, and conjugal genes, respectively. Arrows indicate the translation orientation of the coding genes. Red flags highlight the positions of inverted repeats.

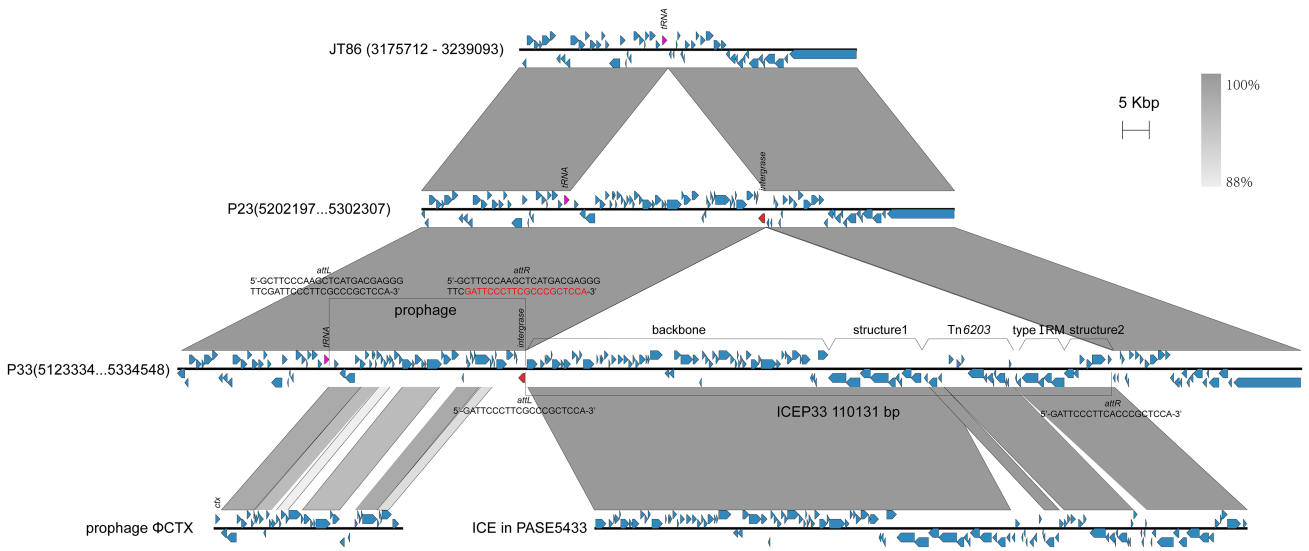

FIGURE 3 | Comparison of partial chromosomes. A prophage integrated into the chromosome first, and then an ICE integrated next to the prophage. The *attL* and *attR* of prophage and ICE are, respectively, labeled. The overlapping att site is marked red. Red arrows represent the genes which ICE and prophage integrate adjacent to. The ICE is divided into four parts.

The antimicrobial resistance genes are organized within a single class I integron integrated in transposon Tn*6203*. In addition, there is a Tn*4378*-like transposon carrying a mercury resistance operon (*mer*) in Tn*6203*. With the exception of the resistance segment, ICEP33 could roughly be divided into four parts: backbone, structure 1, type I restriction and modification (RM) system, and structure 2 (**Figure 3**). The backbone contains genes encoding a bacteriophage P4-like integrase, conjugative apparatuses, and genes for DNA processing and replication. The type I RM is possibly required for ICE self-maintenance (Hu et al., 2015a). Structure 1 and structure 2 contain genes encoding proteins, such as cold shock domain-containing protein, S8 family peptidase and LysR family transcriptional regulator. These structures might be acquired through multiple recombination events during the ICE evolution.

The insertion of ICE is flanked by two attachment (*att*) sites at both ends of the sequence (*attL* and *attR*; Bellanger et al., 2011; Johnson and Grossman, 2015). In P33, the *attL* is 5'-GATTCCCTTCGCCCGCTCCA-3' and the *attR* is 5'-GATTCCCTTCACCCGCTCCA-3'. These site-specific integrations mediated by the bacteriophage P4-like integrase are typically found within the tRNA gene

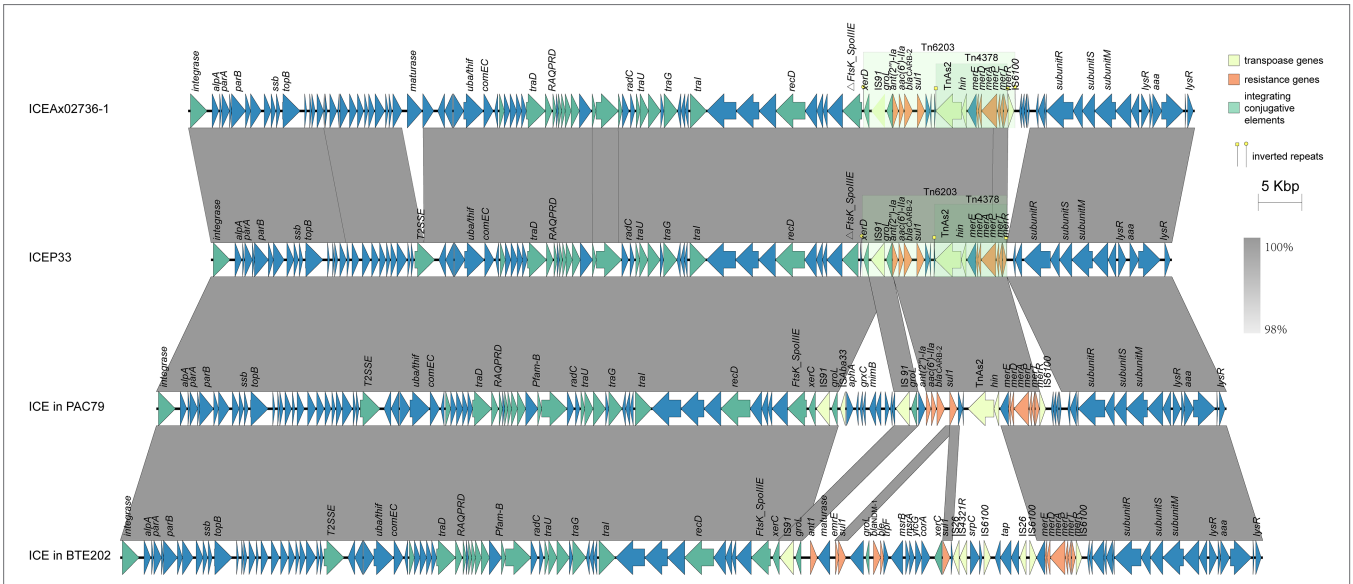

FIGURE 4 | Detailed structure and comparison of similar ICEs. Yellow, orange, and green arrows represent transposase genes, resistance genes, and integrating conjugative elements, respectively. Arrows indicate the translation orientation of the coding genes. Two green shades denote Tn*6203* and Tn*4378*.

(Ravatn et al., 1998a,b; Wozniak and Waldor, 2010; Johnson and Grossman, 2015). However, ICEP33 is integrated approximately 37-kb downstream of $tRNA^{Gly}$. We found an intact prophage sequence inserted next to the $tRNA^{Gly}$ causing 46 bp direct repeats, which contain the *att* site of ICEP33 (**Figure 3**). This prophage is 36.7 kb in length with an average GC content of 63.8% and 48 predicted ORFs. The prophage encodes 42 phage proteins and 33 of them are similar to P2-like phage ΦCTX (AB008550.1). Compared to ΦCTX, the prophage in P33 lacks the cytotoxin gene (*ctx*) and contains a different integrase gene. We propose that the evolution of this genetic section of the bacterial chromosome happened in succession, with integration of the prophage into the chromosome similar to JT86 (CP062219.1) occurring first, forming the genomic organization that is also observed in P23. In a second step, an ICE integrated next to the prophage and eventually leading to the structure observed in P33 (**Figure 3**). ICEs with bacteriophage P4-like integrase are often found adjacent to phages that target the same *att* site (Botelho et al., 2018). Our study provides a possible order of their insertion. However, whether there is an interaction in integration between ICE and prophage is unclear.

ICEP33 Belongs to *clc*-Like Family

Two large families of ICEs exist in *P. aeruginosa*, the pKLC102 family and the *clc*-like family, which includes *clc* (AJ617740), PAGI-2 (AF440523), and PAGI-3 (AF440524; Kung et al., 2010). ICEP33 is similar to PAGI-15 (KX196168.1) and PAGI-16 (KX196169.1), which were defined as *clc*-like ICEs (Hong et al., 2016), indicating that ICEP33 belongs to the same family. These ICEs all share a similar bipartite structure: the conserved part adjacent to the integration site as backbone and the variable part that consisted of unique cargo ORFs (Kung et al., 2010). ICEP33-like ICEs were also found in other bacteria, such as *Achromobacter xylosoxidans* strain X02736 (GCA_000517225.1; Hu et al., 2015a), *Bordetella trematum* strain E202 (CP049957.1), *P. aeruginosa* strain SE5443 (CP046405.1), and C79 (CP040684.1; **Figures 3, 4**). The antibiotic resistance genetic load is the main difference between them. Compared to the most similar sequence ICEAx02736-1, they both carry the same resistance genes embedded in Tn*6203* modules. In P33, the right end of Tn*6203* was truncated by IS6100 and four predicted ORFs, which led to the loss of an inverted or direct repeat. In addition, it appears that a gene encoding group II intron reverse transcriptase/maturase had inserted into the middle of the gene encoding a DEAD/DEAH box helicase. Interestingly, these ICEs in **Figures 3, 4** are found in different bacterial species in China, indicating that this type of ICE is present in a variety of hosts and may be an important molecular mechanism for the dissemination of resistance genes in the country.

CONCLUSION

In this study, four *P. aeruginosa* strains were isolated from a single patient in an intensive care unit. The horizontal transmission of the antibiotic resistance genes in those strains was hypothesized to be mediated by mobile elements IS*26* and ICEs. In this work, a novel plasmid pP33-2 encoding bla_{KPC-2} is described, which likely originates from an IS*26*-mediated insertion into the position of T4SS; subsequently, a deletion of the IS*26* and a partial removal of the T4SS occurred during evolution. In addition, the resistance genes embedded in the transposon Tn*6203* became part of ICEP33 that was found in the same strain. ICEP33, which belongs to *clc*-like family is integrated adjacent to a prophage sequence. The appearance of the novel bla_{KPC-2}

plasmid and the integration of the ICE has created a new type of MDR *P. aeruginosa* strain, which creates a high risk of a regional epidemic carbapenem-resistant clone, bringing more challenges to the clinical treatment of infections caused by *P. aeruginosa*.

DATA AVAILABILITY STATEMENT

The datasets presented in this study can be found in online repositories. The names of the repository/repositories and accession number(s) can be found at: https://www.ncbi.nlm.nih.gov/genbank/ (CP065417-CP065418, CP065412-CP065416, JAEMVM000000000, and JAEMVL000000000).

AUTHOR CONTRIBUTIONS

XH, YY, and HC designed the study. HC, YZ, DH, and YL performed the experiments. HC and YZ analyzed the data. HC drafted the article. XH, YY, SL, and BL revised the article. All authors have approved the final article.

FUNDING

This study was supported by the National Natural Science Foundation of China (grant no. 81830069).

ACKNOWLEDGMENTS

We thank Dr. Mark Toleman, Cardiff University, School of Medicine for critically reading the manuscript.

SUPPLEMENTARY MATERIAL

The Supplementary Material for this article can be found online at: https://www.frontiersin.org/articles/10.3389/fmicb.2021.674974/full#supplementary-material

REFERENCES

Bellanger, X., Morel, C., Gonot, F., Puymege, A., Decaris, B., and Guedon, G. (2011). Site-specific accretion of an integrative conjugative element together with a related genomic island leads to cis mobilization and gene capture. *Mol. Microbiol.* 81, 912–925. doi: 10.1111/j.1365-2958.2011.07737.x

Botelho, J., Roberts, A. P., Leon-Sampedro, R., Grosso, F., and Peixe, L. (2018). Carbapenemases on the move: it's good to be on ICEs. *Mob. DNA* 9:37. doi: 10.1186/s13100-018-0141-4

Botelho, J., Grosso, F., and Peixe, L. (2019). Antibiotic resistance in *Pseudomonas aeruginosa* – mechanisms, epidemiology and evolution. *Drug Resist. Updat.* 44:100640. doi: 10.1016/j.drup.2019.07.002

Cai, J. C., Zhang, R., Hu, Y. Y., Zhou, H. W., and Chen, G. X. (2014). Emergence of *Escherichia coli* sequence type 131 isolates producing KPC-2 carbapenemase in China. *Antimicrob. Agents Chemother.* 58, 1146–1152. doi: 10.1128/AAC.00912-13

Camacho, C., Coulouris, G., Avagyan, V., Ma, N., Papadopoulos, J., Bealer, K., et al. (2009). BLAST+: architecture and applications. *BMC Bioinf.* 10:421. doi: 10.1186/1471-2105-10-421

Carraro, N., and Burrus, V. (2015). The dualistic nature of integrative and conjugative elements. *Mob. Genet. Ele.* 5, 98–102. doi: 10.1080/2159256X.2015.1102796

Chen, L., Hu, H., Chavda, K. D., Zhao, S., Liu, R., Liang, H., et al. (2014a). Complete sequence of a KPC-producing IncN multidrug-resistant plasmid from an epidemic *Escherichia coli* sequence type 131 strain in China. *Antimicrob. Agents Chemother.* 58, 2422–2425. doi: 10.1128/AAC.02587-13

Chen, L., Mathema, B., Chavda, K. D., DeLeo, F. R., Bonomo, R. A., and Kreiswirth, B. N. (2014b). Carbapenemase-producing *Klebsiella pneumoniae*: molecular and genetic decoding. *Trends Microbiol.* 22, 686–696. doi: 10.1016/j.tim.2014.09.003

Chen, Y. T., Lin, J. C., Fung, C. P., Lu, P. L., Chuang, Y. C., Wu, T. L., et al. (2014c). KPC-2-encoding plasmids from Escherichia coli and *Klebsiella pneumoniae* in Taiwan. *J. Antimicrob. Chemother.* 69, 628–631. doi: 10.1093/jac/dkt409

CLSI (2020). *Performance Standards for Antimicrobial Susceptibility Testing*. 30th Edn CLSI supplement M100. Wayne, PA, USA: Clinical and Laboratory Standards Institute.

Dai, X., Zhou, D., Xiong, W., Feng, J., Luo, W., Luo, G., et al. (2016). The IncP-6 plasmid p10265-KPC from *Pseudomonas aeruginosa* carries a novel DeltaISEc33-associated bla KPC-2 gene cluster. *Front. Microbiol.* 7:310. doi: 10.3389/fmicb.2016.00310

Garcillan-Barcia, M. P., Redondo-Salvo, S., Vielva, L., and de la Cruz, F. (2020). MOBscan: automated annotation of MOB relaxases. *Methods Mol. Biol.* 2075, 295–308. doi: 10.1007/978-1-4939-9877-7_21

Harmer, C. J., and Hall, R. M. (2015). IS26-mediated precise excision of the IS26-aphA1a translocatable unit. *MBio* 6:e01866-01815. doi: 10.1128/mBio.01866-15

Harmer, C. J., Moran, R. A., and Hall, R. M. (2014). Movement of IS26-associated antibiotic resistance genes occurs via a translocatable unit that includes a single IS26 and preferentially inserts adjacent to another IS26. *MBio* 5, e01801–e01814. doi: 10.1128/mBio.01801-14

He, S., Hickman, A. B., Varani, A. M., Siguier, P., Chandler, M., Dekker, J. P., et al. (2015). Insertion sequence IS26 reorganizes plasmids in clinically isolated multidrug-resistant bacteria by replicative transposition. *MBio* 6:e00762. doi: 10.1128/mBio.00762-15

Hong, J. S., Yoon, E. J., Lee, H., Jeong, S. H., and Lee, K. (2016). Clonal dissemination of *Pseudomonas aeruginosa* sequence type 235 isolates carrying blaIMP-6 and emergence of blaGES-24 and blaIMP-10 on novel genomic islands PAGI-15 and -16 in South Korea. *Antimicrob. Agents Chemother.* 60, 7216–7223. doi: 10.1128/AAC.01601-16

Horcajada, J. P., Montero, M., Oliver, A., Sorli, L., Luque, S., Gomez-Zorrilla, S., et al. (2019). Epidemiology and treatment of multidrug-resistant and extensively drug-resistant *Pseudomonas aeruginosa* infections. *Clin. Microbiol. Rev.* 32:e00031-19. doi: 10.1128/CMR.00031-19

Hu, F., Guo, Y., Yang, Y., Zheng, Y., Wu, S., Jiang, X., et al. (2019a). Resistance reported from China antimicrobial surveillance network (CHINET) in 2018. *Eur. J. Clin. Microbiol. Infect. Dis.* 38, 2275–2281. doi: 10.1007/s10096-019-03673-1

Hu, Y., Zhu, Y., Ma, Y., Liu, F., Lu, N., Yang, X., et al. (2015a). Genomic insights into intrinsic and acquired drug resistance mechanisms in *Achromobacter xylosoxidans*. *Antimicrob. Agents Chemother.* 59, 1152–1161. doi: 10.1128/AAC.04260-14

Hu, Y. Y., Gu, D. X., Cai, J. C., Zhou, H. W., and Zhang, R. (2015b). Emergence of KPC-2-producing *Pseudomonas aeruginosa* sequence type 463 isolates in Hangzhou, China. *Antimicrob. Agents Chemother.* 59, 2914–2917. doi: 10.1128/AAC.04903-14

Hu, Y. Y., Wang, Q., Sun, Q. L., Chen, G. X., and Zhang, R. (2019b). A novel plasmid carrying carbapenem-resistant gene bla KPC-2 in *Pseudomonas aeruginosa*. *Infect. Drug Resist.* 12, 1285–1288. doi: 10.2147/IDR.S196390

Johnson, C. M., and Grossman, A. D. (2015). Integrative and conjugative elements (ICEs): what they do and how they work. *Annu. Rev. Genet.* 49, 577–601. doi: 10.1146/annurev-genet-112414-055018

Jolley, K. A., Bray, J. E., and Maiden, M. C. J. (2018). Open-access bacterial population genomics: BIGSdb software, the PubMLST.org website and their applications. *Wellcome Open Res.* 3:124. doi: 10.12688/wellcomeopenres.14826.1

Kung, V. L., Ozer, E. A., and Hauser, A. R. (2010). The accessory genome of *Pseudomonas aeruginosa*. *Microbiol. Mol. Biol. Rev.* 74, 621–641. doi: 10.1128/MMBR.00027-10

Li, G., Zhang, Y., Bi, D., Shen, P., Ai, F., Liu, H., et al. (2015). First report of a clinical, multidrug-resistant Enterobacteriaceae isolate coharboring fosfomycin resistance gene fosA3 and carbapenemase gene blaKPC-2 on the same transposon, Tn1721. *Antimicrob. Agents Chemother.* 59, 338–343. doi: 10.1128/AAC.03061-14

Li, X., Xie, Y., Liu, M., Tai, C., Sun, J., Deng, Z., et al. (2018). oriTfinder: a web-based tool for the identification of origin of transfers in DNA sequences of bacterial mobile genetic elements. *Nucleic Acids Res.* 46, W229–W234. doi: 10.1093/nar/gky352

Liu, M., Li, X., Xie, Y., Bi, D., Sun, J., Li, J., et al. (2019). ICEberg 2.0: an updated database of bacterial integrative and conjugative elements. *Nucleic Acids Res.* 47, D660–D665. doi: 10.1093/nar/gky1123

Munoz-Price, L. S., Poirel, L., Bonomo, R. A., Schwaber, M. J., Daikos, G. L., Cormican, M., et al. (2013). Clinical epidemiology of the global expansion of *Klebsiella pneumoniae* carbapenemases. *Lancet Infect. Dis.* 13, 785–796. doi: 10.1016/S1473-3099(13)70190-7

Nascimento, A. P., Ortiz, M. F., Martins, W. M., Morais, G. L., Fehlberg, L. C., Almeida, L. G., et al. (2016). Intraclonal genome stability of the metallo-beta-lactamase SPM-1-producing *Pseudomonas aeruginosa* ST277, an endemic clone disseminated in Brazilian hospitals. *Front. Microbiol.* 7:1946. doi: 10.3389/fmicb.2016.01946

Partridge, S. R., Kwong, S. M., Firth, N., and Jensen, S. O. (2018). Mobile genetic elements associated with antimicrobial resistance. *Clin. Microbiol. Rev.* 31:e00088-17. doi: 10.1128/CMR.00088-17

Ravatn, R., Studer, S., Springael, D., Zehnder, A. J., and van der Meer, J. R. (1998a). Chromosomal integration, tandem amplification, and deamplification in *Pseudomonas putida* F1 of a 105-kilobase genetic element containing the chlorocatechol degradative genes from *Pseudomonas* sp. strain B13. *J. Bacteriol.* 180, 4360–4369. doi: 10.1128/JB.180.17.4360-4369.1998

Ravatn, R., Studer, S., Zehnder, A. J., and van der Meer, J. R. (1998b). Int-B13, an unusual site-specific recombinase of the bacteriophage P4 integrase family, is responsible for chromosomal insertion of the 105-kilobase clc element of *Pseudomonas* sp. strain B13. *J. Bacteriol.* 180, 5505–5514. doi: 10.1128/JB.180.21.5505-5514.1998

Roy Chowdhury, P., Scott, M. J., and Djordjevic, S. P. (2017). Genomic islands 1 and 2 carry multiple antibiotic resistance genes in *Pseudomonas aeruginosa* ST235, ST253, ST111 and ST175 and are globally dispersed. *J. Antimicrob. Chemother.* 72, 620–622. doi: 10.1093/jac/dkw471

Seemann, T. (2014). Prokka: rapid prokaryotic genome annotation. *Bioinformatics* 30, 2068–2069. doi: 10.1093/bioinformatics/btu153

Shen, P., Wei, Z., Jiang, Y., Du, X., Ji, S., Yu, Y., et al. (2009). Novel genetic environment of the carbapenem-hydrolyzing beta-lactamase KPC-2 among Enterobacteriaceae in China. *Antimicrob. Agents Chemother.* 53, 4333–4338. doi: 10.1128/AAC.00260-09

Shi, L., Liang, Q., Feng, J., Zhan, Z., Zhao, Y., Yang, W., et al. (2018). Coexistence of two novel resistance plasmids, blaKPC-2-carrying p14057A and tetA(A)-carrying p14057B, in *Pseudomonas aeruginosa*. *Virulence* 9, 306–311. doi: 10.1080/21505594.2017.1372082

Smillie, C., Garcillan-Barcia, M. P., Francia, M. V., Rocha, E. P., and de la Cruz, F. (2010). Mobility of plasmids. *Microbiol. Mol. Biol. Rev.* 74, 434–452. doi: 10.1128/MMBR.00020-10

Tacconelli, E., Carrara, E., Savoldi, A., Harbarth, S., Mendelson, M., Monnet, D. L., et al. (2018). Discovery, research, and development of new antibiotics: the WHO priority list of antibiotic-resistant bacteria and tuberculosis. *Lancet Infect. Dis.* 18, 318–327. doi: 10.1016/S1473-3099(17)30753-3

van Duin, D., and Doi, Y. (2017). The global epidemiology of carbapenemase-producing Enterobacteriaceae. *Virulence* 8, 460–469. doi: 10.1080/21505594.2016.1222343

Varani, A., He, S., Siguier, P., Ross, K., and Chandler, M. (2021). The IS6 family, a clinically important group of insertion sequences including IS26. *Mob. DNA* 12:11. doi: 10.1186/s13100-021-00239-x

Wick, R. R., Judd, L. M., Gorrie, C. L., and Holt, K. E. (2017). Unicycler: resolving bacterial genome assemblies from short and long sequencing reads. *PLoS Comput. Biol.* 13:e1005595. doi: 10.1371/journal.pcbi.1005595

Wozniak, R. A., and Waldor, M. K. (2010). Integrative and conjugative elements: mosaic mobile genetic elements enabling dynamic lateral gene flow. *Nat. Rev. Microbiol.* 8, 552–563. doi: 10.1038/nrmicro2382

Wurdemann, D., and Tummler, B. (2007). In silico comparison of pKLC102-like genomic islands of *Pseudomonas aeruginosa*. *FEMS Microbiol. Lett.* 275, 244–249. doi: 10.1111/j.1574-6968.2007.00891.x

Yu, G. (2020). Using ggtree to visualize data on tree-like structures. *Curr. Protoc. Bioinformatics* 69:e96. doi: 10.1002/cpbi.96

Zankari, E., Hasman, H., Cosentino, S., Vestergaard, M., Rasmussen, S., Lund, O., et al. (2012). Identification of acquired antimicrobial resistance genes. *J. Antimicrob. Chemother.* 67, 2640–2644. doi: 10.1093/jac/dks261

Conflict of Interest: The authors declare that the research was conducted in the absence of any commercial or financial relationships that could be construed as a potential conflict of interest.

frontiers in Microbiology

ORIGINAL RESEARCH
published: 21 July 2021
doi: 10.3389/fmicb.2021.698478

Complete Genome Sequences of Two Novel KPC-2-Producing IncU Multidrug-Resistant Plasmids From International High-Risk Clones of *Escherichia coli* in China

Wenhao Wu[1,2†], Lingling Lu[3†], Wenjia Fan[1], Chun Chen[4], Dazhi Jin[5], Hongying Pan[1] and Xi Li[5*]*

[1] Department of Infectious Diseases, Zhejiang Provincial People's Hospital, People's Hospital of Hangzhou Medical College, Hangzhou, China, [2] Medical College, Qingdao University, Qingdao, China, [3] Adicon Clinical Laboratories, Hangzhou, China, [4] Department of Pneumology, Zhejiang Provincial People's Hospital, People's Hospital of Hangzhou Medical College, Hangzhou, China, [5] Centre of Laboratory Medicine, Zhejiang Provincial People's Hospital, People's Hospital of Hangzhou Medical College, Hangzhou, China

The rapidly increasing prevalence of *Klebsiella pneumoniae* carbapenemase 2 (KPC-2)-producing bacteria has become a serious challenge to public health. Currently, the bla_{KPC-2} gene is mainly disseminated through plasmids of different sizes and replicon types. However, the plasmids carrying the bla_{KPC-2} gene have not been fully characterized. In this study, we report the complete genome sequences of two novel bla_{KPC-2}-harboring incompatibility group U (IncU) plasmids, pEC2341-KPC and pEC2547-KPC, from international high-risk clones of *Escherichia coli* isolated from Zhejiang, China. Two KPC-2-producing *E. coli* isolates (EC2341 and EC2547) were collected from clinical samples. Whole-genome sequencing (WGS) analysis indicated that EC2341 and EC2547 belonged to the ST410 and ST131 clones, respectively. S1-nuclease pulsed-field gel electrophoresis (S1-PFGE), Southern blot and conjugation experiments confirmed the presence of the bla_{KPC-2} gene on the pEC2341-KPC plasmid and that this was a conjugative plasmid, while the bla_{KPC-2} gene on the pEC2547-KPC plasmid was a non-conjugative plasmid. In addition, plasmid analysis further revealed that the two bla_{KPC-2}-harboring plasmids have a close evolutionary relationship. To the best of our knowledge, this is the first report of *E. coli* strains carrying the bla_{KPC-2} gene on IncU plasmids. The emergence of the IncU-type bla_{KPC-2}-positive plasmid highlights further dissemination of bla_{KPC-2} in *Enterobacteriaceae*. Therefore, effective measures should be taken immediately to prevent the spread of these bla_{KPC-2}–positive plasmids.

Keywords: *E. coli*, KPC-2, IncU plasmid, high-risk clones, whole genome sequencing

OPEN ACCESS

Edited by:
Yi-Wei Tang,
Cepheid, United States

Reviewed by:
Jeong Hwan Shin,
Inje University Busan Paik Hospital, South Korea
Charles William Stratton,
Vanderbilt University Medical Center, United States

****Correspondence:***
Xi Li
lixi_0611@163.com
Hongying Pan
hypanzjsrmyy@126.com

† These authors have contributed equally to this work and share first authorship

Specialty section:
This article was submitted to Antimicrobials, Resistance and Chemotherapy, a section of the journal Frontiers in Microbiology

Received: *21 April 2021*
Accepted: *23 June 2021*
Published: *21 July 2021*

Citation:
Wu W, Lu L, Fan W, Chen C, Jin D, Pan H and Li X (2021) Complete Genome Sequences of Two Novel KPC-2-Producing IncU Multidrug-Resistant Plasmids From International High-Risk Clones of Escherichia coli in China. Front. Microbiol. 12:698478. doi: 10.3389/fmicb.2021.698478

INTRODUCTION

The rapidly increasing prevalence of KPC-producing bacteria has become a serious challenge to public health (Suay-García and Pérez-Gracia, 2019). At the time of writing (April 2021), 82 variants of KPC enzymes (KPC-1 to KPC-82) have been identified among gram-negative bacteria worldwide[1]. Among these carbapenemases, KPC-2 was first identified from a *Klebsiella pneumoniae* strain in the United States in 2003 (Smith Moland et al., 2003) and attracted extensive attention because of its rapid worldwide dissemination. Currently, the bla_{KPC-2} gene is prevalent in *K. pneumoniae* strains, and the sequence type 258 (ST258) clone has successfully spread worldwide (Munoz-Price et al., 2013).

Although not as common as in *K. pneumoniae*, the bla_{KPC-2} gene has also been identified in *Escherichia coli* strains. Some reports, including two from our group, have recently found that the bla_{KPC-2} gene was present in the ST131-type *E. coli* strains, which are international multidrug-resistant high-risk clones (Du et al., 2020; Wang et al., 2020). KPC-2-producing *E. coli* strains were isolated not only from humans but also from animals, such as cattle (Vikram and Schmidt, 2018), swine (Liu et al., 2018) and cats (Sellera et al., 2018). Unfortunately, bla_{KPC-2} has also been identified in environmental samples [urban rivers (Xu et al., 2015), drinking water (Mahmoud et al., 2020), and vegetables (Wang et al., 2018)], indicating its presence in the environment. In addition, bla_{KPC-2} was further disseminated through plasmids of different sizes and replicon types (Mathers et al., 2017), such as the pKpQIL-like plasmid (Chen et al., 2014b), the IncFIA plasmid (Chen et al., 2014a), the IncI2 plasmid (Chen et al., 2013), the IncX3 plasmid (Fuga et al., 2020), the IncP-6 plasmid (Hu et al., 2019) and the IncN plasmid (Schweizer et al., 2019). The movement of bla_{KPC} plasmids into *E. coli* strains that are known pathogens of urinary tract and intra-abdominal infections raises clinical concerns (Bratu et al., 2007). Plasmid transfer will further lead to continued spread of resistance and limit clinical treatment options (Chen et al., 2014). However, plasmids carrying the bla_{KPC-2} gene have not been fully characterized.

In the present study, we reported the complete sequences of two novel bla_{KPC-2}-harboring IncU plasmids from international high-risk clones of *E. coli* ST131 and ST410 isolates from China. In addition, the whole genome sequence revealed that the two bla_{KPC-2}-positive plasmids have a close evolutionary relationship.

MATERIALS AND METHODS

Bacterial Strains

In a retrospective study, 109 carbapenem-resistant *Enterobacteriaceae* strains were isolated from June 2018 to September 2019. Common carbapenemase genes (bla_{KPC}, bla_{NDM}, bla_{VIM}, and bla_{IMP}) were amplified, and the positive products were sequenced. Two KPC-2-producing *E. coli* strains were included in this study and further identified by the VITEK MS system (bioMérieux, Marcy-l'Etoile, France).

Antimicrobial Susceptibility Testing

Antimicrobial susceptibility testing was carried out using the broth microdilution method according to the protocol of CLSI guidelines (CLSI, 2020). Minimum inhibitory concentrations (MICs) were interpreted according to the guideline document established by Clinical and Laboratory Standards Institute (CLSI, 2020). For tigecycline and polymyxin E, the MIC results were categorized in accordance with the breakpoints defined by the European Committee on Antimicrobial Susceptibility Testing criteria[2]. *E. coli* ATCC 25922 was used as a quality control strain.

S1-PFGE and Southern Blot Hybridization

The plasmid location of the bla_{KPC-2} gene was determined by Southern blot experiments according to the previous study (Wang et al., 2020). Briefly, whole chromosomal DNA was digested with S1-nuclease (TaKaRa, Japan). The digested fragments were electrophoresed on a CHEF-mapper XA pulsed-field gel electrophoresis (PFGE) system (Bio-Rad, United States) for 18 h at 14°C. The DNA fragments were transferred to a positively charged nylon membrane (Millipore, United States) and then hybridized with a digoxigenin-labeled bla_{KPC-2}-specific probe. The fragments was detected by an NBT/BCIP color detection kit (Roche, Germany). The *Salmonella enterica* serotype *Braenderup* H9812 was used as the size marker.

Conjugation Experiments

A filter-mating experiment was performed with *E. coli* J53 as the recipient strain and bla_{KPC-2}-positive isolates as the donor strains. Transconjugants were selected on Mueller-Hinton agar plates supplemented with 300 mg/L sodium azide and 100 mg/L ampicillin. The transconjugants were confirmed by PCR sequencing and antimicrobial susceptibility testing.

Whole Genome Sequencing and Plasmid Analysis

Total genomic DNA extraction and analysis were carried out according to previously described methods (Wang et al., 2020). Briefly, the QIAamp DNA MiniKit (Qiagen, Valencia, CA, United States) was used to extract the genomic DNA of two strains for genome sequencing. A NextEra XT DNA library preparation kit (Illumina, Inc., Cambridge, United Kingdom) was used to prepare the DNA library. Genomic DNA was sequenced on an Illumina HiSeq^{TM} 4000 instrument with a 150-bp paired-end approach at a depth of approximately 200×. The CLC Genomics Workbench 10.0 was used to assemble the raw reads of the strains into draft genomes using. In addition, a Pacific Biosciences RSII DNA sequencing system (PacBio, Menlo Park, CA, United States) was used to obtain the complete genomes of strains EC2341 and EC2547. The resulting sequences were *de novo* assembled using the Hierarchical Genome Assembly Process (HGAP_Assembly.2) with the default settings of the SMRT Analysis v2.3.0 software package.

[1]http://www.ncbi.nlm.nih.gov/pathogens/submit_beta_lactamase/

[2]http://www.eucast.org/clinical_breakpoints

The Rapid Annotation using Subsystems Technology (RAST) annotation website server[3] was used to annotate the genomes. A schematic map of the linear comparison of the two bla_{KPC-2}-positive plasmids and their related plasmids was generated with EasyFig 2.2.2 (Sullivan et al., 2011). Multi-locus sequence typing (MLST) of the strain and incompatibility typing of the bla_{KPC-2}-positive plasmid were performed with the assistance of the PlasmidFinder-1.3 server and the MLST 2.0 server, which are available at the Center for Genomic Epidemiology[4].

In addition, plasmid stability was determined according to a previous study (Li et al., 2018).

Nucleotide Sequence Accession Number

The complete sequences of the plasmids pEC2341-KPC (accession number CP072979) and pEC2547-KPC (accession number CP072981) were deposited in DDBJ/EMBL/GenBank.

RESULTS AND DISCUSSION

Isolate Characteristics

In the present study, two KPC-2-producing isolates were collected from a teaching hospital in Zhejiang, China. *E. coli* strains EC2341 and EC2547 were isolated from urine and sputum, respectively. The antimicrobial susceptibility testing results showed that the bla_{KPC-2}-positive isolates were resistant to carbapenems, cephalosporins, amoxicillin/clavulanate, ciprofloxacin, and amikacin but were susceptible to colistin, tigecycline and ceftazidime-avibactam (**Table 1**).

The MLST results showed that *E. coli* strains EC2547 and EC2341 belonged to ST131 and ST410, respectively. The ST131 clone-type *E. coli* strain emerged in the mid-2000s and has spread worldwide (Can et al., 2015). Similar to clone lineage of ST131, the *E. coli* ST410 strain has been confirmed as another successful clone in *E. coli* (Schaufler et al., 2016). Furthermore, these two clone-type *E. coli* strains have gained a further selective advantage due to acquisition of carbapenem resistance (Du et al., 2020; Lee and Choi, 2020). In addition, other resistance genes, such as $bla_{CTX-M-3}$, $bla_{CTX-M-27}$, *fosA3*, and *qnrS1*, were also detected in the *E. coli* strains by analysis of the genome sequences. Multiple resistance genes were identified in the ST410 and ST131 strains, indicating that these two clone-type strains might be more capable of acquiring resistance genes.

Notably, these two international high-risk clones have caused a wide variety of clinical infections (Roer et al., 2018; Wang et al., 2020) and are associated with treatment failure because of their high virulence potential (Can et al., 2015). In the present study, multiple potential virulence factors were identified by VirulenceFinder analysis of *E. coli* EC2341 and EC2547 strains, such as *ompA* (outer membrane protein A), *fdeC* (adhesin), and *fepC* (iron-enterobactin transporter). bla_{KPC-2} was present in the ST131 and ST410 strains, further supporting the results that these two clone types may become a successful lineage of KPC-2-producing *E. coli* strains.

[3]https://rast.nmpdr.org/

[4]http://www.genomicepidemiology.org/

IncU-Type Plasmid Carrying the bla_{KPC-2} Gene

To ascertain the plasmid location of the bla_{KPC-2} gene, S1-PFGE was performed followed by Southern blot experiments. The bla_{KPC-2} gene was located on two plasmids of different sizes, ca. 80 Kb and ca. 100 Kb (data not shown). The transferability of the two bla_{KPC-2}-positive plasmids was further determined by filter mating experiments. The EC2341 isolate tested could successfully transfer its carbapenem-resistance to *E. coli* strain J53 (**Table 1**), while the EC2547 isolate could not transfer its carbapenem resistance. Additionally, the bla_{KPC-2}-positive plasmids were both stable in the two isolates by plasmid stability experiments. In the absence of antibiotics, the randomly selected strains all carried the bla_{KPC-2}-positive plasmid that was identical to the parental isolate after 12 rounds of subculture on MH agar.

Incompatibility plasmid classification showed that the two bla_{KPC-2}-positive plasmids were both grouped into IncU replicon types. The IncU plasmid incompatibility group was assigned in 1981 (Sirgel et al., 1981) and is a unique group of mobile elements with highly conserved backbone functions and variable antibiotic resistance gene cassettes (Tschäpe et al., 1981; Rhodes et al., 2000). The IncU incompatibility group has been isolated from a number of *Aeromonas* spp. and *E. coli* strains from natural and clinical environments (Tschäpe et al., 1981; Sandaa and Enger, 1994; Adams et al., 1998; Rhodes et al., 2000). Various resistance genes have also been described for IncU plasmids, such as *qnrS2*, *aac(6′)-Ib-cr*, *aadA1* and *aadA2, sulI* and *sulII, dfrA16 dfrIIc (dfrB3)* and *catAII* (Sørum et al., 2003). However, carbapenem-resistant IncU plasmids have not been found previously. In this study, the bla_{KPC-2} gene was confirmed to be carried on the IncU plasmids. To the best of our knowledge, this is the first report of *E. coli* strains carrying the bla_{KPC-2} gene on IncU plasmids. Our study further demonstrated that plasmids harboring the bla_{KPC-2} gene were diverse.

Sequence Analysis of bla_{KPC-2} IncU Plasmids

Two entire sequences were obtained to further characterize the IncU plasmids carrying bla_{KPC-2}. Sequence analysis showed that plasmid pEC2341_KPC was 76,952 bp in size, had 51.9% G + C content, and harbored 133 predicted ORFs (**Figure 1A**). The core region of pEC2341_KPC includes a replication module (*repE*), one transfer (*tra*) system, and a stability operon (*stbAB* and *umuCD*). Four antimicrobial resistance genes, *qnrS1*, $bla_{CTX-M-13}$, bla_{TEM-1}, and *drfA14*, were detected in this plasmid except for the bla_{KPC-2} gene. In addition, a class 1 integron-like element was also detected in this plasmid. The element is a *dfrA14* gene with its 3′-conserved sequence truncated by the insertion of an *IS*6100 element. Sequence alignments revealed that the plasmid sequences were almost identical to those previously reported plasmids pECN-580 (KF914891) of *E. coli* ECN580 (97% coverage, 99.97% identity) in China (Chen et al., 2014c) and pCRKP-1-KPC (KX928750) of *K. pneumoniae* CRKP-1-KPC (96% coverage, 99.90% identity) in China (unpublished data) (**Figure 2**).

Plasmid pEC2547 contained bla_{KPC-2} and was 94,462 bp in size, with an average G + C content of 49.3% (**Figure 1B**). Compared with plasmid pEC2341_KPC, two other antimicrobial resistance genes, *aar-3* and *acc(6′)Ib*, were identified in this plasmid. Two class 1 integron-like elements were identified in pEC2547_KPC. The first element is same as that in pEC2341_KPC. The second element is an *IntI1-aac(6′)-Ib-cr-aar-3-Tn3* gene cassette located downstream of the bla_{KPC-2} gene.

TABLE 1 | Antibiotic susceptibility used in this study (mg/L).

Strains	AMC	FEP	CAZ	ETP	IPM	MEM	CZA	AMK	CIP	TGC	CST
EC2341	128	>128	>128	64	8	16	0.25	4	>128	<0.0625	0.125
EC2341-J53	64	>128	32	64	4	8	<0.125	4	1	<0.0625	0.25
EC2547	128	>128	>128	>64	8	32	0.125	8	>128	<0.0625	0.125
E. coli ATCC 25922	4	0.125	0.125	0.125	0.125	0.125	<0.125	0.5	0.125	0.125	0.125

Drug susceptibility was determined with broth microdilution method according to the Clinical Laboratory Standards Institute (CLSI) guidelines. AMC, amoxicillin clavulanate; FEP, cefepime; CAZ, ceftazidime; ETP, ertapenem; IPM, imipenem; MEM, meropenem; CZA, ceftazidime-avibactam; AMK, amikacin; CIP, ciprofloxacin; TGC, tigecycline; CST, colistin.

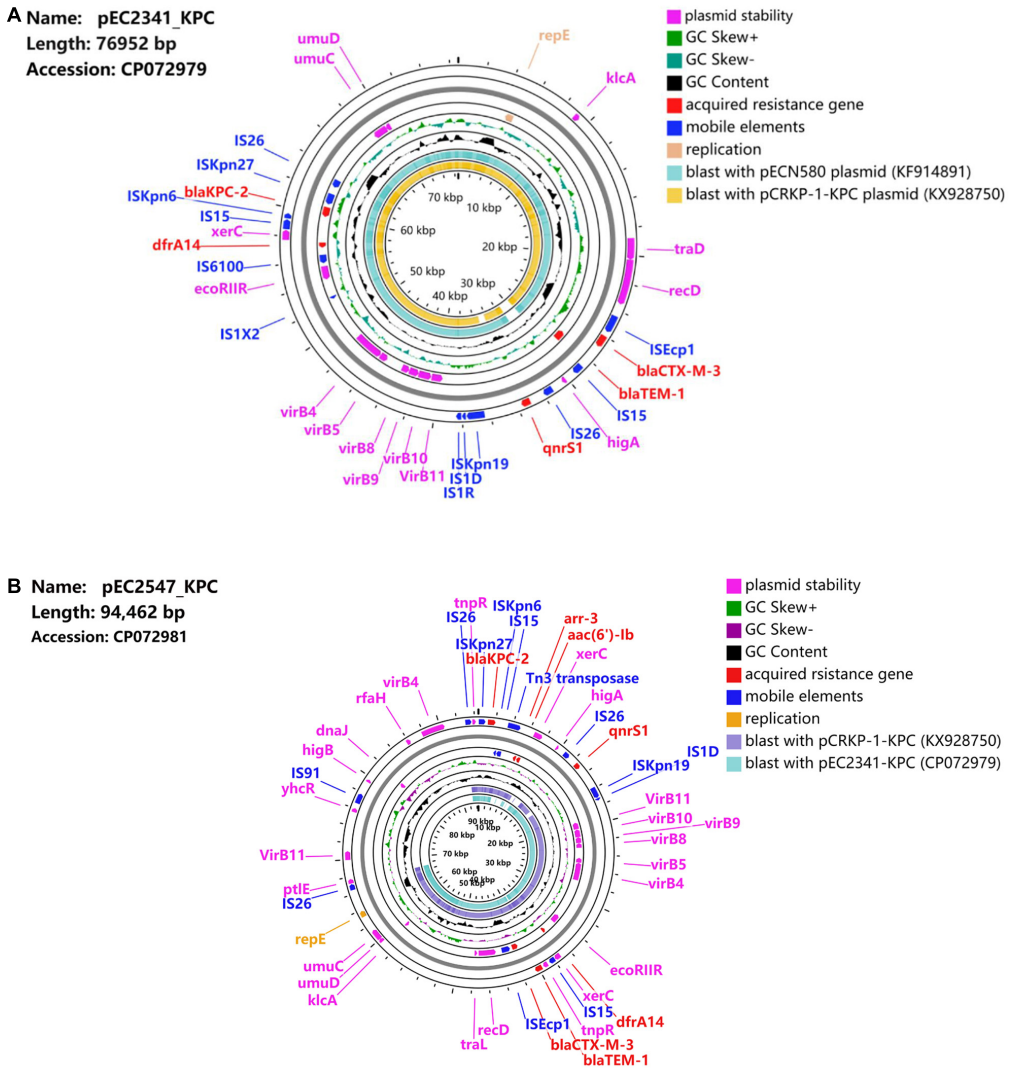

FIGURE 1 | (A) Schematic map of plasmid pEC2341_KPC. Sequence alignment between pECN580 (accession number KF914891) and pCRKP-1-KPC (accession number KX928750) is the outer circle in orange and teal. **(B)** Schematic map of plasmid pEC2547_KPC. Sequence alignment between pEC2341-KPC (accession number CP072979) and pCRKP-1-KPC (accession number KX928750) is the outer circle in teal and blue.

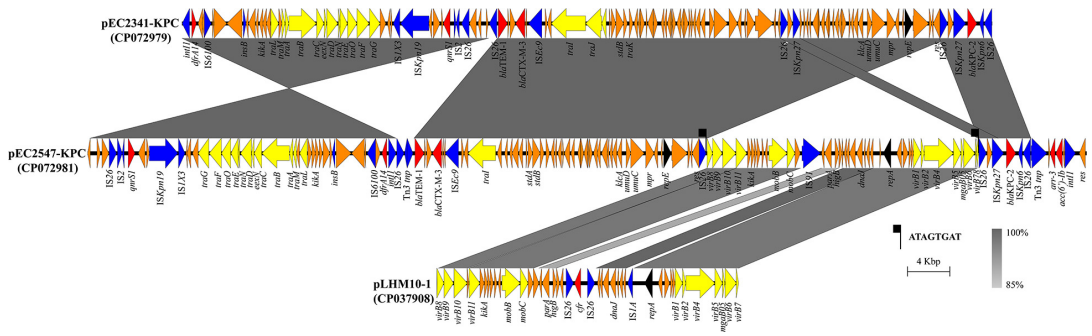

FIGURE 2 | Linear characterization of the plasmids pEC2341-KPC and pEC2547-KPC with closely related plasmid. The gray regions between plasmids indicate nucleotide identity (85–100%) by BLASTn. Arrows indicate predicted ORFs. Primary structural characteristics of plasmids pEC2341-KPC (CP072979), pEC2547-KPC (CP072981), and pLHM10-1 (CP037908). Colored arrows represent open reading frames, with red, yellow, blue, and orange representing antibiotic resistance gene, plasmid transfer related genes, mobile elements and common function genes, respectively.

Notably, sequencing analysis further indicated that pEC2547 might evolve from plasmid pEC2341_KPC of *E. coli* EC2341 (67% coverage, 100% identity) (**Figure 2**). Compared with plasmid pEC2341_KPC, an approximately 24-kb sequence flanked by two *IS*26 elements was carried on plasmid pEC2547, which resulted in disruption of the transfer systems of this plasmid. Consistent with our conjugate transfer results, the EC2547 isolate could not transfer its carbapenem resistance to *E. coli* strain J53. The 24-kb sequence was further aligned to an unnamed plasmid of *E. coli* strain LHM10-1 (GenBank accession number CP037908) with 89% coverage and 96.52% identity. This 24-kb composite transposon-like element flanking with two IS26 elements undergoes replicative transposition by the 8-bp target site duplication (TSD) (ATAGTGAT). *IS*26 elements have been demonstrated to undergo frequent intramolecular transposition and facilitate recombination between the plasmid or the chromosome (He et al., 2015). These findings suggest that the plasmid pEC2547 was composed of the pEC2341_KPC plasmid and an unnamed plasmid of *E. coli* strain LHM10-1, which was a composite transposon formed by *IS*26 (**Figure 2**).

In addition, the bla_{KPC-2} gene carried on the two plasmids was preceded by *IS*26, *IS*Kpn27, and *IS*Kpn6, and followed by *IS*26. In China, bla_{KPC-2} genetic environments can be classified into three main types: Tn4401 with the *IS*Kpn7-bla_{KPC-2}-*IS*Kpn6 core structure, Tn1722-based unit transposons with the *IS*Kpn27-bla_{KPC-2}-*IS*Kpn6 core structure and *IS*26-based composite transposons with the *IS*Kpn27-bla_{KPC-2}-*IS*Kpn6 core structure (Wang et al., 2015). In this study, bla_{KPC-2} genes were both located in an approximately 5-kb composite transposon-like element with the *IS*Kpn27 insertion sequence upstream and the *IS*Kpn6 insertion sequence downstream of the element and flanked by two IS26 elements bracketed by *IS*26, which belonged to the *IS*26-based composite transposon. *IS*26-based composite transposons are mainly carried by IncN-type plasmids. Our plasmids belonged to the IncU type, which led to speculation that the *IS*26 elements may promote recombination between the plasmids and explain the movement of the new IncU regions.

CONCLUSION

Overall, we describe here the complete sequences of two novel bla_{KPC-2}-positive IncU plasmids from *E. coli* isolates. The two bla_{KPC-2}-harboring plasmids have a close evolutionary relationship, which highlighted the diversity of these highly promiscuous plasmids. The spread of bla_{KPC-2} harboring multidrug-resistant plasmids, e.g., pEC2341-KPC and pEC2547-KPC, into the international high-risk clones *E. coli* ST131 and ST410, presents tremendous challenges for clinicians. It is important for the IncU-type plasmid to further disseminate bla_{KPC-2} in *Enterobacteriaceae* in order for it to be maintained. Therefore, effective measures should be taken immediately to prevent the spread of these bla_{KPC-2}–positive plasmids.

DATA AVAILABILITY STATEMENT

The complete sequences of the plasmids pEC2341-KPC (accession number CP072979) and pEC2547-KPC (accession number CP072981) were deposited in DDBJ/EMBL/GenBank).

ETHICS STATEMENT

The Ethics Committee of the Zhejiang Provincial People's Hospital exempted this study from review because the present study focused on bacteria.

AUTHOR CONTRIBUTIONS

XL and HP conceived and designed the experiments. WW, LL, and WF performed the experiments. CC and DJ analyzed the data. WW and XL wrote the manuscript. All authors read and approved the final manuscript.

FUNDING

This study was supported by the Public Technology Research Projects of Zhejiang Province, China (LGD21H190001), Natural Science Foundation of Zhejiang Province, China (Q18H010007), and Medical and Health Research Project (2020KY420). The funders had no role in study design, data collection and analysis, decision to publish, or preparation of the manuscript.

REFERENCES

Adams, C. A., Austin, B., Meaden, P. G., and Mcintosh, D. (1998). Molecular characterization of plasmid-mediated oxytetracycline resistance in *Aeromonas salmonicida*. *Appl. Environ. Microbiol.* 64, 4194–4201. doi: 10.1128/aem.64.11.4194-4201.1998

Bratu, S., Brooks, S., Burney, S., Kochar, S., Gupta, J., Landman, D., et al. (2007). Detection and spread of *Escherichia coli* possessing the plasmid-borne carbapenemase KPC-2 in Brooklyn, New York. *Clin. Infect. Dis.* 44, 972–975. doi: 10.1086/512370

Can, F., Azap, O. K., Seref, C., Ispir, P., Arslan, H., and Ergonul, O. (2015). Emerging *Escherichia coli* O25b/ST131 clone predicts treatment failure in urinary tract infections. *Clin. Infect. Dis.* 60, 523–527. doi: 10.1093/cid/ciu864

Chen, L., Chavda, K. D., Al Laham, N., Melano, R. G., Jacobs, M. R., Bonomo, R. A., et al. (2013). Complete nucleotide sequence of a bla_{KPC}-harboring IncI2 plasmid and its dissemination in New Jersey and New York hospitals. *Antimicrob. Agents Chemother.* 57, 5019–5025. doi: 10.1128/aac.01397-13

Chen, L., Chavda, K. D., Melano, R. G., Hong, T., Rojtman, A. D., Jacobs, M. R., et al. (2014a). Molecular survey of the dissemination of two bla_{KPC}-harboring IncFIA plasmids in New Jersey and New York hospitals. *Antimicrob. Agents Chemother.* 58, 2289–2294. doi: 10.1128/aac.02749-13

Chen, L., Chavda, K. D., Melano, R. G., Jacobs, M. R., Koll, B., Hong, T., et al. (2014b). Comparative genomic analysis of KPC-encoding pKpQIL-like plasmids and their distribution in New Jersey and New York Hospitals. *Antimicrob. Agents Chemother.* 58, 2871–2877. doi: 10.1128/aac.00120-14

Chen, L., Hu, H., Chavda, K. D., Zhao, S., Liu, R., Liang, H., et al. (2014c). Complete sequence of a KPC-producing IncN multidrug-resistant plasmid from an epidemic *Escherichia coli* sequence type 131 strain in China. *Antimicrob. Agents Chemother.* 58, 2422–2425. doi: 10.1128/aac.02587-13

Chen, L., Mathema, B., Chavda, K. D., Deleo, F. R., Bonomo, R. A., and Kreiswirth, B. N. (2014). Carbapenemase-producing *Klebsiella pneumoniae*: molecular and genetic decoding. *Trends Microbiol.* 22, 686–696. doi: 10.1016/j.tim.2014.09.003

CLSI (2020). *Performance Standards for Antimicrobial Susceptibility Testing CLSI Supplement M100*, 30th Edn. Wayne, PA: Clinical and Laboratory Standards Institute.

Du, X., Huang, J., Wang, D., Zhu, Y., Lv, H., and Li, X. (2020). Whole genome sequence of an *Escherichia coli* ST131 strain isolated from a patient with bloodstream infection in China co-harbouring bla(KPC-2), bla(CTX-M-3), bla(CTX-M-14), qnrS1, aac(3)-IIa and aac(6′)-Ib-cr genes. *J. Glob. Antimicrob. Resist.* 22, 700–702. doi: 10.1016/j.jgar.2020.06.027

Fuga, B., Ferreira, M. L., Cerdeira, L. T., De Campos, P. A., Dias, V. L., Rossi, I., et al. (2020). Novel small IncX3 plasmid carrying the *bla*(KPC-2) gene in high-risk *Klebsiella pneumoniae* ST11/CG258. *Diagn. Microbiol. Infect. Dis.* 96:114900. doi: 10.1016/j.diagmicrobio.2019.114900

He, S., Hickman, A. B., Varani, A. M., Siguier, P., Chandler, M., Dekker, J. P., et al. (2015). Insertion sequence IS26 reorganizes plasmids in clinically isolated multidrug-resistant bacteria by replicative transposition. *mBio* 6:e00762.

Hu, X., Yu, X., Shang, Y., Xu, H., Guo, L., Liang, Y., et al. (2019). Emergence and characterization of a novel IncP-6 plasmid harboring *bla* (KPC-2) and *qnrS2* genes in *Aeromonas taiwanensis* isolates. *Front. Microbiol.* 10:2132. doi: 10.3389/fmicb.2019.02132

Lee, M., and Choi, T. J. (2020). Species transferability of *Klebsiella pneumoniae* Carbapenemase-2 isolated from a high-risk clone of *Escherichia coli* ST410. *J. Microbiol. Biotechnol.* 30, 974–981. doi: 10.4014/jmb.1912.12049

Li, X., Fu, Y., Shen, M., Huang, D., Du, X., Hu, Q., et al. (2018). Dissemination of *bla*(NDM-5) gene via an IncX3-type plasmid among non-clonal *Escherichia coli* in China. *Antimicrob. Resist. Infect. Control* 7:59.

Liu, X., Liu, H., Wang, L., Peng, Q., Li, Y., Zhou, H., et al. (2018). Molecular characterization of extended-spectrum β-lactamase-producing multidrug resistant *Escherichia coli* from Swine in Northwest China. *Front. Microbiol.* 9:1756. doi: 10.3389/fmicb.2018.01756

Mahmoud, N. E., Altayb, H. N., and Gurashi, R. M. (2020). Detection of carbapenem-resistant genes in *Escherichia coli* isolated from drinking water in khartoum, Sudan. *J. Environ. Public Health* 2020:2571293.

Mathers, A. J., Stoesser, N., Chai, W., Carroll, J., Barry, K., Cherunvanky, A., et al. (2017). Chromosomal integration of the *Klebsiella pneumoniae* carbapenemase gene, *bla*(KPC), in klebsiella species is elusive but not rare. *Antimicrob. Agents Chemother.* 61:e01823-16.

Munoz-Price, L. S., Poirel, L., Bonomo, R. A., Schwaber, M. J., Daikos, G. L., Cormican, M., et al. (2013). Clinical epidemiology of the global expansion of *Klebsiella pneumoniae* carbapenemases. *Lancet Infect. Dis.* 13, 785–796. doi: 10.1016/s1473-3099(13)70190-7

Rhodes, G., Huys, G., Swings, J., Mcgann, P., Hiney, M., Smith, P., et al. (2000). Distribution of oxytetracycline resistance plasmids between aeromonads in hospital and aquaculture environments: implication of Tn1721 in dissemination of the tetracycline resistance determinant *tet A*. *Appl. Environ. Microbiol.* 66, 3883–3890. doi: 10.1128/aem.66.9.3883-3890.2000

Roer, L., Overballe-Petersen, S., Hansen, F., Schønning, K., Wang, M., Røder, B. L., et al. (2018). *Escherichia coli* sequence type 410 is causing new international high-risk clones. *mSphere* 3:e00337-18.

Sandaa, R. A., and Enger, O. (1994). Transfer in marine sediments of the naturally occurring plasmid pRAS1 encoding multiple antibiotic resistance. *Appl. Environ. Microbiol.* 60, 4234–4238. doi: 10.1128/aem.60.12.4234-4238.1994

Schaufler, K., Semmler, T., Wieler, L. H., Wöhrmann, M., Baddam, R., Ahmed, N., et al. (2016). Clonal spread and interspecies transmission of clinically relevant ESBL-producing *Escherichia coli* of ST410–another successful pandemic clone? *FEMS Microbiol. Ecol.* 92:fiv155. doi: 10.1093/femsec/fiv155

Schweizer, C., Bischoff, P., Bender, J., Kola, A., Gastmeier, P., Hummel, M., et al. (2019). Plasmid-mediated transmission of KPC-2 carbapenemase in *Enterobacteriaceae* in critically Ill patients. *Front. Microbiol.* 10:276. doi: 10.3389/fmicb.2019.00276

Sellera, F. P., Fernandes, M. R., Ruiz, R., Falleiros, A. C. M., Rodrigues, F. P., Cerdeira, L., et al. (2018). Identification of KPC-2-producing *Escherichia coli* in a companion animal: a new challenge for veterinary clinicians. *J. Antimicrob. Chemother.* 73, 2259–2261.

Sirgel, F. A., Coetzee, J. N., Hedges, R. W., and Lecatsas, G. (1981). Phage C-1: an IncC group; plasmid-specific phage. *J. Gen. Microbiol.* 122, 155–160. doi: 10.1159/000149385

Smith Moland, E., Hanson, N. D., Herrera, V. L., Black, J. A., Lockhart, T. J., Hossain, A., et al. (2003). Plasmid-mediated, carbapenem-hydrolysing beta-lactamase, KPC-2, in *Klebsiella pneumoniae* isolates. *J. Antimicrob. Chemother.* 51, 711–714. doi: 10.1093/jac/dkg124

Sørum, H., L'abée-Lund, T. M., Solberg, A., and Wold, A. (2003). Integron-containing IncU R plasmids pRAS1 and pAr-32 from the fish pathogen *Aeromonas salmonicida*. *Antimicrob. Agents Chemother.* 47, 1285–1290. doi: 10.1128/aac.47.4.1285-1290.2003

Suay-García, B., and Pérez-Gracia, M. T. (2019). Present and future of carbapenem-resistant *Enterobacteriaceae* (CRE) infections. *Antibiotics* 8:122. doi: 10.3390/antibiotics8030122

Sullivan, M. J., Petty, N. K., and Beatson, S. A. (2011). Easyfig: a genome comparison visualizer. *Bioinformatics* 27, 1009–1010. doi: 10.1093/bioinformatics/btr039

Tschäpe, H., Tietze, E., and Koch, C. (1981). Characterization of conjugative R plasmids belonging to the new incompatibility group IncU. *J. Gen. Microbiol.* 127, 155–160. doi: 10.1099/00221287-127-1-155

Vikram, A., and Schmidt, J. W. (2018). Functional bla(KPC-2) sequences are present in U.S. beef cattle feces regardless of antibiotic use. *Foodborne Pathog. Dis.* 15, 444–448. doi: 10.1089/fpd.2017.2406

Wang, D., Mu, X., Chen, Y., Zhao, D., Fu, Y., Jiang, Y., et al. (2020). Emergence of a clinical *Escherichia coli* sequence type 131 strain carrying a chromosomal bla (KPC-2) gene. *Front. Microbiol.* 11:586764. doi: 10.3389/fmicb.2020.586764

Wang, J., Yao, X., Luo, J., Lv, L., Zeng, Z., and Liu, J. H. (2018). Emergence of *Escherichia coli* co-producing NDM-1 and KPC-2 carbapenemases from a retail vegetable, China. *J. Antimicrob. Chemother.* 73, 252–254. doi: 10.1093/jac/dkx335

Wang, L., Fang, H., Feng, J., Yin, Z., Xie, X., Zhu, X., et al. (2015). Complete sequences of KPC-2-encoding plasmid p628-KPC and CTX-M-55-encoding p628-CTXM coexisted in *Klebsiella pneumoniae*. *Front. Microbiol.* 6:838. doi: 10.3389/fmicb.2015.00838

Xu, G., Jiang, Y., An, W., Wang, H., and Zhang, X. (2015). Emergence of KPC-2-producing *Escherichia coli* isolates in an urban river in Harbin, China. *World J. Microbiol. Biotechnol.* 31, 1443–1450. doi: 10.1007/s11274-015-1897-z

Conflict of Interest: LL was employed by company Adicon Clinical Laboratories.

The remaining authors declare that the research was conducted in the absence of any commercial or financial relationships that could be construed as a potential conflict of interest.

frontiers in Microbiology

ORIGINAL RESEARCH
published: 30 August 2021
doi: 10.3389/fmicb.2021.691406

The Emergence of Novel Sequence Type Strains Reveals an Evolutionary Process of Intraspecies Clone Shifting in ICU-Spreading Carbapenem-Resistant *Klebsiella pneumoniae*

Dongdong Zhao[1,2,3†], Qiucheng Shi[4†], Dandan Hu[1,2,3], Li Fang[1,2,3], Yihan Mao[1,2,3], Peng Lan[1,2,3], Xinhong Han[1,2,3], Ping Zhang[1,2,3], Huangdu Hu[1,2,3], Yanfei Wang[1,2,3], Jingjing Quan[1,2,3], Yunsong Yu[1,2,3] and Yan Jiang[1,2,3]*

[1] Department of Infectious Diseases, Sir Run Run Shaw Hospital, Zhejiang University School of Medicine, Hangzhou, China, [2] Key Laboratory of Microbial Technology and Bioinformatics of Zhejiang Province, Hangzhou, China, [3] Regional Medical Center for National Institute of Respiratory Diseases, Sir Run Run Shaw Hospital, Zhejiang University School of Medicine, Hangzhou, China, [4] Department of Clinical Laboratory, National Clinical Research Center for Child Health, The Children's Hospital, Zhejiang University School of Medicine, Hangzhou, China

OPEN ACCESS

Edited by:
Shaolin Wang,
China Agricultural University, China

Reviewed by:
Sophia Vourli,
University General Hospital Attikon, Greece
Xiaoming Wang,
Nanjing Agricultural University, China

***Correspondence:**
Yan Jiang
jiangy@zju.edu.cn

† These authors have contributed equally to this work and share first authorship

Specialty section:
This article was submitted to Antimicrobials, Resistance and Chemotherapy, a section of the journal Frontiers in Microbiology

Received: 06 April 2021
Accepted: 03 August 2021
Published: 30 August 2021

Citation:
Zhao D, Shi Q, Hu D, Fang L, Mao Y, Lan P, Han X, Zhang P, Hu H, Wang Y, Quan J, Yu Y and Jiang Y (2021) The Emergence of Novel Sequence Type Strains Reveals an Evolutionary Process of Intraspecies Clone Shifting in ICU-Spreading Carbapenem-Resistant Klebsiella pneumoniae. Front. Microbiol. 12:691406. doi: 10.3389/fmicb.2021.691406

Carbapenem-resistant *Klebsiella pneumoniae* (CRKP) is an urgent public health problem worldwide, and its rapid evolution in the clinical environment has been a major concern. A total of 99 CRKP isolates spreading in the intensive care unit (ICU) setting were included and subjected to whole-genome sequencing, and their sequence types (STs), serotype loci, and virulence determinants were screened based on genome data. The phylogenetic structure was reconstructed based on the core genome multilocus sequence typing method. Regions of recombination were assessed. Biofilm formation, serum resistance assays, and a *Galleria mellonella* infection model were used to evaluate strain virulence. A novel ST, designated ST4496, emerged in the ICU and spread for 6 months before its disappearance. ST4496 was closely related to ST11, with only a single-allele variant, and ST11 is the most dominant clinical clone in China. Recombination events occurred at capsule biosynthesis loci and divided the strains of ST11 and its derivative ST4496 into three clusters, including ST11-KL47, ST11-KL64, and ST4496-KL47. The phylogenetic structure indicated that ST11-KL47 was probably the origin of ST11-related strain evolution and presented more diversity in terms of both sequence similarity and phenotypes. ST4496-KL47 cluster strains presented less virulence than ST11-KL64, which was probably one of the factors preventing the former from spreading widely. In conclusion, ST4496-KL47 was probably derived from ST11-KL47 via intraspecies shifting but was less competitive than ST11-KL64, which also evolved from ST11-KL47 and developed increased virulence via capsule biosynthesis locus recombination. ST11-KL64 has the potential to be the predominant CRKP clone in China.

Keywords: virulence, capsule biosynthesis locus, intraspecies shifting, recombination, carbapenem-resistant

INTRODUCTION

Klebsiella pneumoniae is a common cause of community- and hospital-acquired infections (Paczosa and Mecsas, 2016; Bengoechea and Sa Pessoa, 2019). In recent decades, carbapenem-resistant *K. pneumoniae* (CRKP) has emerged as a major clinical concern worldwide with few treatment options (Munoz-Price et al., 2013; Grundmann et al., 2017). More worrisome is the emergence of hypervirulence-associated genetic determinants in CRKP, which may lead to even higher mortality and morbidity (Gu et al., 2018).

The capsule of *K. pneumoniae* confers resistance to antimicrobial peptides, phagocytosis, and complement-mediated killing and contributes to its ability to thrive in the environment or in a host. More than 77 capsular types (K-types) have been reported in clinical isolates of *K. pneumoniae*, and recombination events involving the capsule biosynthesis (cps) region are frequently observed within several dominant sequence type (ST) clones, such as CG258 (ST258, ST512, ST11, etc.) isolates (Wyres et al., 2015; Chiarelli et al., 2020). In China, ST11 is believed to be the most dominant CRKP clone, with a prevalence greater than 60% (Zhang et al., 2017; Wang et al., 2018). The diversity of K-type capsule polysaccharides is one of the important forces driving the extensive evolution of these bacteria and has been proven to be associated with virulence (Zhao et al., 2020; Zhou et al., 2020). Enhanced virulence may lead to subclonal replacement and thus to great challenges in clinical management and infection control (Zhou et al., 2020).

In this study, we observed an intraspecies shift in CRKP at our center, and we attempted to decipher the underlying mechanisms by determining the genetic and phenotypic diversity of related groups.

MATERIALS AND METHODS

CRKP Isolates

A common CRKP surveillance was conducted from January 1, 2017, at Sir Run Run Shaw Hospital, Zhejiang, China, which is a 1,200-bed tertiary medical center. A novel ST closely related to ST11 with a single-locus variant in *mdh* (allele: 1, C59T) was identified. Sixteen isolates with the novel ST (designated ST4496) were collected between January 2017 and May 2017. A rough *mdh* allele polymerase chain reaction analysis and subsequent sequencing screening were then applied to the isolates that were collected 2 months before January 2017 and after May 2017. Only two isolates from late December 2016 were found to harbor the novel *mdh* variant and were later identified as ST4496 by sequencing all seven alleles.

Altogether, 18 non-duplicated ST4496 CRKP isolates were detected, and the clinical data of the corresponding patients were collected from electronic medical records. All of the contemporaneous (from January to May 2017) CRKP isolates from the same intensive care unit (ICU) ward were collected and sequenced, resulting in a total of 99 CRKP isolates.

Species identification was performed by using matrix-assisted laser desorption ionization time-of-flight mass spectrometry (Bruker Daltonics, Bremen, Germany) and verified by genome sequencing. Isolates were considered carbapenem-resistant if the minimal inhibitory concentrations (MICs) of meropenem or imipenem were $\geq$ 4 mg/L or the MIC of ertapenem was $\geq$ 2, in accordance with the Clinical and Laboratory Standards Institute guidelines (2017).

The project was approved by the Ethical Review Committee of Sir Run Run Shaw Hospital (no. 20191231-20).

Whole-Genome Sequencing

Genomic DNA was extracted using the QIAamp DNA Minikit (Qiagen, Hilden, Germany) according to the manufacturer's recommendations and subsequently sequenced on the Illumina HiSeq X Ten platform (Illumina, San Diego, CA, United States) via a 150-bp paired-end approach. The generated short reads were *de novo* assembled using CLC Genomics Workbench 9.5.1 software, and the draft genome contigs were used for further analysis. One strain was also subjected to long-read sequencing using a MinION Sequencer (Nanopore, Oxford, United Kingdom). The *de novo* hybrid assembly of both short (Illumina) and long (Nanopore) reads was performed using Unicycler v0.4.8 in conservative mode (Wick et al., 2017).

ST, K-Type, and Virulence Gene Analysis

Multilocus sequence typing (MLST) was performed by using the CGE database,[1] and the novel ST was submitted to Institut Pasteur to obtain the specific ST number. The K-types were identified with Kaptive, and virulence genes were identified using the Institut Pasteur database[2] (Wyres et al., 2016). Virulence genes [i.e., siderophore system yersiniabactin (*ybtAEPQSTUX*), salmochelin (*iroBCDN*), aerobactin (*iucABCDiutA*), and polysaccharide regulator *rmpA*/*rmpA2* genes] were chosen as genotypic biomarkers for virulence evaluation (Russo et al., 2018; Turton et al., 2019; Lan et al., 2020).

Core Genome MLST and Recombination Analysis

All 99 assembled genomes were imported into Ridom Seqsphere + 4.1.9 (Ridom GmbH, Germany) for core genome MLST (cgMLST) analysis according to the default parameters. *K. pneumoniae* NTUH-K2044 (GenBank accession no. NC_012731.1) was used as a reference with a standard set of 2,358 genes for gene-by-gene comparisons, and the minimum spanning tree was constructed.

ST11-KL64, ST11-KL47, and ST4496 were subjected to further phylogenetic and recombination analyses. Genome alignment was established by using Snippy[3] with the default parameters. Recombination analysis was performed by using Gubbins (Croucher et al., 2015), and the complete genome acquired by long-read sequencing was used as a reference. The region of recombination was extracted and annotated with Prokka (rapid prokaryotic genome annotation) (Seemann, 2014) and PHAST (PHAge Search Tool). Figures illustrating the phylogenetic

[1] http://www.genomicepidemiology.org/

[2] https://bigsdb.pasteur.fr/klebsiella/klebsiella.html

[3] https://github.com/tseemann/snippy

and recombination results were produced with Phandango (Hadfield et al., 2018).

Biofilm Formation

Microtiter dish biofilm formation assays were used to determine the capacity of biofilm formation, with minor modifications (Naparstek et al., 2014). Briefly, bacteria [10^7 colony-forming units (CFU)/mL] were inoculated into Mueller Hinton (MH) medium in polystyrene microtiter 96-well plates (Grenier Bio-One, Frickenhausen, Germany) and incubated at 37°C for 20 h. The biofilm that formed in each well was quantified via crystal violet (Sigma, St. Louis, MO, United States) staining followed by elution with 95% ethanol and optical density (OD) measurements (OD595). Three independent cultures for each strain and quantification in four wells for each culture were performed.

Serum Resistance Assay

Serum resistance was determined by comparing the lag phase of the growth curve in MH broth or MH broth with 10% pooled normal human serum (1 mL serum mixed with 9 mL MH broth), which was collected from healthy volunteers. Three independent cultures for each strain were grown overnight until saturation and diluted 1:1,000 in MH broth or MH broth with 10% pooled normal human serum. Three replicates of each culture were aliquoted into a flat-bottom 100-well plate (0.2 mL/well). Growth curves were determined by measuring the OD at 600 nm every 5 min for 20 h using a Bioscreen C MBR machine (Oy Growth Curves Ab Ltd., Finland). The lag phase was estimated based on the OD600 curves using an R script defined as previously described (Hua et al., 2017).

Galleria mellonella Infection Model

A *Galleria mellonella* infection model was used to evaluate the virulence level among different CRKP clone groups. For strain assessment, bacteria from a freshly streaked plate were grown overnight and underwent 10-fold serial dilutions in 1 × phosphate-buffered saline (PBS). Prior to inoculation into *G. mellonella* larvae, bacterial cells were washed with PBS and then diluted to an appropriate cell density, as determined by measuring the OD at 600 nm. Groups of 30 larvae (∼200 mg; Yuejiayin, Tianjin, China) were stored in the dark at 4°C prior to use. For virulence evaluation, every larva was infected with 10-μL aliquots of 1×10^6 CFU bacteria ($n = 10$) via the last left proleg by using a 10-μL Hamilton syringe. Survival was monitored every 3 h up to 24 h postinfection at 37°C. Experiments were performed in triplicate.

Statistical Analysis

A two-tailed Mann–Whitney *U*-test was used to calculate the differences between all pairs of the ST11-KL47, ST11-KL64, and ST4496-KL47 groups regarding the median number of different core genes, biofilm formation, and the lag phase of the growth curve in MH broth or MH broth with 10% human serum. The survival rates of *G. mellonella* were evaluated using Kaplan–Meier survival curves and analyzed with the log-rank (Mantel–Cox) test. The mean numbers of bases involved in recombination were compared among these three clone groups by using one-way analysis of variance. All p-values ≤ 0.05 were considered statistically significant.

RESULTS

Clinical Characteristics of Patients Infected With ST4496 Strains

The novel allele and ST were submitted to the administrator of the Pasteur database and assigned as ST4496 with an mdh335 allele (allelic profile of 3-3-335-1-1-1-79 for *gapA*, *infB*, *mdh*, *pgi*, *phoE*, *rpoB*, and *tonB*, respectively).

The clinical characteristics of the patients infected with ST4496 strains are presented in **Table 1**. All 18 isolates were collected from the ICU. Notably, none of the isolates originated from blood or primary abscesses, and the patients tended to show a good prognosis, even though five of them were discharged against medical advice because of uncontrolled underlying conditions. Moreover, the relatively good outcomes of the majority of the patients receiving no effective antimicrobials for CRKP indicated a colonized status of the strains rather than an infectious status. The non-invasive clinical manifestations indicated a hypovirulent character of the ST4496 CRKP.

cgMLST for Contemporaneous CRKP

Altogether, 99 contemporaneous isolates were included in the cgMLST analysis and the subsequent phylogenetic analysis. K-type was also considered as capsule synthesis loci are recombination hotspots in multidrug-resistant *K. pneumoniae* and are associated with virulence.

The minimum spanning tree based on the cgMLST profiles is presented in **Figure 1**. The results showed that ST11 (70/99) accounted for the majority of CRKP isolates, among which KL64 and KL47 were the overwhelmingly dominant serotypes. ST4496 (18/99) was the second most common ST, and all of the isolates with this ST belonged to the KL47 serotype. There were five ST15 isolates, and the remaining six isolates included five distinct STs. ST4496 and ST11 were closely related to each other but displayed relatively long distances from other STs. ST4496 showed a shorter phylogenetic distance from ST11-KL47 strains than from ST11-KL64 based on the core gene difference. As ST4496 strains have never previously been detected at this center or reported in any other studies, it is logical to believe that they may have originated from ST11-KL47.

ST4496-KL47 ($n = 18$), ST11-KL64 ($n = 58$), and ST11-KL47 ($n = 8$) were selected for further analysis, as these three groups were very closely related to each other according to cgMLST and were the predominant CRKP groups. Notably, ST11-KL47 exhibited greater genetic diversity than the other two clusters; among the clusters, the median number of different core genes between each pair of strains within the group was 25 in ST11-KL47 vs. 5 in ST11-KL64 and 2 in ST4496-KL47, and these differences were significant (both $p < 0.0001$; **Figure 2A**).

TABLE 1 | Clinical characteristics of the patients infected with ST4496 CRKP.

Isolates	Time of isolation	Origin	Department	Underlying conditions	Clinical outcome	Antimicrobials
NST-1	21/12/2016	Bile	ICU	Severe acute pancreatitis	Improved	Cefoperazone and sulbactam, tigecycline
NST-2	26/12/2016	Ascites	ICU	Pseudomyxoma peritonei	Improved	Imipenem
NST-3	05/01/2017	Sputum	ICU	Colon cancer	Improved	Amoxicillin and clavulanic acid
NST-4	09/01/2017	Urine	ICU	Bladder cancer	Improved	Cefoperazone and sulbactam
NST-5	16/01/2017	Sputum	ICU	Sepsis	Improved	Cefoperazone and sulbactam, tigecycline
NST-6	26/01/2017	Ascites	ICU	Hepatic carcinoma	Improved	Imipenem
NST-7	26/01/2017	Sputum	ICU	Heart failure	Improved	Moxifloxacin, imipenem
NST-8	02/02/2017	Urine	ICU	Deep vein thrombosis, GI bleeding	Improved	Cefoperazone and sulbactam
NST-9	02/02/2017	Purulent discharge from surgical site	ICU	Femoral artery embolectomy, atrial fibrillation, heart failure	Against-advice discharge	Amoxicillin and clavulanic acid, cefepime
NST-10	02/02/2017	Sputum	ICU	Brain ischemia	Improved	Piperacillin and tazobactam
NST-11	11/03/2017	Sputum	ICU	Esophageal cancer, pyothorax, respiratory failure	Against-advice discharge	Tigecycline, meropenem
NST-12	22/03/2017	Sputum	ICU	Brain hemorrhage	Improved	Meropenem
NST-13	22/03/2017	Sputum	ICU	GI bleeding	Improved	Piperacillin and tazobactam
NST-14	23/03/2017	Sputum	ICU	Cerebral infarction, pulmonary infection	Against-advice discharge	Amoxicillin and clavulanic acid, cefepime
NST-15	02/04/2017	Sputum	ICU	Brain hemorrhage	Improved	Cefoperazone and sulbactam
NST-16	05/04/2017	Ascites	ICU	Acute generalized suppurative peritonitis, exploratory laparotomy	Improved	Imipenem, Tigecycline
NST-17	10/04/2017	Purulent discharge from surgical site	ICU	Esophageal perforation from foreign body, mediastinal abscess	Against-advice discharge	Imipenem
NST-18	02/05/2017	Urine	ICU	Malignant tumor of the meninges, lymphoma suspected	Against-advice discharge	Cefoperazone and sulbactam

Phylogenetic and Recombination Analysis

Further phylogenetic analysis was performed on 84 isolates and revealed three distinct clusters, corresponding to ST11-KL47, ST4496-KL47, and ST11-KL64 (**Figure 3**). The strains in cluster ST11-KL47 had longer branches, continuing to show more genetic diversity than the other two clusters. The mean number of bases involved in recombination in ST11-KL64 was 270,666.7, whereas 56,866.6 and 10,879.2 bases were found in ST11-KL47 and ST4496-KL47, respectively ($p < 0.0001$). The three major regions of recombination were annotated, and the largest region corresponded to the K locus and O locus (149,594 bases), deciphering the K-type and LPS shifts. The other two regions were *fimA*/*oqxAB* (27,879 bases) and the prophage sequence (45,116 bases).

Virulence Genes

Several key virulence genes were screened, including the capsular polysaccharide regulator *rmpA* or *rmpA2*, and siderophore systems (yersiniabactin, salmochelin, and aerobactin). Yersiniabactin was the most common of these genes and was found in all strains, whereas salmochelin was not found in three lineages, ST11-KL47, ST11-KL64, and ST4496-KL47. However, great differences in other virulence genes were observed among the three lineages. Among ST11-KL64 isolates, not only did the majority (56/58, 96.6%) possess aerobactin/*rmpA2** genes [*rmpA2** indicates a frameshift mutation compared to empirical *rmpA2* gene (Zhou et al., 2020)], but a relatively high proportion (15/58, 25.9%) also carried the *rmpA* gene. Only one isolate of ST11-KL47 contained aerobactin and the empirical *rmpA2* gene. The ST4496 isolates carried no targeted virulence genes beyond the yersiniabactin gene cluster *ybtAEPQSTUX*.

Phenotypic Assessment

All eight ST11-KL47 isolates were included in the following phenotypic analysis. For biofilm formation and serum resistance assays, eight isolates were randomly chosen as representatives for the phenotypic assessment of ST4496-KL47 and ST11-KL64, respectively. In the biofilm formation assay, the OD measurements indicated that ST4496-KL47 isolates produced the least biofilm, whereas ST11-KL64 isolates produced the most biofilm. The differences between the three groups were significant (median OD595 values in ST11-KL47, ST11-KL64, and ST4496-KL47 of 0.4264, 0.8531, and 0.2340, respectively, **Figure 2B**). Greater diversity in biofilm formation was observed for ST11-KL47 than for ST11-KL64 and ST4496-KL47. In the serum resistance assay, similar lag phases were detected for the three groups in the MH broth (**Figure 2C**). However, a significantly prolonged lag phase was observed for ST4496-KL47 and some

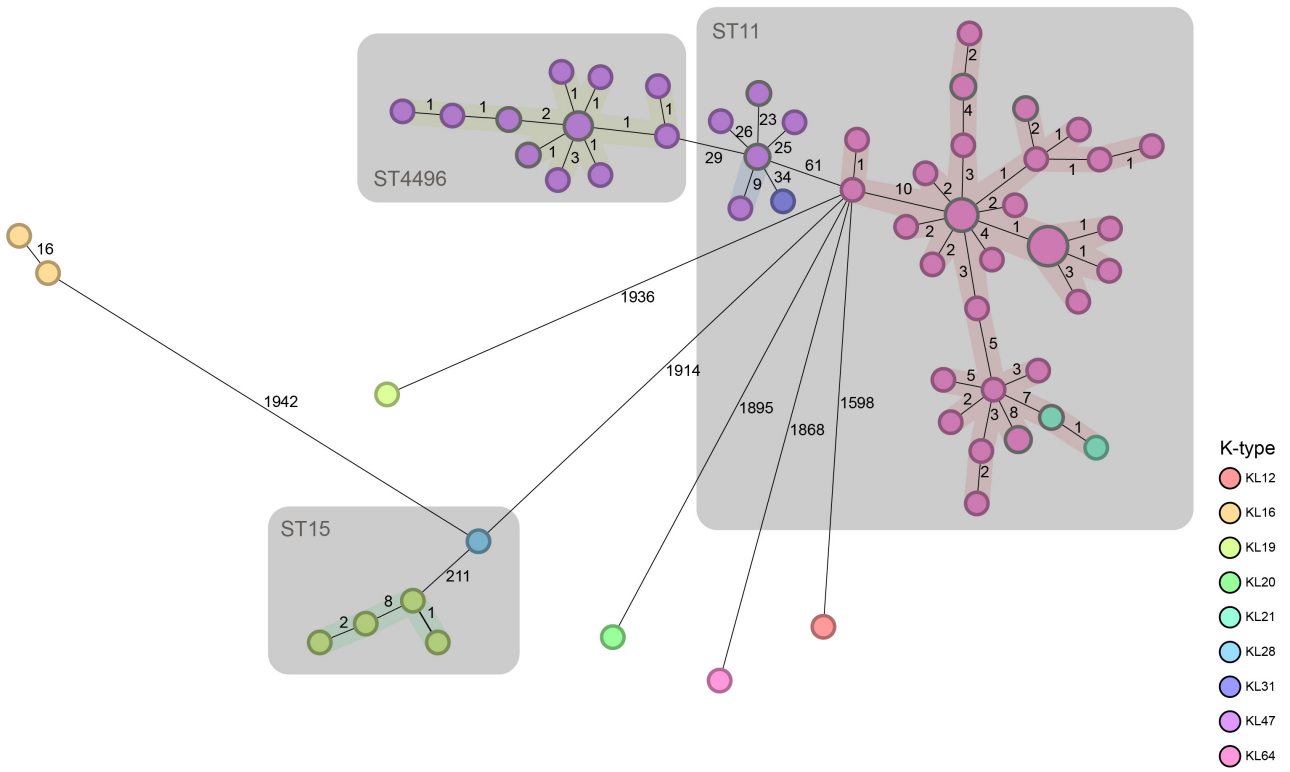

FIGURE 1 | Minimum spanning tree based on the cgMLST profiles of contemporaneous CRKP strains. cgMLST profiles are represented by circles, and the size of the circle is proportional to the number of isolates with an identical cgMLST profile. The color of each circle is encoded by the K-type, and the length of lines connecting the cgMLST profiles is proportional to the number of core gene differences between circles. A gray zone surrounds a group of circles that share the same sequence type.

of the ST11-KL47 isolates in MH broth with 10% human serum relative to ST11-KL64. The differences between ST11-KL47 and ST4496-KL47 or between ST11-KL64 and ST4496-KL47 were significant ($p < 0.0001$). Similarly, greater variation in the lag phase in MH broth with 10% pooled normal human serum was observed in ST11-KL47 (**Figure 2D**). Furthermore, we generated a *G. mellonella* infection model to evaluate the virulence among these three groups. The survival percentage of *G. mellonella* larvae in the ST11-KL64 group was significantly lower than that in the ST11-KL47 or ST4496-KL47 group, indicating that the ST11-KL64 isolates had the highest virulence compared to other KL47 serotype isolates (**Figure 4**).

DISCUSSION

In this study, a novel ST with one single-locus variant in *mdh* emerged in the ST11 CRKP and was assigned ST4496. Unlike other successful descendants (e.g., ST258) of ST11, ST4496 did not show successful persistence or dissemination in the hospital setting. The characteristics of patients infected with ST4496 indicated a hypovirulent nature, as ST4496 strains mostly presented colonization rather than infection, and no bloodstream infection involving ST4496 was detected. We presumed that hypovirulence was mainly responsible for the restriction of the spread of ST4496 after it caused occasional outbreaks in the hospital setting for a couple of months.

There are growing reports of convergent evolution of resistance and virulence in *K. pneumoniae*. Although convergence can result from hypervirulent strains gaining multidrug resistance (MDR) elements or MDR strains gaining virulence elements, MDR clones are more likely to acquire virulence genes than hypervirulent clones are to acquire resistance genes (Wyres et al., 2019). Following sporadic reports of isolates showing the phenomenon of convergence in clinical isolates, there has recently been growing evidence of increasing virulence in the CRKP population, especially in the dominant ST11 clone in China (Shen et al., 2020; Zhao et al., 2020; Zhou et al., 2020). To reveal the genotypic and phenotypic basis of this convergence, novel ST4496 isolates and contemporary CRKP isolates were included in the present study. The K-type was also investigated because it has been proven to be associated with virulence, and recent evidence showed that the previously prevalent ST11-KL47 has been gradually replaced by ST11-KL64, which was derived from an ST11-KL47–like ancestor through recombination (Zhao et al., 2020; Zhou et al., 2020).

From the cgMLST analysis and the derived minimum spanning tree, we can see that ST4496-KL47, ST11-KL64, and ST11-KL47 were closely related to each other and were the predominant CRKP groups. The relationships of the three groups

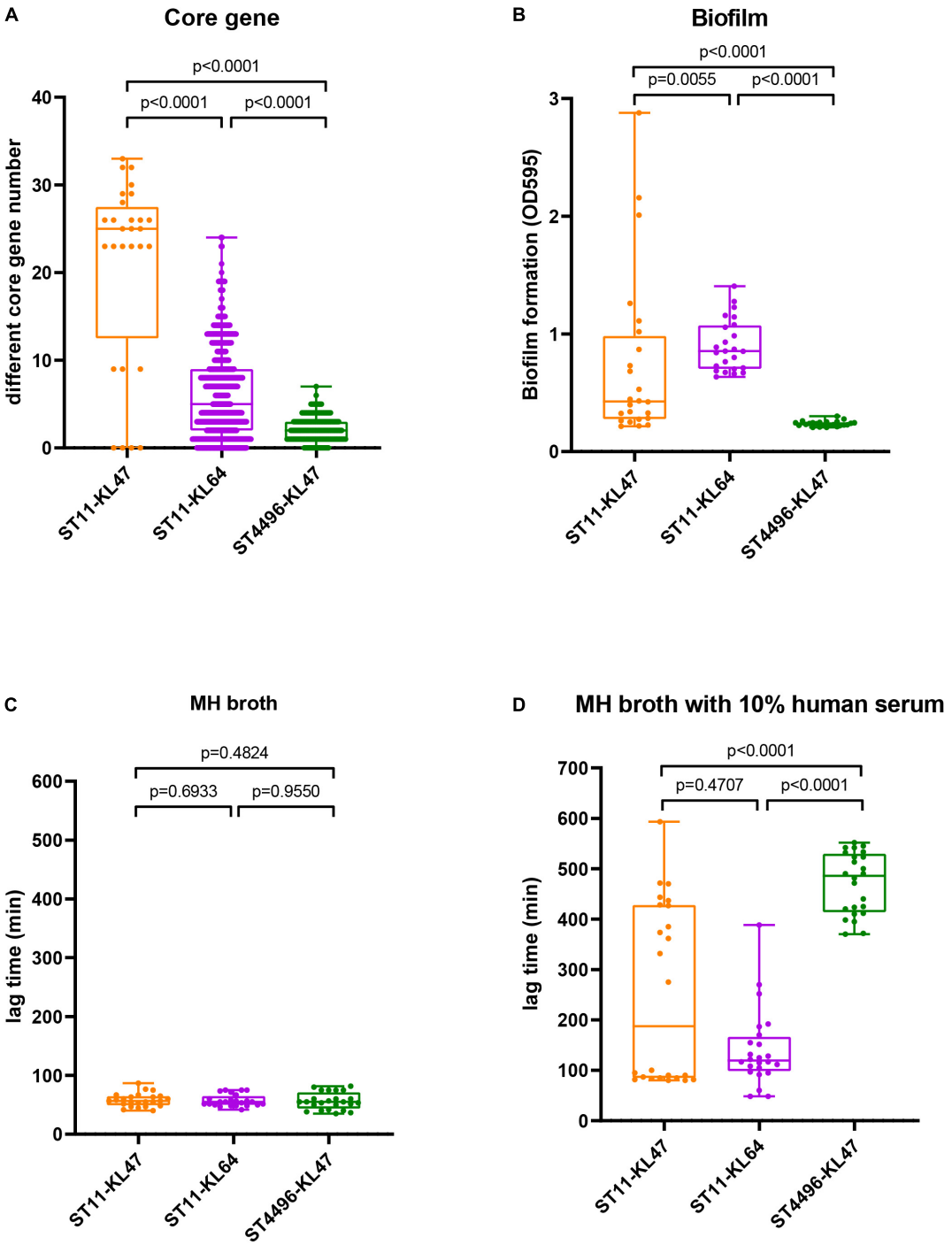

FIGURE 2 | Genetic evidence and phenotypic manifestations among the ST11-KL47, ST11-KL64, and ST4496-KL47 groups: **(A)** The distribution of different core gene numbers between each pair of strains within the group; **(B)** biofilm formation (OD595); **(C)** lag phase in MH broth; **(D)** lag phase in MH broth with 10% human serum. The middle lines represent the median value for each group. Error bars indicate the region from the lowest to highest values in each group.

were further confirmed by single-nucleotide polymorphism (SNP)–based phylogenetic and recombination analysis. ST11-KL47 is much more diverse genetically. Since it has been reported that enhanced virulence promotes the replacement of ST11-KL47 by ST11-KL64 (Zhou et al., 2020), it is logical to presume that different levels of virulence may be one of the factors leading to the different fates of the three CRKP groups, that is, the disappearance of ST4496-KL47, the decrease in ST11-KL47, and the proliferation of ST11-KL64, although both ST4496-KL47 and ST11-KL64 may have evolved from ST11-KL47.

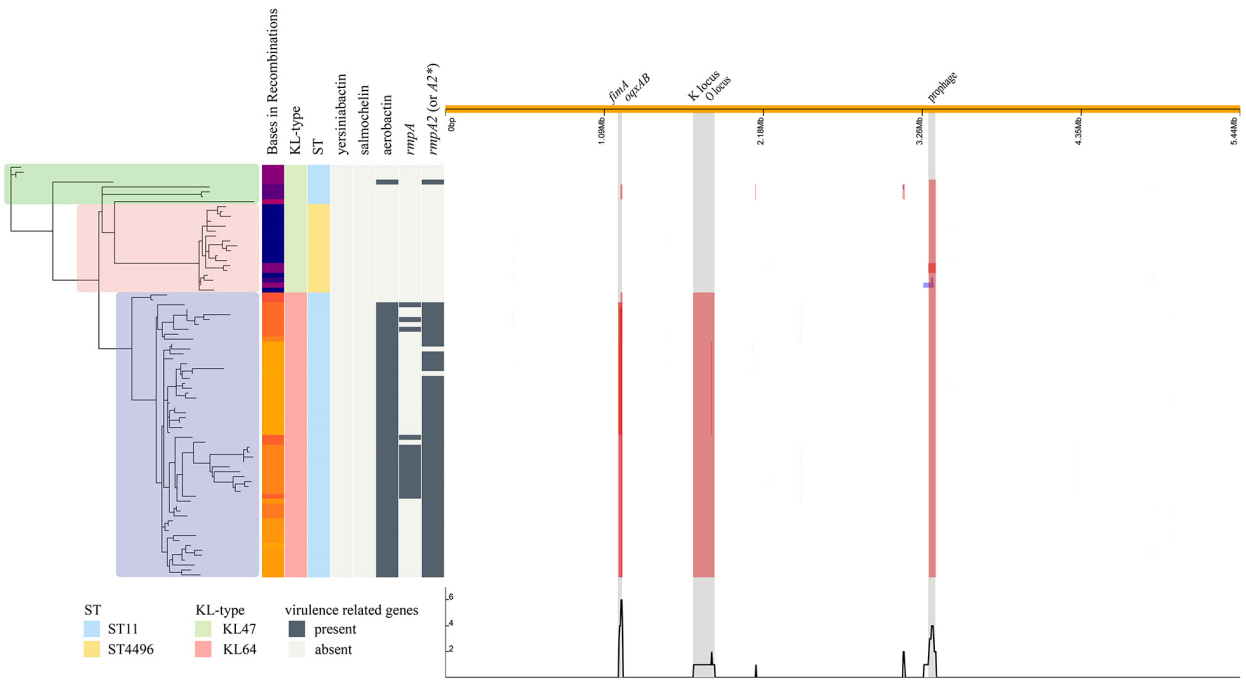

FIGURE 3 | Phylogenetic structure combined with the molecular characteristics and the regions of recombination in the ST11-KL47, ST4496-KL47, and ST11-KL64 strains. The SNP-based phylogenetic tree is shown to the left; green zone, ST11-KL47; pink zone, ST4496-KL47; blue zone, ST11-KL64. The distributions of bases in recombinations, KL type, ST type, and some virulence-related genes are shown in the middle. The three major regions of recombination are shown to the right, and the largest region corresponds to the K locus and O locus.

This assumption was supported by the fact that enhanced virulence of ST11-KL64 and weakened virulence of ST4496-KL47 were observed both genetically and phenotypically. Genetically, ST11-KL64 has the most virulence genes, and ST4496-KL47 has the fewest virulence genes. As previously reported, *iuc* (the aerobactin locus) is important for the production of siderophores to promote iron acquisition, and some researchers have even considered aerobactin as an indicator of hypervirulent *K. pneumoniae* (Zhang et al., 2016). The presence of *rmpA/A2*, which encodes regulators of mucoid phenotype genes, is strongly associated with the phenotype of hypermucoviscosity. Positivity for *iuc*, *rmpA*, and *rmpA2* (or *rmpA2**) may indicate the presence of a virulence plasmid (Wyres et al., 2020).

Virulence levels were further determined by phenotypic tests. First, the observation of biofilm formation supported bacterial adhesion to indwell medical devices and potentially better survival in adverse environmental conditions, which may lead to drug ineffectiveness and failure to eradicate infection (O'Toole et al., 2000; Zheng et al., 2018). Previous studies have shown that biofilm formation ability is associated with genetic factors such as *iucA* and *rmpA/rmpA2* in *K. pneumoniae* (Zheng et al., 2018). Second, a significantly prolonged lag phase was observed for ST4496-KL47 and some of the ST11-KL47 isolates in MH broth with 10% human serum. In fact, some ST4496-KL47 and ST11-KL47 isolates failed to grow in MH broth with a higher concentration of human serum (20%) over a 20-h period (data not shown). A shorter lag phase may indicate a relatively high serum resistance ability of ST11-KL64. Finally, the highest virulence level in ST11-KL64 isolates was also observed based on the *G. mellonella* infection model, implying that this clone was more likely to cause pandemic outbreaks than other KL47 serotype isolates.

Relative to ST4496-KL47 and ST11-KL64, diversity is much higher in ST11-KL47 based on both genetic evidence and phenotypic findings. This is consistent with the fact that this group is much more ancient and has therefore had a higher chance to evolve and develop greater diversity.

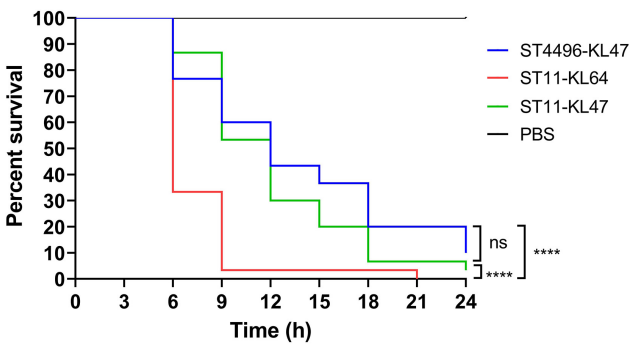

FIGURE 4 | Percent survival curve of *G. mellonella* infected with ST11-KL64 isolates (red line), ST11-KL47 isolates (green line), and ST4496-KL47 (blue line). ns, no significant difference; ****$p < 0.0001$.

Our findings are relevant for understanding the risk of carbapenem-resistant hypervirulent *K. pneumoniae* strains as highly virulent MDR strains may be able to persist and be disseminated in hospital settings and may even spread to community settings, leading to public health disasters (Chen and Kreiswirth, 2018). The early detection and containment of spreading through comprehensive infection control measures could be the most feasible solution to this problem.

This work provides a glimpse of intraspecies shifts from one hospital, and a preliminary investigation has been conducted. Certainly, more studies are needed to verify this assumption. To better understand the mechanisms of evolution, we should pay attention to "unsuccessful" evolution as well as successful evolution. Thus, unsuccessful ST4496 could be an excellent reference when studying the evolution of *K. pneumoniae*.

CONCLUSION

The present study provided further evidence that virulence enhancement in ST11-KL64 was the reason for intraspecies replacement, as further demonstrated by the disappearance of ST4496-KL47, with weakened virulence. The results indicate that ST11-KL64 has the potential to be the predominant CRKP strain in China, and it seems that the convergent evolution of virulence and resistance in *K. pneumoniae* is inevitable under current antimicrobial strategies and infection control policies.

DATA AVAILABILITY STATEMENT

The datasets presented in this study can be found in online repositories. The names of the repository/repositories and accession number(s) can be found below: NCBI BioProject, accession numbers: PRJNA747841 and PRJEB34922.

AUTHOR CONTRIBUTIONS

DZ and QS participated in the design of the study, performed the bioinformatics analysis, and drafted the manuscript. DH, LF, and YM performed Genomic DNA extraction and prepared for illumine sequencing. PL and JQ participated in the bioinformatics analysis and generated some figures. XH and PZ performed biofilm formation assay. HH and YW performed serum resistance assay. YJ and YY conceived of the study, participated in its design and coordination and helped to draft the manuscript. All authors read and approved the final manuscript.

FUNDING

This work was supported by the National Natural Science Foundation of China (No. 81830069), the China International Medical Foundation for Young Scientists (No. Z-2018-35-2003), and the Key Research and Development Program of Zhejiang (No. 2015C03046).

REFERENCES

Bengoechea, J. A., and Sa Pessoa, J. (2019). *Klebsiella pneumoniae* infection biology: living to counteract host defences. *FEMS Microbiol. Rev.* 43, 123–144. doi: 10.1093/femsre/fuy043

Chen, L., and Kreiswirth, B. N. (2018). Convergence of carbapenem-resistance and hypervirulence in *Klebsiella pneumoniae*. *Lancet Infect. Dis.* 18, 2–3. doi: 10.1016/S1473-3099(17)30517-0

Chiarelli, A., Cabanel, N., Rosinski-Chupin, I., Zongo, P. D., Naas, T., Bonnin, R. A., et al. (2020). Diversity of mucoid to non-mucoid switch among carbapenemase-producing *Klebsiella pneumoniae*. *BMC Microbiol.* 20:325. doi: 10.1186/s12866-020-02007-y

Croucher, N. J., Page, A. J., Connor, T. R., Delaney, A. J., Keane, J. A., Bentley, S. D., et al. (2015). Rapid phylogenetic analysis of large samples of recombinant bacterial whole genome sequences using Gubbins. *Nucleic Acids Res.* 43:e15. doi: 10.1093/nar/gku1196

Grundmann, H., Glasner, C., Albiger, B., Aanensen, D. M., Tomlinson, C. T., Andrasevic, A. T., et al. (2017). Occurrence of carbapenemase-producing *Klebsiella pneumoniae* and *Escherichia coli* in the European survey of carbapenemase-producing *Enterobacteriaceae* (EuSCAPE): a prospective, multinational study. *Lancet Infect. Dis.* 17, 153–163. doi: 10.1016/S1473-3099(16)30257-2

Gu, D., Dong, N., Zheng, Z., Lin, D., Huang, M., Wang, L., et al. (2018). A fatal outbreak of ST11 carbapenem-resistant hypervirulent *Klebsiella pneumoniae* in a Chinese hospital: a molecular epidemiological study. *Lancet Infect. Dis.* 18, 37–46. doi: 10.1016/S1473-3099(17)30489-9

Hadfield, J., Croucher, N. J., Goater, R. J., Abudahab, K., Aanensen, D. M., and Harris, S. R. (2018). Phandango: an interactive viewer for bacterial population genomics. *Bioinformatics* 34, 292–293. doi: 10.1093/bioinformatics/btx610

Hua, X., Liu, L., Fang, Y., Shi, Q., Li, X., Chen, Q., et al. (2017). Colistin resistance in *Acinetobacter baumannii* MDR-ZJ06 revealed by a multiomics approach. *Front. Cell. Infect. Microbiol.* 7:45. doi: 10.3389/fcimb.2017.00045

Lan, P., Shi, Q., Zhang, P., Chen, Y., Yan, R., Hua, X., et al. (2020). Core genome allelic profiles of clinical *Klebsiella pneumoniae* strains using a random forest algorithm based on multilocus sequence typing scheme for hypervirulence analysis. *J. Infect. Dis.* 221(Suppl. 2), S263–S271. doi: 10.1093/infdis/jiz562

Munoz-Price, L. S., Poirel, L., Bonomo, R. A., Schwaber, M. J., Daikos, G. L., Cormican, M., et al. (2013). Clinical epidemiology of the global expansion of *Klebsiella pneumoniae* carbapenemases. *Lancet Infect. Dis.* 13, 785–796. doi: 10.1016/S1473-3099(13)70190-7

Naparstek, L., Carmeli, Y., Navon-Venezia, S., and Banin, E. (2014). Biofilm formation and susceptibility to gentamicin and colistin of extremely drug-resistant KPC-producing *Klebsiella pneumoniae*. *J. Antimicrob. Chemother.* 69, 1027–1034. doi: 10.1093/jac/dkt487

O'Toole, G., Kaplan, H. B., and Kolter, R. (2000). Biofilm formation as microbial development. *Annu. Rev. Microbiol.* 54, 49–79. doi: 10.1146/annurev.micro.54.1.49

Paczosa, M. K., and Mecsas, J. (2016). *Klebsiella pneumoniae*: going on the offense with a strong defense. *Microbiol. Mol. Biol. Rev.* 80, 629–661. doi: 10.1128/MMBR.00078-15

Russo, T. A., Olson, R., Fang, C. T., Stoesser, N., Miller, M., MacDonald, U., et al. (2018). Identification of biomarkers for differentiation of hypervirulent *Klebsiella pneumoniae* from classical *K. pneumoniae*. *J. Clin. Microbiol.* 56:e00776. doi: 10.1128/JCM.00776-18

Seemann, T. (2014). Prokka: rapid prokaryotic genome annotation. *Bioinformatics* 30, 2068–2069. doi: 10.1093/bioinformatics/btu153

Shen, P., Berglund, B., Chen, Y., Zhou, Y., Xiao, T., Xiao, Y., et al. (2020). Hypervirulence markers among non-ST11 strains of carbapenem- and multidrug-resistant *Klebsiella pneumoniae* isolated from patients with bloodstream infections. *Front. Microbiol.* 11:1199. doi: 10.3389/fmicb.2020.01199

Turton, J., Davies, F., Turton, J., Perry, C., Payne, Z., and Pike, R. (2019). Hybrid resistance and virulence plasmids in "high-risk" clones of *Klebsiella*

pneumoniae, including those carrying bla_{NDM-5}. *Microorganisms* 7:326. doi: 10.3390/microorganisms7090326

Wang, Q., Wang, X., Wang, J., Ouyang, P., Jin, C., Wang, R., et al. (2018). Phenotypic and genotypic characterization of carbapenem-resistant *Enterobacteriaceae*: data from a longitudinal large-scale CRE study in China (2012-2016). *Clin. Infect. Dis.* 67(suppl. 2), S196–S205. doi: 10.1093/cid/ciy660

Wick, R. R., Judd, L. M., Gorrie, C. L., and Holt, K. E. (2017). Unicycler: resolving bacterial genome assemblies from short and long sequencing reads. *PLoS Comput. Biol.* 13:e1005595. doi: 10.1371/journal.pcbi.1005595

Wyres, K. L., Gorrie, C., Edwards, D. J., Wertheim, H. F., Hsu, L. Y., Van Kinh, N., et al. (2015). Extensive capsule locus variation and large-scale genomic recombination within the *Klebsiella pneumoniae* clonal group 258. *Genome Biol. Evol.* 7, 1267–1279. doi: 10.1093/gbe/evv062

Wyres, K. L., Lam, M. M. C., and Holt, K. E. (2020). Population genomics of *Klebsiella pneumoniae*. *Nat. Rev. Microbiol.* 18, 344–359. doi: 10.1038/s41579-019-0315-1

Wyres, K. L., Wick, R. R., Gorrie, C., Jenney, A., Follador, R., Thomson, N. R., et al. (2016). Identification of *Klebsiella* capsule synthesis loci from whole genome data. *Microb. Genom.* 2:e000102. doi: 10.1099/mgen.0.000102

Wyres, K. L., Wick, R. R., Judd, L. M., Froumine, R., Tokolyi, A., Gorrie, C. L., et al. (2019). Distinct evolutionary dynamics of horizontal gene transfer in drug resistant and virulent clones of *Klebsiella pneumoniae*. *PLoS Genet.* 15:e1008114. doi: 10.1371/journal.pgen.1008114

Zhang, R., Liu, L., Zhou, H., Chan, E. W., Li, J., Fang, Y., et al. (2017). Nationwide surveillance of clinical carbapenem-resistant *Enterobacteriaceae* (CRE) strains in China. *EBioMedicine* 19, 98–106. doi: 10.1016/j.ebiom.2017.04.032

Zhang, Y., Zhao, C., Wang, Q., Wang, X., Chen, H., Li, H., et al. (2016). High prevalence of hypervirulent *Klebsiella pneumoniae* infection in China: geographic distribution, clinical characteristics, and antimicrobial resistance. *Antimicrob. Agents Chemother.* 60, 6115–6120. doi: 10.1128/AAC.01127-16

Zhao, J., Liu, C., Liu, Y., Zhang, Y., Xiong, Z., Fan, Y., et al. (2020). Genomic characteristics of clinically important ST11 *Klebsiella pneumoniae* strains worldwide. *J. Glob. Antimicrob. Resist.* 22, 519–526. doi: 10.1016/j.jgar.2020.03.023

Zheng, J. X., Lin, Z. W., Chen, C., Chen, Z., Lin, F. J., Wu, Y., et al. (2018). Biofilm formation in *Klebsiella pneumoniae* bacteremia strains was found to be associated with CC23 and the presence of WCAG. *Front. Cell. Infect. Microbiol.* 8:21. doi: 10.3389/fcimb.2018.00021

Zhou, K., Xiao, T., David, S., Wang, Q., Zhou, Y., Guo, L., et al. (2020). Novel subclone of carbapenem-resistant *Klebsiella pneumoniae* sequence type 11 with enhanced virulence and transmissibility, China. *Emerg. Infect. Dis.* 26, 289–297. doi: 10.3201/eid2602.190594

Conflict of Interest: The authors declare that the research was conducted in the absence of any commercial or financial relationships that could be construed as a potential conflict of interest.

Publisher's Note: All claims expressed in this article are solely those of the authors and do not necessarily represent those of their affiliated organizations, or those of the publisher, the editors and the reviewers. Any product that may be evaluated in this article, or claim that may be made by its manufacturer, is not guaranteed or endorsed by the publisher.

frontiers in Microbiology

ORIGINAL RESEARCH
published: 13 September 2021
doi: 10.3389/fmicb.2021.661798

Global Expansion of Linezolid-Resistant Coagulase-Negative Staphylococci

*Vladimir Gostev[1,2], Semen Leyn[3], Alexander Kruglov[4†], Daria Likholetova[1,5], Olga Kalinogorskaya[1], Marina Baykina[4], Natalia Dmitrieva[6], Zlata Grigorievskaya[6], Tatiana Priputnevich[7], Lyudmila Lyubasovskaya[7], Alexey Gordeev[7] and Sergey Sidorenko[1,2]**

[1] Department of Medical Microbiology and Molecular Epidemiology, Pediatric Research and Clinical Center for Infectious Diseases, Saint Petersburg, Russia, [2] Department of Medical Microbiology, North-Western State Medical University Named After I. I. Mechnikov, Saint Petersburg, Russia, [3] Infectious and Inflammatory Disease Center, Sanford Burnham Prebys Medical Discovery Institute, La Jolla, CA, United States, [4] Laboratory of Clinical Microbiology, National Agency for Clinical Pharmacology and Pharmacy, Moscow, Russia, [5] Saint Petersburg State University, Saint Petersburg, Russia, [6] Department of Microbiology, N. N. Blokhin Russian Cancer Research Center, Moscow, Russia, [7] Department of Microbiology, Clinical Pharmacology and Epidemiology, National Medical Research Center for Obstetrics, Gynecology and Perinatology, Moscow, Russia

OPEN ACCESS

Edited by:
Ye Feng,
Zhejiang University, China

Reviewed by:
Adam C. Silver,
University of Hartford, United States
Amy H. Lee,
Simon Fraser University, Canada

***Correspondence:**
Sergey Sidorenko
sidorserg@gmail.com

†Present address:
Alexander Kruglov,
City Hospital No 40, Moscow Department of Health, Moscow, Russia

Specialty section:
This article was submitted to Antimicrobials, Resistance and Chemotherapy, a section of the journal Frontiers in Microbiology

Received: *31 January 2021*
Accepted: *30 July 2021*
Published: *13 September 2021*

Citation:
Gostev V, Leyn S, Kruglov A, Likholetova D, Kalinogorskaya O, Baykina M, Dmitrieva N, Grigorievskaya Z, Priputnevich T, Lyubasovskaya L, Gordeev A and Sidorenko S (2021) Global Expansion of Linezolid-Resistant Coagulase-Negative Staphylococci. Front. Microbiol. 12:661798. doi: 10.3389/fmicb.2021.661798

Coagulase-negative staphylococci (CoNS) for a long time were considered avirulent constituents of the human and warm-blooded animal microbiota. However, at present, *S. epidermidis*, *S. haemolyticus*, and *S. hominis* are recognized as opportunistic pathogens. Although linezolid is not registered for the treatment of CoNS infections, it is widely used off-label, promoting emergence of resistance. Bioinformatic analysis based on maximum-likelihood phylogeny and Bayesian clustering of the CoNS genomes obtained in the current study and downloaded from public databases revealed the existence of international linezolid-resistant lineages, each of which probably had a common predecessor. Linezolid-resistant *S. epidermidis* sequence-type (ST) 2 from Russia, France, and Germany formed a compact group of closely related genomes with a median pairwise single nucleotide polymorphism (SNP) difference of fewer than 53 SNPs, and a common ancestor of this lineage appeared in 1998 (1986–2006) before introduction of linezolid in practice. Another compact group of linezolid-resistant *S. epidermidis* was represented by ST22 isolates from France and Russia with a median pairwise SNP difference of 40; a common ancestor of this lineage appeared in 2011 (2008–2013). Linezolid-resistant *S. hominis* ST2 from Russia, Germany, and Brazil also formed a group with a high-level genome identity with median 25.5 core-SNP differences; the appearance of the common progenitor dates to 2003 (1996–2012). Linezolid-resistant *S. hominis* isolates from Russia demonstrated associated resistance to teicoplanin. Analysis of a midpoint-rooted phylogenetic tree of the group confirmed the genetic proximity of Russian and German isolates; Brazilian isolates were phylogenetically distant. *repUS5*-like plasmids harboring *cfr* were detected in *S. hominis* and *S. haemolyticus*.

Keywords: coagulase-negative staphylococci, linezolid, resistance, genome epidemiology, tedizolid

INTRODUCTION

Coagulase production was introduced as a criterion for the differentiation of members of genus *Staphylococcus* members in 1940 (Fairbrother, 1940). In contrast to the main representative of coagulase-positive staphylococci (*Staphylococcus aureus*), coagulase-negative staphylococci (CoNS) initially were considered avirulent constituents of the human and warm-blooded animal microbiota. However, at present, many CoNS species are recognized as opportunistic pathogens (Coates et al., 2014; Heilmann et al., 2019). The most frequent colonizers of human skin *S. epidermidis, S. haemolyticus,* and *S. hominis* are the main cause of local and bloodstream foreign body–related infections; prosthetic valve endocarditis (Otto, 2012; Becker et al., 2014); and neonatal infections, including bacteremia (Dong and Speer, 2014).

Treatment of CoNS is becoming increasingly complex due to the emergence and rapid spread of methicillin resistance (MR)—a marker of resistance to most beta-lactams (except for ceftaroline and ceftobiprol), mediated by an additional penicillin-binding protein (PBP), designated PBP2a, that has reduced affinity to beta-lactams. After its first description (Kjellander et al., 1963), prevalence of MR among CoNS causing hospital-acquired infections has continuously increased. Publications from the late 2010s confirm high percentages of MR isolates among CoNS causing bacteremia worldwide: 64.2% in the United Kingdom (Henriksen et al., 2018), 64.7% in the United States (Pfaller et al., 2019), and 91% in Iran (Pourakbari et al., 2018).

Methicillin resistance in CoNS is frequently associated with resistance to other antibiotics except for glycopeptides, which for many years were the drugs of choice in the treatment of staphylococcal infections. Over the past decades, treatment options for Gram-positive infections have expanded significantly with new glycopeptides, beta-lactams, lipopetides, glycylcyclins, and oxazolidinones (linezolid and tedizolid). Although linezolid is not registered for the treatment of CoNS infections, it was used off-label for the treatment of meningitis (Krueger et al., 2004; Kruse et al., 2006; Watanabe et al., 2013), ventriculitis (Boak et al., 2006), osteomyelitis (Nam et al., 2008) and prosthetic-joint infections (Ferry et al., 2018) caused by CoNS. However, high rates of oxazolidinone consumption or the use of long courses of therapy promotes resistance (Dortet et al., 2018; Bai et al., 2019). There are four mechanisms of oxazolidinone resistance in CoNS: methylation of 23S rRNA [plasmid-born chloramphenicol–florfenicol resistance (*cfr)* gene], mutations in 23S rRNA and ribosomal proteins (*rpl* genes), and efflux (plasmid-born *optr*A gene) (Long and Vester, 2012; Wang et al., 2015). Resistance due to ribosomal protection (plasmid-born *poxt*A gene) was recently described in enterococci (Antonelli et al., 2018). Isolates harboring the *cfr* gene are resistant to linezolid but susceptible to tedizolid; all other resistance mechanisms confer cross-resistance between both oxazolidinones. Oxazolidinone-resistant CoNS infections and particularly bloodstream infections are associated with poor clinical outcome: high mortality and prolonged hospital stay (Russo et al., 2015).

Recently, several outbreaks of hospital-acquired infections due to oxazolidinone-resistant CoNS were reported from the United States (Tewhey et al., 2014), Brazil (de Almeida et al., 2013), Greece (Karavasilis et al., 2015), Italy (Mendes et al., 2010), France (Dortet et al., 2018), Germany (Layer et al., 2018), China (Cai et al., 2012), and Spain (Seral et al., 2011; Rodríguez-Lucas et al., 2020).

Revealing the genetic structure of bacterial populations is necessary for the identification of their evolution and distribution. Clustering in large databases is most often done using both non-spatial and spatial Bayesian analysis of population structure (BAPS) algorithms developed by Corander et al. (2008). Bayesian evolutionary analysis by sampling trees (BEAST) is used for the estimation of the time of clade formation (or divergence times). It is used to build rooted, time-measured phylogenies inferred using strict or relaxed molecular clock models. Using the combination of BEAST and BAPS (Castillo-Ramirez et al., 2012) several genetically isolated lineages within the MRSA sequence type (ST) 239 clone and chronology of the introduction of these lineages into the specific geographical regions were identified.

In the present study, we describe linezolid-resistant *S. epidermidis* (LRSE), *S. haemolyticus*, and *S. hominis* recovered in several tertiary hospitals in Moscow. Methods of comparative genomics were initially used for the investigation of recovered isolates and followed by comparison with publicly available genomes of oxazolidinone-resistant CoNS. BAPS and chronogram reconstruction using BEAST were implemented to determine clusters and the time of linezolid-resistant CoNS lineage emergence. The possibilities of two scenarios of oxazolidinone resistance dissemination were evaluated: either clonal spread of resistant genetic lineages or emergence of resistance *de novo*.

MATERIALS AND METHODS

Bacterial Strains and Antibiotic Susceptibility

Staphylococcus epidermidis, *S. hominis*, and *S. haemolyticus* isolates (n = 47) demonstrating reduced susceptibility to linezolid were collected in 2014–2018 in six Moscow hospital laboratories and transferred to the central laboratory Pediatric Research and Clinical Centre for Infectious Diseases (PRCCID) together with record forms. Personal data of patients were not included in record forms; ethical approval for the study was not required. Control of CoNS identification was performed in the central laboratory by MALDI-TOF mass spectrometry (Microflex LT, Bruker Daltonics, Germany) following the manufacturer's instructions. Antimicrobial susceptibilities to 22 antibiotics (Molekula, United Kingdom), including linezolid (Sigma-Aldrich, United States), tedizolid (Bayer, Germany), teicoplanin, oritavancin, telavancin, and dalbavancin (Biosynth Carbosynth, United Kingdom) were tested by broth microdilution in cation-adjusted Mueller–Hinton broth (Bio-Rad, Marnes-la-Coquette, France) and interpreted according to The European Committee on Antimicrobial Susceptibility Testing (EUCAST) (2020) recommendations

(Breakpoint tables for interpretation of MICs and zone diameters, Version 10.0, 2020.[1]).

Population Analysis Profile

A population analysis profile (PAP) was performed according to the microdilution modification proposed in a previous study (Pfeltz et al., 2001). Four dilutions (10^{-1}, 10^{-3}, 10^{-5}, and 10^{-7}) of the initial suspension (10^8 CFU/mL) of each strain were prepared. Three 10-μL droplets of each dilution were plated on vancomycin-containing brain–heart infusion agar plates (0.5, 1, 1.5, 2.0, 3.0, 4.0, 6.0, 4.0, 8.0, 12.0, and 16.0 mg/mL). The inoculated plates were incubated for 48 h at 37°C. Plated droplets containing 5–50 CFU were selected for counting, and the average number of colonies per vancomycin concentration was determined. Plots showing the log10 CFU in the presence of each concentration of vancomycin were constructed. Area under curve (AUC) was calculated using the R 3.6.3 base package with trapezoidal rule. The ratio of AUC for CoNS to AUC of control hetero-resistant strain *Staphylococcus aureus* Mu50 under the study was calculated (AUC_{CoNS}/AUC_{Mu50}). Isolates demonstrating $AUC_{CoNS}/AUC_{Mu50} \geq 0.9$ were considered to be hetero-resistant.

Whole Genome Sequencing

Genomic DNA was extracted using a PureLink™ Genomic DNA Mini Kit (Invitrogen™, CA, United States) with preliminary lysis of the cells being done with 1 mg/mL lysostaphin (Sigma-Aldrich, United States). The Nextera XT Kit (Illumina, San Diego, CA, United States) was used for DNA library preparation followed by sample indexing and amplification according to the manufacturer's protocol. DNA libraries were sequenced on a MiSeq instrument (Illumina, San Diego, CA, United States). Quality check data on sequencing reads is presented in **Supplementary Table 1**.

Genome Assembling and Annotation

Sequence reads were filtered and trimmed using the trimmomatic 0.32 (Bolger et al., 2014) under default settings for Illumina raw data. Read quality and length distribution were analyzed with FastQC 0.11.9 (Brown et al., 2017). *De novo* contigs were assembled with SPAdes 3.14.0 (Bankevich et al., 2012). Bowtie 2 2.3.5 (Langmead and Salzberg, 2012) and SAMtools 1.10 (Li et al., 2009) software were used for detection of SNP's conferred antibiotic resistance, including oxazolidinones resistance. Prediction of single nucleotide polymorphism (SNP) effects was done with SNPeff 4.3t (Cingolani et al., 2012) using filtered (minimum SNP coverage 10 and quality Phred per base > 20) and deduplicated reads after SAMtools processing. The following genomes were used as reference: *S. epidermidis* ATCC 12228 (NC_004461.1), *S. hominis* FDAARGOS_746 (NZ_CP046306.1), and *S. haemolyticus* ATCC 29970 (NZ_CP035291.1). Genomes were annotated with PROKKA 1.14.5 (Seemann, 2014), MLST typing, resistance, and virulence gene typing were done using MLST 2.18.0[2] and abricate 0.9.8[3] scripts, respectively.

Inclusion of Genome Data From Previous Studies

For phylogenetic reconstruction in addition to Moscow genomes, data from previous studies—outbreaks in France (Dortet et al., 2018) and the United States (Tewhey et al., 2014)—were included in the study. These data were downloaded from the NCBI Sequence Read Archive (SRA) (BioProjects PRJEB22222 and PRJNA239883, respectively), assembled, and annotated using methods listed in the previous section. Additionally, 460 genomes of *S. epidermidis*, 60 genomes of *S. hominis,* and 205 genomes of *S. haemolyticus* were downloaded from the NCBI GenBank using the list of genomes from the PATRIC database (update July 2019) (Wattam et al., 2017). The genomes included for phylogenetic analysis are listed in the data set (**Supplementary Table 2**).

Phylogenetic and Pan-Genome Analysis

Pan-genomic analysis was done with Roary 3.13.0 (Page et al., 2015), and gene content comparison was done with scoary 1.6.16 (Brynildsrud et al., 2016). Genomes of the CoNS were *in silico* genotyped against the PubMLST database update July 2020 (Jolley and Maiden, 2010) using MLST script 2.18.0 (see text footnote 2).

To produce a core genome alignment for phylogenetic tree reconstruction, we developed a nucmer aligner wrapper named panmap (available on[4]). Panmap uses nucmer 3.9.4 (Kurtz et al., 2004) to create a pairwise alignment for every genome against a reference contigs [in our case, we used the complete chromosome of *S. epidermidis* BPH0662 (NZ_LT571449.1), of *S. hominis* FDAARGOS_136 (NZ_CP014107.1), and *S. haemolyticus* JCSC1435 (NC_007168.1)]. Then, it uses reference contig annotations for every region—gene or intergenic—to produce counts of gapped positions. A gapped position is defined as a position in which the proportion of gaps is above some threshold. If the proportions of gapped positions in a region are higher than a second threshold, then the whole region is dropped. Otherwise, the whole region is kept. Both thresholds were set to 1%. We implemented this annotation-based region-to-region approach to keep as much information about distance between SNPs as possible as Gubbins 2.4.1 (Croucher et al., 2015)—the program that identifies potential recombination regions—uses SNP density information. Using Gubbins 2.4.1, we removed potential regions of recombination from the core genome alignment. The resulting alignment was used for phylogenetic tree reconstruction by IQ-tree 1.6.12 software with ModelFinder and ultrafast bootstraps (Nguyen et al., 2015; Kalyaanamoorthy et al., 2017; Hoang et al., 2018). The substitution model chosen by ModelFinder was TVMe + ASC + R4. The substitution model was chosen based on the ModelFinder results under default parameters. Long branches that did not contain genomes of interest were removed from the trees. The core genome

[1]http://www.eucast.org

[2]https://github.com/tseemann/mlst

[3]https://github.com/tseemann/abricate

[4]https://github.com/sleyn/panmap

alignment was clustered using BAPS with the rhierBAPS R package 1.0.1 (Cheng et al., 2013; Tonkin-Hill et al., 2018) with the expected number of populations set as 20 and maximum depth of clustering set as two. Intra- and inter-group pairwise comparison of the number of SNPs was carried out using R script pairwise_snp_differences[5] (**Supplementary Table 3**).

Timed Phylogeny Analysis

Timed phylogeny calculation was used for the genetically closest groups of CoNS. Several genome groups were chosen: LRSE belonging to ST2 (n = 76), all (susceptible and resistance to linezolid) ST22 isolates (n = 27), and *S. hominis* ST2 (n = 20). BEAST 2.6.4 was used to generate a timed phylogeny (chronogram) assuming a relaxed lognormal clock and, with coalescent constant tree prior, 10 million iterations of a gamma site model with an HKY substitution model. Tree convergence was confirmed using BEAST's Tracer 1.7.1 program (Suchard et al., 2018) using the recommended criterion (ESS > 200). TreeAnnotator was then used to identify the maximum clade credibility (MCC) tree using a 10% burn-in. The resulting tree was visualized using FigTree 1.4.4.

Annotation and Mapping of Resistance Data

Analysis of resistance-related SNPs was done for SNPs known to cause linezolid resistance: 23S rRNA (G2576T, C2534T, T2504A *Escherichia coli* numbering), ribosomal proteins L3 (Ala157Arg, Asp159Tyr, Met156Thr, Gly152Asp, His146Arg, Gly137Val, Leu101Val), L4 (Asn158Ser), and L2 (Val112Ile, Ile75Thr) with a potential role of oxazolidinone-resistant. *mecA*, *cfr* genes, and mutations in *rpoB* that conferred multidrug resistance were also mapped. The sequence of 23S rRNA was extracted using barrnap tool 0.9[6]. Other genes were extracted with designed in the study Riddikulus script[7]. Genes were aligned by MAFFT 7.407 (Katoh and Standley, 2013). SNPs were extracted using Unipro UGENE software 37.0 (Okonechnikov et al., 2012). Calculation of the total number of acquired resistance genes for each genome was done with abricate 0.9.8 (see text footnote 3).

Seventeen proteins associated with decreased glycopeptide susceptibility in *S. aureus* (MprF, Pbp123, WalKR, GraSR, VraSRT, RpoBC, YycIH, Cmk, and MsrR) were selected for analysis, and homology proteins were extracted from *S. epidermidis* and *S. hominis* genomes. Frequency of amino acids substitution (AAS) was compared across the all-genome data set in linezolid-resistant genomes and linezolid-susceptible genomes. AAS with frequency below the threshold of 5 and 1% for *S. epidermidis* and *S. hominis*, respectively, were excluded. For possible associations between mutations and linezolid-resistance phenotype multiple correspondence analysis (MCA) was applied using factoextra R package 1.0.7.

Visualization and annotations of phylogenetic trees were done using ITOL 6.1.1 (Letunic and Bork, 2016). Plasmid structural comparison was done with Mauve 2.4.0 (Darling et al., 2004).

Accession Numbers

Genomic data have been deposited in NCBI Sequence Read Archive (SRA) and all reads are available from BioProject PRJNA384130 (SRA id: SRR5482186—SRR5482205 and SRR8427123—SRR8427149).

RESULTS

Linezolid-Resistant CoNS in Moscow Hospitals

The first two LRSE isolates were recovered at site A in 2014 and 2015 from patients with catheter-associated bloodstream infections in the intensive care unit. These isolates belonged to genetic lineage ST23. Emergence and dissemination of LRSE (ST2, *ST22*), linezolid-resistant *S. hominis* (ST2), and *S. haemolyticus* (ST1) were observed in several Moscow hospitals (A to F), in 2016–2018.

Different combinations of mutations in 23S rRNA and *rlp3* genes and acquisition of the *cfr* gene mediated resistance to oxazolidinones (**Table 1**). To estimate the number of modified copies of 23S rRNA, we aligned sequence reads on the target

[5]https://github.com/MDU-PHL/pairwise_snp_differences

[6]https://github.com/tseemann/barrnap

[7]https://github.com/dariader/Riddikulus

TABLE 1 | Characterization of Oxazolidinone-resistant CoNS isolated in Moscow hospitals.

Species	MLST	N	Sites	Source	MIC, mg/L		*cfr*	SNPs	
					LNZ	TDZ		*23S rRNA**	*rpl3*
S. epidermidis	ST2	6	E	Blood, sputum, intubation tube	>32	2–4	–	G2576T, (G2602T)	–
		2	F	Intubation tube, feces	>32	16	–	G2576T, (G2602T)	Gly137Val, His146Arg, Met156Thr
	ST23	2	A	Blood	32	2	–	G2576T, (G2602T)	–
	ST22	20	A, B, D, E	Blood	>32	>32	–	C2534T, (C2560T), T2504A, (T2530A)	Asp159Tyr, Gly152Asp
S. hominis	ST2	10	A,C,D,E	Blood	>32	4–8	–	G2576T, (G2603T)	Met156Thr, Val154Leu
		6	A,F	Blood, feces, sputum	>32	4–8	+	G2576T, (G2603T)	Met156Thr, Val154Leu
S. haemolyticus	ST1	1	A	Blood	>32	0.25	+	–	–

**Mutation in 23S rRNA according to E. coli numbering, in brackets mutation according to Staphylococcus numbering (NC_004461.1, NZ_CP046306.1, and NZ_CP035291.1).*

fragment of the reference sequence, and in all isolates, the specific SNPs were detected in 99% of the reads without mixed alleles. These data suggest that mutations are present in all copies of 23S rRNA.

All CoNS isolates demonstrated a high level of linezolid resistance (MIC $\geq$ 32 mg/L). The majority of isolates demonstrated tedizolid MIC $\leq$ 16.0 mg/L. A high level of tedizolid resistance (MIC $\geq$ 32 mg/L) was detected in ST22 isolates carrying double substitution in 23S rRNA. Only one *S. haemolyticus* isolate carrying the *cfr* gene as a single mechanism of resistance demonstrated susceptibility to tedizolid (MIC = 0.25 mg/L).

LRSE, belonging to ST2 and ST22, harbored *mec*–cassette of *SCCmec* III–like type with intact recombinase genes *ccrA3*, *ccrB3*, *mec*-complex class A, and *psm-mecA* regions. ST23 isolates carried *SCCmec* V–like type without the *psm-mecA* region. All *S. hominis* harbored intact SCC*mec* III with *psm-mecA* region. The *S. haemolyticus* isolate lacked SCC*mec* elements with only the *mecA* gene.

CoNS isolates under the study demonstrated high levels of associated resistance to aminoglycosides, fluoroquinolones, macrolides/lincosamides, tetracycline, co-trimoxazole, fusidic acid, rifampicin, and mupirocin but retained susceptibility to ceftaroline, tigecycline, and daptomycin. Resistance phenotypes were confirmed by the detection of corresponding genotypes (**Supplementary Table 4**). Isolates belonging to ST22 demonstrated susceptibility to erythromycin (despite the presence of intact macrolide resistance genes *msrA* and *mphC*) and resistance to clindamycin (L-phenotype). The phenotype is associated with T2504A point mutation (Liakopoulos et al., 2009).

Molecular Epidemiology of LRSE

Analysis of the *S. epidermidis* population identified a pan-genome consisting of 31,036 genes and 731 core ortholog gene clusters. Phylogenetic analysis of genomes was based on extraction of a 74,628 nt long core genome after alignment.

Bayesian analysis of population structure divided the *S. epidermidis* population into eight clusters (**Figure 1** and **Supplementary Figure 1**), but LRSE genomes were found only in two of them: BAPS clusters 2 and 3 consisting mainly of *mecA*-positive isolates of human origin (from infected persons and carriers). *S. epidermidis* belonging to other clusters (1 and 4–8) were isolated from different sources: environmental samples, animals, and humans and were characterized by maximum diversity and represented by different STs.

BAPS Cluster 2

Bayesian analysis of population structure cluster 2 consisted mostly of ST2 (n = 260) and a minor number of other STs. Part of LRSE in the cluster forms a compact group of closely related ST2 genomes from Russia, France, and Germany, all of them harbored a mutation in the 23S rRNA gene (G2576T) and *rpoB* gene (Asp471Glu and Ile527Met). LRSE from France carried an additional mutation in *rpl3* (Met156Thr). Part of LRSE from France and Germany harbored the *cfr* gene. Other LRSE were represented by distantly related ST2 and ST23 genomes from the United States, Brazil, and Germany. A pairwise SNP difference between LRSE and linezolid-susceptible ST2 isolates revealed a low level of identity with a median of 191 SNPs with lower and upper interquartile range (IQR): 181–545. LRSE of ST2 demonstrated high genomic identity with a median pairwise SNP difference of 43 SNPs with lower and upper IQR: 16–53 SNPs. A subgroup of isolates from France, Germany, and Russia demonstrated an even higher level of similarity (**Supplementary Table 3**). Intragroup SNP differences between genomes from the same country varied from 2 to 27 and intergroup from 44 to 52. BAPS cluster 2 also includes a group of seven highly similar ST23 isolates from the United States with a median pairwise SNP difference of 35 SNPs (IQR: 29–39).

The timed phylogeny analysis of all LRSE ST2 isolates showed that they could have emerged in the 1960s with a large confidence interval: 1915–1994 (**Figure 2**). A common ancestor of LRSE isolates from Russia, France, and Germany appeared in 1998 (1986–2006) before introduction of linezolid in practice. We can assume two scenarios for the appearance of LRSE in Russia: independent formation (site E) and importation (site F) from Germany. At the same time, the progenitor of the Russian isolates appeared in 2002 (1996–2008). In Brazil and the United States, LRSE isolates emerged independently in 1960–1970.

BAPS Cluster 3

Bayesian analysis of population structure cluster 3 included ST5, ST2, ST22, ST23, ST186, ST7, ST16, and ST35. Two groups of LRSE were detected within this cluster. The first group included LRSE of ST22 and its single-locus variant ST186 from Russia, France, and the United States. ST22 from Russia and France carried two mutations in 23S rRNA (C2534T and T2504A), and two mutations in *rpl3* (Asp159Tyr and Gly152Asp). Part of the Russian isolates carried a mutation of the *rpoB* gene (His481Asn). ST186 from the United States carried C2534T mutations and harbored the *cfr* gene. The pairwise SNP difference between LRSE and linezolid-susceptible ST22 isolates demonstrated a low level of identity with a median pairwise SNP difference of 214.5 (IQR: 204–233). LRSE from Russia and France were highly similar with a median pairwise SNP difference of 40 (IQR: 35.75–48.25). LRSE of ST186 from the United States were genetically distant from Russian and French isolates with a median pairwise SNP difference of more than 1,000 (**Supplementary Table 3**).

All ST22 isolates were included in BEAST analysis (**Figure 3**), a majority of them were LRSE, and a few were susceptible to linezolid. ST22 has a common time of origin in 1992 (1975–2000), but the LRSE sublineage widespread in France and Russia emerged in 2011 (2008–2013), and further divergence continued. Russian isolates from center A, B, and D are descended from a common ancestor with isolates from France, whose time of origin was 2011 (2009–2013). All isolates are compactly localized and have a short spreading period (which is also reflected in short branches on the chronogram), which indicates a clonal spread. Russian isolates from site E formed a separate cluster and were susceptible to rifampicin due to a wild type of *rpoB*.

The second group of LRSE within BAPS cluster 3 consisted of ST5 isolates from France (n = 23), and the United States (n = 2), and ST23 isolates from the United States (n = 2) and

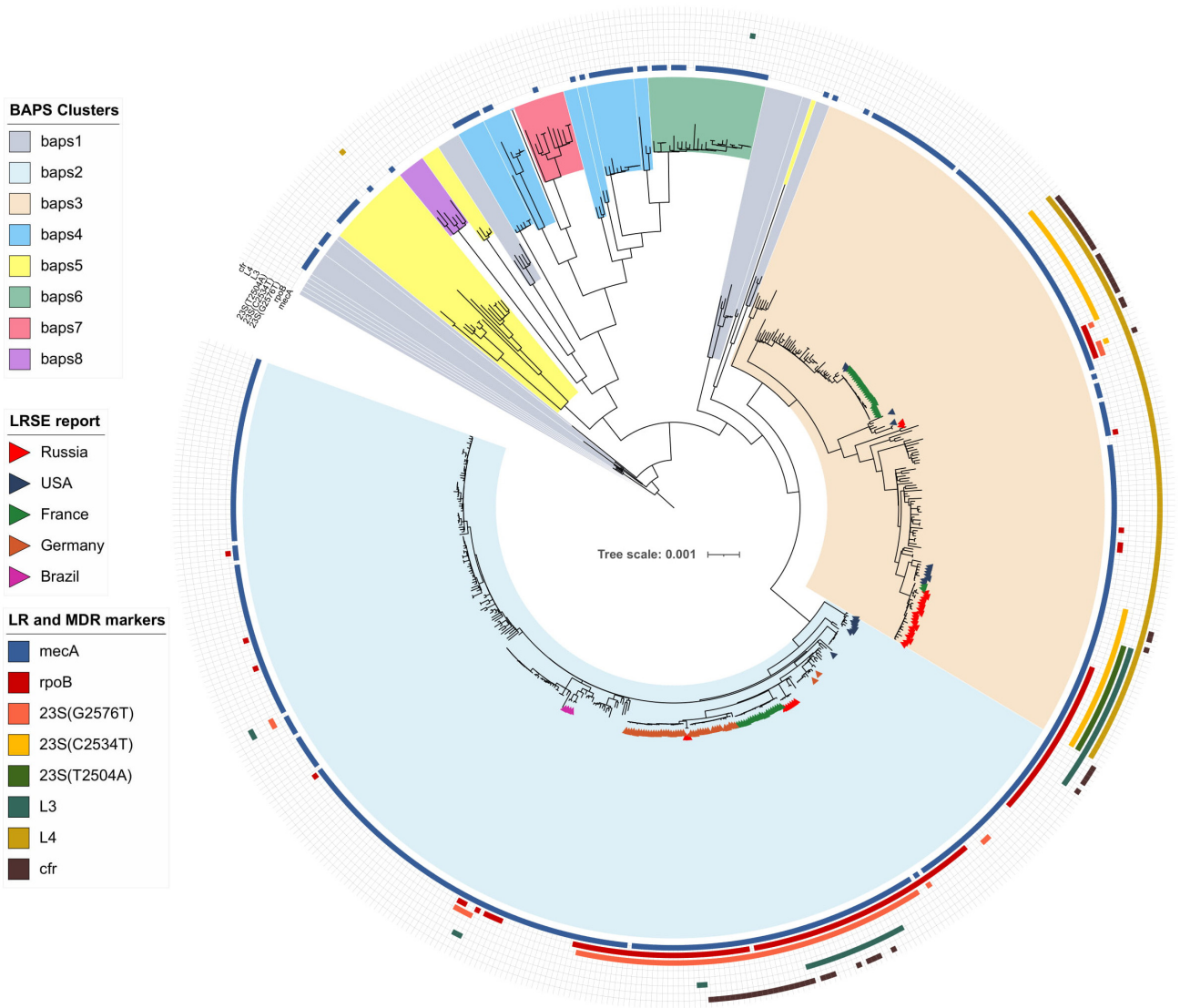

FIGURE 1 | Maximum-likelihood phylogeny of *S. epidermidis* population (*n* = 554) with mapped data of linezolid resistance and multidrug resistance data. Background color fill is matched to BAPS clustering. LRSE isolate is marked triangles: from Russia (current study), the United States (Tewhey et al., 2014), France (Dortet et al., 2018), Germany (unpublished data, only metadata is available BioProject PRJNA314440), and Brazil (unpublished data, only metadata is available from BioProjects PRJNA419710, PRJNA419705, PRJNA419706, and PRJNA419711). Annotation from inner to outer circle: presence *mecA*, mutations in *rpoB* (rifampin resistance), linezolid resistance (mutations in 23S rRNA, *rpl3, rpl4* genes and presence of *cfr*). Full zoom scalable view of phylogenetic tree with additional data and names of strains and description of calculated acquired resistance genes are available in **Supplementary Figure 1**.

Russia (*n* = 2). LRSE of ST23 harbored mutations in 23S RNA (G2576T or C2534T) and *rpoB* (Asp471Glu and Ile527Met), and one isolate carried the *cfr* gene. LRSE of ST5 carried a C2534T mutation and harbored the *cfr* gene. LRSE of ST23 were characterized by significant heterogeneity between BAPS clusters and between all LRSE of ST23 with median pairwise SNP difference of 4,204 (IQR: 4,167–4,252) SNPs and 4,196 (IQR: 37–4,245), respectively. LRSE of ST5 from France were highly similar with a median pairwise SNP difference of 5 (IQR: 2–7) SNP. Two isolates from Russia were also similar, but four isolates from the United States of ST23 and ST5, belonging to BAPS 3 and located close to the Russian isolates, revealed a high level of heterogeneity with a median pairwise SNP difference of 7,165 (IQR: 1,955.5–7,167.5).

In two genomes from Russia (CNS243, CNS244 from site F) and one from the United States (strain DAR4891, BioProject PRJNA308322) belonging to the ST2 rare mutation in *rpl*3, Gly137Val was detected together with a G2576T mutation in 23S rRNA. The role of this SNP in linezolid resistance development is unknown. Mutations in *rpl*2 (Val112Ile and Ile75Thr) and *rpl4* (Asn158Ser) were detected in LRSE and linezolid-susceptible isolates from epidemic sequence types from BAPS cluster 3.

Analysis of distribution of acquired resistance genes in the population shows that the highest mean count of determinants

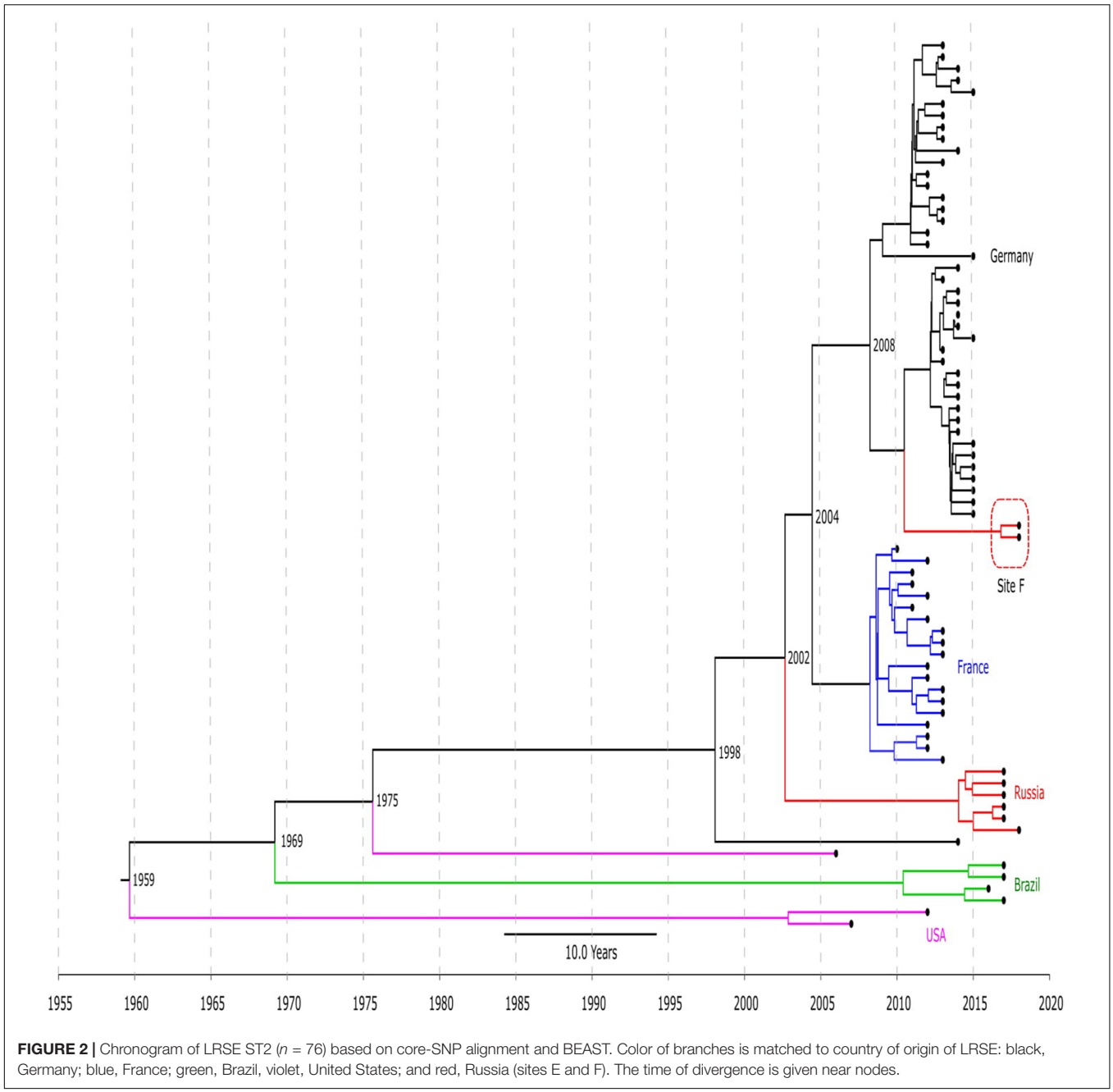

FIGURE 2 | Chronogram of LRSE ST2 (*n* = 76) based on core-SNP alignment and BEAST. Color of branches is matched to country of origin of LRSE: black, Germany; blue, France; green, Brazil, violet, United States; and red, Russia (sites E and F). The time of divergence is given near nodes.

per genome was in genomes of BAPS clusters 2 (6.1) and 3 (5.9). The mean count of resistance genes in the LRSE subpopulation was 6.9.

Phylogenetic Analysis of *S. hominis*

The pan-genome of *S. hominis* consisted of 7,798 genes, and the core genome included 1,185 genes. Phylogenetic analysis of genomes was based on extraction of 50,332 nt long core genome after alignment. The *S. hominis* population formed six BAPS clusters (**Figure 4**). The 1–3 BAPS clusters were localized closely to the root; they included *mecA*-negative isolates from healthy humans, animals, insects, and environmental specimens with different new unregistered MLST allelic profiles. Comparative analysis of genomes of these clusters showed a high number of core SNPs: for the BAPS 1 cluster, the pairwise median SNP difference was 4,197 (IQR: 3,538.5–4,915), and for BAPS 3, 2,860 SNPs (IQR: 348–7,694). The pairwise median SNP difference of all BAPS clusters is presented in **Supplementary Table 3**.

BAPS clusters 4–6 consisted of ST1, ST2, ST18, ST29, and ST47. Isolates of BAPS cluster 6 belonged to ST2, and they demonstrated high level genome identity with median 25.5 core SNP differences (IQR: 15–92); the cluster included linezolid-resistant isolates: 16 from Russia (current study), one from Lübeck, Germany (LRKNS031 unpublished, data from

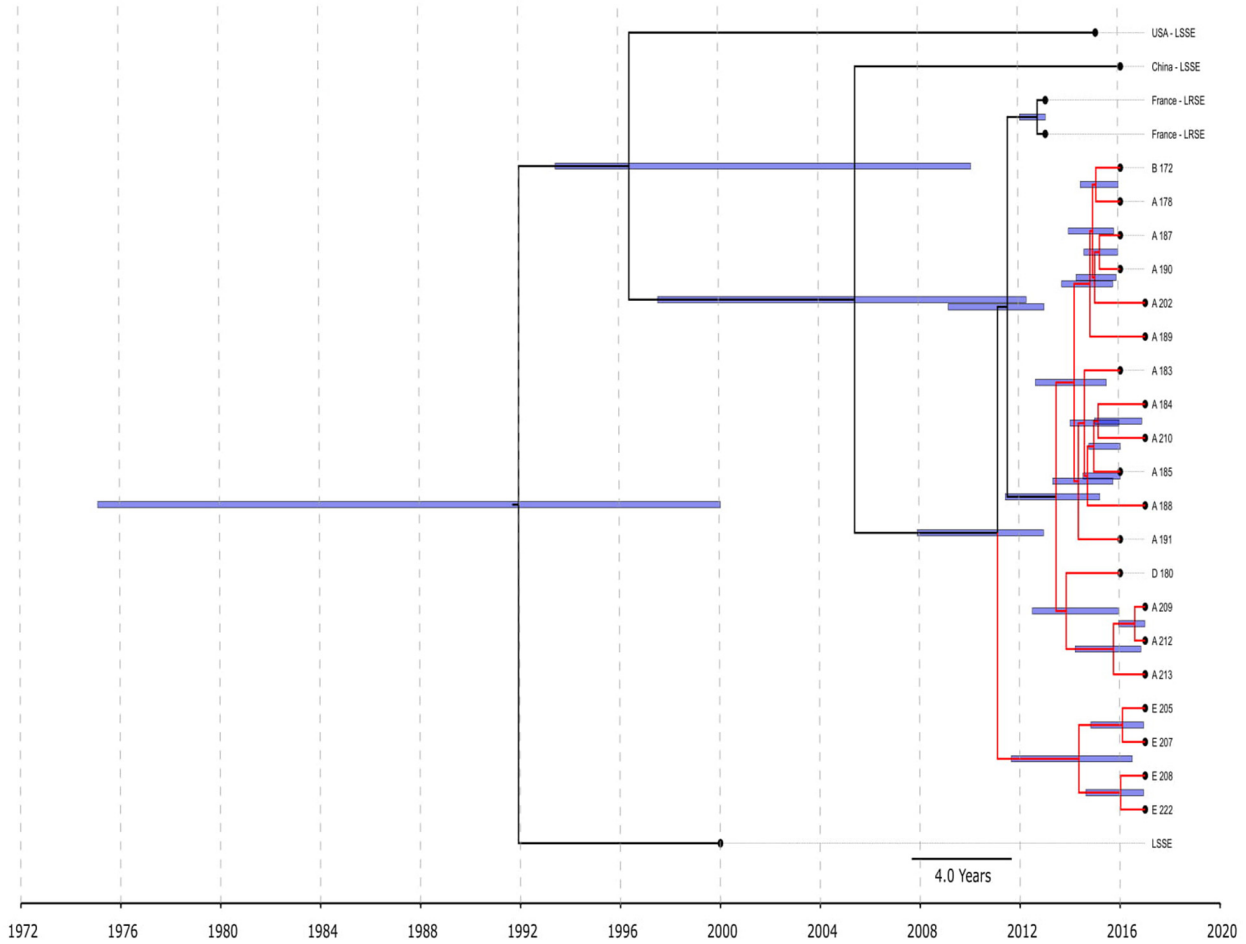

FIGURE 3 | Chronogram of *S. epidermidis* ST22 (*n* = 25) based on core-SNP alignment and BEAST. Three linezolid-susceptible *S. epidermidis* from different countries were included in the analysis. LRSE ST22 from Russia (red branches) and France were included in the analysis. Title of Russian isolates is matched of site isolation. 95% CI of time appearance (blue bars) shown near the nodes.

BioProject PRJNA314440), and two from Brazil (unpublished, data from BioProjects PRJNA419707 and PRJNA419709). One isolate from Sweden in BAPS cluster 6 was linezolid susceptible. All isolates carried a mutation in *rpoB* (Asn481His). Phylogenetic analysis of a midpoint rooted tree of BAPS cluster 6 (**Figure 5**) revealed the genetic proximity of the Russian and German isolates; they carried identical mutations in *23S rRNA* (G2603T) and *rpl3* (Met156Thr, Val154Leu). Six Russian isolates carried *cfr* also; most of them were isolated from site F. Isolates with double mechanism resistance and isolates with only mutation in 23S rRNA shared the same core genetic background with a minimum SNP difference. Brazilian isolates were phylogenetically distant; they carried identical mutations in *23S rRNA* but different mutations in *rpl3* (Met156Thr, Phe147Leu). The timed phylogeny analysis (**Figure 5**) showed that the BAPS 6 cluster of the *S. hominis* ST2 appeared in 1993 (95% CI: 1982–1998). The appearance of the common progenitor of linezolid-resistant *S. hominis* dates to 2003 (1996–2012) soon after introduction of linezolid into clinical practice in 2001, emergence of resistance *de novo* looks more probable.

Phylogenetic Analysis of *S. haemolyticus*

The pan-genome of *S. haemolyticus* consists of 13,524 genes. The population of *S. haemolyticus* was divided into four BAPS clusters based on the extraction of 45,692 core SNPs after alignment of 1,032 core genes (**Figure 6**). BAPS cluster 1 included 82.6% of available *S. haemolyticus* isolates that were recovered at different times from different sources and belonged to 15 different STs, the cluster demonstrated a relatively low-level genome identity with median core-SNP differences of 651 SNPs (IQR: 481–806). A majority (77%) of isolates were *mecA*-positive and carried an average of 6.7 resistant genes per genome. Oxazolidinone-resistant *S. haemolyticus* isolates from Moscow (ST1) and the United States (ST4) (Tewhey et al., 2014) belonged to BAPS cluster 1 and were genetically distant.

Staphylococcus haemolyticus and *S. hominis* Plasmids Carrying *cfr* Genes

One *S. haemolyticus* and six *S. hominis* isolates carried *cfr*-harboring plasmids of approximately 38,000 bp size (only

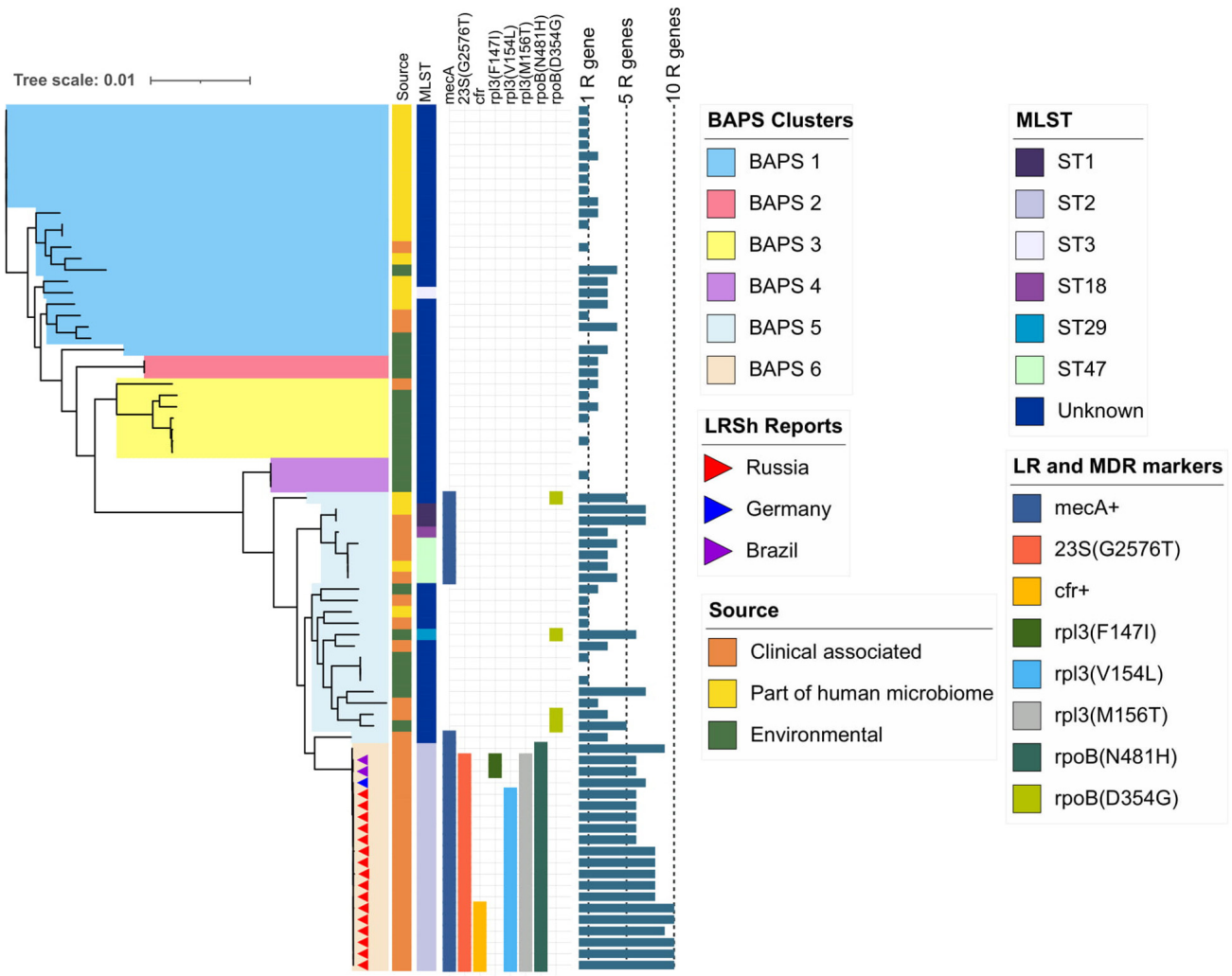

FIGURE 4 | Maximum-likelihood phylogeny of *S. hominis* population (76 genomes) based on core-SNP alignment. Background color fill is matched to BAPS clustering (BAPS 1 to BAPS 6). Linezolid-resistant *S. hominis* isolates (LRSh reports) marked as triangles on the tree. Annotation included source of genomes, MLST, linezolid resistance markers (LR): 23S rRNA mutation G2576T, rpl3 (Phe147Ile, Val154Leu, and Met156Thr), *cfr*; and multidrug-resistance markers (MDR): *mecA* and mutations in *rpoB* (Asn481His, Asp354Gly); bar chart is matched to the number of acquired resistance genes from 0 to 10 genes per genome (1R gene to 10R genes). The following genes were screened (mutations were not included): *aac(6')-aph(2'')*, *aadD*, *ant(6)-Ia*, *ant(9)-Ia*, *aph(3')-III*, *blaZ*, *cat*, *ermC*, *fexA*, *cfr*, *fosB*, *fosD*, *fusB*, *fusC*, *lnu(A)*, *lsa(B)*, *mecA*, *mph(C)*, *msr(A)*, *str*, *tetK*, *tetL*, *vgaA*, and *vgaB*.

de novo assembled contigs were studied). BLAST analysis of the plasmid sequence revealed in GenBank several similar plasmids, which formed two clusters (**Supplementary Figure 2**). The first cluster included plasmids from *S. haemolyticus* (current study, Moscow), MRSA from the United States (Mendes et al., 2008) and Ireland (Shore et al., 2016), *S. cohnii* from China (Chen et al., 2013), and *S. epidermidis* from France (Dortet et al., 2018). The analysis of core genes of these plasmids revealed differences in no more than five SNPs. The second cluster included similar plasmids from *S. hominis*. They differed from the first cluster in no more than 408 SNPs. Plasmids from both clusters share 90% nucleotide identity and harbored replication gene *repUS5*, which was included in incompatibility group 18 (Inc18). The *Cfr*-gene in all considered plasmids was colocated together with the *fexA* gene coding phenicol resistance.

Decreased Susceptibility to Glycopeptide in Linezolid-Resistant CoNS

Eight *S. hominis* ST2 and one *S. epidermidis* ST23 isolates demonstrated teicoplanin resistance with MIC = 16 mg/L. At the same time, the MIC of vancomycin was in range 1–4 mg/L (**Table 2**). However, the median parameter of AUC_{MU50}/AUC_{CoNS} with vancomycin across all isolates was 0.74 (0.38–0.98). Nine isolates demonstrated a hetero-resistant phenotype with AUC_{MU50}/AUC_{CoNS} range from 0.90 to 0.99

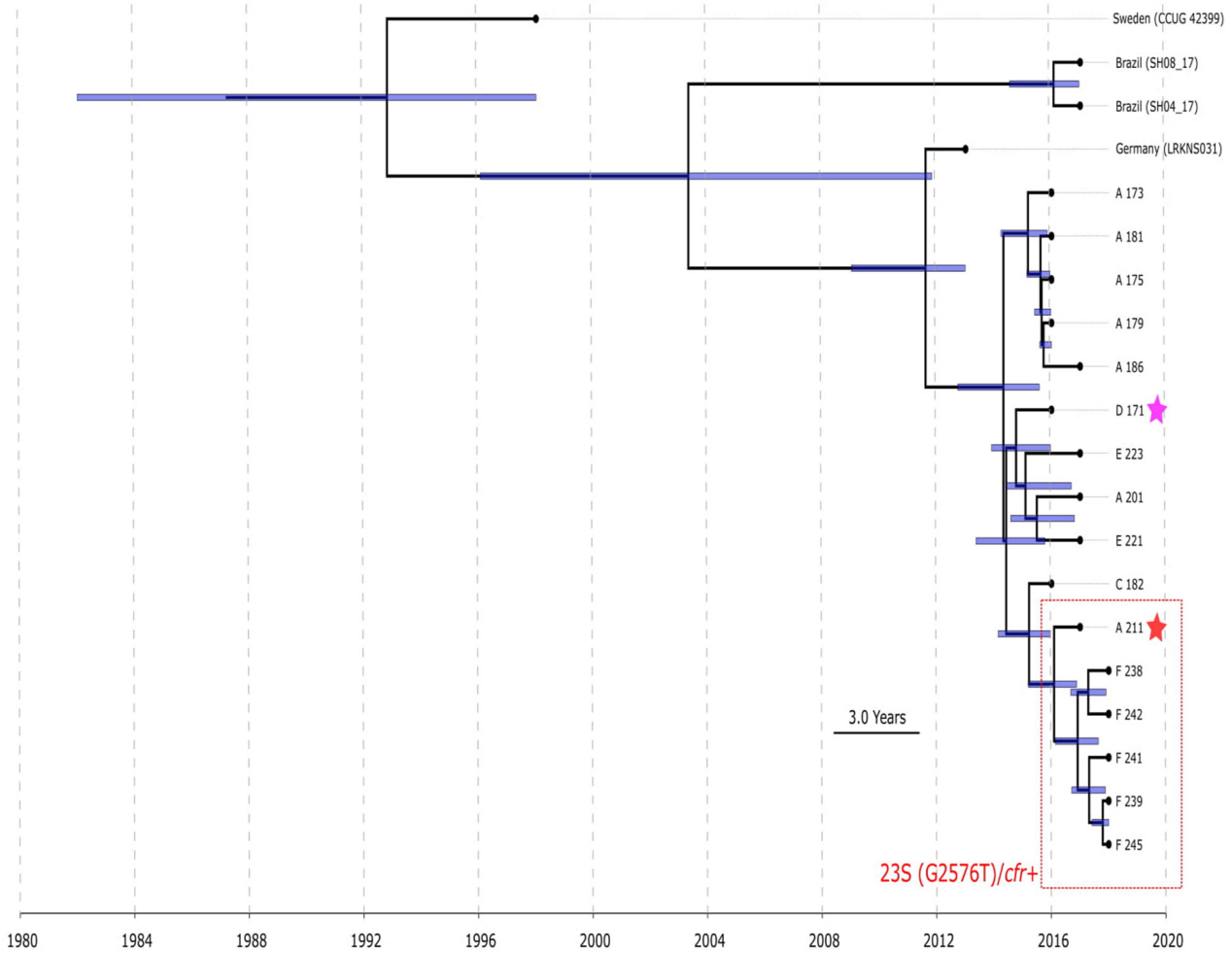

FIGURE 5 | Chronogram of *S. hominis* ST2 (BAPS cluster 6, *n* = 20) based on core-SNP alignment and BEAST. The violet star marks first time isolated oxazolidinone-resistant *S. hominis* in Russia, red star—first isolated cfr-positive *S. hominis*. Sites of appearance oxazolidinone-resistant *S. hominis* is shown on the figure (A, C–F). In addition to Russian isolates, this cluster included (blue names of strains): isolate LRKNS031 (linezolid-resistant *S. hominis* from Germany, BioProject PRJNA314440), two isolates from Brazil (BioProject PRJNA419707 and BioProject PRJNA419709) and linezolid-susceptible isolate CCUG 42399 from Sweden. 95% CI of time appearance (blue bars) shown near the nodes.

(**Supplementary Table 4**). Correlation between susceptibility to rifampicin (including mutations in *rpoB*) and PAP/AUC as well as correlation between teicoplanin and vancomycin levels of susceptibility were not found (**Supplementary Figure 3C**). However, a moderate positive correlation ($R = 0.27$, $p < 0.05$) was found between two parameters: AUC_{MU50}/AUC_{CoNS} and teicoplanin susceptibility (**Figure 7**). The new lipoglycopeptides (oritavancin, dalbavancin, and telavancin) demonstrated high potency with an MIC range from 0.03 to 0.125 mg/L (**Table 2** and **Supplementary Table 4**). For *S. hominis* isolates, possible genetic markers associated with teicoplanin resistance were identified. These include the plasmid homolog of teicoplanin resistance–related proteins (*tcaA*), localized together with the *cfr* and *fexA*. However, in the *cfr*-positive isolate of *S. haemolyticus* (CNS200), this gene is also present on the plasmid, but the teicoplanin MIC level was 2 mg/L. Other mutations were also identified only in teicoplanin-resistant isolates. In particular, the Tyr75Asn mutation in the protein with unknown function with the Duf420 domain; mutation of Gly95Glu in the protein containing the DedA family protein domain; mutation (G → T) in the upstream region of DNA polymerase III subunit beta.

Using genomic data of all isolates included in the study, we analyzed the possible association of linezolid-resistance in *S. epidermidis* and *S. hominis* isolates with a decrease susceptibility to glycopeptides. For this purpose, 17 amino acid sequences of homologous proteins involved in the decreased susceptibility to glycopeptides in *S. aureus* were analyzed. A total of 45 mutation variants were identified, including missense and frameshift mutations. Using MCA analysis, the distribution of these mutations in the proteins was not associated with the LRSE genomes (**Supplementary Figure 3B**). However, it was found that the following mutations: YycH (Ser379Ala), RpoB (Ser486Tyr), GraS (Asn2Asp), and GraR (Glu224Gly) are most common in LRSE ($p < 0.01$), then in the other groups (heat

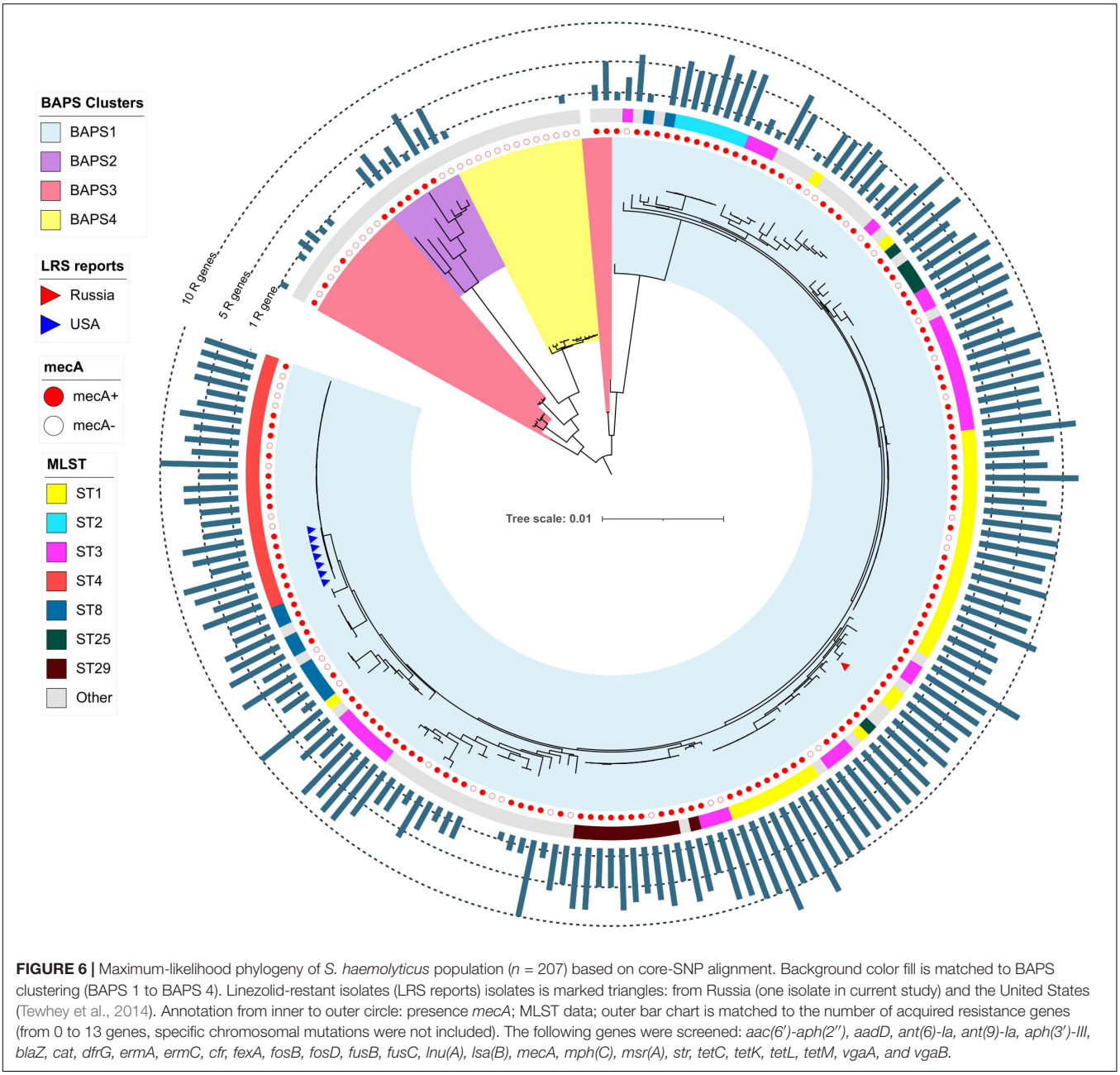

FIGURE 6 | Maximum-likelihood phylogeny of *S. haemolyticus* population (*n* = 207) based on core-SNP alignment. Background color fill is matched to BAPS clustering (BAPS 1 to BAPS 4). Linezolid-restant isolates (LRS reports) isolates is marked triangles: from Russia (one isolate in current study) and the United States (Tewhey et al., 2014). Annotation from inner to outer circle: presence *mecA*; MLST data; outer bar chart is matched to the number of acquired resistance genes (from 0 to 13 genes, specific chromosomal mutations were not included). The following genes were screened: *aac(6′)-aph(2″), aadD, ant(6)-Ia, ant(9)-Ia, aph(3′)-III, blaZ, cat, dfrG, ermA, ermC, cfr, fexA, fosB, fosD, fusB, fusC, lnu(A), lsa(B), mecA, mph(C), msr(A), str, tetC, tetK, tetL, tetM, vgaA, and vgaB.*

TABLE 2 | Glycopeptide and lipoglycopeptides susceptibility and PAP analysis in linezolid-resistant coagulase-negative staphylococci.

	MLST	*n*	Range MIC, mg/L							PAP/AUC		AAS* in RpoB		
			VAN	TEC	DLB	TLV	ORI	DAP	RIF	Range	M**	D471E	H481N	I527M
LRSE	ST2	8	1–4	0.25–4	0.03–0.06	0.06–0.125	<0.06	0.25–0.5	>4	0.38–0.9	0.59	+	–	+
	ST22	16	1–2	0.125–4	<0.03	0.03–0.125	<0.06	0.125–0.5	0.25–1	0.37–0.99	0.76	–	+	–
	ST22	4	2–4	4	<0.03	0.06–0.125	<0.06	0.25–0.5	<0.03	0.75–0.98	0.85	–	–	–
	ST23	2	2–4	2 and 16	0.06	0.125	0.125	0.5	>4	0.67–0.85	NA	+	–	+
LRSH	ST2	16	1–2	4–16	0.03–0.125	0.06–0.125	0.03–0.125	0.125–0.5	0.5–2	0.40–0.9	0.75	–	+	–

*NA, not applicable; VAN, vancomycin; TEC, teicoplanin; DLB, dalbavancin; TLV, telavancin; ORI, oritavancin; DAP, daptomycin; RIF, rifampicin. *amino acid substitution, **median.*

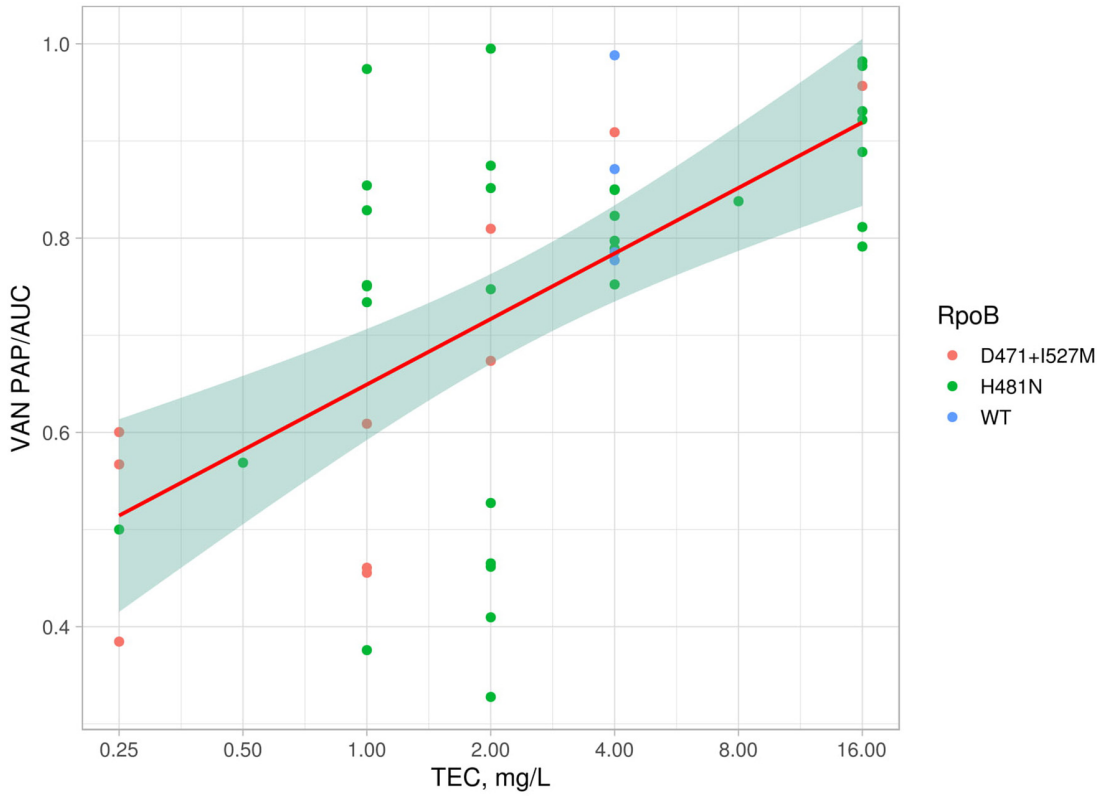

FIGURE 7 | Linear model and confidence interval plot with PAP/AUC data and teicoplanin MICs. Each point represented by AAS in RpoB (WT—wild type).

map of frequency of occurrence mutations is presented in the **Supplementary Figure 3A**). There were no significant differences in the prevalence of these mutations between linezolid-resistant and linezolid-susceptible *S. hominis*.

DISCUSSION

In 2018, the main representative of CoNS group *S. epidermidis* was recognized by the European Centre for Disease Prevention and Control (2018) as a public health threat. The decision was based on the results of a study (Lee et al., 2018). The authors described the international spread of three hospital-adapted, multidrug-resistant lineages of *S. epidermidis*. Among the multidrug-resistant *S. epidermidis* isolates included in the study, the 18 isolates from Germany, France, and Ireland demonstrated resistance to linezolid, 14 of them belonged to ST2, three to ST5, and one to ST23. In the current study, we examined the international spread of LRSE in more detail. We also analyzed the dissemination of linezolid-resistant lineages of other common human skin colonizers: *S. hominis* and *S. haemolyticus*.

Evaluation of pairwise core-SNP differences between isolates of the same group (intragroup comparison) or between isolates of different groups (intergroup comparison) is a powerful tool for the assessment of the level of similarity between bacteria. However, criteria for different levels of similarity or identity are not established, making it difficult to interpret the results and differentiate lineages that have independently acquired resistance to oxazolidinones from lineages originating from a common resistant precursor. In this case, additional approaches could be used, such as BAPS and BEAST, for more detailed analysis of *Staphylococcus* phylogenomic.

In the current study using several approaches, we uncovered the existence of three international LRSE lineages, which largely coincides with the clustering of the *S. epidermidis* obtained in the study (Lee et al., 2018). The first lineage was represented by ST2 BAPS cluster 2 with highly similar isolates from France, Germany, and Russia harboring identical mutations in 23S rRNA and *rpoB*. The SNP difference between genomes from the same country (intragroup) was less than between genomes from different countries (intergroup). The time-scaled tree analysis showed that a common ancestor for LRSE ST2 from European countries and Russia appeared in 1998 (1986–2006) before introduction of linezolid in clinical practice, which indicates a greater likelihood of independent formation of LRSE in various countries. However, possible import of isolates can be observed for isolates from site F, which are in the same clade with LRSE from Germany. After dissemination to different regions, the lineage probably continues to evolve, thus the sublineage in France acquired additional a mutation in *rpl3*-Met156Thr, and some isolates in Germany and France acquired *cfr* genes.

The second LRSE lineage included ST22 isolates from France and Russia and its single-locus variant ST186 from the United States. Two ST22 isolates from France (Dortet et al., 2018) and 20 from Russia demonstrated high levels of intra- and intergroup similarity; they have identical mutations in 23S rRNA and *rpl3*, which suggests the existence of a common resistant precursor that appeared in 2011 (2008–2013). Isolates of this lineage harbored a maximal number of acquired resistance genes between all studied genomes. This genetic lineage may be common not only in Russia and France. ST22 LRSE carrying the same mutations in 23S and *rpl3* were reported from Greece and Turkey (Karavasilis et al., 2015; Freitas et al., 2018; Papadimitriou-Olivgeris et al., 2020). The whole genome sequencing (WGS) data in the mentioned publication are lacking, and it is impossible to evaluate the level of similarity between ST22 isolates from different sources. Seven ST186 isolates from the United States were genetically distant from the ST22 subgroup.

The third LRSE lineage included highly similar ST5 isolates from France (n = 23) and the United States (n = 2), *cfr* genes, and the 23S rRNA SNP at position 2,534 mediated oxazolidinone resistance in this subgroup. In this case, neither the international spread of LRSE nor the independent acquisition of the plasmid by representatives of closely related genetic lineages can be ruled out.

S. hominis is a poorly studied species among CoNS, and it is an uncommon causative agent of different opportunistic infections, including life-threatening nosocomial (d'Azevedo et al., 2008) and neonatal bacteremia's (Chaves et al., 2005). ST16, ST23, and ST2 are major lineages associated with human infections (Zhang et al., 2013). In this study, we found emergence and spread of linezolid-resistant ST2 lineage in Russia, Germany, and Brazil. BEAST analysis revealed that time of divergence of linezolid-resistant *S. hominis* was 2003 (1996–2012). The greatest genetic relationship with isolates from Russia demonstrated a single isolate from Germany. Linezolid-resistant *S. hominis* were previously reported from Europe (Musumeci et al., 2016; Drăgulescu et al., 2018) and Brazil (de Almeida et al., 2013; Chamon et al., 2014); however, data on MLST typing and/or WGS of these isolates are lacking. Six isolates from Russia carried simultaneous mutations in genes 23S rRNA and plasmid-born *cfr*. This combination of resistance mechanisms was previously described only in Romania (Drăgulescu et al., 2018). It cannot be ruled out that the spread of linezolid-resistant *S. hominis* ST2 is underestimated.

Several linezolid-resistant *S. hominis* from Russia demonstrated resistance to teicoplanin while maintaining susceptibility to vancomycin. To our knowledge, only a few reports dealing with teicoplanin-resistant *S. hominis* are published (Cercenado et al., 1996; d'Azevedo et al., 2008). We propose that resistance is caused by mutations in hypothetical proteins with Duf420 and DedA domains. The DedA family membrane proteins are widely represented in Gram-negative and Gram-positive bacteria; however, their biological functions are unknown. In one study, it was shown that DedA protein is associated with colistin resistance in *Burkholderia* (Panta et al., 2019). Further studies are needed for understanding of glycopeptide-resistance mechanisms in CoNS.

Staphylococcus haemolyticus is also an opportunistic pathogen and the second most frequent CoNS isolated from human blood cultures. In the study of Cavanagh et al. (2014), the population structure based on analysis of the core-genomes of a large collection of clinical European *S. haemolyticus* isolates showed predominance of one single cluster of genomes. All genomes from Cavanagh's study were included in the current work, and a majority of them were in BAPS cluster 1. This cluster included highly similar linezolid-resistant isolates from the United States (Tewhey et al., 2014) and genetically distant isolate from Russia. Linezolid-resistant *S. haemolyticus* were previously reported from Europe (Rodriguez-Aranda et al., 2009), China (Jian et al., 2018), and India (Brijwal et al., 2016; Mittal et al., 2019); however, data on MLST typing and\or WGS of these isolates are lacking.

A limitation of the study is the impossibility to characterize mobilomes from the short reads of the studied genomes. We were able to demonstrate that *cfr* harboring plasmids from *S. hominis* and *S. haemolyticus* belonged to different clusters of *repUS5*-like plasmids widely disseminated in the *S. aureus* population (Mendes et al., 2008; Chen et al., 2013; Dortet et al., 2018). Lack of epidemiological data supporting this assumption is another limitation of the study. We also have no information about the level of consumption of antibiotics, including linezolid in participating hospitals, which may indicate in favor of the local formation of resistance.

Noteworthy is the small number of available complete genomes of linezolid-resistant strains of CoNS that are not associated with the main genetic lineages. Many linezolid-resistant clones may be quickly eliminated from circulation, and only evolutionarily successful ones remain. However, likely, isolates obtained from local outbreaks were mainly included in the studies with genome-wide sequencing. Larger studies using whole genome sequencing are needed to better understand the molecular epidemiology of linezolid-resistant CoNS.

CONCLUSION

CoNS are part of the human microbiome and are frequent contaminants of implants and medical devices. The importance of CoNS in the future is likely to increase as the use of invasive technologies in medicine increases, which will require new approaches to antibiotic therapy and, possibly, wider use of oxazolidinones. At present, the global population of linezolid-resistant CoNS is represented by a limited number of homogeneous genetic lineages and a small number of unrelated isolates. The leading mechanisms of resistance are mutations in the 23S rRNA and ribosomal protein genes; resistance due to *cfr* production is relatively rare. The geographic dissemination of resistance to linezolid is mediated by both the spread of resistant clones (LRSE ST22) and the formation of resistance *de novo* in closely related lineages of (LRSE ST2 and *S. hominis* ST2). The rate of further dissemination of resistance in the future is likely to depend on the consumption of oxazolidinones; however, it is almost impossible to predict which of the resistance mechanisms will dominate. Whole genome sequencing should become the main tool in the surveillance of the spread of linezolid-resistant CoNS.

DATA AVAILABILITY STATEMENT

Genomic data have been deposited in NCBI Sequence Read Archive (SRA) and all reads are available from BioProject PRJNA384130 (SRA id: SRR5482186–SRR5482205 and SRR8427123–SRR8427149).

AUTHOR CONTRIBUTIONS

SS, VG, and AK conceived and designed the study. SL and DL analyzed the data. OK, MB, ND, ZG, TP, LL, and AG performed the experiments. All authors have read and agreed to the published version of the manuscript.

FUNDING

This study was supported by the Institutional grant 001-05, Pediatric Research and Clinical Center for Infectious Diseases.

SUPPLEMENTARY MATERIAL

The Supplementary Material for this article can be found online at: https://www.frontiersin.org/articles/10.3389/fmicb.2021.661798/full#supplementary-material

Supplementary Figure 1 | Maximum-likelihood phylogeny of *S. epidermidis* population based on core-SNP alignment with additional data and names of strains and description of calculated acquired resistance genes.

Supplementary Figure 2 | Structure alignment of *cfr*-harboring plasmids.

Supplementary Figure 3 | (A) Heat map of the distribution of AAS in proteins associated with decreased susceptibility to glycopeptides in *S. epidermidis*; **(B)** Results of MCA analysis; **(C)** Distribution of isolates with PAP data, genotypes, and variants of mutations in RpoB.

Supplementary Table 1 | Quality of sequence data.

Supplementary Table 2 | Genomes included in the study.

Supplementary Table 3 | Pairwise SNP differences between genomes of CoNS.

Supplementary Table 4 | Description of resistance phenotypes and genotypes of Russian linezolid resistant isolates including MICs and PAP data.

REFERENCES

Antonelli, A., D'andrea, M. M., Brenciani, A., Galeotti, C. L., Morroni, G., Pollini, S., et al. (2018). Characterization of poxtA, a novel phenicol-oxazolidinone-tetracycline resistance gene from an MRSA of clinical origin. *J. Antimicrob. Chemother.* 73, 1763–1769. doi: 10.1093/jac/dky088

Bai, B., Hu, K., Zeng, J., Yao, W., Li, D., Pu, Z., et al. (2019). Linezolid consumption facilitates the development of linezolid resistance in *Enterococcus faecalis* in a tertiary-care hospital: a 5-year surveillance study. *Microb. Drug Resist.* 25, 791–798. doi: 10.1089/mdr.2018.0005

Bankevich, A., Nurk, S., Antipov, D., Gurevich, A. A., Dvorkin, M., Kulikov, A. S., et al. (2012). SPAdes: a new genome assembly algorithm and its applications to single-cell sequencing. *J. Comput. Biol.* 19, 455–477. doi: 10.1089/cmb.2012.0021

Becker, K., Heilmann, C., and Peters, G. (2014). Coagulase-negative *Staphylococci*. *Clin. Microbiol. Rev.* 27, 870–926.

Boak, L. M., Li, J., Spelman, D., Du Cros, P., Nation, R. L., and Rayner, C. R. (2006). Successful treatment and cerebrospinal fluid penetration of oral linezolid in a patient with coagulase-negative *Staphylococcus ventriculitis*. *Ann. Pharmacother.* 40, 1451–1455. doi: 10.1345/aph.1h029

Bolger, A. M., Lohse, M., and Usadel, B. (2014). Trimmomatic: a flexible trimmer for illumina sequence data. *Bioinformatics* 30, 2114–2120. doi: 10.1093/bioinformatics/btu170

Brijwal, M., Dhawan, B., Rawre, J., Sebastian, S., and Kapil, A. (2016). Clonal dissemination of linezolid-resistant *Staphylococcus haemolyticus* harbouring a G2576T mutation and the cfr gene in an Indian hospital. *J. Med. Microbiol.* 65, 698–700. doi: 10.1099/jmm.0.000279

Brown, J., Pirrung, M., and Mccue, L. A. (2017). FQC dashboard: integrates FastQC results into a web-based, interactive, and extensible FASTQ quality control tool. *Bioinformatics* 33, 3137–3139. doi: 10.1093/bioinformatics/btx373

Brynildsrud, O., Bohlin, J., Scheffer, L., and Eldholm, V. (2016). Rapid scoring of genes in microbial pan-genome-wide association studies with Scoary. *Genome Biol.* 17:238.

Cai, J. C., Hu, Y. Y., Zhang, R., Zhou, H. W., and Chen, G. X. (2012). Linezolid-resistant clinical isolates of meticillin-resistant coagulase-negative staphylococci and *Enterococcus faecium* from China. *J. Med. Microbiol.* 61, 1568–1573. doi: 10.1099/jmm.0.043729-0

Castillo-Ramirez, S., Corander, J., Marttinen, P., Aldeljawi, M., Hanage, W. P., Westh, H., et al. (2012). Phylogeographic variation in recombination rates within a global clone of methicillin-resistant *Staphylococcus aureus*. *Genome Biol.* 13:R126.

Cavanagh, J. P., Hjerde, E., Holden, M. T., Kahlke, T., Klingenberg, C., Flægstad, T., et al. (2014). Whole-genome sequencing reveals clonal expansion of multiresistant *Staphylococcus haemolyticus* in European hospitals. *J. Antimicrob. Chemother.* 69, 2920–2927. doi: 10.1093/jac/dku271

Cercenado, E., Garcia-Leoni, M. E., Diaz, M. D., Sanchez-Carrillo, C., Catalan, P., De Quiros, J. C., et al. (1996). Emergence of teicoplanin-resistant coagulase-negative staphylococci. *J. Clin. Microbiol.* 34, 1765–1768.

Chamon, R. C., Iorio, N. L., Cavalcante, F. S., Teodoro, C. R., De Oliveira, A. P., Maia, F., et al. (2014). Linezolid-resistant *Staphylococcus haemolyticus* and *Staphylococcus hominis*: single and double mutations at the domain V of 23S rRNA among isolates from a Rio de Janeiro hospital. *Diagn. Microbiol. Infect. Dis.* 80, 307–310. doi: 10.1016/j.diagmicrobio.2014.09.011

Chaves, F., Garcia-Alvarez, M., Sanz, F., Alba, C., and Otero, J. R. (2005). Nosocomial spread of a *Staphylococcus hominis* subsp. novobiosepticus strain causing sepsis in a neonatal intensive care unit. *J. Clin. Microbiol.* 43, 4877–4879. doi: 10.1128/jcm.43.9.4877-4879.2005

Chen, H., Wu, W., Ni, M., Liu, Y., Zhang, J., Xia, F., et al. (2013). Linezolid-resistant clinical isolates of enterococci and *Staphylococcus cohnii* from a multicentre study in China: molecular epidemiology and resistance mechanisms. *Int. J. Antimicrob. Agents* 42, 317–321. doi: 10.1016/j.ijantimicag.2013.06.008

Cheng, L., Connor, T. R., Siren, J., Aanensen, D. M., and Corander, J. (2013). Hierarchical and spatially explicit clustering of DNA sequences with BAPS software. *Mol. Biol. Evol.* 30, 1224–1228. doi: 10.1093/molbev/mst028

Cingolani, P., Platts, A., Wang Le, L., Coon, M., Nguyen, T., Wang, L., et al. (2012). A program for annotating and predicting the effects of single nucleotide polymorphisms, SnpEff: SNPs in the genome of *Drosophila melanogaster* strain w1118; iso-2; iso-3. *Fly* 6, 80–92. doi: 10.4161/fly.19695

Coates, R., Moran, J., and Horsburgh, M. J. (2014). Staphylococci: colonizers and pathogens of human skin. *Future Microbiol.* 9, 75–91. doi: 10.2217/fmb.13.145

Corander, J., Marttinen, P., Siren, J., and Tang, J. (2008). Enhanced Bayesian modelling in BAPS software for learning genetic structures of populations. *BMC Bioinformatics* 9:539. doi: 10.1186/1471-2105-9-539

Croucher, N. J., Page, A. J., Connor, T. R., Delaney, A. J., Keane, J. A., Bentley, S. D., et al. (2015). Rapid phylogenetic analysis of large samples of recombinant bacterial whole genome sequences using Gubbins. *Nucleic Acids Res.* 43:e15.

Darling, A. C., Mau, B., Blattner, F. R., and Perna, N. T. (2004). Mauve: multiple alignment of conserved genomic sequence with rearrangements. *Genome Res.* 14, 1394–1403. doi: 10.1101/gr.2289704

d'Azevedo, P. A., Trancesi, R., Sales, T., Monteiro, J., Gales, A. C., and Pignatari, A. C. (2008). Outbreak of *Staphylococcus hominis* subsp. novobiosepticus bloodstream infections in Sao Paulo city, Brazil. *J. Med. Microbiol.* 57, 256–257. doi: 10.1099/jmm.0.47345-0

de Almeida, L. M., De Araujo, M. R., Sacramento, A. G., Pavez, M., De Souza, A. G., Rodrigues, F., et al. (2013). Linezolid resistance in Brazilian *Staphylococcus*

hominis strains is associated with L3 and 23S rRNA ribosomal mutations. *Antimicrob. Agents Chemother.* 57, 4082–4083. doi: 10.1128/aac.00437-13

Dong, Y., and Speer, C. P. (2014). The role of *Staphylococcus epidermidis* in neonatal sepsis: guarding angel or pathogenic devil? *Int. J. Med. Microbiol.* 304, 513–520. doi: 10.1016/j.ijmm.2014.04.013

Dortet, L., Glaser, P., Kassis-Chikhani, N., Girlich, D., Ichai, P., Boudon, M., et al. (2018). Long-lasting successful dissemination of resistance to oxazolidinones in MDR *Staphylococcus epidermidis* clinical isolates in a tertiary care hospital in France. *J. Antimicrob. Chemother.* 73, 41–51. doi: 10.1093/jac/dkx370

Drăgulescu, E.-C., Codiță, I., Nistor, I., Coldea, I. L., and Șerban, R. (2018). Linezolid resistant *Staphylococcus hominis* isolated in a paediatric Romanian hospital. *Rom. Biotechnol. Lett.* 23, 13255–13263.

European Centre for Disease Prevention and Control (2018). *Multidrug-Resistant Staphylococcus Epidermidis – 8 November 2018*. Stockholm: ECDC.

Fairbrother, R. W. (1940). Coagulase production as a criterion for the classification of the staphylococci. *J. Pathol. Bacteriol.* 50, 83–88. doi: 10.1002/path.1700500112

Ferry, T., Batailler, C., Conrad, A., Triffault-Fillit, C., Laurent, F., Valour, F., et al. (2018). Correction of linezolid-induced myelotoxicity after switch to tedizolid in a patient requiring suppressive antimicrobial therapy for multidrug-resistant *Staphylococcus epidermidis* prosthetic-joint infection. *Open Forum Infect. Dis.* 5:ofy246.

Freitas, A. R., Dilek, A. R., Peixe, L., and Novais, C. (2018). Dissemination of *Staphylococcus epidermidis* ST22 with stable, high-level resistance to linezolid and tedizolid in the Greek-Turkish region (2008-2016). *Infect. Control Hosp. Epidemiol.* 39, 492–494. doi: 10.1017/ice.2018.5

Heilmann, C., Ziebuhr, W., and Becker, K. (2019). Are coagulase-negative staphylococci virulent? *Clin. Microbiol. Infect.* 25, 1071–1080. doi: 10.1016/j.cmi.2018.11.012

Henriksen, A. S., Smart, J., and Hamed, K. (2018). Comparative activity of ceftobiprole against coagulase-negative staphylococci from the BSAC bacteraemia surveillance programme, 2013–2015. *Eur. J. Clin. Microbiol. Infect. Dis.* 37, 1653–1659. doi: 10.1007/s10096-018-3295-6

Hoang, D. T., Chernomor, O., Von Haeseler, A., Minh, B. Q., and Vinh, L. S. (2018). UFBoot2: improving the ultrafast bootstrap approximation. *Mol. Biol. Evol.* 35, 518–522. doi: 10.1093/molbev/msx281

Jian, J., Chen, L., Xie, Z., and Zhang, M. (2018). Dissemination of cfr-mediated linezolid resistance among *Staphylococcus* species isolated from a teaching hospital in Beijing, China. *J. Int. Med. Res.* 46, 3884–3889. doi: 10.1177/0300060518781636

Jolley, K. A., and Maiden, M. C. (2010). BIGSdb: scalable analysis of bacterial genome variation at the population level. *BMC Bioinformatics* 11:595. doi: 10.1186/1471-2105-11-595

Kalyaanamoorthy, S., Minh, B. Q., Wong, T. K. F., Von Haeseler, A., and Jermiin, L. S. (2017). ModelFinder: fast model selection for accurate phylogenetic estimates. *Nat. Methods* 14, 587–589. doi: 10.1038/nmeth.4285

Karavasilis, V., Zarkotou, O., Panopoulou, M., Kachrimanidou, M., Themeli-Digalaki, K., Stylianakis, A., et al. (2015). Wide dissemination of linezolid-resistant *Staphylococcus epidermidis* in Greece is associated with a linezolid-dependent ST22 clone. *J. Antimicrob. Chemother.* 70, 1625–1629.

Katoh, K., and Standley, D. M. (2013). MAFFT multiple sequence alignment software version 7: improvements in performance and usability. *Mol. Biol. Evol.* 30, 772–780. doi: 10.1093/molbev/mst010

Kjellander, J. O., Klein, J. O., and Finland, M. (1963). *In vitro* activity of penicillins against *Staphylococcus Albus*. *Proc. Soc. Exp. Biol. Med.* 113, 1023–1031. doi: 10.3181/00379727-113-28563

Krueger, W. A., Kottler, B., Will, B. E., Heininger, A., Guggenberger, H., and Unertl, K. E. (2004). Treatment of meningitis due to methicillin-resistant *Staphylococcus epidermidis* with linezolid. *J. Clin. Microbiol.* 42, 929–932. doi: 10.1128/jcm.42.2.929-932.2004

Kruse, A. J., Peerdeman, S. M., Bet, P. M., and Debets-Ossenkopp, Y. J. (2006). Successful treatment with linezolid and rifampicin of meningitis due to methicillin-resistant *Staphylococcus epidermidis* refractory to vancomycin treatment. *Eur. J. Clin. Microbiol. Infect. Dis.* 25, 135–137. doi: 10.1007/s10096-006-0097-z

Kurtz, S., Phillippy, A., Delcher, A. L., Smoot, M., Shumway, M., Antonescu, C., et al. (2004). Versatile and open software for comparing large genomes. *Genome Biol.* 5:R12.

Langmead, B., and Salzberg, S. L. (2012). Fast gapped-read alignment with Bowtie 2. *Nat. Methods* 9, 357–359. doi: 10.1038/nmeth.1923

Layer, F., Vourli, S., Karavasilis, V., Strommenger, B., Dafopoulou, K., Tsakris, A., et al. (2018). Dissemination of linezolid-dependent, linezolid-resistant *Staphylococcus epidermidis* clinical isolates belonging to CC5 in German hospitals. *J. Antimicrob. Chemother.* 73, 1181–1184. doi: 10.1093/jac/dkx524

Lee, J. Y. H., Monk, I. R., Goncalves Da Silva, A., Seemann, T., Chua, K. Y. L., Kearns, A., et al. (2018). Global spread of three multidrug-resistant lineages of *Staphylococcus epidermidis*. *Nat. Microbiol.* 3, 1175–1185. doi: 10.1038/s41564-018-0230-7

Letunic, I., and Bork, P. (2016). Interactive tree of life (iTOL) v3: an online tool for the display and annotation of phylogenetic and other trees. *Nucleic Acids Res.* 44, W242–W245.

Li, H., Handsaker, B., Wysoker, A., Fennell, T., Ruan, J., Homer, N., et al. (2009). The sequence alignment/map format and SAMtools. *Bioinformatics* 25, 2078–2079. doi: 10.1093/bioinformatics/btp352

Liakopoulos, A., Neocleous, C., Klapsa, D., Kanellopoulou, M., Spiliopoulou, I., Mathiopoulos, K. D., et al. (2009). A T2504A mutation in the 23S rRNA gene responsible for high-level resistance to linezolid of *Staphylococcus epidermidis*. *J. Antimicrob. Chemother.* 64, 206–207. doi: 10.1093/jac/dkp167

Long, K. S., and Vester, B. (2012). Resistance to linezolid caused by modifications at its binding site on the ribosome. *Antimicrob. Agents Chemother.* 56, 603–612. doi: 10.1128/aac.05702-11

Mendes, R. E., Deshpande, L. M., Castanheira, M., Dipersio, J., Saubolle, M. A., and Jones, R. N. (2008). First report of cfr-mediated resistance to linezolid in human staphylococcal clinical isolates recovered in the United States. *Antimicrob. Agents Chemother.* 52, 2244–2246. doi: 10.1128/aac.00231-08

Mendes, R. E., Deshpande, L. M., Farrell, D. J., Spanu, T., Fadda, G., and Jones, R. N. (2010). Assessment of linezolid resistance mechanisms among *Staphylococcus epidermidis* causing bacteraemia in Rome, Italy. *J. Antimicrob. Chemother.* 65, 2329–2335. doi: 10.1093/jac/dkq331

Mittal, G., Bhandari, V., Gaind, R., Rani, V., Chopra, S., Dawar, R., et al. (2019). Linezolid resistant coagulase negative staphylococci (LRCoNS) with novel mutations causing blood stream infections (BSI) in India. *BMC Infect. Dis.* 19:717. doi: 10.1186/s12879-019-4368-6

Musumeci, R., Calaresu, E., Gerosa, J., Oggioni, D., Bramati, S., Morelli, P., et al. (2016). Resistance to linezolid in *Staphylococcus* spp. clinical isolates associated with ribosomal binding site modifications: novel mutation in domain V of 23S rRNA. *New Microbiol.* 39, 269–273.

Nam, J. R., Kim, M. S., Lee, C. H., and Whang, D. H. (2008). Linezolid treatment for osteomyelitis due to *Staphylococcus epidermidis* with reduced vancomycin susceptibility. *J. Korean Neurosurg. Soc.* 43, 307–310. doi: 10.3340/jkns.2008.43.6.307

Nguyen, L. T., Schmidt, H. A., Von Haeseler, A., and Minh, B. Q. (2015). IQ-TREE: a fast and effective stochastic algorithm for estimating maximum-likelihood phylogenies. *Mol. Biol. Evol.* 32, 268–274. doi: 10.1093/molbev/msu300

Okonechnikov, K., Fursov, M., Golosova, O., and Team, T. U. (2012). Unipro UGENE: a unified bioinformatics toolkit. *Bioinformatics* 28, 1166–1167. doi: 10.1093/bioinformatics/bts091

Otto, M. (2012). Molecular basis of *Staphylococcus epidermidis* infections. *Semin. Immunopathol.* 34, 201–214. doi: 10.1007/s00281-011-0296-2

Page, A. J., Cummins, C. A., Hunt, M., Wong, V. K., Reuter, S., Holden, M. T., et al. (2015). Roary: rapid large-scale prokaryote pan genome analysis. *Bioinformatics* 31, 3691–3693. doi: 10.1093/bioinformatics/btv421

Panta, P. R., Kumar, S., Stafford, C. F., Billiot, C. E., Douglass, M. V., Herrera, C. M., et al. (2019). A DedA family membrane protein is required for *Burkholderia thailandensis* colistin resistance. *Front. Microbiol.* 10:2532. doi: 10.3389/fmicb.2019.02532

Papadimitriou-Olivgeris, M., Kolonitsiou, F., Karamouzos, V., Tsilipounidaki, K., Nikolopoulou, A., Fligou, F., et al. (2020). Molecular characteristics and predictors of mortality among Gram-positive bacteria isolated from bloodstream infections in critically ill patients during a 5-year period (2012–2016). *Eur. J. Clin. Microbiol. Infect. Dis.* 39, 863–869. doi: 10.1007/s10096-019-03803-9

Pfaller, M. A., Flamm, R. K., Duncan, L. R., Shortridge, D., Smart, J. I., Hamed, K. A., et al. (2019). Ceftobiprole activity when tested against contemporary bacteria causing bloodstream infections in the United States (2016–2017).

Diagn. Microbiol. Infect. Dis. 94, 304–313. doi: 10.1016/j.diagmicrobio.2019.01.015

Pfeltz, R. F., Schmidt, J. L., and Wilkinson, B. J. (2001). A microdilution plating method for population analysis of antibiotic-resistant staphylococci. *Microb. Drug Resist.* 7, 289–295. doi: 10.1089/10766290152652846

Pourakbari, B., Mahmoudi, S., Moradzadeh, M., Mahzari, M., Ashtiani, M. T. H., Tanzifi, P., et al. (2018). Antimicrobial resistance patterns of the gram-positive bacteria isolated from children with bloodstream infection in an Iranian referral hospital: a 6-year study. *Infect. Disord. Drug Targets* 18, 136–144. doi: 10.2174/1871526517666170821164343

Rodriguez-Aranda, A., Daskalaki, M., Villar, J., Sanz, F., Otero, J. R., and Chaves, F. (2009). Nosocomial spread of linezolid-resistant *Staphylococcus haemolyticus* infections in an intensive care unit. *Diagn. Microbiol. Infect. Dis.* 63, 398–402. doi: 10.1016/j.diagmicrobio.2008.12.008

Rodríguez-Lucas, C., Rodicio, M. R., Càmara, J., Domínguez, M. Á, Alaguero, M., and Fernández, J. (2020). Long-term endemic situation caused by a linezolid- and meticillin-resistant clone of *Staphylococcus epidermidis* in a tertiary hospital. *J. Hosp. Infect.* 105, 64–69.

Russo, A., Campanile, F., Falcone, M., Tascini, C., Bassetti, M., Goldoni, P., et al. (2015). Linezolid-resistant staphylococcal bacteraemia: a multicentre case-case-control study in Italy. *Int. J. Antimicrob. Agents* 45, 255–261. doi: 10.1016/j.ijantimicag.2014.12.008

Seemann, T. (2014). Prokka: rapid prokaryotic genome annotation. *Bioinformatics* 30, 2068–2069. doi: 10.1093/bioinformatics/btu153

Seral, C., Saenz, Y., Algarate, S., Duran, E., Luque, P., Torres, C., et al. (2011). Nosocomial outbreak of methicillin- and linezolid-resistant *Staphylococcus epidermidis* associated with catheter-related infections in intensive care unit patients. *Int. J. Med. Microbiol.* 301, 354–358. doi: 10.1016/j.ijmm.2010.11.001

Shore, A. C., Lazaris, A., Kinnevey, P. M., Brennan, O. M., Brennan, G. I., O'connell, B., et al. (2016). First report of cfr-carrying plasmids in the pandemic sequence type 22 methicillin-resistant *Staphylococcus aureus* staphylococcal cassette chromosome mec type IV clone. *Antimicrob. Agents Chemother.* 60, 3007–3015. doi: 10.1128/AAC.02949-15

Suchard, M. A., Lemey, P., Baele, G., Ayres, D. L., Drummond, A. J., and Rambaut, A. (2018). Bayesian phylogenetic and phylodynamic data integration using BEAST 1.10. *Virus Evol.* 4:vey016. doi: 10.1093/ve/vey016

Tewhey, R., Gu, B., Kelesidis, T., Charlton, C., Bobenchik, A., Hindler, J., et al. (2014). Mechanisms of linezolid resistance among coagulase-negative staphylococci determined by whole-genome sequencing. *MBio* 5:e00894-14.

The European Committee on Antimicrobial Susceptibility Testing (EUCAST) (2020). *Breakpoint Tables for Interpretation of MICs and Zone Diameters.* Version 10.0, 2020. Växjö: The European Committee on Antimicrobial Susceptibility Testing.

Tonkin-Hill, G., Lees, J. A., Bentley, S. D., Frost, S. D. W., and Corander, J. (2018). RhierBAPS: an R implementation of the population clustering algorithm hierBAPS. *Wellcome Open Res.* 3:93. doi: 10.12688/wellcomeopenres.14694.1

Wang, Y., Lv, Y., Cai, J., Schwarz, S., Cui, L., Hu, Z., et al. (2015). A novel gene, optrA, that confers transferable resistance to oxazolidinones and phenicols and its presence in *Enterococcus faecalis* and *Enterococcus faecium* of human and animal origin. *J. Antimicrob. Chemother.* 70, 2182–2190. doi: 10.1093/jac/dkv116

Watanabe, S., Tanaka, A., Ono, T., Ohta, M., Miyamoto, H., Tauchi, H., et al. (2013). Treatment with linezolid in a neonate with meningitis caused by methicillin-resistant *Staphylococcus epidermidis*. *Eur. J. Pediatr.* 172, 1419–1421. doi: 10.1007/s00431-013-1978-7

Wattam, A. R., Davis, J. J., Assaf, R., Boisvert, S., Brettin, T., Bun, C., et al. (2017). Improvements to PATRIC, the all-bacterial bioinformatics database and analysis resource center. *Nucleic Acids Res.* 45, D535–D542.

Zhang, L., Thomas, J. C., Miragaia, M., Bouchami, O., Chaves, F., D'azevedo, P. A., et al. (2013). Multilocus sequence typing and further genetic characterization of the enigmatic pathogen, *Staphylococcus hominis*. *PLoS One* 8:e66496. doi: 10.1371/journal.pone.0066496

Conflict of Interest: The authors declare that the research was conducted in the absence of any commercial or financial relationships that could be construed as a potential conflict of interest.

Publisher's Note: All claims expressed in this article are solely those of the authors and do not necessarily represent those of their affiliated organizations, or those of the publisher, the editors and the reviewers. Any product that may be evaluated in this article, or claim that may be made by its manufacturer, is not guaranteed or endorsed by the publisher.

frontiers in Microbiology

ORIGINAL RESEARCH
published: 07 October 2021
doi: 10.3389/fmicb.2021.742040

Combining CRISPR-Cas12a-Based Technology and Metagenomics Next Generation Sequencing: A New Paradigm for Rapid and Full-Scale Detection of Microbes in Infectious Diabetic Foot Samples

Yixin Chen[1†], Ya Shi[2†], Weifen Zhu[1†], Jiaxing You[3], Jie Yang[3], Yaping Xie[4], Hanxin Zhao[1], Hongye Li[3], Shunwu Fan[3], Lin Li[1] and Chao Liu[3*]*

[1] Department of Endocrinology, Zhejiang University School of Medicine Sir Run Run Shaw Hospital, Hangzhou, China, [2] Hangzhou Digital Micro Biotech Co., Ltd., Hangzhou, China, [3] Department of Orthopedics, Zhejiang University School of Medicine Sir Run Run Shaw Hospital, Hangzhou, China, [4] Department of Hematology, Affiliated Hangzhou First People's Hospital, Zhejiang University School of Medicine, Hangzhou, China

Introduction: Diabetic foot infections (DFIs) pose a huge challenge for clinicians. *Staphylococcus aureus*, including methicillin-resistant *S. aureus* (MRSA), is one of the most significant pathogens of DFI. Early pathogen identification will greatly benefit the diagnosis and treatment of the disease. However, existing diagnostic methods are not effective in early detection.

Methods: We developed an assay that coupled loop-mediated isothermal amplification (LAMP) and clustered regularly interspaced short palindromic repeats (CRISPR) techniques to enable quick and specific detection of *Staphylococcus aureus* and differentiate MRSA in samples from patients with DFI. Furthermore, the results were compared using a reference culture, quantitative real-time polymerase chain reaction (qRT-PCR), and metagenomics next generation sequencing (mNGS).

Results: The CRISPR-LAMP assay targeting *nuc* and *mecA* successfully detected *S. aureus* strains and differentiated MRSA. The limit of detection (LoD) of the real-time LAMP for *nuc* and *mecA* was 20 copies per microliter reaction in comparison to two copies per μL reaction for the qRT-PCR assay. The specificity of the LAMP-CRISPR assay for *nuc* was 100%, without cross-reactions with non-*S. aureus* strains. Evaluating assay performance with 18 samples from DFI patients showed that the assay had 94.4% agreement (17/18 samples) with clinical culture results. The results of mNGS for 8/18 samples were consistent with those of the reference culture and LAMP-CRISPR assay.

Conclusion: The findings suggest that the LAMP-CRISPR assay could be promising for the point-of-care detection of *S. aureus* and the differentiation of MRSA in clinical samples. Furthermore, combining the LAMP-CRISPR assay and mNGS provides an advanced platform for molecular pathogen diagnosis of DFI.

Keywords: diabetic foot infections, *Staphylococcus aureus*, loop-mediated isothermal amplification, clustered regularly interspaced short palindromic repeats, metagenomics next generation sequencing

OPEN ACCESS

Edited by:
Shaolin Wang,
China Agricultural University, China

Reviewed by:
Polly H. M. Leung,
Hong Kong Polytechnic University, Hong Kong, SAR China
Artur J. Sabat,
University Medical Center Groningen, Netherlands

****Correspondence:***
Lin Li
3312012@zju.edu.cn
Chao Liu
liuchaozju@zju.edu.cn

† These authors have contributed equally to this work and share first authorship

Specialty section:
This article was submitted to Antimicrobials, Resistance and Chemotherapy, a section of the journal Frontiers in Microbiology

Received: *15 July 2021*
Accepted: *14 September 2021*
Published: *07 October 2021*

Citation:
Chen Y, Shi Y, Zhu W, You J, Yang J, Xie Y, Zhao H, Li H, Fan S, Li L and Liu C (2021) Combining CRISPR-Cas12a-Based Technology and Metagenomics Next Generation Sequencing: A New Paradigm for Rapid and Full-Scale Detection of Microbes in Infectious Diabetic Foot Samples. Front. Microbiol. 12:742040. doi: 10.3389/fmicb.2021.742040

INTRODUCTION

Diabetic foot ulcers, one of the most critical complications of diabetes mellitus, has become a significant public health problem. When patients with diabetic foot ulcers first consult physicians, over half of them have complications with diabetic foot infections (DFIs) (Prompers et al., 2006; Jia et al., 2017). Treatment of DFI requires precise evaluation of infection conditions, pathogen confirmation of infectious ulcers, appropriate selection of antibiotics, and surgical intervention, if necessary (Lipsky et al., 2012). DFI patients are often challenged by the complexity of intricate ulceration and moderate to severe infections, even sepsis. Broad-spectrum empirical antimicrobials would be the primary option for clinicians to hinder the further deterioration of infectious conditions and lower medical risks, which increases antibiotic exposure and selective pressure that contribute to the development of multi-drug resistant microorganisms. Nevertheless, a rapid, accessible, and accurate diagnostic test for pathogenic identification is valuable for clinical procedures.

Staphylococcus aureus is the dominant pathogen of DFI. The resistance rate of *S. aureus* to methicillin fluctuated between 15–30% (Eleftheriadou et al., 2010). It has been shown that infections caused by methicillin-resistant *S. aureus* (MRSA) are linked to higher mortality rates and greater consumption of medical resources than infections caused by methicillin-sensitive *S. aureus* (MSSA) (Cosgrove et al., 2003; Filice et al., 2010). Bacterial culture, quantitative real-time polymerase chain reaction (qRT-PCR) (Buchan et al., 2015; Ellem et al., 2015; Silbert et al., 2017), and metagenomics next generation sequencing (mNGS) (Charalampous et al., 2019; Kalan et al., 2019; Zou et al., 2020) are typically used to identify *S. aureus* and discriminate between MSSA and MRSA. Although traditional culture is the gold standard for pathogen diagnosis, it is time-consuming, and delayed results cannot provide timely clinical guidance. qRT-PCR has a shortened detection time; however, it has not been widely applied because of its high requirements for equipment and laboratory staff. mNGS, a novel detection method, is still not commonly accessible because of its high cost in terms of time, funding, instrumentation, and technical expertise.

In recent years, the application of isothermal amplification combined with clustered regularly interspaced short palindromic repeats (CRISPR) has been developed for pathogen diagnosis (Li et al., 2019). An innovative discovery reported that RNA-guided DNA binding activated Cas12a for both site-specific double-stranded DNA (dsDNA) *cis*-cleavage and indiscriminate single-stranded DNA (ssDNA) *trans*-cleavage. With the guidance of a single CRISPR RNA (crRNA), Cas12a recognizes a TTTN protospacer-adjacent motif (PAM) and binds to crRNA-complementary dsDNA (Li et al., 2018a,b). This indicates that the high specificity of the CRISPR/Cas12a assay is determined by PAM and crRNA. The coupling of isothermal amplification and *trans*-ssDNA repetitive cutting results in double-magnifying biosensing signals, indicating the high sensitivity of the assay. It has been proven to enable a rapid and accurate detection of the human papillomavirus and a new coronavirus (resulting in the disease referred to as COVID-19) in patient samples (Chen et al., 2018; Broughton et al., 2020).

In this study, we developed an assay coupling loop-mediated isothermal amplification (LAMP) and *trans*-cleavage of Cas12a for the quick and specific detection of *S. aureus* and the differentiation of MRSA in samples of patients with DFI. Furthermore, the results were compared with standard methods, including bacterial culture, qRT-PCR, and mNGS.

Abbreviations: DFI, diabetic foot infections; MRSA, methicillin-resistant *Staphylococcus aureus*; MSSA, methicillin-sensitive *Staphylococcus aureus*; LAMP, loop-mediated isothermal amplification; CRISPR, clustered regularly interspaced short palindromic repeats; mNGS, metagenomics next generation sequencing; qRT-PCR, quantitative real-time polymerase chain reaction; ssDNA, single-stranded DNA; dsDNA, double-stranded DNA; crRNA, CRISPR RNA; PAM, protospacer-adjacent motif; LoD, limit of detection; DNB, DNA nanoballs; RCA, rolling circle replication; NTC, no template control.

MATERIALS AND METHODS

Nucleic Acid Preparation

DNA extraction from the tissues of DFI patients was performed using QuickExtract^{TM} DNA Extraction Solution (Lucigen, Beijing, China). Quick DNA extractions were finished after incubation at 65°C for 10 min and 98°C for 2 min. The sequences of *nuc* (*S. aureus*-specific gene) and *mecA* (encoding penicillin-binding protein-2a) were obtained from a public database. LAMP primers were designed against regions of *nuc* and *mecA* using PrimerExplorer v.5. with compatible gRNAs (**Supplementary Table 1**). The gRNA was designed with a TTTN structure (PAM) at the right end. The length of gRNA was 20-25bp, and the GC content was 40–60%. The design was assured to avoid the combination of gRNA and primer dimer (**Table 1**). The primers and gRNAs were obtained from Shanghai General Biotech Co., Ltd. (Shanghai, China).

Real-Time Polymerase Chain Reaction Assay

A 20-μL system was used to conduct the real-time PCR assay for the detection of *nuc* and *mecA* with the following specifications: Forward primer for *nuc* gene: 5′-ACTGTAACTTTGGCACTGG-3′; Reverse primer for *nuc* gene: 5′-GCAGATACCTCATTACCTGC-3′; Probe: 5′-[6FAM]-ATCGCAACGACTGGCGCTA-[BHQ1]-3′ [12]; Forward primer for *mecA* gene: AAAACTAGGTGTTGGTGAAGATATACC; Reverse primer for *mecA* gene: GAAAGGATCTGTACTGGGTTAATCAG; Probe: [6FAM]-TTCACCTTGTCCGTAACCTGAATCAGCT-[BHQ1] (Sabet et al., 2007). Real-time PCR assays were performed using the Premix Ex Taq^{TM} (Probe qPCR) Kit (TaKara Biomedical Technology Co., Ltd., Beijing, China). Ten microliters Premix Ex Taq (Probe qPCR) (2×), 0.2 μM forward primer, 0.2 μM

TABLE 1 | gRNA sequences for *nuc* and *mecA*.

gRNA	sequence (5′-3′)
nuc-gRNA	UAAUUUCUACUAAGUGUAGAUUACAUUAAUUUAACCGUAUCA
mecA-gRNA	UAAUUUCUACUAAGUGUAGAUUGCCAACCUUUACCAUCGAUU

reverse primer, 0.1 μM probe, and 2 μL DNA templates of different concentrations were included in the reaction system. The temperature cycling conditions were 95°C for 30 s, followed by 40 cycles of 95°C for 5 s, and 60°C for 30 s. The reaction was performed using the StepOne^{TM}Plus Real-Time PCR System (Applied Biosystems, Inc., Carlsbad, CA, United States).

Real-Time Loop-Mediated Isothermal Amplification Assay

The real-time LAMP assay was conducted in a 25-μL mixture containing 1 × Bst DNA polymerase buffer (New England Biolabs, Beijing, China), 0.4 μM FIP primers, 0.4 μM BIP primers, 0.2 μM LF primers, 0.2 μM LB primers, 0.1 μM F3 primers F3, 0.1 μM B3 primers, 1.4 μM dNTPs (New England Biolabs), 8U Bst DNA polymerase (New England Biolabs), 8 mM $MgSO_4$ (New England Biolabs), 1 × SYBR Green I (Thermo Fisher Scientific, Inc., Waltham, MA, United States), and 2 μL of DNA templates of different concentrations. Real-time LAMP assays of *nuc* and *mecA* were conducted in the same reaction system, except for the primers. The LAMP reaction solution was covered with 40 μL mineral oil. The reaction was performed at 65°C for 60 min in a StepOne^{TM} Plus Real-Time PCR System (Applied Biosystems, Inc., Carlsbad, CA, United States) and terminated at 80°C for 5 min. The fluorescence information was collected every 30 s during the reaction.

Loop-Mediated Isothermal Amplification-Clustered Regularly Interspaced Short Palindromic Repeats Assay

The LAMP system contained the same mixture as the real-time LAMP assay. The fluorescent dyes were added into the system and the LAMP reagents covered with 40 μL of mineral oil. The LAMP reaction was followed by the admixture of CRISPR reaction solution (preloaded inside the lid) to the LAMP amplification solution by centrifugation. The 20 μL CRISPR reaction solution contained 1 × NEBuffer 2.1, reaction buffer, 0.2 μM EnGen® Lba Cas12a (Cpf1) (New England Biolabs), 0.6 μM gRNA, 2.5 μM CRISPR probes, and 1 U/μL RNA inhibitor (Thermo Fisher Scientific, Inc., Waltham, MA, United States). Sequence information of gRNA is shown in **Table 1**. The CRISPR reaction was conducted in a ProFlex PCR System (Applied Biosystems, Inc., Carlsbad, CA, United States) at 37°C for 5 min. After the reaction, the visualized results were observed using a simple fluorescence reader.

Sensitivity and Specificity of Loop-Mediated Isothermal Amplification-Clustered Regularly Interspaced Short Palindromic Repeats Assay

Amplification of *S. aureus* genomic DNA, including *nuc* and *mecA*, was performed using outer primers (F3 and B3, **Supplementary Table 1**). The lengths of the PCR products of *nuc* and *mecA* were 248 bp and 208 bp, respectively. The PCR product was purified using the TAKARA gel DNA fragment recovery kit, and the purified product was ligated to the pMD18-T vector (2692 bp). The recombinant plasmids were transformed into *Escherichia coli* DH5α competent cells. LB growth medium containing 10 μg/mL ampicillin was used to screen positive colonies. Plasmids of *E. coli* that comprised the pMD18-T vector and *nuc* (248 bp)/*mecA* (208 bp) were extracted using the TaKaRa MiniBEST Plasmid Purification Kit (TaKaRa, 9760). We then measured the concentration of plasmids and calculated the DNA copy number [$6.02 \times 10^{23} \times$ concentration (ng/μL) $\times 10^9$/(DNA sequence length × 660)]. The concentration of plasmids containing *nuc* was 3.26 ng/μL. The DNA copy number of *nuc* was 1.0×10^9 copies per μl, calculated according to the above formula. The concentration of plasmids containing *mecA* was 12 ng/μL, and the copy number was 3.78×10^9 copies per μl. The plasmids were serially diluted to 1:10. Isothermal amplifications of the dilutions were repeatedly performed three times, and the limit of detection (LoD) was determined as the minimum DNA copy number of the diluted plasmids that could amplify the target genomic DNA.

Genomic DNA from 14 strains of *staphylococci* species was analyzed using the LAMP-CRISPR assay to examine the specificity of the LAMP assay. The strains were *S. epidermidis, S. hominis, S. cohnii, S. warneri, S. haemolyticus, S. aureus, S. capitis, S. saprophyticus, S. pasteuri, S. saprophyticus* ATCC® 15305, *S. haemolyticus* ATCC ®29970, *S. epidermidis* ATCC ®14990, *S. caprae,* and *S. aureus* subsp. *sureus* ATCC ®12600.

Metagenomic Next-Generation Sequencing

After DNA extractions using a DNeasy Blood and Tissue Kit (Qiagen, 69504, Shenzhen, China), DNA was fragmented using a Bioruptor Pico instrument to generate 200–300-bp fragments (Bioruptor Pico protocols). Then, libraries were constructed by MGIEasy (MGIEasy universal DNA library prep kit) as follows: first, the DNA fragments were subjected to end-repair sequencing, and A-tailing was added to one tube. Subsequently, the resulting DNA was ligated with bubble-adaptors that included barcode sequences and then amplified by the PCR method. Quality control was carried out using bioanalyzer (Agilent 2100, Agilent Technologies, Santa Clara, CA, United States) to assess DNA concentrations and fragment size. Qualified libraries were pooled together to make a single strand DNA circle (ssDNA circle), and then, DNA nanoballs (DNB) were generated by rolling circle replication (RCA). The final DNBs were loaded into the sequence chip and sequenced on the BGISEQ platform using 50 bp/single-end sequencing. Finally, optical signals were collected using a high-resolution imaging system, and then, these signals were transformed into digital information, which can be decoded into DNA sequence information.

Reference Culture Method and Antimicrobial Susceptibility Test

The sample culture broths were plated on blood agar and incubated for 18–48 h. Identification of S. aureus and examination of antimicrobial susceptibility were conducted using

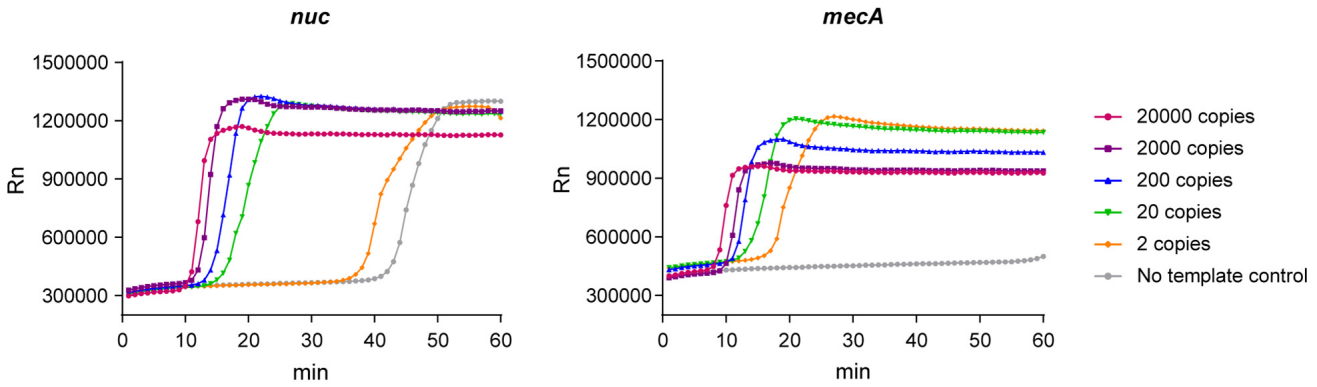

FIGURE 1 | Amplification curves of the real-time LAMP assay for *nuc* and *mecA*.

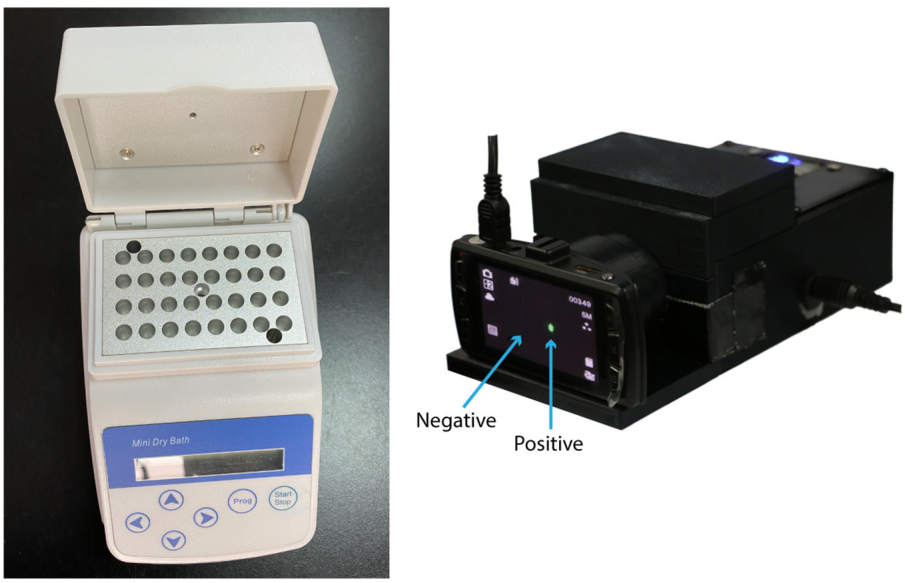

FIGURE 2 | Portable equipment for the LAMP assay and fluorescence visualization.

a fully automatic vitek-2 compact system (Biomerieux, Shanghai, China). The results were interpreted on the basis of the guidelines (M100, 28th edition) established by the Clinical and Laboratory Standards Institute (CLSI, 2018).

Human Clinical Sample Collection

Tissues of infected ulcers were acquired from DFI patients at their first visit to the outpatient clinic or the Department of Emergency at Sir Run Run Shaw Hospital. After the wound was cleaned with saline solution, DFU tissue with the size of a rice grain was taken out with a blade and immediately sent to the laboratory for DNA extraction. The study was approved by the Human Research Ethics Committee of Sir Run Run Shaw Hospital.

Statistical Methods

All reactions were repeated three times, the CT value of the real-time PCR is shown as "mean ± standard deviation" (x ± s).

RESULTS

Real-Time Loop-Mediated Isothermal Amplification Assay for nuc and mecA

We conducted a real-time LAMP assay for amplifying nuc and mecA with seven dilutions. The amplification curves of the dilutions with serial concentrations are shown in **Figure 1**. The LAMP assay was able to amplify genomic DNA targets. There was no stable fluorescent signal obtained when the genomic DNA template was at two copies per μL reaction.

Visual Detection Assay With Clustered Regularly Interspaced Short Palindromic Repeats/Cas12a

Next, we used the CRISPR/Cas12a system to realize the visual readout of the targeted amplicons, based on the collateral DNA

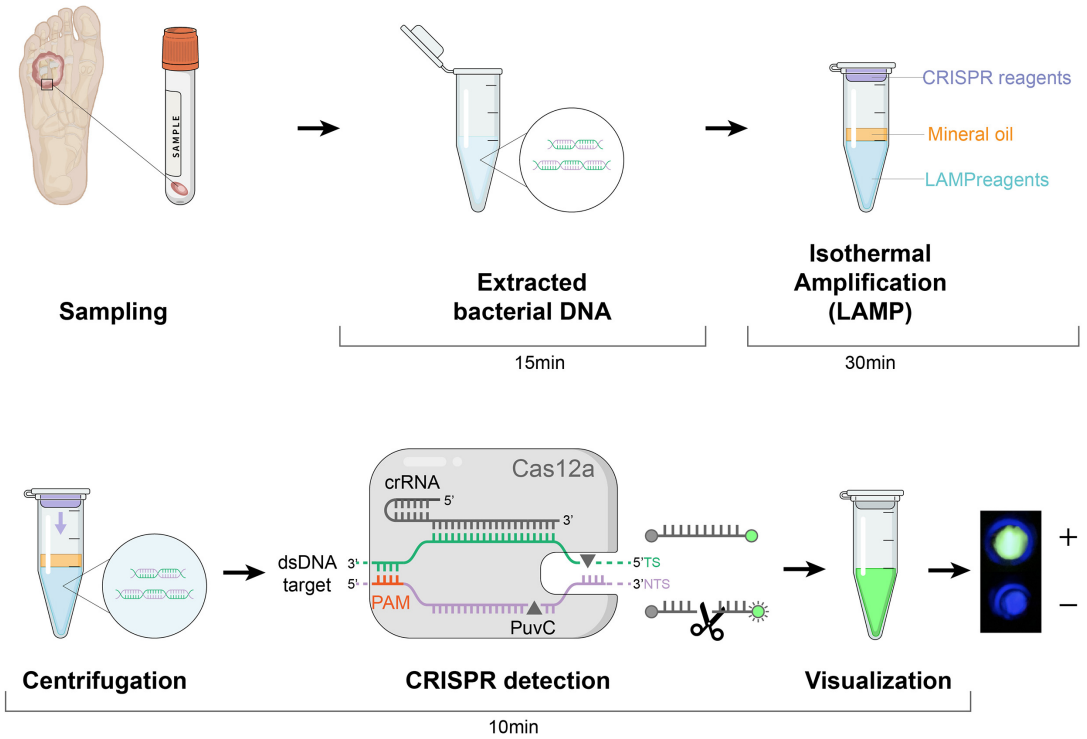

FIGURE 3 | Schematic of the LAMP-CRISPR assay workflow. Quick DNA extraction was used as an input to the LAMP-CRISPR system (LAMP preamplification and Cas12-based detection for *nuc* and *mecA*). The result is visualized by a fluorescence reader.

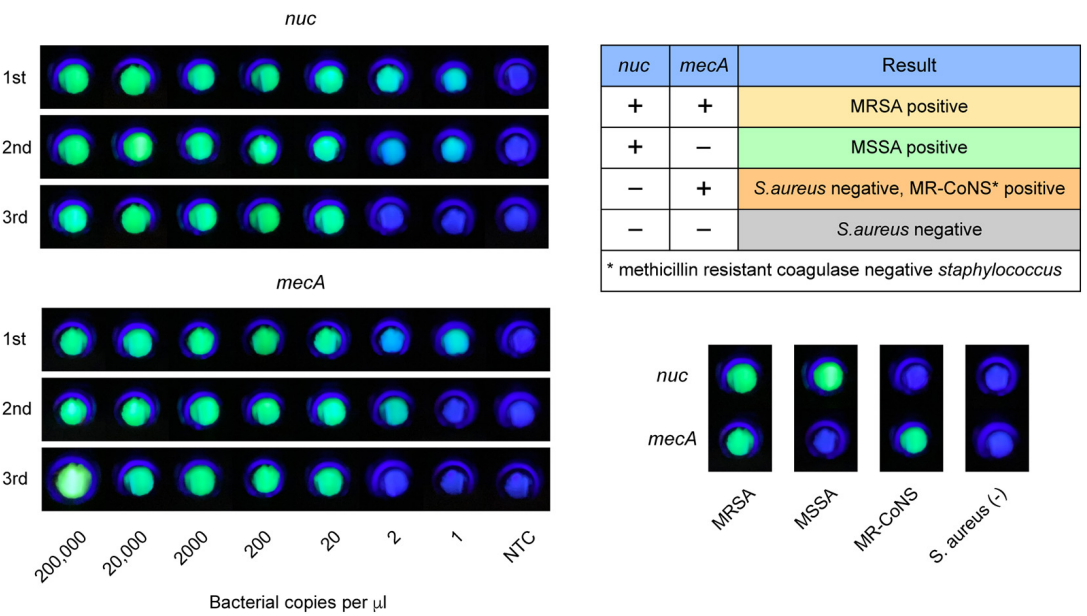

nuc	*mecA*	Result
+	+	MRSA positive
+	–	MSSA positive
–	+	*S.aureus* negative, MR-CoNS* positive
–	–	*S.aureus* negative

* methicillin resistant coagulase negative *staphylococcus*

FIGURE 4 | LAMP-CRISPR assay readout. Fluorescent results of MRSA, MSSA, MR-CoNS, and *S. aureus* are presented at the bottom right. *Nuc* detection indicates *S. aureus* positive. MRSA identification requires positive for both *nuc* and *mecA*.

cleavage activity of the Cas12a effector. The cleaved ssDNA reporters produced fluorescent signals, which could be seen through a portable fluorescence reader (**Figure 2**). The entire procedure and explanation of the results are presented in **Figure 3**. Pre-loading of the CRISPR reagents inside the lid avoided the need to open the cap during the process. We

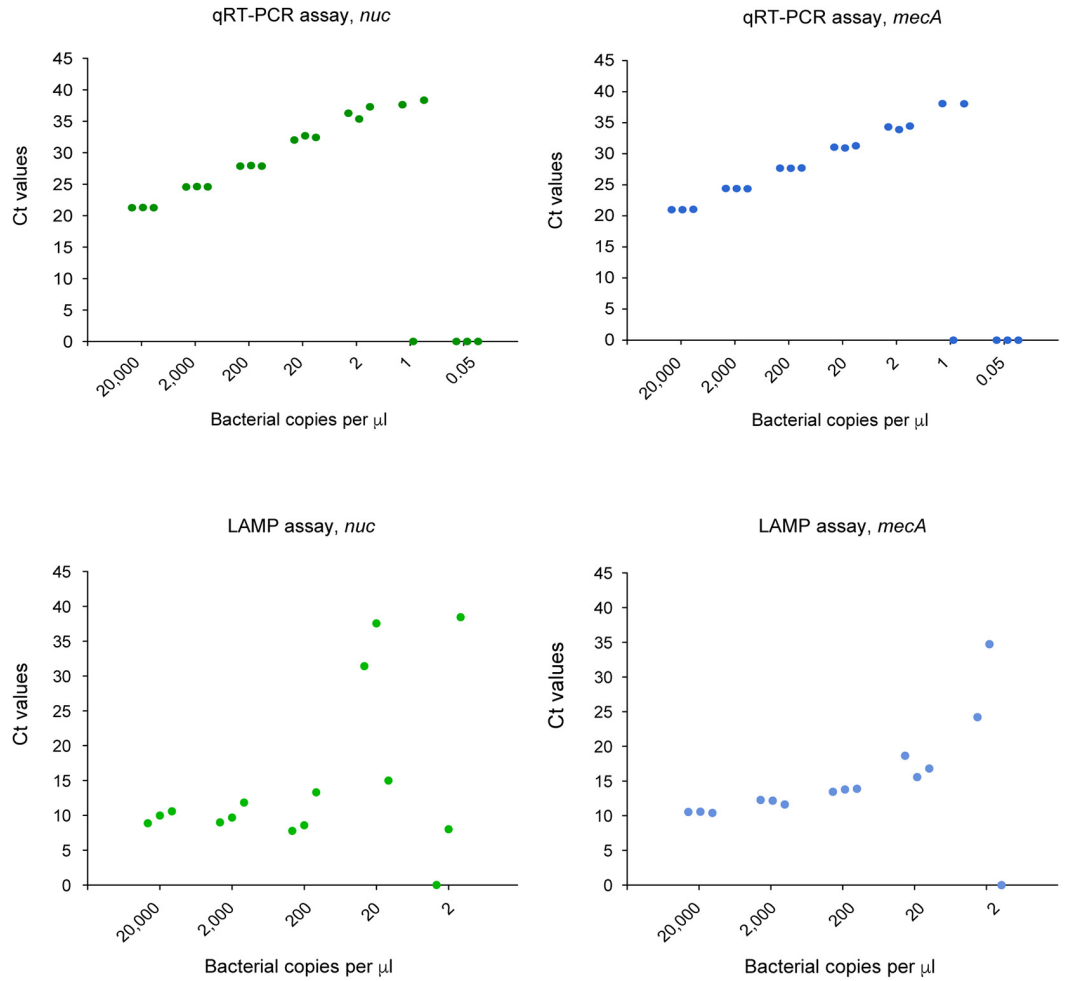

FIGURE 5 | LoD of the qRT-PCR and CRISPR-LAMP assay for *nuc* and *mecA*.

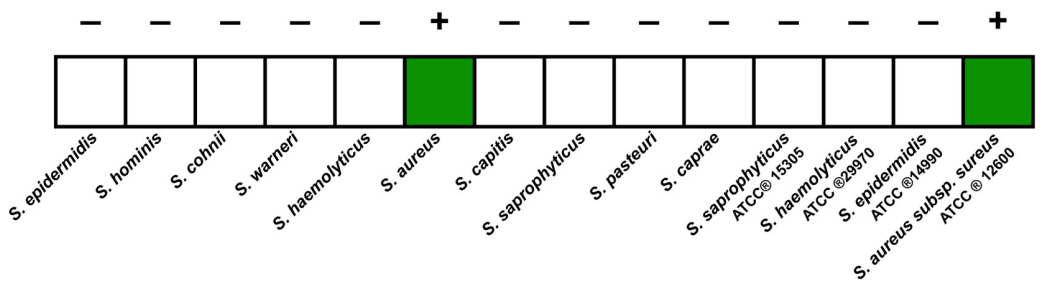

FIGURE 6 | Results of the LAMP-CRISPR assay for 14 strains of *staphylococci* species.

performed this assay for detecting *nuc* and *mecA* with serial dilutions. Green fluorescence was observed when the DNA sample was 2×10^5, 2×10^4, 2×10^3, 2×10^2, and 2×10^1 copies, which was referred to as a positive result. No green fluorescence signal was seen for a sample of 2×10^0 copies, one copy, and the no template control (NTC) (**Figure 4**). The interpretation of the genetic results for bacterial identification are illustrated in **Figure 4**.

Sensitivity of the Loop-Mediated Isothermal Amplification-Clustered Regularly Interspaced Short Palindromic Repeats Assay

We compared the LoD of the LAMP assay relative to the qRT-PCR assay for the detection of *S. aureus* and MRSA. A standard scatter plot was plotted using seven serial dilutions with three

TABLE 2 | Results of 18 samples from DFI patients using the LAMP-CRISPR assay, real-time PCR, and the reference culture.

Patient	LAMP-CRISPR		Real-time PCR		Culture
	nuc	*mecA*	*nuc*	*mecA*	
1	+	–	+(38.337)	–	MSSA
2	–	–	–	–	*Proteus vulgaris*
3	–	–	–	–	*Klebsiella pneumoniae*
4	–	–	–	37.454	*Klebsiella pneumoniae*
5	+	+	+(26.836)	+ (27.123)	MRSA
6	–	–	–	–	*Acinetobacter baumannii*
7	–	–	–	–	*Staphylococcus hominis*
8	+	+	+(35.05)	+ (31.203)	MSSA,*Staphylococcus pippi**
9	–	–	–	–	*Pseudomonas aeruginosa*
10	–	–	–	–	*Proteus vulgaris*
11	+	–	+(24.945)	–	MSSA
12	–	–	–	–	*Proteus vulgaris*
13	+	–	+(28.193)	–	MSSA
14	–	–	–	37.217	*Morganella morganii*
15	+	+	+(30.227)	+ (29.936)	MRSA
16	–	–	–	–	*Enterococcus faecalis*
17	–	–	–	–	*Staphylococcus epidermidis*
18	–	–	–	–	*Proteus mirabilis*

**Methicillin resistant-coagulase negative staphylococcus.*

replicates at each dilution (**Figure 5**). The LoD of the LAMP assay for *nuc* was 20 copies per μL reaction in comparison to two copies per μL reaction for the qRT-PCR assay. For *mecA*, the LoD of the LAMP assay was 20 copies per μL reaction, versus two copies per μL reaction for the qRT-PCR assay.

Specificity of the Loop-Mediated Isothermal Amplification-Clustered Regularly Interspaced Short Palindromic Repeats Assay

We tested the extracted DNA templates from strains of several staphylococcus species using the LAMP-CRISPR assay with primers for *nuc*. These strains included ten isolates, including *S. epidermidis*, *S. hominis*, *S. cohnii*, *S. warneri*, *S. haemolyticus*, *S. aureus*, *S. capitis*, *S. saprophyticus*, *S. pasteuri*, and *S. caprae*, and four purchased strains, including *S. saprophyticus* ATCC® 15305, *S. haemolyticus* ATCC ®29970, *S. epidermidis* ATCC ®14990, and *S. aureus* subsp. *aureus* ATCC ®12600. Positive results were generated only for DNA samples from *S. aureus* (**Figure 6**). It was confirmed that the LAMP-CRISPR assay for *nuc* could specifically detect *S. aureus*, with no cross-reactions to other staphylococcal families.

Application of the Loop-Mediated Isothermal Amplification-Clustered Regularly Interspaced Short Palindromic Repeats Assay to the Diabetic Foot Infection Patient Samples

Clinical validation of this assay was performed using 18 samples of isolated strains from DFI ulcers. Confirmatory qRT-PCR was used to establish target gene detected by the LAMP-CRISPR assay. The results of the two molecular methods were compared to those of the gold-standard culture method (**Table 2**). For *S. aureus* detection, six samples were *nuc*-positive as per the CRISPR-LAMP assay and *S. aureus*-positive by culture. For

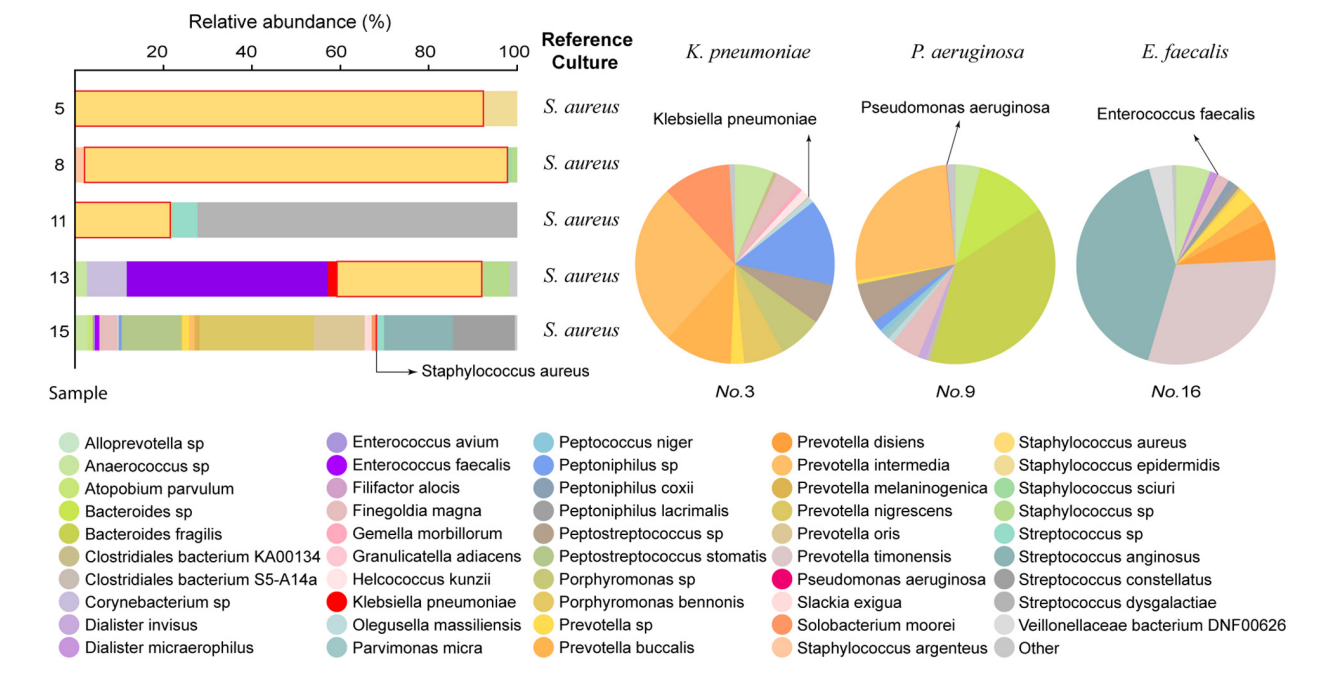

FIGURE 7 | Comparison of mNGS data to the reference culture. In the left 100% stacked columns, the column representing *S. aureus* is framed by a red line.

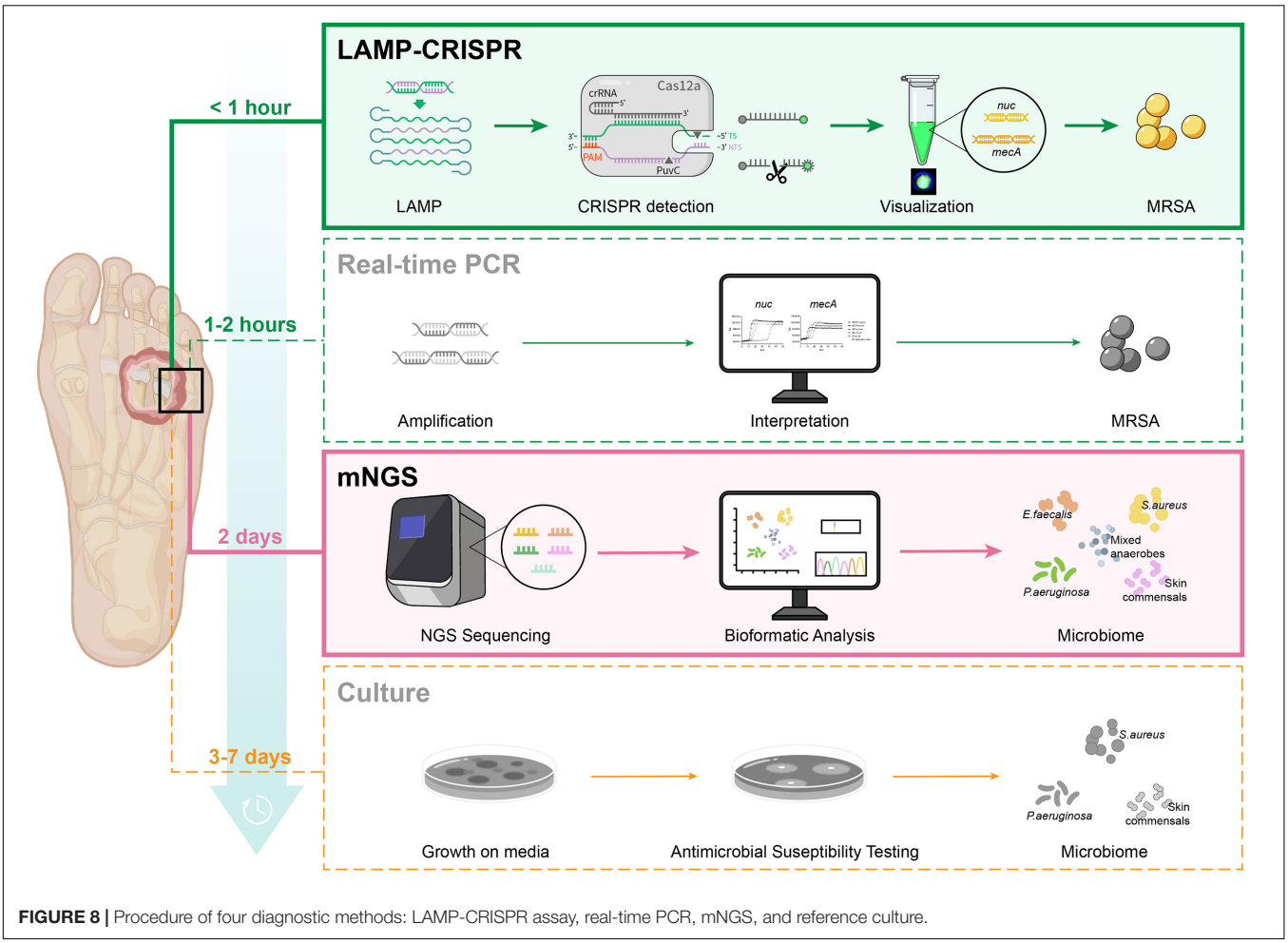

FIGURE 8 | Procedure of four diagnostic methods: LAMP-CRISPR assay, real-time PCR, mNGS, and reference culture.

MRSA detection, two samples were positive for both *nuc* and *mecA* as per the CRISPR-LAMP assay and MRSA-positive by culture. One discordant sample (No. 8) was positive for both *nuc* and *mecA* as per the LAMP-CRISPR assay and MRSA-negative by culture. The results showed that MSSA was mixed with methicillin-resistant *Staphylococcus pippi*.

Metagenomics Next Generation Sequencing Analysis

After LAMP-CRISPR and qRT-PCR analysis, 8/18 samples were selected for mNGS. The culture growth of these eight samples indicated pathogens commonly seen in clinical practice, such as *S. aureus*, *Enterococcus faecalis*, *Pseudomonas aeruginosa*, *and Klebsiella pneumoniae*. The results of the mNGS analysis are listed in **Supplementary Material** (**Supplementary Table 2**). The mNGS results were consistent with the reference culture (**Figure 7**).

DISCUSSION

Here, we combined the CRISPR-Cas12a-based technique with LAMP to develop a rapid diagnostic assay for the detection of *S. aureus* in samples directly from patients with DFI.

TABLE 3 | Comparison of the LAMP-CRISPR assay to real-time PCR, mNGS, and the reference culture.

	LAMP-CRISPR	Real-time PCR	mNGS	Culture
Assay sample-to-result time	<1 h	1–2 h	2 days	3–7 days
Sensitivity	High	High	High	Low
Specificity	High	High	Low	High
complex laboratory infrastructure required	No	Yes	Yes	Yes
Cost	Inexpensive	Inexpensive	Expensive	Inexpensive

The CRISPR-LAMP assay targeting *nuc* and *mecA* successfully identified *S. aureus* strains and differentiated MRSA from MSSA. The entire procedure was brief and contamination-free. Visualization of the results through a simple device also made them easy to interpret. This molecular assay could be promising for the point-of-care detection of *S. aureus* from clinical samples at some underprovided hospitals and areas.

MRSA can be transmitted by contact between the medical staff and patients. Infection-control precautions, such as the primary isolation of patients with MRSA infection and disinfection of the clinic environment after every diabetic foot patient with MRSA infection, can prevent cross-transmission of MRSA

(Lecornet et al., 2007). Early detection of MRSA can alert hospital staff to carry out the necessary precautions to reduce the spread of MRSA among patients. With the worldwide prevalence of MRSA isolates and frequent exposure to vancomycin, the appearance of vancomycin-intermediate *S. aureus* (Centers for Disease Control and Prevention (CDC), 2002; Chang et al., 2003) as well as vancomycin-resistant *S. aureus* (Centers for Disease Control and Prevention (CDC), 1997) strains have been identified globally. Early discrimination between MSSA and MRSA could reduce the inappropriate use of broad-spectrum antimicrobials and decrease the selective pressure that initiates the emergence and spread of resistance in bacteria (Gardete and Tomasz, 2014).

A potential weakness of this assay was the partial disagreement between the phenotype and genotype of microorganisms, which was also observed in other molecular strategies such as GeneOhm MRSA or Xpert MRSA assays (Buchan et al., 2015). Microbes that were *mecA*-negative might contain *mecC*, which was recently discovered and identified as a novel resistance gene in MRSA (Lakhundi and Zhang, 2018). DFI is often caused by multiple bacteria (Lipsky et al., 2012), which indicates that the culture growth of a clinical sample could be a mixture of *S. aureus* and coagulase-negative *Staphylococcus*, both of which can carry the *mecA* gene. Therefore, apart from being caused MRSA alone, the double positivity of *nuc* and *mecA* could be explained by mixed Staphylococcal isolates. This discrepancy was observed in one patient (No. 8). Using long-range PCR may encompass the amplicons, including both *nuc* and *mecA*, from a single strain that can uniquely identify MRSA (McClure et al., 2020). This will compensate for the current deficiency of the LAMP or regular PCR assays and improve specificity.

We then compared this novel LAMP-CRISPR assay with the reference culture, using qRT-PCR and mNGS methods (**Figure 8**). Compared to other diagnostic technologies, the CRISPR-LAMP assay enabled the detection of targeted genes at very low DNA concentrations within 1 h, which is faster than qRT-PCR and no complex infrastructure was required (**Table 3**). DFI is a rapidly progressing and relatively critical disease that may lead to disability and mortality. CRISPR-LAMP detection could aid clinicians in selecting targeted antibiotics and prevent the spread of multi-drug resistant microbes. Application of the CRISPR-LAMP assay optimizes the early treatment of DFI and complements the current paradigm for clinical diagnostics.

We also chose several representative samples for mNGS. mNGS can unbiasedly identify multiple microbes and address the limitations in pathogen width. It provides comprehensive information on the microbial profile of DFIs, including some rare pathogens that cannot be detected by conventional methods. mNGS can also provide quantitative data on the microbial concentration in the sample by counting sequenced reads, which is useful for polymicrobial samples (Wei et al., 2019). Study of the microbiome can potentially improve the diagnosis and treatment of DFIs. This revolutionary genetic approach further advances the management procedure of DFIs, which is becoming a rising trend in the clinical detection of infectious diseases. With the rapid determination of pathogens via CRISPR-LAMP and comprehensive supplementation of the bacterial spectrum by mNGS, a combination of these two methods can realize a timely and accurate pathogenic diagnosis of DFIs.

CONCLUSION

Targeting both *nuc* and *mecA*, our LAMP-CRISPR assay has proven to be a rapid (within 1 h) and effective method for detecting *S. aureus* and distinguishing MRSA from MSSA in DFI samples. Due to its convenient visualized readout and portable nature, this method is promising for improving point-of-care detection. mNGS can provide comprehensive information for the microbiome study of DFI samples. Combining the LAMP-CRISPR technique and mNGS expanded and improved the pathogen diagnostic routine of DFI.

DATA AVAILABILITY STATEMENT

The data presented in this study are deposited in the EBI Metagenomics repository, accession numbers ERR6769676–ERR6769683.

ETHICS STATEMENT

The studies involving human participants were reviewed and approved by Human Research Ethics Committee of Sir Run Run Shaw Hospital. The patients/participants provided their written informed consent to participate in this study.

AUTHOR CONTRIBUTIONS

CL, LL, and YC conceived and designed the study. YC was the major contributor in manuscript writing. YS, YC, and WZ completed the laboratory procedures. JaY, JeY, HL, and SF collected the samples of DFI patients and managed the diagnosis and treatment of patients. HZ analyzed the mNGS Data. YX proofread the first draft of the manuscript. CL and LL reviewed the manuscript. All authors agree to be accountable for the content of the work.

FUNDING

Zhejiang Province Medical and Health Science Project (grant numbers 2021454695, 2021KY881, and 2019323752), Hangzhou Municipality Medical and Health Science Project (grant number A20200297).

SUPPLEMENTARY MATERIAL

The Supplementary Material for this article can be found online at: https://www.frontiersin.org/articles/10.3389/fmicb.2021.742040/full#supplementary-material

Supplementary Table 1 | The sequences of the LAMP primers for *nuc* and *mecA*, and the CRISPR probe.

Supplementary Table 2 | The results of the mNGS analysis. The highlights in the table represent the consistent microbials detected both by the mNGS and reference culture.

REFERENCES

Prompers, L., Huijberts, M., Apelqvist, J., Jude, E., Piaggesi, A., Bakker, K., et al. (2006). High prevalence of ischaemia, infection and serious comorbidity in patients with diabetic foot disease in Europe. Baseline results from the Eurodiale study. *Diabetologia* 50, 18–25.

Jia, L., Parker, C. N., Parker, T. J., Kinnear, E. M., Derhy, P. H., Alvarado, A. M., et al. (2017). Incidence and risk factors for developing infection in patients presenting with uninfected diabetic foot ulcers. *PLoS One* 12:e0177916. doi: 10.1371/journal.pone.0177916

Lipsky, B. A., Berendt, A. R., Cornia, P. B., Pile, J. C., Peters, E. J. G., Armstrong, D. G., et al. (2012). 2012 Infectious Diseases Society of America clinical practice guideline for the diagnosis and treatment of diabetic foot infections. *Clin. Infect. Dis.* 54, e132–e173.

Eleftheriadou, I., Tentolouris, N., Argiana, V., Jude, E., and Boulton, A. J. (2010). Methicillin-resistant *Staphylococcus aureus* in diabetic foot infections. *Drugs* 70, 1785–1797. doi: 10.2165/11538070-000000000-00000

Cosgrove, S. E., Sakoulas, G., Perencevich, E. N., Schwaber, M. J., Karchmer, A. W., and Carmeli, Y. (2003). Comparison of mortality associated with methicillin-resistant and methicillin-susceptible *Staphylococcus aureus* bacteremia: a meta-analysis. *Clin. Infect. Dis.* 36, 53–59.

Filice, G. A., Nyman, J. A., Lexau, C., Lees, C. H., Bockstedt, L. A., Como-Sabetti, K., et al. (2010). Excess costs and utilization associated with methicillin resistance for patients with *Staphylococcus aureus* infection. *Infect. Control Hosp. Epidemiol.* 31, 365–373. doi: 10.1086/651094

Buchan, B. W., Allen, S., Burnham, C.-A. D., McElvania TeKippe, E., Davis, T., Levi, M., et al. (2015). Comparison of the next-generation Xpert MRSA/SA BC assay and the GeneOhm StaphSR assay to routine culture for identification of *Staphylococcus aureus* and methicillin-resistant *S. aureus* in positive-blood-culture broths. *J. Clin. Microbiol.* 53, 804–809. doi: 10.1128/jcm.03108-14

Ellem, J. A., Olma, T., and O'Sullivan, M. V. N. (2015). Rapid detection of methicillin-resistant *Staphylococcus aureus* and methicillin-susceptible *S. aureus* directly from positive blood cultures by use of the BD Max StaphSR assay. *J. Clin. Microbiol.* 53, 3900–3904. doi: 10.1128/jcm.02155-15

Silbert, S., Gostnell, A., Kubasek, C., and Widen, R. (2017). Evaluation of the BD Max StaphSR assay for detecting methicillin-resistant *Staphylococcus aureus* (MRSA) and methicillin-susceptible *S. aureus* (MSSA) in ESwab-collected wound samples. *J. Clin. Microbiol.* 55, 2865–2867. doi: 10.1128/jcm.00641-17

Kalan, L. R., Meisel, J. S., Loesche, M. A., Horwinski, J., Soaita, I., Chen, X., et al. (2019). Strain- and species-level variation in the microbiome of diabetic wounds is associated with clinical outcomes and therapeutic efficacy. *Cell Host Microbe* 25, 641–645. doi: 10.1016/j.chom.2019.03.006

Zou, M., Cai, Y., Hu, P., Cao, Y., Luo, X., Fan, X., et al. (2020). Analysis of the composition and functions of the microbiome in diabetic foot osteomyelitis based on 16S rRNA and metagenome sequencing technology. *Diabetes* 69, 2423–2439. doi: 10.2337/db20-0503

Charalampous, T., Kay, G. L., Richardson, H., Aydin, A., Baldan, R., Jeanes, C., et al. (2019). Nanopore metagenomics enables rapid clinical diagnosis of bacterial lower respiratory infection. *Nat. Biotechnol.* 37, 783–792. doi: 10.1038/s41587-019-0156-5

Li, Y., Li, S., Wang, J., and Liu, G. (2019). CRISPR/Cas Systems towards next-generation biosensing. *Trends Biotechnol.* 37, 730–743. doi: 10.1016/j.tibtech.2018.12.005

Li, S.-Y., Cheng, Q.-X., Liu, J.-K., Nie, X.-Q., Zhao, G.-P., and Wang, J. (2018a). CRISPR-Cas12a has both *cis*- and *trans*-cleavage activities on single-stranded DNA. *Cell Res.* 28, 491–493.

Li, S.-Y., Cheng, Q.-X., Wang, J.-M., Li, X.-Y., Zhang, Z.-L., Gao, S., et al. (2018b). CRISPR-Cas12a-assisted nucleic acid detection. *Cell Discov.* 4:20 .

Chen, J. S., Ma, E., Harrington, L. B., Da Costa, M., Tian, X., Palefsky, J. M., et al. (2018). CRISPR-Cas12a target binding unleashes indiscriminate single-stranded DNase activity. *Science* 360, 436–439. doi: 10.1126/science.aar6245

Broughton, J. P., Deng, X., Yu, G., Fasching, C. L., Servellita, V., Singh, J., et al. (2020). CRISPR–Cas12-based detection of SARS-CoV-2. *Nat. Biotechnol.* 395, 470–478.

Sabet, N. S., Subramaniam, G., Navaratnam, P., and Sekaran, S. D. (2007). Detection of mecA and ermA genes and simultaneous identification of *Staphylococcus aureus* using triplex real-time PCR from Malaysian *S. aureus* strain collections. *Int. J. Antimicrob. Agents* 29, 582–585. doi: 10.1016/j.ijantimicag.2006.12.017

CLSI (2018). *Performance standards for antimicrobial susceptibility testing; twenty-sixth informational supplement. CLSI document M100-S28*. Wayne: Clinical and Laboratory Standards Institute.

Lecornet, E., Robert, J., Jacqueminet, S., Van Georges, H., Jeanne, S., Bouilloud, F., et al. (2007). Preemptive isolation to prevent methicillin-resistant *Staphylococcus aureus* cross-transmission in diabetic foot. *Diabetes Care* 30, 2341–2342. doi: 10.2337/dc07-0743

Centers for Disease Control and Prevention (CDC) (2002). *Staphylococcus aureus* resistant to vancomycin–United States, 2002. *MMWR Morb. Mortal. Wkly. Rep.* 51, 565–567.

Chang, S., Sievert, D. M., Hageman, J. C., Boulton, M. L., Tenover, F. C., Downes, F. P., et al. (2003). Infection with vancomycin-resistant *Staphylococcus aureus* containing the vanA resistance gene. *N. Engl. J. Med.* 348, 1342–1347.

Centers for Disease Control and Prevention (CDC) (1997). *Staphylococcus aureus* with reduced susceptibility to vancomycin–United States, 1997. *MMWR Morb. Mortal. Wkly. Rep.* 46, 765–766.

Gardete, S., and Tomasz, A. (2014). Mechanisms of vancomycin resistance in *Staphylococcus aureus*. *J. Clin. Invest.* 124, 2836–2840. doi: 10.1172/jci68834

Lakhundi, S., and Zhang, K. (2018). Methicillin-resistant *Staphylococcus aureus*: molecular characterization, evolution, and epidemiology. *Clin. Microbiol. Rev.* 31, 5–103.

McClure, J. A., Conly, J. M., Obasuyi, O., Ward, L., Ugarte-Torres, A., Louie, T., et al. (2020). A novel assay for detection of methicillin-resistant *Staphylococcus aureus* directly from clinical samples. *Front. Microbiol.* 11:1295. doi: 10.3389/fmicb.2020.01295

Wei, G., Steve, M., and Charles, Y. C. (2019). Clinical metagenomic next-generation sequencing for pathogen detection. *Annu. Rev. Pathol.* 14, 319–338.

Conflict of Interest: YS was employed by Hangzhou Digital-Micro Biotech Co., Ltd.

The remaining authors declare that the research was conducted in the absence of any commercial or financial relationships that could be construed as a potential conflict of interest.

frontiers in Microbiology

ORIGINAL RESEARCH
published: 08 October 2021
doi: 10.3389/fmicb.2021.724935

Phenotypic Antimicrobial Susceptibility and Genotypic Characterization of Clinical *Ureaplasma* Isolates Circulating in Shanghai, China

Hongxia Ma[1†], Xuemei Zhang[2†], Xiaoxing Shi[3], Jun Zhang[4] and Yunheng Zhou[5*]*

[1]Department of Health Management Medicine, Shanghai East Hospital, Tongji University School of Medicine, Shanghai, China, [2]Department of Oncology, Shanghai East Hospital, Tongji University School of Medicine, Shanghai, China, [3]Department of Clinical Laboratory, Shanghai Provincial Crops Hospital of Chinese People's Armed Police Forces, Shanghai, China, [4]Department of Clinical Laboratory, Sir Run Run Shaw Hospital Zhejiang University School of Medicine, Hangzhou, China, [5]Department of Clinical Laboratory, Zhabei Central Hospital of Jing'an District, Shanghai, China

OPEN ACCESS

Edited by:
Yi-Wei Tang,
Cepheid, United States

Reviewed by:
Alba Pérez-Cataluña,
Institute of Agrochemistry and Food Technology (IATA), Spain
Dazhi Jin,
Hangzhou Medical College, China

***Correspondence:**
Jun Zhang
jameszhang2000@zju.edu.cn
Yunheng Zhou
hongniwan@aliyun.com

[†]These authors have contributed equally to this work

Specialty section:
This article was submitted to Antimicrobials, Resistance and Chemotherapy, a section of the journal Frontiers in Microbiology

Received: *14 June 2021*
Accepted: *08 September 2021*
Published: *08 October 2021*

Citation:
Ma H, Zhang X, Shi X, Zhang J and Zhou Y (2021) Phenotypic Antimicrobial Susceptibility and Genotypic Characterization of Clinical Ureaplasma Isolates Circulating in Shanghai, China. Front. Microbiol. 12:724935. doi: 10.3389/fmicb.2021.724935

There is a growing global concern regarding the rise of antimicrobial resistance among *Ureaplasma* spp. isolates. However, studies on the antimicrobial susceptibility profiles, resistance mechanisms, and clonality of *Ureaplasma* spp. clinical isolates are still limited and cover only some geographic regions. Firstly, *Ureaplasma* species from the urogenital tracts of patients in Shanghai, China, were isolated by using the culture medium (A8 and 10B broth), and identified the genotype by polymerase chain reaction (PCR). Secondly, the antimicrobial susceptibility tests were determined by using broth microdilution assay. Then, the resistance genetic determinants to fluoroquinolones (FQs), macrolides, and tetracyclines were investigated through PCR/DNA sequencing. Finally, the molecular epidemiology of *Ureaplasma* species was studied by multilocus sequence typing (MLST). Among 258 isolates, *Ureaplasma parvum* (UPA) and *Ureaplasma urealyticum* (UUR) were found in 226 (87.60%) and 32 (12.40%) isolates, respectively. The minimum inhibitory concentrations (MICs) of 258 *Ureaplasma* spp. strains ranged from 0.015 to 64 μg/ml for all 11 kinds of antimicrobials. Regardless of species, the isolates were most sensitive to AZI (1.94%), JOS (3.49%), and CLA (4.23%). Among them, there were 39 (15.12%) multidrug-resistant (MDR) strains, including 32 UPA isolates. The resistance rates of UPA to CIP (91.59%), and ROX (36.28%) were significantly higher than those of UUR. Twenty six FQ-resistant isolates had amino acid substitutions in *gyrA* and in *parC* (Ser83Leu). Mutations were detected in genes encoding ribosomal proteins L4 (Thr84Ile) and L22 (Ser81Pro) in macrolide-resistant isolates. *Tet*(M) was found in four UPA isolates. These mutations were mainly found in UPA isolates. Sequence type 1 (ST1) was the predominant ST, which contained 18 isolates. In conclusion, this study showed a higher resistance rate (especially to ROX and CIP), higher substitution rate, and higher MDR rate among UPA strains. The most active antimicrobial agents were AZI, JOS, and CLA. Identifying UPA or UUR in clinical isolates could help clinicians to choose appropriate drugs for treatment. The main resistance mechanisms may involve gene substitution of Ser83Leu in *parC* and Ser81Pro in L22. ST1 was the predominant ST of *Ureaplasma* isolates with MDR to FQs and macrolides in Shanghai, China.

Keywords: *Ureaplasma* spp., drug resistance, urogenital tract samples, multilocus sequence typing, resistance mechanism, multidrug resistance

INTRODUCTION

Ureaplasma spp. are among the best characterized mycoplasmal bacteria because they are tightly associated with the urogenital tract pathology in humans (Beeton and Spiller, 2017). Owing to their small genome and limited metabolic and biosynthetic capacities, *Ureaplasma* spp. are dependent on an exogenous supply of amino acids and require a close association with host cells for survival. As a result, *Ureaplasma* spp. infections have emerged as a clinical issue in a large group of patients with various diseases, such as nonchlamydial and nongonococcal urethritis (Beeton et al., 2019), prostatitis, cervicitis, as well as pelvic inflammatory disease (Hartmann, 2009). To date, reports have indicated that *Ureaplasma* spp. could be related to adverse neonatal and pregnancy outcomes, including miscarriage and meningitis in newborns (Waites, et al., 2005; Capoccia et al., 2013; Sprong et al., 2020), fatal hyperammonemia in adults (Bharat et al., 2015).

Ureaplasma spp. have no cell wall and belong to the class *Mollicutes*; they are characterized by small cell size and genome (Hartmann, 2009). Based on molecular analyses, human *Ureaplasma* spp. are now divided into *Ureaplasma parvum* (UPA) and *Ureaplasma urealyticum* (UUR), which contain at least 14 serovars: UPA (serovars 1, 3, 6, and 14) and UUR (serovars 2, 4, 5, and 7–13; Robertson et al., 2002).

Because *Ureaplasma* spp. lack cell wall and folic acid synthesis capacity, they are naturally insusceptible to β-lactams, sulfonamides, and trimethoprim (Beeton and Spiller, 2017). However, they are generally considered susceptible to tetracyclines, fluoroquinolones (FQs), and macrolides, which interfere with bacterial protein synthesis or DNA replication (Sweeney et al., 2016). In 2011, the Clinical and Laboratory Standards Institute (CLSI) issued the document M43-A: a standard method for performing and validating *in vitro* susceptibility tests for clinical *Ureaplasma* spp. (Clinical and Laboratory Standards Institute, 2011). CLSI M43-A highlights the requirement for standardized media (10B broth or A8 agar). The document lists only five kinds of selected antimicrobials with breakpoints. However, most laboratories lack the capability to cultivate, isolate, and purify fastidious bacteria such as *Ureaplasma* spp. Only a few studies have characterized antimicrobial resistance levels of *Ureaplasma* spp. in China and other countries (Zhang et al., 2014a; Fernández et al., 2016).

We have recently reported the relationship between *Ureaplasma* spp. infection, male infertility, and semen quality, and determined the minimum inhibitory concentrations (MICs) of some antimicrobials for *Ureaplasma* spp. (Zhou et al., 2018b; Wang et al., 2019). Although some studies have evaluated acquired resistance against several of the above-mentioned agents, the detailed mechanisms underlying the resistance and clonality of *Ureaplasma* spp. are still scarce and are limited to several geographic regions (Pereyre et al., 2007; Beeton et al., 2009; Leli et al., 2012; De Francesco et al., 2013; Schneider et al., 2015; Fernández et al., 2016). Therefore, the aim of this study was to study the genotype, the antimicrobial susceptibility; corresponding molecular resistance mechanisms; multidrug resistance (MDR) and sequence type (ST) distribution and clonality of large-scale clinical *Ureaplasma* spp. isolated from the urogenital tracts of patients in Shanghai, China.

MATERIALS AND METHODS

Clinical Specimens and Species Identification

The study was approved by the Ethics Committee of Shanghai Crops Hospital of Chinese People's Armed Police (No. 20121206). Clinical specimens were collected from the urogenital tracts of patients (33 men and 225 women; medium age, 28.40 years; age range, 19–54 years) between 2013 and 2014 in three departments (i.e., departments of dermatology, gynecology and obstetrics, and infertility) of the Shanghai Crops Hospital of Chinese People's Armed Police. The specimens were collected by picking up endocervical cells or vaginal secretion using sterile swabs in women and from urethral secretions or semen in men.

The secretions were inoculated directly on the selective solid culture medium (A8) and the liquid culture medium at 37°C in an atmosphere of 5% CO_2; the results were observed after 48 and 72 h. Liquefied semen was inoculated in the broth medium (100 μl) and on the selective agar medium in parallel (20 μl). Due to an increase in pH caused by *Ureaplasma* spp. growth, a phenol red indicator was added to media to display a color change. A Leitz Orthoplan microscope was used for direct examination of colonies at 100× magnification. Colonies of *Ureaplasma* spp. were identified presumptively by their characteristic echinus appearance (brown and tiny) on A8 agar in the presence of the Mn indicator (Viscardi, 2010).

Isolation and Purification

A single *Ureaplasma* spp. colony was placed into 10B broth media under microscope for purification at 37°C. After the color of the liquid medium had changed into light pink or peach after approximately 16–18 h of incubation, the liquid medium was measured and adjusted to pH 7.0; then, the purified strains were identified by PCR and stored in multiple aliquots at −80°C in fetal bovine serum in strains bank of Shanghai Crops Hospital. The selective medium agar (A8) and the liquid medium (10B broth) kits and reference strains (ATCC 33175 and ATCC 15488) were provided by Zhongaisheng Hebei Bioscience Technology Inc. (Xingtai, China).

For *Ureaplasma* spp. samples, genomic DNA extraction was performed using a Takara DNA Minikit (Shiga, Japan). These samples were reconfirmed by amplification of the *Ureaplasma* spp.-specific urease gene (a 430-bp DNA product) using U4 and U5 primers. Detection of 284 *Ureaplasma* spp. isolates was done using DNA sequences of the UM-1 primers (UMS125 and UMA226; Blanchard et al., 1993; Teng et al., 1994; Cunningham et al., 2013) and/or 16S-rRNA gene primers UMS 57-UMA 222 for the detection of UPA (327 bp), as well as UMS 170-UMA 263 for the detection of UUR (476 bp; Kong et al., 2000; Xie et al., 2009).

Antimicrobial Susceptibility Testing

In this study, 11 antimicrobials were used, including macrolides [erythromycin (ERY), azithromycin (AZI), roxithromycin (ROX), clarithromycin (CLA), josamycin (JOS)], FQs [levofloxacin (LEV), moxifloxacin (MXF), ciprofloxacin (CIP)], and

tetracyclines [tetracycline (TET), doxycycline (DOX), and minocycline (MIN)]. All agents (Sigma-Aldrich, St. Louis, MO, United States) were obtained in a powdered form of known purity and were diluted in accordance with their respective manufacturer's instructions. The MICs were determined in duplicate by broth microdilution performed in 96-well microtiter plates in accordance with the Clinical and Laboratory Standards (CLSI) guidelines and previous reports (Kechagia et al., 2008; Clinical and Laboratory Standards Institute, 2011) using a range of antimicrobial concentrations from 0.0625 to 128 μg/ml in 10B broth (Zhong ai sheng). American Type Culture Collection (ATCC) 33,175 (*Ureaplasma urealyticum*) was used as a quality control strain in each broth microdilution assay.

Briefly, we first quantified these organisms for use in MIC determination; then, the frozen culture aliquots were thawed and enriched, where one part was used for colony counting and the rest was stored at 4°C for 48 h for MIC. Next, all the antimicrobials were added to 96-well plates in duplicate. The 96-well plates were placed in a biosafety cabinet, dried at room temperature overnight, and then stored at 4°C for use. Then, the microdilution plates were incubated in ambient air at 37°C until the color change of the positive growth control due to the phenol red pH indicator after approximately 16–24 h of incubation. The MIC was then determined as the lowest concentration of an antimicrobial agent that did not show any color change at the time of the growth control's color change. The MIC_{50} and MIC_{90} values were recorded.

Analysis of Macrolide, FQ and Tetracycline Resistance Mechanisms

Among FQ-resistant isolates ($n = 31$; MIC ≥ 32 μg/ml), the quinolone resistance-determining regions (QRDRs) of the *gyrA*, *gyrB*, *parC*, and *parE* genes were studied by PCR/DNA sequencing. Primers were designed for amplification, and PCR-amplified DNA was sequenced in both directions to verify the existence by previously described methods (Bébéar et al., 1999, 2000). The *tet*(M) gene was assessed by PCR using Blanchard et al. (1992) primers and cycling conditions described previously in a total of 20 tetracycline-resistant isolates (15 UPA and five UUR isolates) and 59 tetracycline-susceptible isolates (Blanchard et al., 1992). For all macrolide-resistant isolates ($n = 59$, 51 UPA and eight UUR isolates), PCR amplification and sequencing were performed for both 23S rRNA alleles and the genes encoding ribosomal proteins L4 and L22 (Pereyre et al., 2007; Beeton et al., 2009; Fernández et al., 2016).

The acquired sequences were analyzed using DNAStar Lasergene 7.1 and were translated into protein sequences by blastx in NCBI. Nucleotide mutations in the 23S rRNA alleles as well as amino acid substitutions in L4 and L22, *gyrA*, *gyrB*, *parC*, and *parE* were identified by comparison with wild-type sequences, i.e., *Ureaplasma parvum* serovar 3 str. ATCC 700970 (GenBank accession numbers AF222894), UPA ATCC 700970, *Ureaplasma urealyticum* serovar 10 str. ATCC 33699 (GenBank accession numbers CP001184; Pereyre et al., 2007; Schneider et al., 2015; Fernández et al., 2016), and UPA serovar 3 str. SV3F4 (GenBank accession numbers AP 014584; Wu et al., 2014).

Multilocus Sequence Typing

Multilocus sequence typing (MLST; involving the *ftsH*, *rpl22*, *valS*, and *thrS* genes) was performed on a selection of 59 isolates (51 UPA and eight UUR isolates) that were resistant to FQs and macrolides as well as partially susceptible to tetracyclines (Fernández et al., 2016). Population structures of 59 *Ureaplasma* spp. isolates were predicted by eBURST. All the STs were analyzed.

Statistical Analysis

Data analysis was performed using SPSS, version 21. The Chi-square test was used for comparison of qualitative variables. $p < 0.05$ was considered statistically significant.

RESULTS

Species Identification and Prevalence of Resistance in *Ureaplasma* spp.

Of the 258 tested specimens, 226 (87.60%) were only positive for UPA and 32 (12.40%) were only positive for UUR (**Table 1**). There was no significant difference in the distribution of *Ureaplasma* spp. between the two genders ($p > 0.05$). More than 40% of all the *Ureaplasma* spp. were isolated from patients aged 19–25 years. There was no significant difference in the distribution of UPA and UUR isolates among the age groups ($p > 0.05$; **Table 2**).

The detailed results for the MIC range, MIC_{50} and MIC_{90} values, and the antimicrobial resistance of *Ureaplasma* spp. (UPA and UUR) are shown in **Table 3**. The MICs of 258 *Ureaplasma* spp. strains ranged from 0.015 to 64 μg/ml for all 11 kinds of antimicrobials *in vitro*. Among them, ciprofloxacin had the least effective activity (MIC_{50} of 16 μg/ml and MIC_{90} of 64 μg/ml) against *Ureaplasma* spp. CLA was the most active

TABLE 1 | Distribution of *Ureaplasma* spp. species isolated from 258 cases between female and male.

	UPA (N %)	UUR (N %)	Total (N %)
Female	196 (87.11%)	29 (12.89%)	225 (87.21%)
male	30 (90.91%)	3 (9.09%)	33 (12.79%)
Total	226 (87.60%)	32 (12.40%)	258 (100%)

UPA, Ureaplasma parvum; UUR, Ureaplasma urealyticum.

TABLE 2 | The distribution of *Ureaplasma* spp. of 258 cases from the urogenital tracts of patients among different age groups.

Age group (range, years)	UPA (N %)	UUR (N %)	Total (N %)
19–25	98 (88.29%)	13 (11.71%)	111 (43.02%)
26–30	63 (86.30%)	10 (13.70%)	73 (28.29%)
31–35	31 (93.94%)	2 (6.06%)	33 (14.44%)
>35	34 (82.93%)	7 (17.07%)	41 (16.55%)
Total	226 (87.60%)	32 (12.40%)	258 (100%)

UPA, Ureaplasma parvum; UUR, Ureaplasma urealyticum.

TABLE 3 | Antimicrobial *in vitro* resistance profiles of 258 clinical *Ureaplasma* spp. isolates.

	ERY N (%)	AZI N (%)	ROX N (%)	CLA N (%)	JOS N (%)	LEV N (%)	MXF N (%)	CIP N (%)	TET N (%)	DOX N (%)	MIN N (%)
UPA	39 (17.26)	4 (1.77)	82 (36.28)	9 (3.98)	6 (2.65)	167 (73.89)	61 (27.00)	207 (91.59)	39 (17.2)	22 (9.73)	18 (7.96)
UUR	6 (18.75)	1 (3.2)	3 (9.37)	3 (9.37)	3 (9.37)	21 (65.63)	11 (34.37)	25 (78.12)	6 (18.75)	7 (21.87)	6 (18.75)
p value	0.806	-	0.002	-	-	0.395	0.403	0.027	0.806	0.042	-
Total	45 (17.44)	5 (1.94)	85 (32.95)	12 (4.23)	9 (3.49)	188 (72.87)	72 (27.91)	232 (89.92)	45 (17.44)	29 (11.24)	24 (9.30)
MIC range	0.03–64	0.015–16	0.03–64	0.015–16	0.015–16	0.03–64	0.03–64	0.03–64	0.015–16	0.015–16	0.015–16
MIC_{50}	2	1	1	0.125	0.125	8	1	16	0.5	0.25	0.5
MIC_{90}	16	4	8	0.5	1	64	16	64	8	2	4

TABLE 4 | Occurrence of ROX-CIP and MDR among *Ureaplasma* spp.

Ureaplasma spp. (N %)	ROX-CIP	MDR	Total
UPA	67 (29.65%)	32 (14.16%)	226 (87.60%)
UUR	10 (31.25%)	7 (21.87%)	32 (12.40%)
Total	77 (29.84%)	39 (15.12%)	258 (100%)

ROX-CIP: both resistant to roxithromycin (ROX) and ciprofloxacin (CIP). MDR, multi-drug resistance: resistant to at least one agent in ≥3 antimicrobial categories: macrolides, tetracyclines, and fluoroquinolones. UPA, Ureaplasma parvum; UUR, Ureaplasma urealyticum.

antimicrobial with an MIC_{50} of 0.125 μg/ml and MIC_{90} of 0.5 μg/ml. ERY was the least effective among macrolides (MIC_{50} of 2 μg/ml and MIC_{90} of 16 μg/ml). DOX was the most active tetracycline, with MIC_{50} of 0.25 μg/ml and MIC_{90} of 2 μg/ml.

According to the CLSI, the top three drug resistance rates of *Ureaplasma* spp. were those to CIP (89.92%), LEV (72.87%), and ROX (32.95%). Among them, the drug resistance rates of UPA were as follows: CIP (91.59%), and ROX (36.28%); they were significantly higher than those of UUR. The most active antimicrobial agents were AZI (1.94%), JOS (3.49%), CLA (4.23%), and MIN (9.30%). Of the 258 *Ureaplasma* spp. strains, there were 77(29.84%) isolates uniformly resistant to ROX and CIP, and 39(15.12%) MDR isolates; both of them were dominated by UPA strains (**Table 4**).

Molecular Characterization of Antimicrobial Resistance

In the comparison with the relative DNA and protein sequences of reference strains, none of the isolates possessed mutations in 23S rRNA. A Thr84Ile mutation was detected in the ribosomal protein L4 of one roxithromycin-resistant UPA isolate. A Ser81Pro mutation was detected in the ribosomal protein L22 of seven *Ureaplasma* spp. isolates (five roxithromycin-resistant UPA isolates, one erythromycin-resistant UPA isolate, and an UPA isolate resistant to roxithromycin and erythromycin); the latter also had another mutation, Lys91Asn in the protein L22.

The comparison between the QRDR DNA sequences of reference strains and the QRDRs of FQ-resistant isolates ($n = 31$; MIC ≥ 32 μg/ml) revealed no mutations in *gyrB* or *parE* in any of the isolates. However, *gyrA* and *parC* quinolone resistance-associated mutations were found. One FQ-resistant UPA isolate showing a levofloxacin MIC of 32 μg/ml harbored a Val120Phe mutation in *gyrA*, but no QRDR mutations were found in *gyrA* of FQ-resistant UUR isolates. The most frequent mutation was Ser83Leu in *parC*, which was present in 22 (88%) and three (50%) of the FQ-resistant UPA and UUR isolates, respectively. Among 32 MDR UPA isolates, there were 14 cases of mutation in *parC* S83L (Ser83Leu); 2 isolates with Ser83Leu (Ser81Pro) and 1 isolates with *Tet*(M) Screening of the *tet*(M) gene, which is associated with tetracycline resistance, was performed among 79 isolates. Two tetracycline-resistant UPA isolates were positive for this gene, but two tetracycline-susceptible UPA isolates also harbored this gene.

Multilocus Sequence Typing

Among the 59 *Ureaplasma* spp. isolates resistant to FQs and macrolides, the *ftsH* gene and *thrS* gene, with the highest discriminatory power, had 10 alleles and 8 alleles, respectively, while the *rpL22* gene and *valS* gene had four and three alleles, respectively.

The lineage of the 21 STs in 59 strains was analyzed, and two major clonal complexes (CC1 and CC2) were revealed by the eBURST package. ST2 was the predicted ancestor, highlighted in the blue circle, while the other STs are displayed in the yellow circle. The size of the circle reflects the number of isolates in the relevant ST, and STs are represented as numbers. Twenty one STs appeared among the 59 clinical isolates. ST1 was the predominant ST, which contained 18 UPA isolates. CC1 contained the vast majority of 17 STs in 44 isolates, while the remaining four STs (ST9, ST52, ST101, and ST161) were singletons (**Figure 1**).

DISCUSSION

In recent years, many questions regarding the role of *Ureaplasma* spp. as human pathogens, therapeutic strategies, and the antimicrobial susceptibility of individual species remain open. In this study, we examined the antimicrobial susceptibility, resistance mechanisms, and ST distribution of contemporary 258 clinical *Ureaplasma* spp. isolated from 2013 to 2014 in Shanghai, China. Few previous studies have focused on the individual UPA and UUR distributions in clinical *Ureaplasma* spp. samples (Kawai et al., 2015; Schneider et al., 2015; Yang et al., 2020). In our study, the positive rate of UPA among clinical *Ureaplasma* spp. isolates of the urogenital tract was 87.60%, similar to a recent estimate obtained by Fernández et al. (2016) in the United States. Studies of the frequencies

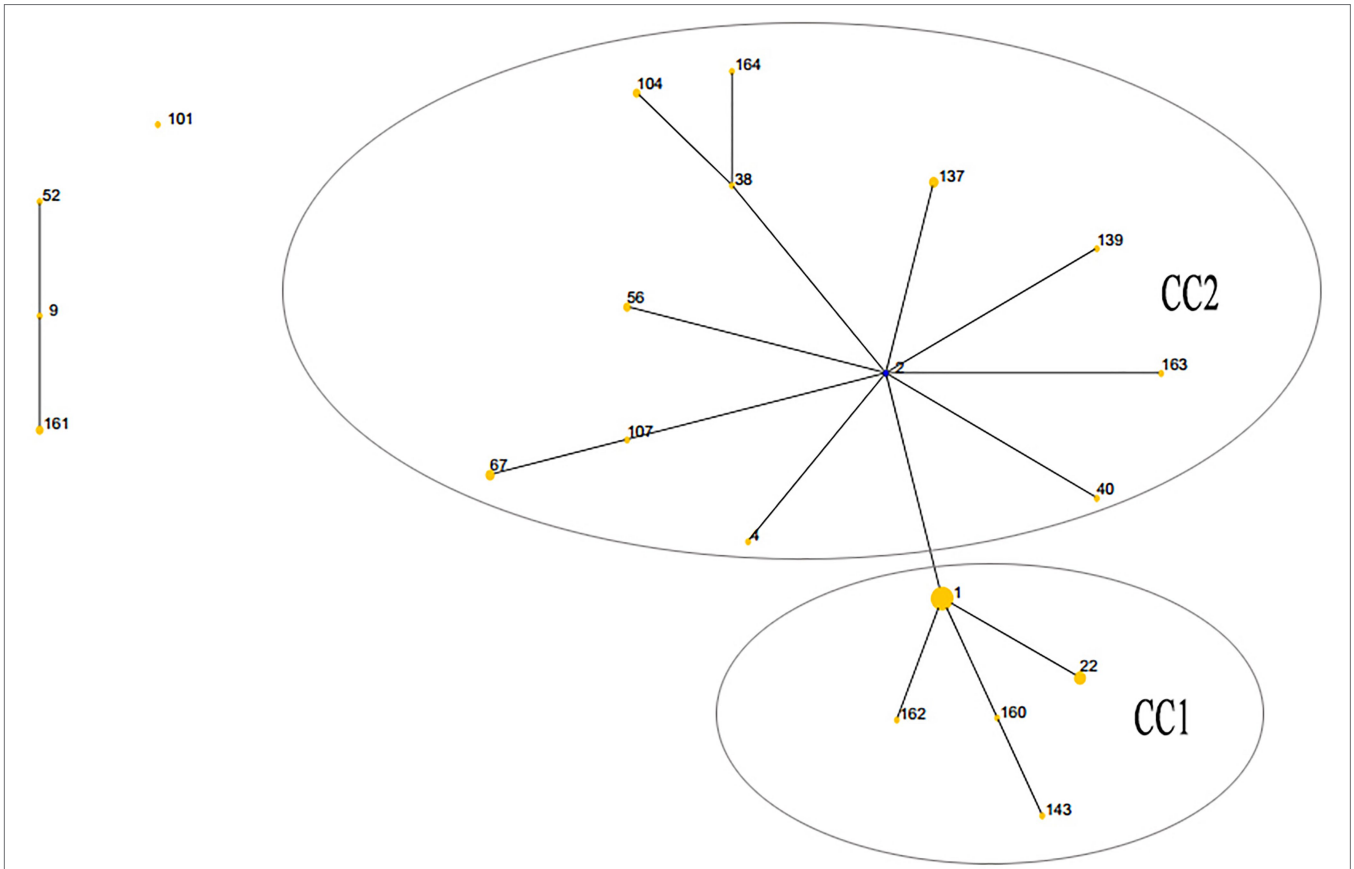

FIGURE 1 | Population structures of 59 *Ureaplasma* spp. isolates resistant to quinolones and macrolides predicted by eBURST. CC, clonal complex.

of individual species may be useful for further analyses of their clinical characteristics.

The continuous increase in the prevalence of *Ureaplasma* spp. raised questions regarding their antimicrobial resistance (Zeng et al., 2016; Zhou et al., 2018a). Here, we analyzed the susceptibility of *Ureaplasma* spp. to 11 kinds of antimicrobial drugs. As expected, UPA and UUR had low resistance to most macrolides and tetracyclines, while their resistance to LEV (72.87%) was very high. While the resistance to macrolides is less than 5% in most countries, our study showed a higher rate of ERY (17.44%) and ROX (32.95%) resistance among clinical strains from Shanghai. Additionally, our results significantly differed from those of previous reports. For instance, Fernández et al. have reported a lower resistance rate to LEV (6%) and no macrolide resistance among the 250 clinical isolates in the United States (Fernández et al., 2016). Some domestic studies of *Ureaplasma* spp. strains indicated a 20.09% resistance rate to LEV (Zhu et al., 2012), less than 10% to macrolides (Song et al., 2014), and 76.9% to LEV (Song et al., 2015). In addition, *Ureaplasma* spp. exhibited high resistance to CIP (100%) and to ERY (100% in Tunisia and 80% in South Africa; Redelinghuys et al., 2014; Boujemaa et al., 2020).

Higher resistance rates to ERY, ROX, and LEV may be attributed to the following four factors. First, our study population (87.21% women with border age distribution) may have had higher antimicrobial exposure (especially to macrolides and FQs) and higher resistance levels. Kobayashi et al. found that each age group over 30 years had significantly higher odds of receiving FQs for treatment compared with women between 18 and 29 years (Kobayashi et al., 2016). However, in Europe and the United States, the macrolide resistance rates of *M. pneumoniae* are substantially lower than those in Asia (Waites et al., 2017). Second, these overall figures indicate that resistance rates vary significantly among countries; in some instances, there are even dramatic differences within the same country, which may be related to the different strategy or preference of antimicrobials usage in different areas (Yang et al., 2020). Third, another explanation for this variation may be related to the shortcomings of different Mycoplasma testing kits and the reference broth microdilution method currently used to estimate the antimicrobial susceptibility of *Ureaplasma* spp. Schneider et al. reported that there was conflicting results from the IST 2 kit and standard broth microdilution was observed for CIP and AZI (Schneider et al., 2015). Namely, the Mycoplasma IST2 assay identifies a number of false positives and does not conform to the approved CLSI guidelines (Beeton et al., 2009, 2015). The accuracy of some reports is still questionable since there are no standardized methods for *in vitro* susceptibility testing and no MIC interpretive breakpoints were designated before 2011. Of note, acidic pH and incubation time affect erythromycin MICs (Kenny and Cartwright, 1993).

Furthermore, mutations, biofilm formation, and the distribution pattern of species or serovars of *Ureaplasma* spp. can also lead to this phenomenon. The top three drug resistance rates of *Ureaplasma* spp. were those to CIP, LEV, and ROX. Among CIP and ROX, the drug resistance rates of UPA were significantly higher than those of UUR. The drug resistance rates to AZI, CLA, JOS, and MIN were very low (less than 10%) regardless of *Ureaplasma* spp.

The relationship and the molecular mechanism between the antimicrobial susceptibility and genotype of *Ureaplasma* spp. have seldom been reported (Song, 2019). Valentine-King and Brown (2017) reported a trend to higher MIC of UUR compared with UPA. The resistance rates were different for different kinds of antimicrobial between UUR and UPA (Fernández et al., 2016). Therefore, analyses of resistance rates of *Ureaplasma* spp. require more data to properly explain and interpret the observed trends.

In this study, we also studied *Ureaplasma* spp. resistance mechanisms to the above-mentioned drugs. As described previously, FQ resistance has been attributed to mutations in *gyrA*, *gyrB*, S83L, S83W, and S84P mutations in the *parC* genes and *parE* genes (Pereyre et al., 2007; Beeton et al., 2015; Kawai et al., 2015; Schneider et al., 2015; Fernández et al., 2016; Valentine-King and Brown, 2017; Meygret et al., 2018). A sequence analysis of the QRDRs revealed that the resistance mechanism of FQ-resistant isolates involves mutations at position 248 (C-T) of *parC*, which leads to a substitution of Ser83 by Leu, followed by a Val120Phe substitution, which was mostly found in UPA isolates. As in previous studies, Beeton et al. (2009) also found that about 80% of isolates were UUR, and the *ParC* Ser83Leu mutation was largely found in all FQ-resistant *Ureaplasma* spp. We found that three FQ-resistant UPA isolates and three FQ-resistant UUR isolates among 31 *Ureaplasma* spp. isolates with high MICs (≥32 μg/ml) for LEV, MXF and CIP did not harbor QRDR mutations, suggesting the existence of other undescribed resistance mechanisms in these isolates.

Macrolide resistance has been related to mutations in domain V of 23S rRNA, ribosomal proteins L4 and L22, similar to the mechanism underlying *Mycoplasma pneumoniae* resistance (Schneider et al., 2015; Song et al., 2015, 2019). The macrolide resistance of *Ureaplasma* spp. is still a controversial issue. The A2066G (A to G) mutation and C2243N (T or C) mutation in the 23S rRNA may be associated with *Ureaplasma* spp. macrolide resistance in the Chinese population (Meng et al., 2008; Song et al., 2019). We analyzed the aforementioned resistance traits for 59 *Ureaplasma* spp. isolates showing drug resistance to macrolides; while none of the isolates possessed mutations in the 23S rRNA, we found a mutation in the L4 protein gene and two mutations of the L22 protein gene in eight macrolide-resistant UPA isolates. Yang et al. (2020) reported double alterations (A121S and T141I) or a single mutation (D66N) in L22 within five strains, including one sample harboring an S21A substitution in L4 at the same time. In addition, Pereyre et al. detected two mutations (Lys91Asn and Ala94Asp) in the ribosomal protein L22 and three mutations (Thr70Lys, Gly71Val, and Trp65Arg) in the ribosomal protein L4 (Pereyre et al., 2007); the Lys91Asn mutation in L22 of an erythromycin-resistant UPA isolate was also found in one UPA isolate resistant to erythromycin and roxithromycin and harboring another mutation, Ser81Pro, in our study. The most resistance mechanism to macrolides included the gene mutations in L4 and L22 ribosomal proteins.

The presence of *tet*(M) has been reported in both tetracycline-susceptible and -resistant *Ureaplasma* spp. isolates. In this study, the prevalence of *tet*(M) gene (5.1%, 4/79) was lower than in other reports (Kenny and Cartwright, 1993; Teng et al., 1994; Pereyre et al., 2007; Kotrotsiou et al., 2015). We also found that the *tet*(M) gene may not be a specific indicator of tetracycline-resistant *Ureaplasma* spp. isolates.

In this study, uniform resistance to ROX and CIP was the most frequently observed pattern (29.84%) among *Ureaplasma* spp. isolates; an elevated MDR rate among *Ureaplasma* spp. (15.12%) was detected, particularly among UPA isolates. Zhu et al. (2016) reported only 1.08% MDR of *Ureaplasma* spp. in Nanjing, China, while Boujemaa et al. found an elevated MDR rate (37.62%) with 60.71% of UUR strains and 28.76% of UPA being MDR (Boujemaa et al., 2020). To the best of our knowledge, this is the first report of a higher MDR rate of *Ureaplasma* spp. isolates in Shanghai, China.

To study the molecular epidemiology and population structure of *Ureaplasma* spp., an MLST approach based on four housekeeping genes (*ftsH*, *rpL22*, *valS*, and *thrS*) was first developed by Zhang et al. (2014b) who used 14 serovar reference strains and 269 clinical strains. ST1 and ST22 were the predominant STs and contained 68 and 70 isolates, respectively. Zhang et al. (2014a) also found that isolates of CC1 were UPA and those of CC2 were UUR. CC2 was found more often in symptomatic patients with vaginitis, tubal obstruction, and cervicitis. In addition, two recent studies evaluated the molecular epidemiology of clinical *Ureaplasma* spp. isolates in the United States and Switzerland, making reference to the research of Zhang et al.; these studies suggested the association of molecular epidemiology of *Ureaplasma* spp. isolates with pathogenicity or spread of antimicrobial resistance (Schneider et al., 2015; Fernández et al., 2016). We found that ST1 (18 UPA isolates) was the predominant ST among 59 MDR isolates, followed by ST22 (5 UPA isolates). Among 18 ST1 UPA isolates, there was higher MDR rate (8 cases, 44.44%) and the mutations found as the following: *parC* gene (4 cases), GyrA/*parC* (one case), and L22: S81P (one case). ST1 was the main clone both in Hangzhou (Zhang et al., 2014a) and Shanghai, which may hypothesize that ST1 can be associated with spread of the urogenital tracts of different populations or the antimicrobial resistance. MLST is a well-accepted way for illustrating the diversity and population structure of different bacterial species compared to any other molecular subtyping method. As the strain numbers of STs were very limited, it was difficult to draw any decisive conclusions on any possible correlations between STs and pathologies or molecular resistance mechanisms of *Ureaplasma* spp.

In conclusion, using a large number of clinical isolates, which were mainly obtained from women, this study addressed the lack of data in China related to the antimicrobial susceptibility of *Ureaplasma* spp. The prevalence of antimicrobial resistance in *Ureaplasma* spp., especially that to ERY, ROX, and LEV, is markedly higher in China than in European countries. The most active

antimicrobial agents were AZI, JOS, and CLA. Identifying UPA or UUR in clinical isolates could help clinicians to choose appropriate drugs for treatment. For UPA in particular, ERY, ROX, and FQs should be used with caution due to the relatively high rate of MDR. ST1 was the predominant ST of *Ureaplasma* isolates with MDR to FQs and macrolides in Shanghai, China. The main resistance mechanisms may involve gene substitution of Ser83Leu in *parC* and Ser81Pro in L22, in addition to other, undescribed mechanisms. One of the limitations of this study is that it did not provide sufficient data to better understand the epidemiology of *Ureaplasma* spp. in China. Future work should extend our investigations to address the resistance mechanisms related to the spread of antimicrobial resistance, particularly MDR strains, and the difference in drug resistance in different *Ureaplasma* spp.

DATA AVAILABILITY STATEMENT

The datasets presented in this study can be found in online repositories. The names of the repository/repositories and accession number(s) can be found at: https://www.ncbi.nlm.nih.gov/genbank/MZ700119-MZ700176 for ftsH, MZ710758 – MZ710815 for valS, MZ710816 – MZ710874 for rpL22, MZ710875 – MZ710931 for thrS.

ETHICS STATEMENT

The studies involving human participants were reviewed and approved by the Ethics Committee of Shanghai Crops Hospital of Chinese People's Armed Police. Written informed consent for participation was not required for this study in accordance with the national legislation and the institutional requirements.

AUTHOR CONTRIBUTIONS

HM, JZ, and YZ contributed to conception and design of the study. HM, XZ, XS, and YZ performed the experimental studies and analysis. HM, XZ, and YZ wrote the section of the manuscript. All authors contributed to the article and approved the submitted version.

FUNDING

This work was financially supported by the Key Programs of Science and Technology Commission Foundation of Changning District, Shanghai (CNKW2016Z05), the Jiangxi Provincial Health Technology Project (20202114), the National Natural Science Foundation of China (NSFC81370047), and Natural Science Foundation of Shanghai (13ZR1449700).

ACKNOWLEDGMENTS

We thank LetPub (www.letpub.com) for its linguistic assistance during the preparation of this manuscript.

REFERENCES

Bébéar, C. M., Grau, O., Charron, A., Renaudin, H., Gruson, D., and Bébéar, C. (2000). Cloning and nucleotide sequence of the DNA gyrase (gyrA) gene from Mycoplasma hominis and characterization of quinolone-resistant mutants selected in vitro with trovafloxacin. *Antimicrob. Agents Chemother.* 44, 2719–2727. doi: 10.1128/AAC.44.10.2719-2727.2000

Bébéar, C. M., Renaudin, J, Charron, A., Renaudin, H., de Barbeyrac, B., Schaeverbeke, T., et al. (1999). Mutations in the gyrA, parC, and parE genes associated with fluoroquinolone resistance in clinical isolates of Mycoplasma hominis. *Antimicrob. Agents Chemother.* 43, 954–956. doi: 10.1128/AAC.43.4.954

Beeton, M. L., Chalker, V. J., Jones, L. C., Maxwell, N. C., and Spiller, O. B. (2015). Antibiotic resistance among clinical *Ureaplasma* isolates recovered from neonates in England and Wales between 2007 and 2013. *Antimicrob. Agents Chemother.* 60, 52–56. doi: 10.1128/AAC.00889-15

Beeton, M. L., Chalker, V. J., Maxwell, N. C., Kotecha, S., and Spiller, O. B. (2009). Concurrent titration and determination of antibiotic resistance in *Ureaplasma* species with identification of novel point mutations in genes associated with resistance. *Antimicrob. Agents Chemother.* 53, 2020–2027. doi: 10.1128/AAC.01349-08

Beeton, M. L., Payne, M. S., and Jones, L. (2019). The role of *Ureaplasma* spp. in the development of nongonococcal urethritis and infertility among men. *Clin. Microbiol. Rev.* 32:e00137. doi: 10.1128/CMR.00137-18

Beeton, M. L., and Spiller, O. B. (2017). Antibiotic resistance among *Ureaplasma* species isolates: cause for concern? *J. Antimicrob. Chemother.* 72, 330–337. doi: 10.1093/jac/dkw425

Bharat, A., Cunningham, S. A., Scott Budinger, G. R., Kreisel, D., DeWet, C. J., Gelman, A. E., et al. (2015). Disseminated *Ureaplasma* infection as a cause of fatal hyperammonemia in humans. *Sci. Transl. Med.* 7:258.re3. doi: 10.1126/scitranslmed.aaa8419

Blanchard, A., Crabb, D. M., Dybvig, K., Duffy, L. B., and Cassell, G. H. (1992). Rapid detection of tetM in mycoplasma hominis and Ureaplasma urealyticum by PCR: tetM confers resistance to tetracycline but not necessarily to doxycycline. *FEMS Microbiol. Lett.* 95, 277–281. doi: 10.1016/0378-1097(92)90442-q

Blanchard, A., Hentschel, J., Duffy, L., Baldus, K., and Cassell, G. H. (1993). Detection of Ureaplasma urealyticum by polymerase chain reaction in the urogenital tract of adults, in amniotic fluid, and in the respiratory tract of newborns. *Clin. Infect. Dis.* 17(Suppl. 1), S148–S153. doi: 10.1093/clinids/17.supplement_1.s148

Boujemaa, S., Mlik, B., Ben Allaya, A., Mardassi, H., and Ben Abdelmoumen Mardassi, B. (2020). Spread of multidrug resistance among *Ureaplasma serovars*, Tunisia. *Antimicrob. Resist. Infect. Control* 9:19. doi: 10.1186/s13756-020-0681-5

Capoccia, R., Greub, G., and Baud, D. (2013). *Ureaplasma urealyticum*, *mycoplasma hominis* and adverse pregnancy outcomes. *Curr. Opin. Infect. Dis.* 26, 231–240. doi: 10.1097/QCO.0b013e328360db58

Clinical and Laboratory Standards Institute (2011). *Methods for Antimicrobial Susceptibility Testing for Human Mycoplasmas; Approved Guideline*. CLSI document M43-A. Wayne, PA: Clinical and Laboratory Standards Institute.

Cunningham, S. A., Mandrekar, J. N., Rosenblatt, J. E., and Patel, R. (2013). Rapid PCR detection of *Mycoplasma hominis*, *Ureaplasma urealyticum*, and *Ureaplasma parvum*. *Int. J. Bacteriol.* 2013, 1–7. doi: 10.1155/2013/168742

De Francesco, M. A., Caracciolo, S., Bonfanti, C., and Manca, N. (2013). Incidence and antibiotic susceptibility of *Mycoplasma hominis* and *Ureaplasma urealyticum* isolated in Brescia, Italy, over 7 years. *J. Infect. Chemother.* 19, 621–627. doi: 10.1007/s10156-012-0527-z

Fernández, J., Karau, M. J., Cunningham, S. A., Greenwood-Quaintance, K. E., and Patela, R. (2016). Antimicrobial susceptibility and clonality of clinical *Ureaplasma* isolates in the United States. *Antimicrob. Agents Chemother.* 60, 4793–4798. doi: 10.1128/AAC.00671-16

Hartmann, M. (2009). Genital mycoplasmas. *J. Dtsch. Dermatol. Ges.* 7, 371–377. doi: 10.1111/j.1610-0387.2008.06965.x

Kawai, Y., Nakura, Y., Wakimoto, T., Nomiyama, M., Tokuda, T., Takayanagi, T., et al. (2015). In vitro activity of five quinolones and analysis of the quinolone resistance-determining regions of gyrA, gyrB, parC, and parE in Ureaplasma parvum and Ureaplasma urealyticum clinical isolates from perinatal patients in Japan. *Antimicrob. Agents Chemother.* 59, 2358–2364. doi: 10.1128/AAC.04262-14

Kechagia, N., Bersimis, S., and Chatzipanagiotou, S. (2008). Incidence and antimicrobial susceptibilities of genital mycoplasmas in outpatient women with clinical vaginitis in Athens, Greece. *J. Antimicrob. Chemother.* 62, 122–125. doi: 10.1093/jac/dkn158

Kenny, G. E., and Cartwright, F. D. (1993). Effect of pH, inoculum size, and incubation time on the susceptibility of *Ureaplasma urealyticum* to erythromycin *in vitro*. *Clin. Infect. Dis.* 17(Suppl. 1), S215–S218. doi: 10.1093/clinids/17.supplement_1.s215

Kobayashi, M., Shapiro, D. J., Hersh, A. L., Sanchez, G. V., and Hicks, L. A. (2016). Outpatient antibiotic prescribing practices for uncomplicated urinary tract infection in women in the United States, 2002–2011. *Open. Forum. Infect. Dis.* 3:ofw159. doi: 10.1093/ofifid/ofw159

Kong, F., Ma, Z., James, G., Gordon, S., and Gilbert, G. L. (2000). Species identification and subtyping of Ureaplasma parvum and Ureaplasma urealyticum using PCR-based assays. *J. Clin. Microbiol.* 38, 1175–1179. doi: 10.1128/JCM.38.3.1175-1179.2000

Kotrotsiou, T., Exindari, M., Diza, E., Gioula, G., Melidou, A., and Malisiovas, N. (2015). Detection of the *tetM* resistance determinant among phenotypically sensitive *Ureaplasma* species by a novel real-time PCR method. *Diagn. Microbiol. Infect. Dis.* 81, 85–88. doi: 10.1016/j.diagmicrobio.2014.10.013

Leli, C., Mencacci, A., Bombaci, J. C., D'Alò, F., Farinelli, S., Vitali, M., et al. (2012). Prevalence and antimicrobial susceptibility of *Ureaplasma urealyticum* and *Mycoplasma hominis* in a population of Italian and immigrant outpatients. *Infez. Med.* 20, 82–87.

Meng, D. Y., Xue, W. C., Ma, X. B., and Wang, L. (2008). Transition mutations in 23S rRNA account for acquired resistance to macrolides in *Ureaplasma urealyticum*. *Microb. Drug Resist.* 14, 183–186. doi: 10.1089/mdr.2008.0817

Meygret, A., Le Roy, C., Renaudin, H., Bébéar, C., and Pereyre, S. (2018). Tetracycline and fluoroquinolone resistance in clinical *Ureaplasma* spp. and *Mycoplasma hominis* isolates in France between 2010 and 2015. *J. Antimicrob. Chemother.* 73, 2696–2703. doi: 10.1093/jac/dky238

Pereyre, S., Métifiot, M., Cazanave, C., Renaudin, H., Charron, A., Bébéar, C., et al. (2007). Characterisation of *in vitro*-selected mutants of *Ureaplasma parvum* resistant to macrolides and related antibiotics. *Int. J. Antimicrob. Agents* 29, 207–211. doi: 10.1016/j.ijantimicag.2006.09.008

Redelinghuys, M. J., Ehlers, M. M., Dreyer, A. W., Lombaard, H. A., and Kock, M. M. (2014). Antimicrobial susceptibility patterns of *Ureaplasma* species and mycoplasma hominis in pregnant women. *BMC Infect. Dis.* 14:171. doi: 10.1186/1471-2334-14-171

Robertson, J. A., Stemke, G. W., Davis, J. W. Jr., Harasawa, R., Thirkell, D., Kong, F., et al. (2002). Proposal of *Ureaplasma parvum* sp. nov. and emended description of *Ureaplasma urealyticum* (Shepard et al. 1974). *Int. J. Syst. Evol. Microbiol.* 52, 587–597. doi: 10.1099/00207713-52-2-587

Schneider, S. C., Tinguely, R., Droz, S., Hilty, M., Dona, V., Bodmer, T., et al. (2015). Antibiotic susceptibility and sequence type distribution of *Ureaplasma* species isolated from genital samples in Switzerland. *Antimicrob. Agents Chemother.* 59, 6026–6031. doi: 10.1128/AAC.00895-15

Song, T., Huang, J., Liu, Z., Zhang, Y., Kong, Y., and Ruan, Z. (2019). Antibiotic susceptibilities and genetic variations in macrolide resistance genes of *Ureaplasma* spp. isolated in China. *New Microbiol.* 42, 225–227.

Song, J., Qiao, Y., Kong, Y., Ruan, Z., Huang, J., Song, T., et al. (2015). Frequent topoisomerase IV mutations associated with fluoroquinolone resistance in *Ureaplasma* species. *J. Med. Microbiol.* 64, 1315–1320. doi: 10.1099/jmm.0.000153

Song, T., Ye, A., Xie, X., Huang, J., Ruan, Z., Kong, Y., et al. (2014). Epidemiological investigation and antimicrobial susceptibility analysis of *Ureaplasma* species and *Mycoplasma* hominis in outpatients with genital manifestations. *J. Clin. Pathol.* 67, 817–820. doi: 10.1136/jclinpath-2014-202248

Sprong, K. E., Mabenge, M., Wright, C. A., and Govender, S. (2020). *Ureaplasma* species and preterm birth: current perspectives. *Crit. Rev. Microbiol.* 46, 169–181. doi: 10.1080/1040841X.2020.1736986

Sweeney, E. L., Dando, S. J., Kallapur, S. G., and Knox, C. L. (2016). The human *Ureaplasma* species as causative agents of chorioamnionitis. *Clin. Microbiol. Rev.* 30, 349–379. doi: 10.1128/CMR.00091-16

Teng, L. J., Zheng, X., Glass, J. I., Watson, H. L., Tsai, J., and Cassell, G. H. (1994). *Ureaplasma urealyticum* biovar specificity and diversity are encoded in multiple-banded antigen gene. *J. Clin. Microbiol.* 32, 1464–1469. doi: 10.1128/jcm.32.6.1464-1469.1994

Valentine-King, M. A., and Brown, M. B. (2017). Antibacterial resistance in *Ureaplasma* species and *Mycoplasma hominis* isolates from urine cultures in college-aged females. *Antimicrob. Agents Chemother.* 61, e01104–e01117. doi: 10.1128/AAC.01104-17

Viscardi, R. M. (2010). *Ureaplasma* species: role in diseases of prematurity. *Clin. Perinatol.* 37, 393–409. doi: 10.1016/j.clp.2009.12.003

Waites, K. B., Katz, B., and Schelonka, R. L. (2005). *Mycoplasmas* and *Ureaplasmas* as neonatal pathogens. *Clin. Microbiol. Rev.* 18, 757–789. doi: 10.1128/CMR.18.4.757-789.2005

Waites, K. B., Xiao, L., Liu, Y., Balish, M. F., and Atkinson, T. P. (2017). *Mycoplasma pneumoniae* from the respiratory tract and beyond. *Clin. Microbiol. Rev.* 30, 747–809. doi: 10.1128/CMR.00114-116

Wang, N., Liu, W., Zhou, Y., and Liu, Y. (2019). *In vitro* activities of Nemonoxacin and other antimicrobial agents against human *Mycoplasma* and *Ureaplasmas* isolates and their defined resistance mechanisms. *Front. Microbiol.* 10:1890. doi: 10.3389/fmicb.2019.01890

Wu, H. N., Nakura, Y., Motooka, D., Nakamura, S., Nishiumi, F., Ishino, S., et al. (2014). Complete genome sequence of *Ureaplasma parvum* Serovar 3 strain SV3F4, isolated in Japan. *Genome Announc.* 2, e00256–e00214. doi: 10.1128/genomeA.00256-14

Xie, X. M., Huang, K. S., Li, W. H. (2009). Species identification genotyping of Ureaplasma in urogenital tract of male with secondary infertility and its clinical application. *J. Reprod. Med.* 18, 25–28.

Yang, T., Pan, L., Wu, N., Wang, L., Liu, Z., Kong, Y., et al. (2020). Antimicrobial resistance in clinical *Ureaplasma* spp. and *Mycoplasma hominis* and structural mechanisms underlying quinolone resistance. *Antimicrob. Agents Chemother.* 64:e02560-19. doi: 10.1128/AAC.02560-19

Zeng, X. Y., Xin, N., Tong, X. N., Wang, J. Y., and Liu, Z. W. (2016). Prevalence and antibiotic susceptibility of Ureaplasma urealyticum and mycoplasma hominis in Xi'an, China. *Eur. J. Clin. Microbiol. Infect. Dis.* 35, 1941–1947. doi: 10.1007/s10096-016-2745-2

Zhang, J., Kong, Y., Feng, Y., Huang, J., Song, T., Ruan, Z., et al. (2014a). Development of a multilocus sequence typing scheme for Ureaplasma. *Eur. J. Clin. Microbiol. Infect. Dis.* 33, 537–544. doi: 10.1007/s10096-013-1981-y

Zhang, J., Kong, Y., Ruan, Z., Huang, J., Song, T., Song, J., et al. (2014b). Correlation between Ureaplasma subgroup 2 and genitourinary tract disease outcomes revealed by an expanded multilocus sequence typing (eMLST) scheme. *PLoS One* 9:e104347. doi: 10.1371/journal.pone.0104347

Zhou, Y. H., Ma, H. X., Shi, X. X., and Liu, Y. (2018b). Ureaplasma spp. in male infertility and its relationship with semen quality and seminal plasma components. *J. Microbiol. Immunol. Infect.* 51, 778–783. doi: 10.1016/j.jmii.2016.09.004

Zhou, Y. H., Ma, H. X., Yang, Y., and Gu, W. M. (2018a). Prevalence and antimicrobial resistance of Ureaplasma spp. and mycoplasma hominis isolated from semen samples of infertile men in Shanghai, China from 2011-2016. *Eur. J. Clin. Microbiol. Infect. Dis.* 37, 729–734. doi: 10.1007/s10096-017-3167-5

Zhu, X., Li, M., Cao, H., Yang, X., and Zhang, C. (2016). Epidemiology of *Ureaplasma urealyticum* and *Mycoplasma hominis* in the semen of male outpatients with reproductive disorders. *Exp. Ther. Med.* 12, 1165–1170. doi: 10.3892/etm.2016.3409

Zhu, C. T., Liu, J. M., Ling, Y., Dong, C. L., Wu, T. T., Yu, X. Y., et al. (2012). Prevalence and antimicrobial susceptibility of Ureaplasma urealyticum and *Mycoplasma hominis* in Chinese women with genital infectious diseases. *Indian J. Dermatol. Venereol. Leprol.* 78, 406–407. doi: 10.4103/0378-6323.95480

Conflict of Interest: The authors declare that the research was conducted in the absence of any commercial or financial relationships that could be construed as a potential conflict of interest.

be evaluated in this article, or claim that may be made by its manufacturer, is not guaranteed or endorsed by the publisher.

frontiers in Microbiology

ORIGINAL RESEARCH
published: 03 December 2021
doi: 10.3389/fmicb.2021.725391

In silico Evolution and Comparative Genomic Analysis of IncX3 Plasmids Isolated From China Over Ten Years

Baomo Liu[1,2†], Yingyi Guo[1†], Ningjing Liu[1], Jiong Wang[1], Feifeng Li[1], Likang Yao[1] and Chao Zhuo[1]*

[1] State Key Laboratory of Respiratory Disease, The First Affiliated Hospital of Guangzhou Medical University, Guangzhou, China, [2] Department of Respiratory Medicine, The First Affiliated Hospital of Sun Yat-sen University, Guangzhou, China

IncX3 plasmids are correlated with the dissemination and acquisition of carbapenem resistance in *Enterobacteriaceae* and have been prevalent in China over the last 10 years. Since the distribution characteristics of IncX3 plasmids across China as well as their evolutionary traits for 10 years remain unclear, here we conducted a retrospective literature review and *in silico* comparative analysis of IncX3 plasmids in publicly available IncX3 plasmid genomes. IncX3 plasmids distributed in 17 provinces or cities were extracted for analysis, which tend to be specifically associated with hospital-isolated *Escherichia coli* ST410 from phylogroup A. Although the backbones of IncX3 plasmids have remained highly conservative over the last 10 years, the bla_{NDM} resistance genetic contexts on these plasmids could fall into five subtypes, among which AR_N1_I has been identified in *Enterobacter cloacae174* chromosome and AR_N5_I was simultaneously located on IncF and IncA/C plasmids. This suggests that the bla_{NDM} resistance gene environment can spread between different plasmids, between different bacterial genera, or between strains and plasmids, highlighting that it is imperative to adopt more stringent infection control measures targeting IncX3 plasmid spread.

Keywords: IncX3 plasmid, bla_{NDM}, carbapenem, *Escherichia coli*, genome

OPEN ACCESS

Edited by:
Yi-Wei Tang,
Cepheid, United States

Reviewed by:
Jian-Hua Liu,
South China Agricultural University, China
Abdullah Kilic,
Wake Forest University, United States

***Correspondence:**
Chao Zhuo
chao_sheep@263.net

[†] These authors have contributed equally to this work

Specialty section:
This article was submitted to Antimicrobials, Resistance and Chemotherapy, a section of the journal Frontiers in Microbiology

Received: *15 June 2021*
Accepted: *19 October 2021*
Published: *03 December 2021*

Citation:
Liu B, Guo Y, Liu N, Wang J, Li F, Yao L and Zhuo C (2021) In silico Evolution and Comparative Genomic Analysis of IncX3 Plasmids Isolated From China Over Ten Years. Front. Microbiol. 12:725391. doi: 10.3389/fmicb.2021.725391

INTRODUCTION

IncX3 plasmids were discovered 10 years ago, since Ho et al. (2012) first isolated the bla_{NDM}/IncX3 plasmid pNDM-HN380 in China in 2011. IncX3 seems to be the most common plasmid-incompatible type for carrying bla_{NDM} in China and even the world (Ma et al., 2020). However, no previous research has investigated the distribution characteristics of IncX3 plasmids across China as well as their evolutionary traits over the last 10 years. A substantial number of plasmid whole genome sequences from China have been reported over the last few decades, which make it possible to conduct long-term and large-scale plasmid comparison and evolutionary analysis.

Therefore, the current study using published literature about IncX3 plasmids isolated from China and the IncX3 plasmid complete gene sequence deposited in NCBI was presented (i) to describe the prevalence of IncX3 plasmids across China over approximately 10 years, (ii) to identify the genetic context of IncX3 plasmids to further clarify the mechanisms related to antibiotic resistance gene transfer, and (iii) to explore the diversity of IncX3 plasmids and refine the IncX3 subgroup. This project provided an excellent opportunity to facilitate the understanding

of the mechanisms of IncX3 plasmids' high prevalence in China and the mechanism of the wide dissemination of carbapenem-resistant strains.

MATERIALS AND METHODS

Search Strategy

We searched the PubMed database for published research of IncX3 separated in China before August 15, 2020. There was no language restriction. Keywords included ("China" and "IncX3").

Article inclusion criteria: (1) the strain containing the IncX3 plasmid was isolated from China; and (2) the basic information of the strain can be queried in the article, including strain species, isolation dates, cities, and specimen sources.

Exclusion criteria: (1) the strains and plasmids were not isolated from China; (2) there was no bacterial species information of the plasmid host; and (3) all other basic information except the plasmid name is missing.

Referring to selected literature and GenBank online information, we collected the basic information of all IncX3 plasmids including specimen sources, isolation dates, cities, and MLST types (see section "Results" in detail).

Plasmid Replicon Verification and Database Construction

We took the Rep sequence of the IncX3 plasmid deposited in the PlasmidFinder database as a reference and used BLASTN to verify the incompatibility group of the extracted plasmid sequence (homology >90%, coverage >90%). The hit rate of BLASTN was manually reviewed, and only published sequences were included in our IncX3 plasmid database.

Antibiotic Resistance Gene Annotation

We used Mega-BLAST (*e* value ≤0.0001, identity ≥70%) against the ResFinder database to compare and annotate antibiotic resistance genes located in plasmids and then performed a manual inspection.

Comparative Genomics Analysis of IncX3 Plasmids

The bla_{NDM}/IncX3 plasmid pNDM-HN380 (GenBank accession number: JX104760.1) in *Klebsiella pneumoniae* strain HN380 was adopted as a reference plasmid for comparison. BLAST was used to compare all completely sequenced IncX3 plasmids with pNDM-HN380. We counted the number of hits in different regions of pNDM-HN380 to determine the conserved regions. Annotation of the complete gene sequence was performed using Prokka for all collected plasmids.

Plasmid Backbone Recognition, Multiple Sequence Alignment, and Visualization

Mauve was used to perform multiple sequence alignment of plasmid DNA sequences to identify backbone genes. Plasmid backbone genes were defined as regions of plasmid DNA whose sequences were highly conserved in all aligned genomes.

The local blast + method was used for pairwise comparison to determine the plasmid group. Snippy software was applied to identify single-nucleotide polymorphism (SNP), insertion, or deletion changes between the reference plasmid pNDM-HN380 and other plasmids. Visualization of the comparison results was generated by Easyfig software, and the produced pictures were marked with gene names using Adobe Illustrator CC 2019 software.

RESULTS

The Distribution and Host Characteristics of IncX3 Plasmids Reported in China

By searching "China and IncX3" in the PubMed database, the genome sequences and basic information of 84 IncX3 plasmids involving 60 documents were collected (see **Supplementary Table 1** for all collected plasmid information).

From 2011 to 2021, a total of 84 non-duplicate collected IncX3 plasmids were reported in 13 provinces or cities across China, namely, Shandong, Jiangsu, Zhejiang, Guangdong, Shaanxi, Chongqing, Sichuan, Henan, Hong Kong, Beijing, Shanghai, Hunan, and Jiangxi. In this collection, the reported IncX3 plasmid-containing strains were isolated from clinical specimens (60.7%, 51/84, blood, urine, or sputum), livestock animals (17.9%, 15/84), life environment (such as sewage samples and surface of subway instruments), anal swab screening of admitted patients, and retail food meat.

The collected isolates carrying IncX3 plasmids were inspected further. The hosts of IncX3 plasmids involved 15 species. *Escherichia coli* (51.2%, 43/84), *K. pneumoniae* (23.8%, 20/84), and *Enterobacter cloacae* (7.1%, 6/84) were the most common hosts. The IncX3 plasmid was also sporadically distributed in 12 other species of *Enterobacteriaceae*, namely, *Citrobacter freundii*, *Salmonella Typhimurium*, *Cronobacter sakazakii*, *K. aerogenes*, *K. quasipneumoniae*, *Klebsiella oxytocin*, *Klebsiella oxytoca*, *Kluyvera cryocrescens*, *M. morganii*, *Proteus mirabilis*, *Raoultella planticola*, *Raoultella ornithinolytica*, and *Salmonella Lomita*.

A remarkable diversity of sequence types (STs) was identified among IncX3 plasmid-containing *E. coli* isolates. Among the 43 *E. coli* isolates, 17 different STs were noted. The preferred STs seemed to be ST48 (6/33), ST410 (4/33), ST156 (4/33), ST167 (3/33), ST1114 (2/33), ST10 (2/33), ST617 (2/33), and ST641 (2/33). The other *E. coli* isolates belonged to single diverse STs (including ST46, ST3835, ST224, ST-744, ST44, ST1236, ST448, ST3076, and ST8809). It is worth noting that all ST48 *E. coli* were isolated from animals and ST410s were from clinical patients and hospital environments.

We also obtained phylotype data of 16 *E. coli* strains in our collection. Phylotype data suggested that more than half (68.8%, 11/16) belonged to non-pathogenic phylogroup A. Phylogroup B included three strains, and the remaining two strains belong to group C. Phylogroup A strains have been isolated from various sources, including clinical specimens, animals, human colonization, and environment. Four types of bla_{NDM}

variants (bla_{NDM-1}, bla_{NDM-5}, bla_{NDM-7}, and bla_{NDM-21}) were identified in IncX3 plasmid-carrying phylogroup A strains.

Carbapenem Resistance Genes Carried on IncX3 Plasmids

All the collected IncX3 plasmids were positive for carbapenemase genes, among which 81 (96.4%) of them were NDM-positive and 3 (3.6%) were OXA181-positive. The IncX3 plasmid carried eight types of NDM variants, namely, NDM-1 (22.2%, 18/81), NDM-5 (67.9%, 55/81), NDM-7 (3/81), NDM-21 (1.2%, 1/81), NDM-13 (1.2%, 1/81), NDM-17 (1.2%, 1/81), NDM-19 (1.2%, 1/81), and NDM-20 (1.2%, 1/81). No bla_{KPC}-carrying IncX3 plasmid was recorded in China.

Notably, bla_{NDM-5} was the most prevalent carbapenemase gene in the IncX3 plasmids, followed by the bla_{NDM-1} subtype. The bla_{NDM-5}-carrying IncX3 plasmids included plasmids from clinical specimens, livestock animals, life environment, anal swab screening of admitted patients, and retail food, indicating the wide dissemination of NDM-5-producing carbapenem-resistant isolates mediated by quick transfer of IncX3 plasmids. Interestingly, IncX3 plasmids containing the bla_{NDM-1} gene could be recovered from patient clinical specimens, rectal swabs, and hospital environments, which showed a preferred in-hospital spread for this gene subtype.

Whole Genome Sequence Grouping of IncX3 Plasmids

Among the 84 plasmids collected, a total of 76 IncX3 plasmid complete genome sequences were finally obtained. The analysis using Mauve and BlastN software identified that all 76 plasmids could be divided into nine subgroups by comparing sequences, that is, pNDM-HN380 (group1), pNDM_MGR194 (group2), pOXA181_EC14828 (group3), MH10T (group4), pNDM-BJ03 (group5), pGZ2-NDM (group6), pWLK-NDM (group7), pNDM5-LDR (group8), and pNDM5-GZ04_A (group9).

Comparison of plasmid sequences revealed nine distinct types, mainly because of the variety of the genetic load region (**Table 1**). Researchers have referred to "the gene load region" as the fragments containing inserted sequences and different resistance genetic context (Ho et al., 2012). For example, for the first featured IncX3 plasmid pNDM-HN380, the gene load region was between the *resolvase* gene and *hns* gene, and involved bla_{SHV}, bla_{NDM}, and their surrounding mobile genetic elements (*IS26*, *Tn3*, and *tnpA*).

The gene load region of the nine subgroups differed in resistance gene composition and mobile genetic elements. Most of the gene load regions (6/9) included resistance genes, more than just the carbapenemase gene as shown in **Table 1**.

IncX3 Plasmid Backbone Region Was Highly Conserved

The gene organization of the IncX3 plasmid backbones was nearly identical to that of plasmid pNDM-HN380, and the counterparts shared >95% amino acid identities (**Figure 1** and **Supplementary Table 2**). Among 75 plasmids compared with pNDM-HN380, only 21 plasmid backbones had a single-nucleotide change, or insertion/deletion of a single nucleotide, indicating that the IncX3 backbone has been highly conserved for 10 years.

TABLE 1 | IncX3 plasmid gene load regions.

Name	Carbapenemase	Size (bp)	Other resistance genes
pNDM-HN380	NDM-1	23,031	bla_{SHV-12}
pNDM-BJ03	NDM-1	31,079	bla_{SHV-12}
pWLK-NDM	NDM-1	45,279	$ampC^{f}$, *tetA*, *tetR*
pMGR194	NDM-5	15,157	–
MH10T	NDM-5	12,803	–
pGZ2-NDM	NDM-5	39,545	$tmrB^{a}$, tap^{b}, $ant1^{c}$, $emrE^{d}$,
pNDM5-LDR	NDM-5	19,975	–
pNDM5-GZ04_A	NDM-5	26,207	$mphA^{e}$, *tap*
pOXA181_EC14828	OXA-181	15,371	*qnrS1*

[a] *Tunicamycin resistance protein, which is a nucleotide antibiotic produced by the actinomycete Streptomyces lysosuperficus. It can inhibit the reproduction of viruses with envelopes (glycoproteins). It can inhibit the formation of glycoprotein by inhibiting the transfer of N-acetylglucosamine-1-phosphate to monophosphate long alcohol.*
[b] *Scaini et al. (2019).*
[c] *Prabhu et al. (2017).*
[d] *Saleh et al. (2018).*
[e] *Fong et al. (2017).*
[f] *Cephalosporinase.*

Subtype of bla_{NDM} Genetic Contexts Located in IncX3 Plasmids and Exploring the Mechanisms of Resistance Gene Transfer

The bla_{NDM} genetic contexts identified fell into five groups according to the comparison analysis, including AR_N1_I–AR_N1_III and AR_N5_I–AR_N5_II (**Figure 2**). Among them, AR_N1 corresponds to bla_{NDM-1} genetic context and AR_N5 means bla_{NDM-5} genetic context. Deletion or insertion of mobile gene elements (i.e., IS5 or IS125) and ORFs of unknown functions (i.e., *groL* and *groS*) accounted for the majority of the variations of these gene environments.

To detect the location of all bla_{NDM} genetic contexts other than IncX3 plasmids to discover the potential of transposon transfer, we searched all identified genetic context subtypes in the NCBI database. Surprisingly, we found that the genetic structure of AR_N1_I was nearly identical to a chromosome-encoded fragment containing bla_{NDM-1} in *Enterobacter cloacae174* (accession number: CP020528, 1628321. . .1645166, **Figure 3**), whose gene composition of the chromosome-encoded fragment was flanked by *IS26*, in addition to holding AR_N1_I genetic context.

DISCUSSION

Previous studies have sporadically reported that the presence of IncX3 plasmids mediated the dissemination of carbapenem-resistant *Enterobacteriaceae* strains in China (Yang et al., 2020; Zhai et al., 2020; Zhou et al., 2020). However, no previous

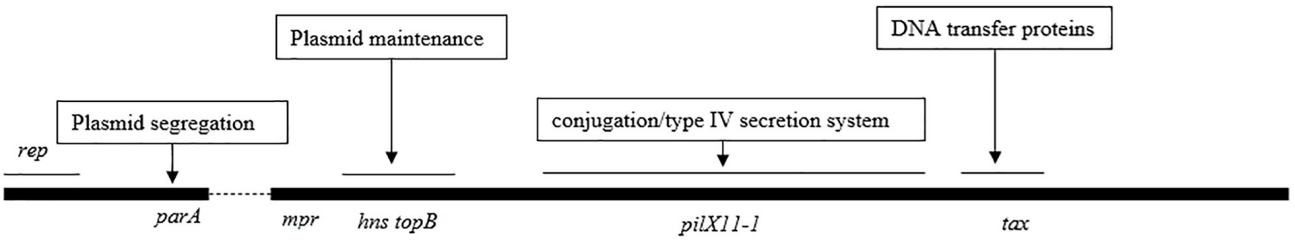

FIGURE 1 | Plasmid backbone region map (dotted line indicates gene load region).

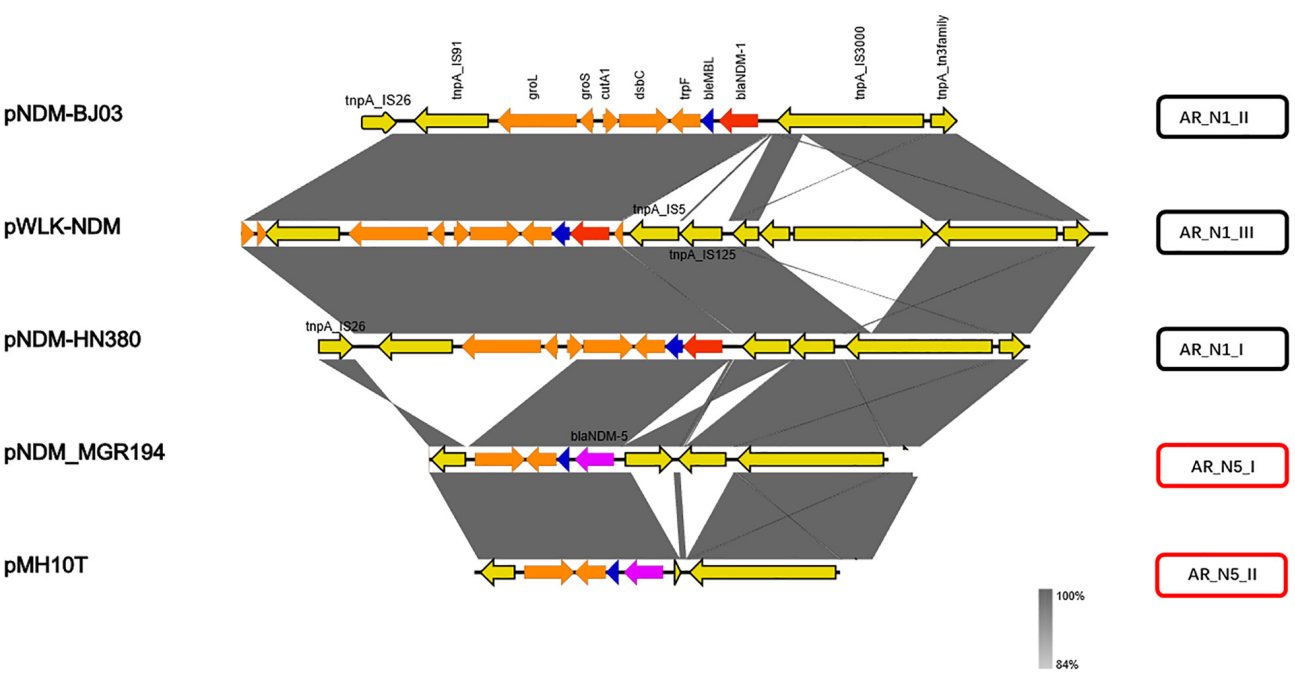

FIGURE 2 | Summary of sub-classifications of resistance gene environment.

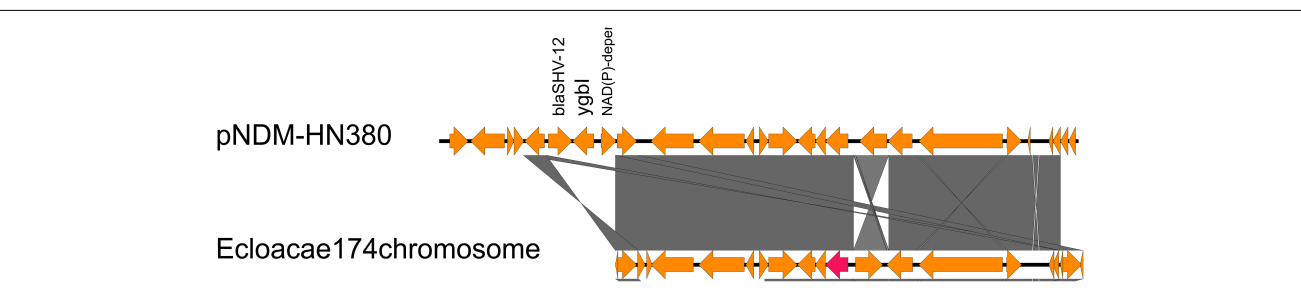

FIGURE 3 | Comparison of AR_N1_I structure of pNDM-HN380 with the *Enterobacter cloacae 174* chromosome gene fragment in NCBI.

research has investigated the distribution characteristics of IncX3 plasmids across China as well as their evolutionary traits over the last 10 years. This study provided a comprehensive and updated prevalence and sequence characteristic profile of carbapenem-resistant IncX3 plasmids isolated from various sources in China. We have performed large-scale and long-term *in silico* analyses of reported IncX3 plasmids to elucidate IncX3 plasmid structural features over 10 years.

IncX3 plasmids are the most prevalent in *E. coli* and *K. pneumoniae* but sparse in other *Enterobacteriaceae*, where phylogroup A and ST410 *E. coli* isolated from patients seems to be the preferred host for IncX3 plasmids, highlighting that more infection control measures should be the target at these

emerging specific associations between plasmids and bacterial clones. Consistently, Ma et al. (2020) demonstrated that IncX3 plasmids could often transfer to phylogroup A *E. coli* successfully and maintain high stability. The study of Huang et al. (2021) published in 2021 has found that bla_{NDM}/IncX3 plasmids tend to be concentrated in ST410 *E. coli*, which also belongs to phylotype A. Our team also found a large number of ST410 *E. coli* with bla_{NDM}-carrying IncX3 plasmids (data not shown).

The IncX3 plasmid carries at least eight kinds of bla_{NDM} gene variants, among which bla_{NDM-5} is dominant. The bla_{NDM-5}-carrying IncX3 plasmids were recovered from diverse sources, indicating the wide dissemination of NDM-5-producing carbapenem-resistant isolates mediated by quick transfer of IncX3 plasmids. However, bla_{NDM-1}-carrying IncX3 plasmids were mainly distributed in the hospital, which show more limited dissemination compared with $bla_{\mathrm{NDM-5}}$.

We further divided carbapenem resistance genes and surrounding structural fragments obtained from IncX3 plasmid into five subtypes, AR_N1_I–AR_N1_III and AR_N5_I–AR_N5_II. The sub-classification of bla_{NDM} genetic contexts can help researchers understand the structural characteristics of resistance genes and explore its transmission mechanism. Our results found that AR_N1_I is highly homologous to bla_{NDM-1} surrounding fragments encoded by *Enterobacter cloacae174* chromosome, indicating that bla_{NDM-1} surrounding fragments could transfer between the IncX3 plasmid and *Enterobacter* chromosome. In 2020, Zou et al. (2020) reported that the genetic environment containing bla_{NDM-5} could be divided into five subtypes. Among them, Type A corresponds to the AR_N5_I genetic environment in our study. The Type A genetic environment has been the most common (50%) genetic environment containing bla_{NDM}, suggesting that the AR_N5_I genetic environment has an advantage in assisting the wide spread of bla_{NDM-5}. Besides, the AR_N5_I genetic environment is also distributed on the IncF and IncA/C plasmids, and the IncA/C plasmid is a well-known broad host plasmid (Douarre et al., 2020), suggesting that the dissemination of bla_{NDM} gene will cross genus, not only limited to *Enterobacteriaceae* bacteria.

Therefore, the bla_{NDM-5} genetic context carried by IncX3 plasmids can spread between different plasmids, between different bacterial genera, or between strains and plasmids. This suggests that controlling the spread of IncX3 plasmids has significant meaning for controlling the quick occurrence of carbapenem-resistant bacteria.

The genes on the backbone are responsible for maintaining the basic functions of the plasmid, including conjugation transfer and plasmid progeny distribution. The comparative analysis of the plasmid backbone region shows that the IncX3 backbone genes have been highly conservative for the last 10 years. This suggests that the IncX3 plasmid backbone gene itself has the advantage of mediating the wide spread of bla_{NDM}. The theory of plasmid biology shows that high conjugation efficiency, powerful distribution system, and low fitness cost are three factors to ensure the long-term existence and wide spread of plasmids (Zwanzig, 2021). The T4SS system in the backbone region guarantees the efficiency of plasmid self-conjugation (Costa et al., 2020); the *parAB* distribution system ensures that progeny plasmids can be assigned to the offspring host, promoting plasmid stability (Sheng et al., 2020). Further research into backbone gene function will facilitate the deep investigation of IncX3 plasmid fitness mechanisms in China.

CONCLUSION

In this study, our data indicate that carbapenem-resistant gene-carrying IncX3 plasmids tend to be specifically associated with hospital-isolated *E. coli* ST410 from phylogroup A. Although the backbones of IncX3 plasmids remained highly conservative over the last 10 years, the bla_{NDM} resistance genetic contexts on plasmid could fall into five subtypes, among which AR_N1_I has been identified in *Enterobacter cloacae174* chromosome and AR_N5_I was simultaneously located on IncF and IncA/C plasmids. This suggests that the bla_{NDM} resistance gene environment can spread between different plasmids, between different bacterial genera, or between strains and plasmids, highlighting that it is imperative to adopt more stringent infection control measures targeting IncX3 plasmid spread.

DATA AVAILABILITY STATEMENT

The datasets presented in this study can be found in online repositories. The names of the repository/repositories and accession number(s) can be found in the article/**Supplementary Material**.

AUTHOR CONTRIBUTIONS

CZ, BL, and YG conceived and designed the experiments and wrote the manuscript. NL, JW, FL, and LY searched PubMed and collected IncX3 plasmid information. BL and YG performed the bioinformatic analysis. All authors provide critical input to the manuscript and endorsed the final version.

FUNDING

The research was supported by the National Natural Science Foundation of China (Project Nos. 81772238 and 81861138056) and the Guangzhou Municipal Science and Technology Bureau (Project No. 201607020044).

ACKNOWLEDGMENTS

We thank Jingjie Song from Shenzhen People's Hospital for helping us to analyze the WGS data.

SUPPLEMENTARY MATERIAL

The Supplementary Material for this article can be found online at: https://www.frontiersin.org/articles/10.3389/fmicb.2021.725391/full#supplementary-material

REFERENCES

Costa, T. R. D., Harb, L., Khara, P., Zeng, L., Hu, B., and Christie, P. J. (2020). Type IV secretion systems: advances in structure, function, and activation. *Mol. Microbiol.* 115, 436–452. doi: 10.1111/mmi.14670

Douarre, P. E., Mallet, L., Radomski, N., Felten, A., and Mistou, M. Y. (2020). Analysis of COMPASS, a new comprehensive plasmid database revealed prevalence of multireplicon and extensive diversity of IncF plasmids. *Front. Microbiol.* 11:483. doi: 10.3389/fmicb.2020.00483

Fong, D. H., Burk, D. L., Blanchet, J., Yan, A. Y., and Berghuis, A. M. (2017). Structural basis for kinase-mediated macrolide antibiotic resistance. *Structure* 25, 750.e5–761.e5. doi: 10.1016/j.str.2017.03.007

Ho, P. L., Li, Z., Lo, W. U., Cheung, Y. Y., Lin, C. H., Sham, P. C., et al. (2012). Identification and characterization of a novel incompatibility group X3 plasmid carrying bla NDM-1 in *Enterobacteriaceae* isolates with epidemiological links to multiple geographical areas in China. *Emerg. Microbes. Infect.* 1:e39. doi: 10.1038/emi.2012.37

Huang, Y. S., Tsai, W. C., Li, J. J., Chen, P. Y., Wang, J. T., Chen, Y. T., et al. (2021). Increasing New Delhi metallo-beta-lactamase-positive *Escherichia coli* among carbapenem non-susceptible *Enterobacteriaceae* in Taiwan during 2016 to 2018. *Sci. Rep.* 11:2609. doi: 10.1038/s41598-021-82166-8

Ma, T., Fu, J., Xie, N., Ma, S., Lei, L., Zhai, W., et al. (2020). Fitness Cost of bla_{NDM-5}-Carrying p3R-IncX3 Plasmids in Wild-Type NDM-Free *Enterobacteriaceae*. *Microorganisms* 8:377. doi: 10.3390/microorganisms8030377

Prabhu, D., Vidhyavathi, R., and Jeyakanthan, J. (2017). Computational identification of potent inhibitors for Streptomycin 3″-adenylyltransferase of *Serratia marcescens*. *Microb. Pathog.* 103, 94–106. doi: 10.1016/j.micpath.2016.12.015

Saleh, M., Bay, D. C., and Turner, R. J. (2018). Few conserved amino acids in the small multidrug resistance transporter EmrE influence drug polyselectivity. *Antimicrob. Agents Chemother.* 62:e00461-18. doi: 10.1128/AAC.00461-18

Scaini, J. L. R., Camargo, A. D., Seus, V. R., von Groll, A., Werhli, A. V., da Silva, P. E. A., et al. (2019). Molecular modelling and competitive inhibition of a *Mycobacterium tuberculosis* multidrug-resistance efflux pump. *J. Mol. Graph. Model.* 87, 98–108. doi: 10.1016/j.jmgm.2018.11.016

Sheng, D., Chen, X., Li, Y., Wang, J., Zhuo, L., and Li, Y. (2020). ParC, a new partitioning protein, is necessary for the active form of ParA From Myxococcus pMF1 plasmid. *Front. Microbiol.* 11:623699. doi: 10.3389/fmicb.2020.623699

Yang, L., Li, J., Zha, L., Wang, K., Qi, K., Qiu, S., et al. (2020). OXA-181-producing extraintestinal pathogenic *Escherichia coli* sequence Type 410 Isolated from a dog in portugal. *Infect. Drug. Resist.* 64:e02298-19. doi: 10.1128/AAC.02298-19

Zhai, R., Fu, B., Shi, X., Sun, C., Liu, Z., Wang, S., et al. (2020). Contaminated in-house environment contributes to the persistence and transmission of NDM-producing bacteria in a Chinese poultry farm. *Environ. Int.* 139:105715. doi: 10.1016/j.envint.2020.105715

Zhou, H., Zhang, K., Chen, W., Chen, J., Zheng, J., Liu, C., et al. (2020). Epidemiological characteristics of carbapenem-resistant *Enterobacteriaceae* collected from 17 hospitals in Nanjing district of China. *Antimicrob. Agents. Chemother.* 9:15. doi: 10.1186/s13756-019-0674-4

Zou, H., Jia, X., Liu, H., Li, S., Wu, X., and Huang, S. (2020). Emergence of NDM-5-Producing *Escherichia coli* in a teaching hospital in chongqing, China: IncF-Type plasmids may contribute to the prevalence of bla NDM- 5. *Front. Microbiol.* 11:334. doi: 10.3389/fmicb.2020.00334

Zwanzig, M. (2021). The ecology of plasmid-coded antibiotic resistance: a basic framework for experimental research and modeling. *Comput. Struct. Biotechnol. J.* 19, 586–599. doi: 10.1016/j.csbj.2020.12.027

Conflict of Interest: The authors declare that the research was conducted in the absence of any commercial or financial relationships that could be construed as a potential conflict of interest.

Publisher's Note: All claims expressed in this article are solely those of the authors and do not necessarily represent those of their affiliated organizations, or those of the publisher, the editors and the reviewers. Any product that may be evaluated in this article, or claim that may be made by its manufacturer, is not guaranteed or endorsed by the publisher.

Advantages of publishing in Frontiers

OPEN ACCESS
Articles are free to read for greatest visibility and readership

FAST PUBLICATION
Around 90 days from submission to decision

HIGH QUALITY PEER-REVIEW
Rigorous, collaborative, and constructive peer-review

TRANSPARENT PEER-REVIEW
Editors and reviewers acknowledged by name on published articles

Frontiers
Avenue du Tribunal-Fédéral 34
1005 Lausanne | Switzerland

Visit us: www.frontiersin.org
Contact us: frontiersin.org/about/contact

REPRODUCIBILITY OF RESEARCH
Support open data and methods to enhance research reproducibility

DIGITAL PUBLISHING
Articles designed for optimal readership across devices

FOLLOW US
@frontiersin

IMPACT METRICS
Advanced article metrics track visibility across digital media

EXTENSIVE PROMOTION
Marketing and promotion of impactful research

LOOP RESEARCH NETWORK
Our network increases your article's readership